NASA Contractor Report 181893

STUDIES OF AEROTHERMAL LOADS GENERATED IN REGIONS OF SHOCK/SHOCK INTERACTION IN HYPERSONIC FLOW

Michael S. Holden, John R. Moselle, and Jinho Lee

CALSPAN-UB RESEARCH CENTER
Buffalo, New York

Contract NAS1-17721
October 1991

National Aeronautics and Space Administration

Langley Research Center
Hampton, Virginia 23665-5225

ABSTRACT

Experimental studies have been conducted to examine the aerothermal characteristics of shock/shock/boundary layer interaction regions generated by single and multiple incident shocks. An extensive review made of the literature on this subject showed that there was significant lack of detailed high-quality experimental data in the high Mach number and Reynolds number flow regime. The experimental studies presented here were conducted over a Mach number range from 6 to 19 for a range of Reynolds numbers to obtain both laminar and turbulent interaction regions. Detailed heat transfer and pressure measurements were made for a range of interaction types and incident shock strengths over a transverse cylinder, with emphasis on the types III and IV interaction regions. These measurements indicated that the peak heat transfer and pressure increased with the occurrence of transition in the shear layer generated in both type III and type IV interactions, and with increasing Mach number. For some type IV interactions with flowfield configurations close to those for maximum heating, a flow instability was observed which caused large temporal variations in the peak heating. For completely laminar interactions in high Mach number, low Reynolds number flows, the structure of the type IV flowfield and the resulting heat transfer and pressure levels appear to be strongly influenced by viscous effects in the shear layers. The measurements made in this study were compared with the simple Edney, Keyes and Hains models for a range of interaction configurations and freestream conditions. For interactions where transition occurred in the shear layer, the peak pressures were in general agreement with the predictions for types III and IV interactions; however, the predictions employing laminar stagnation-point heating rates for type IV interactions must be enhanced to account for radiated noise generated in the transitional shear layer. For fully laminar flow conditions in a type III interaction, experimental results were in good agreement with the simple predictions; however, the pressures and heating rates in a type IV interaction were significantly overpredicted if multiple compressions were assumed in the inviscid jet. The effect of sweeping the interaction is to lower the heating and pressure levels in roughly the same proportions to the reductions observed when sweeping a cylinder in the absence of the interaction. The studies of multiple-shock interaction demonstrated that the largest heat loads are generated on the cylinder if the shocks coalesce before they are incident on the cylinder. The complex flowfields and aerothermal loads generated by multiple-shock impingement, while not generating as large peak loads, provide important test cases for code prediction. It will be difficult to accurately predict the maximum heating in shock/shock-interaction regions over a large and important part of the flight regime, because free-shear-layer transition can take place at low Reynolds numbers, in either single- or multiple-shock/shock interactions, and because of the occurrence of flow instabilities for type IV interactions. The detailed heat transfer and pressure measurements presented in this report provide a good basis for evaluating the accuracy of simple prediction methods and detailed numerical solutions for laminar and transitional regions of shock/shock interactions.

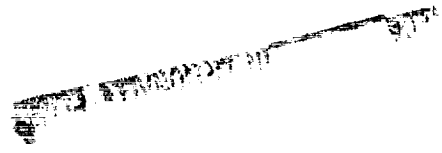

NOMENCLATURE

A, B, N	Constant Used in Peak-Heating Correlation
a	Speed of Sound
C^*	$(\mu^*/\mu_\infty)T_\infty/T^*$
C_h, St	$= q/(\rho_\infty U_\infty (H_o - H_w))$, Stanton Number
C_p	Pressure Coefficient, Equation 4.9
$\overline{C_p}$	Specific Heat at Constant Pressure
c	Specific Heat; Chord Length, Figure 42
$c(T)$	Specific Heat, Appendix A
D	Cylinder Diameter
d	Heat-Penetration Depth of Substrate, Appendix A
F_{shape}	Shape Factor $1/2^{(N-1)/2}$, where $N = 1, 2$
f	Characteristic Frequency (Hz)
H	Total Enthalpy
h	$= q/(T_{aw} - T_w)$, Heat Transfer Coefficient
$k(T), k, K$	Thermal Conductivity
ℓ_{SL}	Length of Shear Layer, Figure 2
M	Mach Number
M_1	Incident Mach Number
M_2	Convective Mach Number $= (U_2 - U_3)/a_2$, Figure 4
OL	Shock-Generator Angle, Table I
P	Pressure; Separation Point, Figure 19
Pr	Prandtl Number
P_{ratio}	Non-Dimensional Pressure Ratio
p	Static Pressure
p_0'	Undisturbed Stagnation Pressure
$Q, q(\dot{q})$	Heat Transfer (Rate)
$\overline{q}_\infty$	Dynamic Pressure
q_{FR}, Q_{FR}	Fay-Riddell Heat Transfer, Reference 49
R	Reattachment Point, Figure 19
$\overline{R}$	Gas Constant (=1717.91 ft-lb/slug/°R)

NOMENCLATURE (cont.)

Re	$= U\ell/\nu$, Reynolds Number
Re_D	$= \rho_\infty U_\infty D/\mu_\infty$
Re_d	Attachment-Line Reynolds Number, Equation 5.7a
Re_{d_*}	Reference Attachment-Line Reynolds Number, Equation 5.10b
R_{LE}	Leading-Edge Body Radius, Figure 11
r	Implicit Marching-Step Size, Appendix A
SL	Shear Layer, Figure 1
St_A	Attachment-Line Stanton Number
s	Laplace Variable, Appendix A
T	Temperature (°R)
TS	Transmitted Shock, Figure 1
t	Time; Thickness of Blunt Leading Edge or Nose
t_{max}	Length of Time for which Semi-infinite Solid Assumption is Valid, Appendix A
U, V	Velocity
U_R	Width of Reattachment Region
V	Characteristic Velocity, Figure 42
X, x	Normal Distance Measured in to Surface, Body Surface Coordinate
Y, y	Normal Distance Measured Away from Surface

GREEK SYMBOLS

α	$= k(T)/(\rho c(T))$, Appendix A
$\bar{\alpha}$	Reattachment Angle
β	Shock and Initial Shear-Layer Angles, Figure 15
$\bar{\beta}$	Pressure-Gradient Parameter (= 0 to 2)
γ	Specific Heat Ratio ($\sim$1.4, Ideal Gas)
Λ	Bow-Shock Standoff Distance, Figure 9b
$\Lambda\ell$	Width of Supersonic Jet, Figure 3
δ	Boundary Layer Thickness
δ_{SL}	Width of Shear Layer, Figure 2
Γ	$(\gamma - 1)/(\gamma + 1)$
ζ	Parameter Used in Equation 5.5

NOMENCLATURE (cont.)

η	Non-Dimensional Distance, Appendix A
$\bar{\eta}$	Non-Dimensional Length Scale, Equation 5.7b
θ	Angular Position on the Cylinder Model
$\bar{\theta}$	Angular Position on the Cylinder Model, Figure 12
κ	$= D_n/(\varrho_\infty U^2 t)$
λ	Dummy Variable, Appendix A
λ, Λ	Swept Angle
$\bar{\lambda}$	Model Sweep Angle, Table I
μ	Viscosity
ν	Kinematic Viscosity
ξ	Kirchoff Transformation Variable, Appendix A
ϱ	Density
τ	Non-Dimensional Time
ϕ	Orbital Angle of Attack, Figure 13
ω	Radial Frequency

SUBSCRIPTS

*	Reference Value
0	Undisturbed Value
1	Initial Value
1, 2, 3, 4, 5, 6, 7, 8	Regions in Type III and Type IV interactions as illustrated by Figures 2 and 12a(c)
A	At Attachment Line
aw, AW	Adiabatic Wall Value
b, B	At Body
D	Diameter
e	Edge Condition
FR, F – R	Fay-Riddell Values, Reference 49
IDEAL	Ideal Value
i	Incident
LAM	Laminar-Flow Value
LE	At Leading Edge

NOMENCLATURE (cont.)

max	Maximum Peak Value
peak	Peak Value
R	At Reattachment Region, Figure 19
$Real$	Real Value
ref, REF	Reference Value
SL	Shear-Layer Value
$STAG, stag$	At Stagnation Region
s	Shear-Layer Value
w, W	Wall Value
∞, INF	Freestream Value

Table of Contents

Table of Contents (cont.)

List of Figures

List of Figures (cont.)

List of Figures (cont.)

List of Figures (cont.)

List of Tables

[redacted] INTENTIONALLY BLANK

Section 1
INTRODUCTION

The heating rates generated on blunt bodies by a shock incident on the bow shock in the stagnation region can be orders of magnitude greater than the stagnation value in the absence of the interaction and, therefore, are of considerable interest to designers of hypersonic vehicles. Initial studies by Edney[1] of flowfields and large heating loads generated in shock/shock interaction regions demonstrate that, for certain incident-shock/bow-shock configurations, the pressure recovered on the body can be orders of magnitude larger than the undisturbed-flow pitot pressure, which, in turn, causes a corresponding heat transfer rate increase in the stagnation region. Edney and, later, others[2,3] showed that six different flow configurations can be generated, depending on the strength of the incident shock and its point of intersection with the bow shock. Figure 1 shows the various flow patterns developed for the incident-shock/bow-shock configurations as defined by Edney. Types I, II, and V are interactions where the shock propagates to the surface of the body, resulting in a shock/boundary layer interaction. A type VI interaction results in an expansion-fan boundary layer interaction, which does not cause significant aerothermal-load enhancement. However, types III and IV interactions (shown in Figures 2 and 3) result in large heating and pressure loads and are of the greatest interest to researchers.

The peak heating developed in regions of type III interaction are generated on the body just downstream of the reattachment point of the free shear layer. This reattachment phenomenon is very similar to the reattachment of separated shear layers developed over spiked bodies, highly indented nose shapes, and compression ramps. The development of the shear layer and the peak heating developed in these flows are strongly dependent upon whether the shear layer is laminar or turbulent, as demonstrated in extensive studies of separated flows by Holden[4]. These studies (and many others) have shown that the stability of the laminar flow in both the free shear layer and the attached boundary layer increases with local Mach number. However, in general, transition of the free shear layer occurs at Reynolds numbers an order of magnitude smaller than for attached boundary layers. To provide a guide in determining which correlation to employ in the semi-empirical prediction techniques, Edney[1] and, later, Birch and Keyes[5] correlated shear-layer transition measurements from separated-flow studies and shock/shock-interaction measurements. The transition correlation developed by Birch and Keyes is shown in Figure 4. This correlation suggests that, in hypersonic flows, shear layers with Reynolds numbers of approximately 5×10^4 will be transitional in character. Employing the analogy between reattachment heating in separated flows and that induced in regions of shock/shock interaction, Keyes and Hains[2] (based on the work of Bushnell and Weinstein[5a]) suggested the relationships shown in Figure 2 for estimating the heating rates for type III interactions. While such correlation techniques may be considered outmoded by current computational procedures for modeling the transitional shear layers and boundary layers, the correlation techniques still represent a useful engineering tool.

A type IV interaction is generated when an oblique shock is incident close to the normal region of the bow shock, as illustrated in Figure 1. In high Reynolds number flows, shock/shock interaction produces an essentially inviscid slipstream—which Edney termed a "jet"—in which the supersonic flow is efficiently compressed by a series of compression and expansion waves. This jet, which is bounded by shear layers, is terminated by a normal shock just ahead of the surface to produce a narrow stagnation region. The efficient compression process produces high pressures and large velocity gradients in the small stagnation

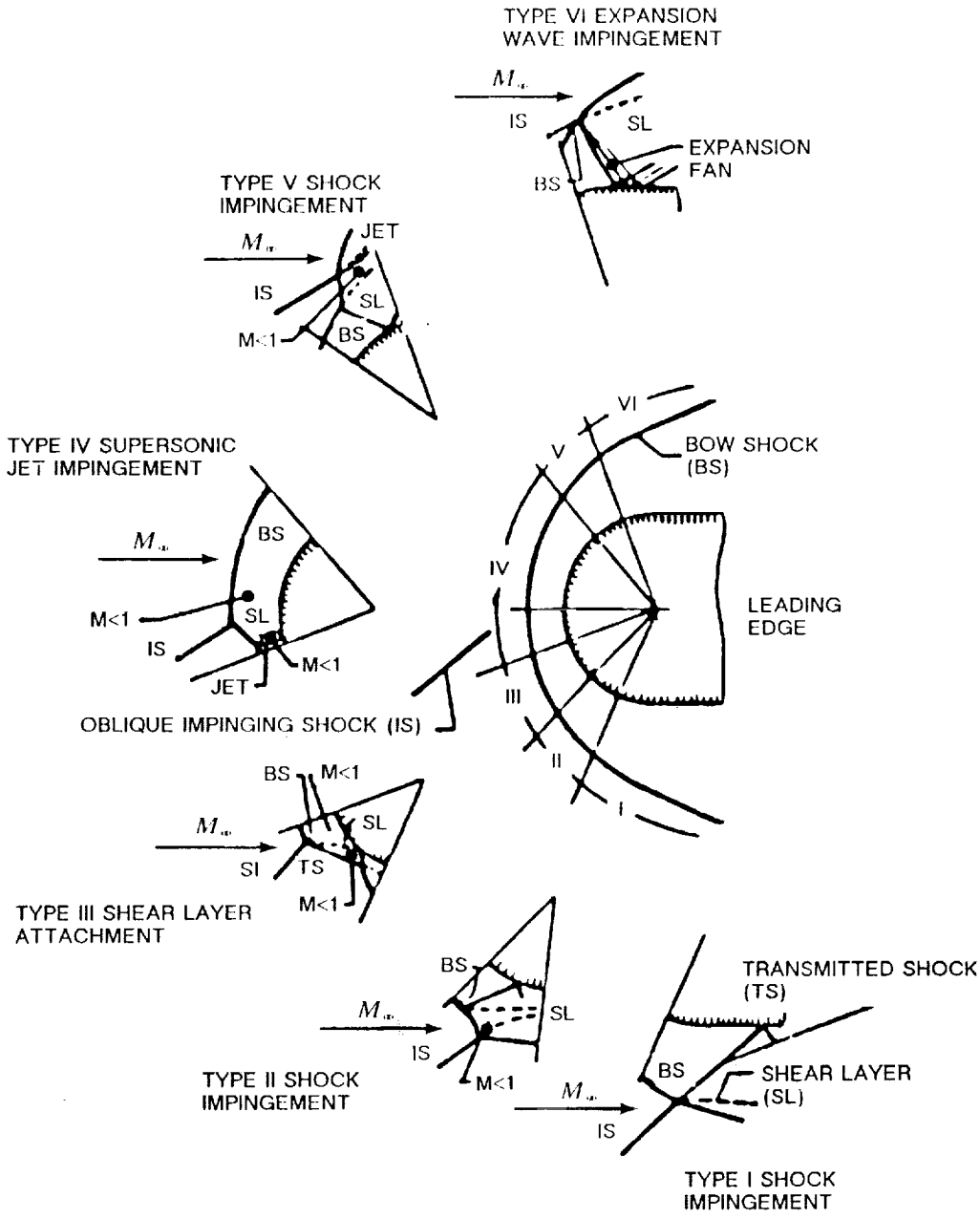

Figure 1 SIX TYPES OF SHOCK-WAVE INTERFERENCE PATTERNS

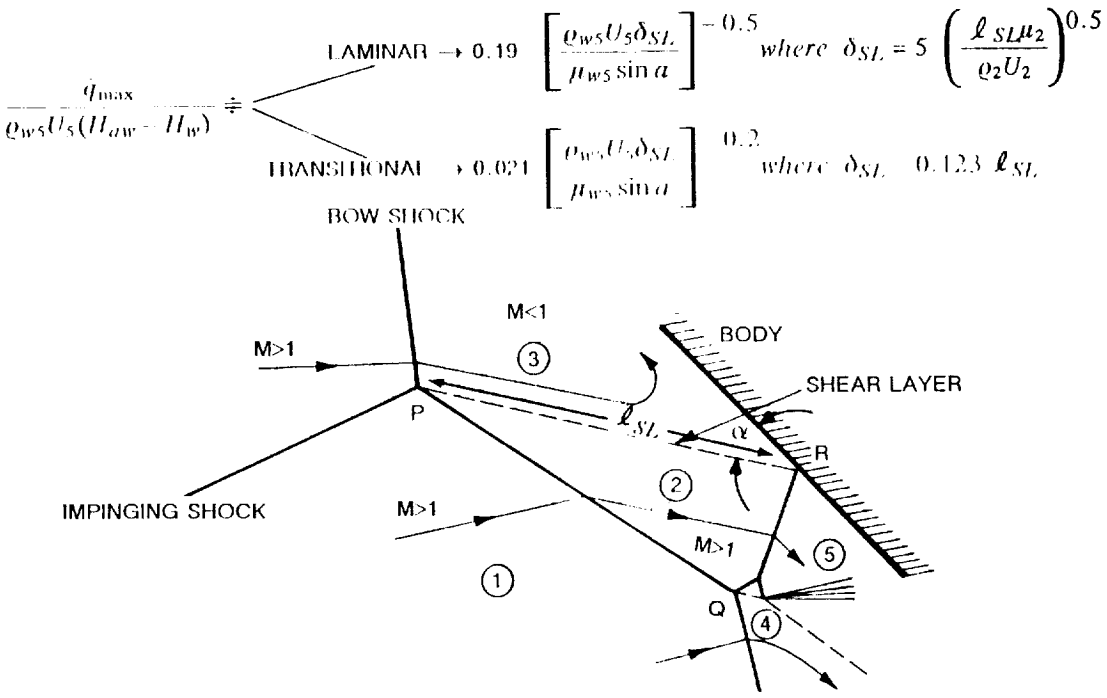

Figure 2 SCHEMATIC DIAGRAM OF TYPE III INTERFERENCE

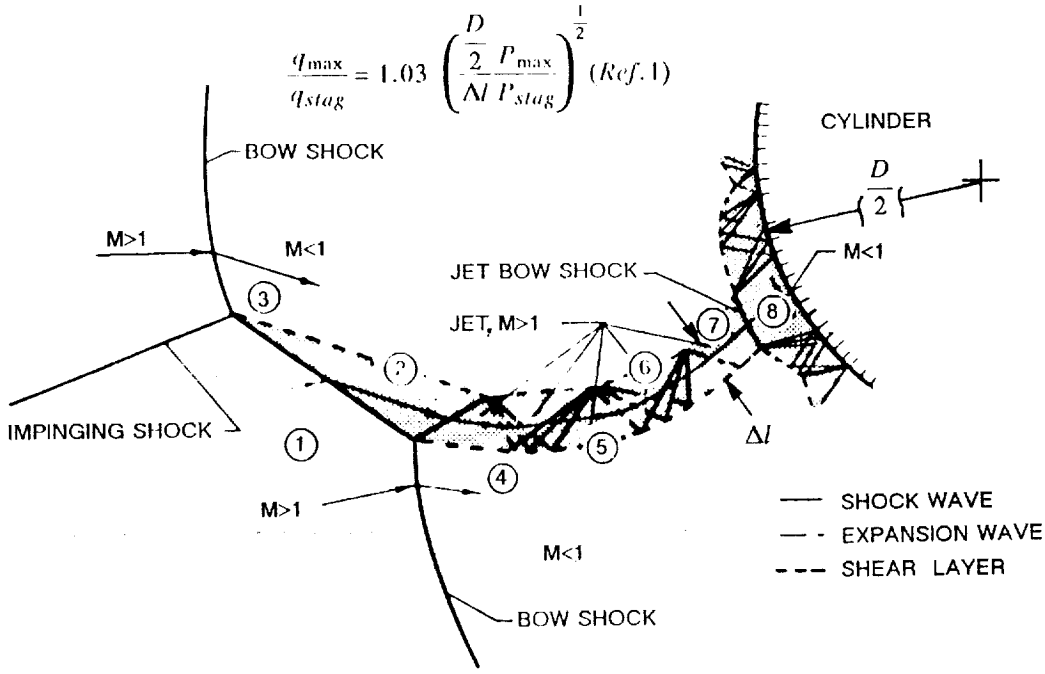

Figure 3 SCHEMATIC DIAGRAM OF A TYPE IV INTERFERENCE PATTERN IMPINGING ON A CYLINDER (After Reference 22)

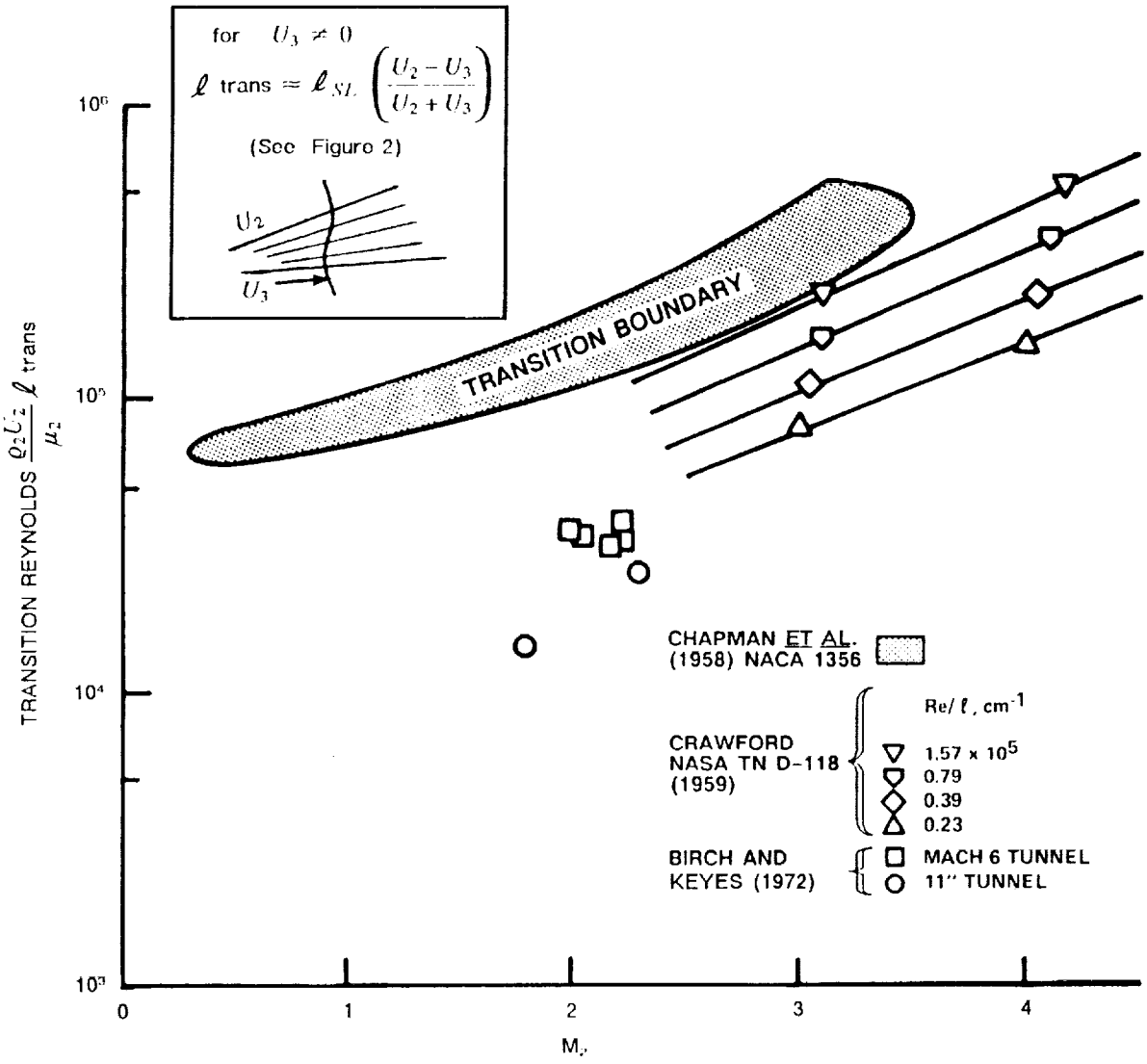

Figure 4 VARIATION OF TRANSITION REYNOLDS NUMBER WITH CONVECTIVE MACH NUMBER

region that can cause large heating rates relative to the heating generated by undisturbed flow. A simple relationship, suggested by Edney, for estimating the ratio of type IV heating to the undisturbed value is shown in Figure 3. However, with increasing Mach number and decreasing Reynolds number, the laminar shear layers that bound the jet can influence the characteristics of the jet to the point that the structure of the stagnation regions is significantly modified. Under such conditions, viscous effects can significantly reduce the heating levels at the base of the jet, as will be seen later. Alternatively, if the shear layer upstream of the jet is transitional, the disturbances generated in the stagnation regions of the jet may significantly enhance the peak heating levels.

In this report, we present an experimental study to investigate the effects of Mach number and Reynolds number on the detailed distributions of pressure and heat transfer in regions of shock/shock interaction over a transverse cylinder at Mach 6 to 19. Additional studies of the aerothermal characteristics of regions of multiple-shock/shock interaction and a preliminary study of sweep effects on regions of shock/shock interactions are presented. We first review some of the results of earlier studies of regions of shock/shock interaction. We then discuss the objectives and design of the present experimental program. The models and instrumentation employed in this study are presented, together with the test procedures employed. The results of the experimental program are then presented and discussed. Detailed listings of the model configurations, test conditions, and measurements of pressure and heat transfer, together with Schlieren photographs, are presented in appendices.

Section 2
REVIEW OF EARLIER STUDIES

Studies of the aerothermal loads generated by shock/shock/boundary layer interaction, or "interference heating," began shortly after the advent of supersonic flight and construction of supersonic wind tunnels. Most of the earlier studies were concerned with the aerodynamic loads generated by shock/shock interaction. However the structural failure of the pylon supporting the dummy ramjet engine in X-15 flight tests[6] and the burning up of the nosetip model in a sled test conducted by the Air Force[7] provide graphic demonstrations (Figures 5 and 6) of the searing heating loads that can be generated in the regions of shock/shock interaction. One of the most definitive studies of shock/shock interaction resulted from an investigation of "anomalous heating rates" by Edney[1]. Other major studies of interference heating have been formulated to investigate the aerothermal loads from (i) shock incident on a fin, wing or pylon; (ii) nosetip/body shock interaction on indented nosetips and spiked bodies; and (iii) impingement of shocks onto inlet cowl lips and injector struts. A chronological summary of various investigations is given in Table 1.

Investigations of "shock impingement" heating began in the early 60's with studies of the oblique shock incident on swept and unswept fins. These early efforts were motivated by observations of unusually high heating rates generated during flow-visualization studies of various uninstrumented supersonic aircraft configurations at NASA/Langley. The first definitive investigations of shock-interaction heating were wind tunnel and free-flight studies conducted in supersonic flows (up to Mach 5.5), designed by Newlander[8] and Carter and Carr[9] to measure the heating in regions of shock impingement on unswept cylinders. A typical model configuration for Newlander's investigation, along with the associated heating rates, is shown in Figure 7. Similar heating rates are shown in Figure 8 for the free-flight investigation of Carter and Carr. These studies revealed heating enhancements 5 to 10 times higher than the reference stagnation heating value in the presence of shock/shock interaction. Measurements on similar configurations were conducted in hypersonic flows by Francis[10]. Beckwith[11] and Bushnell[12,13] measured the interference heating on a swept cylinder close to its junction with a wedge, while Jones[14] studied a fin/plate interference at Mach 6. Bushnell's[12] earlier work focused on the interference heating problem caused by the root region of a wedge-swept cylinder configuration, and, initially, analysis of localized effects of shock/shock interactions was not pursued. However, in a subsequent study, Bushnell[13] isolated both the effects of shock/shock interactions and the effects of separated root region. By supporting the cylinder away from the shock generator, he removed the separated region at the wedge/cylinder junction. A typical result of peak-heating expectations based on Bushnell's work, and the typical model configuration, is given in Figures 9a and 9b.

Also, during the mid-60's, studies were being conducted for the Air Force Flight Dynamics Laboratory (AFFDL) in the Arnold Engineering Development Center (AEDC) facilities by Siler and Deskin[15], Gulbran et al.,[16,17] Knox,[18] and Ray and Palko.[19] Again, the emphasis in this work was on leading-edge shock impingement and was a direct result of AFFDL's experience with high heat loading observed during their supersonic aircraft testing programs. Siler's investigation of leading-edge surface heat transfer yielded heating enhancements of 5 times the values without shock impingement. The high heat rates caused by the shock/shock interaction are illustrated in Figure 10. This test was conducted in AEDC's Tunnel F, using nitrogen as the test gas at Mach 19. The investigation(s) of Ray and Palko were

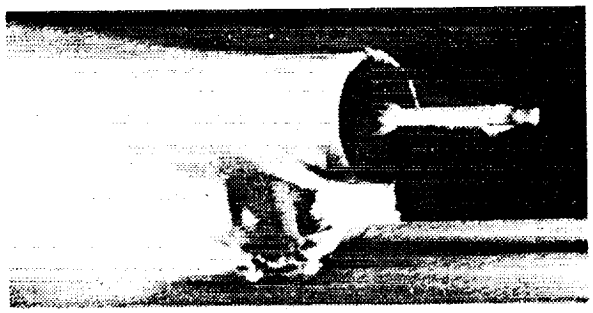

Figure 5a SLED IN MOTION AT 7,000 FPS ON TEST TRACK AT HOLLOMAN AFB

Figure 5b SLED ON TEST TRACK AT HOLLOMAN AFB AND RESULTING INTERACTION-HEATING DAMAGE

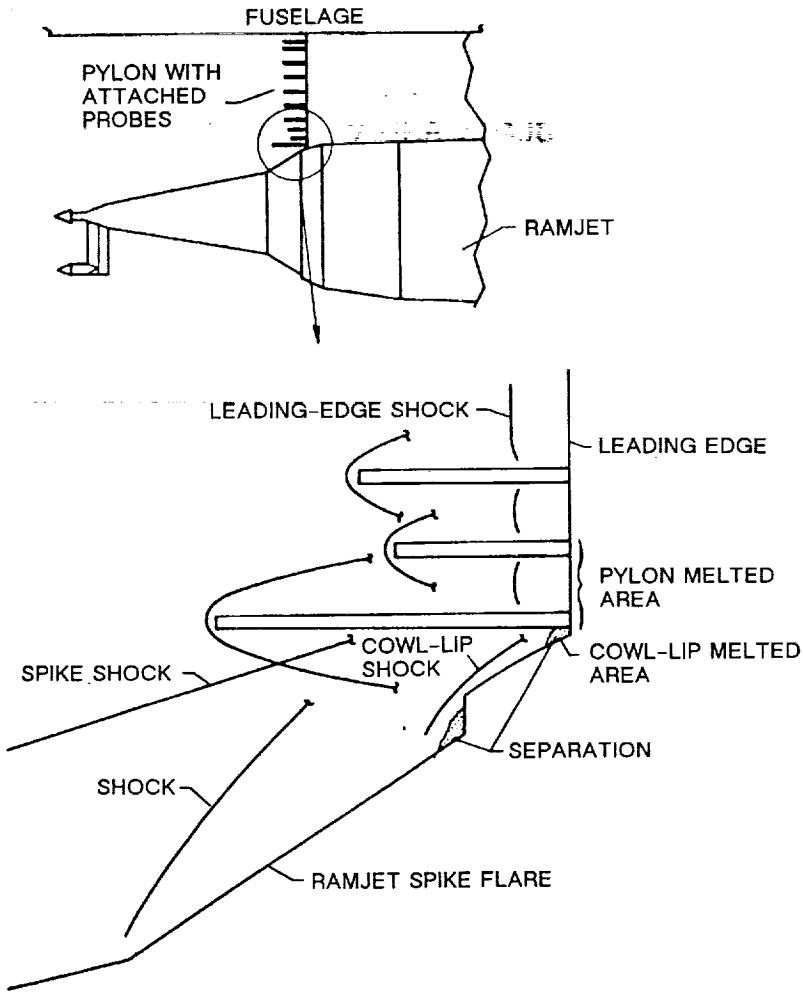

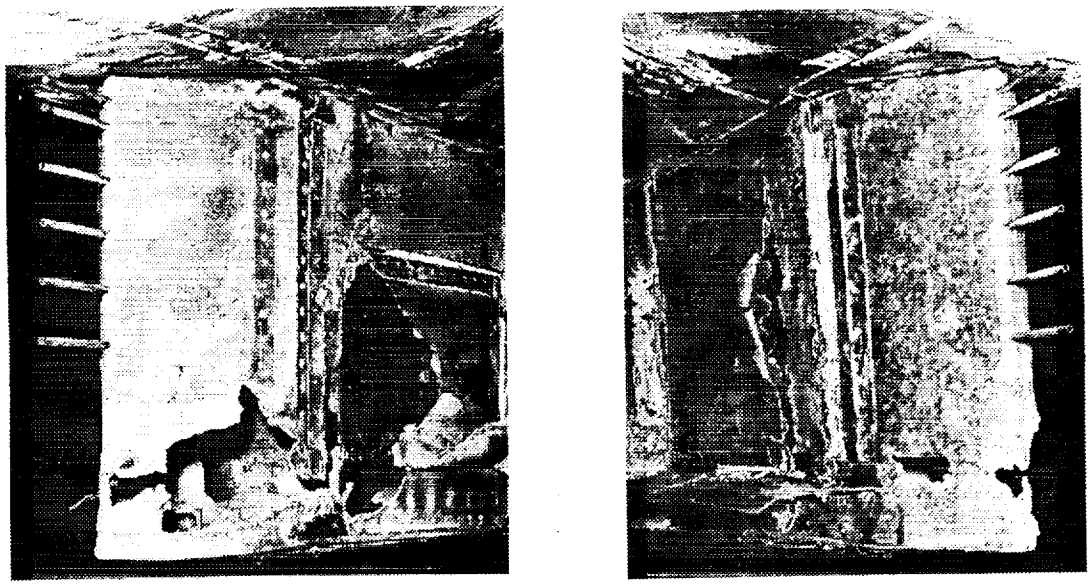

Figure 6 DAMAGE TO X-15 PYLON RESULTING FROM SHOCK/SHOCK INTERACTIONS

Table 1. SUMMARY OF SHOCK-INTERFERENCE INVESTIGATIONS

Author and Date	Reference number	M_∞	Re_∞/ft	Fin diameter, t, in.	Shock-generator angle, OL, deg	Model sweep angle, Λ, deg	Measurements: Static Pressure p	Measurements: Heat Transfer q	Visualization: Schlieren	Visualization: Oil	$\frac{\dot{q}_{max}}{\dot{q}_{ref}}$	Remarks
Newlander (1961)	8	2.65 3.51 4.44	1.32×10^6 to 4.56×10^6	2.796	16.25	0		x		x	1.8 2.0 3.1	Wedge and fin mounted on flat plate. Partially immersed in boundary layer. Thermocouple/stainless steel model.
Carter and Carr (1961)	9	2.0		0.75	*	0			x			*Not applicable. Shock generated by hemisphere/cylinder.
		2.53 to 5.5	15.96×10^6 to 30.01×10^6		*	0		x			0.1 to 0.5 (M_∞ = 3) 1.5 to 2	Free flight to 10,500-ft altitude. Thermocouple/thin-wall stainless steel cylinder.
Beckwith (1964)	11	4.15	17.28×10^6 to 43.21×10^6	1.10	0	20	x	x	x		2.5	Thermocouple/stainless steel model.
Jones (1964)	14	6.0	0.7145×10^6 to 8.76×10^6	1.06	0	60	*x	x	x	x	1 to 3	*Only at Re/ft = 10×10^6. Model yawed up to 30°.
Siler and Deskin (1964)	15	19.0	0.287×10^6	2.00	0 to 40	0 to 60	x	x	x		2.5 to 5	34 stainless steel colorimeter-type transducer based on a thermocouple.
Bushnell (1965)	12	8.0	0.924×10^6 to 1.05×10^6	1.00	12	45 and 60	x	x	x		3 to 5	Thin thermocouple/thin-wall model.
Francis (1965)	10	9.0	1.15×10^6 to 1.757×10^6	1.00	*6.34	0		x	x		1 to 4	*Cone and wedge with one cylinder and one wedge fin, both fixed.
Knox (1965)	18	~18	0.05×10^6 to 0.15×10^6	–	–	–	x	–	x	–	–	
Ray and Palko (1965)	19	6, *8, 10	0.567×10^6 to 3.6×10^6	2.00	0 to 60	0 to 60	x	x	x	x	2.5 to 5	*Data not presented for $M_\infty = 8$.
Gulbran et al. (1965)	17	~8.0	$\sim 3 \times 10^6$							X		Forward-facing step, plate/wedge, fin model with swept angle, bluntness. Temperature paint.
Gulbran et al. (1967)	16	~16	0.2×10^6	2	–	–	x	x	x	–	–	Thermistor heat-flux gage.
Heirs and Loubsky (1967)	20	14	0.095×10^6	1.00	0 to 15	0, 22.5, 45		x	x	x	10	Luminous photographs supplement Schlieren photographs. Chromel-constantan thermocouples thin-wall leading-edge model.
Jones, Bushnell, and Hunt (1967)	37	8	0.57×10^6	–	0	0	x	x	0		9	Phase-changing paint "Tension Shell" model.
Bushnell (1968)	13	8	0.503×10^6 to 5.03×10^6		12	0.76	x	x	x		x	Mica/glass model, temp.-sensitive paint.
Edney (1968)	1	4.6 7	1.24×10^6 to 14.42×10^6 0.335×10^6 to 2.334×10^6		0 to 15 0 to 5		x	x	x		10	Axisymmetric blunt bodies and fins. Thin-film gages.
Watts (1968)	6											Flight data only. Pressure data later reported by Burcham and Nugent (1970).
Young, Kaufman, and Korkegi (1968)	29	3, 5	0.5396×10^6 to 1.418×10^6	0.75	0	0	x		x	x		
Rogers (1971)	23	8,10	10^6	–	0	0	x	x	x	–	~4	1/80-scale straight-wing shuttle model, thin-film H/T gages.
Haslett et al. (1972)	31	8	0.360×10^6 to 3.59×10^6	1.00	1.5 to 15		x	+x	*x		1.15	*Shadowgraphs also. +Thermocouple and phase-change coating data.
Holden (1972)	53	6.5 to 13	10×10^6 to 100×10^6		0 to 20		x	x	x		50	Thin-film H/T gage.
Kaufman and Korkegi (1972)	25	2.5, 3.0	0.6×10^6	0.394	0	0	x	x	x			Only pressures reported.
Ginoux and Matthews (1973)	32	2.25	0.405×10^6 to 0.87×10^6	1.78	6		x	x			~3	Copper/constantan thermocouple-hollow cylinder.
Keyes and Hains (1973)	2	6-20	1×10^6 to 7.8×10^6	1.92	30		x	x	x		7.5 to 17	347 Stainless steel models, pressure model, temp-paint/epoxy model.
Tannehill et al. (1976)	27	5.95	0.186×10^6	1.92								Computational solution to N.S. compared to
Wieting and Holden ('88)	38	6,8	0.5×10^6 to 4.9×10^6	3.00	10 to 15	0	x	x	x		5 to 18	Thin-film gages.
Holden, Wieting, Moselle and Glass (1988)	28	6-18	0.5×10^6 to 20×10^6	3.00	10 to 15	0	x	x	x		5 to 28	Thin-film gages.
Glass, Holden, and Wieting (1989)	57	8	1.5×10^6	3	12.5*	15° 30°	x	x	x		5 to 18	*Swept angles.

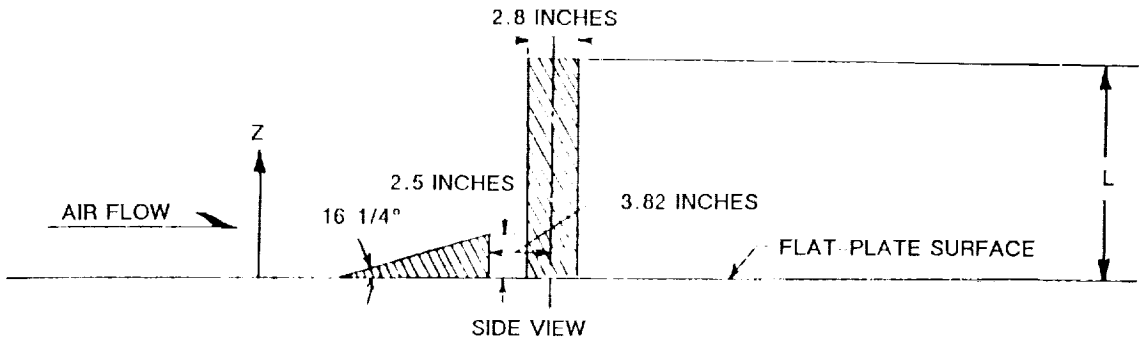

M_∞	$\frac{U_\infty L}{\nu_\infty}$	h
2.65	3.95×10^6	0.01661
2.65	2.65	.01356
2.65	1.60	.00959
3.51	3.95	.01472
3.51	2.75	.01231
3.51	1.60	.00938
4.44	4.50	.01282
4.44	3.20	.01071
4.44	2.15	.00871

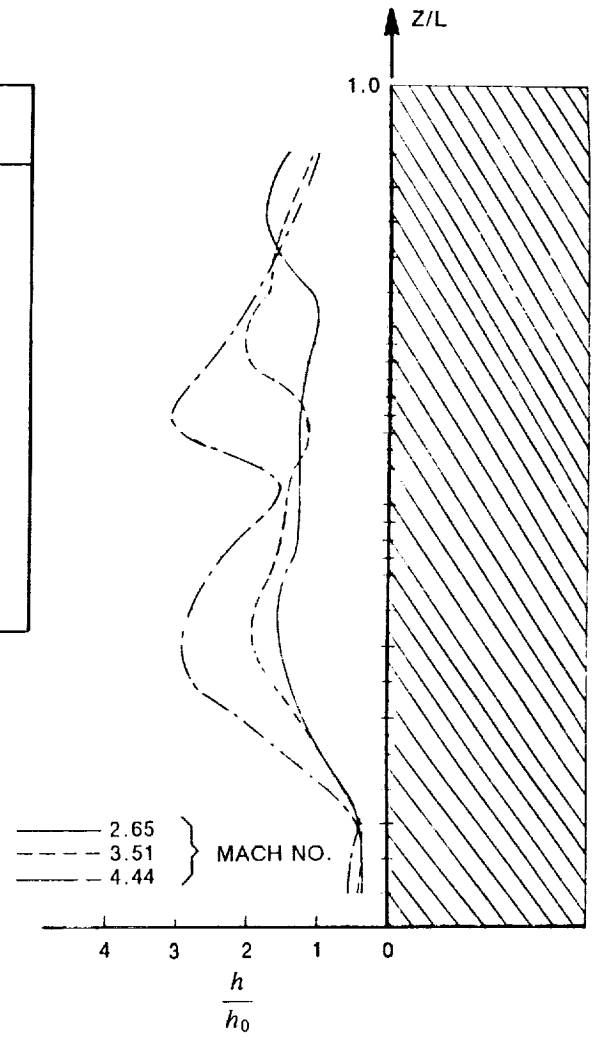

Figure 7 SHOCK IMPINGEMENT HEATING ON A RIGHT CIRCULAR CYLINDER AT MACH NUMBERS BETWEEN 2.65 AND 4.44 IN INVESTIGATION OF NEWLANDER (Ref. 8)

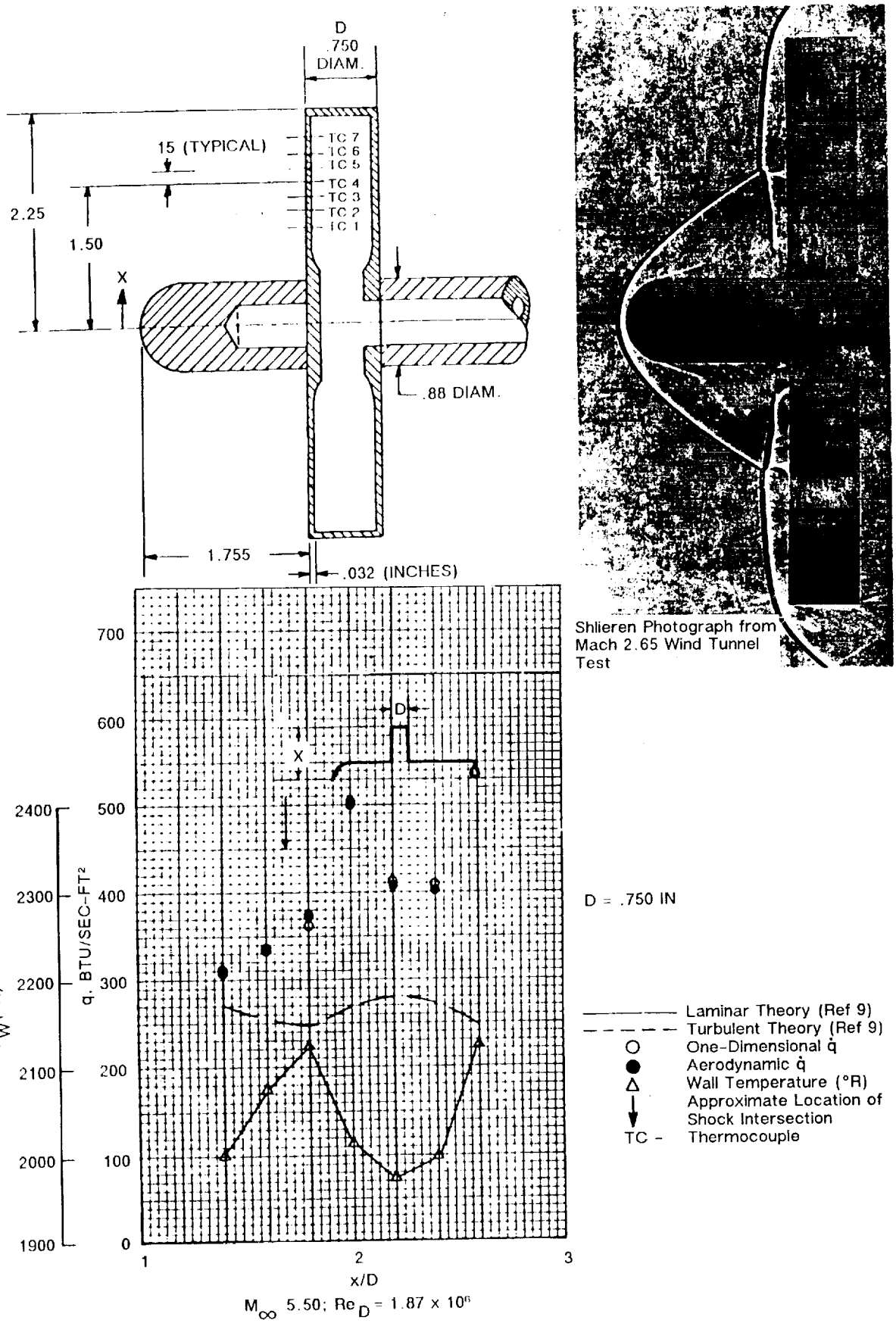

Figure 8 FREE-FLIGHT SHOCK INTERFERENCE MEASUREMENTS OF HEAT TRANSFER ON UNSWEPT CYLINDER AT MACH NUMBERS UP TO 5.5 (Ref. 9)

HEAT TRANSFER TO LEADING EDGE WITH AND WITHOUT GROOVES (TO TRIP THE BOUNDARY LAYER)
$M_\infty = 8$; X /D ≈ 12

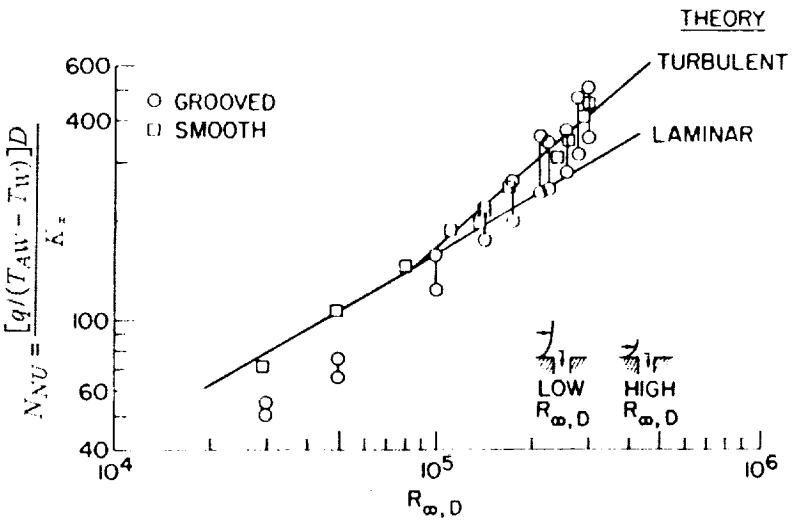

TYPICAL MODEL CONFIGURATIONS FOR SWEPT LEADING EDGE STUDY

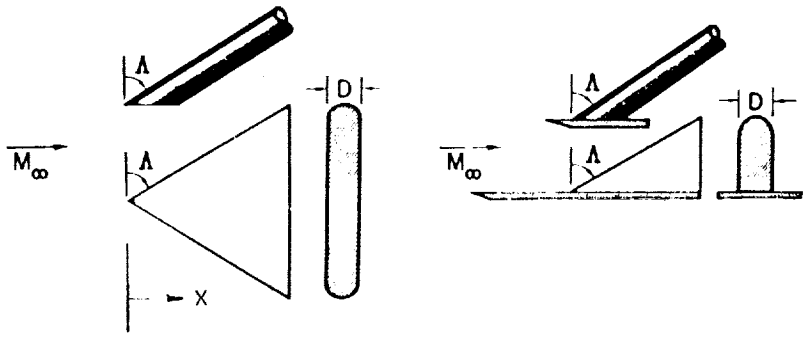

Figure 9a EFFECTS OF SHOCK IMPINGEMENT ON PEAK-HEATING INVESTIGATION OF BUSHNELL (Ref. 12, 13)

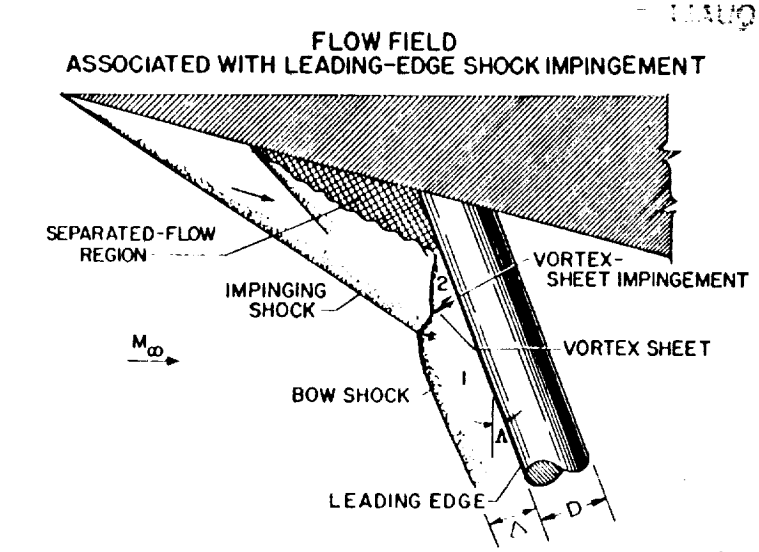

Figure 9b ILLUSTRATION OF INTERFERENCE PATTERN GENERATED BY A HYPERSONIC WING/FUSELAGE JUNCTION AND A TYPICAL WIND TUNNEL MODEL USED (Ref. 12, 13)

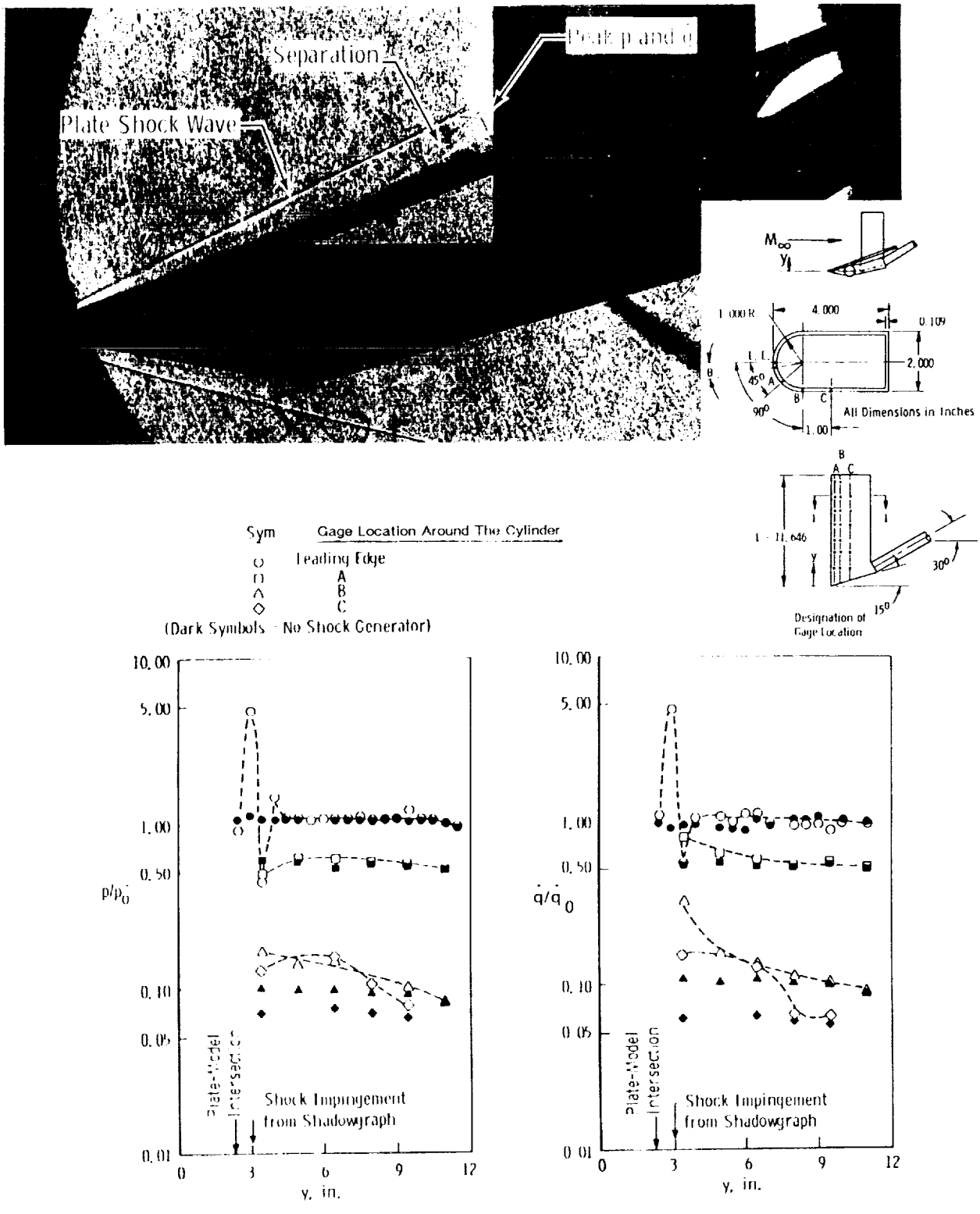

Figure 10 PRESSURE AND HEAT TRANSFER DISTRIBUTION MEASUREMENTS OF SILER AND DESKIN (Ref. 15) (using N_2 at Mach 19)

conducted in AEDC Tunnels B and C, again with a wedge/cylinder model configuration. These studies were conducted in air at Mach 6 to 10. The peak heat transfer rates observed here were 3 to 4 times the undisturbed rate. It is clear that, in these studies as well as in the earlier work, the density of instrumentation was insufficient to define the distribution and peak heating in the interaction region.

At NASA/Ames, Heirs and Loubsky[20] also studied the effects of shock impingement on the heat transfer to a cylindrical leading edge in the Ames shock tunnel at Mach 14. This latter study highlighted a number of problems associated with measurement of the large heat transfer rates and gradients generated in the interaction regions. More specifically, in the experiments of Heirs and Loubsky, and in many of the other studies, the conductivities of the model surfaces were such that the measured peak heating and the distribution of heating rates were significantly reduced by heat conduction along the model surface. Although a correction procedure can be used, it can be highly inaccurate, particularly if the actual heat transfer distribution is unsteady. The long response time of the instrumentation used in the past made it impossible to resolve unsteady movement in the interaction region. Even with these difficulties in instrumentation, the measured peak heat rates on an unswept cylinder impinged by an externally generated shock wave were estimated to be 10 times those of the undisturbed values. This study also concluded that increasing the swept angle of the cylinder will alleviate the heat loading. At larger swept angles, the heat transfer rates could be adequately analyzed through the use of a simple two-dimensional boundary layer solution with swept-cylinder transformation, as discussed later. A typical prediction for an unswept configuration as compared with an experimental result at Mach 14 is illustrated in Figure 11.

In one of the most significant investigations of shock/shock-interaction phenomena, Edney[1] identified the basic flowfield structure in regions of shock/shock interaction for a number of shock geometries and suggested simple prediction methods to estimate the aerothermal loads generated by them. The work of Edney provided valuable insights to various types of inviscid and viscous interaction problems and will be discussed further in detail. Following this major work (cited earlier), a series of studies were initiated by NASA/Langley to develop more accurate methods for predicting shock interaction heating with application to the design of the Shuttle project. The work of Keyes and Hains[2] and, later, Keyes and Morris[22] extended the experimental work of Edney and provided some simple prediction techniques with which to estimate the aerodynamic loads, as well as peak heating-rate measurements. The work of Keyes and Hains, in particular, focused on the various types of interactions that could occur on the surface of shuttle/tank configurations. This investigation led to the conclusion that a Type IV interaction could occur on a shuttle/tank configuration, increasing the local heating rate up to 20 times that of the undisturbed freestream heating rate. The test results, model configuration, and typical locations of the interaction are illustrated in Figures 12a and 12b. The heat transfer measurements made in the Keyes and Haines work were deduced from phase-change paint techniques, which have slow response and are accurate to only $\pm 30\%$. However, the evaluation of the flowfield characteristics represents an important contribution. The computer program written by Morris and Keyes[21] provides particularly useful information in this regard. Measurements of the shock impingement heat loads on the shuttle were also performed in a number of other studies made with models of the orbiter (Rogers[23]) and the orbiter/tank (Lanning[24] and Ginoux[33]).

During the mid-60's to early 70's, the Air Force, motivated by their experience with the X-aircraft testing program, supported work on shock impingement on blunt fins (Kaufman[25]) and inlets (Craig[3]) as well as (at the Von Karman Institute) on conical bodies and cylinders. The works of Kaufman[30,31] were directed to study of the detailed structure of the separation and interaction regions of a blunt fin mounted on a flat plate. The focus of these works was to study detailed flow structure by various means of flow

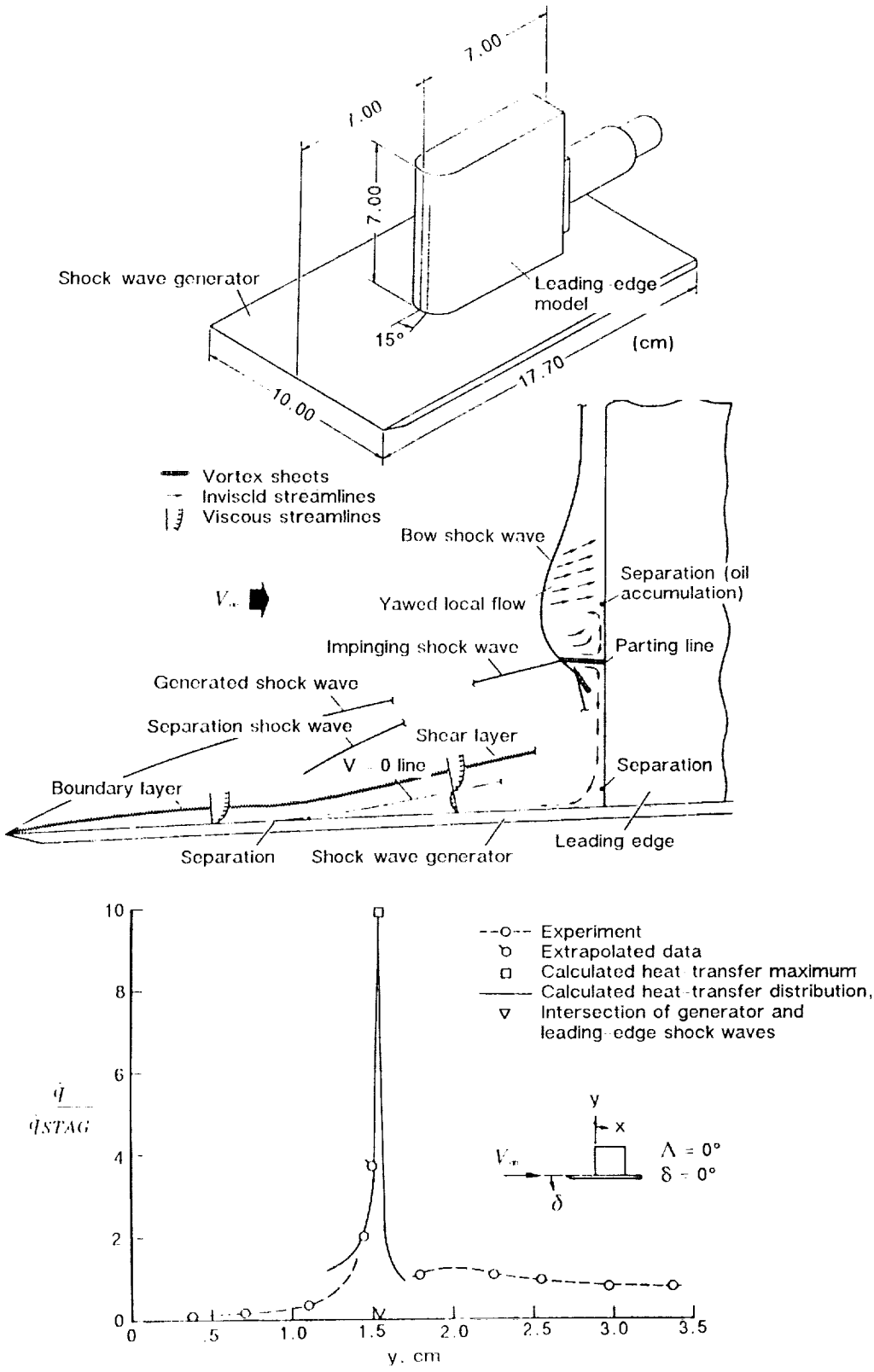

Figure 11 SPANWISE HEAT TRANSFER DISTRIBUTION ON STAGNATION LINE OF THE BLUNT LEADING-EDGE INVESTIGATION OF HEIRS AND LOUBSKY (Ref. 20)

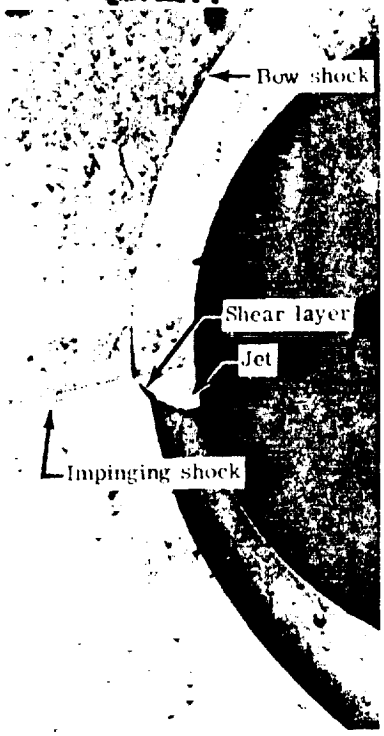

L-73-254

(a) Schlieren photograph.

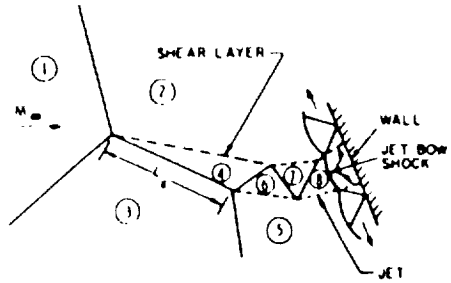

JET BOW SHOCK IN REGION (8)

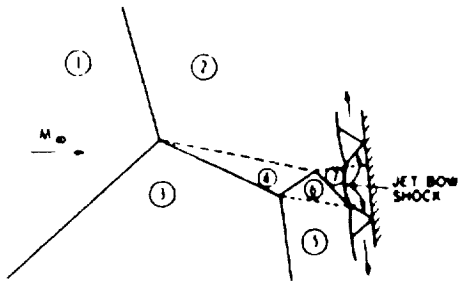

JET BOW SHOCK IN REGION (7)

(c) Interference patterns.

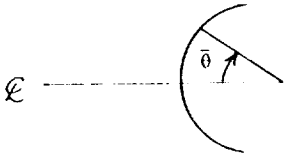

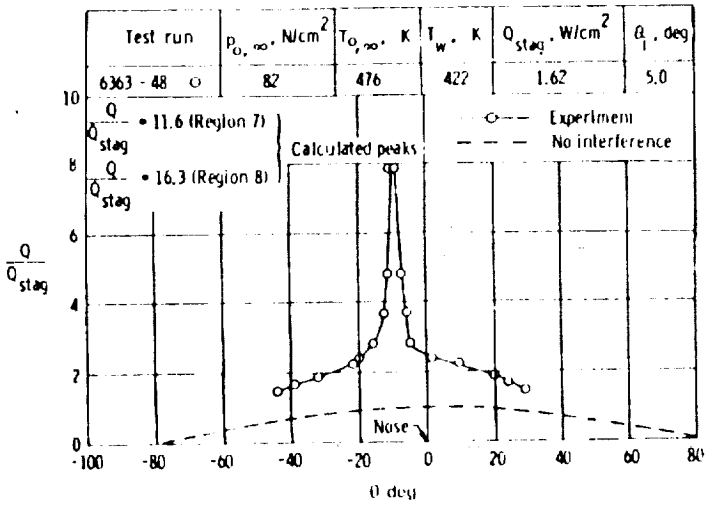

(b) Heat-transfer distribution.

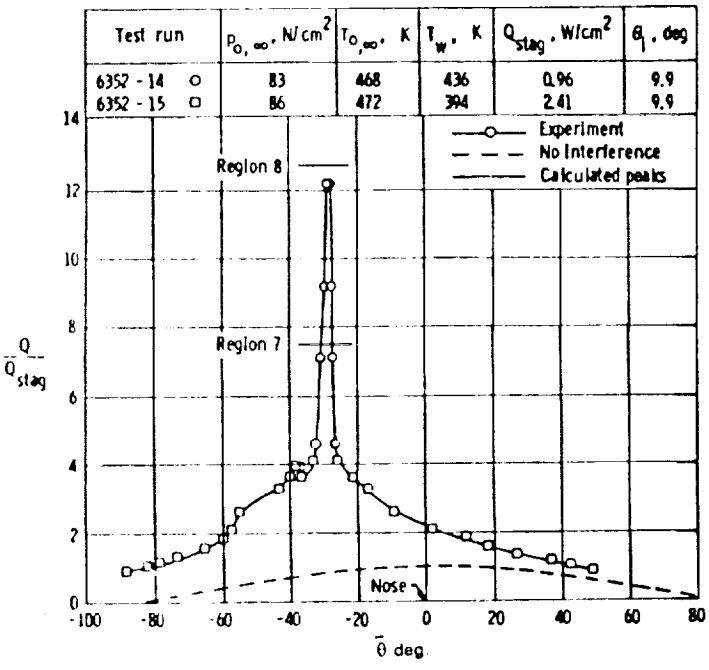

(d) Heat-transfer distribution.

Figure 12a TYPE IV INTERACTION(S) AND ASSOCIATED HEAT TRANSFER DISTRIBUTIONS ON A HEMISPHERE AT MACH 5.94. INVESTIGATION OF KEYES AND HAINS (Ref. 2)

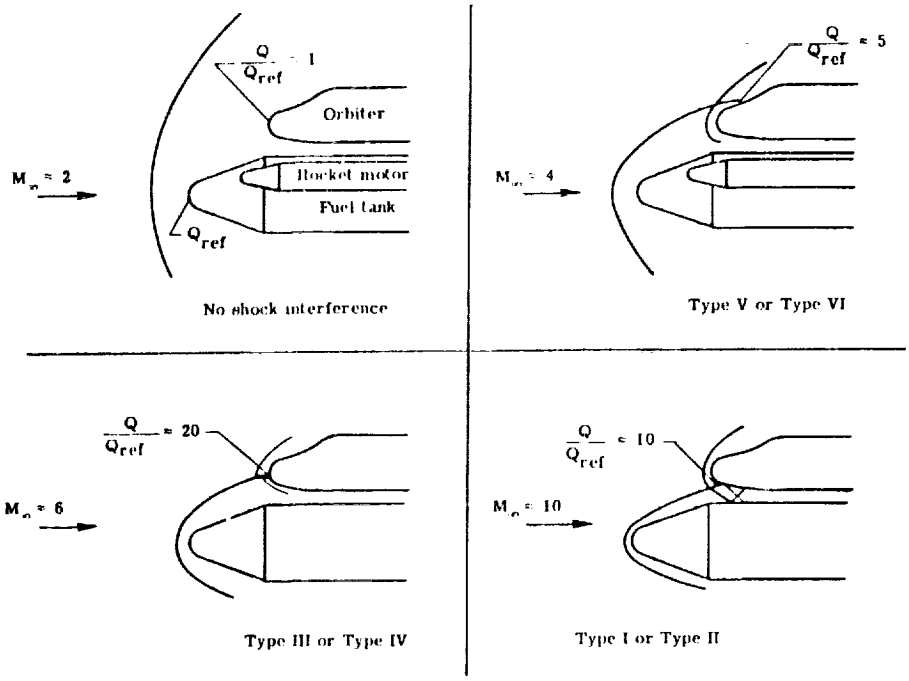

Shock interference heating during ascent of a mated shuttle configuration.

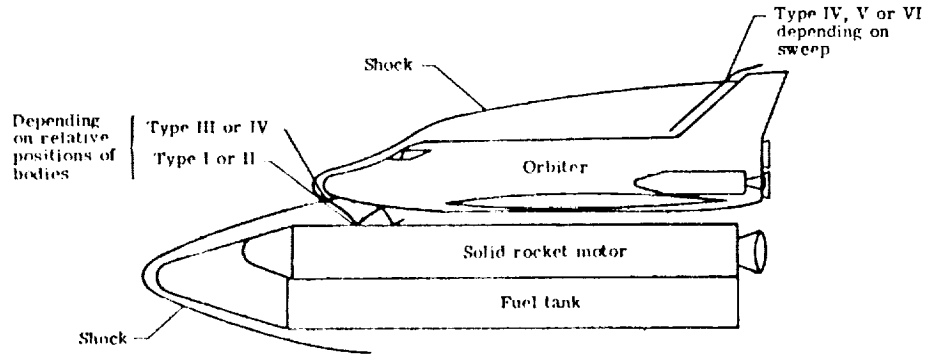

Locations of types of interference heating on mated configuration at $M_\infty = 20$.

Figure 12b TYPES III AND IV SHOCK INTERFERENCE PATTERNS GENERATED DURING ASCENT OF A MATED SHUTTLE CONFIGURATION (Ref. 2)

visualization and to perform detailed pressure measurements. Although the abnormal peak heat rates were observed, no heat transfer data were reported. The later efforts of Haslett and Kaufman focused heavily on heat load measurements, and on complex geometrical configurations. The tested configurations included various combinations of the orbital model with a flat-plate receiver and models of the shuttle fuel tanks (Figure 13). These combinations of models, along with surface-mounted heat transfer gages, were used to validate a typical empirical heat-load amplification correlation function, an example of which is given in Figure 14. The orbiter/tank configuration was used along with heat-sensitive paint to predict residual heat loading on the shuttle fuel-tank system during the separation stage of the shuttle flight. In the results illustrated in Figure 13, peak heating is shown to be as much as 30 times the undisturbed values. The work of Craig and Ortwerth[3] was directed specifically toward cowl lip heating, which currently is a problem of major concern in the design of the National AeroSpace Plane (NASP). Studies by Gulbran et al.[16,17] and work by Ginoux and Matthews[32,33] provided further measurements and analysis of shock/shock-interaction problems occurring on blunt bodies.

In a later work, Ginoux[33] studied the types III and IV shock/shock interaction produced on a wedge/cylinder model configuration. However, only small increases in the peak heat rates were observed, because of the weak interaction regions generated by the low freestream Mach number used in this investigation. Typical geometrical configurations and distributions of heat transfer are shown in Figure 15.

The heating loads developed in regions of shear-layer impingement were measured in a number of studies on spiked bodies (Holden[34]), indented nose shapes (Holden[35,36]) and Tension Shells (Jones, Bushnell, and Hunt[37]). In these studies, the interaction regions were generated by the interaction between the nosetip shock and the body shock, as illustrated by Figures 16, 17, and 18. In most cases, the basic mechanism for heating enhancement was the reattachment of a free shear layer (axisymmetric), although there were a number of cases where a free jet was formed. Figures 17 and 18 show some of the typical heat transfer distributions developed along the body surfaces. The investigation of the flowfield around a tension shell by Jones, Bushnell, and Hunt[37] utilized phase-changing paint to measure heat transfer rate; the test gas of tetrafluoromethane was used in an attempt to evaluate the effects of γ on the interaction. The investigations of spiked bodies[34] and indented nose tips[35,36] used high-frequency thin-film instrumentation to measure heat transfer distribution. A graphic illustration of the damage caused by the enormous heating rates in reattachment regions on spiked bodies was provided by sled tests conducted at Holloman Air Force Base. As shown in Figure 6, the shock-induced heating loads caused significant damage to the sled and its runners.

The techniques used to provide simple predictions of the flowfields and peak heating levels in regions of shock/shock interaction are founded on the flowfield analysis developed by Edney[1]. The basic approach employed by Edney was expanded and incorporated into a numerical code by Keyes and Hains.[2] Edney defined the basic flowfield structures for the various incident-shock/bow-shock configurations (Figures 1, 2 and 3) and formulated techniques to quantify the flowfield structure and estimate the pressure and heating levels at the body surface in the interaction regions. For a type IV interaction (where the jet-like flowfield structure was postulated to be inviscid in nature), a simple stagnation-point heating relationship was formulated to estimate the peak heating in the interaction region. For a type III interaction, the heating at the attachment point of the free shear layer to the surface was estimated from semi-empirical relationships based on correlations of reattachment heating rates. The correlation was developed from measurements over compression ramps, base-cavity flows, and spiked bodies. Edney justified this approach by drawing the analogy between these latter flowfields and those produced in regions of shock/

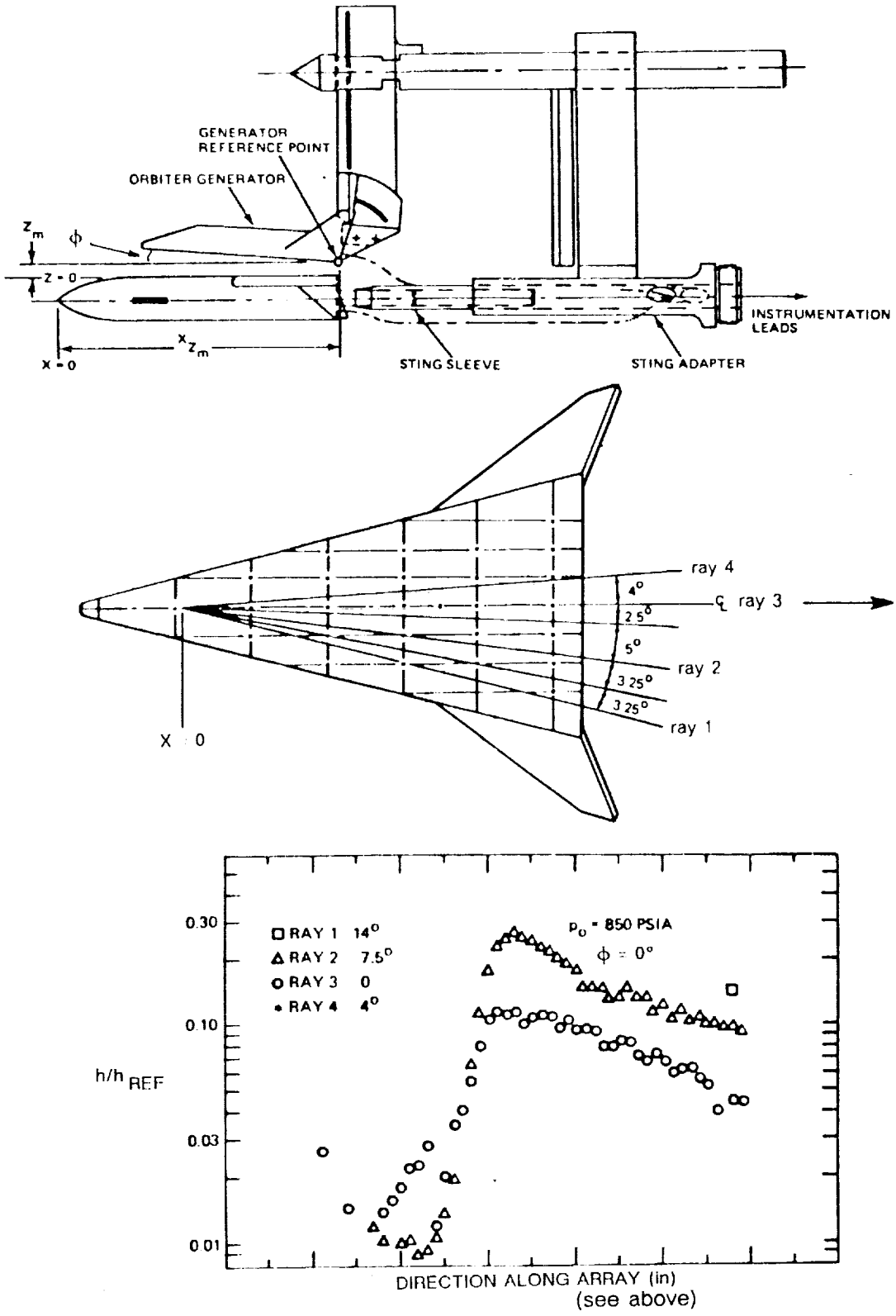

Figure 13 INTERFERENCE HEATING DISTRIBUTION ON ORBITER CAUSED BY BOOSTER (Ref. 31)

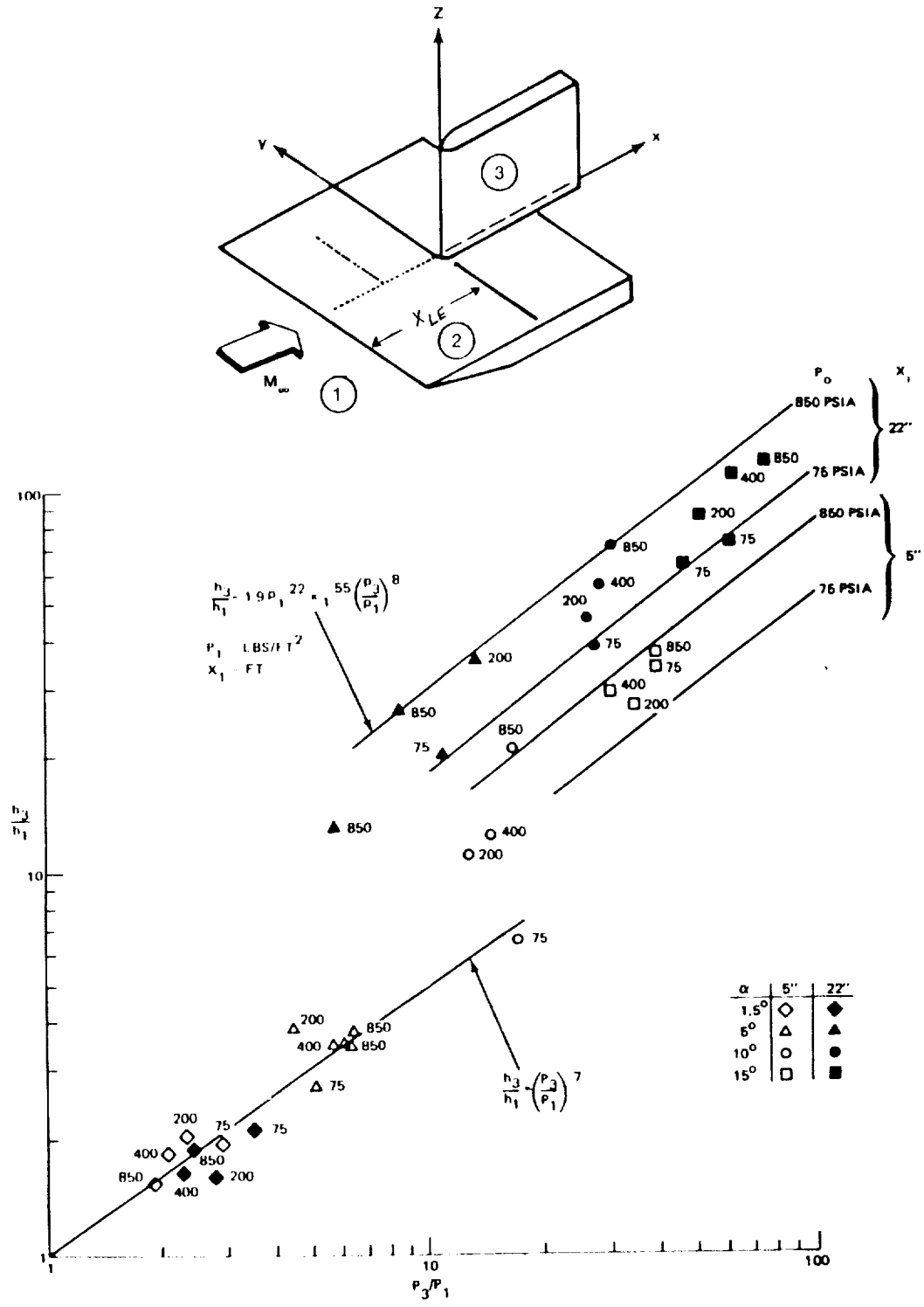

1- UPSTREAM OF SHOCK 2-DOWNSTREAM OF REFLECTED SHOCK

Figure 14 SHOCK INTERFERENCE HEATING ON BLUNT CYLINDER AT MACH 3. INVESTIGATION OF KAUFMAN (Refs. 30 and 31)

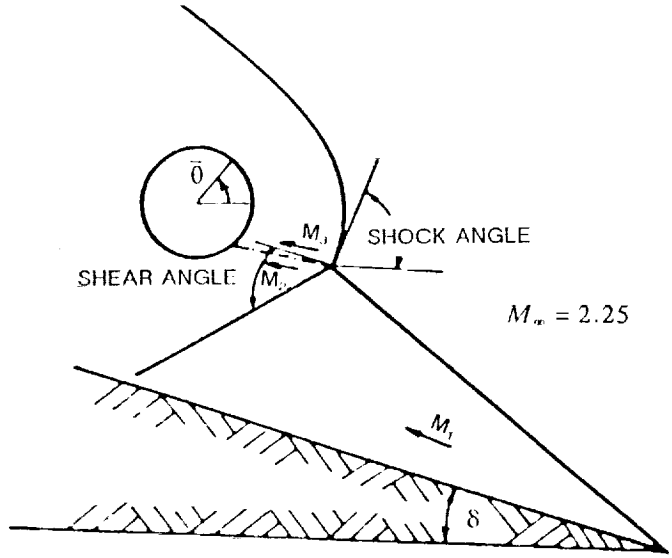

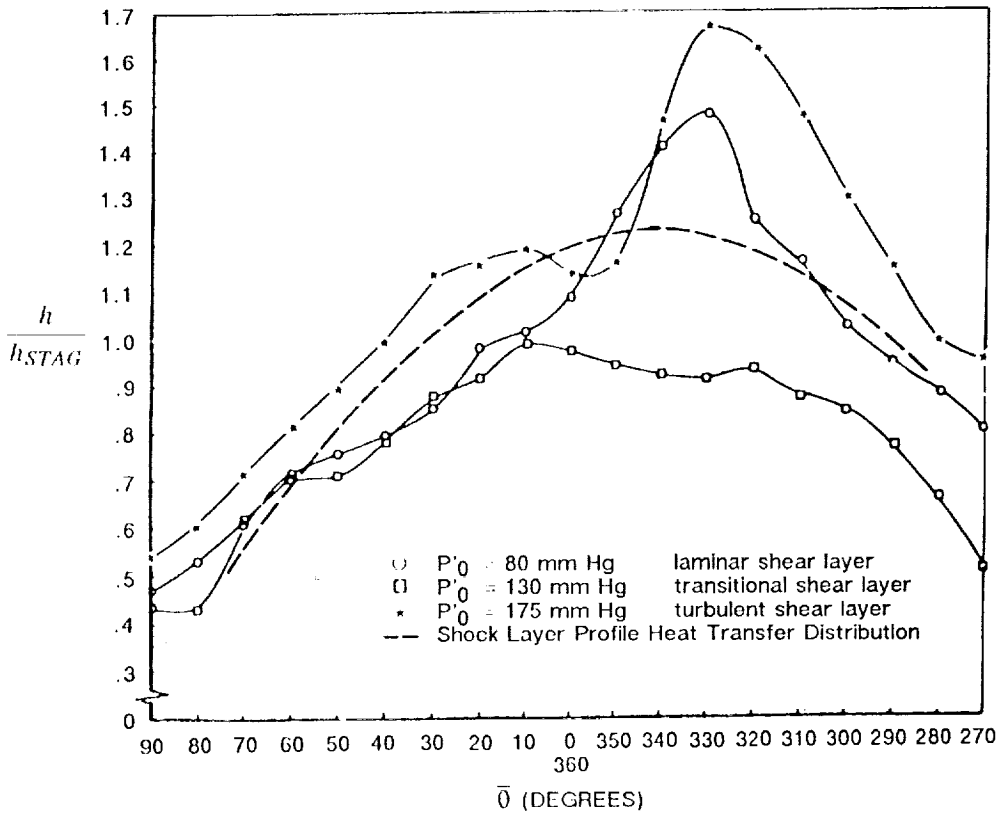

Figure 15 INTERFERENCE HEATING ON RIGHT CIRCULAR CYLINDER AT MACH 2.25. INVESTIGATION OF GINOUX (Ref. 32)

ORIGINAL PAGE IS
OF POOR QUALITY

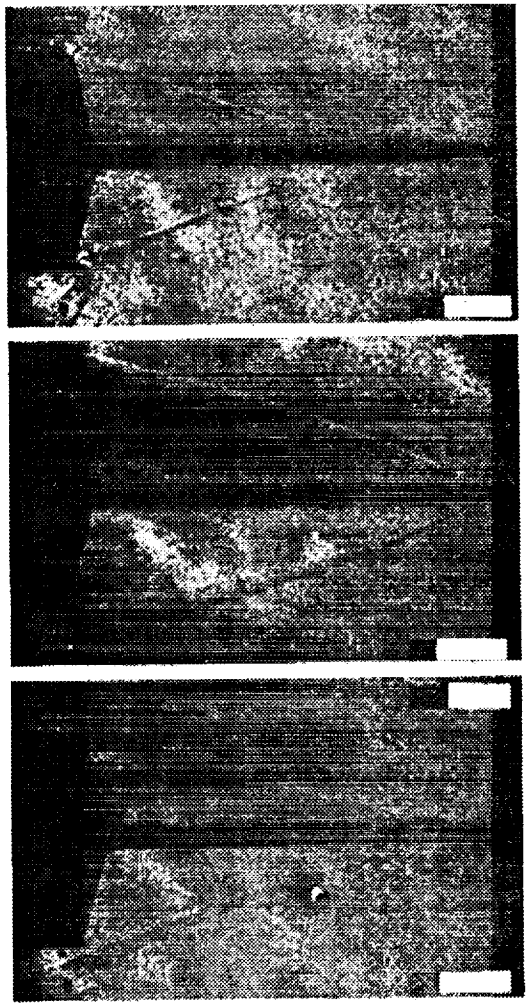

Figure 16 TYPICAL SCHLIEREN PHOTOGRAPHS OF INTERFERENCE-HEATING FLOW PATTERNS GENERATED BY A SPIKED BODY DURING STUDIES CONDUCTED AT CALSPAN (Ref. 34)

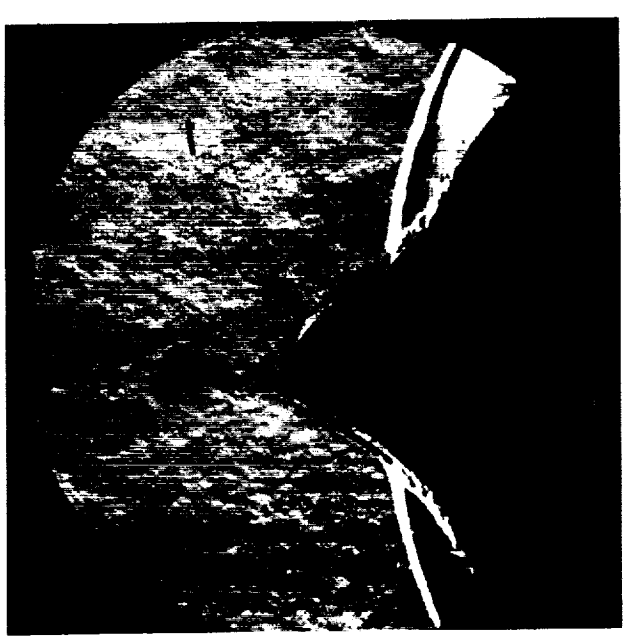

(a) MACH 11

(b) MACH 13

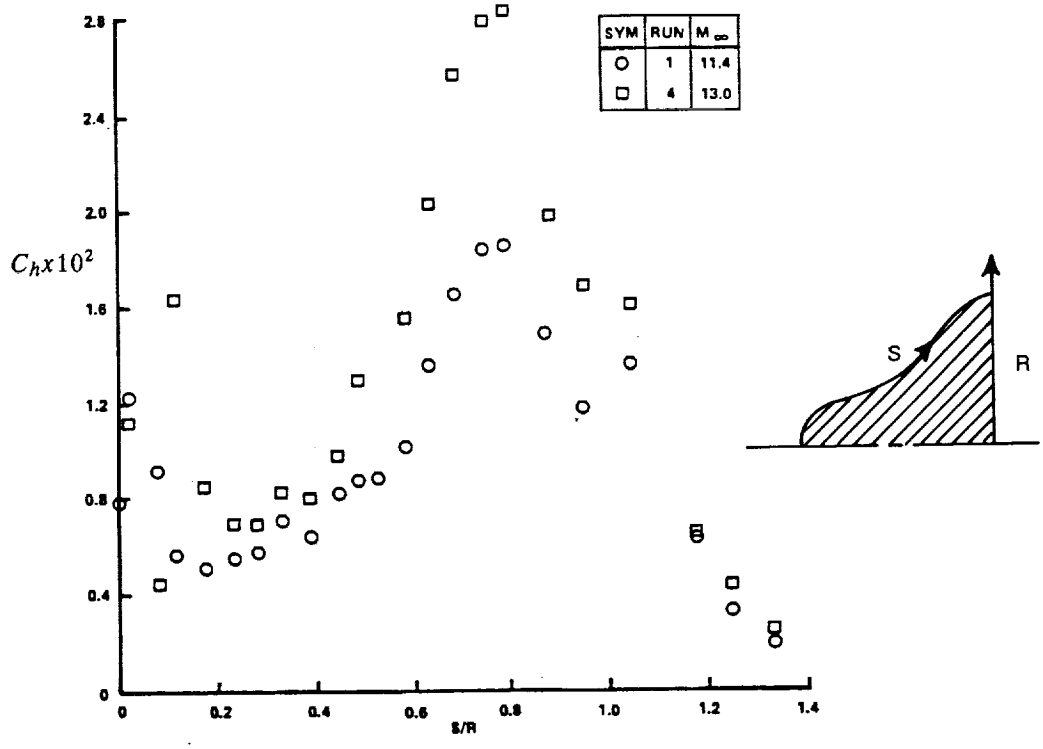

Figure 17 SHOCK/SHOCK-INTERACTION HEATING ON INDENTED NOSE TIP (Ref. 36)

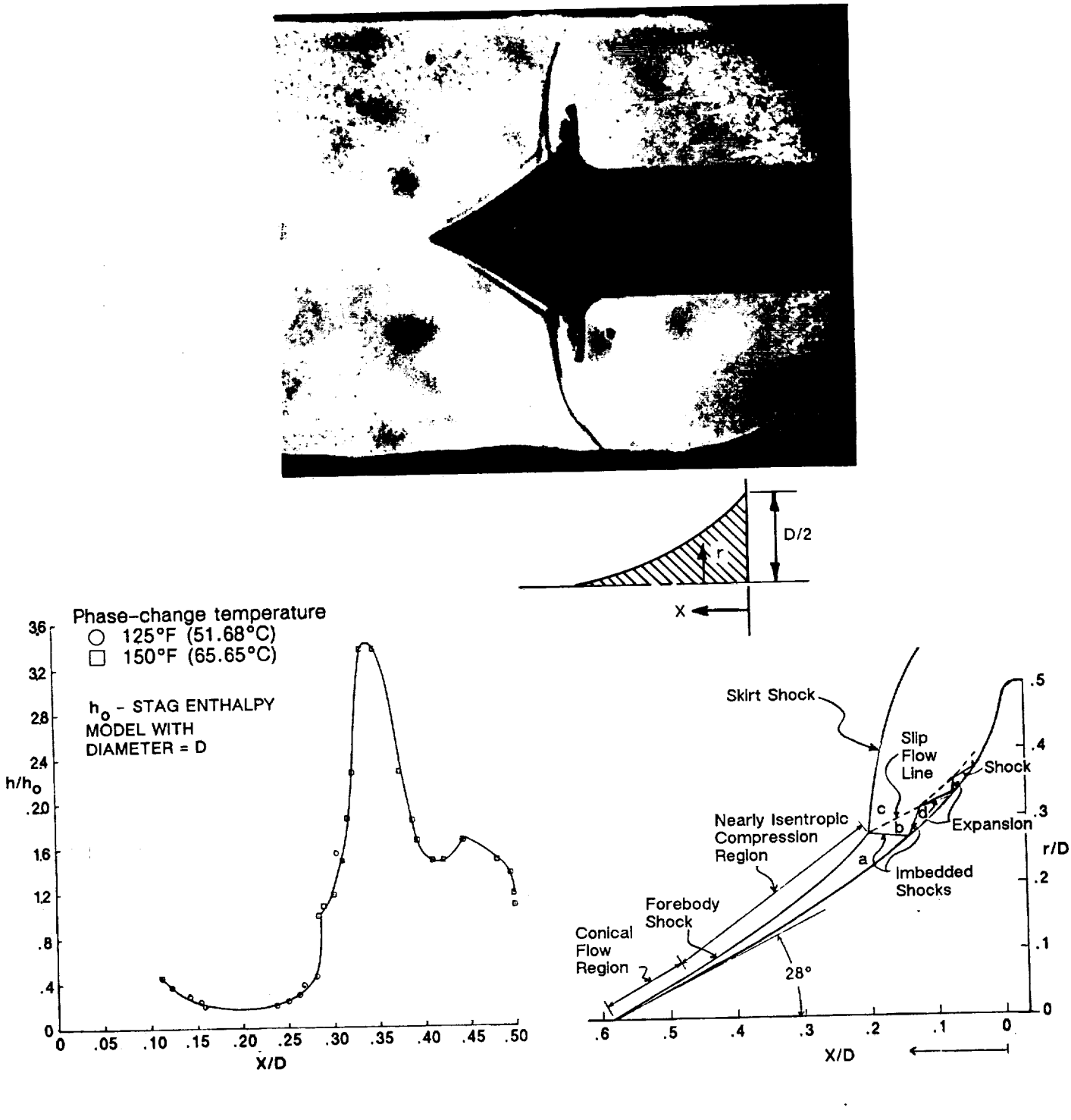

Figure 18 SHOCK/SHOCK-INTERACTION HEATING ON "TENSION SHELLS." INVESTIGATION OF JONES, BUSHNELL AND HUNT (Ref. 37)

shock interaction, as illustrated by Figure 19. However, previous experimental studies have shown that these correlations of attachment heating are reasonably accurate only when the flows are either fully laminar or turbulent. Thus, a type III interaction, which is generated by a transitional shear layer, is intrinsically transitional in nature and is extremely difficult to predict, regardless of the computational technique employed. However, in hypersonic flows where the Reynolds numbers are low enough to maintain a laminar slipstream (shear layer), shear layers bounding the jet formed in a type IV interaction influence the peak heating, as illustrated by the results of the present study.

Because the basic flowfield structure in regions of shock/shock interaction is controlled by principally inviscid phenomena, it is not surprising that numerical techniques to solve the Navier–Stokes equations that have good shock-capturing properties along with high grid resolution have been used successfully to predict the basic flow structure and surface pressure distributions of these flows, as illustrated by the computations of Tannehill et al. (Figure 20). However, a substantial grid refinement is required, as illustrated by the studies of Klopfer and Yee[39] and Stewart et al.[40] to predict the surface heating. Furthermore, without an adequate transition model, it is difficult to accurately predict the heating levels for a type IV interaction occurring at Reynolds numbers of approximately 10^4.

The major problem with the earlier experimental studies of shock/shock interaction was that they lacked the instrumentation to provide adequate accuracy and resolution of the heating and pressure distributions in the interaction regions and were not able to develop high Mach number, high Reynolds number interactions. Also, in most cases, the heat transfer instrumentation employed suffered from problems associated with lateral heat conduction and low frequency response. In the studies presented in this report, we employed instrumentation with the spatial and temporal resolution necessary to determine the detailed distribution of surface properties. We were able to identify the basic character of the boundary layer on the body for type III and type IV interactions because of the intrinsically high frequency response of our thin-film heat transfer instrumentation. The emphasis in these studies was placed on an investigation of Mach number effects on the heating levels and pressure distribution in regions of types III and IV interactions. The Reynolds number was varied in the present studies to investigate the effect of shear-layer transition on surface heating. We also investigated the effects of multiple-shock impingement and the effects of sweep in these flows by using a number of geometrical configurations of the shock/shock-interaction model.

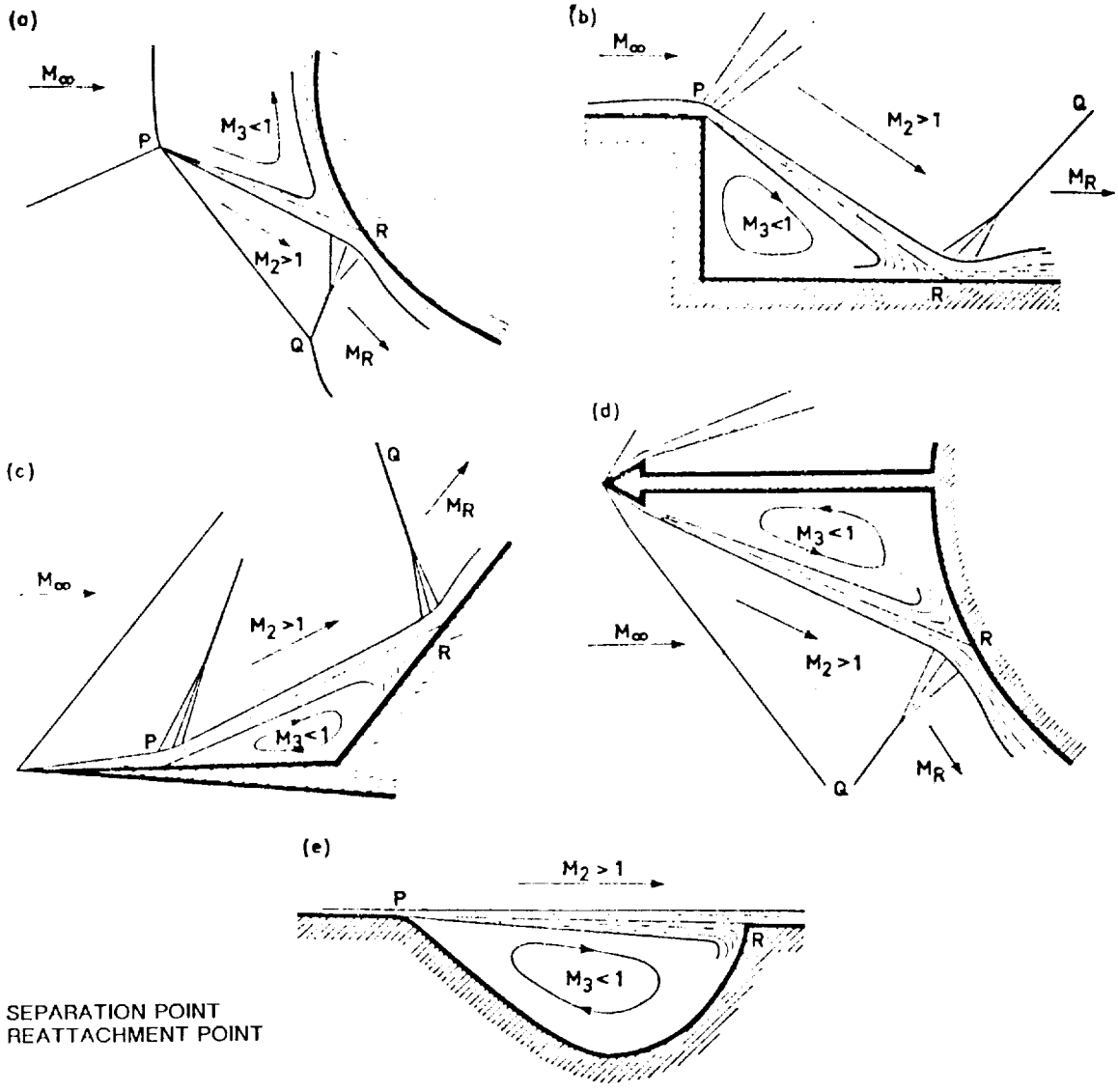

Figure 19 ANALOGY BETWEEN TYPE III AND REATTACHING SHEAR LAYERS (Ref. 1)

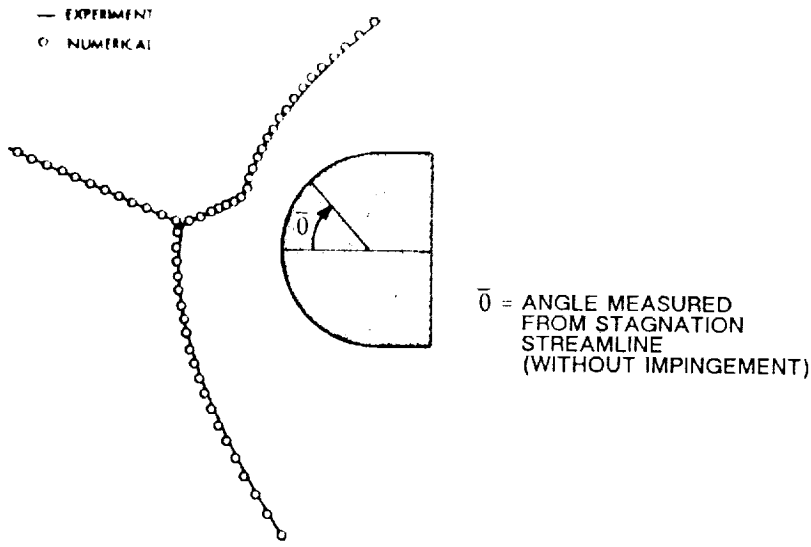

Comparison of shock shapes.

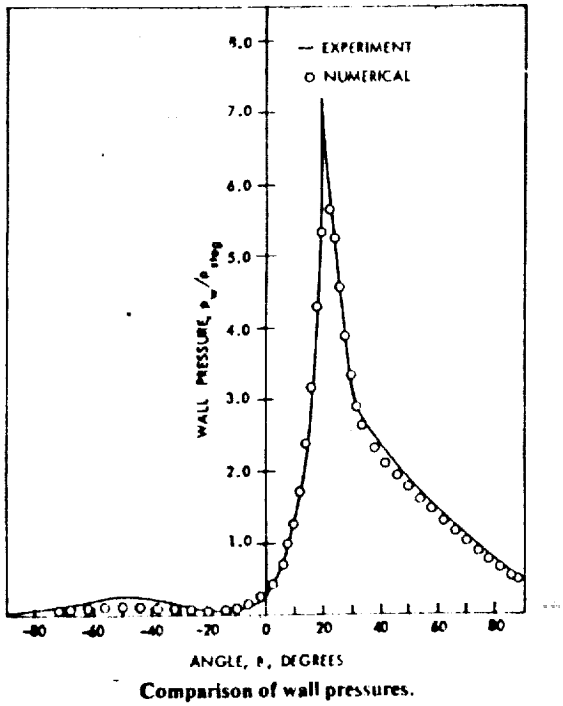

Comparison of wall pressures.

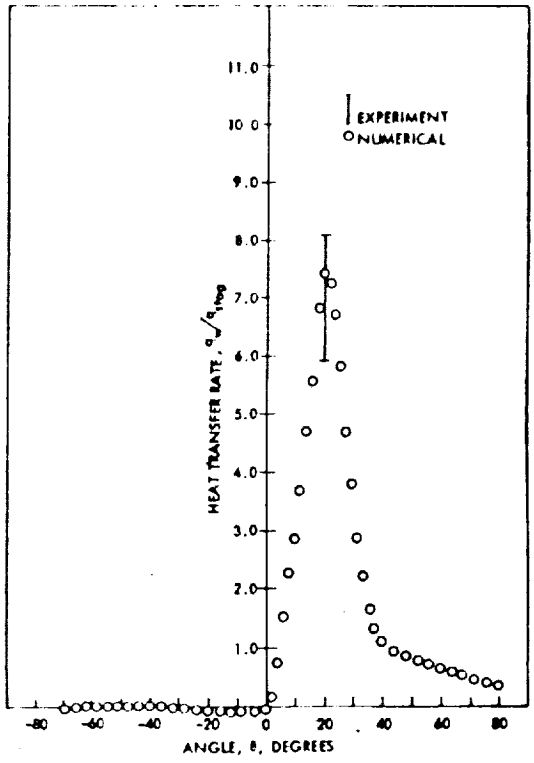

Comparison of surface heat transfer rates.

Figure 20 COMPARISON BETWEEN NUMERICAL PREDICTIONS OF TANNEHILL ET AL. USING NAVIER-STOKES EQUATIONS AND MEASUREMENTS OF KEYES AND HAINS (Refs. 26 and 27)

Section 3
EXPERIMENTAL PROGRAM

3.1 PROGRAM OBJECTIVE AND DESIGN

The objective of the present studies was to provide detailed pressure and heat transfer measurements as well as Schlieren photographs to define the structure and properties of regions of shock/shock interaction at Mach numbers from 6 to 19. The emphasis in these studies was placed on type III and type IV interactions, for these provide the largest aerothermal loads. Studies were performed over a range of Reynolds numbers to explore the effects of transition on the heating rates. Measurements were also performed for fully laminar conditions to provide a data set that could be compared with theory without transition or turbulence modeling problems.

The first group of studies explored the aerothermal characteristics of the interaction between a planar shock and the shock layer ahead of a cylinder, supported perpendicular to the flow. The primary objective of this study was to investigate the effects of Mach number and Reynolds number on the magnitude and distribution of heating caused by various types of shock/shock interaction on the cylinder. The Mach number range from 6 to 19 was of particular interest here, because the type III and type IV interactions generated at these Mach numbers cause large aerothermal loads. The condition of the shear layer, either laminar or turbulent, generated by a type III interaction, and upstream of or surrounding the jet for a type IV interaction, is the other major factor that controls the peak heating levels generated by the shock/shock interactions. The Mach number and Reynolds number in the shock layer adjacent to the shear layer are believed to be the most important parameters controlling transition of the shear layer, which, in turn, is controlled by the Mach number and Reynolds number of the freestream. Measurements were made at Mach 6, 8, and 16 for Reynolds numbers large enough to ensure generation of turbulent shear layers by the shock/shock interactions. The majority of the studies at Mach numbers from 11 to 19 were conducted for Reynolds numbers where the shear layers were determined to be fully laminar, based on analysis of the measured thin-film gage characteristics.

The second series of studies investigated the aerothermal loads associated with the impingement of two oblique shocks in the stagnation region of a cylinder model at a Mach number of 8. The objective was to determine whether the heating levels generated by the interactions of two oblique shocks with the bow shock would generate significantly lower heating loads than a single shock of the same overall strength. This investigation arose from questions concerning the impingement of multiple shocks from the compression ramp of ramjet inlets on the cowl lip. In these experiments, the effects of the relative strengths of the two incident shocks and their positions relative to the bow shock were studied. In particular, attempts were made to determine whether the heating loads would be substantially reduced by preventing the two ramp shocks from coalescing before they impinged on the bow shock. Measurements were made to determine the relative magnitudes of the heating loads developed for a single impinging shock and a pair of focused shocks with the same overall turning angle.

The third, and final, investigation was a preliminary study to examine the effects of sweeping the interaction regions on the peak heating generated on the surface of the cylinder. In addition to problems of obtaining quasi-two-dimensional flows over the models, questions associated with transition of the boundary layer on the swept cylinder in the absence of the shock/shock interaction are an important

issue. The latter two studies were conducted at a range of Reynolds numbers and at a freestream Mach number of 8.

A number of key problems must be solved before a meaningful experimental study of shock/shock interaction at hypersonic speeds can be conducted. First, a blockage-free flow between the shock generator and the cylinder must be obtained while, at the same time, preventing expansion at the trailing edge of the shock generator from influencing the shock/shock interaction. Also, a 3-inch-diameter cylinder is required to accurately define the characteristics of the interaction regions, consistent with the 0.010-inch gage spacing employed with our thin-film instrumentation. These constraints required that we use a shock generator 4 feet in length and 18 inches in width to obtain two-dimensional flow over the centerline of the model. Large experimental facilities are required for such experimental studies. We designed models with shock-generator angles between 10 and 15 degrees based on Edney's prediction technique, to give the maximum interference heating enhancement. In the multiple-shock interaction investigation, the two turning angles were selected so that the total turning angle was always between 12.5 and 13.5 degrees.

3.2 EXPERIMENTAL FACILITIES, MODELS, INSTRUMENTATION, AND FLOW VISUALIZATION

3.2.1 Experimental Facilities

The experimental studies were conducted in Calspan 48-inch and 96-inch shock tunnels at Mach numbers of 6.5, 8.0, 11.7, 15.6, 16.3, and 18.9. The facilities and their performance are described in Reference 43. The freestream conditions at which the current experimental program was conducted are plotted on the map of Mach number versus unit Reynolds number shown in Figure 21a. Test conditions A, B, D, and E were obtained in the 48-inch tunnel, and test condition C was obtained in the 96-inch tunnel. At Mach numbers of 6.5 and 8, the Reynolds numbers were sufficiently large that the interactions generated transitional to turbulent shear layers. We obtained completely laminar interactions at Mach numbers between 11 and 19 and transitional interactions at Mach 11 and 16.5.

The operation of the shock tunnel in the reflected-shock mode is shown with the aid of the wave diagram in Figure 21b. The tunnel is started by rupturing a double diaphragm, permitting high-pressure helium in the driver section to expand into the driven section. This generates a normal shock, which propagates through the low-pressure air. A region of high-temperature, high-pressure air is produced between this normal-shock front and the gas interface (often referred to as the contact surface) between the driver and driven gases. When the primary or incident shock strikes the end of the driven section, it is reflected, leaving a region of almost stationary, high-pressure, heated air. This air is then expanded through a nozzle to the desired freestream conditions in the test section.

The duration of the flow in the test section is controlled by the interactions between the reflected shock, the gas interface, and the leading expansion wave generated by the non-stationary expansion process occurring in the driver section. We normally control the initial conditions of the gases in the driver and driven sections so that the gas interface becomes transparent to the reflected shock interaction. This is known as operating under "tailored interface" conditions. Under these conditions, the test time is controlled by the time taken for the driver/driven interface to reach the throat, or for the leading expansion wave to deplete the reservoir of pressure behind the reflected shock. The flow duration is, therefore, either driver-gas-limited or expansion-limited. Figure 21c shows the flow duration in the test section as a function of the Mach number of the incident shock. Here, it can be seen that, for operation at low

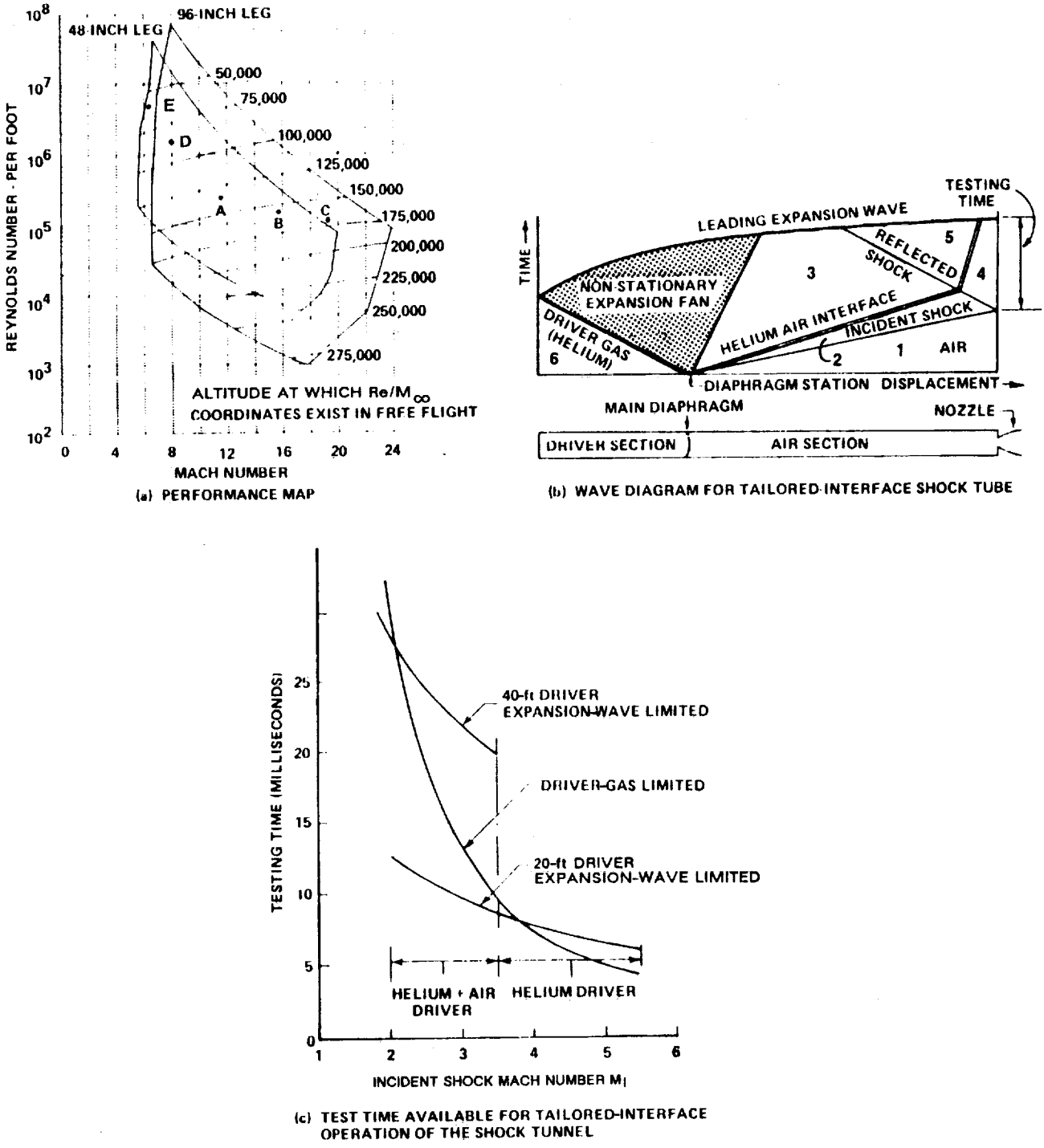

Figure 21 PERFORMANCE CHARACTERISTICS OF CALSPAN'S SHOCK TUNNEL

incident-shock Mach numbers, running times of over 25 milliseconds can be obtained with a long driver section. When performed under these latter conditions at high pressures and high Reynolds numbers, the test running times are of the same magnitude or longer than for piston-driven tunnels (Needham,[42] Holden[4,41]) with comparable stagnation temperatures and the same reservoir conditions. However, the flow quality is superior to those of piston-driven tunnels, because the test gas is processed by a simple reflected shock. Unlike the piston-driven tunnels, freestream conditions of the shock tunnels can be calculated with high accuracy. Note that, when sensitive high-frequency instrumentation is used in the very severe heating conditions encountered in shock/shock interaction regions in hypersonic flow, running for longer than 20 milliseconds can result in damage to, or destruction of, the sensing elements.

3.2.2 Models

Three basic models were used in these experimental studies, associated respectively with the single-shock/bow-shock interaction studies, the studies of multiple-shock/bow-shock interaction, and, finally, the investigation of sweep on the shock/shock interaction.

The model used in the studies of the planar single-shock/bow-shock interactions is shown in Figure 22. The highly instrumented 3-inch-diameter cylinder was supported by two side arms, so that it could be translated both parallel and perpendicular to the back of the shock generator and rotated about its axis. The length of the shock generator and its position relative to the circular cylinder were adjustable. In general, the position of shock impingement was controlled by adjusting the position of both the cylinder and the shock generator. The cylinder was heavily instrumented with heat transfer and pressure instrumentation as illustrated in Figure 23. As shown, the instrumentation was concentrated in a high-density region on the cylinder to provide the resolution needed to define the peak heating and the large heat transfer gradients generated in type III and type IV interaction regions. In almost all of the experiments, the cylinder was rotated so that this high-density segment was positioned in the interaction region. A listing of the gage positions on the cylinder is given in Table 2.

Schematic diagrams for the model used in the multiple-shock/bow-shock interaction study are shown in Figures 24a and 24b. For this study, new shock generators and ramps were constructed to provide a range of shock strengths and relative positions for the two incident shocks. The angles of the shock-generator plate and the ramp were varied to change the strengths of the two incident shocks. The positions of the intersections of the incident shocks with the bow shock ahead of the cylinder were controlled by translating the ramp and the shock-generator plate relative to the support system and to each other, as well as by adjusting the elevation and streamwise location of the cylinder. Again, the cylinder was rotated to place high-density instrumentation segments in the interaction region.

The model used in the preliminary studies of swept-shock/shock interactions was designed to place the incident shock along the attachment line of the swept cylinder (Figure 24b). To do this, we swept the leading edge of the shock-generator plate and mounted it on multi-angled support blocks to place the leading edge in the same horizontal plane as the swept cylinder. The cylinder support brackets were redesigned to allow the cylinder to be swept, leaving the centerpoint at the same axial location as the unswept configuration. Similarly, the shock-generator system was designed to place the center of the shock generator at the same axial station as its unswept counterpart. Again, the vertical and horizontal positions of the cylinder were used to control the type of shock/shock being studied. The shock generator's length and angles were measured in the pitch plane. For swept cylinder shock/shock-interaction

ORIGINAL PAGE
BLACK AND WHITE PHOTOGRAPH

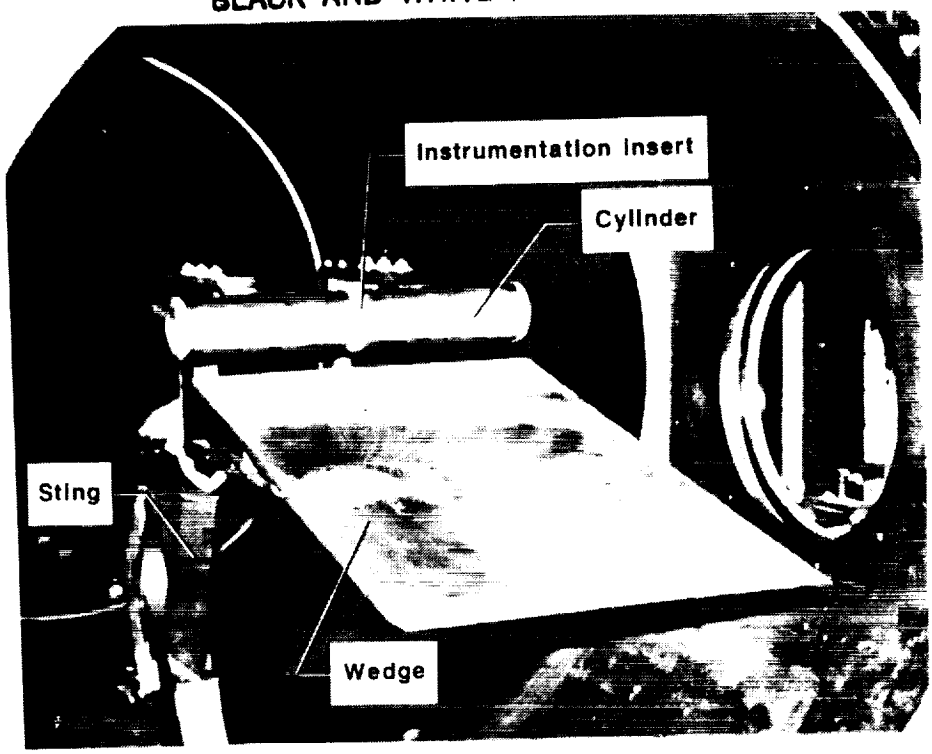

Figure 22 SHOCK INTERFERENCE MODEL MOUNTED IN CALSPAN'S 48-INCH HYPERSONIC SHOCK TUNNEL

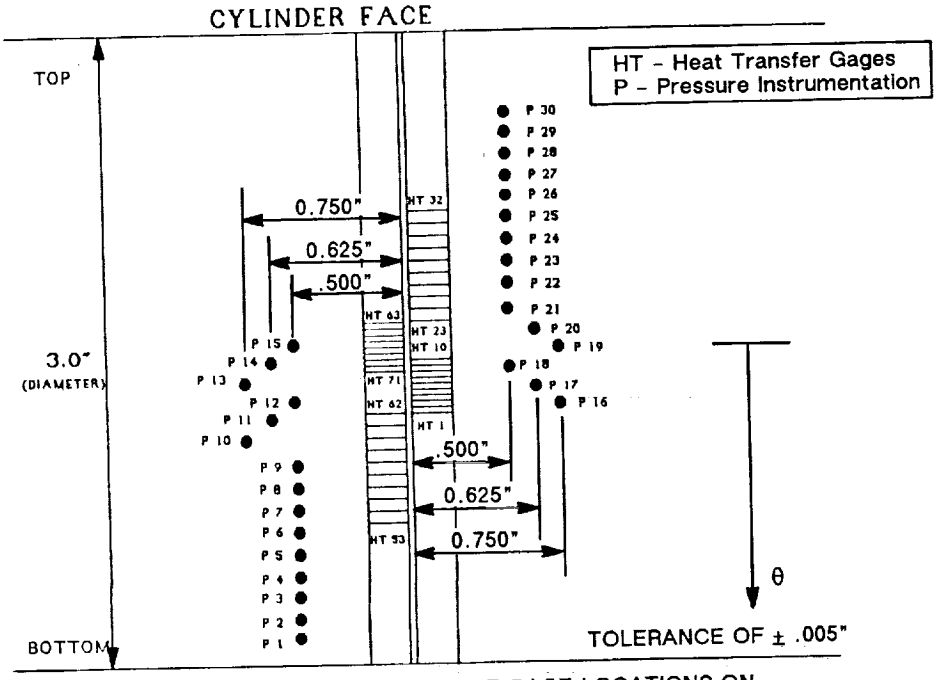

HEAT TRANSFER AND PRESSURE GAGE LOCATIONS ON SHOCK/SHOCK-INTERACTION MODEL (CYLINDER)

Figure 23 INSTRUMENTATION SCHEMATIC DIAGRAM FOR SHOCK INTERFERENCE MODEL

Table 2. SUMMARY OF GAGE POSITIONS ON CYLINDER

GAGE	DEGREES FROM P 30	INCHES FROM P 30
P 30	0.000	0.0000
P 28	14.324	0.3750
P 26	28.648	0.7500
P 25	35.810	0.9375
P 24	42.972	1.1250
P 23	50.134	1.3125
P 22	57.296	1.5000
P 21	64.458	1.6875
P 20	69.232	1.8125
P 15	71.620	1.8750
P 19	74.007	1.9375
P 14	76.394	2.0000
P 18	78.782	2.0625
P 13	81.169	2.1250
P 17	83.556	2.1875
P 12	85.944	2.2500
P 16	88.331	2.3125
P 11	90.718	2.3750
P 10	95.493	2.5000
P 9	102.655	2.6875
P 7	116.979	3.0625
P 5	131.303	3.4375
P 3	145.627	3.8125
P 1	159.951	4.1875
HT 42	22.208	0.5814
HT 41	25.428	0.6657
HT 40	28.648	0.7500
HT 39	31.868	0.8343
HT 38	35.088	0.9186
HT 37	38.308	1.0029
HT 36	41.524	1.0871
HT 35	44.744	1.1714
HT 32	48.128	1.2600
HT 34	48.128	1.2600
HT 31	51.184	1.3400
HT 33	51.184	1.3400
HT 30	54.240	1.4200
HT 72	55.386	1.4500
HT 73	56.341	1.4750
HT 29	57.296	1.5000
HT 74	57.296	1.5000
HT 75	58.251	1.5250
HT 76	59.206	1.5500
HT 77	60.161	1.5750
HT 28	60.352	1.5800
HT 78	61.115	1.6000
HT 79	62.070	1.6250
HT 80	63.025	1.6500
HT 27	63.407	1.6600
HT 81	63.980	1.6750
HT 26	66.463	1.7400
HT 25	69.519	1.8200
HT 11	70.833	1.8544
HT 12	71.627	1.8752
HT 13	72.422	1.8960
HT 24	72.575	1.9000
HT 14	73.216	1.9168
HT 15	74.011	1.9376
HT 16	74.805	1.9584
HT 17	75.600	1.9792
HT 23	75.630	1.9800
HT 18	76.394	2.0000
HT 63	76.394	2.0000
HT 19	77.189	2.0208
HT 64	77.349	2.0250
HT 20	77.983	2.0416
HT 65	78.304	2.0500
HT 21	78.778	2.0624
HT 66	79.259	2.0750
HT 22	79.572	2.0832
HT 101	79.572	2.0832
HT 67	80.214	2.1000
HT 102	80.367	2.1040
HT 103	81.161	2.1248
HT 68	81.169	2.1250
HT 104	81.956	2.1456
HT 69	82.124	2.1500
HT 105	82.750	2.1664
HT 70	83.079	2.1750
HT 10	83.537	2.1870
HT 106	83.556	2.1875
HT 71	84.034	2.2000
HT 9	84.339	2.2080
HT 107	84.351	2.2083
HT 8	85.142	2.2290
HT 108	85.145	2.2291
HT 109	85.940	2.2499
HT 7	85.944	2.2500
HT 6	86.734	2.2707
HT 110	86.734	2.2707
HT 111	87.529	2.2915
HT 5	87.533	2.2916
HT 112	88.323	2.3123
HT 4	88.331	2.3125
HT 113	89.118	2.3331
HT 3	89.129	2.3334
HT 114	89.916	2.3540
HT 43	89.916	2.3540
HT 2	89.928	2.3543
HT 62	90.730	2.3753
HT 1	90.730	2.3753
HT 44	93.102	2.4374
HT 61	93.786	2.4553
HT 45	96.287	2.5208
HT 60	96.841	2.5353
HT 46	99.469	2.6041
HT 59	99.897	2.6153
HT 47	102.655	2.6875
HT 58	102.953	2.6953
HT 48	105.841	2.7709
HT 57	106.009	2.7753
HT 49	109.026	2.8543
HT 56	109.064	2.8553
HT 55	112.120	2.9353
HT 50	112.208	2.9376
HT 54	115.176	3.0153
HT 51	115.394	3.0210
HT 53	118.232	3.0953
HT 52	118.579	3.1044

HT = HEAT TRANSFER; P = PRESSURE

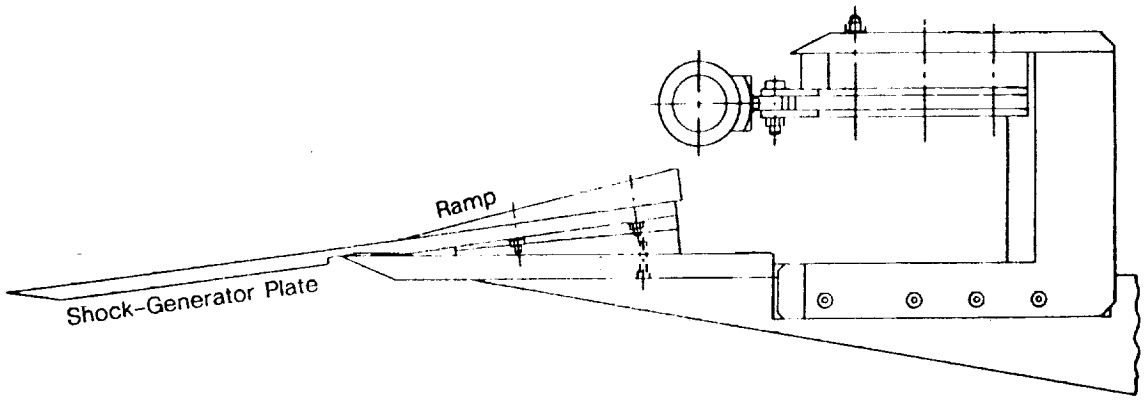

B – DIMENSION FROM BACK OF WEDGE TO BACK OF PLATE (BOW TO TOP)
H – HORIZONTAL DISTANCE BETWEEN CYLINDER FACE AND TOP OF PLATE
V – VERTICAL DISTANCE BETWEEN CYLINDER AXIS AND TOP OF PLATE
A – MODEL GAGE LOCATED AT HORIZONTAL PLANE (STAGNATION POINT)
C – SHOCK-GENERATOR PLATE ANGLE IN PITCH PLANE
D – RAMP ANGLE
W – RAMP LENGTH
P – SHOCK-GENERATOR PLATE LENGTH

SWEEP ANGLE IS THE ANGLE OF SHOCK-GENERATOR PLATE AND CYLINDER RELATIVE TO THE PERPENDICULAR TO FLOW DIRECTION

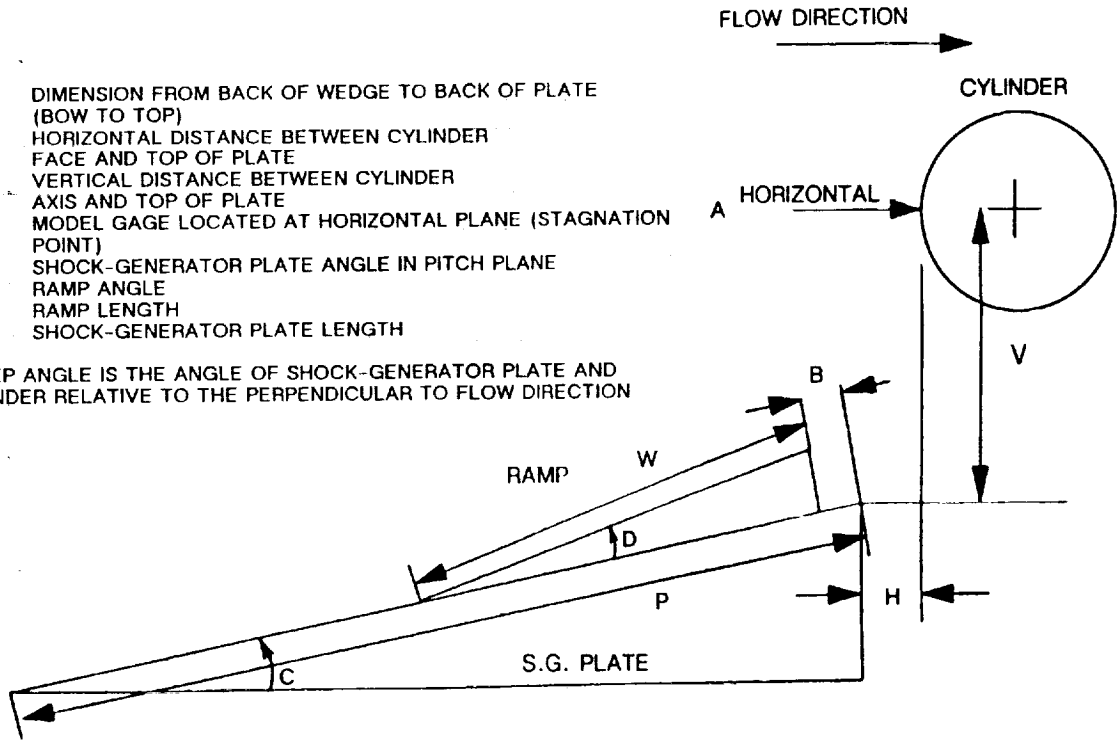

Figure 24a SCHEMATIC DIAGRAM OF MULTIPLE-SHOCK-INTERACTION MODEL (See Table 3 for dimensions for each test configuration.)

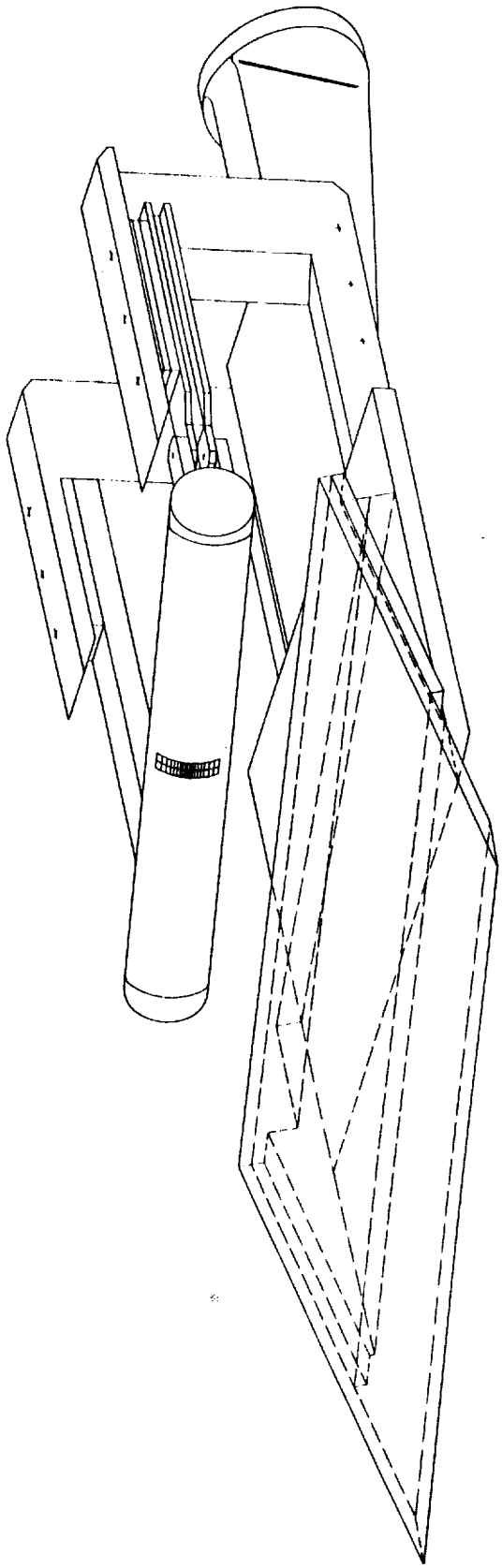

Figure 24b MODEL FOR STUDIES OF SWEPT-SHOCK/SHOCK INTERACTIONS

studies, all dimensions were measured in a plane perpendicular to the cylinder axis, except for angles "C" and "P," which were measured in the pitch plane.

3.2.3 Heat Transfer Instrumentation

The large heat transfer gradients generated in the interaction regions on the cylinder can be significantly distorted by lateral heat conduction unless the heat transfer instrumentation is mounted on an insulating surface. Because our platinum thin-film gages are mounted on a Pyrex substrate, they are well-suited for this application. However, with heating rates up to 1000 Btu/ft^2/sec, the rise in surface temperature during the shock tunnel's short run times can also lead to problems with data analysis and interpretation. The platinum films indicated in Figure 23 are deposited on cylindrical glass inserts, forming a continuous circumferential surface. Two sets of circumferential inserts were employed with overlapping gage positions to check the accuracy of the measurements. These gages, which have a width of 0.005 inch and a spacing of 0.010 inch, have a 1-microsecond response time and, therefore, can easily follow the instabilities occurring in shock/shock interaction regions. The gage positions are listed in Table 2.

Thin-film gages have been used extensively at Calspan and elsewhere to detect transition. The transient response of these gages is such that they can detect turbulent bursts that occur in transitional boundary layers and the unsteady nature of the heat transfer beneath turbulent boundary layers. Thus, this measurement technique provides an excellent method of determining the nature of the boundary layer at the attachment point of the jet on the cylinder model.

For the thin-film heat transfer instrumentation, the uncertainties associated with the gage calibration and the recording equipment are estimated to be ±5% for the levels of heating obtained in the current studies. The basic unsteady nature of some of the type III and type IV shock/shock interactions observed in the studies produced cyclic variations of typically up to ±15%.

3.2.4 Pressure Instrumentation

We used both flush-mounted and orifice pressure gages in these studies to obtain measurements of the mean and fluctuating pressure levels through the interaction regions. Calspan piezoelectric pressure gages were connected to a series of short, closely spaced orifices to obtain the mean pressure distribution around the model. Larger high-frequency Kulite transducers (0.062 inch in diameter) were flush-mounted to the surface of the model in key areas of the flow. Their positions and gage numbers are listed in Table 2.

The uncertainties in the pressure measurements associated with the calibration and recording apparatus are ±3%. Again, the variations associated with the unsteady nature of the fluid dynamics can be as large as ±15%.

3.2.5 Flow Visualization

We used a single pass-Schlieren system with a focal length of 10 feet for flow visualization in these studies. The horizontal knife edge used in these studies was adjusted to give between 15 and 50% cutoff. A single microsecond spark was triggered close to the end of the steady run time. The tunnel windows have 16-inch diameters.

Section 4
TEST PROCEDURES

4.1 INTRODUCTION

Two aspects of this experimental program make the reduction of the measurements unique. First, for some test configurations, the heat transfer rates were so large that gage temperature increases of over 500°F were not uncommon for the 15-millisecond run times that were generated in the 48-inch Shock Tunnel fitted with a 40-foot-long driver. Second, in a significant number of cases with type IV interactions, unsteady oscillations were observed in the jet impingement region. Large flow instabilities were observed for typical frequencies of 2 to 10 kHz. These problems, coupled with the large number of measurements recorded on two separate data systems with significantly different characteristics, stimulated the development of a new, faster and more complete data reduction capability. This new reduction and presentation system provides on-line reduction, plotting, and analysis capabilities for measurements in unsteady flows with very large heat transfer rates.

Analyzing Hypersonic Shock Tunnel voltage time-history data acquired by the PDP-11/73 (also known as the Digital Data Acquisition System (DDAS) II, as discussed in Section 4.3.4) or NAVCOR facilities is an integral part of Calspan's data-reduction process. Until recently, the software did not provide a convenient means for merging time histories from the two independent data-collection systems. The computer program CUBRED was designed to permit integration of raw voltage files for subsequent analysis of temporal and frequency-related phenomena. Additionally, the program was extended to include some new features and offline processing capabilities. The Rae-Taulbee algorithm (Appendix A), which accounts for variable thermal properties, is now used as an alternative to the Cooke-Felderman numerical technique for computing heat transfer profiles. Calspan-UB Research Center's (CUBRC's) COMPAQ 386 personal computer was chosen for the new software implementation because of its simplicity, computational speed, and portability for this internally funded program.

The architectures of the data-collection devices differ greatly. The sample spacing, number of samples, and test duration in DDAS II acquired files may vary. NAVCOR files, on the other hand, have 300 samples spaced 50 microseconds apart over 14.95 milliseconds. A separate computer program is used to merge NAVCOR and PDP files. NAVCOR raw voltage time histories on merged files are altered to conform to the DDAS II run specifications. Potentially, a total of 177 channels (128 from DDAS II, 49 from NAVCOR) may be examined and archived efficiently.

4.2 EVALUATION OF STAGNATION AND FREESTREAM TEST CONDITIONS

The stagnation and freestream test conditions (Table 3) were determined based on measurements of the incident-shock-wave speed, U_i, the initial temperature of the test gas (in the driven tube), T_1, the initial pressure of the test gas, p_1, and the pressure behind the reflected shock wave, p_o. We calculated the incident-shock-wave Mach number, $M_i = U_i/a_1$, where the speed of sound, a_1, is a function of p_1 and T_1. The freestream Mach number, M_∞, was determined from correlations of M_∞ with M_i and p_o. These correlations were based on previous airflow calibrations of the A and D nozzles used.

Freestream test conditions of pressure, temperature, Reynolds number, etc., were computed based on isentropic expansion of the test gas from the conditions behind the reflected shock wave to the freestream

Table 3. SUMMARY OF TEST CONDITIONS

RUN NO.	M_∞	Re/ft	STGN GAGE†	MODEL CLEARANCES V* (in.)	MODEL CLEARANCES H* (in.)	ANGLE C* (deg)	LENGTH P* (in.)	RAMP ANGLE D* (deg)	RAMP LENGTH W* (in.)	RAMP DIST. B* (in.)	MODEL SWEEP (deg)	TEST TYPE
9	6.35	4.5E+06	P18	N/A	N/A	N/A	N/A	N/A	N/A	N/A	0.00	SINGLE SHOCK
10	6.35	4.4E+06	P18	3.20	0.09	10.0	26.5	N/A	N/A	N/A	0.00	SINGLE SHOCK
11	6.35	4.4E+06	P18	3.50	0.05	10.0	26.5	N/A	N/A	N/A	0.00	SINGLE SHOCK
12	6.35	4.3E+06	P21	3.34	0.06	10.0	26.5	N/A	N/A	N/A	0.00	SINGLE SHOCK
13	6.35	4.4E+06	P18	3.34	0.06	10.0	26.5	N/A	N/A	N/A	0.00	SINGLE SHOCK
14	6.36	4.7E+06	P23	3.55	0.09	10.0	26.5	N/A	N/A	N/A	0.00	SINGLE SHOCK
15	6.33	2.4E+06	P23	3.55	0.09	10.0	26.5	N/A	N/A	N/A	0.00	SINGLE SHOCK
16	8.02	1.4E+06	P23	2.95	0.06	10.0	26.5	N/A	N/A	N/A	0.00	SINGLE SHOCK
17	8.06	1.5E+06	P23	2.95	0.06	10.0	26.5	N/A	N/A	N/A	0.00	SINGLE SHOCK
18	8.03	1.5E+06	P21	2.86	0.50	10.0	26.5	N/A	N/A	N/A	0.00	SINGLE SHOCK
19	8.03	1.5E+06	P21	2.78	0.50	10.0	26.5	N/A	N/A	N/A	0.00	SINGLE SHOCK
20	7.94	7.6E+05	P21	2.78	0.50	10.0	26.5	N/A	N/A	N/A	0.00	SINGLE SHOCK
21	8.03	1.6E+06	P21	2.89	0.59	12.5	26.5	N/A	N/A	N/A	0.00	SINGLE SHOCK
22	7.95	7.7E+05	P21	2.89	0.59	12.5	26.5	N/A	N/A	N/A	0.00	SINGLE SHOCK
24	8.14	3.8E+06	P21	2.89	0.59	12.5	26.5	N/A	N/A	N/A	0.00	SINGLE SHOCK
26	8.03	1.5E+06	HT39	3.36	0.63	12.5	26.5	N/A	N/A	N/A	0.00	SINGLE SHOCK
27	8.03	1.5E+06	P21	2.95	0.31	15.0	26.5	N/A	N/A	N/A	0.00	SINGLE SHOCK
28	7.93	7.2E+05	P21	2.95	0.31	15.0	26.5	N/A	N/A	N/A	0.00	SINGLE SHOCK
29	8.03	1.5E+06	P23	3.19	0.31	15.0	26.5	N/A	N/A	N/A	0.00	SINGLE SHOCK
30	8.15	1.8E+06	P11	2.31	0.75	15.0	26.5	N/A	N/A	N/A	0.00	SINGLE SHOCK
31	8.03	1.5E+06	P18	N/A	N/A	N/A	N/A	N/A	N/A	N/A	0.00	SINGLE SHOCK
32	6.38	5.0E+06	P18	N/A	N/A	N/A	N/A	N/A	N/A	N/A	0.00	SINGLE SHOCK
33	11.00	4.3E+06	P21	2.00	0.44	10.0	26.5	N/A	N/A	N/A	0.00	SINGLE SHOCK
34	11.01	4.4E+06	P21	2.25	0.44	10.0	26.5	N/A	N/A	N/A	0.00	SINGLE SHOCK
35	11.02	4.5E+06	P21	2.72	1.81	10.0	26.5	N/A	N/A	N/A	0.00	SINGLE SHOCK
36	11.01	4.3E+06	P21	2.41	1.50	10.0	26.5	N/A	N/A	N/A	0.00	SINGLE SHOCK
37	11.00	4.2E+06	P21	2.41	2.10	10.0	26.5	N/A	N/A	N/A	0.00	SINGLE SHOCK
38	11.00	4.3E+06	P18	N/A	N/A	N/A	N/A	N/A	N/A	N/A	0.00	SINGLE SHOCK
39	12.97	4.7E+06	P18	N/A	N/A	N/A	N/A	N/A	N/A	N/A	0.00	SINGLE SHOCK
40	16.50	1.2E+06	P18	N/A	N/A	N/A	N/A	N/A	N/A	N/A	0.00	SINGLE SHOCK
41	19.14	3.7E+05	P18	N/A	N/A	N/A	N/A	N/A	N/A	N/A	0.00	SINGLE SHOCK
42	16.31	1.0E+06	P21	2.94	0.16	10.0	48.0	N/A	N/A	N/A	0.00	SINGLE SHOCK
43	16.33	1.0E+06	P23	3.63	0.09	10.0	48.0	N/A	N/A	N/A	0.00	SINGLE SHOCK
44	16.27	9.4E+05	P25	3.94	-0.25	10.0	48.0	N/A	N/A	N/A	0.00	SINGLE SHOCK
59	8.04	1.4E+06	P21	2.83	2.76	12.5	26.5	N/A	N/A	N/A	0.00	SINGLE SHOCK
60	8.04	1.4E+06	P21	3.19	1.81	12.5	26.5	N/A	N/A	N/A	0.00	SINGLE SHOCK
61	8.05	1.5E+06	P23	3.08	0.35	12.5	26.5	N/A	N/A	N/A	0.00	SINGLE SHOCK
62	8.05	7.3E+05	P24	3.08	0.35	12.5	26.5	N/A	N/A	N/A	0.00	SINGLE SHOCK
63	7.75	3.7E+05	P24	3.08	0.35	12.5	26.5	N/A	N/A	N/A	0.00	SINGLE SHOCK
64	8.06	1.8E+06	P24	3.08	0.35	12.5	26.5	N/A	N/A	N/A	0.00	SWEPT SHOCK
66	7.94	7.0E+05	P21	3.19	1.81	12.5	26.5	N/A	N/A	N/A	15.00	SWEPT SHOCK
67	8.03	1.5E+06	P21	3.19	1.81	12.5	26.5	N/A	N/A	N/A	15.00	SWEPT SHOCK
68	8.05	1.5E+06	P24	3.43	1.43	12.5	26.5	N/A	N/A	N/A	15.00	SWEPT SHOCK
69	8.04	1.5E+06	P21	3.63	1.43	12.5	26.5	N/A	N/A	N/A	15.00	SWEPT SHOCK

Table 3. SUMMARY OF TEST CONDITIONS (cont.)

RUN NO.	M_∞	Re/ft	STGN GAGE†	MODEL CLEARANCES V* (in.)	MODEL CLEARANCES H* (in.)	ANGLE C* (deg)	LENGTH P* (in.)	RAMP ANGLE D* (deg)	RAMP LENGTH W* (in.)	RAMP DIST. B* (in.)	MODEL SWEEP (deg)	TEST TYPE
70	8.04	1.5E+06	P24	3.63	-0.33	12.5	26.5	N/A	N/A	N/A	15.00	SWEPT SHOCK
71	8.05	1.4E+06	P24	3.31	-0.33	12.5	26.5	N/A	N/A	N/A	15.00	SWEPT SHOCK
72	8.06	1.9E+06	P24	3.31	-0.33	12.5	26.5	N/A	N/A	N/A	15.00	SWEPT SHOCK
73	7.97	7.1E+05	P24	3.31	-0.33	12.5	26.5	N/A	N/A	N/A	15.00	SWEPT SHOCK
74	8.05	1.4E+06	P24	N/A	N/A	N/A	N/A	N/A	N/A	N/A	15.00	SWEPT SHOCK
75	8.04	1.5E+06	P21	3.44	1.34	12.5	26.0	N/A	N/A	N/A	30.00	SWEPT SHOCK
76	8.03	1.5E+06	P21	3.09	1.34	12.5	26.0	N/A	N/A	N/A	30.00	SWEPT SHOCK
77	8.04	1.5E+06	P21	3.44	-0.25	12.5	26.0	N/A	N/A	N/A	30.00	SWEPT SHOCK
78	8.03	1.5E+06	P21	3.24	1.34	12.5	26.0	N/A	N/A	N/A	30.00	SWEPT SHOCK
79	8.05	1.8E+06	P21	3.44	1.34	12.5	26.0	N/A	N/A	N/A	30.00	SWEPT SHOCK
80	7.99	7.1E+05	P21	3.44	1.34	12.5	26.0	N/A	N/A	N/A	30.00	SWEPT SHOCK
81	8.04	1.5E+06	P21	N/A	N/A	N/A	N/A	N/A	N/A	N/A	30.00	SWEPT SHOCK
82	8.04	1.5E+06	P21	3.90	1.58	7.5	36.0	N/A	N/A	N/A	0.00	MULTI SHOCK
83	8.04	1.4E+06	P21	3.97	1.32	7.5	36.0	5.0	14.00	0.05	0.00	MULTI SHOCK
84	8.04	1.4E+06	P21	3.97	1.32	7.5	36.0	5.0	14.00	1.05	0.00	MULTI SHOCK
85	8.04	1.4E+06	P21	3.97	1.32	7.5	36.0	5.0	14.00	1.05	0.00	MULTI SHOCK
86	8.04	1.4E+06	P21	3.97	1.32	7.5	36.0	6.0	11.00	-1.00	0.00	MULTI SHOCK
87	8.04	1.5E+06	P21	3.97	1.32	7.5	36.0	5.0	14.00	-1.00	0.00	MULTI SHOCK
88	8.05	1.7E+06	P21	3.97	1.32	7.5	36.0	5.0	14.00	1.05	0.00	MULTI SHOCK
89	8.04	1.5E+06	P21	4.12	1.32	7.5	36.0	N/A	N/A	N/A	0.00	MULTI SHOCK
90	8.04	1.5E+06	P21	4.00	1.32	7.5	36.0	6.0	11.00	-1.44	0.00	MULTI SHOCK
91	8.04	1.5E+06	P21	4.00	1.32	7.5	36.0	6.0	11.00	-1.44	0.00	MULTI SHOCK
92	8.04	1.5E+06	P21	4.00	1.32	7.5	36.0	6.0	13.25	-2.69	0.00	MULTI SHOCK
93	8.04	1.5E+06	P21	4.00	1.32	7.5	36.0	6.0	13.25	-3.44	0.00	MULTI SHOCK
94	8.04	1.5E+06	P21	4.00	1.32	7.5	36.0	6.0	11.00	-0.25	0.00	MULTI SHOCK
95	8.03	1.5E+06	P24	4.25	1.32	7.5	36.0	6.0	13.25	-0.25	0.00	MULTI SHOCK
98	8.03	1.5E+06	P21	3.41	1.22	12.5	26.0	N/A	N/A	N/A	30.00	SWEPT SHOCK
99	8.30	2.3E+06	P21	2.79	0.22	12.5	26.5	N/A	N/A	N/A	0.00	SINGLE SHOCK
100	8.29	2.2E+06	P21	2.79	0.22	10.0	26.5	N/A	N/A	N/A	0.00	SINGLE SHOCK
101	8.31	2.5E+06	P22	2.89	0.22	12.5	26.5	N/A	N/A	N/A	0.00	SINGLE SHOCK
102	11.70	2.0E+05	P22	3.35	1.86	10.0	46.3	N/A	N/A	N/A	0.00	SINGLE SHOCK
103	11.63	2.0E+05	P22	4.15	-1.40	10.0	46.3	N/A	N/A	N/A	0.00	SINGLE SHOCK
104	11.55	1.7E+05	P22	4.52	-0.62	10.0	44.0	N/A	N/A	N/A	0.00	SINGLE SHOCK
106	15.62	1.6E+05	P24	3.69	-1.40	10.0	46.3	N/A	N/A	N/A	0.00	SINGLE SHOCK
107	15.61	1.6E+05	P22	3.39	-1.40	10.0	46.3	N/A	N/A	N/A	0.00	SINGLE SHOCK
108	15.58	1.6E+05	P22	3.30	-1.40	10.0	46.3	N/A	N/A	N/A	0.00	SINGLE SHOCK
109	18.86	1.9E+05	P22	3.42	1.60	10.0	46.3	N/A	N/A	N/A	0.00	SINGLE SHOCK
110	18.80	1.8E+05	P22	3.85	1.54	10.0	46.3	N/A	N/A	N/A	0.00	SINGLE SHOCK
112	18.84	1.9E+05	P24	3.75	-0.34	10.0	46.3	N/A	N/A	N/A	0.00	SINGLE SHOCK
113	11.63	2.0E+05	P21	3.94	-1.40	10.0	46.3	N/A	N/A	N/A	0.00	SINGLE SHOCK
114	15.67	1.6E+05	P22	3.99	1.10	12.5	44.0	N/A	N/A	N/A	0.00	SINGLE SHOCK
115	15.68	1.7E+05	P21	3.93	2.10	12.5	44.0	N/A	N/A	N/A	0.00	SINGLE SHOCK
116	18.92	2.1E+05	P21	3.99	1.10	12.5	44.0	N/A	N/A	N/A	0.00	SINGLE SHOCK

†STAGNATION-POINT GAGE ID.

*REFER TO MODEL DIAGRAM OF FIGURE 24a.

Mach number. Real-gas effects were taken into account for this expansion under the justified assumption that the gas was in thermochemical equilibrium. In the freestream, the static temperature, T_∞, was sufficiently low that the ideal-gas equation of state, $p_\infty = \rho \overline{R} T_\infty$ was applicable, where $\overline{R}$ is the gas constant for the test gas.

The stagnation enthalpy, H_o, and temperature, T_o, of the gas behind the reflected shock wave (shown as region 4 in Figure 21b) were calculated from:

$$H_o = (H_4/H_1)H_1 \text{ and } T_o = (T_4/T_1)\ T_1 \tag{4.1}$$

where (H_4/H_1) and (T_4/T_1) are functions of U_i (or M_i) and p_1 and are given in Reference 43 for air. H_1 was obtained from Reference 44 for air, knowing p_1 and T_1.

The freestream static temperature was found from the energy equation, knowing H_o and M_∞,

$$T_\infty = \frac{H_o}{\overline{C}_p}\left(\frac{1}{1 + \dfrac{(\gamma - 1)}{2} M_\infty^2}\right) \tag{4.2}$$

where $\overline{C}_p = 6006$ ft-lb/slug/R° and $\gamma = 1.40$.

The freestream static pressure was calculated from

$$p_\infty = \frac{p}{p_p} p_o \left(1 + \frac{(\gamma - 1)}{2} M_\infty^2\right)^{\left(\frac{-\gamma}{\gamma - 1}\right)} \tag{4.3}$$

where

$$\frac{p}{p_p} = \frac{(p_\infty/p_o)_{REAL}}{(p_\infty/p_o)_{IDEAL}} \tag{4.4}$$

is the real-gas correction to the ideal-gas static-to-total pressure ratio as described in Reference 45. The sources for the real-gas data used in this technique are References 46 and 47.

The freestream velocity was determined from

$$U_\infty = M_\infty a_\infty \tag{4.5}$$

where

$$a_\infty = \sqrt{\gamma \overline{R} T_\infty}\ , \tag{4.6}$$

the speed of sound.

The freestream dynamic pressure was found from

$$\bar{q}_\infty = 1/2\gamma p_\infty M_\infty^2 \tag{4.7}$$

and the freestream density then was calculated from the ideal-gas equation of state

$$\varrho_\infty = p_\infty/\bar{R}T_\infty \tag{4.8}$$

where $\bar{R}$ = 1717.91 ft-lb/slug/R° for air. Values of the absolute viscosity, μ, used to compute the freestream Reynolds number per foot were obtained using the technique described in Reference 43.

The test-section pitot pressure, p_o', was determined from $\bar{q}_\infty$ and the ratio (p_o'/q_∞). This ratio has been correlated as a function of M_∞ and H_o for normal-shock waves in air in thermodynamic equilibrium.

For the test conditions at which our studies were conducted, the uncertainty in pitot-pressure measurements from errors in calibration and recording is ±2.5%. The reservoir pressure can be measured with an uncertainty of ±2.0%, and the total enthalpy (H_o) can be determined from the driven-tube pressure and the incident-shock Mach number with an uncertainty of ±1.5%. These measurements combine to yield an uncertainty in the Mach number and dynamic pressure measurements of ±0.8% and ±3.5%, respectively.

4.3 REDUCTION OF MEASUREMENTS OF PRESSURE AND HEAT TRANSFER

4.3.1 Measurement-Time Selection

Measurements were made during the current studies for a number of different test conditions and tunnel configurations. While, in all cases, the basic flowfield stabilized within several milliseconds, we observed oscillations in the heat transfer and pressure records that we believe are local flow instabilities, an intrinsic feature of these flows for some type IV interactions. For example, with a type IV interaction (where the jet tries to impinge normal to the cylinder surface), we observed a movement in the peak heating and pressure that, as discussed in Section 5, suggests that the jet oscillates, deflecting above and below the normal impingement point. In cases where there was some degree of flow unsteadiness, selection of the time and duration over which the data were averaged was based on an exhaustive analysis of all the measurements and flow visualizations made in this program, together with experience gained in many earlier experimental studies. The data were read just preceding the Schlieren photograph of the flow, to avoid electrical interference from the spark source. For runs 9 through 32 in the 48-inch shock tunnel, where we had run times of close to 12 milliseconds, the Schlieren photographs were taken at approximately 10 milliseconds, and the measurements were made typically between 8 and 10 milliseconds. For runs 33 to 44 in the 96-inch shock tunnel (which had steady run times of 5 milliseconds), Schlieren photographs were taken close to the end of the run, and the heat transfer and pressure measurements were made 1 millisecond prior to the Schlieren exposure. For runs 59 through 116, conducted in the 48-inch shock tunnel with the long driver, we obtained test times of over 12 milliseconds. We took Schlieren photographs at approximately 2 milliseconds before the end of the run and made the measurements of heat transfer during the 2 milliseconds just preceding the Schlieren pulse.

4.3.2 Pressure Measurements

The measured voltages from the pressure transducers were reduced to engineering units (psi) by applying the amplifier gains and the transducer calibration factors. The pressures were then converted to absolute pressures (psia) by adding the measured initial vacuum pressure in the test section. The latter was the reference pressure for the transducers. The pressures were then averaged over the time interval of steady flow to obtain an average value for each case. The values of the pressure coefficients, C_p, were calculated from

$$C_p = p/(1/2\varrho_\infty U_\infty^2) \tag{4.9}$$

where p was the measured model pressure (psia).

4.3.3 Heat Transfer Measurements

The thin-film heat transfer gage is a resistance thermometer that reacts to the local surface temperature of the model. The first step of the data reduction was to convert the measured voltage time history for each gage to a temperature time history, taking into account the gage resistance, the current through the gage, the gage calibration factor, and the amplifier gain. The theory of heat conduction was used to relate the surface temperature to the rate of heat transfer. The platinum resistance element has negligible heat capacity and, hence, negligible effect on the Pyrex-substrate surface temperature. The substrate can be characterized as being homogeneous and isotropic. Furthermore, because of the short duration of a shock-tunnel test, the substrate can be treated as a semi-infinite body. The one-dimensional heat conduction equation is

$$\varrho c(T)\frac{\partial T}{\partial t} = \frac{\partial}{\partial y}\left(k(T)\frac{\partial T}{\partial y}\right) \tag{4.10}$$

where ϱ, c, and k are the substrate density, specific heat, and thermal conductivity, respectively; y is the distance normal to the substrate surface; and $T(t)$ is the transient surface temperature rise $(T(0) = 0)$. For a quick look at the data, the Cooke-Felderman method, given below, was used

$$q(t_m) = \left(2\sqrt{(\varrho\frac{ck}{\pi})}\right)\sum_{i=1}^{m}\frac{T(t_i) - T(t_{i-1})}{(t_m - t_1)^{1/2} + (t_m - t_{i-1})^{1/2}} \tag{4.11}$$

where m is the number of time interval steps from $t = 0$ *to* t_m. Inasmuch as the heat transfer gage outputs were sampled at constant time intervals of 50 or 100 μsec and were digitized by DDAS II, this equation provided a straightforward method for calculating the heat transfer rates. The heat transfer rates, $\dot{q}(t)$, were then averaged over a specified time interval during the steady-flow portion of each test run to obtain a value of $\dot{q}$ for each gage. Initially, the heat transfer rates were calculated with time $t = 0$ taken just before the arrival of the airflow. The Cooke-Felderman method is valid for constant values of (ϱck), where c and k are functions of the substrate temperature. However, the final reduction was done using the Rae-Taulbee algorithm to solve the heat-conduction equation numerically to account for the variation of (ϱck) with temperature. A brief summary of this algorithm is provided in Appendix A.

The Stanton number, C_h, based on the freestream conditions, was calculated from the following

$$C_h = \frac{\dot{q}}{\rho_\infty U_\infty (H_o - H_w)} \tag{4.12}$$

where H_w is the enthalpy at the measured wall temperature.

4.3.4 Measurement Recording System

All data were recorded on the 128-channel Calspan DDAS II together with the NAVCOR system described earlier. The DDAS II system consists of 128 Marel Co. Model 117-22 amplifiers, an Analogic ANDS 5400 data acquisition and distribution system, and a Digital Equipment Corp. (DEC) PDP-11/73 computer. The Analogic system functions as a transient-event recorder in that it acquires, digitizes, and stores the data in real time. Immediately after each test run, the data were transferred to the DEC computer for processing and storage.

The Marel amplifiers provide gains up to 1000 for low-level signals, can be AC or DC coupled to the transducers, and have selectable low-pass filters with cutoff frequencies of 300, 1000, or 3000 Hz. The Analogic system contains a sample-and-hold amplifier, a 12-bit analog-to-digital converter, and a 4096-sample memory for each channel.

Section 5
RESULTS AND DISCUSSION

5.1 INTRODUCTION

The three studies discussed here provide detailed experimental measurements and insight into the important aerothermal mechanisms associated with the aerothermal loads induced in regions of single- and multiple-shock/shock interaction in hypersonic flow. These studies were conducted over the Mach number range from 6 to 19 and included measurements in laminar, transitional, and turbulent interactions. A summary of the freestream test conditions used in these studies is given in Table 3. In each study, the emphasis of the investigation was placed on the flows that generated the largest heating loads, and that were of the greatest interest in terms of developing correlations of the aerothermal characteristics of these flows. A major objective was to provide measurements of sufficient definition and accuracy for code evaluation.

In the first of the three studies discussed here, we investigated the effects of Mach number and Reynolds number on the heat transfer and pressure distributions in Types III, IV, and VI shock/shock interaction regions over a cylinder at Mach numbers between 6 and 19. Here, we were principally interested in how the characteristics of the different types of interaction were influenced by Mach number and transition, and in the influence of these parameters on the peak heating in Types III and IV interactions. The results of the 56 experimental studies conducted during this phase of the research are tabulated, together with Schlieren photographs of the flowfield, in Appendix B.

The second investigation was conducted to examine the heating loads and flow structures generated in regions of shock/shock interaction induced by two externally generated shocks impinging in the stagnation region of the cylinder. Here, the emphasis was on determining whether the heating loads generated under multiple-shock impingement conditions, for comparable overall shock strengths, would be greater or less than those generated by a single shock. The experimental studies were conducted at Mach 8, with the principal variable being the relative positions of the two incident shocks and the position of the cylinder. Some measurements were made to define the effects of relative incident-shock strengths. The test conditions, surface measurements, and Schlieren photographs are presented in Appendix C.

A third study was devoted to an investigation of sweep effects on the peak heating levels generated in regions of Type III/IV interaction. Here, the investigation was conducted only at the Mach 8 condition, where we believe the interaction was turbulent. The freestream conditions, pressure, and heat transfer measurements, together with the Schlieren photographs from this study, are presented in Appendix D.

5.2 MEASUREMENT OF HEAT TRANSFER AND PRESSURE DISTRIBUTIONS ON A CYLINDER WITHOUT INCIDENT SHOCK

Measurements of the heat transfer and pressure distributions to the cylinder in the absence of a incident shock, made at the Mach 8 and 16 test conditions, are compared with theory in Figures 25 and 26. The measurements are in good agreement with the Fay and Riddell[49] stagnation-point value and the Kemp, Rose, and Detra[50] distribution.

The Fay-Riddell stagnation-point heat transfer is given by

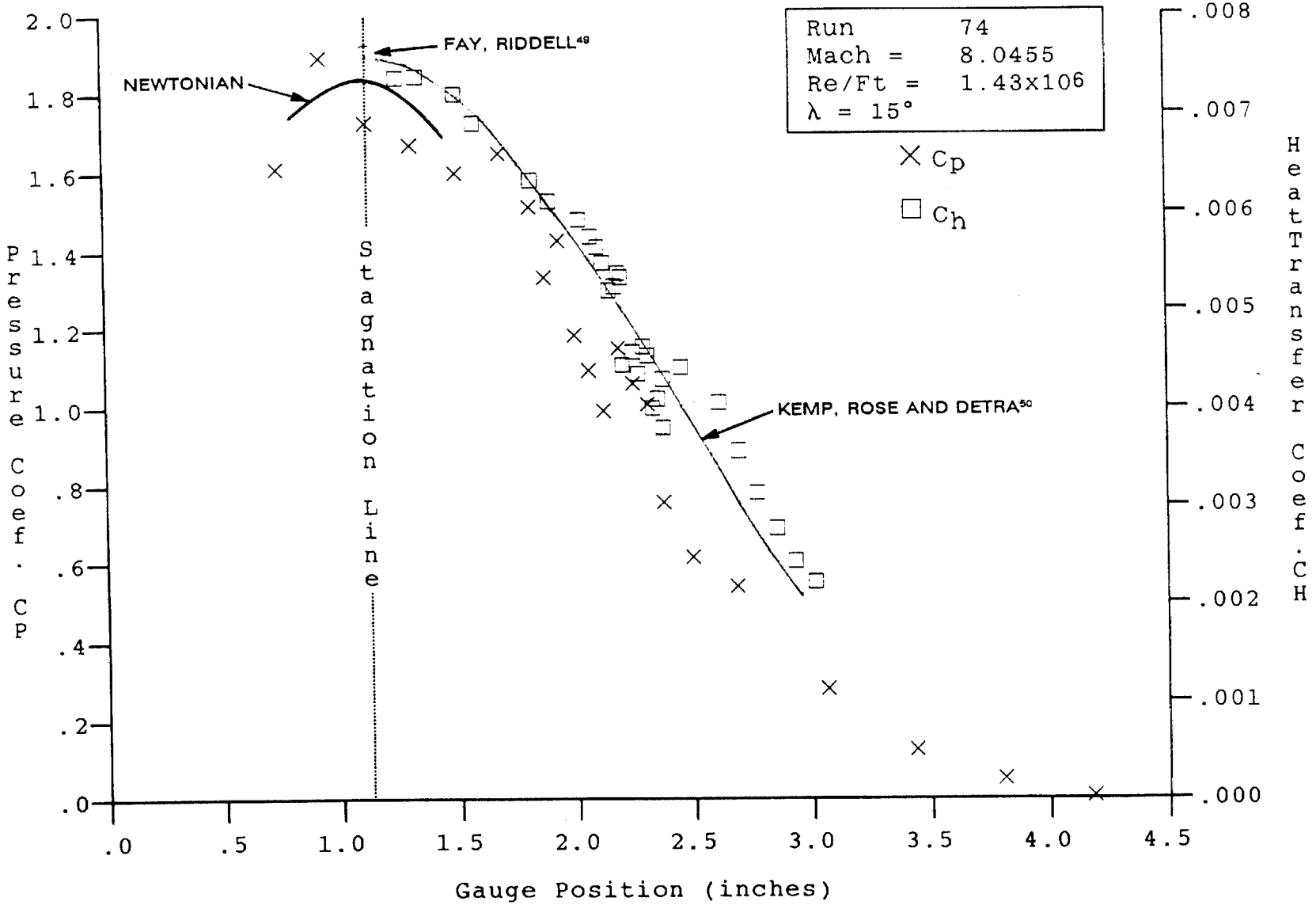

Figure 25 COMPARISONS BETWEEN MEASURED, PREDICTED HEAT TRANSFER AND PRESSURE DISTRIBUTIONS AROUND A CIRCULAR CYLINDER AT MACH 8

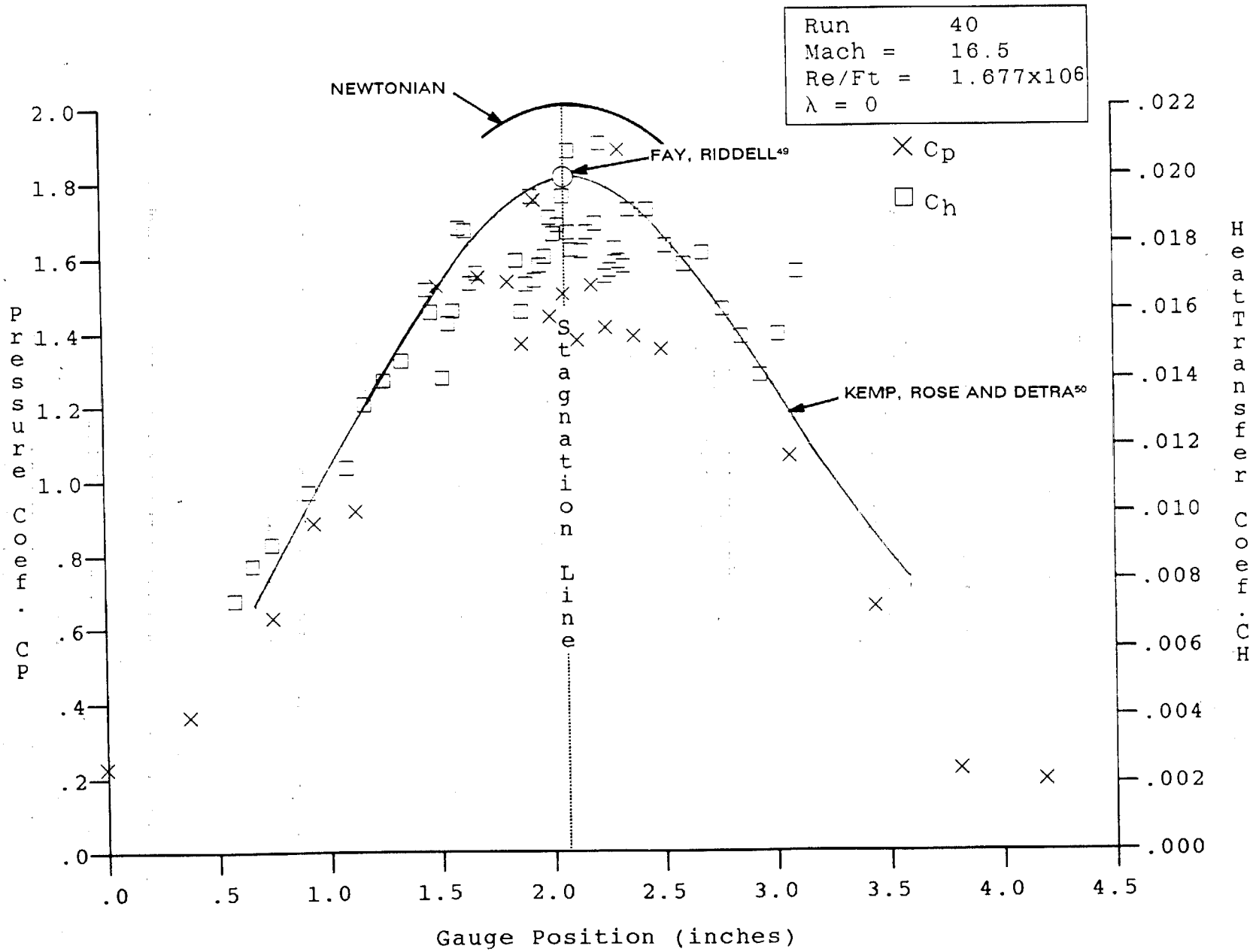

Figure 26 COMPARISONS BETWEEN MEASURED, PREDICTED HEAT TRANSFER AND PRESSURE DISTRIBUTIONS AROUND A CIRCULAR CYLINDER AT MACH 16

$$q_{FR} = F_{shape}\left[\frac{0.944}{Pr^{0.6}}(\varrho_{STAG}\,\mu_{STAG})^{0.4}(\varrho_w\,\mu_w)^{0.1}[H_{STAG} - H_w]\left(\frac{dU_e}{dx}\right)^{1/2}\right] \tag{5.1}$$

where

$$\frac{dU_e}{dx} = \frac{\sqrt{2\overline{R}}}{D/2}\left[T_{STAG}\left[1 - \frac{p_\infty}{p_{STAG}}\right]\right]^{1/2} \tag{5.2}$$

The Kemp, Rose, and Detra heat transfer distribution is given by

$$\frac{q}{q_{STAG}} = \frac{0.89\varrho_w\mu_w U_e}{\sqrt{2\xi}}\left[2\varrho_{STAG}\,\mu_{STAG}\left(\frac{dU_e}{dx}\right)\right]^{-(1/2)}\left(\frac{g_{\eta w}}{g_{\eta STAG}}\right) \tag{5.3}$$

where

$$\frac{g_{\eta w}}{g_{\eta STAG}} = \left(\frac{1 + 0.096\sqrt{\beta}}{1.068}\right)\left(\frac{1 - H_w/H_e}{1 - H_{STAG}/H_e}\right) \tag{5.4}$$

and

$$\xi(x) = \int_0^x \varrho_w\mu_w U_e(D/2)^2 dx \tag{5.5}$$

The Newtonian pressure distribution is given by

$$\frac{p}{p_{STAG}} = 1 - \frac{p_{STAG} - p_\infty}{p_{STAG}}\sin^2\left(\frac{x}{(D/2)}\right) \tag{5.6}$$

5.3 STUDIES OF MACH NUMBER AND REYNOLDS NUMBER EFFECTS ON SINGLE-SHOCK/BOW-SHOCK INTERACTION

5.3.1 Introduction

The current studies were designed to fill the void in the knowledge of shock/shock interaction in the Mach number range from 6 to 19 with measurements of sufficient accuracy and resolution to provide data suitable for detailed code evaluation. At the Mach 11 and 16 conditions, the Reynolds numbers were varied over a wide range to obtain both laminar and turbulent interaction regions. At each Mach number condition, a series of runs were made where the position of the incident shock was varied relative to the cylinder to induce a range of Types III and IV interactions. For numerous Mach number conditions, the freestream Reynolds number was varied to explore both laminar and turbulent interactions. For all of the studies, the cylinder was oriented to place the high-density instrumentation in the region of maximum

heat transfer. Measurements of the distributions of heat transfer and pressure, and the temperature distribution at the time of measurement, for this series of studies are presented in tabular and graphical form in Appendix B.

5.3.2 Discussion of Measurements

The variation of the distribution of heat transfer and pressure around the cylinder, together with the Schlieren photographs of the flow, are shown for a number of incident-shock configurations at the Mach 8 test condition in Figures 27a through 27f. The emphasis here was on obtaining a range of Types III and IV interactions to evaluate the variation in peak heating with the position of the interaction. For the Type IV interaction, where the peak heating region is between 15 and 30 degrees below the horizontal, the distribution of heating and pressure at the base of the jet did not exhibit a region of relatively constant values as might be expected in a stagnation region. Instead, we observed both pressure and heat transfer distributions in this region with large gradients about a peak value. The peak mean values of heat transfer and pressure decreased markedly as the interaction was moved upward toward the horizontal axis (Figure 27b). Our measurements also showed that small flapping instability occurred for interactions where the jet impinged almost normal to the surface, and this resulted in the jet oscillating between the upper and lower surfaces of the horizontal axis (Figure 27b). Under these conditions, where the Type IV interaction was at approximately 20 degrees below horizontal, we observed jet oscillation at frequencies between 3 and 10 kHz, as illustrated in the heat transfer and pressure records shown in Figure 28. In these interactions, and in the Type III interaction regions close to the 30-degree position, the peak heating region was so narrow and the gradients so steep that selecting meaningful peak values was extremely difficult.

While the measurements at Mach 8 were for transitional shear layers, the measurements at Mach 11 were made for a range of Reynolds numbers that we believe resulted in both laminar and turbulent interaction regions over the models. Figures 29a through 29c show the effects of decreasing shock-generator angle. Here, we observe a significant decrease in the heating level as the shear-layer Reynolds number is lowered.

A similar result is observed for the Mach 16 measurements, shown in Figures 30a to 30e, where the heating enchancement factors in laminar flow (Figures 30a through 30d) are a factor of approximately 5 lower than the turbulent value (Figure 30e). The measurements made at Mach 18 for Types III and IV flows (shown in Figures 31a through 31d) were all at Reynolds numbers below which transition occurred in the interaction regions. Figure 31a shows a Type IV interaction configuration, where the jet was deflected upward above the flow centerline and, as observed earlier, the heating rates were greatly reduced. Also, we again see from Figures 31a and 31b that there is not a significant difference in heating rates between Types III and IV flows, where the interaction occurs between 25 and 37 degrees below the centerline. As the interaction is moved lower, the peak heating diminishes rapidly, as illustrated by Figures 31c and 31d. While obtaining an accurate value for the peak heating and pressure is difficult, we have plotted the peak heating versus interaction position for the various Mach numbers in Figures 32a through 32d along with typical Keyes-Hains model predictions. For a transitional or turbulent interaction, peak heating is relatively constant if the interaction region falls between 20 and 40 degrees below the horizontal plane, and the heat transfer falls off rapidly above and below this region. Plotting the ratio of peak heating to the maximum peak heating for all of the turbulent measurements at Mach 6 to Mach 11 (Figure 33a), and for laminar measurements from Mach 11 to 18 (Figure 33b), we see that both sets of measurements indicate a maximum in peak heating occurring at about 26 degrees. The variations in peak pressure and

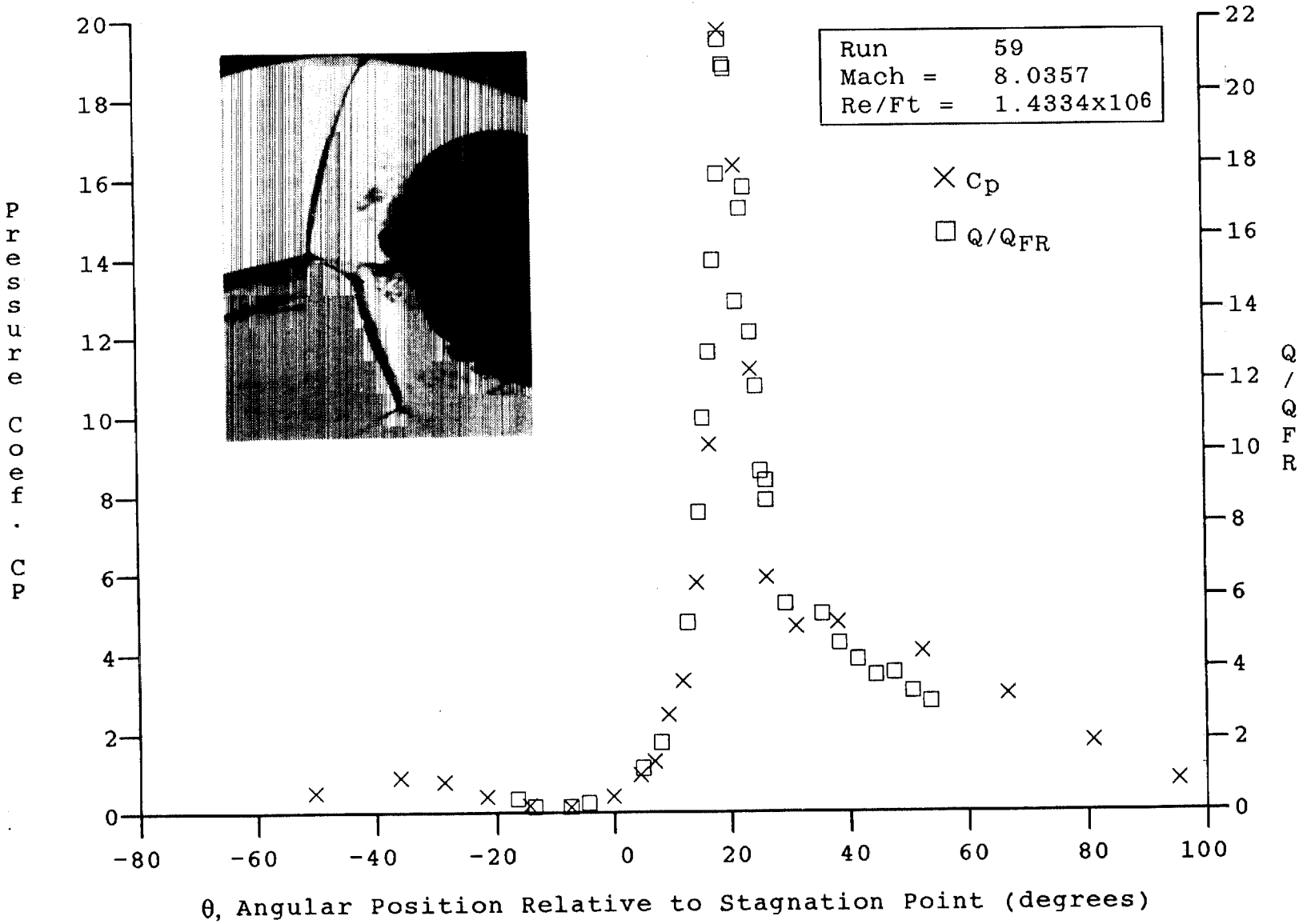

Figure 27a HEAT AND PRESSURE DISTRIBUTIONS IN SHOCK/SHOCK-INTERACTION REGIONS INDUCED BY A 12.5° SHOCK GENERATOR OVER A 3-INCH-DIAMETER CYLINDER AT MACH 8 FOR RUN 59

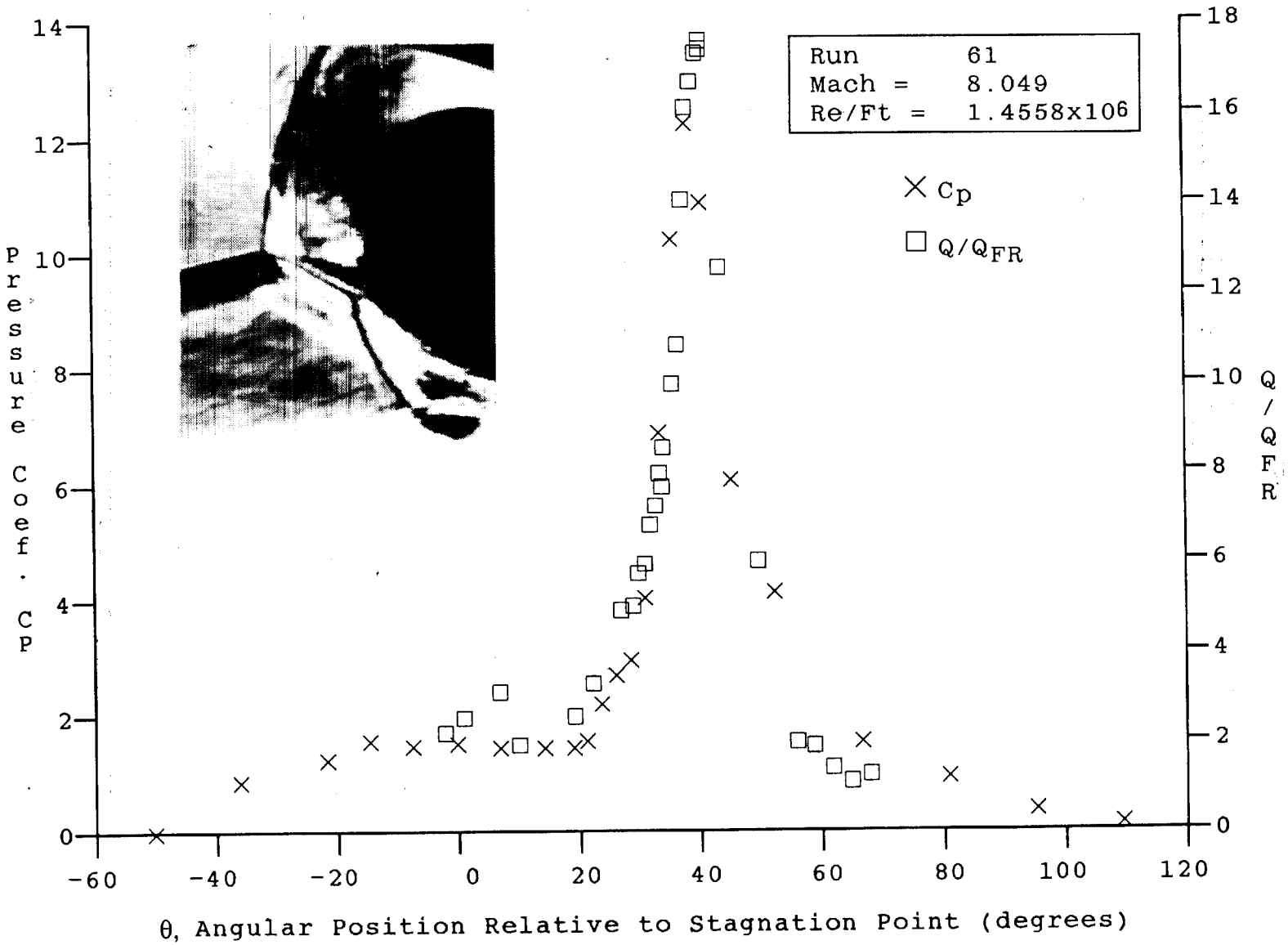

Figure 27b HEAT AND PRESSURE DISTRIBUTIONS IN SHOCK/SHOCK-INTERACTION REGIONS INDUCED BY A 12.5° SHOCK GENERATOR OVER A 3-INCH-DIAMETER CYLINDER AT MACH 8 FOR RUN 61

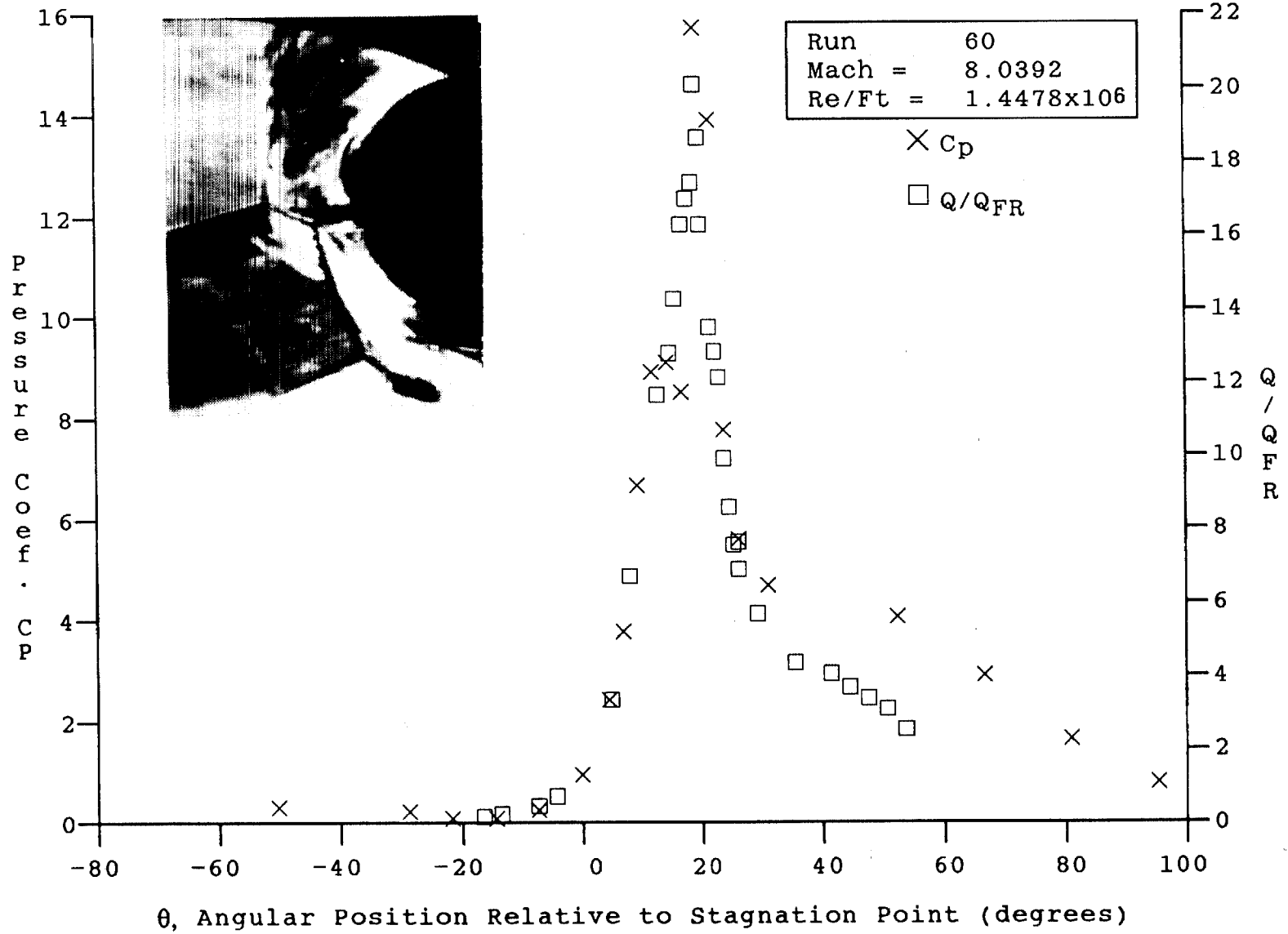

Figure 27c HEAT AND PRESSURE DISTRIBUTIONS IN SHOCK/SHOCK-INTERACTION REGIONS INDUCED BY A 12.5° SHOCK GENERATOR OVER A 3-INCH-DIAMETER CYLINDER AT MACH 8 FOR RUN 60

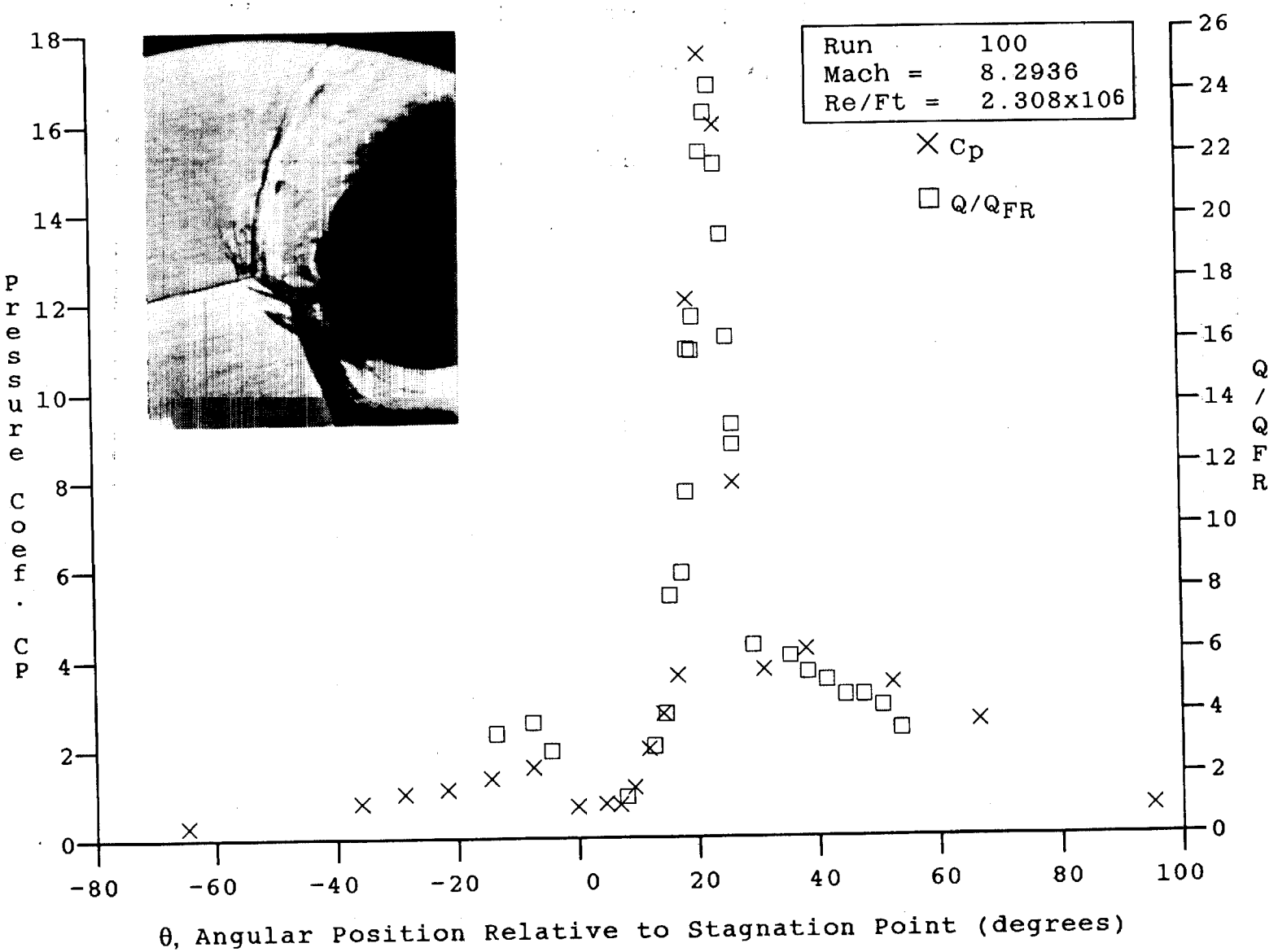

Figure 27d HEAT AND PRESSURE DISTRIBUTIONS IN SHOCK/SHOCK-INTERACTION REGIONS INDUCED BY A 12.5° SHOCK GENERATOR OVER A 3-INCH-DIAMETER CYLINDER AT MACH 8 FOR RUN 100

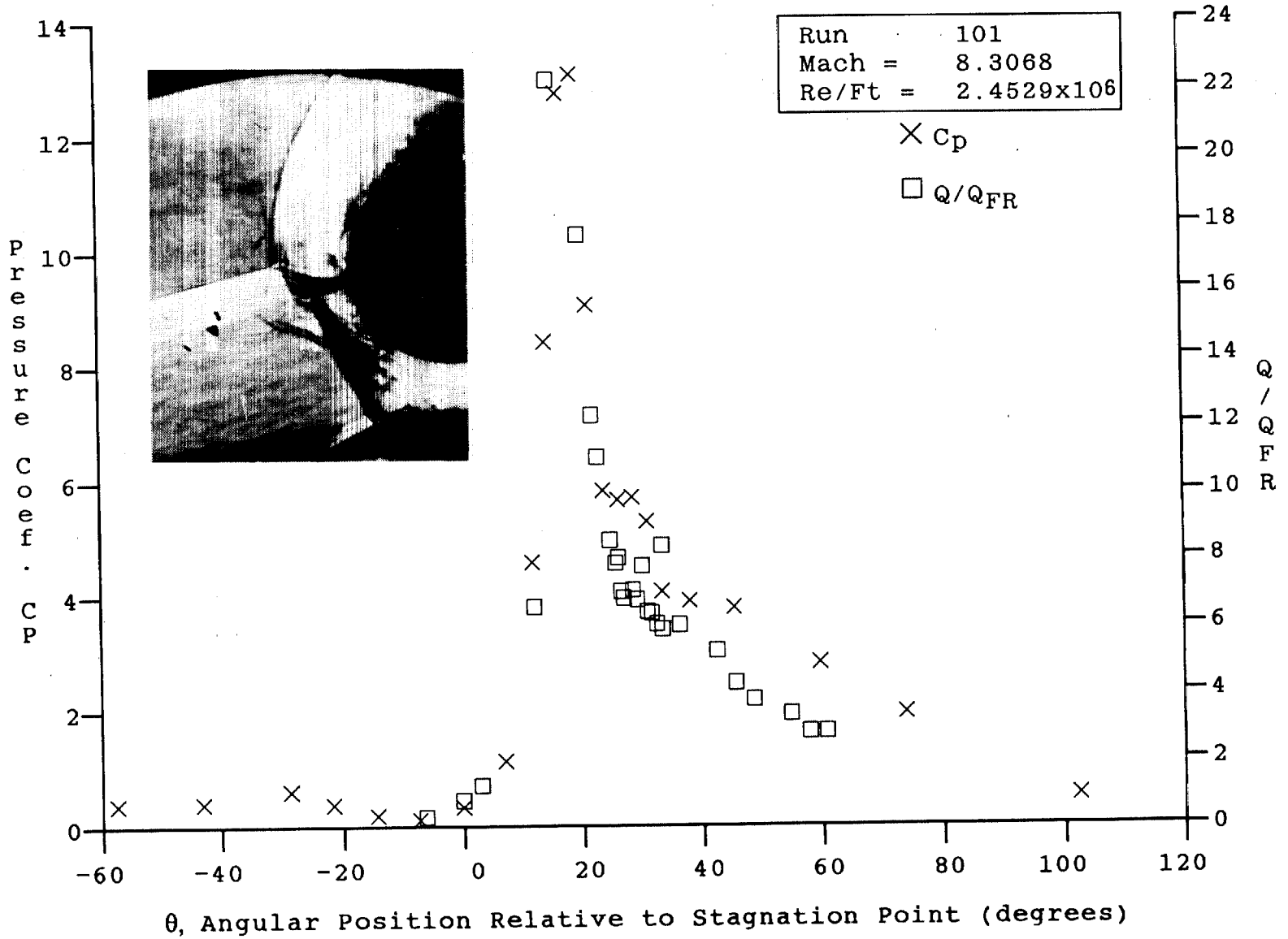

Figure 27e HEAT AND PRESSURE DISTRIBUTIONS IN SHOCK/SHOCK-INTERACTION REGIONS INDUCED BY A 12.5° SHOCK GENERATOR OVER A 3-INCH-DIAMETER CYLINDER AT MACH 8 FOR RUN 101

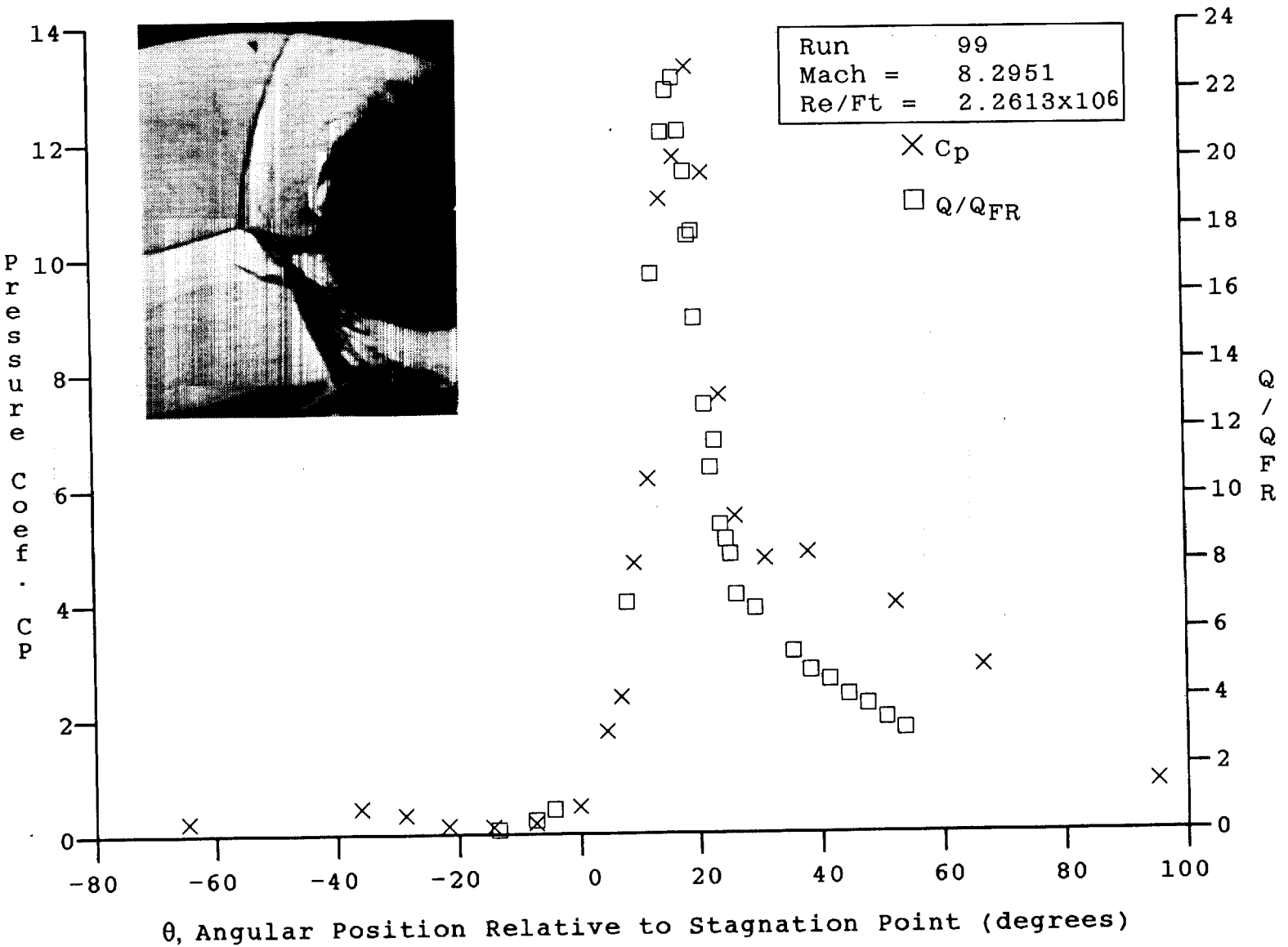

Figure 27f HEAT AND PRESSURE DISTRIBUTIONS IN SHOCK/SHOCK-INTERACTION REGIONS INDUCED BY A 12.5° SHOCK GENERATOR OVER A 3-INCH-DIAMETER CYLINDER AT MACH 8 FOR RUN 99

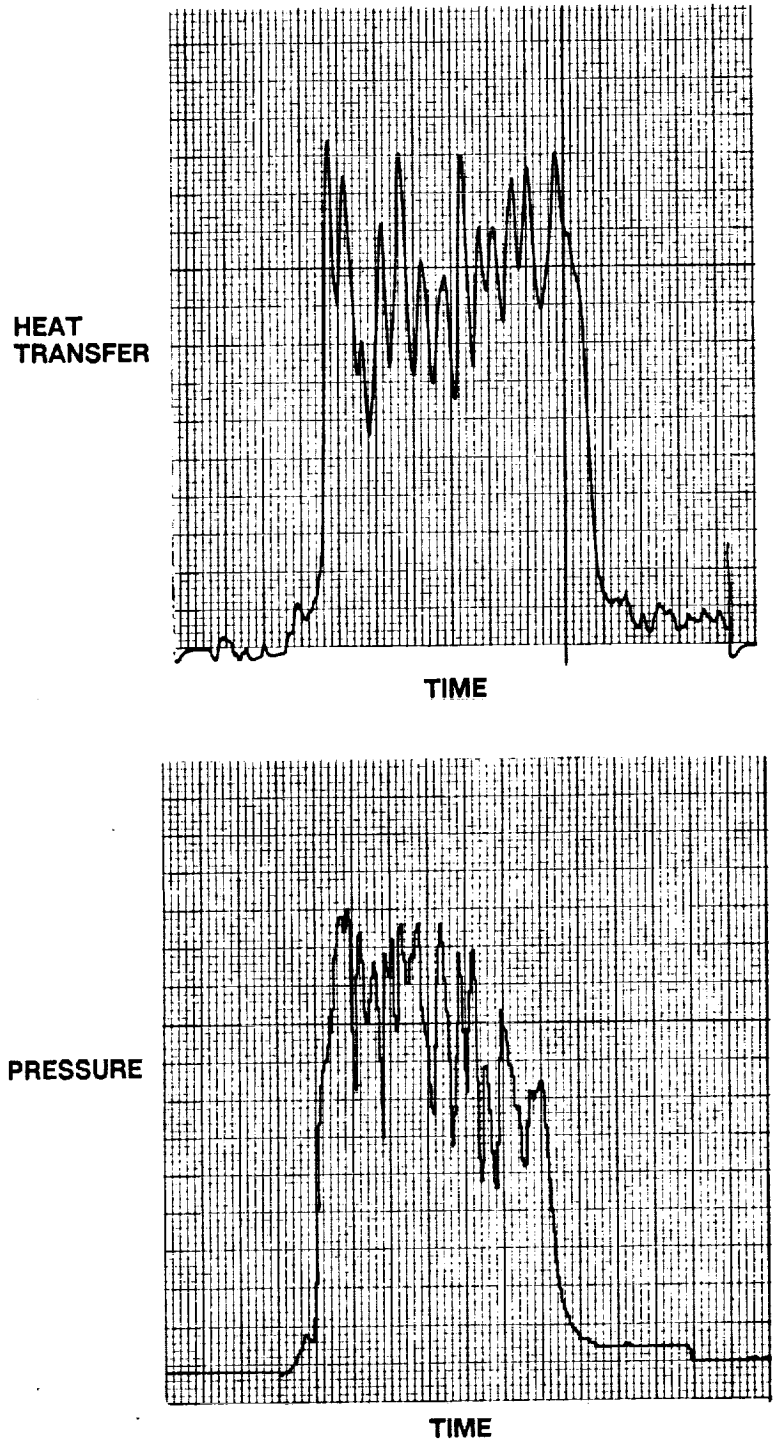

Figure 28 TYPICAL TIME HISTORIES FOR HEAT TRANSFER AND PRESSURE IN TYPE IV INTERACTION REGION AT MACH 8

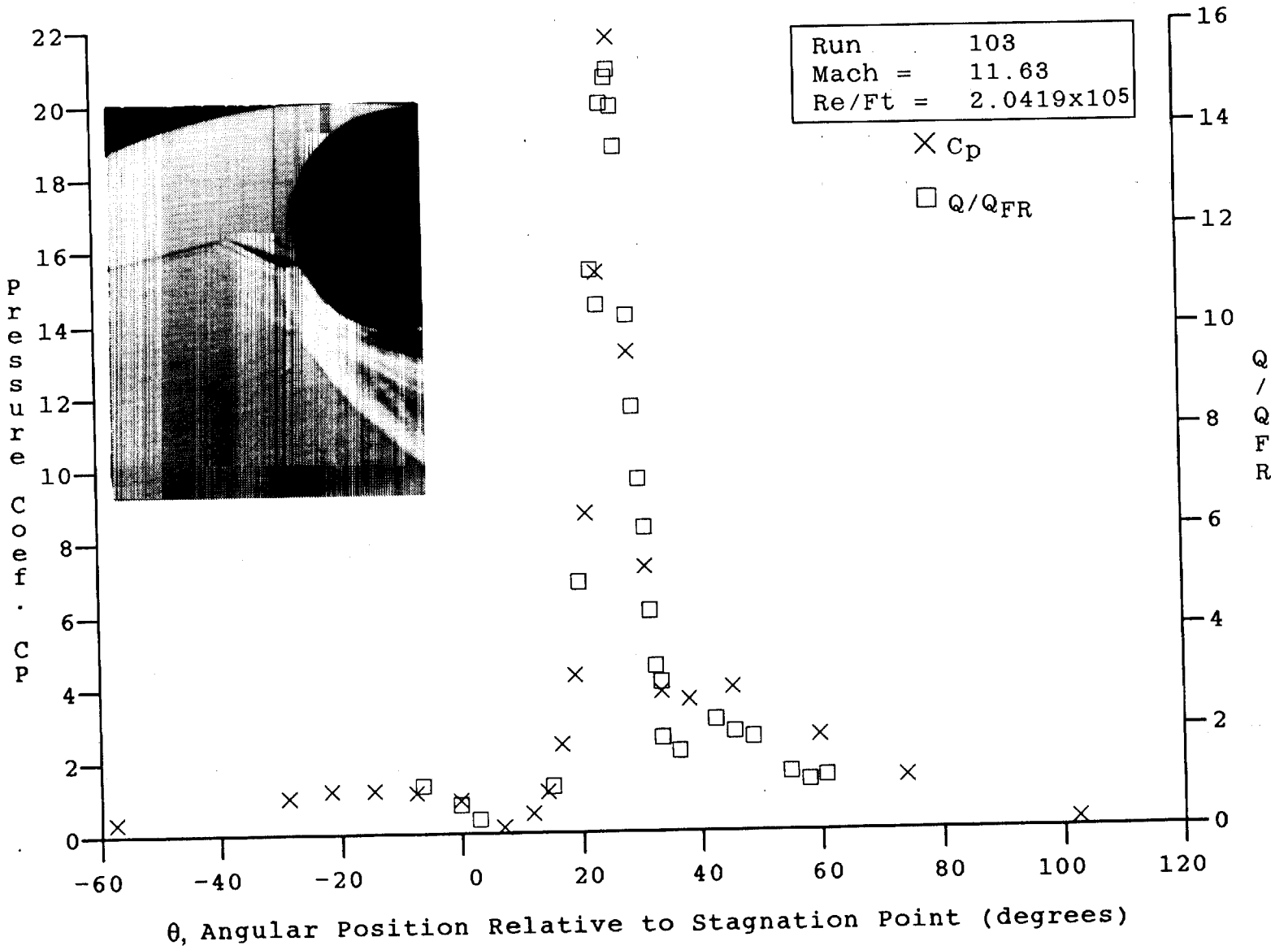

Figure 29a HEAT AND PRESSURE DISTRIBUTIONS IN SHOCK/SHOCK-INTERACTION REGIONS INDUCED BY A 10.0° SHOCK GENERATOR OVER A 3-INCH-DIAMETER CYLINDER AT MACH 11.6 FOR RUN 103

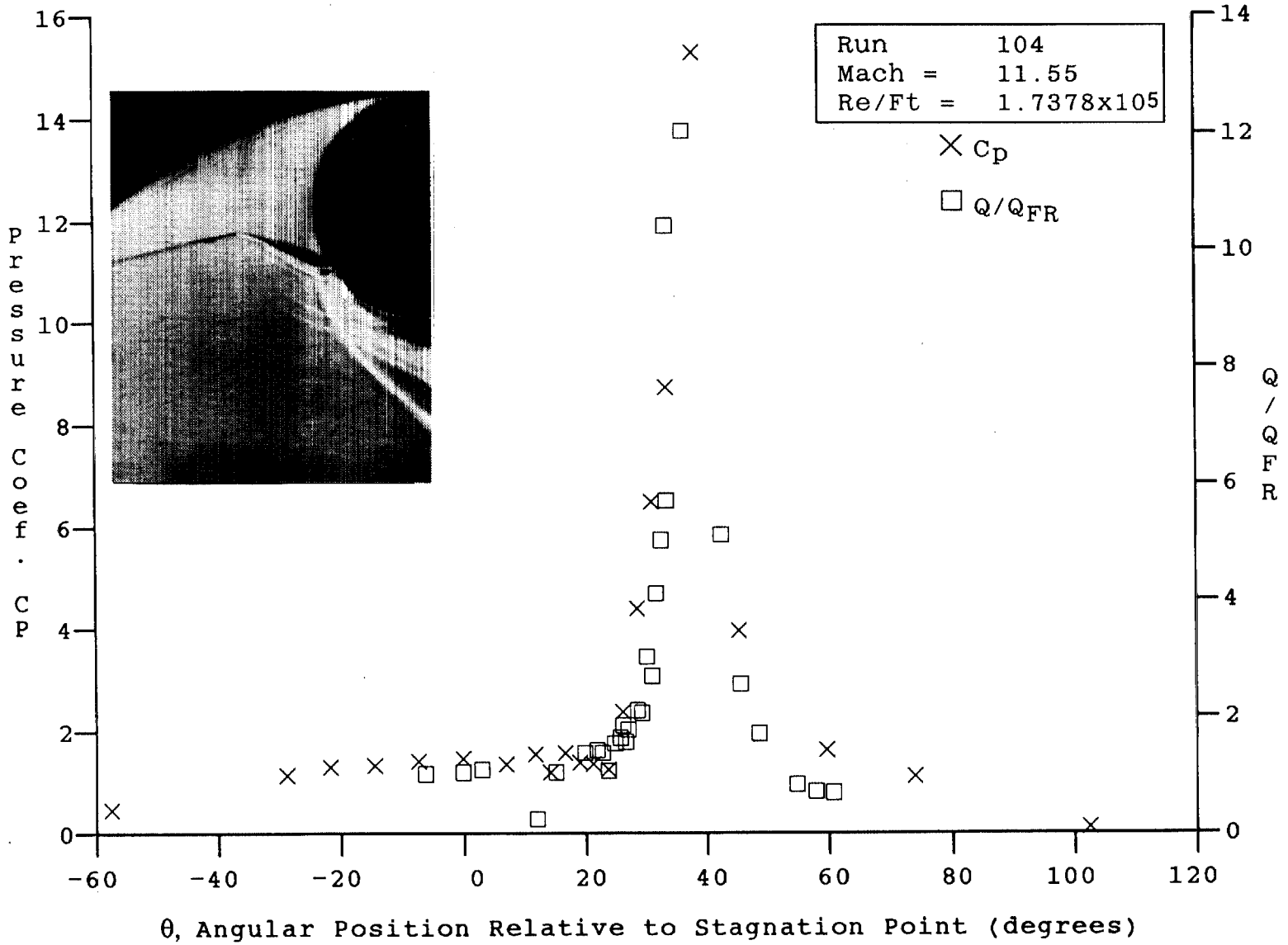

Figure 29b HEAT AND PRESSURE DISTRIBUTIONS IN SHOCK/SHOCK-INTERACTION REGIONS INDUCED BY A 10.0° SHOCK GENERATOR OVER A 3-INCH-DIAMETER CYLINDER AT MACH 11.6 FOR RUN 104

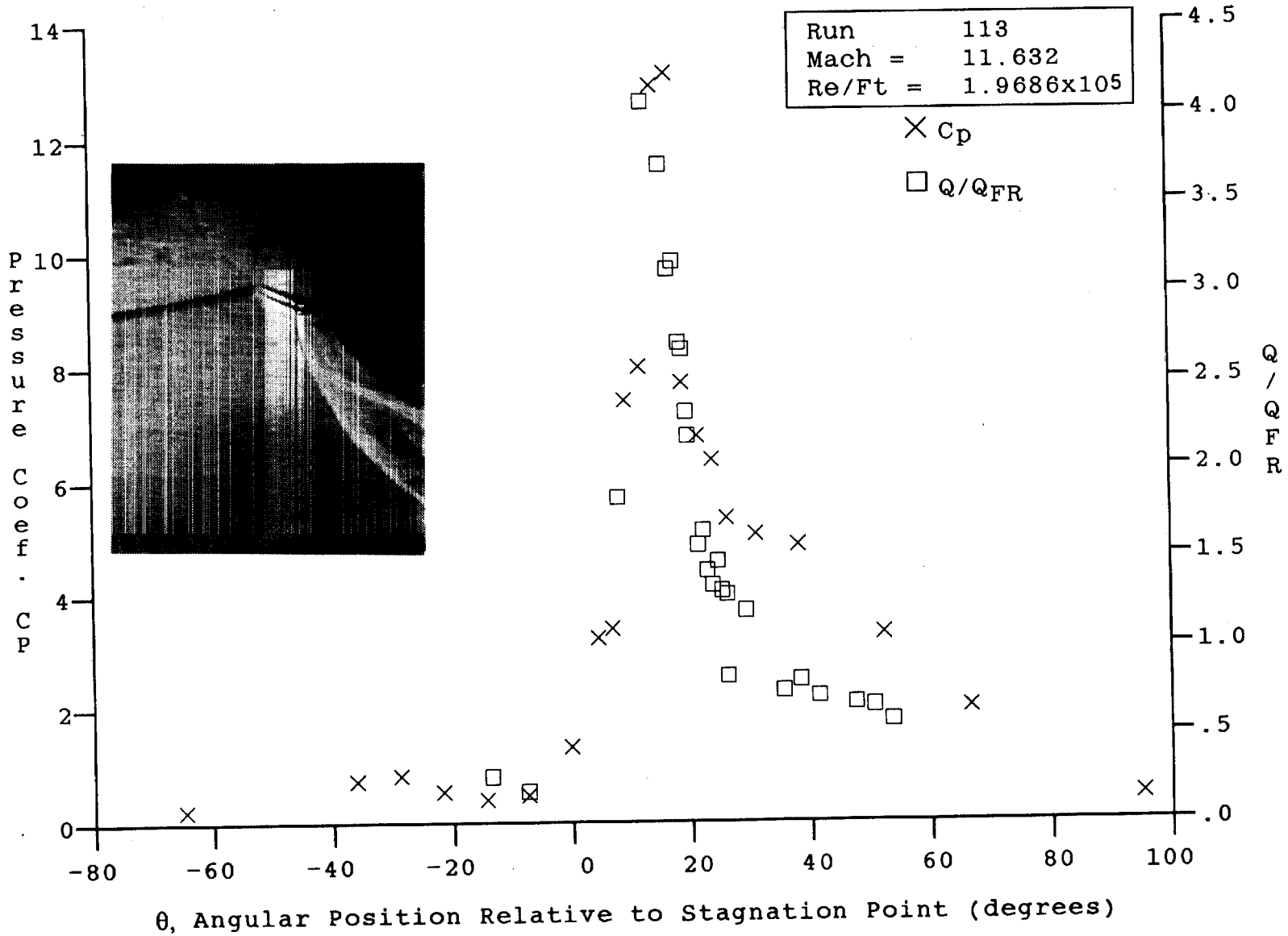

Figure 29c HEAT AND PRESSURE DISTRIBUTIONS IN SHOCK/SHOCK-INTERACTION REGIONS INDUCED BY A 10.0° SHOCK GENERATOR OVER A 3-INCH-DIAMETER CYLINDER AT MACH 11.6 FOR RUN 113

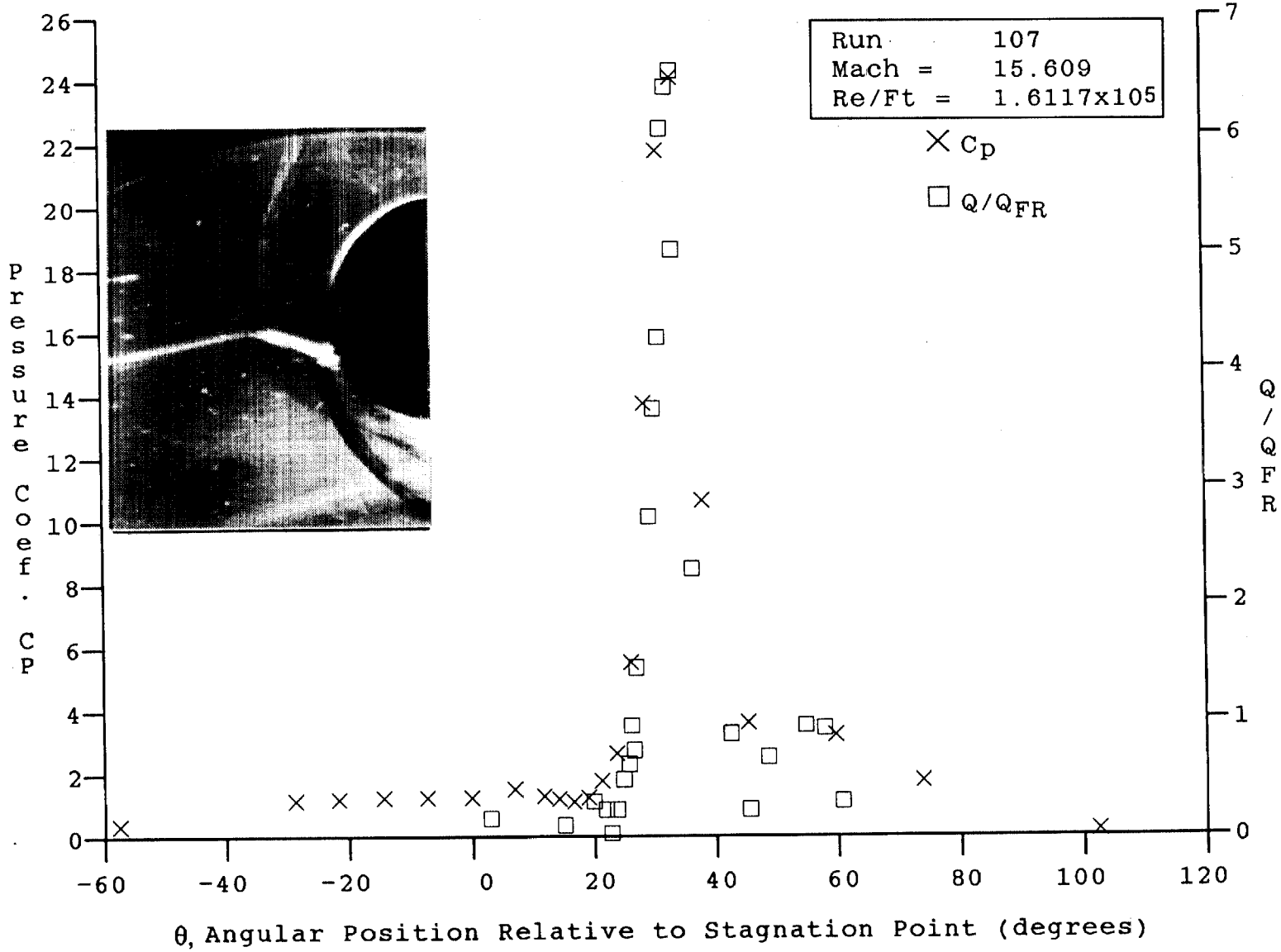

Figure 30a HEAT AND PRESSURE DISTRIBUTIONS IN SHOCK/SHOCK-INTERACTION REGIONS INDUCED BY A 10.0° SHOCK GENERATOR OVER A 3-INCH-DIAMETER CYLINDER AT MACH 15.6 FOR RUN 107

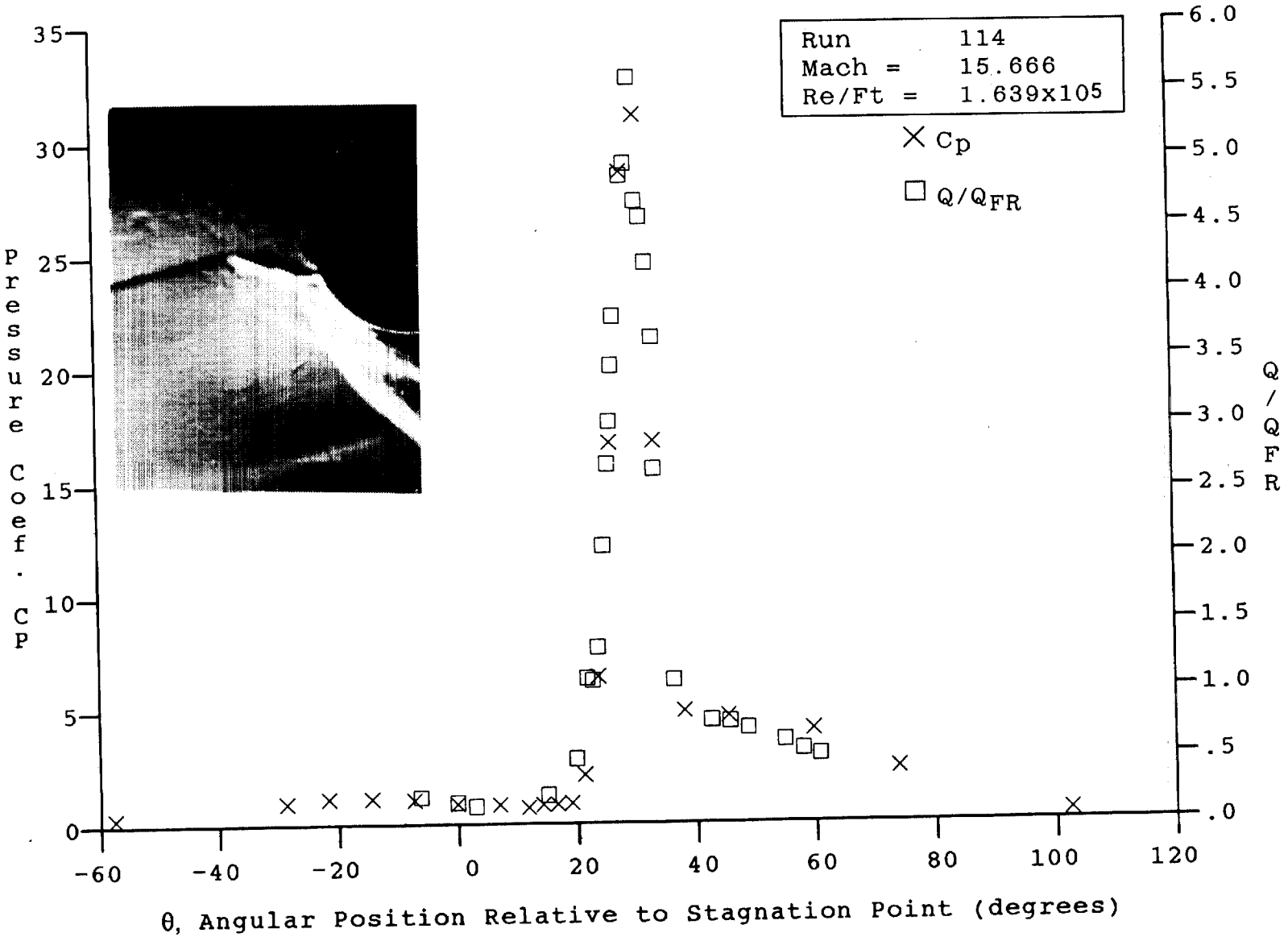

Figure 30b HEAT AND PRESSURE DISTRIBUTIONS IN SHOCK/SHOCK-INTERACTION REGIONS INDUCED BY A 12.5° SHOCK GENERATOR OVER A 3-INCH-DIAMETER CYLINDER AT MACH 15.7 FOR RUN 114

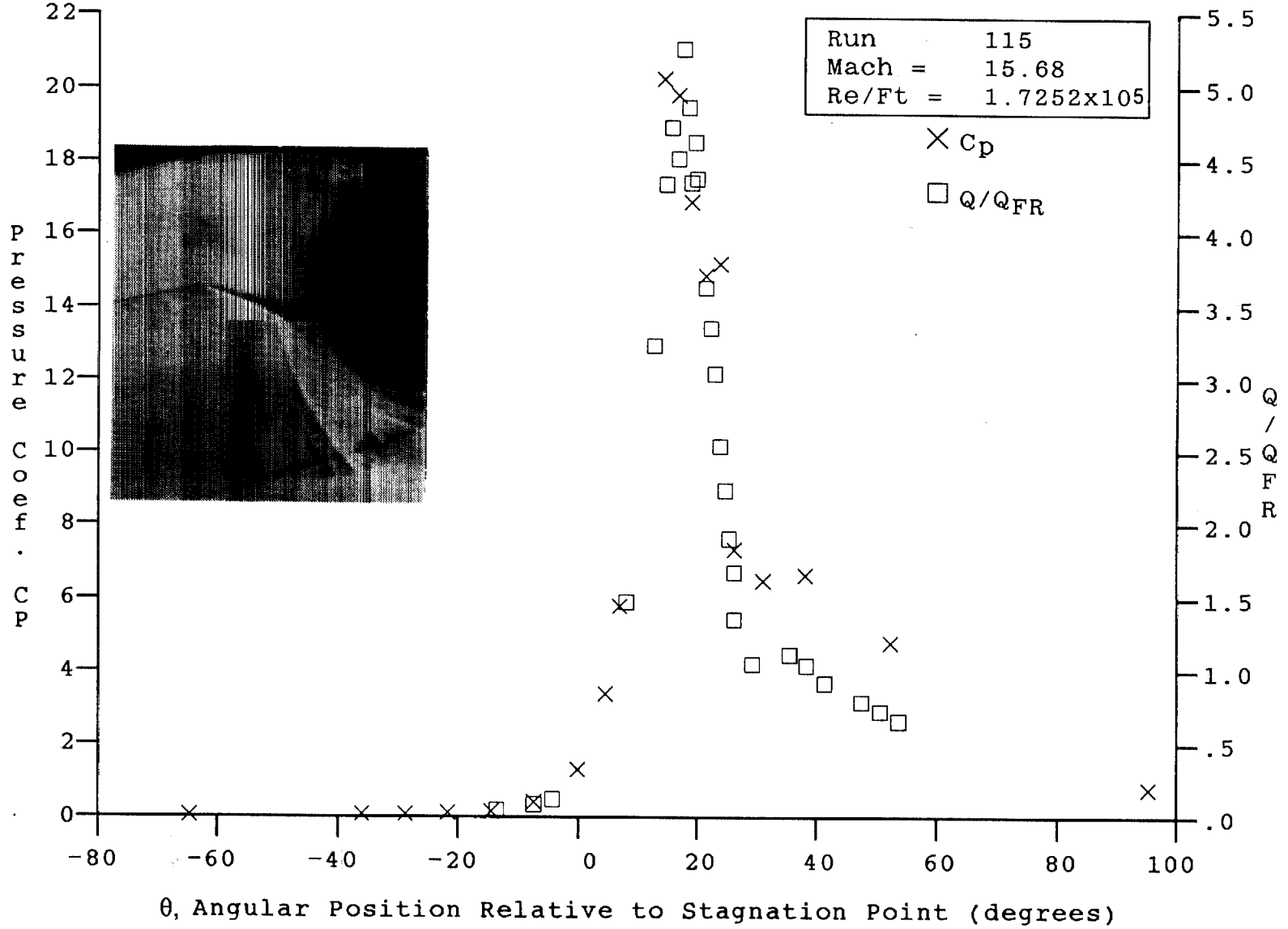

Figure 30c HEAT AND PRESSURE DISTRIBUTIONS IN SHOCK/SHOCK-INTERACTION REGIONS INDUCED BY A 12.5° SHOCK GENERATOR OVER A 3-INCH-DIAMETER CYLINDER AT MACH 15.7 FOR RUN 115

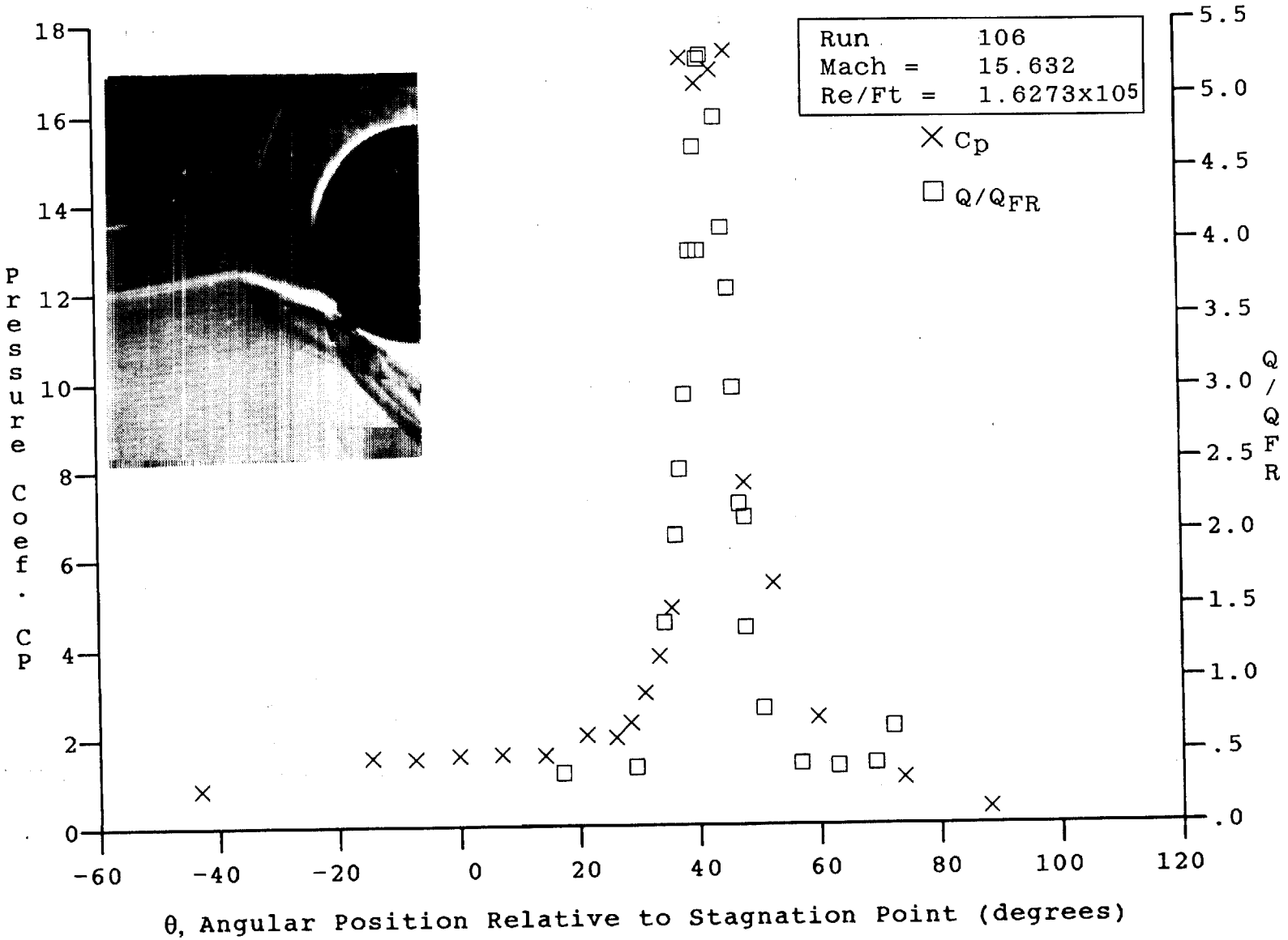

Figure 30d HEAT AND PRESSURE DISTRIBUTIONS IN SHOCK/SHOCK-INTERACTION REGIONS INDUCED BY A 10.0° SHOCK GENERATOR OVER A 3-INCH-DIAMETER CYLINDER AT MACH 15.6 FOR RUN 106

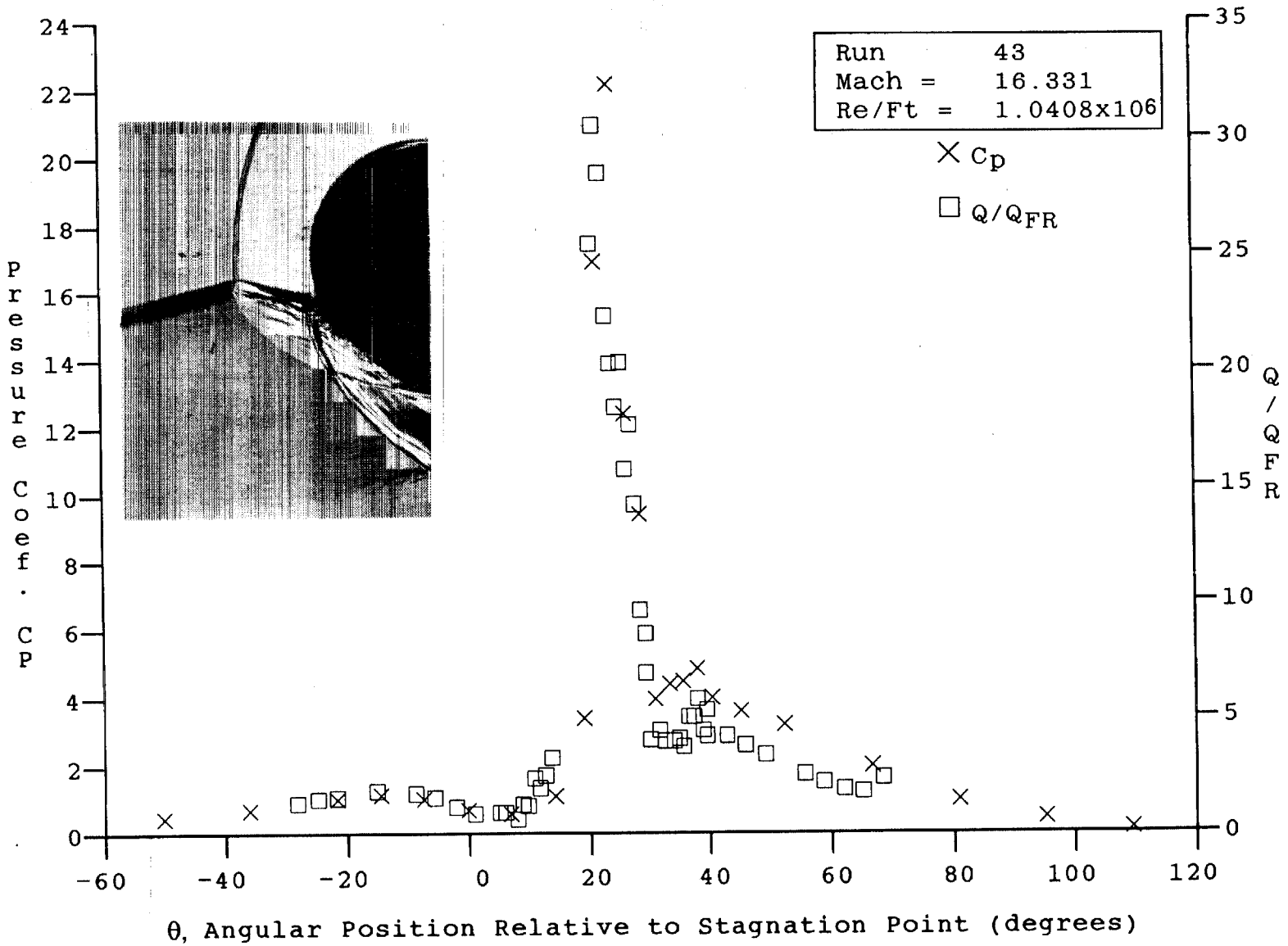

Figure 30e HEAT AND PRESSURE DISTRIBUTIONS IN SHOCK/SHOCK-INTERACTION REGIONS INDUCED BY A 10.0° SHOCK GENERATOR OVER A 3-INCH-DIAMETER CYLINDER AT MACH 16.3 FOR RUN 43

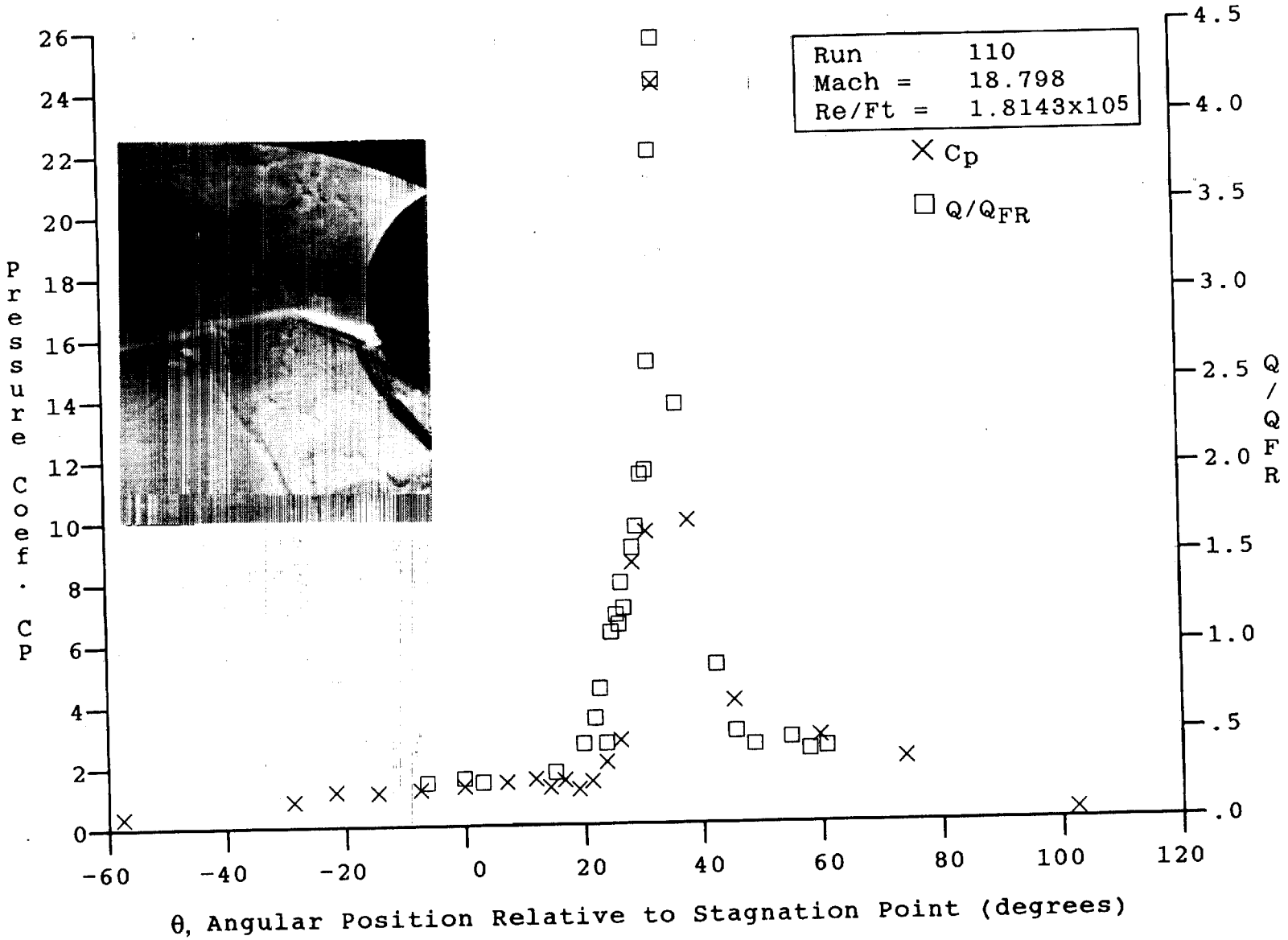

Figure 31a HEAT AND PRESSURE DISTRIBUTIONS IN SHOCK/SHOCK-INTERACTION REGIONS INDUCED BY A 10.0° SHOCK GENERATOR OVER A 3-INCH-DIAMETER CYLINDER AT MACH 18.7 FOR RUN 110

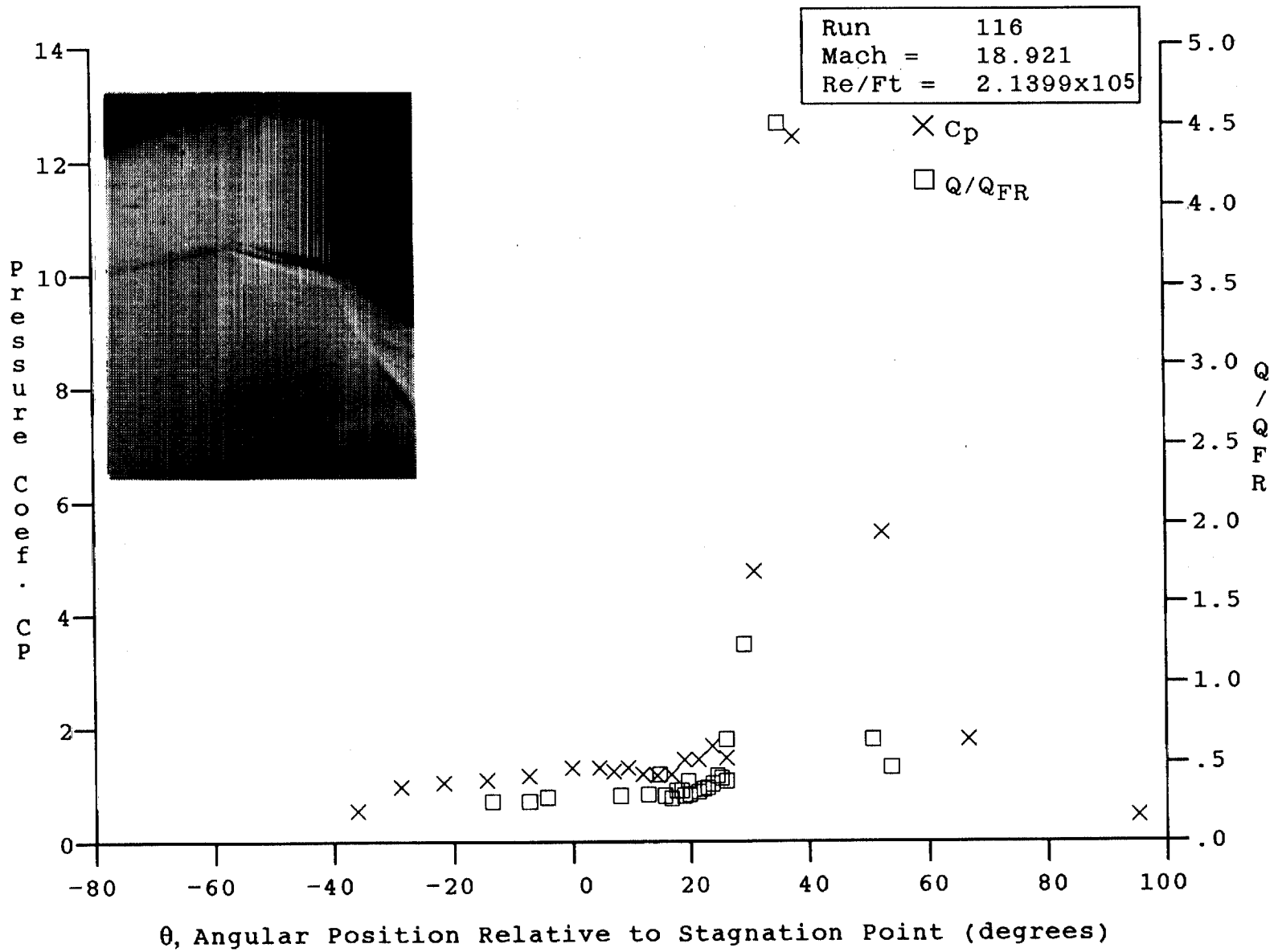

Figure 31b HEAT AND PRESSURE DISTRIBUTIONS IN SHOCK/SHOCK-INTERACTION REGIONS INDUCED BY A 12.5° SHOCK GENERATOR OVER A 3-INCH-DIAMETER CYLINDER AT MACH 18.9 FOR RUN 116

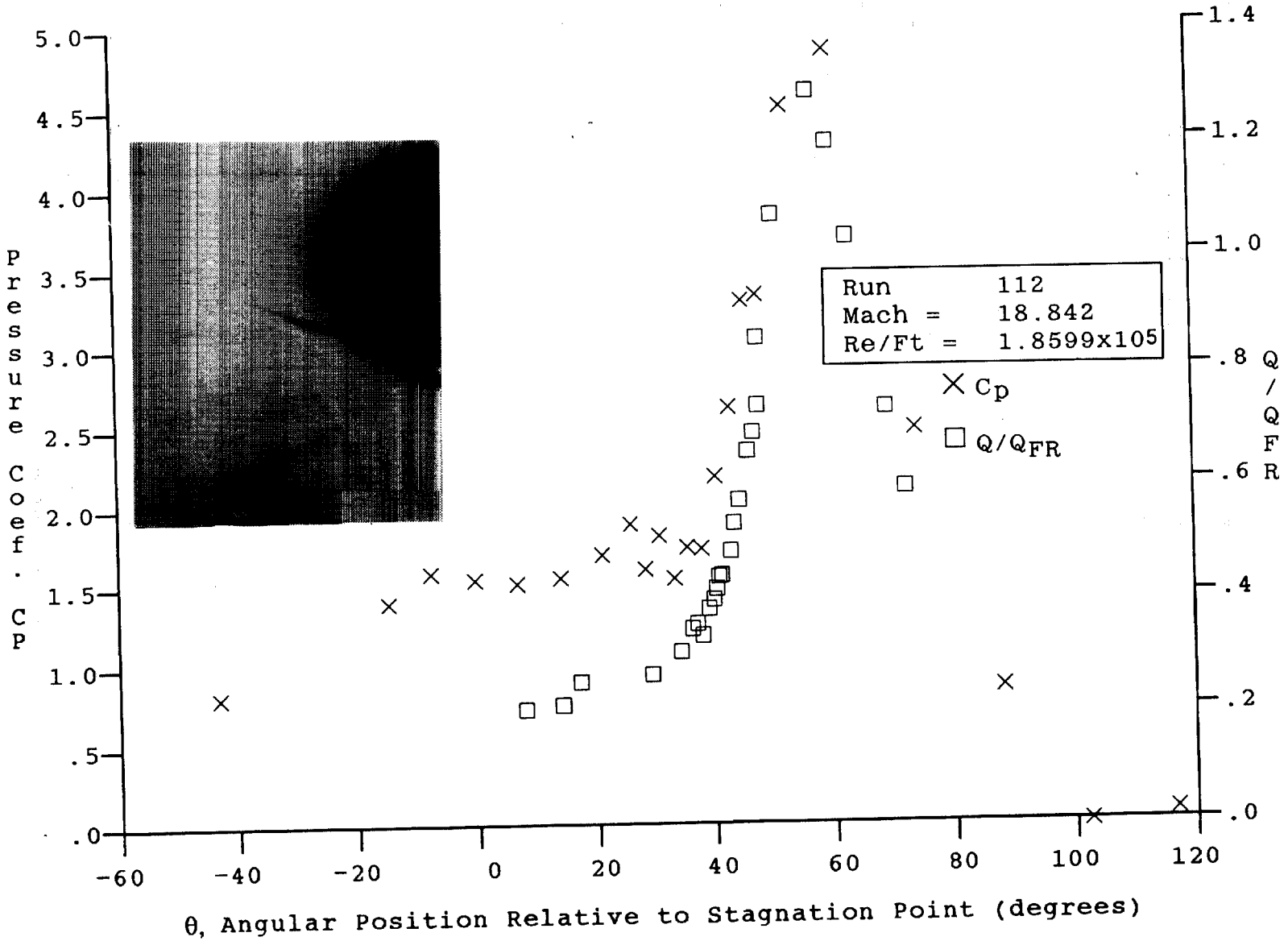

Figure 31c HEAT AND PRESSURE DISTRIBUTIONS IN SHOCK/SHOCK-INTERACTION REGIONS INDUCED BY A 10.0° SHOCK GENERATOR OVER A 3-INCH-DIAMETER CYLINDER AT MACH 18.8 FOR RUN 112

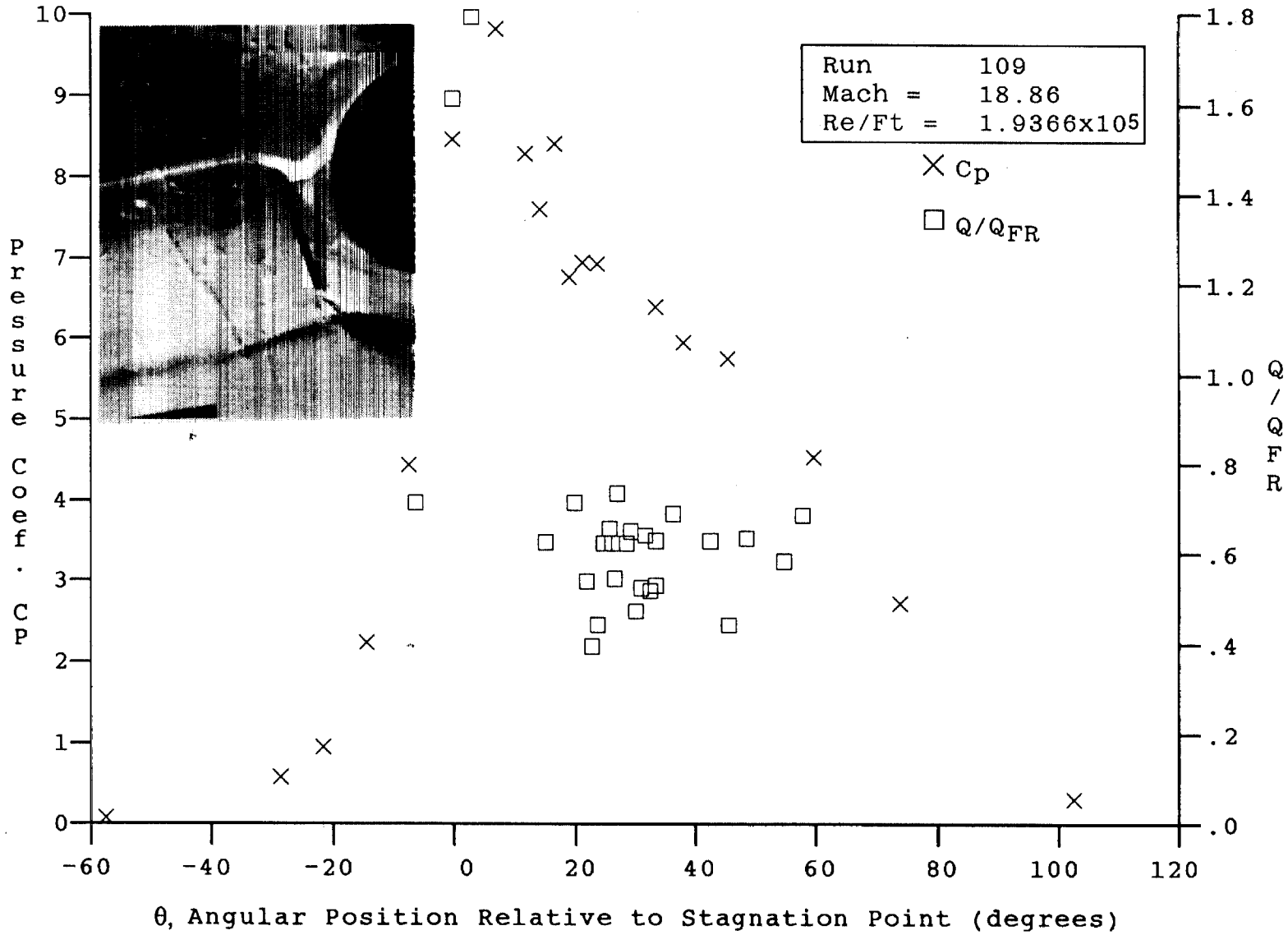

Figure 31d HEAT AND PRESSURE DISTRIBUTIONS IN SHOCK/SHOCK-INTERACTION REGIONS INDUCED BY A 10.0° SHOCK GENERATOR OVER A 3-INCH-DIAMETER CYLINDER AT MACH 18.9 FOR RUN 109

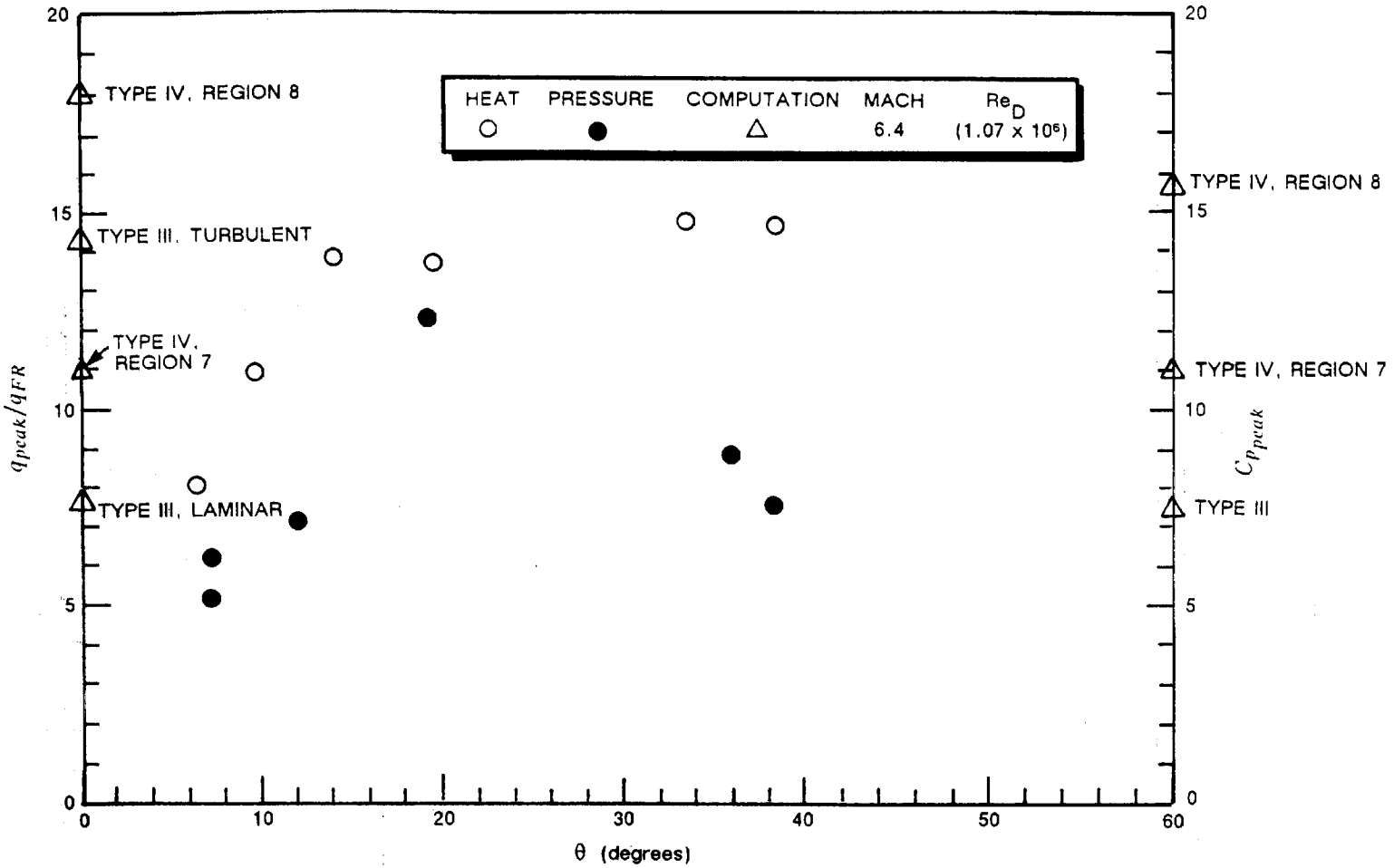

Figure 32a VARIATIONS OF PEAK HEATING AND PRESSURE WITH ANGULAR POSITION OF THE INTERACTION REGION FOR MACH 6.4

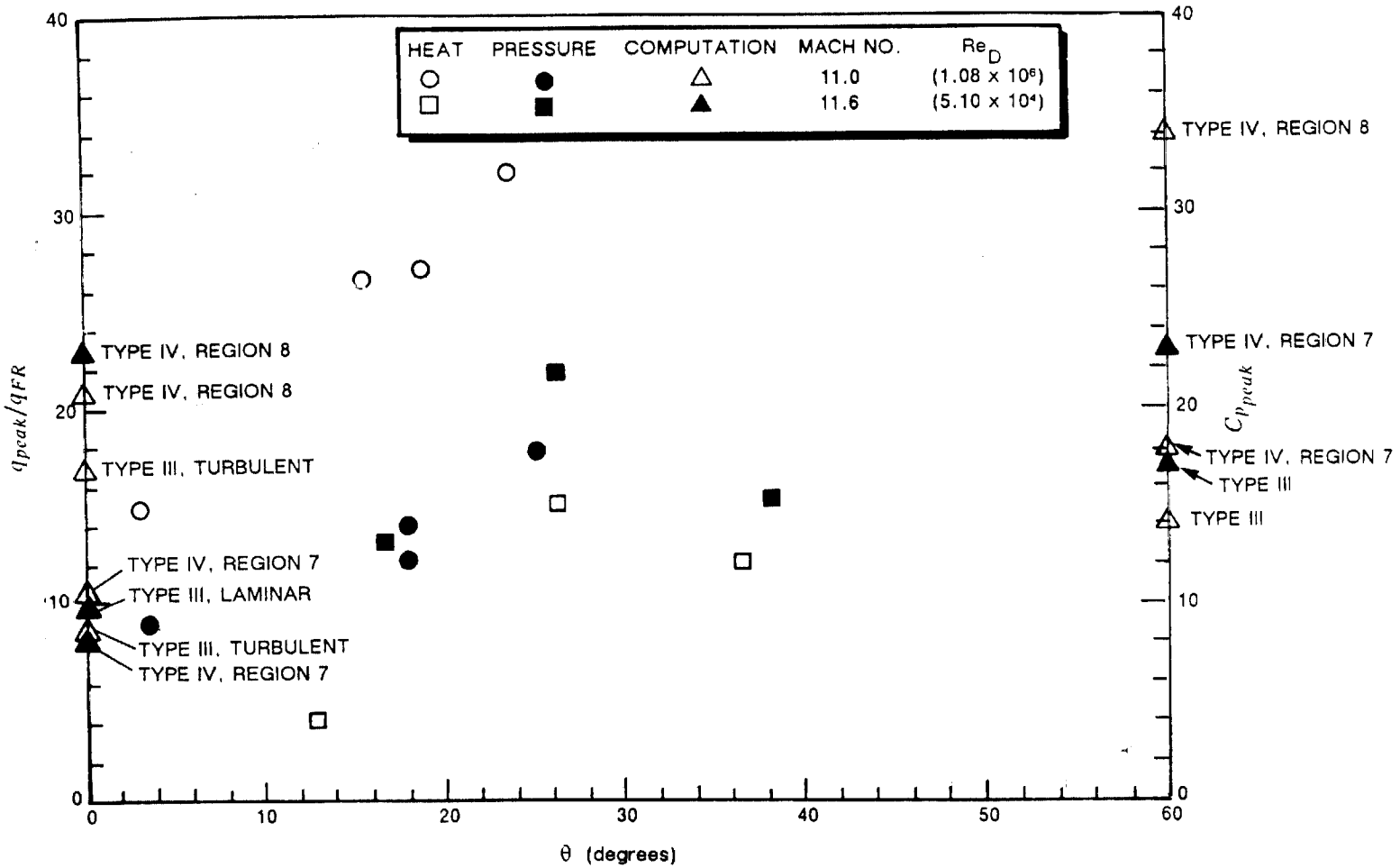

Figure 32b VARIATIONS OF PEAK HEATING AND PRESSURE WITH ANGULAR POSITION OF THE INTERACTION REGION FOR MACH 11.0 AND 11.6

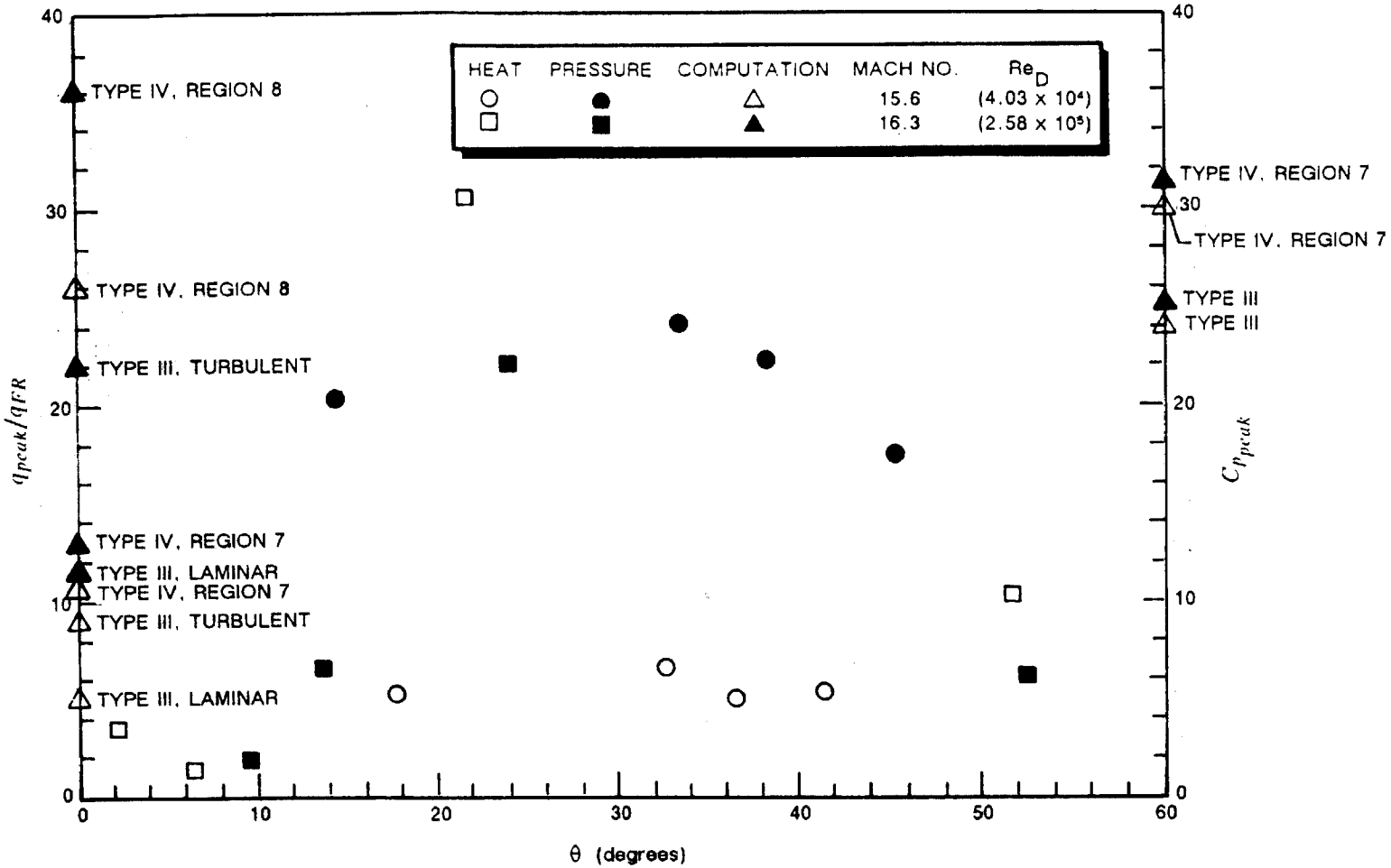

Figure 32c VARIATIONS OF PEAK HEATING AND PRESSURE WITH ANGULAR POSITION OF THE INTERACTION REGION FOR MACH 15.6 AND 16.3

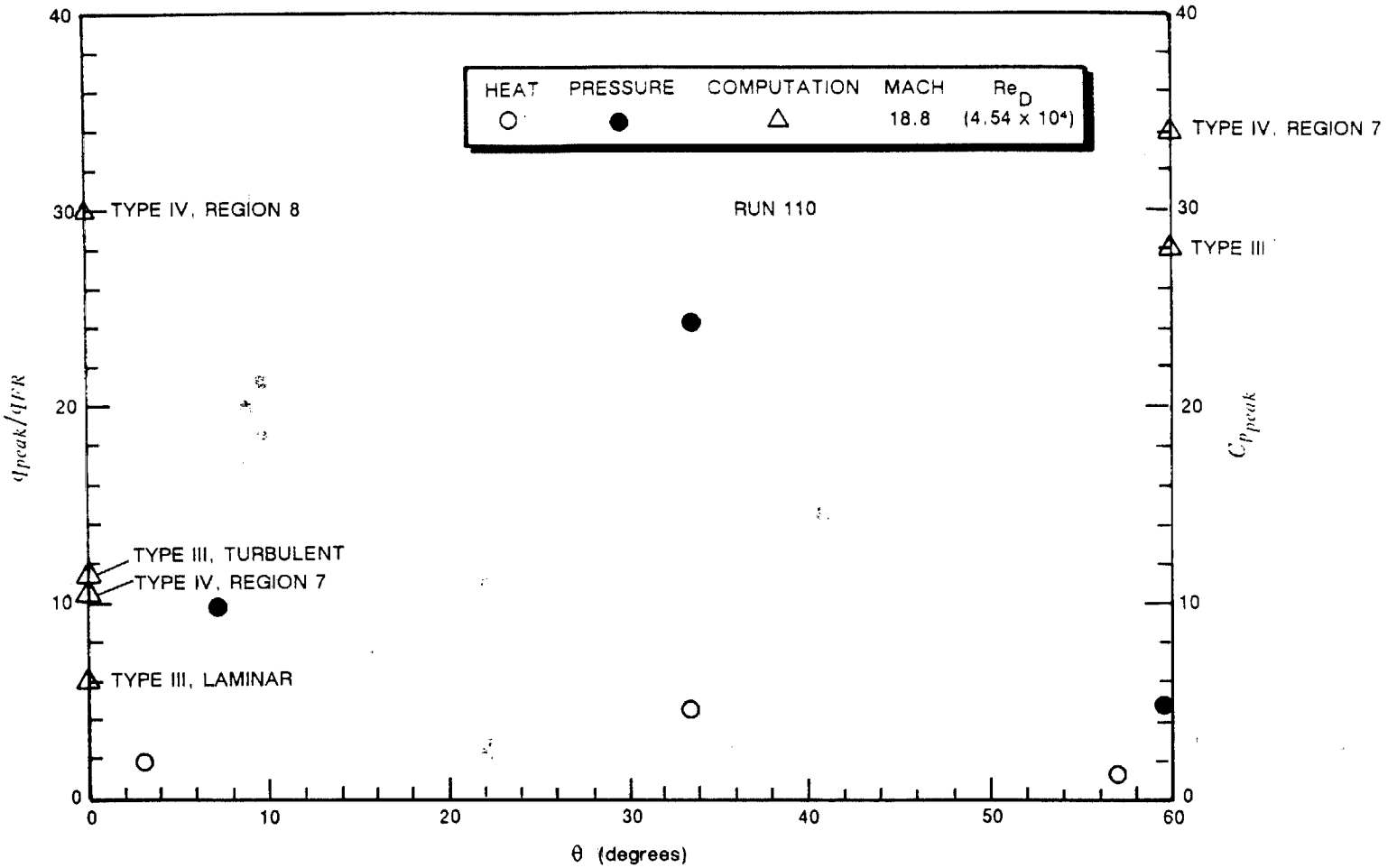

Figure 32d VARIATIONS OF PEAK HEATING AND PRESSURE WITH ANGULAR POSITION OF THE INTERACTION REGION FOR MACH 18.8

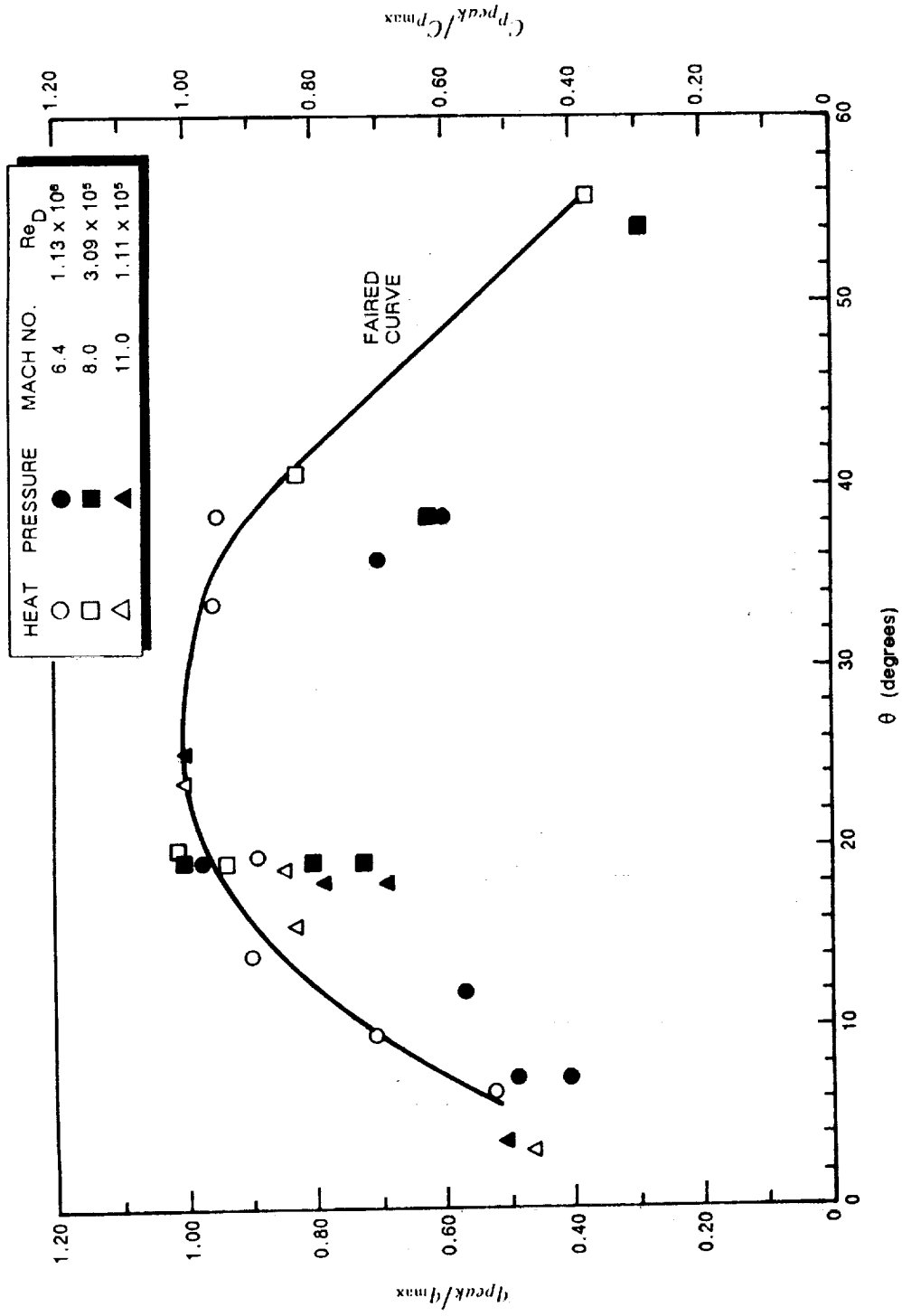

Figure 33a VARIATIONS OF PEAK HEATING AND PRESSURE RATIO WITH ANGULAR POSITION OF TURBULENT INTERACTION FOR MACH 6.4, 8.0, AND 11.0

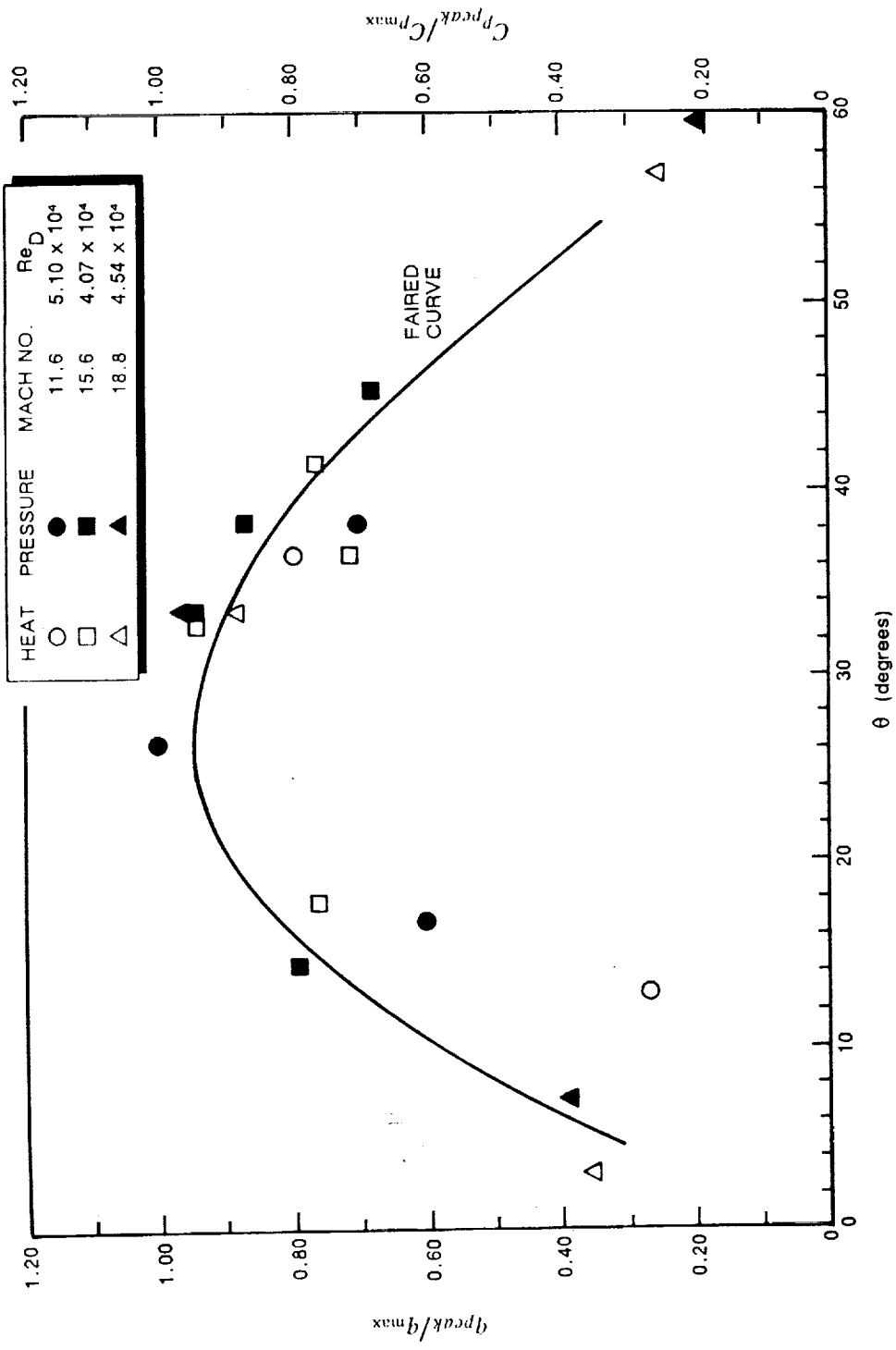

Figure 33b VARIATIONS OF PEAK HEATING AND PRESSURE RATIO WITH ANGULAR POSITION OF LAMINAR INTERACTION FOR MACH 11.6, 15.6, AND 18.8

heating with Mach number are shown in Figures 34a and 34b. We see that, for turbulent flows, the peak heating increases with increasing Mach number, although the measurements at Mach 16 are not significantly larger than those at Mach 11, possibly as a result of transitional effects. For the laminar interaction, the measurements at Mach 11, 16, and 19, all at a Reynolds number of approximately 5×10^4, show decreasing heating with increased Mach number. This may result from viscous effects influencing the recompression process, which otherwise would show an increased pressure recovery with increased freestream Mach number. In support of our contention that we had generated turbulent and transitional shear layers in our studies at Mach 6, 8, 11, and 16 conditions and laminar shear layers at some of the conditions at Mach 11, 16, and 18, we have plotted in Figure 35 the shear-layer Reynolds number in region 2 (Figure 2) for each of the test conditions at which the studies were conducted. Here we also show the free shear-layer transition boundaries from the Birch and Keyes[5] studies and transition measurements in separated shear layers from the experimental studies of Chapman, Kuehn, and Larson[54] and Crawford.[55] Our test conditions fall on each side of the transition boundaries suggested from these earlier studies. The strong influence of shear-layer condition on the heating augmentation in the Types III and IV interactions is shown in the correlation of peak heating versus peak pressure in Figure 36. Here, it can be seen that, while the measurements for the higher shear-layer Reynolds number conditions show enhancement heating factors of from 10 to 40, the laminar factors can be almost an order of magnitude less than these turbulent levels. As in the earlier correlations of the heating levels in the reattachment regions of separated flows (Reference 53), the heating levels in turbulent interaction regions correlate with a power-law relationship with an exponent of 0.85, while the laminar measurements correlate roughly with a 0.5 power exponent.

5.3.3 Comparison with Simple Prediction Techniques

Because of the intrinsically transitional nature of the shock/shock interaction at the lower Mach numbers, predicting the peak heating and pressures in these flows is a difficult task. Particularly for those flows involving shear-layer transition, we would not expect a Navier-Stokes solution employing current turbulence modeling techniques to perform significantly better than those based on simple semi-empirical models of the flow. The influence of the disturbances generated in the transitional/turbulent shear layer upstream of the jet for the type IV interaction on the heating in the stagnation region is not easily modeled. For laminar flows, the significant number of grids required in the shear region and in the stagnation and reattachment regions may also present significant problems for typical computational fluid dynamics (CFD) codes being developed.

To provide some insight into the fluid mechanics of these flows, we have compared our measurements with the Edney/Keyes and Hains models[2] embodied within the Morris and Keyes[21] code. The computations with the Morris and Keyes[21] method were performed for a number of representative cases at Mach numbers from 6 to 19 for both laminar and transitional interactions. The results of these computations are summarized in Table 4. The predicted peak heat transfer and pressure are compared with the measurements at Mach 6, 8, 11, 16, and 18 for the appropriate shear-layer conditions in Figures 32a through 32d. For the Mach 6 conditions, it can be seen that the measured pressure and heat transfer fall between a stagnation region in regions 7 and 8 (Figures 12a and 12c). While the predicted pressure levels for a type III interaction are in good agreement with experiment, the heating levels are underpredicted for a type IV interaction. A similar trend is observed at the turbulent Mach 8 and 11 conditions. For the latter conditions, we hypothesize that the boundary layers in the stagnation regions are influenced by the noise generated by the turbulent shear layers. At Mach 16, the predicted pressure levels for both the laminar

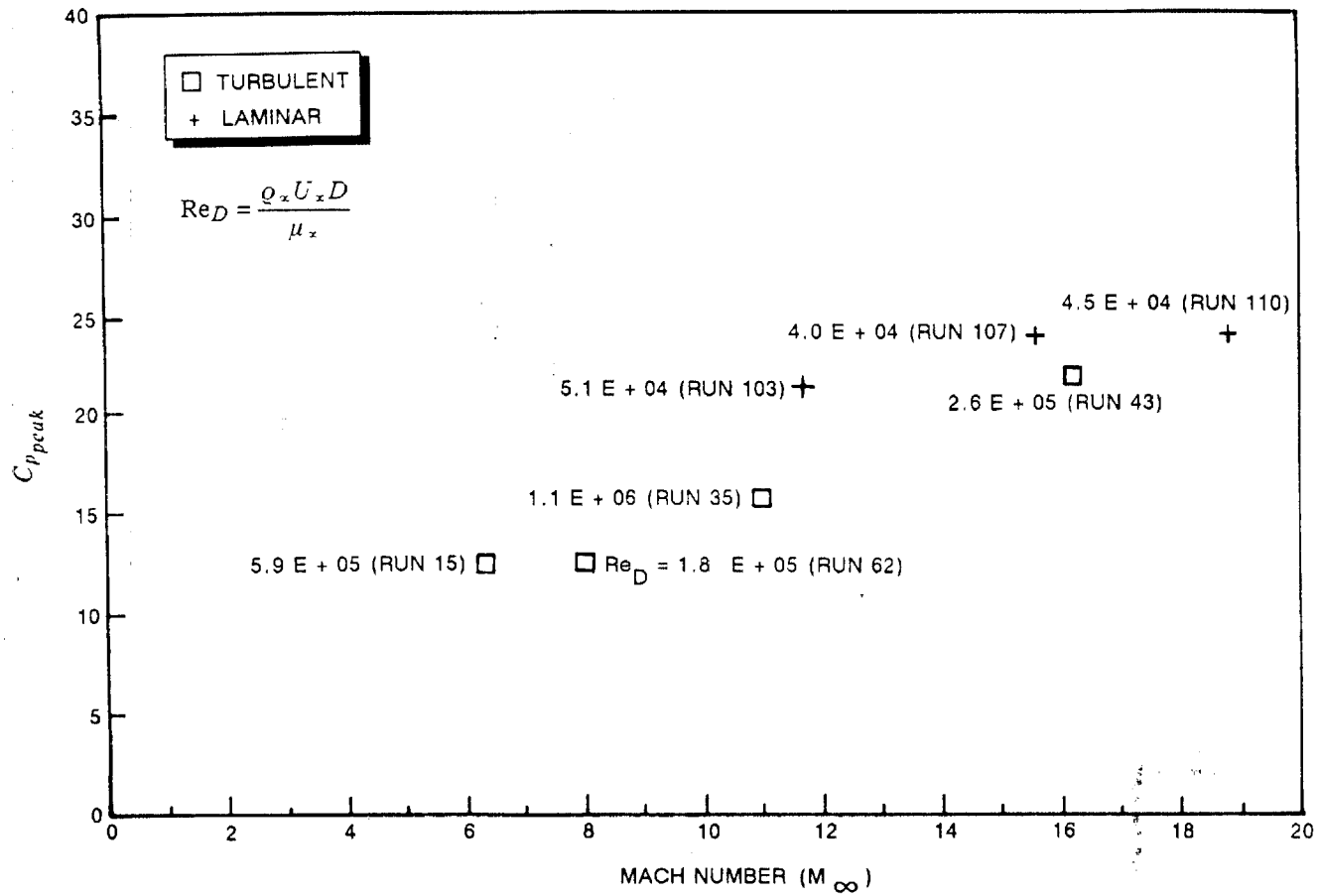

Figure 34a OBSERVED VARIATIONS OF PEAK PRESSURE WITH FREESTREAM MACH NUMBER FOR AN INTERACTION AT θ = 20° LOCATION

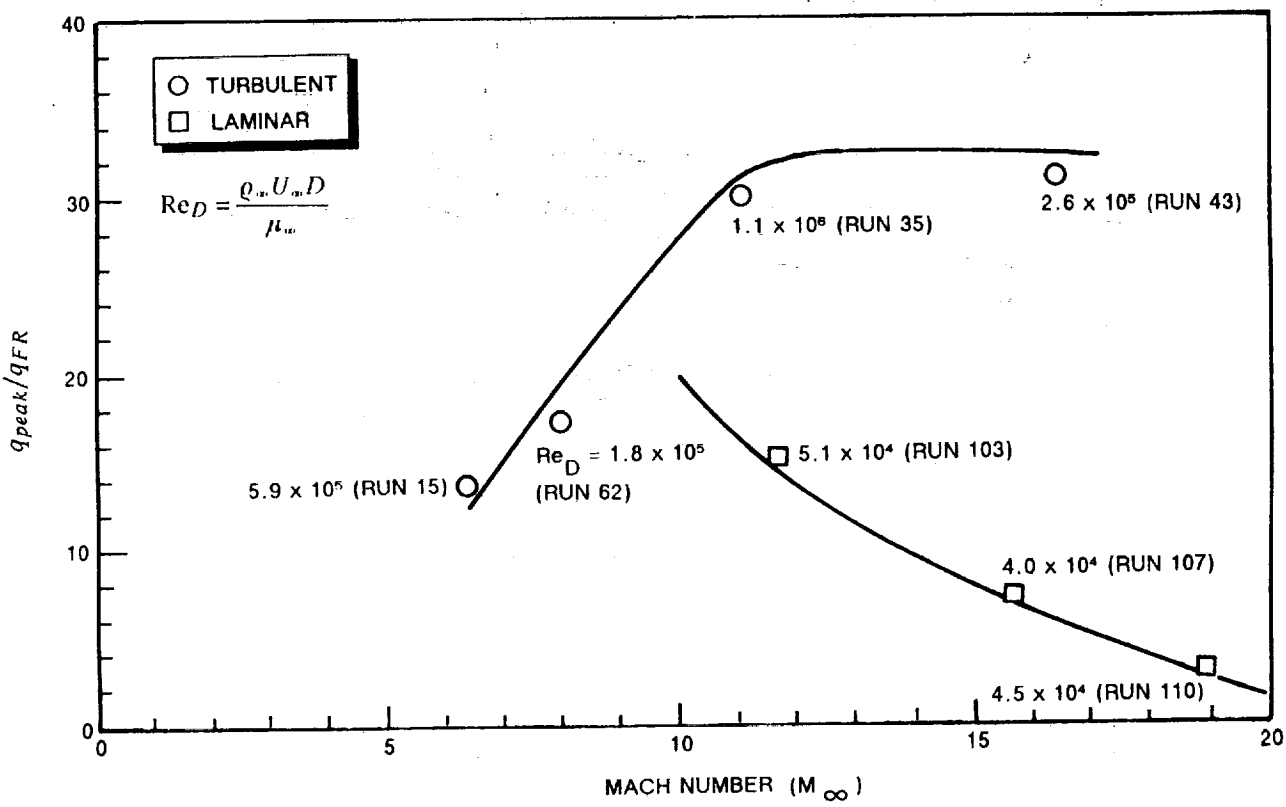

Figure 34b OBSERVED VARIATIONS OF PEAK HEATING WITH FREESTREAM MACH NUMBER FOR AN INTERACTION AT θ = 20° LOCATION

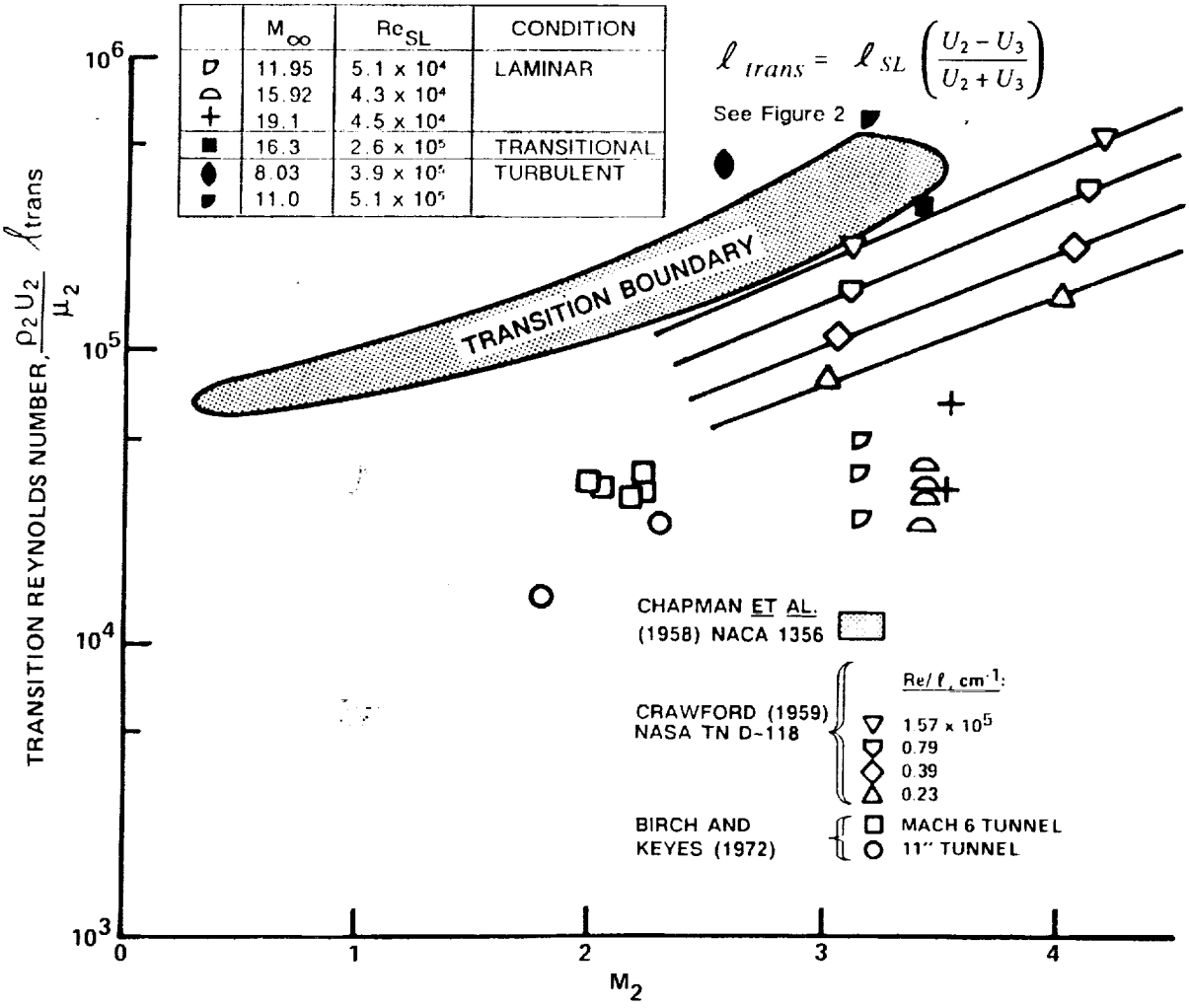

	M_∞	Re_{SL}	CONDITION
▷	11.95	5.1×10^4	LAMINAR
▷	15.92	4.3×10^4	
+	19.1	4.5×10^4	
■	16.3	2.6×10^5	TRANSITIONAL
⬮	8.03	3.9×10^5	TURBULENT
◤	11.0	5.1×10^5	

Figure 35 VARIATION OF TRANSITION REYNOLDS NUMBER WITH CONVECTIVE MACH NUMBER

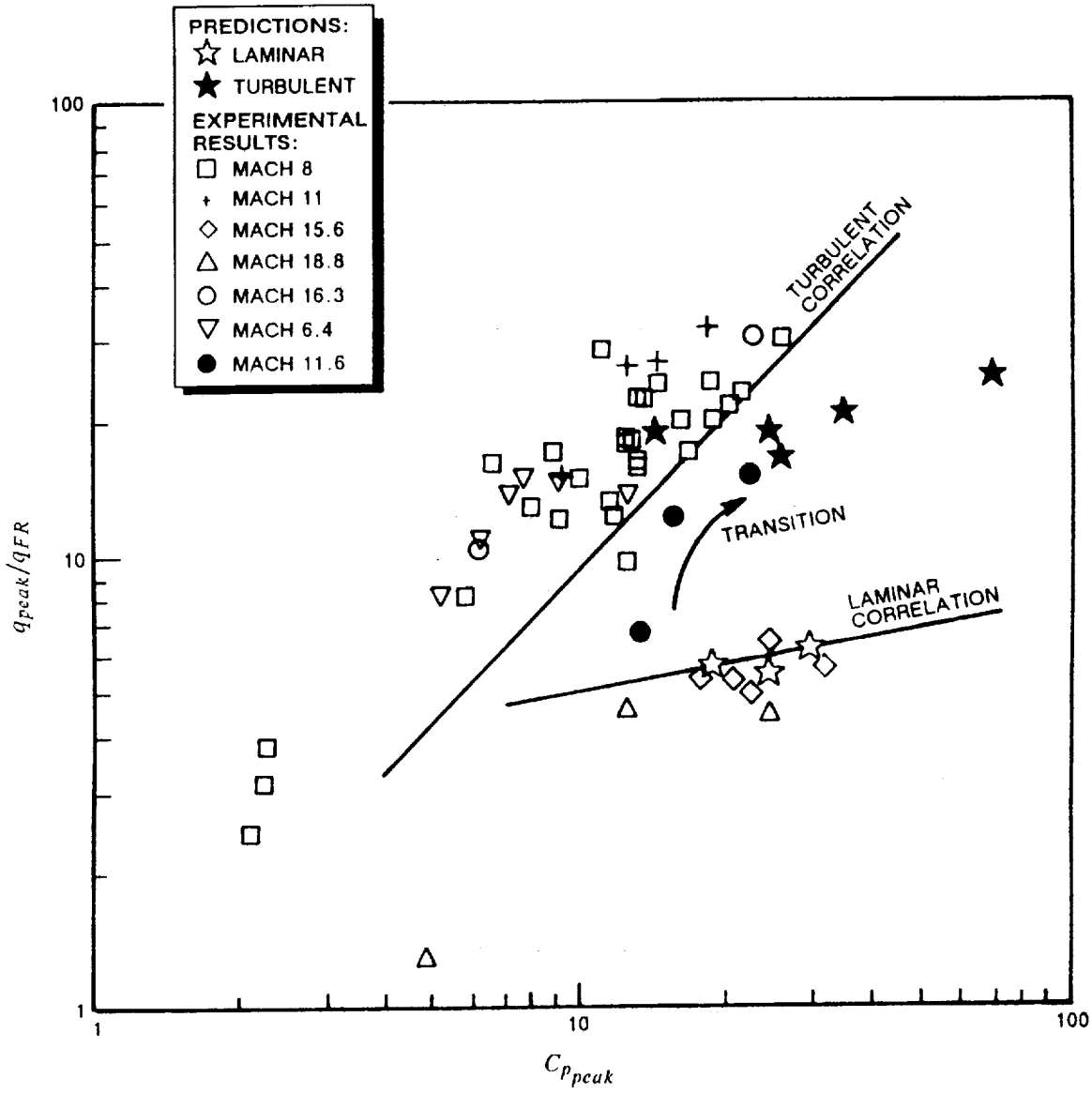

Figure 36 CORRELATION OF PEAK HEATING AND PRESSURE MEASUREMENTS AND COMPARISON WITH PREDICTIONS USING MORRIS AND KEYES COMPUTATIONAL MODEL (Table 4)

Table 4. PREDICTION OF PEAK HEATING RATES AND PRESSURES USING MORRIS AND KEYES COMPUTATIONAL MODEL

Run No.	M_∞	Re_D	Observed Peaks q/q_0	Observed Peaks $P/\bar{q}_\infty$	Observed Peaks θ[1]	$\bar{q}_\infty$ (psia)	q_{FR} (Btu/ft²-sec)[2]	M_{SL}	TYPE III Re_{SL}	TYPE III θ_5 (deg)[3]	TYPE III $P_5/\bar{q}_\infty$	TYPE III q_{max}/q_0 Lam.	TYPE III q_{max}/q_0 Tur.	TYPE IV Re_{SL}	TYPE IV $P/\bar{q}_\infty$ Reg.7[4]	TYPE IV $P/\bar{q}_\infty$ Reg.8[4]	TYPE IV q_{max}/q_0 Reg.7[4]	TYPE IV q_{max}/q_0 Reg.8[4]
10	6.4	1.11E+06	8.08	5.14	6.38	16.5500	48.773	2.17	1.694E+05	25.70	7.43	8.14	14.34	1.938E+05	11.00	15.00	11.16	19.49
11	6.4	1.09E+06	14.75	7.53	33.36	16.4240	49.157	2.17	5.224E+05	25.69	7.39	6.12	11.47	5.992E+05	11.03	15.05	6.31	11.02
12	6.3	1.07E+06	13.90	7.14	13.87	16.5490	50.440	2.17	1.944E+05	25.70	7.52	7.83	14.04	2.221E+05	11.07	15.09	10.34	18.05
13	6.4	1.11E+06	10.97	6.14	9.57	16.7420	49.668	2.17	1.985E+05	25.70	7.40	7.87	14.05	2.277E+05	11.03	15.05	10.34	18.06
14	6.4	1.17E+06	14.68	8.87	38.22	17.2260	49.035	2.17	5.782E+05	25.71	7.35	6.13	11.44	6.342E+05	10.97	14.97	6.18	10.80
15	6.3	5.92E+05	13.67	12.31	19.40	8.1155	31.301	2.17	1.074E+05	25.59	7.30	6.53	10.97	1.234E+05	10.95	14.89	10.13	17.65
21	8.0	3.91E+05	24.35	14.20	17.69	5.7649	40.240	2.65	1.798E+05	31.25	12.18	7.85	14.58	2.000E+05	16.68	27.76	9.06	19.25
22	8.0	1.91E+05	17.87	12.46	15.78	2.8467	28.077	2.63	9.495E+04	31.09	12.09	6.48	11.67	1.059E+05	16.70	27.63	8.77	18.55
26	8.0	3.71E+05	8.00	5.78	55.68	5.6557	41.107	2.65	4.685E+05	31.24	12.24	6.11	12.05	5.215E+05	16.83	28.00	5.52	11.74
34	11.0	1.11E+06	27.08	13.96	18.72	8.3215	43.835	3.04	3.699E+05	34.30	13.77	9.87	17.56	4.019E+05	18.38	34.27	9.58	21.90
35	11.0	1.13E+06	31.95	17.77	23.50	8.4709	44.232	3.04	7.135E+05	34.30	13.70	8.45	15.54	7.758E+05	18.35	34.23	6.95	15.89
36	11.0	1.08E+06	26.59	12.12	15.55	8.1888	43.925	3.04	3.903E+05	34.30	13.84	9.67	17.30	4.240E+05	18.46	34.41	9.25	21.14
37	11.0	1.05E+06	14.86	9.03	3.13	8.1453	44.589	3.04	3.828E+05	34.30	13.93	9.68	17.40	4.159E+05	18.56	34.59	9.28	21.22
42	16.3	2.58E+05	3.50	6.86	2.18	2.2592	48.181	3.58	8.308E+04	37.19	24.66	10.86	22.12	8.877E+04	31.06	69.16	13.29	36.33
43	16.3	2.60E+05	30.56	22.17	21.51	2.2219	46.991	3.58	1.489E+05	37.19	24.43	9.32	19.43	1.592E+05	30.83	68.70	9.87	26.99
44	16.3	2.36E+05	10.36	6.09	51.74	2.1617	48.706	3.58	2.535E+05	20.75X	9.99	4.87	11.40	3.087E+05	31.82	70.80	7.02	19.17
59	8.0	3.58E+05	21.46	19.74	19.10	5.3608	39.332	2.65	1.756E+05	31.25	12.22	7.63	14.23	1.954E+05	16.77	27.90	8.83	18.76
60	8.0	3.62E+05	20.11	15.74	19.10	5.3070	38.463	2.65	1.609E+05	31.25	12.13	7.78	14.36	1.792E+05	16.70	27.79	9.21	19.58
61	8.0	3.64E+05	17.61	12.26	40.62	5.3068	38.342	2.65	3.124E+05	31.25	12.05	6.61	12.62	3.485E+05	16.70	27.82	6.62	14.09
62	8.0	1.83E+05	16.42	12.95	34.38	2.2920	22.019	2.65	1.210E+05	31.25	11.86	5.68	9.90	1.349E+05	16.41	27.32	7.34	15.62
103	11.6	5.10E+04	15.18	21.77	26.24	0.4158	11.509	3.12	2.368E+04	34.84	17.63	5.42	8.89	2.560E+04	23.11	44.30	10.15	23.80
104	11.6	4.34E+04	12.05	15.28	36.49	0.3979	12.300	3.11	2.941E+04	34.77	17.85	4.96	8.50	3.186E+04	23.60	45.08	8.69	20.30
106	15.6	4.07E+04	5.28	17.39	41.37	0.2327	10.297	3.53	2.399E+04	32.25X	17.32	5.00	8.90	2.682E+04	29.60	64.83	9.31	25.02
107	15.6	4.03E+04	6.55	24.10	33.43	0.2307	10.248	3.53	2.057E+04	36.95	23.36	5.60	9.41	2.201E+04	29.59	64.78	10.23	27.48
109	18.9	4.84E+04	1.80	9.85	3.06	0.2613	14.038	3.74	1.603E+04	37.85	28.05	7.09	12.62	1.705E+04	34.68	81.25	13.14	37.81
110	18.8	4.54E+04	4.44	24.21	33.43	0.2624	14.788	3.74	2.471E+04	37.85	28.80	6.38	11.81	2.629E+04	35.47	83.01	10.55	30.34
113	11.6	4.92E+04	4.07	13.14	12.91	0.4193	12.014	3.12	2.030E+04	34.84	17.80	5.64	9.32	2.196E+04	23.36	44.78	10.93	25.62
115	15.7	4.31E+04	5.27	20.24	17.69	0.2295	9.691	3.51	2.443E+04	36.91	22.93	5.33	8.85	2.623E+04	28.41	64.02	9.01	25.42

NOTES:
[1]Angular location on the cylindrical model. (See Figure 23.)
[2]Refer to Equation 5.1 .
[3]"X" appended to the value of θ_5 indicates that a specified shear-layer angle was used instead of the calculated maximum.
[4]Regions (Reg.'s) refer to Figure 3.

and turbulent conditions in zone 8 are significantly larger than those observed from experiment. For a turbulent condition, the experiment is more in line with the heating rates determined from the Keyes and Hains model. Again, in order for the heating rates to be consistent for such a flow configuration, a heating enhancement in the stagnation region is required. At Mach 18, the flows are fully laminar, and the calculated heat transfer and pressure are in reasonable agreement with the measurements for a type III interaction.

Based on correlations of the peak heating measurements with the position of the interaction shown in Figures 32a to 32d, we have determined that the experimental peak pressures for interactions usually occurred at a location 20 degrees below the horizontal axis. These measurements are compared with the code prediction for Mach numbers from 6 to 16 in Figures 37a and 37b. It can be seen that, at the lower Mach number and higher Reynolds number conditions, where the flows are fully turbulent, the measured pressure levels fall between the predicted pressure levels of regions 7 and 8 (Figure 3). However, at the higher Mach numbers, we observe that the measured peak pressures fall well below the prediced pressure level of region 8, at values closer to those in regions 5 and 6 (Figure 3). Thus, under these conditions, it is possible that the viscous shear layers that precede and surround the jet significantly modify its structure and, therefore, the recompression process occurring within the shear layer. In contrast, the measured heat transfer rates in the type IV turbulent interactions at the lower Mach number conditions can exceed the predicted laminar stagnation heat transfer rates, as shown in Figure 37b. As mentioned earlier, we suggest that the larger heating rates result from the strong influence of turbulence in the shear layers, increasing noise level and hence the mixing in the stagnation region. For fully laminar flows at the higher Mach numbers, the heating for the type IV interaction is consistent with a stagnation region between regions 6 and 7 (Figure 3), while the type III predictions are in reasonable agreement with the measurements. Finally, we have plotted the heat transfer and pressure ratios in Figure 36 in the logarithmic format used to examine the power-law relationship in the experimental data. Here, selecting the measurements to be consistent with the earlier observations, we see that predictions are in reasonable agreement with the 0.5 and 0.85 power-law relationships for laminar and turbulent interaction regions, respectively.

5.4 STUDIES OF MULTIPLE-SHOCK/SHOCK INTERACTION

The severity of the aerothermal loads induced by shock/shock interaction has led to speculation on techniques that can be used to reduce loads for configurations such as inlets, where the compression must be captured. Preventing the formation of a single bounding shock and allowing multiple shock impingement on the inlet lip may significantly reduce the peak heating and pressure loads. Here, we briefly discuss the results of a preliminary study to examine such an approach.

We selected two configurations that generated total flow turning angles of 12.5 and 13.5 degrees in 7.5/5.0-degree and 7.5/6.0-degree dual-shock-generation configurations. These configurations were selected to match the interaction strengths developed in the earlier studies. We examined configurations where the two shocks coalesced ahead of the bow shock and where the shocks impinged on either side of the stagnation line. All of the measurements were made at Mach 8 and at a unit Reynolds number of about $1.5 \times 10.^6$ Test conditions, heat transfer and pressure measurements, plots of these quantities, and Schlieren photographs for each test condition are provided in Appendix C.

The pressure and heat transfer distributions for the 7.5/5.0-degree shock-generator studies are shown in Figures 38a through 38e. Starting with the flow configuration where the incident shocks combine ahead of the bow shock (Figure 38a) and translating the shocks relative to the cylinder and to each other, we

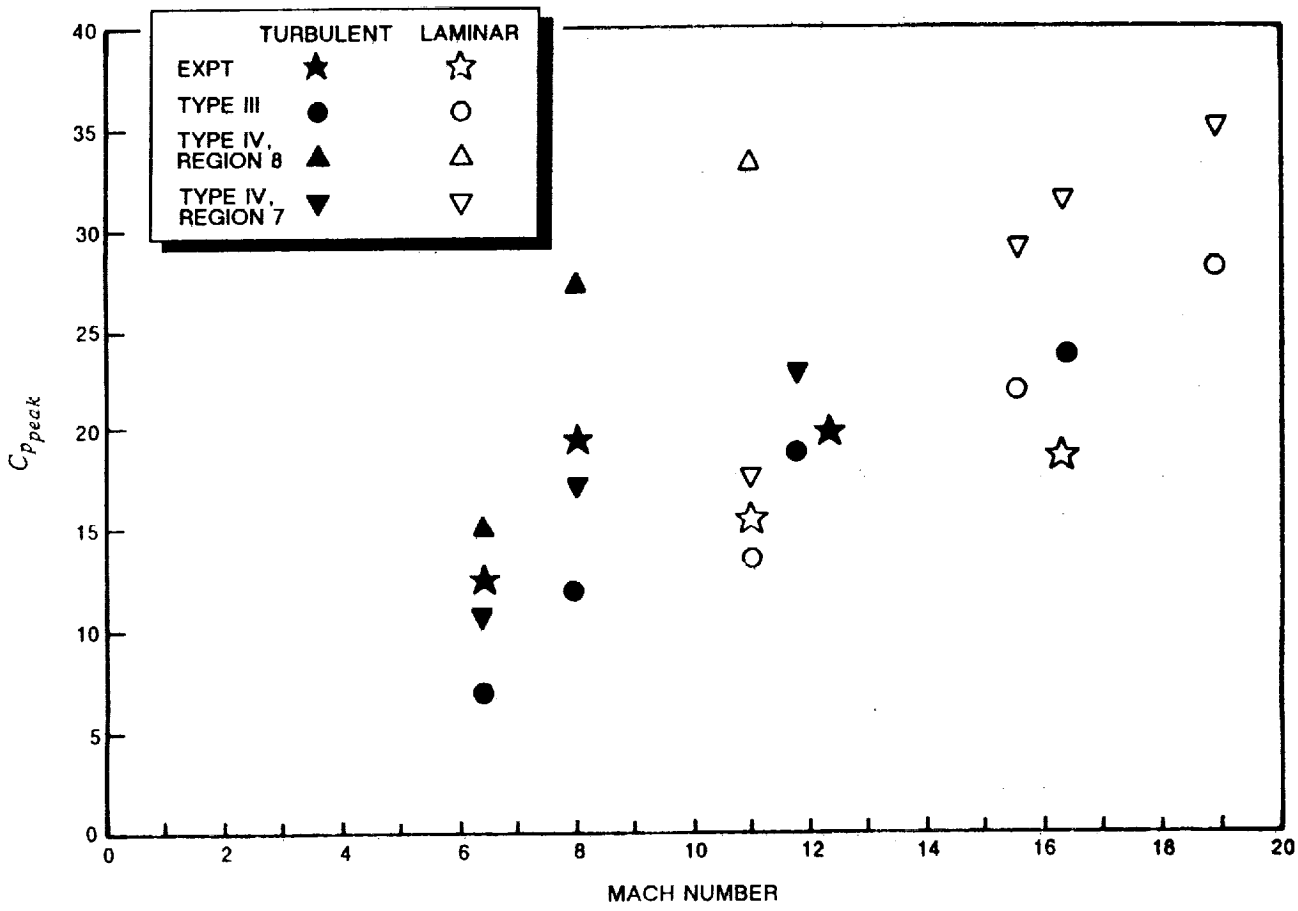

Figure 37a VARIATION OF PEAK PRESSURE WITH FREESTREAM MACH NUMBERS FOR AN INTERACTION AT θ = 20° LOCATION

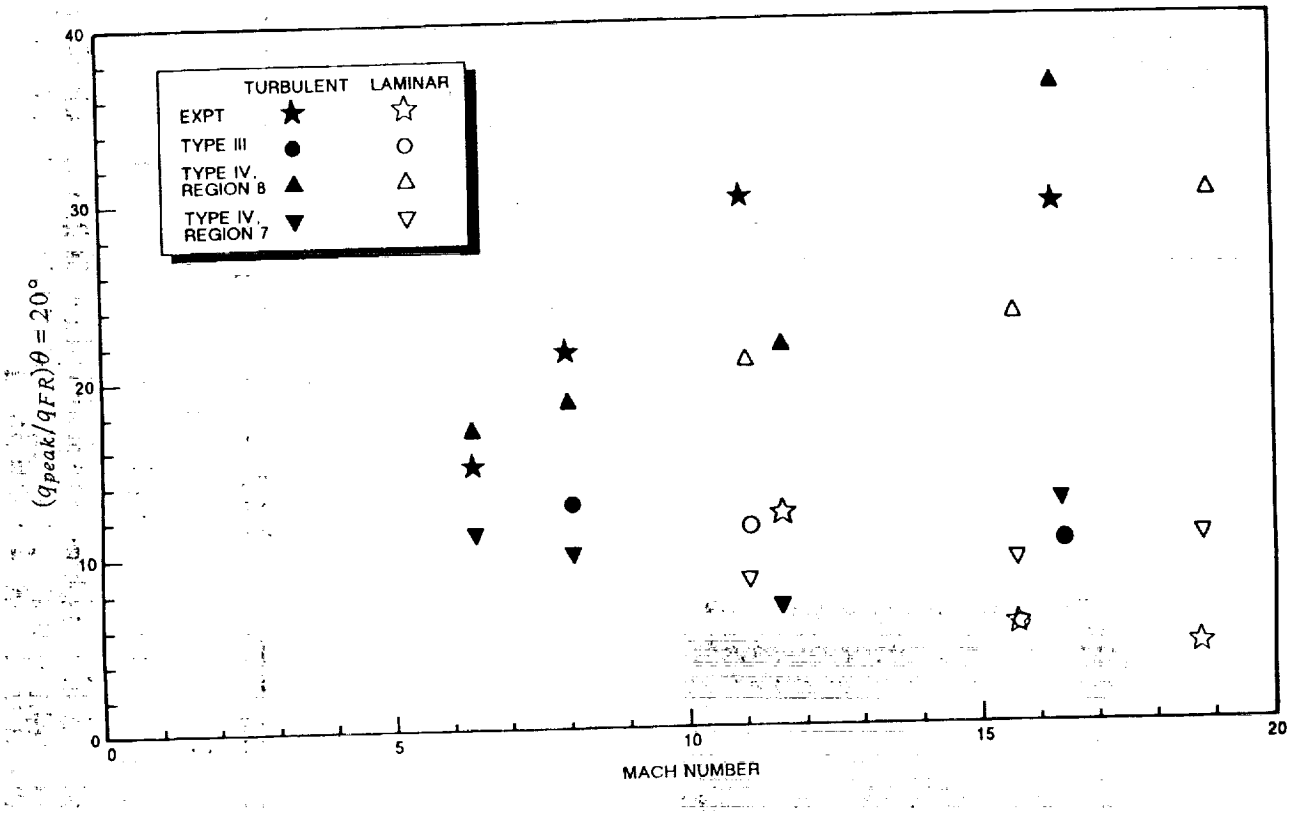

Figure 37b VARIATION OF PEAK HEATING WITH FREESTREAM MACH NUMBERS FOR AN INTERACTION AT θ = 20° LOCATION

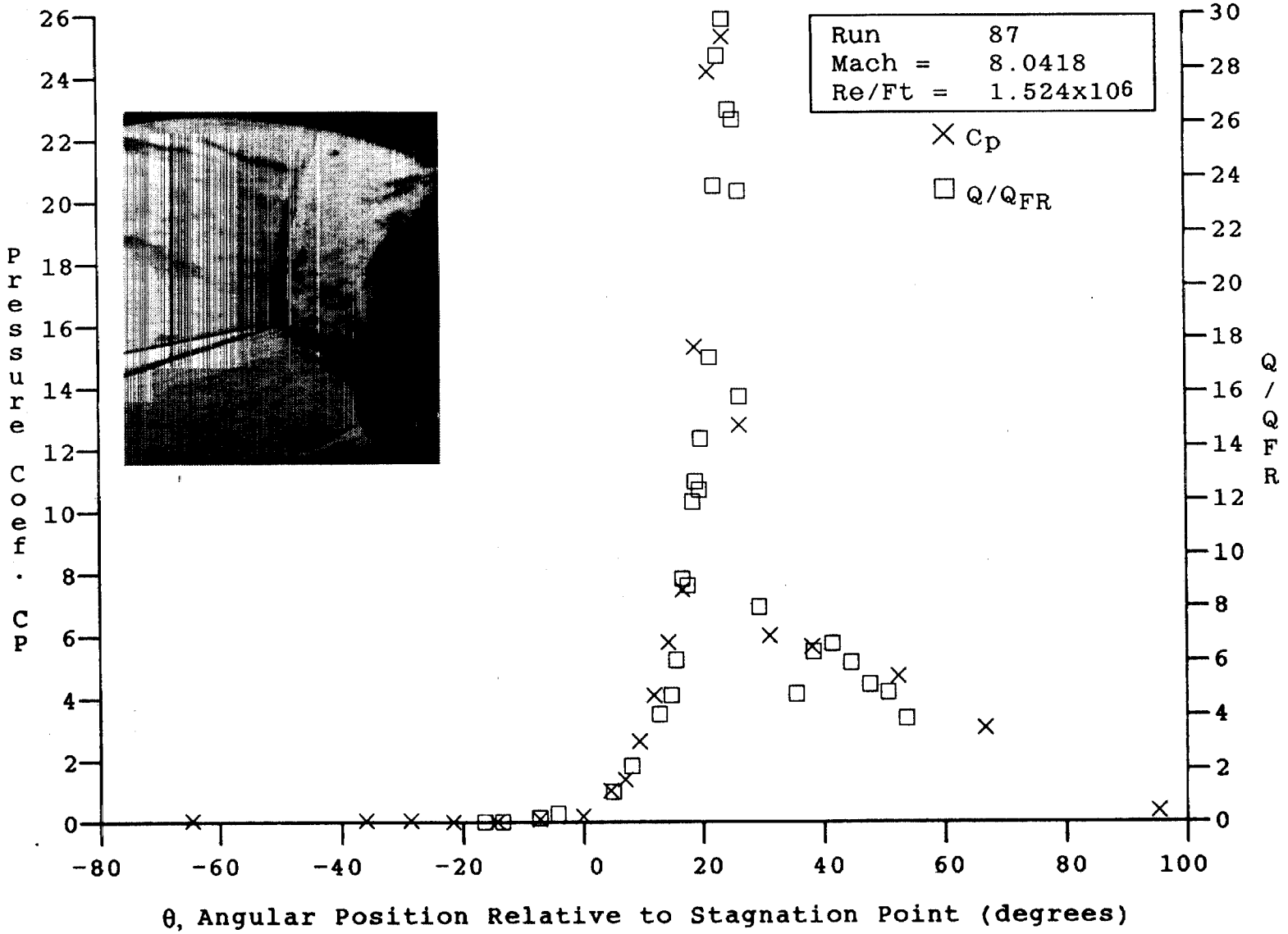

Figure 38a HEAT AND PRESSURE DISTRIBUTIONS IN MULTIPLE-SHOCK-INTERACTION REGIONS INDUCED BY A 7.5/5° SHOCK GENERATOR OVER A 3-INCH-DIAMETER CYLINDER AT MACH 8 FOR RUN 87

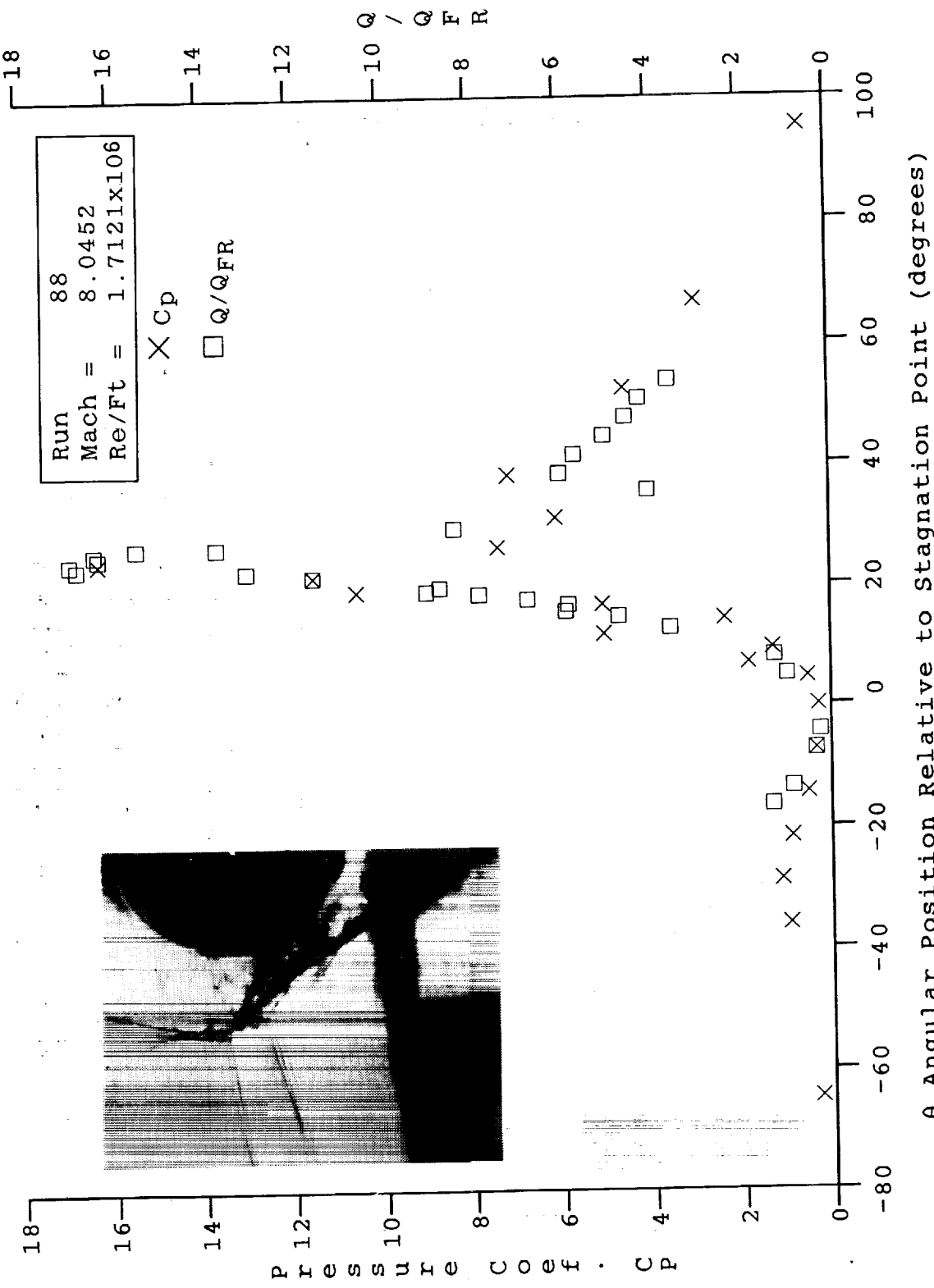

Figure 38b HEAT AND PRESSURE DISTRIBUTIONS IN MULTIPLE-SHOCK-INTERACTION REGIONS INDUCED BY A 7.5/5° SHOCK GENERATOR OVER A 3-INCH-DIAMETER CYLINDER AT MACH 8 FOR RUN 88

C-2

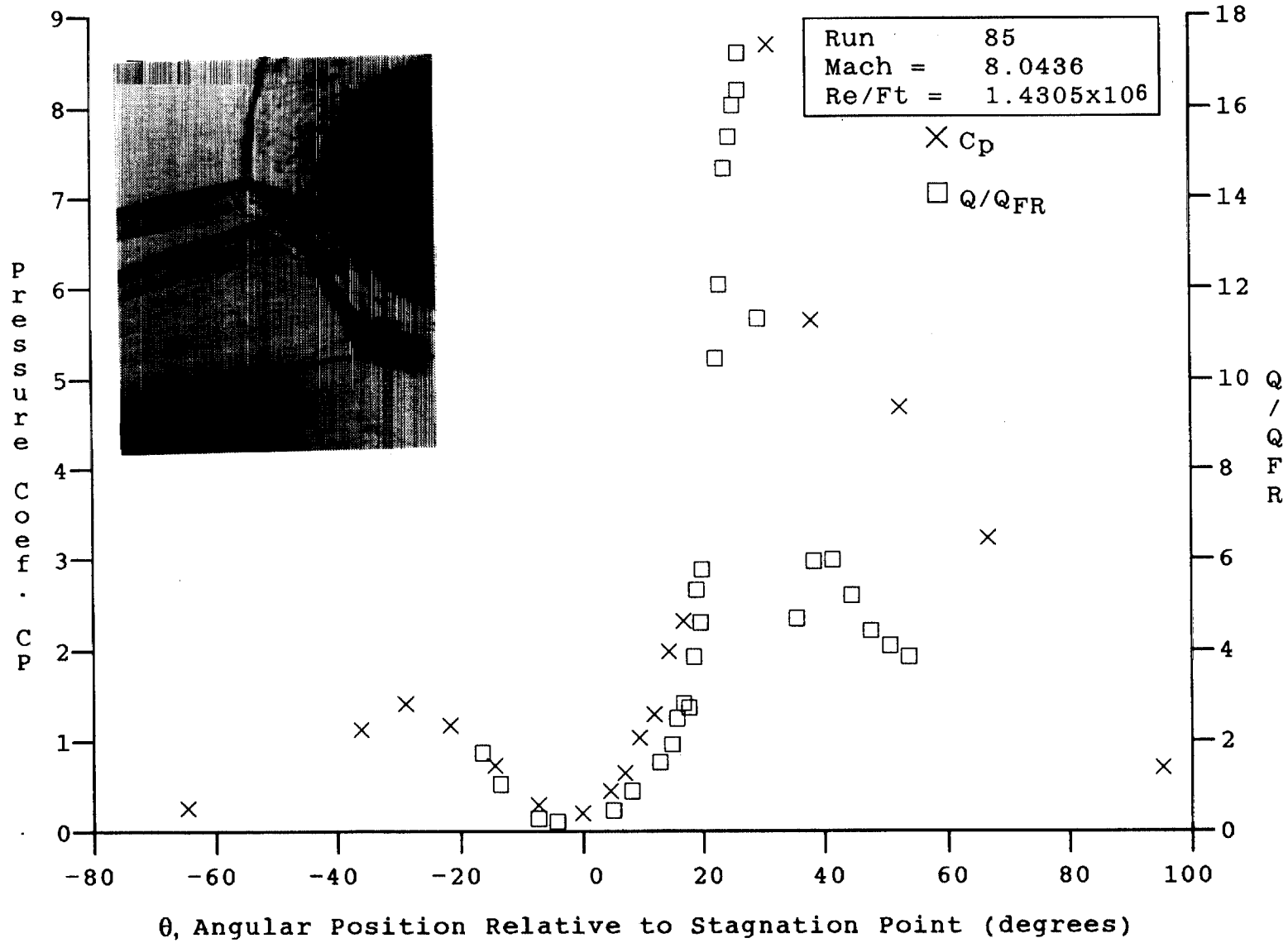

Figure 38c HEAT AND PRESSURE DISTRIBUTIONS IN MULTIPLE-SHOCK-INTERACTION REGIONS INDUCED BY A 7.5/5° SHOCK GENERATOR OVER A 3-INCH-DIAMETER CYLINDER AT MACH 8 FOR RUN 85

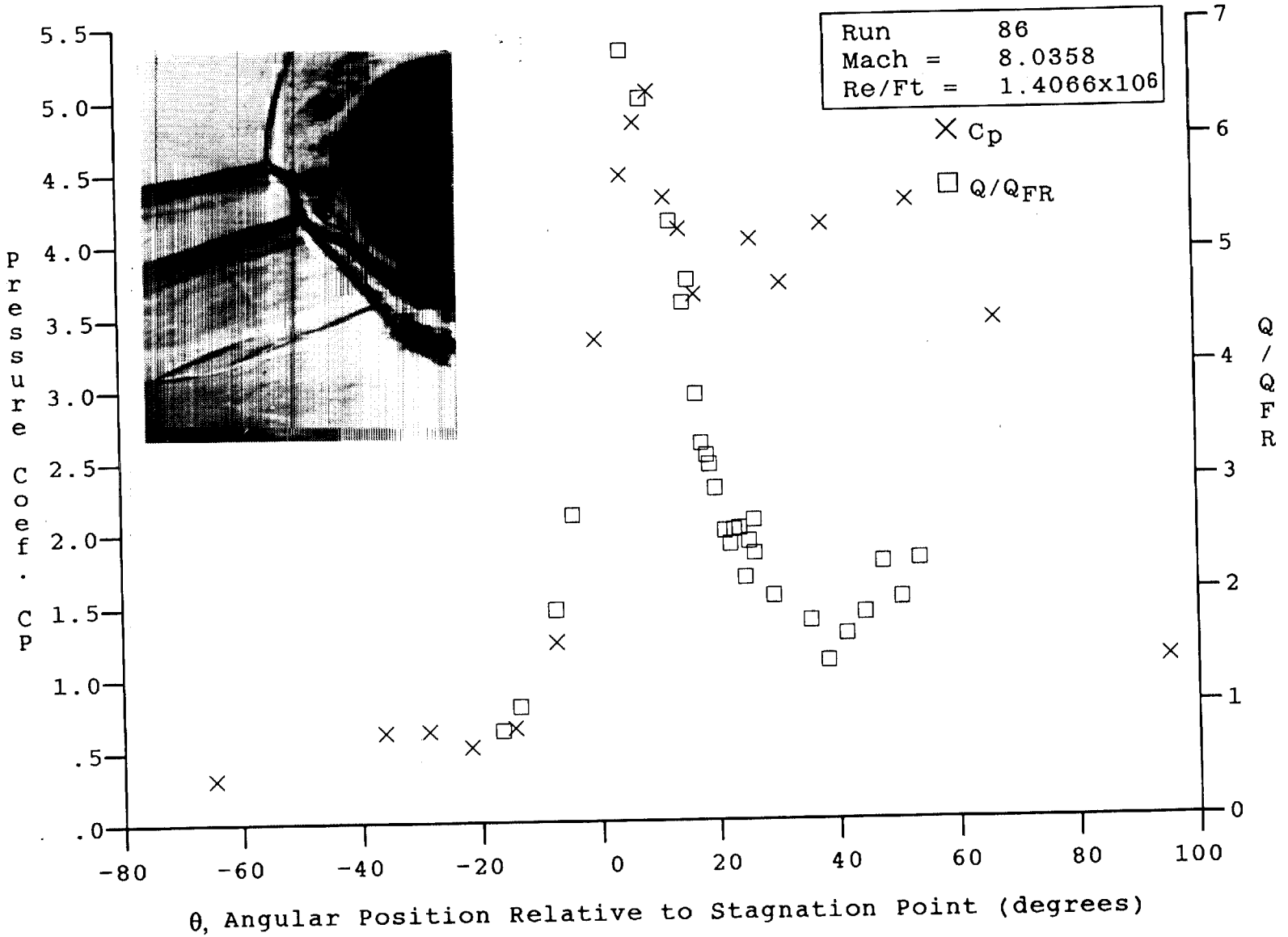

Figure 38d HEAT AND PRESSURE DISTRIBUTIONS IN MULTIPLE-SHOCK-INTERACTION REGIONS INDUCED BY A 7.5/5° SHOCK GENERATOR OVER A 3-INCH-DIAMETER CYLINDER AT MACH 8 FOR RUN 86

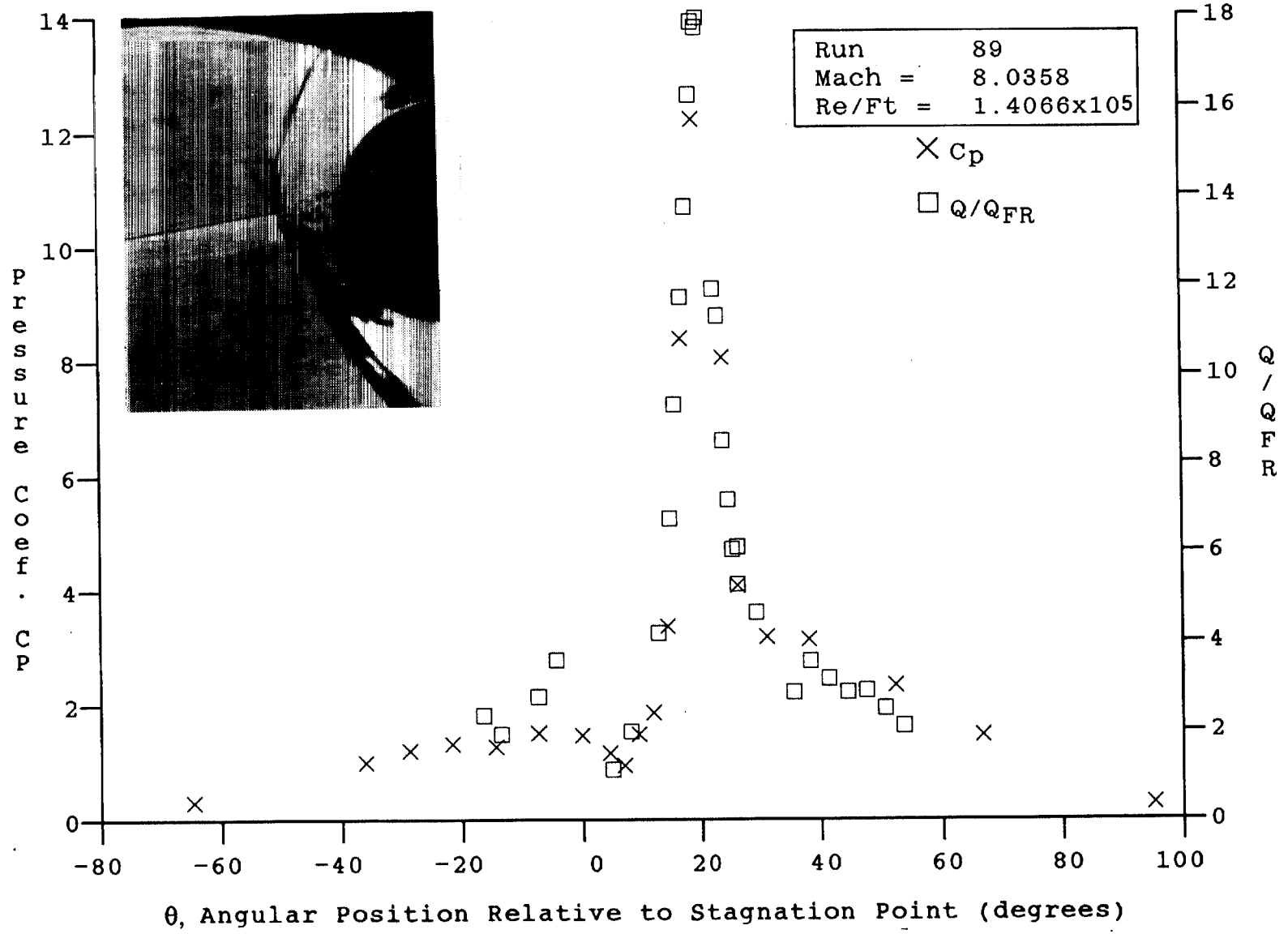

Figure 38e HEAT AND PRESSURE DISTRIBUTIONS IN MULTIPLE-SHOCK-INTERACTION REGIONS INDUCED BY A 7.5/5° SHOCK GENERATOR OVER A 3-INCH-DIAMETER CYLINDER AT MACH 8 FOR RUN 89

observe the following results. First, the peak heating loads are significantly reduced by allowing multiple impingements. Spreading the shocks about the stagnation line results in the greatest reduction in pressure recovery and heating rate, as shown in Figure 38b. Even very small relative displacements, as shown in Figures 38c and 38d, can cause significant heat-loading reductions. The flow configuration in Figure 38d is of particular interest, because of the jet and the shear layer formed in this flow. For completeness, we also show the measurements for the 7.5-degree shock-generator configuration in Figure 38e. A similar flow of interest is shown in Figures 39a through 39e from the 7.5/6.0-degree shock-generator studies. However, enhancement in heat transfer is observed when the shock coalesces ahead of the bow shock. Note that, in this series, separating the shocks does not cause as great a reduction in heating as observed in the 7.5/5.0-degree shock-generator configuration.

5.5 PRELIMINARY STUDIES OF SWEEP EFFECTS ON REGIONS OF SHOCK/SHOCK INTERACTION

5.5.1 Introduction

Regions of shock/shock interaction are seldom two-dimensional in most situations. Therefore, a knowledge of the effects of crossflow is important. One controlled way of studying this effect is to sweep the interaction region, creating a quasi-two-dimensional flow. Practically, this can create problems with end effects and introduce an additional fundamental phenomenon—attachment-line transition. At large Reynolds numbers, the absence of an incident shock sweeping the cylinder introduces a crossflow instability at the attachment line that, if large enough, can result in transition and turbulent heating along the attachment line. With a shock incident on the swept cylinder, we, therefore, have the potentially interesting situation of a shear layer or jet incident on a turbulent attachment line. Thus, the results of these studies must be carefully interpreted to distinguish between sweep and transition effects.

5.5.2 Experimental Studies

This was an intrinsically difficult experiment to conduct, because we were attempting to place the incident shock at the same radial station as the bow shock along the entire length of the cylinder. To achieve this flow configuration, we designed and fabricated inserts that rolled and yawed the shock generator to place its leading edge in the same plane as the stagnation line of the cylinder. Because we have only one Schlieren window station (set), we were unable to align the optics with the axis of the swept cylinder. Therefore, Schlieren photographs, as illustrated by Figure 40, do not provide definitive information on the structure of the flowfield in this situation.

Measurements of heat transfer and pressure around the cylinder were made for sweep angles of 15 and 30 degrees, with a shock-generator angle of 12.5 degrees in the pitch plane. At each sweep angle, the position of the incident shock was varied to search for the maximum heating rates generated by the types III and IV interaction regions. The measurements made in this segment of the program are plotted and tabulated in Appendix D.

5.5.3 Discussion of Measurements

During this segment of the program, 15 test runs were devoted to the preliminary study of sweep effects on shock/shock interaction. The measurements made in these runs (66 through 81 and 98) are presented in Appendix D. All studies were conducted at Mach 8 and a unit Reynolds number of 1.5×10^6 /ft with a shock-generator angle of 12.5 degrees, and cylinder sweep angles of 0, 15, and 30 degrees

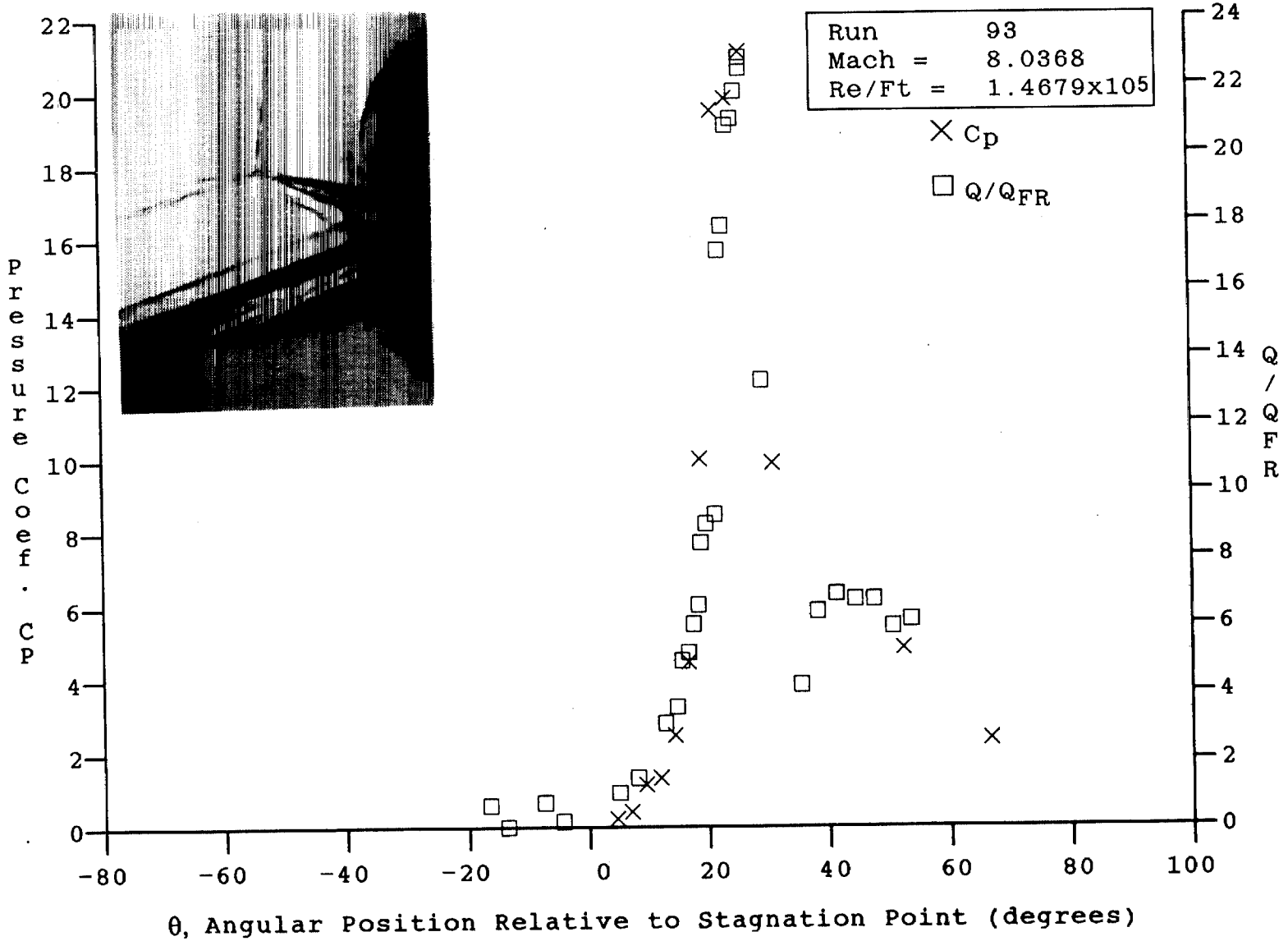

Figure 39a HEAT AND PRESSURE DISTRIBUTIONS IN MULTIPLE-SHOCK-INTERACTION REGIONS INDUCED BY A 7.5/6° SHOCK GENERATOR OVER A 3-INCH-DIAMETER CYLINDER AT MACH 8 FOR RUN 93

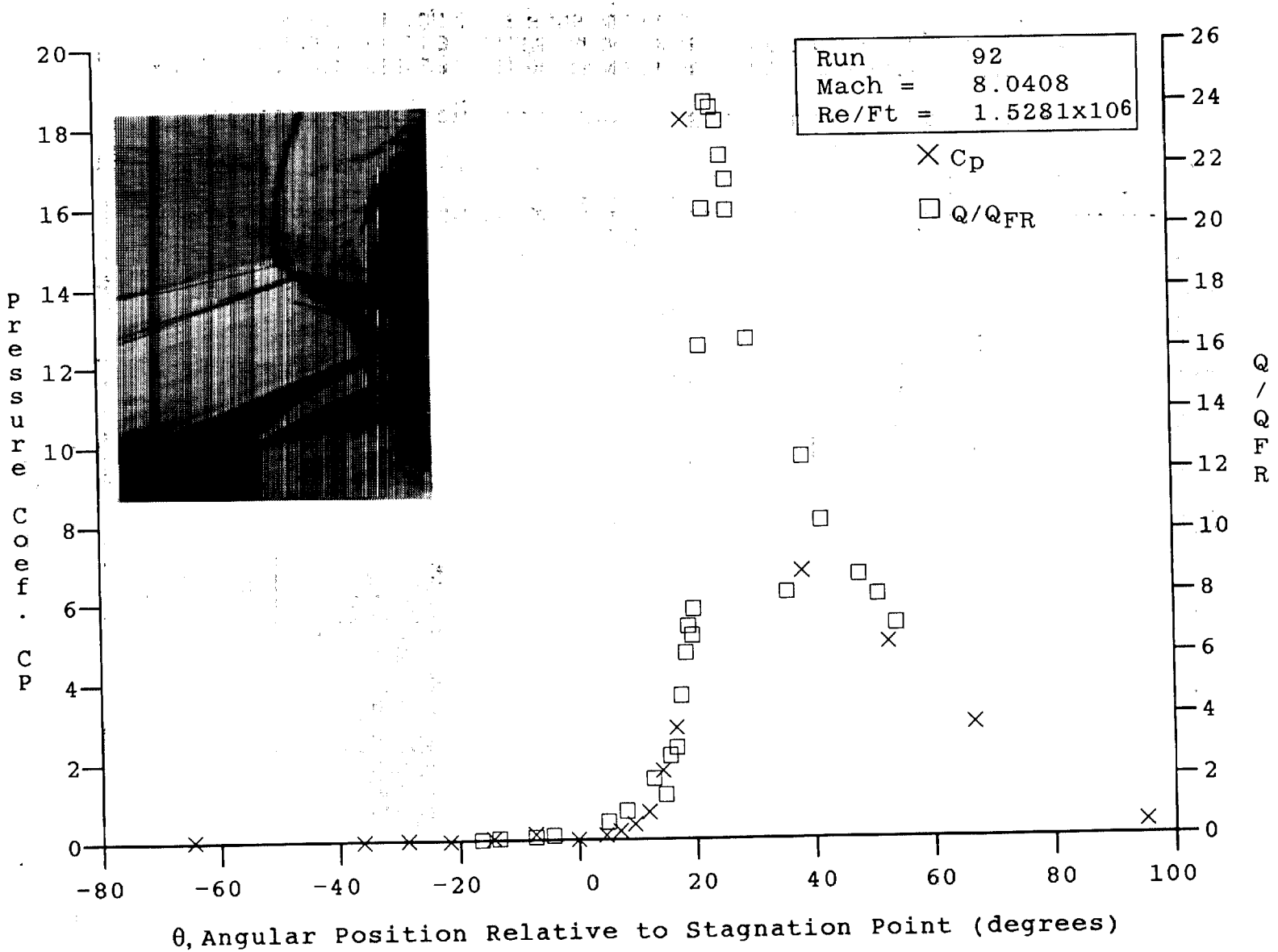

Figure 39b HEAT AND PRESSURE DISTRIBUTIONS IN MULTIPLE-SHOCK-INTERACTION REGIONS INDUCED BY A 7.5/6° SHOCK GENERATOR OVER A 3-INCH-DIAMETER CYLINDER AT MACH 8 FOR RUN 92

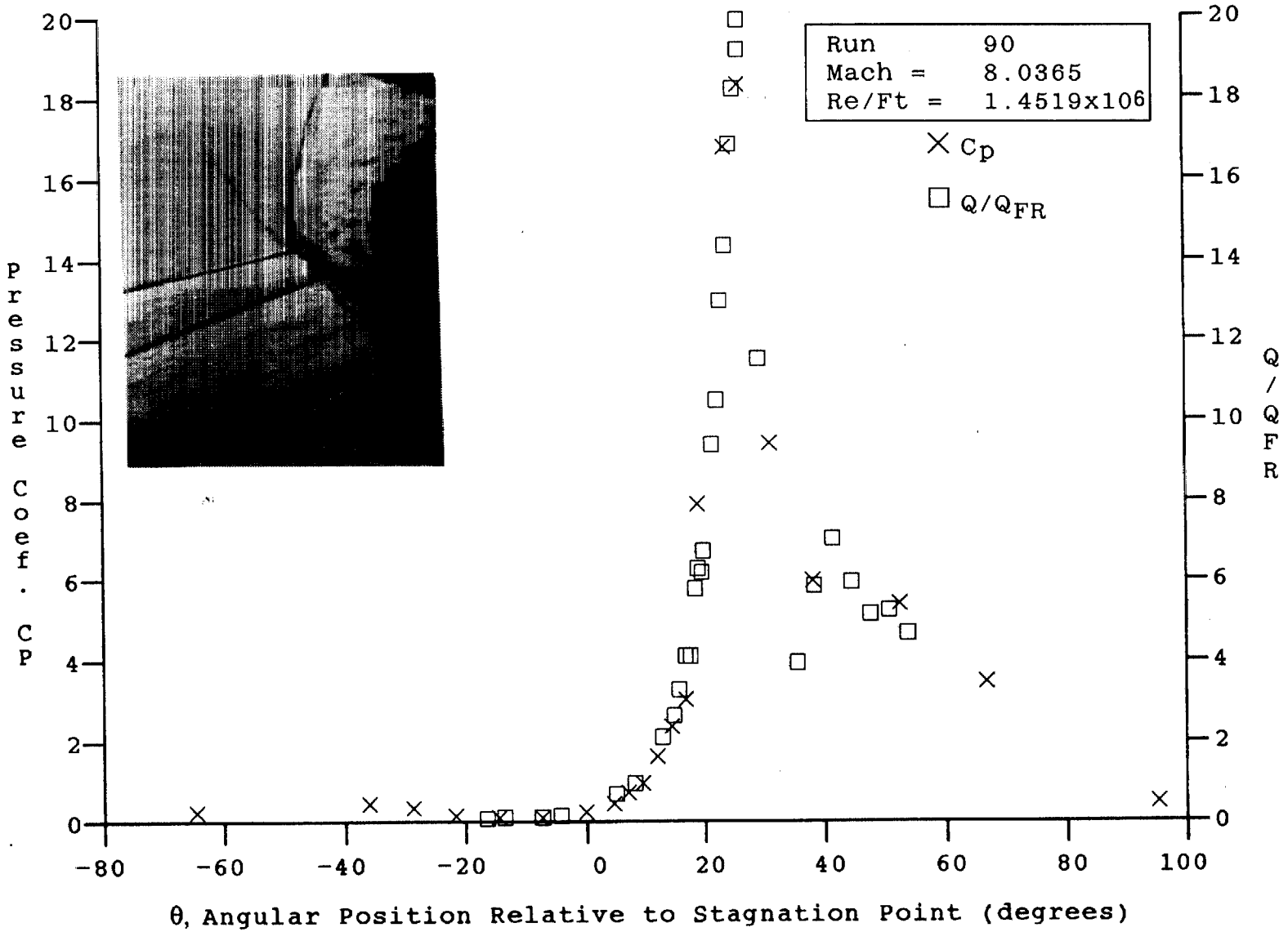

Figure 39c HEAT AND PRESSURE DISTRIBUTIONS IN MULTIPLE-SHOCK-INTERACTION REGIONS INDUCED BY A 7.5/6° SHOCK GENERATOR OVER A 3-INCH-DIAMETER CYLINDER AT MACH 8 FOR RUNS 90 AND 91

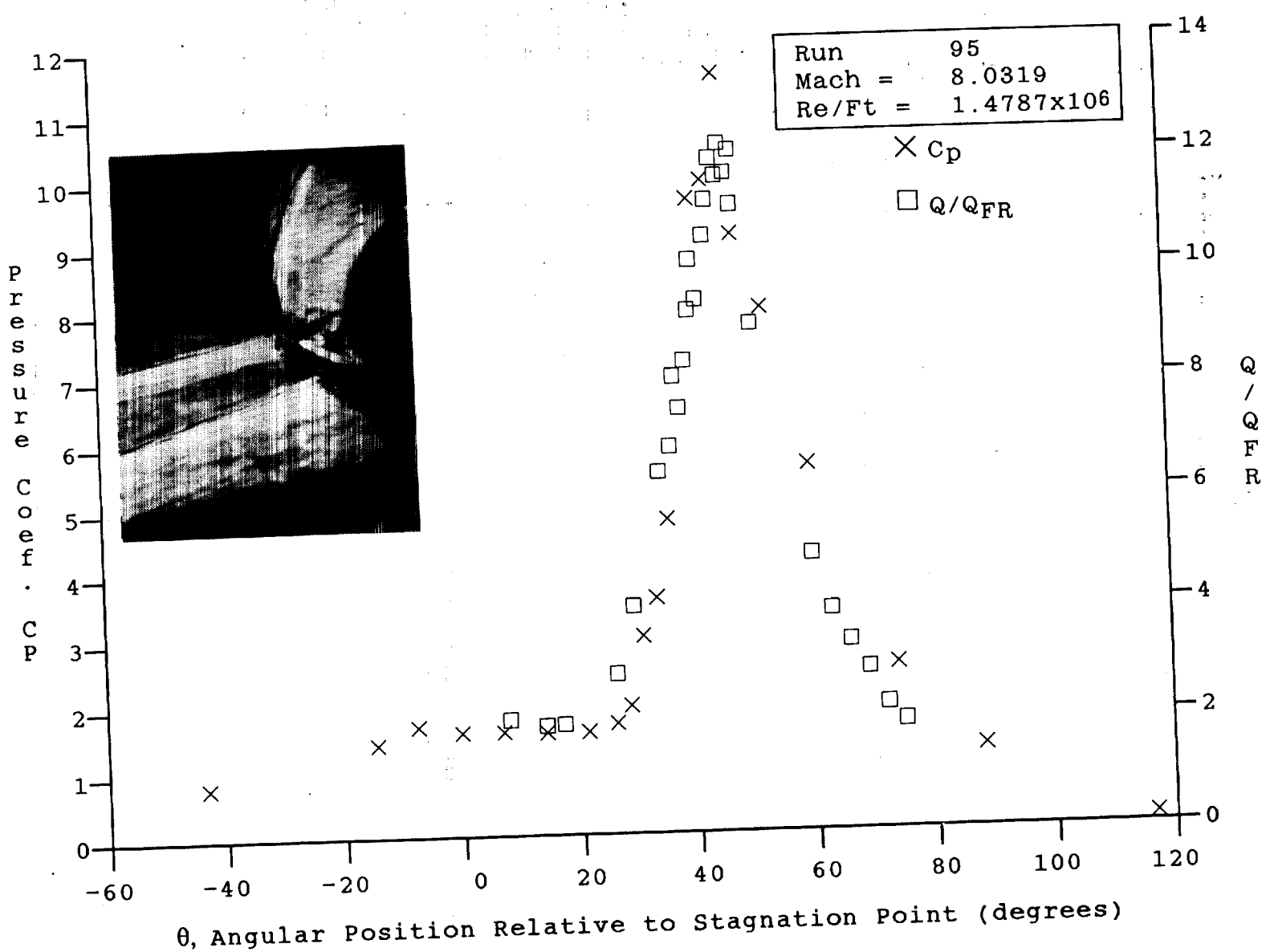

Figure 39d HEAT AND PRESSURE DISTRIBUTIONS IN MULTIPLE-SHOCK-INTERACTION REGIONS INDUCED BY A 7.5/6° SHOCK GENERATOR OVER A 3-INCH-DIAMETER CYLINDER AT MACH 8 FOR RUN 95

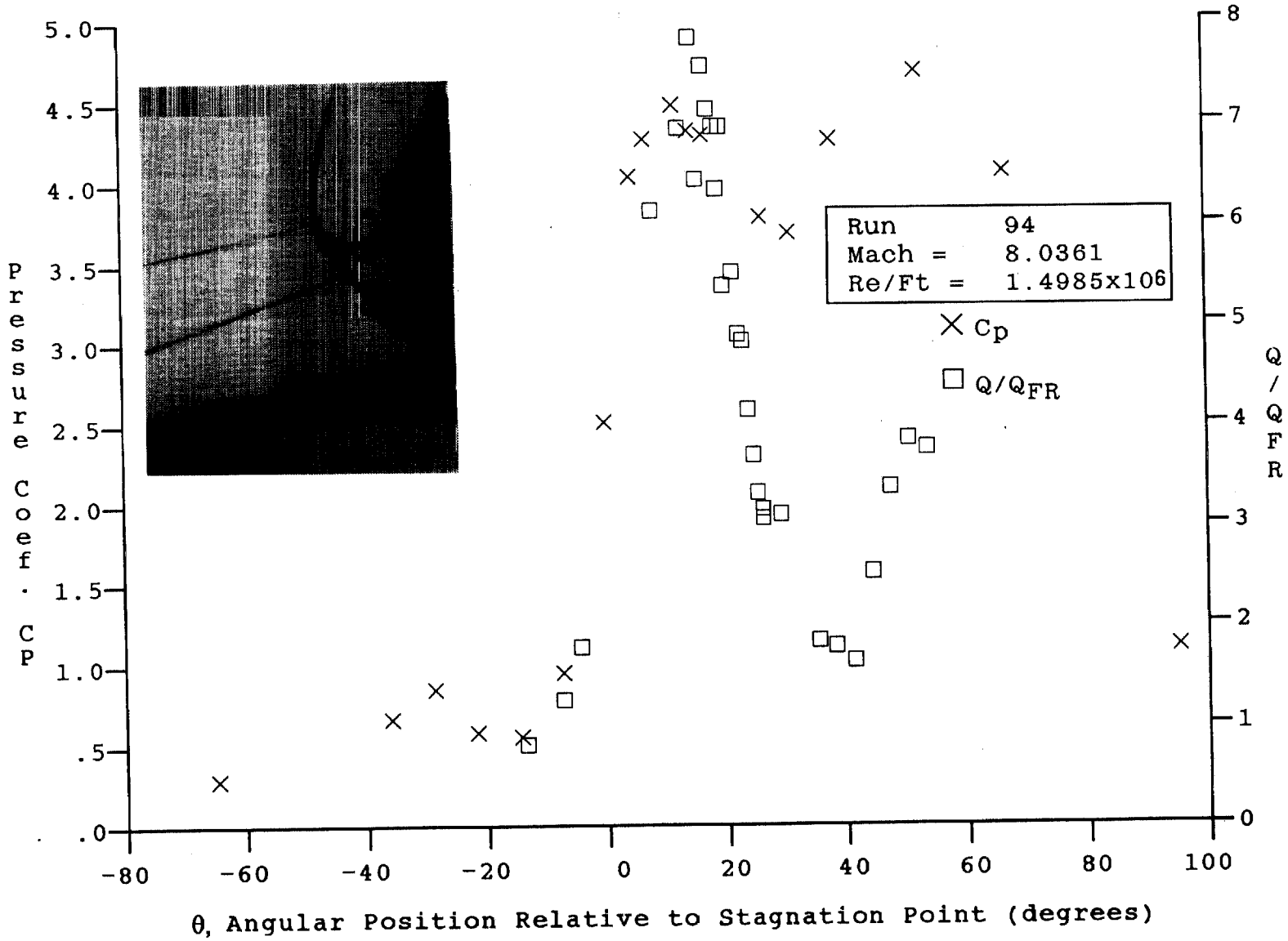

Figure 39e HEAT AND PRESSURE DISTRIBUTIONS IN MULTIPLE-SHOCK-INTERACTION REGIONS INDUCED BY A 7.5/6° SHOCK GENERATOR OVER A 3-INCH-DIAMETER CYLINDER AT MACH 8 FOR RUN 94

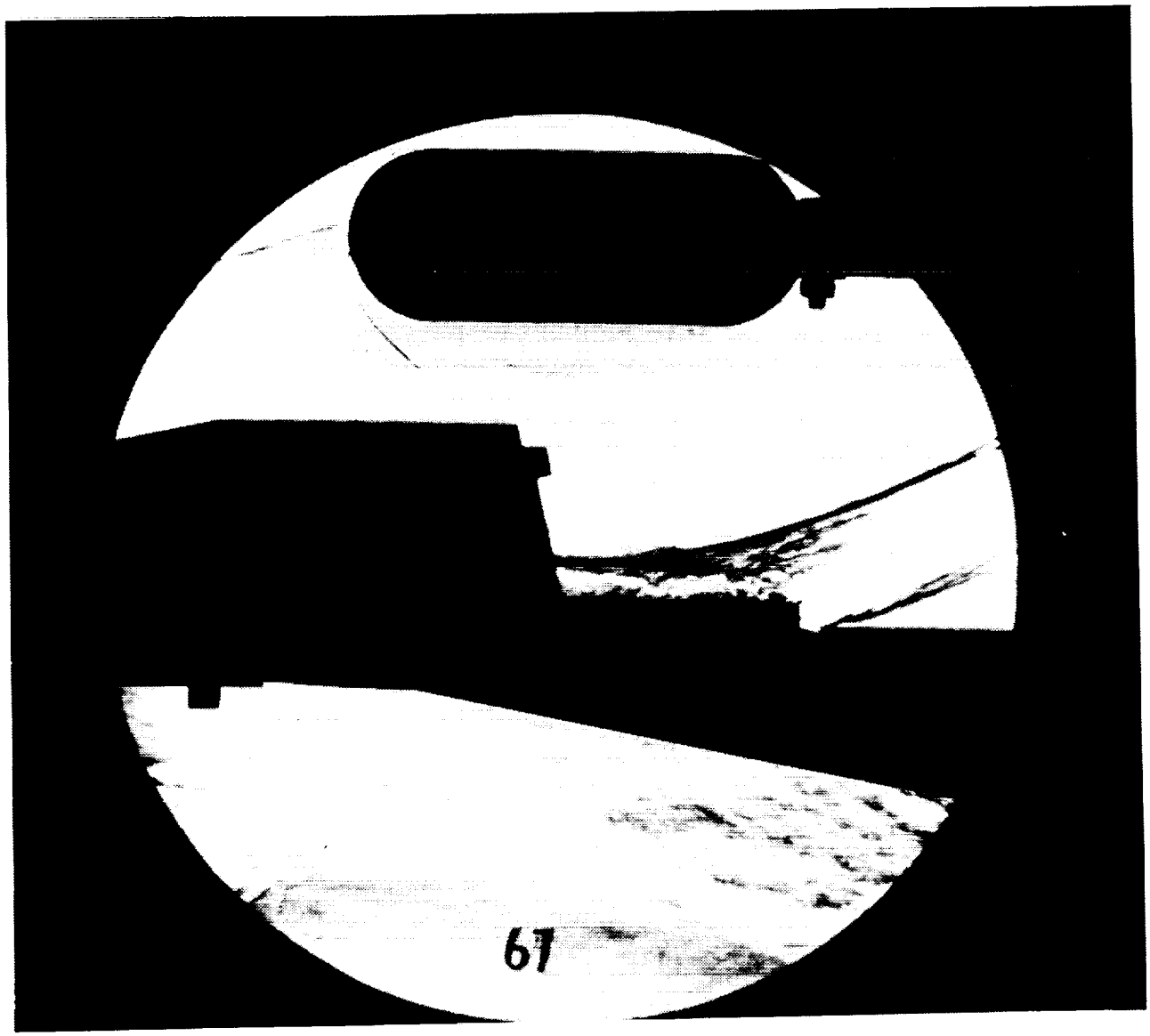

Figure 40 TYPICAL SCHLIEREN PHOTOGRAPH OF 15° SWEPT CYLINDER AT MACH 8

were used in these studies. The lack of good flow visualization hampered these studies, and we spent a large number of runs performing simple positioning of the models to obtain the types III and IV interactions that were of principal interest to us.

The initial runs in this segment of the program (runs 74 and 81) were devoted to evaluating the effects of sweep angle on attachment-line heating. The relatively large Reynolds numbers at which the studies were conducted provided a situation where it might be expected that transition could occur along the attachment line on the swept configurations. Figure 26 shows the laminar flow for a 15-degree swept configuration. Figure 41 shows a correlation of the transition on swept cylinders in terms of the attachment-line Reynolds number based on cylinder diameter (Re_d). The terms and flow configurations are illustrated in Figure 42. The attachment-line Reynolds number is defined as

$$Re_d = \frac{V_A \overline{\eta}}{\nu_A} \tag{5.7a}$$

where the attachment-line characteristic length $\overline{\eta}$ is given by

$$\overline{\eta} = \left[\nu_A \Big/ \left(\frac{dU_A}{d_x} \right)_{x=0} \right]^{1/2} \tag{5.7b}$$

and where the velocity (V_A) and kinematic viscosity (ν_A) are evaluated at the attachment line as shown in Figure 42. The attachment-line Reynolds number can also be reduced to the following expression

$$Re_d = \left(\frac{V_A^2 D}{\nu_A U_\infty U_1} \right)^{1/2} \tag{5.7c}$$

since

$$U_1 = \left[\frac{D}{U_\infty} \left(\frac{dU_A}{d_x} \right)_{x=0} \right] \tag{5.7d}$$

which can be further simplified to

$$\mathrm{Re}_d = \left[\left(\frac{\varrho_\infty D}{\nu_\infty} \right) \frac{\mu_\infty}{\mu_A} \frac{\varrho_A}{\varrho_\infty} \frac{\sin\lambda \tan\lambda}{U_1} \right]^{1/2} \tag{5.7e}$$

based on blunt-body Newtonian assumptions.

The attachment-line density ratio ($\varrho A/\varrho_\infty$) is defined to be

$$\frac{\varrho_A}{\varrho_\infty} = \left[\frac{\gamma+1}{2} M_\infty^2 \cos^2\lambda \right]^{\left(\frac{\gamma}{\gamma-1}\right)} \cdot \left[\frac{\gamma+1}{2\gamma M_\infty^2 \cos^2\lambda - (\gamma-1)} \right]^{\frac{1}{\gamma-1}} \cdot \left[1 + \frac{\gamma-1}{2} M_\infty^2 \cos^2\lambda \right]^{-1} \tag{5.8}$$

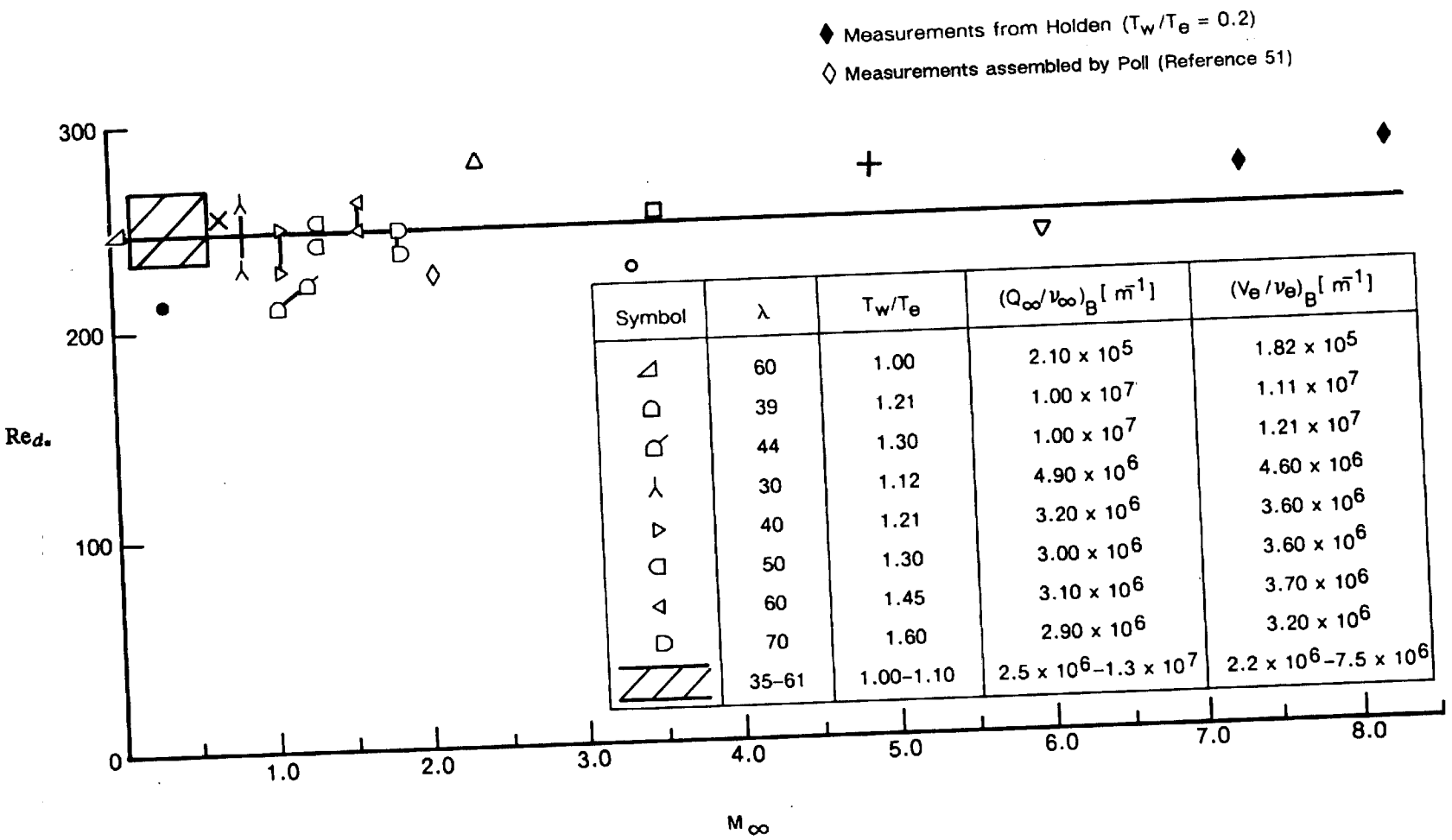

Symbol	λ	T_w/T_e	$(Q_\infty/\nu_\infty)_B$ [m^{-1}]	$(V_e/\nu_e)_B$ [m^{-1}]
◿	60	1.00	2.10×10^5	1.82×10^5
◻	39	1.21	1.00×10^7	1.11×10^7
◻	44	1.30	1.00×10^7	1.21×10^7
⅄	30	1.12	4.90×10^6	4.60×10^6
▷	40	1.21	3.20×10^6	3.60×10^6
◻	50	1.30	3.00×10^6	3.60×10^6
◁	60	1.45	3.10×10^6	3.70×10^6
D	70	1.60	2.90×10^6	3.20×10^6
▨	35–61	1.00–1.10	2.5×10^6–1.3×10^7	2.2×10^6–7.5×10^6

Figure 41 VARIATIONS OF TRANSITION REYNOLDS NUMBER AT THE ONSET OF TRANSITION WITH EDGE MACH NUMBER AND WALL TEMPERATURE

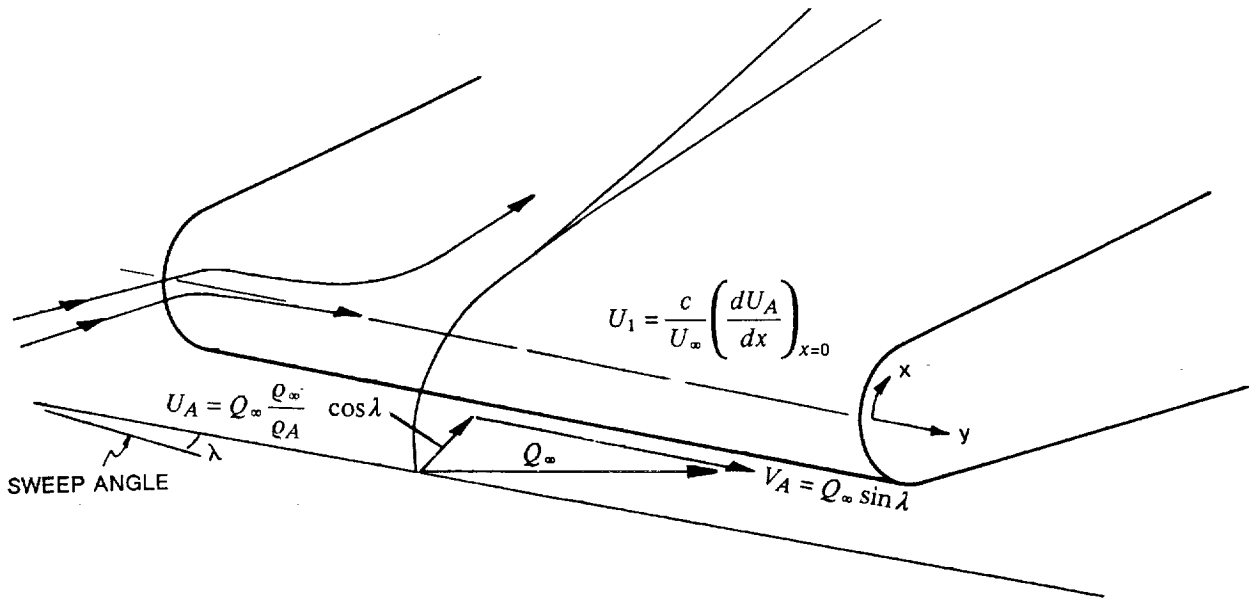

Figure 42 SCHEMATIC DIAGRAM OF FLOWFIELD STRUCTURES IN SWEPT-CYLINDER FLOW CONFIGURATIONS

For swept-cylinder compressible flow, the Stanton number in terms of freestream properties is given as

$$St_A = \frac{0.0689}{2(Pr^{2/3})} \cdot \frac{1}{\mathrm{Re}_d^{0.42}} \tag{5.9}$$

where the reference temperature is given by

$$T_* = T_A + 0.1(T_w - T_A) + 0.6(T_{aw} - T_A) \tag{5.10a}$$

and the reference attachment-line Reynolds number is

$$Re_{d_*} = Re_d[\nu_A/\nu_*]^{1/2} \tag{5.10b}$$

The heat transfer coefficient for laminar and turbulent attachment-line heating can be expressed by the following correlations

$$St_A = \frac{q}{\varrho_\infty U_\infty (h_{aw} - h_w)} = \frac{1.141}{2\,\mathrm{Pr}^{2/3}} \sqrt{\left(\frac{\varrho_A T_A}{\varrho_* T_*}\right)} \sqrt{\left(\frac{\mu_* U_1}{\mu_\infty Re_D}\right)} \cos^{1/2}\lambda \tag{5.11}$$

(for laminar flows)

$$St_A = \frac{q}{\varrho_\infty U_\infty (h_{aw} - h_w)} = \frac{0.0689}{2\,\mathrm{Pr}^{2/3}} \left(\frac{\varrho_A T_A}{\varrho_* T_*}\right)^{0.79} \left(\frac{\mu_* U_1}{\mu_\infty Re_D}\right)^{0.21} \sin^{0.58}\lambda \cos^{0.21}\lambda \tag{5.12}$$

(for turbulent flows.)

The measurements of the stagnation-line heating and the distribution around the 15- and 30-degree swept cylinders are shown in Figures 43a and 43b. It can be seen that, while the measurements on the 15-degree shock-generator configuration are in good agreement with laminar theory, measurements on the 30-degree shock-generator configuration indicate that transition may have taken place. Thus, the occurrence of transition on the 30-degree shock-generator configuration may complicate the interpretation of the shock/shock-interaction measurements.

The measurements made on the swept-shock/shock interactions, which are presented in Appendix D, provided enough information to evaluate the effects of sweep on type III/IV interaction heating. The peak measurements in runs 69 for the 15-degree shock generator and in run 98 for the 30-degree shock generator (Figures 44a and 44b), together with runs 59, 60, and 61 (shown in Figures 27a, 27b, and 27c) for unswept cases, are plotted in Figures 45a and 45b, which show the variation of peak pressure and heat transfer with sweep angle. Reductions of 20 to 30 percent of the stagnation values of pressures and heating rates are seen in these figures. Figure 46 shows the reductions that should occur in the pressure based on Newtonian theory, and in the heat transfer based on the laminar and turbulent theory given in the earlier equations, as the cylinder is put into a swept configuration. The measured swept type III/IV interaction peak pressure and heat transfer measurement can be predicted using these theories within the experimental accuracy.

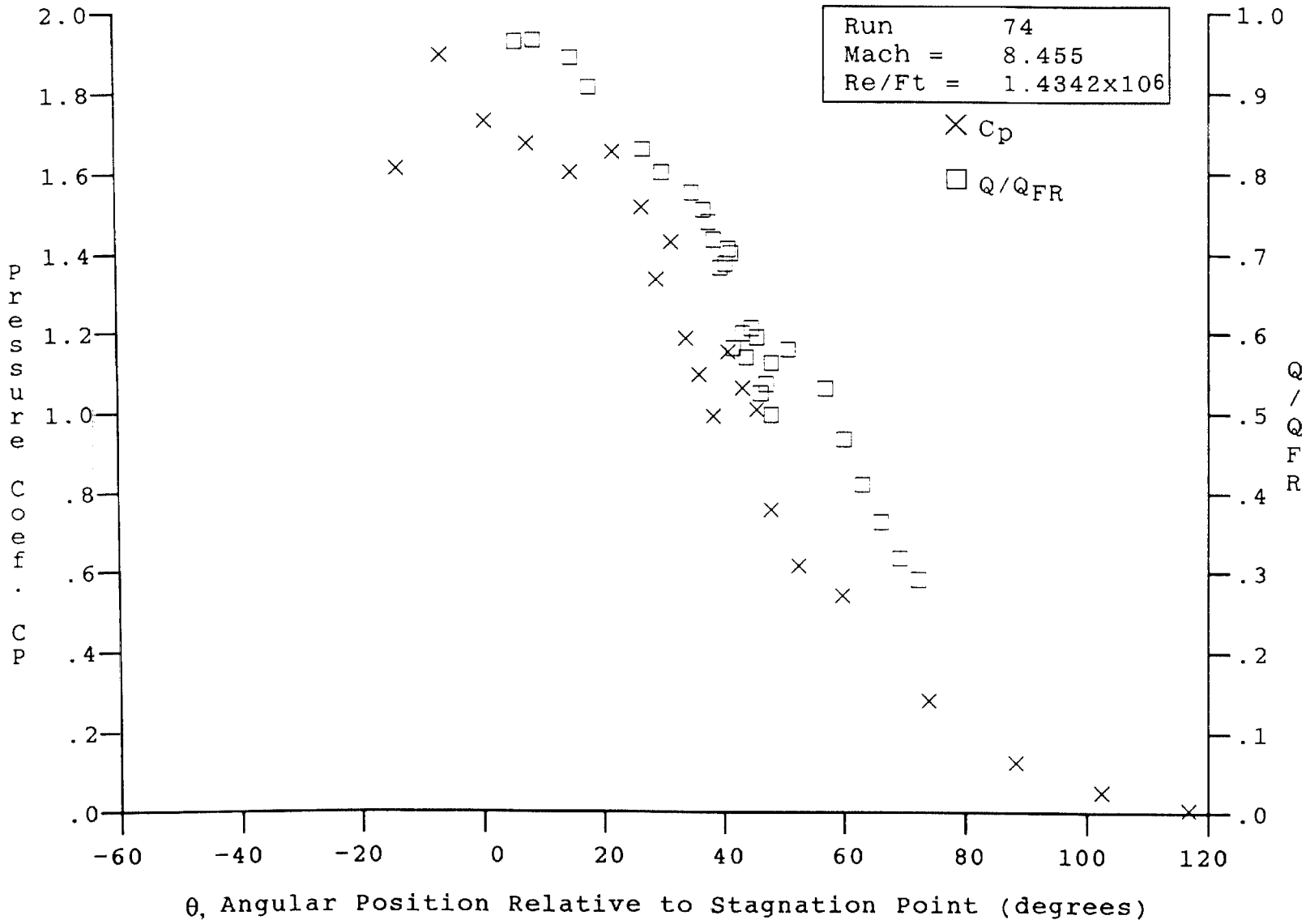

Figure 43a PRESSURE AND HEAT TRANSFER TO SWEPT CYLINDER, $\lambda = 15°$

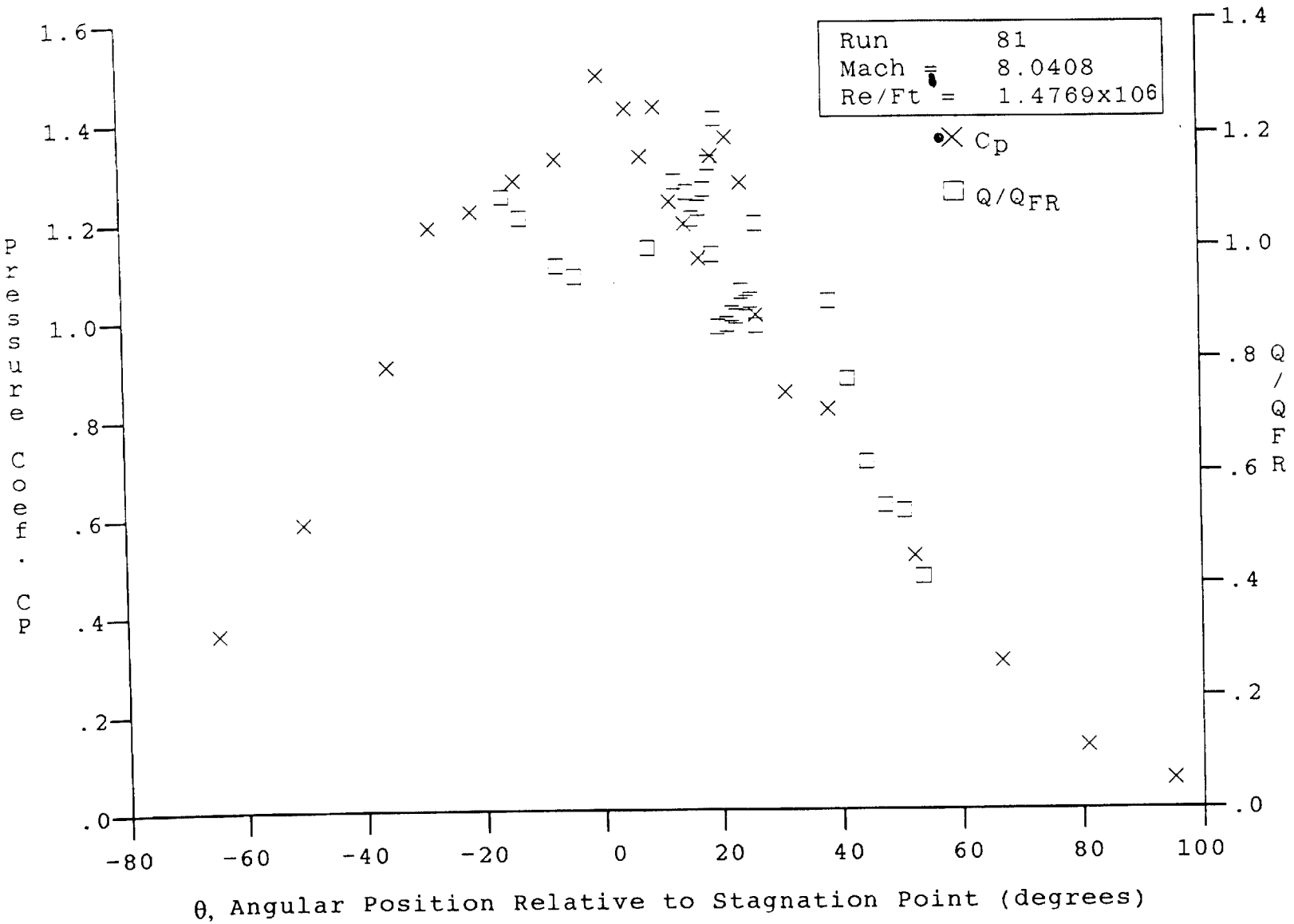

Figure 43b PRESSURE AND HEAT TRANSFER TO SWEPT CYLINDER, $\lambda = 30°$

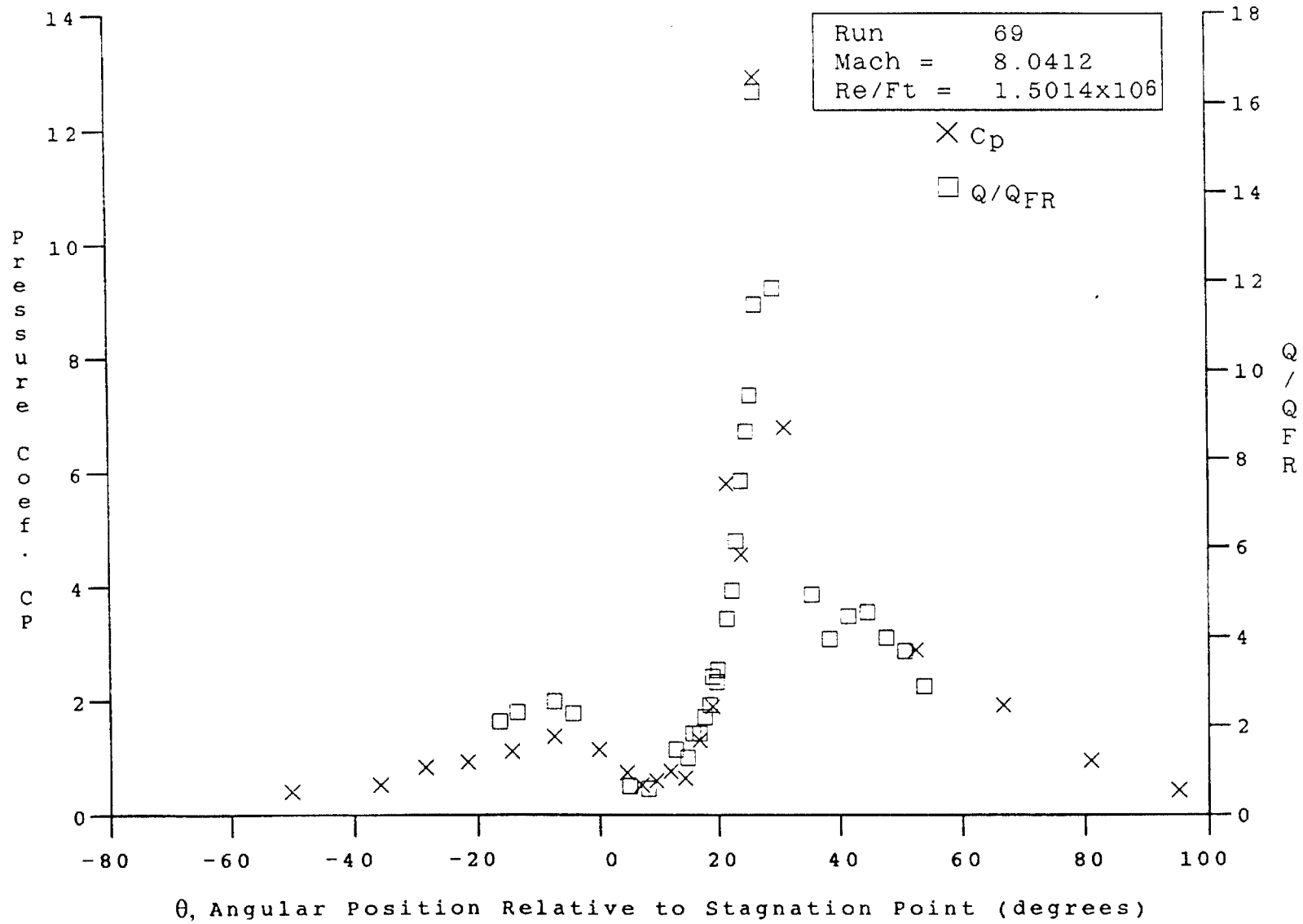

Figure 44a HEAT AND PRESSURE DISTRIBUTIONS IN SHOCK/SHOCK-INTERACTION REGIONS INDUCED BY A 12.5° SHOCK GENERATOR SWEPT AT 15° OVER A 3-INCH-DIAMETER CYLINDER AT MACH 8 FOR RUN 69

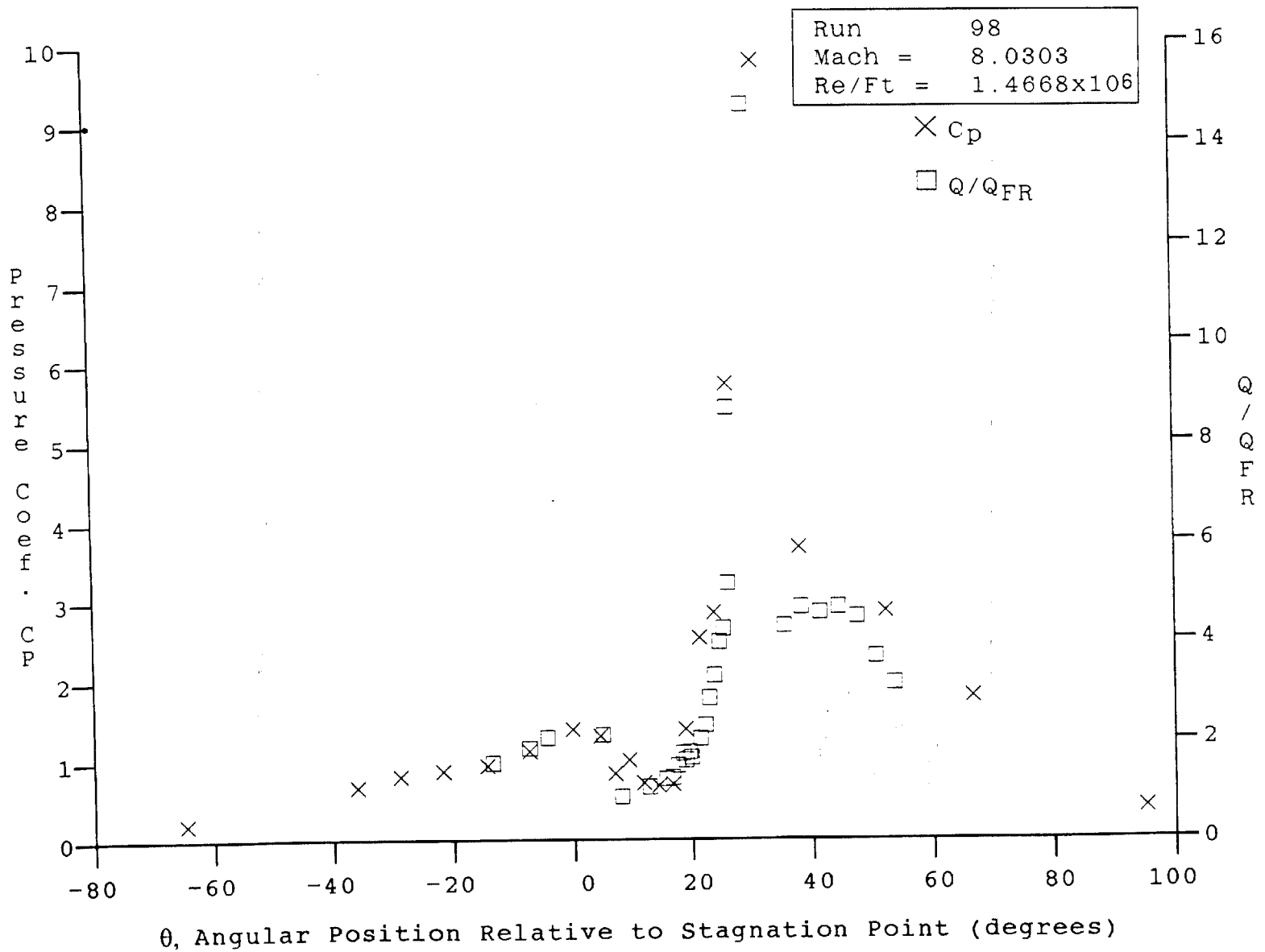

Figure 44b HEAT AND PRESSURE DISTRIBUTIONS IN SHOCK/SHOCK-INTERACTION REGIONS INDUCED BY A 12.5° SHOCK GENERATOR SWEPT AT 30° OVER A 3-INCH-DIAMETER CYLINDER AT MACH 8 FOR RUN 98

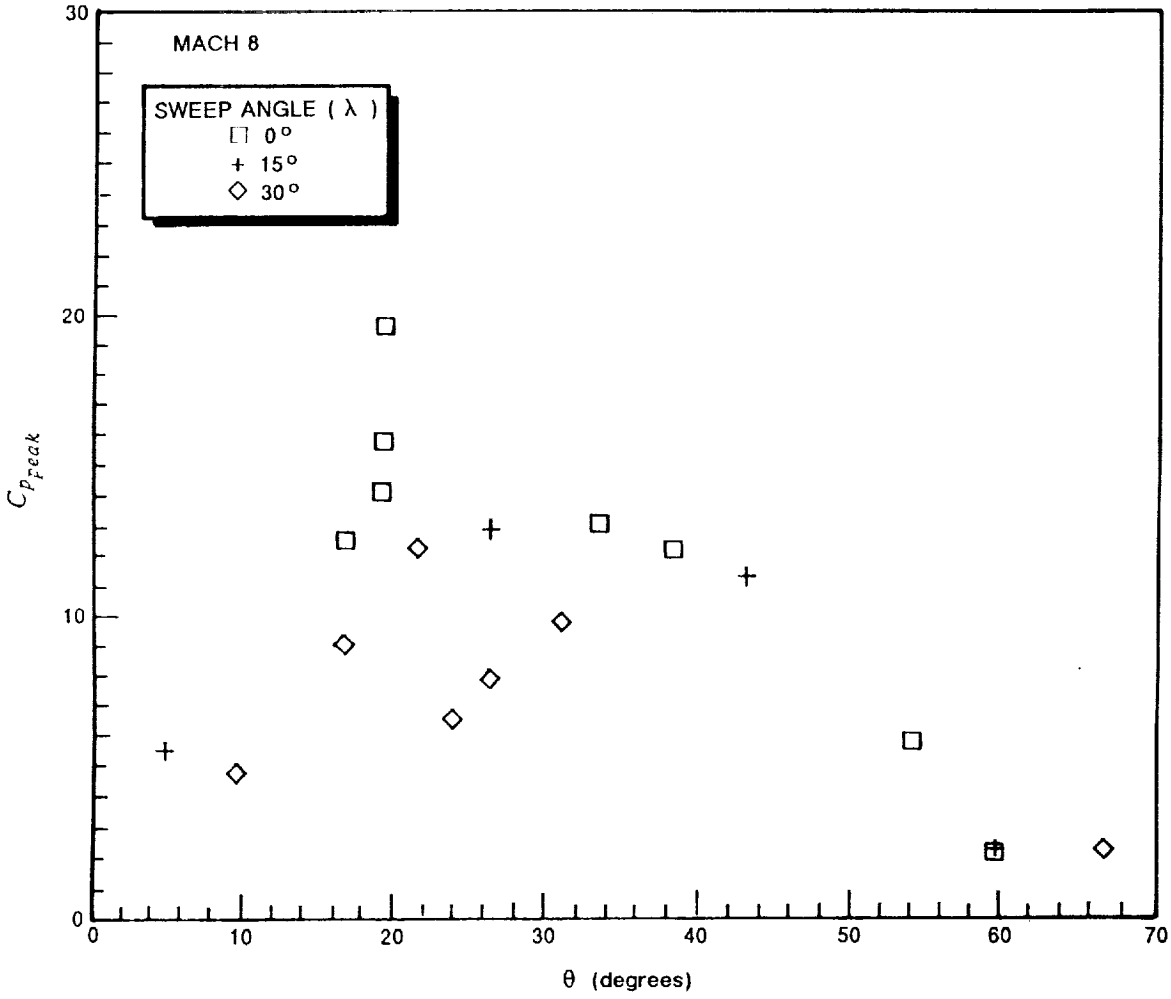

Figure 45a PEAK-PRESSURE MEASUREMENTS FOR SWEPT-SHOCK CONFIGURATION

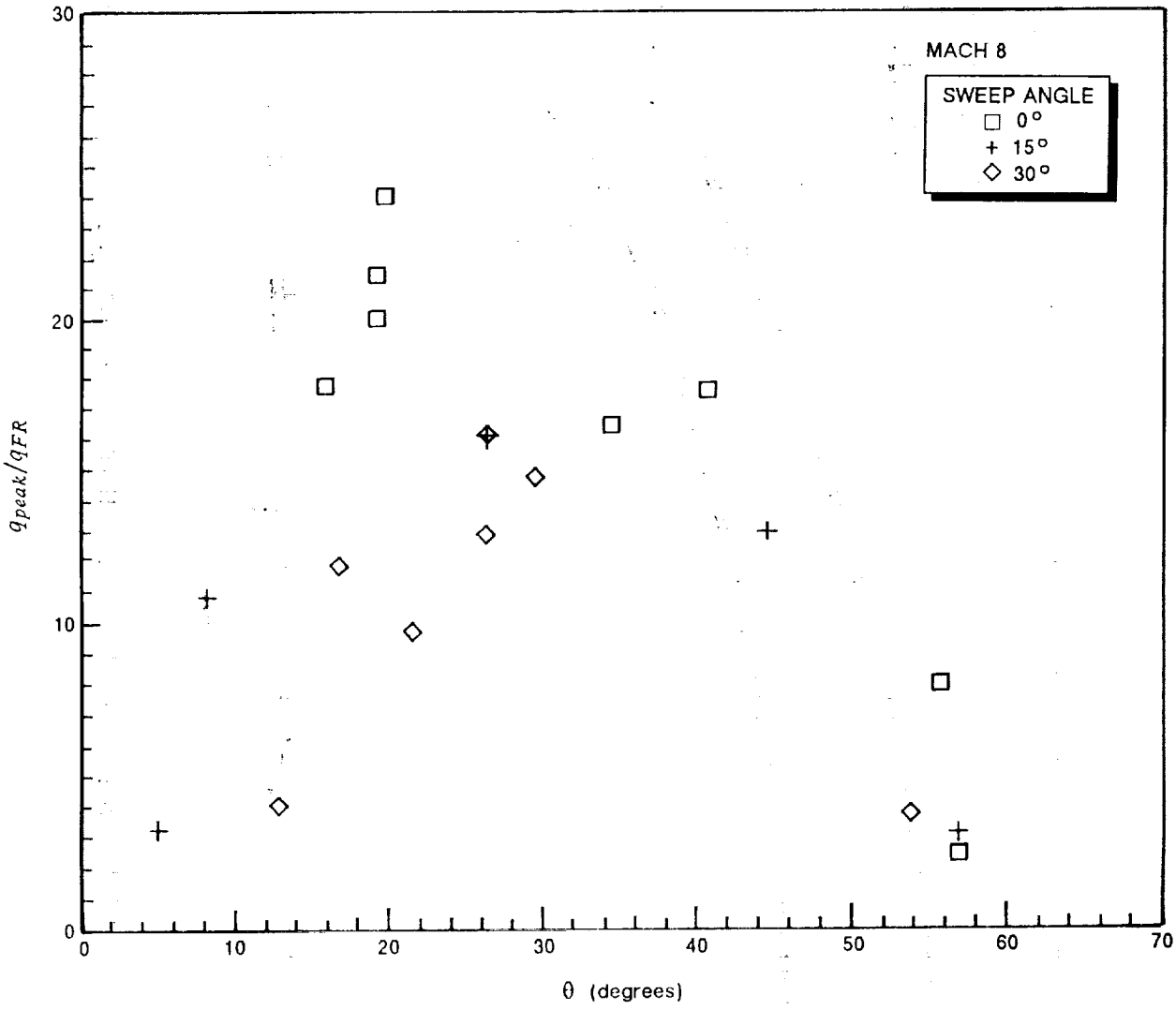

Figure 45b PEAK-HEATING MEASUREMENTS FOR SWEPT-SHOCK CONFIGURATION

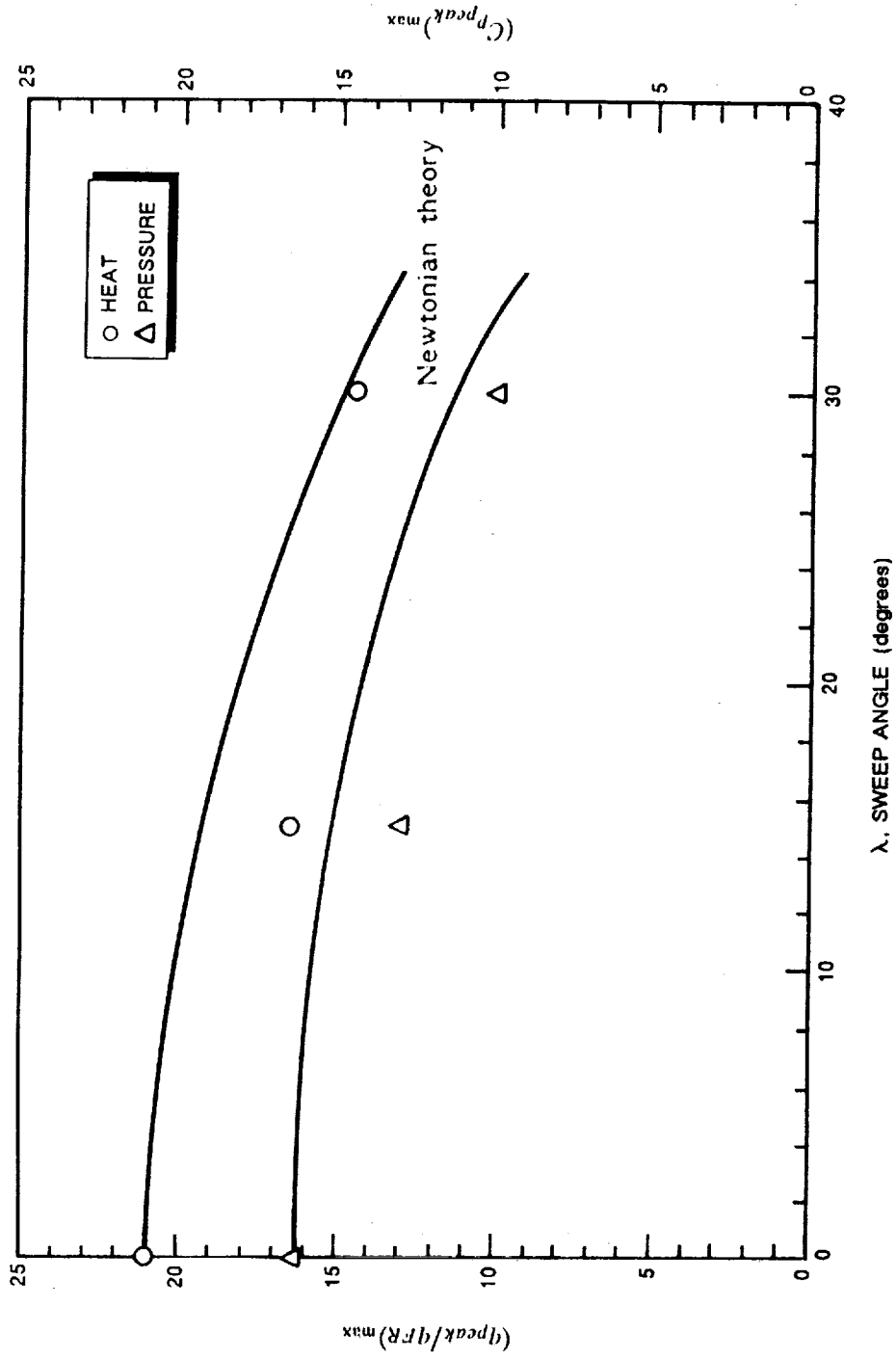

Figure 46 VARIATIONS OF MAXIMUM PEAK HEATING AND PRESSURE WITH SWEEP ANGLE

Section 6
CONCLUSIONS

Studies have been conducted to examine the aerothermal characteristics of two-dimensional regions of shock/shock/boundary layer interaction induced by the impingement of single and multiple incident shocks on the shock layer over a transverse cylinder. It is concluded from review of earlier studies of these flows that, because of a number of problems associated with instrumentation, its resolution, and its accuracy, enhancement of heating levels and the distribution of heat transfer and pressure are inadequate for code validations. The present experimental studies were conducted to obtain detailed measurements in the regions of shock/shock interaction over a Mach number range from 6 to 19 at Reynolds numbers (based on cylinder diameter) from 4×10^4 to 1.2×10^6 to provide much-needed insights into the mechanisms of heating enhancement caused by the shock/shock interactions in hypersonic flows. The magnitude and severity of the heating loads and gradients developed in these flows required the use of short-duration facilities with insulated models to minimize lateral heat distortion.

In the first of the three studies conducted here, detailed pressure and heat transfer measurements were made for a single incident shock on a transverse cylinder for a number of interaction configurations and shock strengths. In this study, in which emphasis was placed on types III and IV interactions, it was found that, for transitional shear-layer flows, the peak pressure and heating increased with increased Mach number. For these transitional/turbulent flows, we believe that type IV interaction heating is enhanced by turbulence in the stagnation region. However, significantly lower enhancement factors were observed when the flows remained laminar for a type IV interaction, and we believe that the modification of the jet flow by viscous effects is an important mecahnism for these flows. Calculations of peak heating and pressure in types II and IV interactions, using the simple Edney/Keyes and Hains methods, were in reasonable agreement for transitional flows if a turbulent heating enhancement factor of approximately 1.3 is employed as a correction to the predicted laminar stagnation heating rate for a type IV interaction. The present study has shown that, for laminar type III interactions in high Mach number flows, the simple Keyes-Hains predictions were in good agreement with the measured peak heat transfer and pressure; however, these levels were significantly overpredicted when the compression processes in the jet for a type IV interaction are influenced by viscous effects.

The studies of multiple-shock/shock interaction demonstrated that the largest heat loads are generated on the cylinder if the shocks coalesce before they impinge on the cylinder bow shock. While the flowfields and aerothermal loads generated by multiple-shock impingement provide excellent test cases for code prediction, the peak heating loads are significantly less than those generated by a single shock of the same strength.

The studies of swept-shock/shock interaction configurations showed that sweeping the model reduces the centerline heating rates. These studies used 15- and 30-degree sweep angles in Mach 8 flows and resulted in 20% to 30% reductions in the heating rates generated by the shock/shock interactions. It was also shown that the peak pressure and heat transfer measurement can be predicted by simple correlative techniques. These studies showed that sweeping the shock/shock interaction regions lowered the heating and pressure levels in roughly the same proportion to that of the observed heat transfer and pressure level reductions resulting from sweeping a cylinder in the absence of the interaction.

Because of the low Reynolds numbers at which transition occurs in these flowfields from either single- or multiple-shock/shock interactions, as well as the occurrence of flow instabilities for type IV interactions, predicting such flows accurately over a large, and important, part of the hypersonic flight regime will continue to be a difficult problem.

Section 7
REFERENCES

1. Edney, B., "Anomalous Heat Transfer and Pressure Distributions on Blunt Bodies at Hypersonic Speeds in the Presence of an Impinging Shock," FFA Report 115, Aeronautical Research Institute of Sweden, 1968.

2. Keyes, J.W. and Hains, F.D., "Analytical and Experimental Studies of Shock Interference Heating in Hypersonic Flow," NASA Report TN D-7139, May 1973.

3. Craig, R.R. and Ortwerth, P.J., "Experimental Study of Shock Impingement on a Blunt Leading Edge with Application to Hypersonic Inlet Design," AFFDL TR-71-10, April 1971.

4. Holden, M.S., "A Review of Aerothermal Problems Associated with Hypersonic Flight," AIAA 24th Aerospace Sciences Meeting, Reno, Nevada, AIAA Paper 86-0207, January 1986.

5. Birch, S.F. and Keyes, J.W., "Transition in Compressible Free Shear Layers," AIAA Journal of Spacecraft, Vol. 9, No. 8, August 1972.

6. Watts, J.D., "Flight Experience with Shock Impingement and Interference Heating on the X-15-2 Research Airplane," NASA TM X-1669, 1968.

7. Korkegi, R., "Survey of Viscous Interactions Associated with High Mach Number Flight," AIAA J., Vol. 9, No. 5, May 1971.

8. Newlander, R.D., "Effects of Shock Impingement on the Distribution of Heat Transfer Coefficients on a Right Circular Cylinder at Mach Numbers of 2.65, 3.51 and 4.44," NASA TN D-642, 1961.

9. Carter, H.S. and Carr, R.E., "Free-Flight Investigation of Heat Transfer to an Unswept Cylinder Subjected to an Incident Shock and Flow Interference From an Upstream Body at Mach Numbers Up to 5.50," NASA TN D-9908.

10. Francis, W. L., "Experimental Heat-Transfer Study of Shock Impingement on Fins in Hypersonic Flow," Journal of Spacecraft and Rockets, Vol. 2, No. 4, July/August 1965, pp. 630-632.

11. Beckwith, I.E., "Experimental Investigation of Heat Transfer and Pressures on a Swept Cylinder in the Vicinity of its Intersection with a Wedge and Flat Plate at Mach Number 4.15 and High Reynolds Numbers," NASA TN D-2020, 1964.

12. Bushnell, D.M., "Interference Heating on a Swept Cylinder in Region of Intersection with a Wedge at Mach Number 8," NASA TN D-3094, 1965.

13. Bushnell, D.M., "Effects of Shock Impingement and Other Factors on Leading Edge Heat Transfer," NASA TN D-4543, 1968.

14. Jones, R.A., "Heat-Transfer and Pressure Investigation of a Fin-Plate Interference Model at a Mach Number of 6," NASA TN D-2028, 1964.

15. Siler, L.G. and Deskin, H.E., "Effect of Shock Impingement on the Heat Transfer and Pressure Distributions on a Cylindrical-Leading Edge Model at Mach Number 19," AEDC-TDR-64-228, 1964.

16. Gulbran, C.E. et al., "Heating in Regions of Interfering Flow Fields. Part II - Leading Edge Shock Impingement," AFFDL TR65-49, Part II, January 1967, Air Force Flight Dynamics Laboratory.

17. Gulbran, C.E. et al., "Heating in Regions of Interfering Flow Fields. Part I - Two- and Three-Dimensional Laminar Interactions at Mach 8," AFFDL TR 65-49, Part I, 1965, Air Force Flight Dynamics Laboratory

18. Knox, C.E., "Measurements of Shock-Impingement Effects on the Heat Transfer and Pressure Distributions on a Hemicylinder Model at Mach Number 19," AEDC-TR-65-245, U.S. Air Force, November 1965.

19. Ray, A.D. and Palko, R.L., "An Investigation of the Effects of Shock Impingement on a Blunt Leading Edge," AEDC-TR-65-153, July 1965.

20. Heirs, R.S. and Loubsky, W.J., "Effects of Shock-Wave Impingement on the Heat Transfer on a Cylindrical Leading Edge," NASA TN D-8859, February 1967.

21. Morris, D.J. and Keyes, W.J., "Computer Programs for Predicting Supersonic and Hypersonic Interference Flow Fields and Heating," NASA TM X-2725, May 1973.

22. Keyes, J.W. and Morris, D.J., "Correlations of Peak Heating in Shock Interference Regions at Hypersonic Speeds," Journal of Spacecraft and Rockets, Vol. 9, No. 8, August 1972, pp. 621-623.

23. Rogers, C.E., "Experimental Investigation of Leading-Edge Shock Impingement and Interaction Heating on a 1/80 Scale Model of a NASA Straight Wing Orbiter Configuration at Mach Numbers 8 and 16," Calspan Advanced Technology Center, Report AA-2977-V-1, August 1971.

24. Lanning, W.D. and Hung, F.T., "Shuttle Ascent and Shock Impingement Aerodynamic Heating Studies (Aerodynamic Heating Data from Shock Impingement Studies Simulating Space Shuttle Ascent)," NASA CR 123538, 1971.

25. Kaufman II, L.G. and Korkegi, R.M., "Shock Impingement Caused by Boundary Layer Separation Ahead of Blunt Fins," ARL 72-118, August 1972.

26. Tannehill, J.C., Holst, T.L., and Rakich, J.V., "Numerical Computation of Two-Dimensional Viscous Blunt Body Flows with an Impinging Shock," AIAA J., Vol. 14, No. 2, February 1976.

27. Tannehill, J.C., Holst, T.L., Rakich, J.F. and Keyes, J.W., "Comparison of a Two-Dimensional Shock Impingement Computation with Experiment," AIAA J., Vol. 14, No. 4, April 1976.

28. Holden, M.S., Wieting, A.R., Moselle, J.R., and Glass, C., "Studies of Aerothermal Loads Generated in Regions of Shock/Shock Interaction in Hypersonic Flow," AIAA Paper 88-0477, January 1988.

29. Young, F., Kaufman, L. II, and Korkegi, R., "Experimental Investigation of Interactions Between Blunt Fin Shock Waves and Adjacent Boundary Layer at Mach Numbers 3 and 5," ARL 68-0214, December 1968.

30. Kaufman, L.II and Korkegi, R., "Shock Impingement Caused by Boundary Layer Separation Ahead of Blunt Fins," ARL 72-0118, August 1972.

31. Haslett, R.A. and Kaufman, L. II, et al., "Interference Heating Due to Shock Impingement," AFFDL TR-72-66, July 1972.

32. Ginoux, J.J. and Matthews, R.D., "Effects of Shock Impingement on Heat Transfer," VKI TN 87, May 1973.

33. Ginoux, J.J. and Matthews, R.D., "Effects of Shock Impingement on Heat Transfer. Part II-Effect of Shear Layer Impingement on Pressure and Heat Transfer Rate Distribution Around a Cylinder," AFOSR-TR-74-0714, February 1974.

34. Holden, M.S., "Accurate Vehicle Experimental Dynamics Program - Final Report," SAMSO-TR-79-47, August 1979.

35. Holden, M.S., "Maneuvering Vehicle Aerodynamics Experiment Program," BMO-TR-82-16, November 1981.

36. Holden, M.S., "Studies of Heat-Transfer and Flow Characteristics of Rough and Smooth Indented Nose Shapes, Part I," AIAA Paper 86-384, January 1986.

37. Jones, R.A., Bushnell, D.M. and Hunt, J.L., "Experimental Flow Field and Heat Transfer Investigation of Several Tension Shell Configurations at Mach Number of 8," NASA TN D-3800, January 1967.

38. Wieting, A.R. and Holden, M.S., "Experimental Study of Shock Wave Interference Heating on a Cylindrical Leading Edge at Mach 6 and 8," AIAA 22nd Thermophysics Conference, Honolulu, Hawaii, AIAA Paper 87-1511, June 1987.

39. Klopfer, G.H. and Yee, H.C., "Viscous Hypersonic Shock-on-Shock Interaction on Blunt Cowl Lips," AIAA Paper 88-0233, January 1988.

40. Stewart, J.R., Thareja, R.R., Wieting, A.R., and Morgan, K., "Application of Finite Element and Remeshing Technique to Shock Interference on a Cylindrical Leading Edge," AIAA Paper 88-0368, January 1988.

41. "Calspan Hypersonic Shock Tunnel, Description and Capabilities Brochure," 1975.

42. Needham, D.A., Elfstrom, G.M., and Stollery, J.L., "Design and Operation of the Imperial College Number 2 Hypersonic Gun Tunnel," Imperial College Aero Report 70-04, May 1970.

43. Lewis, C.H., and Burgess, E.G., III, "Charts of Normal Shock Wave Properties in Imperfect Air (Supplement: M = 1 to 10)," AEDC-TR-196, September 1965.

44. Hilsenrath, J. et al., "Tables of Thermal Properties of Gases," NBS Circular 565, 1955.

45. Reece, J.W., "Test Section Conditions Generated in the Supersonic Expansion of Real Air," Journal of Aeronautical Sciences, Vol. 29, No. 5, May 1962, p. 617, 618.

46. Hilsenrath, J. et al., "Tables of Thermodynamic Properties of Air Including Dissociation and Ionization from 1500°K to 15,000°K," AEDC-TR-59-20, December 1959.

47. Neel, C.A., and Lewis, C.H., "Interpolations of Imperfect Air Thermodynamic Data II - At Constant Pressure," AEDC-TDR-64-184, September 1964.

48. Seymour, P.J., "Techniques for Evaluation of Unsteady Heat Flux From Film Gauges," Master of Science Thesis at State University of New York at Buffalo, 1982.

49. Fay, J.A. and Riddell, F.R., "Theory of Stagnation Point Heat Transfer in Dissociated Air," Journal of the Aeronautical Sciences, Vol. 25, No. 2, February 1958.

50. Kemp, N., Rose, P., and Detra, R., "Laminar Heat Transfer Around Blunt Bodies in Dissociated Air," Journal of Aeronautical Sciences, Vol. 26, July 1959, pp. 421-430.

51. Poll, D.I.A., "The Development of Intermittent Turbulence on a Swept Attachment-Line Including the Effects of Compressibility," The Aeronautical Quarterly, Vol. XXXIV, February 1983, pp. 1-23.

52. Bushnell, D. and Weinstein, L., "Correlation of Peak Heating for Reattachment of Separated Flows," Journal of Spacecraft and Rockets, Vol. 5, No. 11, 1968.

53. Holden, M.S., "Shock Wave-Turbulent Boundary Layer Interaction in Hypersonic Flow," AIAA 10th Aerospace Sciences Meeting, AIAA Paper 72-74, January 1972.

54. Chapman, D.R., Kuehn, D.M., and Larson, H.K., "Investigation of Separated Flows in Supersonic and Subsonic Streams with Emphasis on the Effect of Transition," NASA TR-1356, 1958.

55. Crawford, D.H., "Investigation of Flows Over a Spiked Nose Hemisphere Cylinder at a Mach Number of 6.8," NASA TN D-118, 1959.

56. Vidal, R.J., "Model Instrumentation Techniques for Heat Transfer and Force Measurements in a Hypersonic Shock Tunnel," Cornell Aeronautical Laboratory Report AD-917-A-1, February 1956.

57. Glass, C.E., Holden, M.S., and Wieting, A.R., "Effect of Leading Edge Sweep on Shock Interference at Mach 8," AIAA Paper 89-0271, January 1989.

Appendix A

TECHNIQUES FOR NUMERICAL EVALUATION OF UNSTEADY HEAT FLUX FROM THIN-FILM GAGES

A.1 REVIEW

Since the 1950's, Calspan has used shock tubes for practical research on atmospheric re-entry. As a direct result of these efforts, techniques were developed for measuring surface temperatures in transient conditions. These temperature histories came primarily from thin-film gages consisting of an electrical conducting metal (platinum) mounted on a thermally insulating substrate (Pyrex 7740). A known constant current is passed through the gage, and its response is directly related to the temperature of the gage. Today, these gages are highly refined and extremely small.

The interpretation of the heat flux from the gage signal is based on the assumption that the substrate is a semi-infinite solid. The thermal penetration depth into the layer is known to vary as $\sqrt{(at)}$, where t is the time from test initiation and a is the thermal diffusivity. If d is the depth of the substrate, then it determines the maximum thermal penetration depth and can be used for finding t_{max}, the length of time for which the semi-infinite solid assumption is valid. Thus,

$$t_{max} = \frac{d^2}{a} \tag{A.1}$$

is the maximum test time for which the assumption of a semi-infinite solid still remains valid. Therefore, the analysis that follows is valid only when

$$t < t_{max} = d^2/a$$

As long as this criterion can be satisfied, and as long as departures from one-dimensionality can be neglected, the equations can be developed for a two-layer conducting medium, the first layer being the film itself and the second layer the substrate (Figure A-1). Vidal[56] was the first to completely derive and expand these governing equations. Starting with the basic one-dimensional heat-conduction equation, he was able to show that the first layer can be neglected, at least as it affects the unsteady heat flux.

A.2 SOLUTION FOR CONSTANT THERMAL PROPERTIES

The governing equation for heat conduction in a one-dimensional solid is

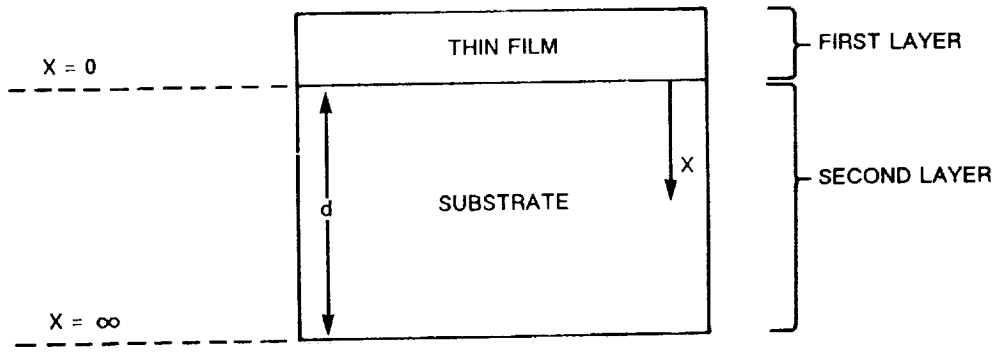

Figure A-1 THIN-FILM GAGE MOUNTED ON SUBSTRATE

$$\frac{\partial}{\partial x}\left[k\frac{\partial T(x,t)}{\partial x}\right] = \varrho c\frac{\partial T(x,t)}{\partial t} \tag{A.2}$$

with a boundary condition of

$$\dot{q}(o,t) = -k\frac{\partial T(x,t)}{\partial x}\bigg|_{x=0} \tag{A.3}$$

at the surface. Also, for a semi-infinite medium, it is necessary to enforce a temperature equal to zero at $x = \infty$ (Figure A-1) for all time. The x-direction will be denoted as penetrating into the substrate.

In general, the thermal conductivity (k), the specific heat (c), and the substrate density (ϱ) are all functions of the temperature (T). It will be assumed for now that the density, the thermal conductivity, and the specific heat are independent of temperature. Note that the assumption of constant thermal properties is *not* true in all situations and usually must be taken into account. With these assumptions, Equation A.2 becomes

$$\frac{\partial^2 T(x,t)}{\partial x^2} = \frac{1}{\alpha}\frac{\partial T(x,t)}{\partial t} \tag{A.4}$$

where $\alpha = \dfrac{k}{\varrho c}$. As before,

$$\dot{q}(o,t) = -k\frac{\partial T(x,t)}{\partial x}\bigg|_{x=0} \tag{A.5}$$

$$T(\infty,t) = 0 \tag{A.6}$$

are the boundary conditions.

Using the Laplace transform method of solution yields

$$\frac{\partial^2 T(x,s)}{\partial x^2} = \frac{1}{\alpha}\, s\, T(x,s) \tag{A.7}$$

with s as the Laplace variable and the initial temperature assumed zero. The boundary conditions become

$$\dot{q}(o,s) = -k\frac{\partial T(o,s)}{\partial x} \tag{A.8}$$

$$T(\infty,s) = 0 \quad . \tag{A.9}$$

The solution is

$$T(x,s) = Ae^{\left(\frac{s}{\alpha}\right)^{1/2}x} + Be^{-\left(\frac{s}{\alpha}\right)^{1/2}x} \tag{A.10}$$

It is easily seen that application of the boundary conditions yields

$$A = 0 \tag{A.11}$$

and

$$B = \frac{\dot{q}(o,s)}{(\varrho ck)^{1/2}(s)^{1/2}} \quad . \tag{A.12}$$

Substituting Equations A.11 and A.12 into Equation A.10 yields Equation A.13

$$T(x,s) = \frac{\dot{q}(o,s)}{(\varrho ck)^{1/2}(s)^{1/2}} e^{-\left(\frac{s}{a}\right)^{1/2} x} \tag{A.13}$$

or

$$T(o,s) = \frac{\dot{q}(o,s)}{(\varrho ck)^{1/2}(s)^{1/2}} \tag{A.14}$$

The solution of Equation A.14 can be transformed back into the time domain to yield an equation relating the surface heat transfer to the surface temperature given by

$$T(o,t) = \frac{1}{(\pi \varrho ck)^{1/2}} \int_o^t \frac{\dot{q}(o,\lambda)}{(t-\lambda)^{1/2}} d\lambda \tag{A.15}$$

Equation A.14 can also be rearranged to yield the heat flux as a function of the surface temperature

$$\dot{q}(o,s) = (\varrho ck)^{1/2}(s)^{1/2} T(o,s) \tag{A.16}$$

$$= s\ T(o,s) \frac{1}{(s)^{1/2}} (\varrho ck)^{1/2} \tag{A.17}$$

Inverting Equation A.17 produces

$$\dot{q}(o,t) = \sqrt{\left(\frac{\varrho ck}{\pi}\right)} \int_o^t \frac{\frac{dT(o,\lambda)}{d\lambda}}{(t-\lambda)^{1/2}} d\lambda \tag{A.18}$$

Equation A.18 can be put in more convenient form through integrating by parts.

Recall that

$$\int_x^y u\,dv = uv \Big|_x^y - \int_x^y v\,du \tag{A.19}$$

Let

$$u = \frac{1}{(t-\lambda)^{1/2}} \tag{A.20}$$

$$du = -\frac{1}{2}(t-\lambda)^{-3/2}dt \tag{A.21}$$

$$dv = \frac{dt(o,\lambda)}{d\lambda}d\lambda \tag{A.22}$$

$$v = T(o,t) - T(o,\lambda) \tag{A.23}$$

It follows that

$$\dot{q}(o,t) = \sqrt{\left(\frac{\varrho ck}{\pi}\right)}\left[\frac{T(o,t)-T(o,\lambda)}{(t-\lambda)^{1/2}} + \frac{1}{2}\int_{o}^{t}\frac{T(o,t)-T(o,\lambda)}{(t-\lambda)^{3/2}}d\lambda\right] \tag{A.24}$$

for $\lambda = 0, T(\lambda) = 0$, which yields

$$\dot{q}(o,t) = \sqrt{\left(\frac{\varrho ck}{\pi}\right)}\left[\frac{T(o,t)}{(t)^{1/2}} + \frac{1}{2}\int_{o}^{t}\frac{T(o,t)-T(o,\lambda)}{(t-\lambda)^{3/2}}d\lambda\right] \tag{A.25}$$

This is now an equation relating surface heat flux to surface temperature. Equations A.15 and A.25 are the general solutions to the heat-conduction equation for constant thermal properties.

A.3 VARIABLE THERMAL PROPERTIES

If the properties do vary with temperature, the governing equation is non-linear. In order to attempt any reasonable solution process, one must first have an equation for the variation of property behavior with temperature.

Miller (Seymour[48]) presents empirical equations in his Appendix A, reproduced here as Figure A-2. As can be plainly seen from this curve, shock tube tests (which produce surface temperature changes from 30 to 150°F) create a change in temperature high enough to produce significant changes in the thermal properties of the substrate.

The physical effect of these property variations is an increase in the thermal conductivity of the substrate with increasing temperature. Thus, a given heat-flux value produces a lower rise in surface temperature than would be produced by a substrate whose properties remained fixed. Conversely, the heat flux inferred from a given surface-temperature history is larger when variable thermal properties are taken into account.

A.4 THE RAE-TAULBEE ALGORITHM

If the effects of variable thermal properties on the instantaneous heat flux are to be accounted for, there appears to be no alternative to solving the heat-conduction equation numerically. (Note, however, that corrections for varying thermal properties on the mean heat transfer rate were proposed by Miller.) Consequently, the constant-property data-reduction procedures must be replaced by a finite-difference solution of the governing equation.

In 1984, Rae (Seymour[48]) proposed a technique utilizing a Crank-Nicholson approach applying the Kirchhoff transformation:

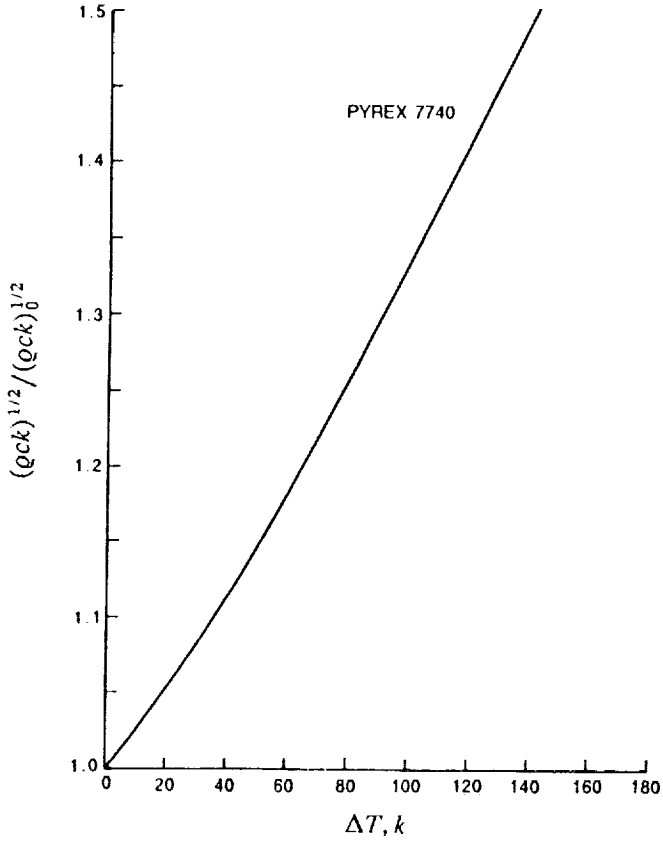

Figure A-2 VARIATION OF THERMAL PROPERTIES WITH TEMPERATURE

$$\xi = \int_{T_{ref}}^{T} \frac{k}{k_{ref}} dT \tag{A.26}$$

Application of this to Equation A.2 yields

$$\frac{\partial \xi}{\partial t} = \alpha \frac{\partial^2 \xi}{\partial x^2} \tag{A.27}$$

where $\alpha = \alpha(T)$.

The actual solved equation is a transformed version of Equation A.27 in which the x coordinate was scaled by the thermal penetration depth

$$\eta = \frac{x}{2(\alpha_{ref}\, t)^{1/2}} \quad \text{and} \quad t = \tau \,. \tag{A.28}$$

In these variables, Equation A.27 becomes

$$\frac{\alpha}{\alpha_{ref}} \frac{\partial^2 \xi}{\partial \eta^2} + 2\eta \frac{\partial \xi}{\partial \eta} = 4\tau \frac{\partial \xi}{\partial \tau} \tag{A.29}$$

This formulation has the advantage that the spatial scale is uniform in time. Numerical solutions using a fixed step size $\Delta\eta$ can then be found, for given values of ξ at the surface, and for ξ approaching 0 when η is on the order of 3 to 5.

The above coordinate transformation is based on the assumption that the thermal penetration depth $\sqrt{(\alpha t)}$ is the significant length scale in the problem. That this is indeed the case can be seen from the analytic solution for the constant-property case for a step-function time variation of the surface heat transfer; the equation shown below, from Carslaw, yields

$$\dot{q}(t) = \dot{q}_o(t) \tag{A.30}$$

$$T(x,t) - T_{initial} = \dot{q}\left\{\frac{2}{k}\left(\frac{\alpha t}{\pi}\right)^{1/2}\exp\left(-\frac{x^2}{4\alpha t}\right) - \frac{x}{k}erfc\left(\frac{x}{2(\alpha t)^{1/2}}\right)\right\} \tag{A.31}$$

In particular, for $x = 0$, Equation A.31 gives

$$T(o,t) - T_{initial} = \dot{q}\frac{2}{k}\sqrt{\left(\frac{\alpha t}{\pi}\right)}. \tag{A.32}$$

Unfortunately, in spite of the obvious advantage of solving the equations for fixed $\Delta\eta$, serious errors can be introduced in the calculation of unsteady heat fluxes. This is because when the heat transfer rate contains a part that fluctuates at frequency ω (the radial frequency $\omega = 2\pi f$ has been used here for convenience), a second length scale enters the problem—namely, $(\alpha/\omega)^{1/2}$, called the skin depth. This can be seen from the classical solution of a sinusoidal surface-temperature variation, from Carslaw. When

$$\Delta T_{surface} = A\cos\omega t\ , \tag{A.33}$$

the solution to Equation (A.2) contains an early time transient plus the solution:

$$\Delta T(x,t) = A\exp\ \{-x(\omega/\alpha x)^{1/2}\}\cos\{\omega t - x(\omega/\alpha)^{1/2}\} \tag{A.34}$$

Thus, the high-frequency portion of the surface-temperature rise has a very shallow penetration, and care must be taken in the numerical work to resolve this thin layer properly.

Solutions of Equation A.29 that use a fixed step size in the η-direction will have a small value of Δx at early time and a large one at late time. It was found, during the course of this research, that, for blade passing frequencies of interest here, this procedure loses accuracy at late time. Accordingly, a revised procedure was adopted.

This revised procedure uses a simple-implicit algorithm given by:

$$\frac{\xi(i,j+1) - \xi(i,j)}{t_{j+1} - t_j} = \alpha(x_j, t_j)\ \frac{\xi(i+1,j+1) - 2\xi(i,j+1) + \xi(i-1,j+1)}{(\Delta x)^2} \tag{A.35}$$

where ξ is defined as before. Equation A.35 was solved on a grid of variable size. At every time step, the boundary condition of zero temperature rise was enforced at a depth of $7(\alpha_{ref}\, t)^{1/2}$. The heat transfer rate

was found from a second-order-accurate expression for the derivative at the surface. As noted in Richtmeyer, this algorithm is capable of following a rapidly fluctuating temperature more accurately than its Crank-Nicholson counterpart.

Implicit numerical procedures work best when the step size ratio

$$r = \frac{\alpha \Delta t}{(\Delta x)^2} \tag{A.36}$$

is in the range 0.25 to 0.5. By varying the quantity r, its optimum value was found to be 0.5 for our particular test conditions and data. The sampling interval Δt is taken, on the basis of the Nyquist sampling theorem, to be inversely proportional to the highest frequency of interest

$$\Delta t \sim \frac{\pi}{\omega} \sim \frac{1}{2f}. \tag{A.37}$$

The spatial step size Δx must be small enough to resolve the skin depth; thus,

$$\Delta x \sim \left(\frac{\alpha}{\omega}\right)^{1/2} \tag{A.38}$$

Therefore, a constant value of the step size ratio (r) of 0.5 or less will satisfy both of these criteria.

Appendix B
SHOCK/SHOCK-INTERACTION STUDY DATA

Test Conditions, Heat Transfer and Pressure Measurements, Schlieren Photographs, and Reduced Data Tabulations

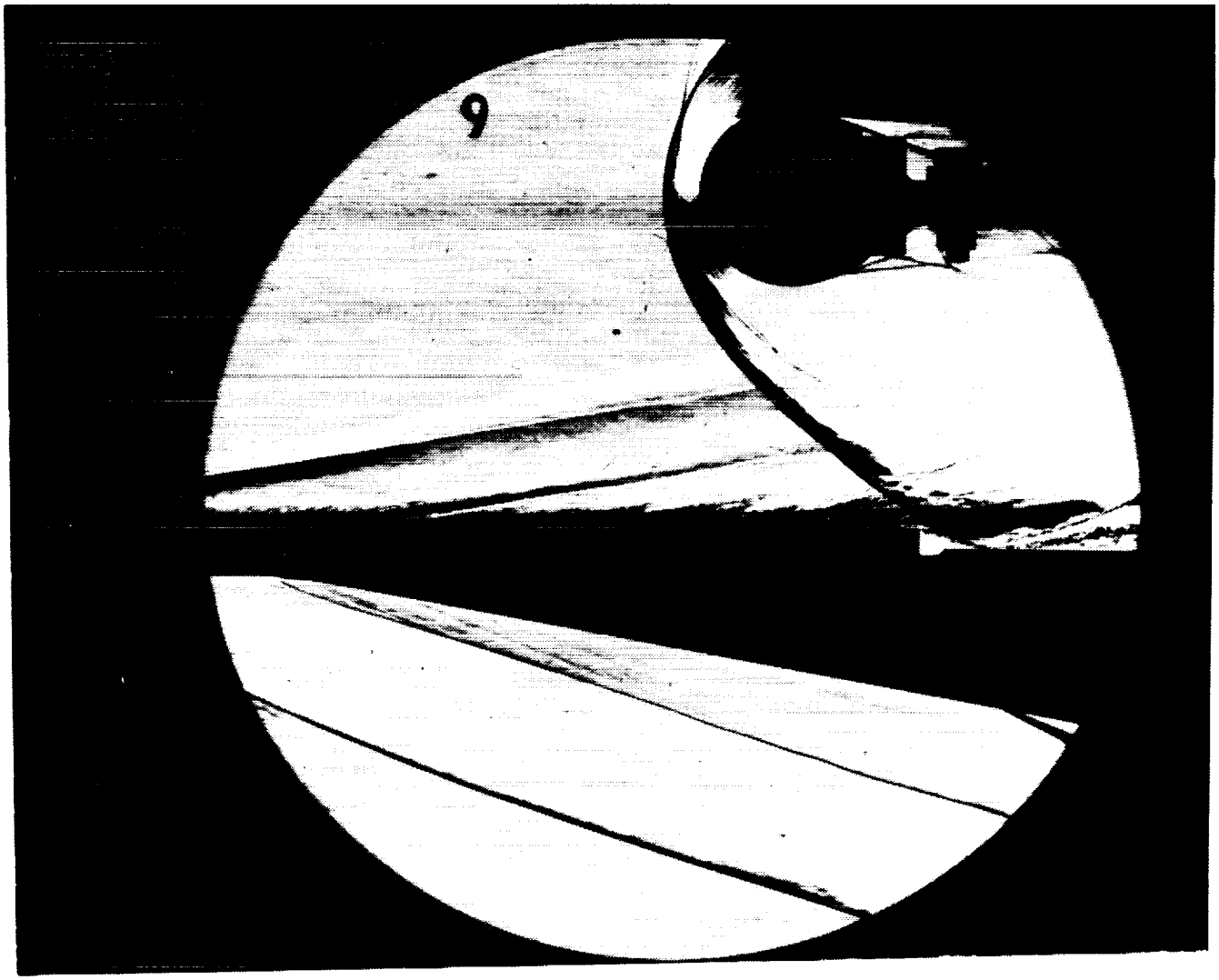

Test Conditions for Run 9 :

Po	= 1.434E+03 PSIA	Reservoir Total Pressure
Ho	= 1.438E-07 (Ft/sec)²	Reservoir Total Enthalpy
To	= 2.243E-03 °R	Reservoir Total Temperature
M	= 6.347E-00	Freestream Mach Number
U	= 5.060E+03 Ft/sec	Freestream Velocity
T	= 2.643E+02 °R	Freestream Temperature
P	= 6.100E-01 PSIA	Freestream Static Pressure
Rho	= 1.937E-04 Slugs/Ft3	Freestream Density
Mu	= 2.155E-07 Slugs/Ft-sec	Freestream Viscosity
Re	= 4.548E+06 1/Ft	Freestream Reynolds Number
Po'	= 3.212E+01 PSIA	Pitot Pressure
Q	= 1.722E+01 PSIA	Dynamic Pressure (½·Rho·U²/144)
Mi	= 2.953E+00	Shock Tube Incident Shock Mach Number
Hw	= 3.183E+06 (Ft/sec)²	Wall Enthalpy (Cp·Tw)
CPf	= 5.808E-02 1/PSIA	Pressure to CP factor (1/Q)
CHf	= 7.093E-05 Ft²-s/BTU	Heat Rate to CH factor (778/(Rho·U·(Ho-Hw))
QoFR	= 5.093E+01 BTU/Ft²-s	Fay-Riddell Heat Transfer to 3" Diam Sphere

Model Configuration Parameter	Value
Stagnation Position (gauge label)	P18
Sweep Angle (degrees)	0.00

Run 9

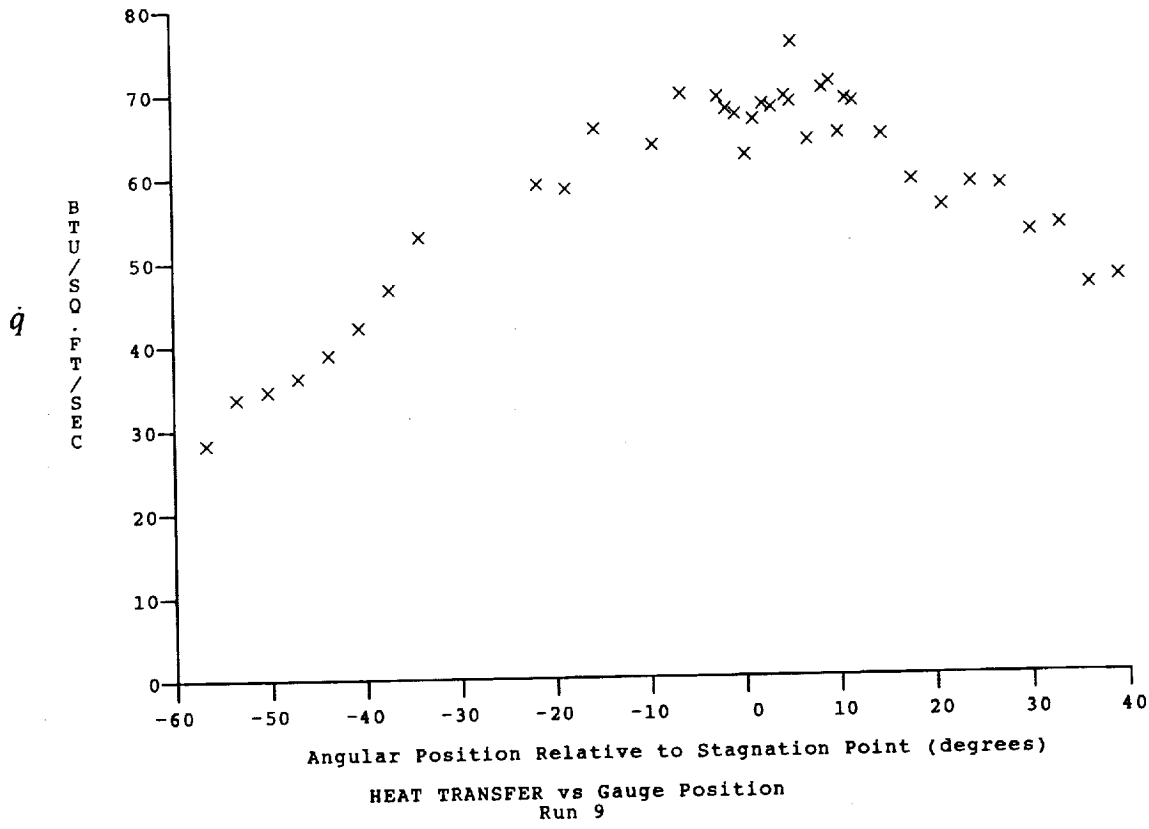

HEAT TRANSFER vs Gauge Position
Run 9

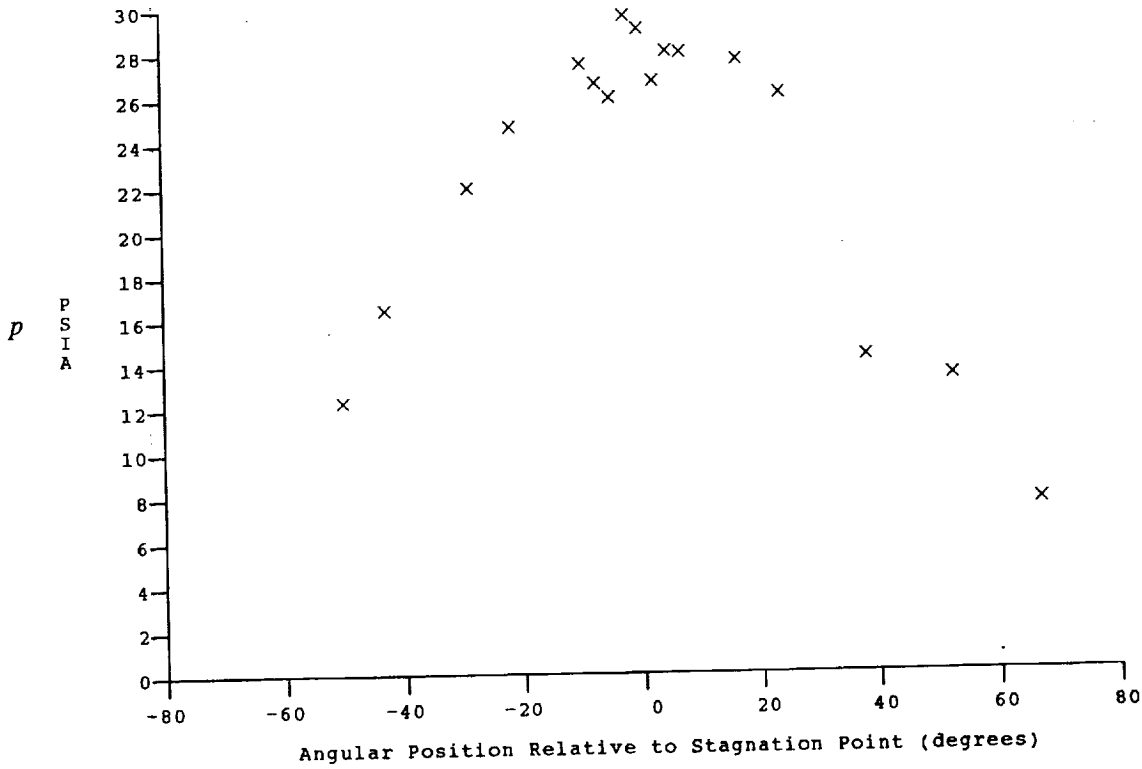

PRESSURE vs Gauge Position
Run 9

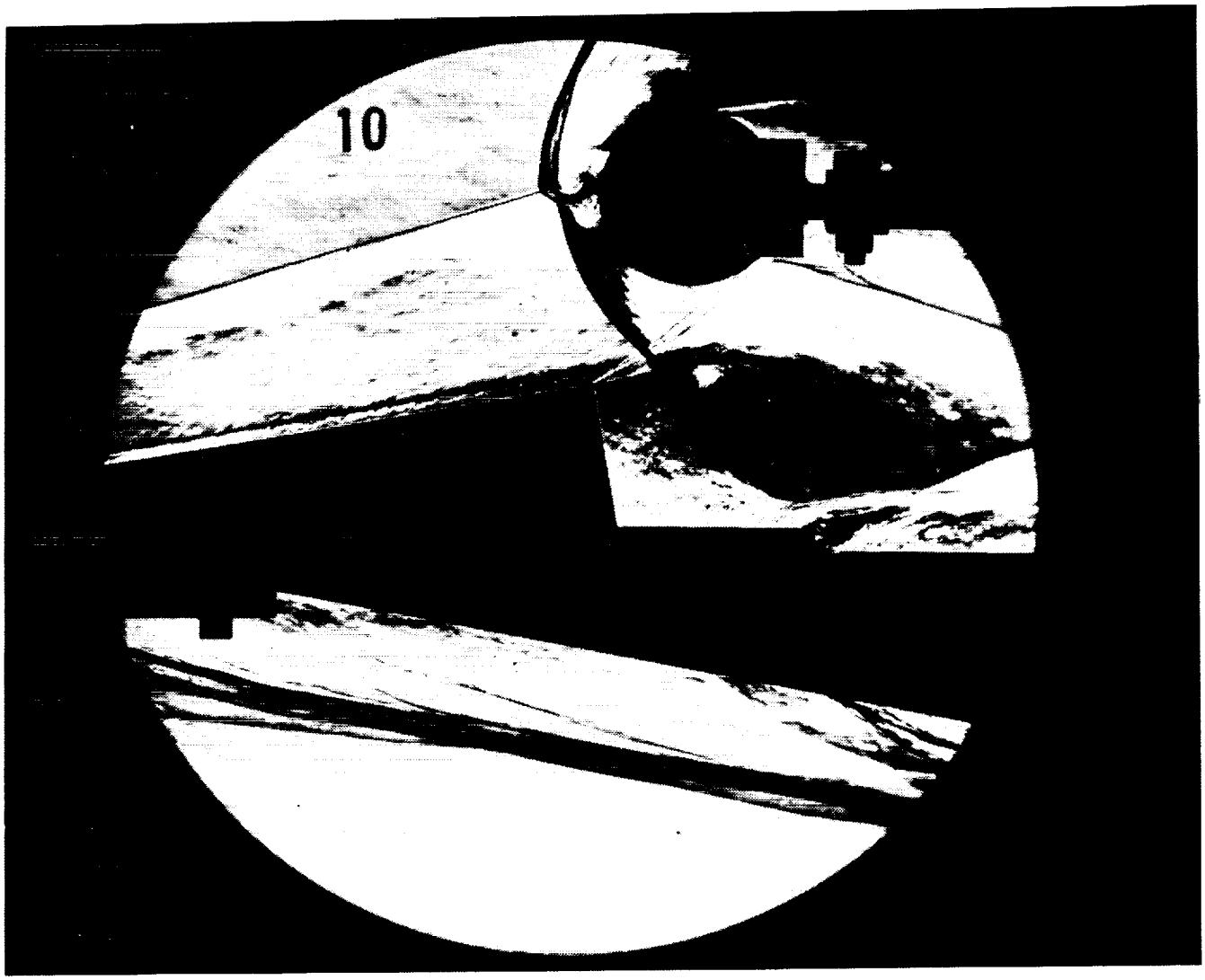

Test Conditions for Run 10 :

Po	= 1.379E-03	PSIA	Reservoir Total Pressure
Ho	= 1.422E-07	(Ft/sec)²	Reservoir Total Enthalpy
To	= 2.223E+03	°R	Reservoir Total Temperature
M	= 6.351E+00		Freestream Mach Number
U	= 5.033E+03	Ft/sec	Freestream Velocity
T	= 2.612E-02	°R	Freestream Temperature
P	= 5.856E-01	PSIA	Freestream Static Pressure
Rho	= 1.881E-04	Slugs/Ft3	Freestream Density
Mu	= 2.132E-07	Slugs/Ft-sec	Freestream Viscosity
Re	= 4.441E+06	1/Ft	Freestream Reynolds Number
Po'	= 3.087E+01	PSIA	Pitot Pressure
Q	= 1.655E+01	PSIA	Dynamic Pressure (½·Rho·U²/144)
Mi	= 2.922E+00		Shock Tube Incident Shock Mach Number
Hw	= 3.183E+06	(Ft/sec)²	Wall Enthalpy (Cp·Tw)
CPf	= 6.042E-02	1/PSIA	Pressure to CP factor (1/Q)
CHf	= 7.441E-05	Ft²-s/BTU	Heat Rate to CH factor (778/(Rho·U·(Ho-Hw))
QoFR	= 4.922E+01	BTU/Ft²-s	Fay-Riddell Heat Transfer to 3" Diam Sphere

Model Configuration Parameter	Value
Stagnation Position (gauge label)	P18
Vertical Distance (inches)	3.20
Horizontal Distance (inches)	0.09
Plate Angle (degrees)	10.00
Plate Length (inches)	26.50
Sweep Angle (degrees)	0.00

Run 10

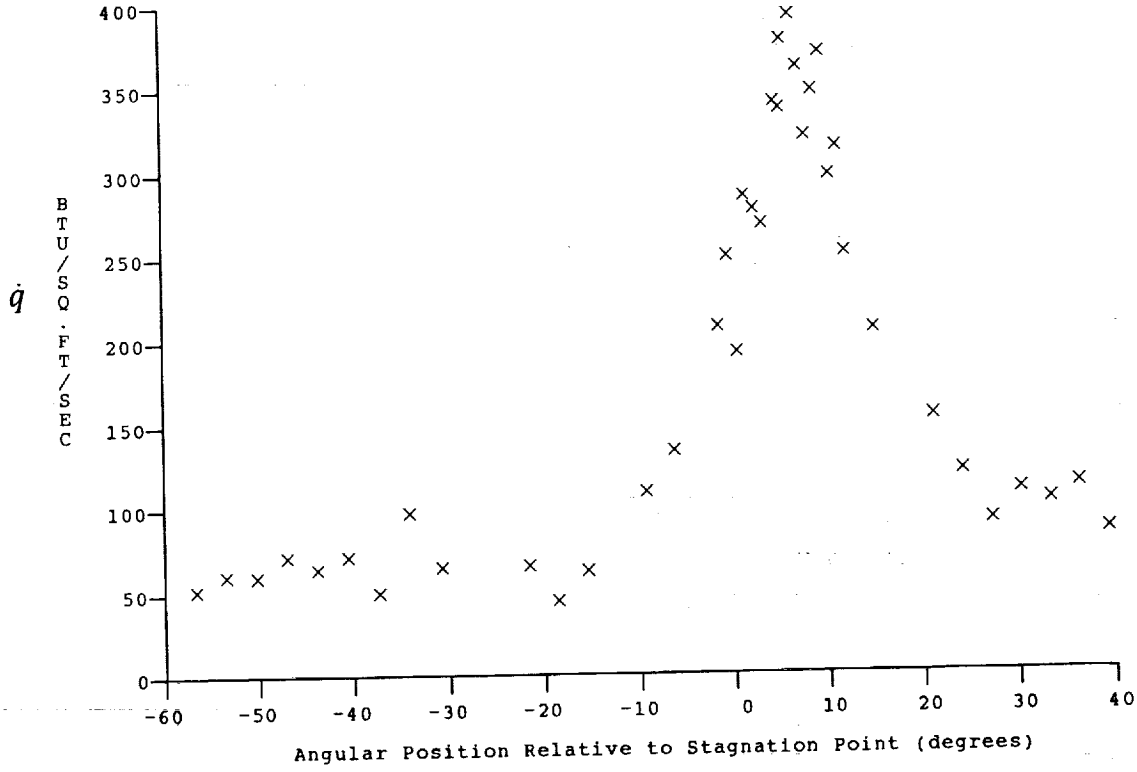

HEAT TRANSFER vs Gauge Position
Run 10

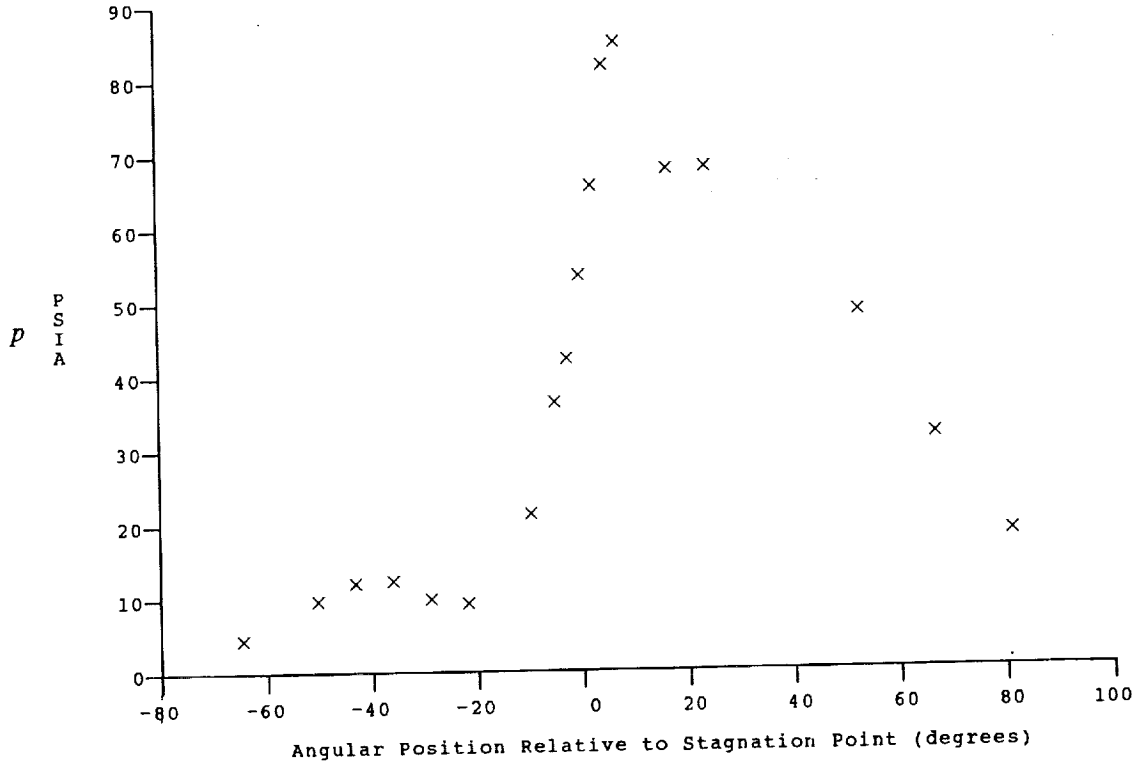

PRESSURE vs Gauge Position
Run 10

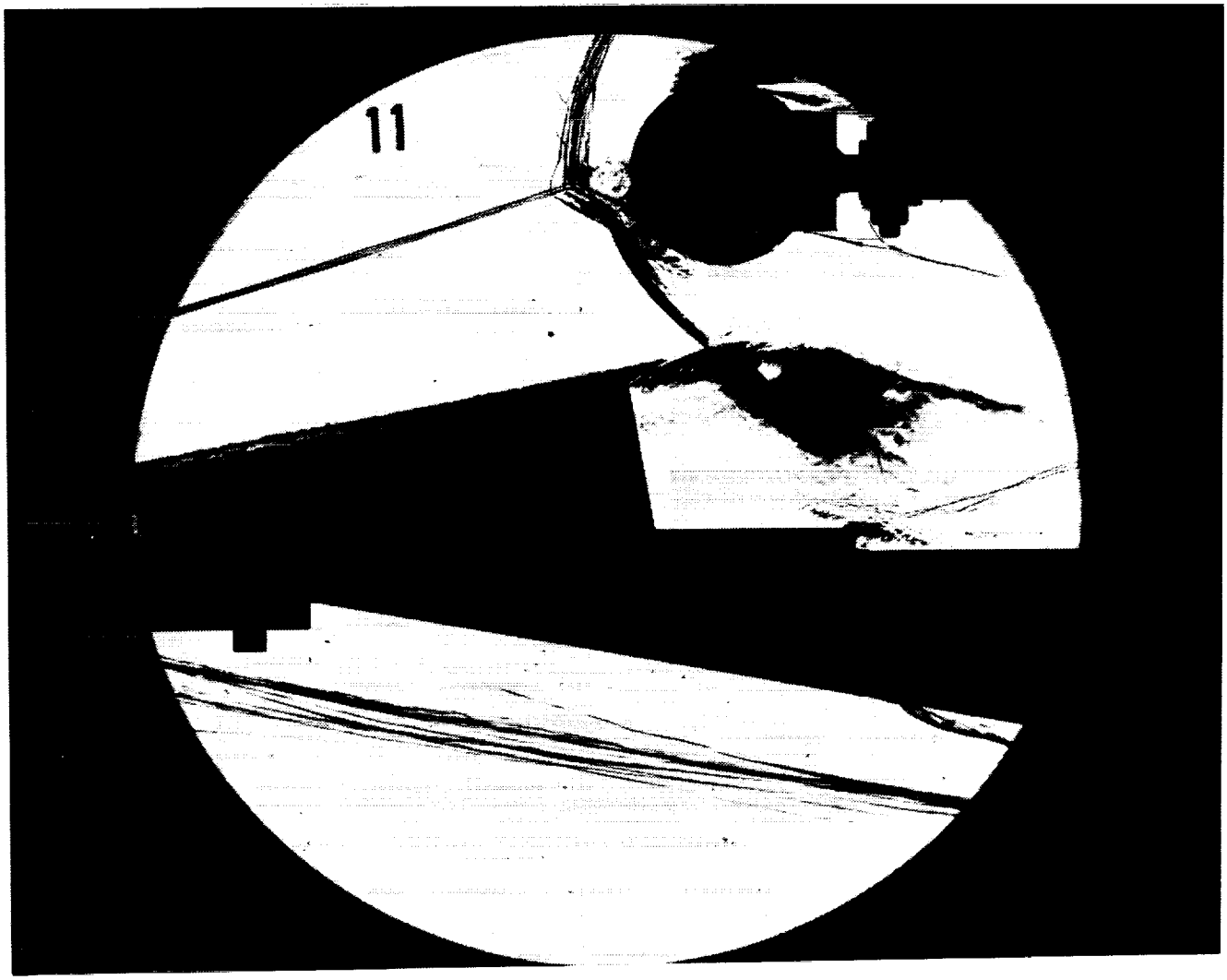

Test Conditions for Run 11 :

Po	= 1.374E-03	PSIA	Reservoir Total Pressure
Ho	= 1.435E+07	(Ft/sec)²	Reservoir Total Enthalpy
To	= 2.241E+03	°R	Reservoir Total Temperature
M	= 6.353E-00		Freestream Mach Number
U	= 5.055E+03	Ft/sec	Freestream Velocity
T	= 2.633E+02	°R	Freestream Temperature
P	= 5.807E-01	PSIA	Freestream Static Pressure
Rho	= 1.851E-04	Slugs/Ft3	Freestream Density
Mu	= 2.148E-07	Slugs/Ft-sec	Freestream Viscosity
Re	= 4.357E+06	1/Ft	Freestream Reynolds Number
Po'	= 3.064E+01	PSIA	Pitot Pressure
Q	= 1.642E+01	PSIA	Dynamic Pressure (½·Rho·U²/144)
Mi	= 2.910E+00		Shock Tube Incident Shock Mach Number
Hw	= 3.183E+06	(Ft/sec)²	Wall Enthalpy (Cp·Tw)
CPf	= 6.089E-02	1/PSIA	Pressure to CP factor (1/Q)
CHf	= 7.449E-05	Ft²-s/BTU	Heat Rate to CH factor (778/(Rho·U·(Ho-Hw))
QoFR	= 4.961E-01	BTU/Ft²-s	Fay-Riddell Heat Transfer to 3" Diam Sphere

Model Configuration Parameter	Value
Stagnation Position (gauge label)	P18
Vertical Distance (inches)	3.55
Horizontal Distance (inches)	0.05
Plate Angle (degrees)	10.00
Plate Length (inches)	26.50
Sweep Angle (degrees)	0.00

Run 11

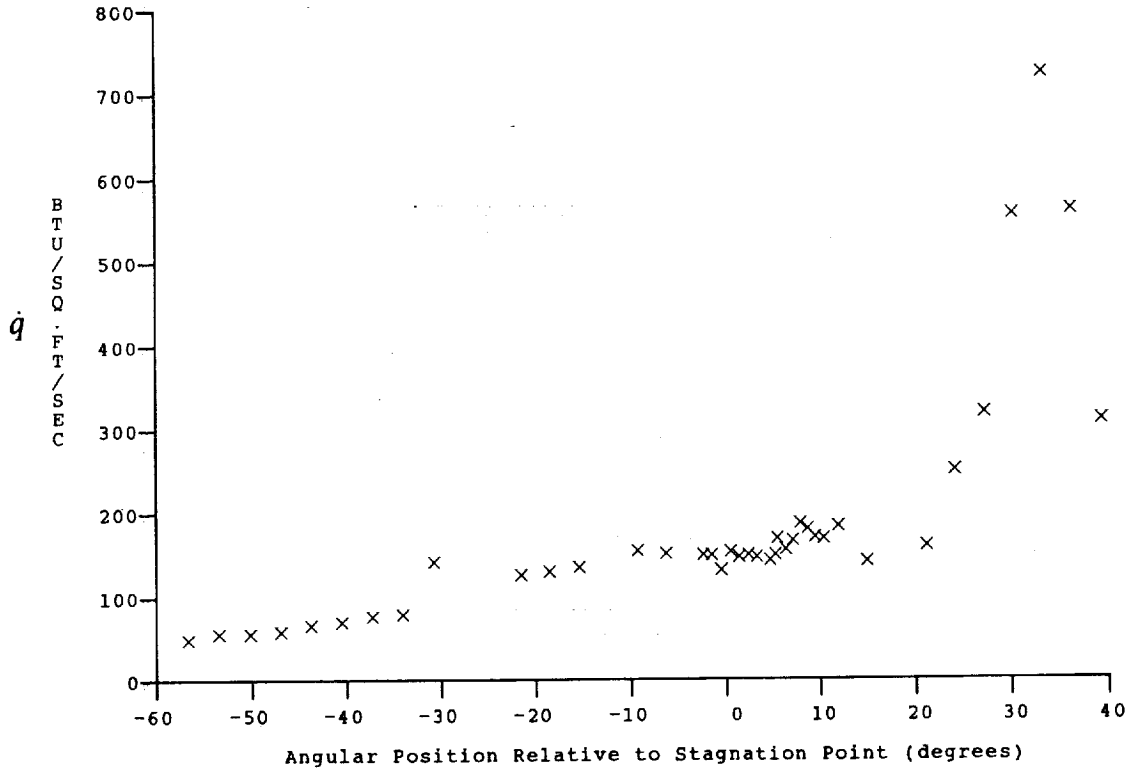

HEAT TRANSFER vs Gauge Position
Run 11

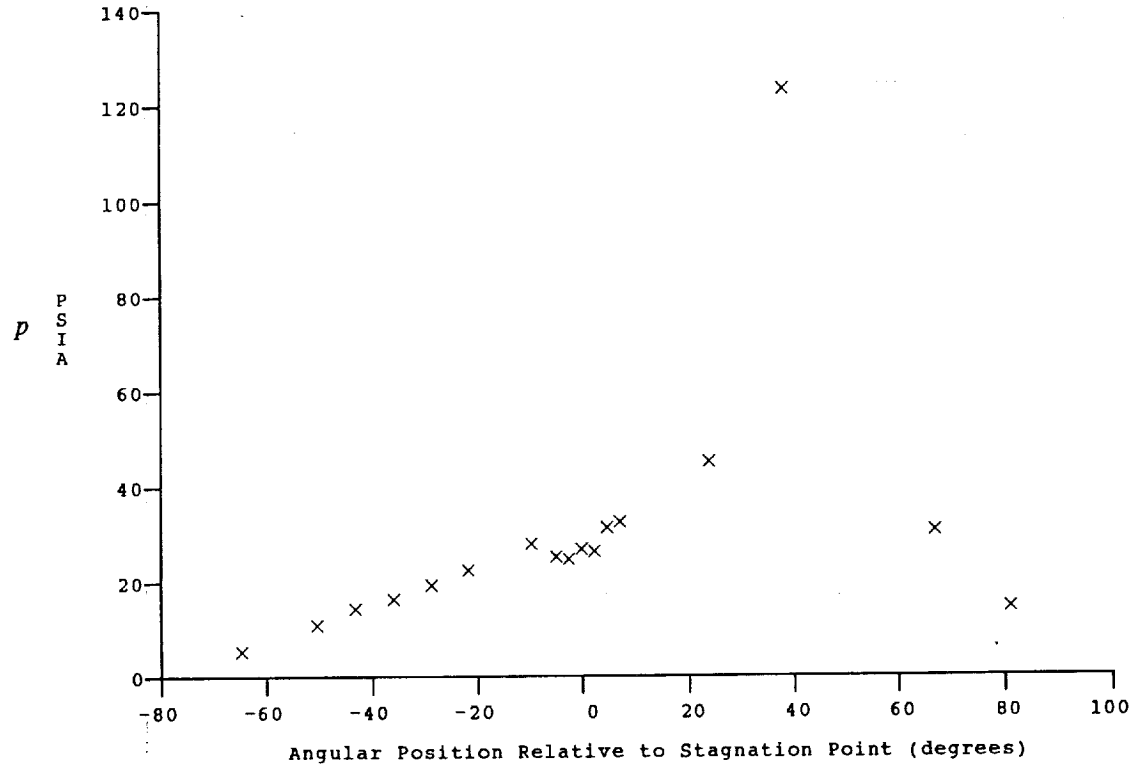

PRESSURE vs Gauge Position
Run 11

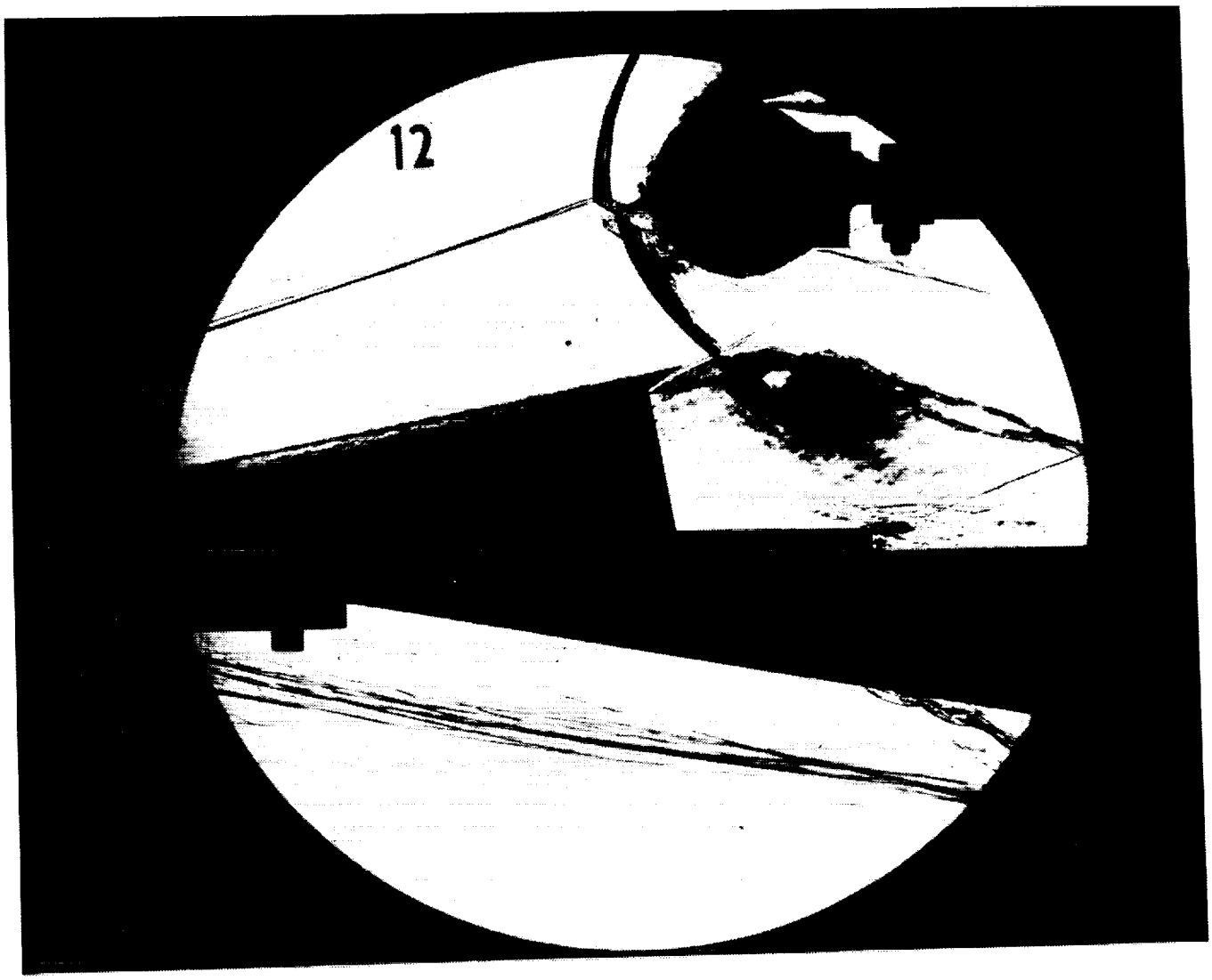

Test Conditions for Run 12 :

Po	= 1.387E-03	PSIA	Reservoir Total Pressure
Ho	= 1.458E+07	(Ft/sec)²	Reservoir Total Enthalpy
To	= 2.275E-03	°R	Reservoir Total Temperature
M	= 6.350E+00		Freestream Mach Number
U	= 5.096E+03	Ft/sec	Freestream Velocity
T	= 2.678E+02	°R	Freestream Temperature
P	= 5.858E-01	PSIA	Freestream Static Pressure
Rho	= 1.836E-04	Slugs/Ft3	Freestream Density
Mu	= 2.181E-07	Slugs/Ft-sec	Freestream Viscosity
Re	= 4.288E+06	1/Ft	Freestream Reynolds Number
Po'	= 3.088E+01	PSIA	Pitot Pressure
Q	= 1.655E+01	PSIA	Dynamic Pressure (½·Rho·U²/144)
Mi	= 2.929E+00		Shock Tube Incident Shock Mach Number
Hw	= 3.183E+06	(Ft/sec)²	Wall Enthalpy (Cp·Tw)
CPf	= 6.043E-02	1/PSIA	Pressure to CP factor (1/Q)
CHf	= 7.300E-05	Ft²-s/BTU	Heat Rate to CH factor (778/(Rho·U·(Ho-Hw))
QoFR	= 5.090E+01	BTU/Ft²-s	Fay-Riddell Heat Transfer to 3" Diam Sphere

Model Configuration Parameter	Value
Stagnation Position (gauge label)	P21
Vertical Distance (inches)	3.34
Horizontal Distance (inches)	0.06
Plate Angle (degrees)	10.00
Plate Length (inches)	26.50
Sweep Angle (degrees)	0.00

Run 12

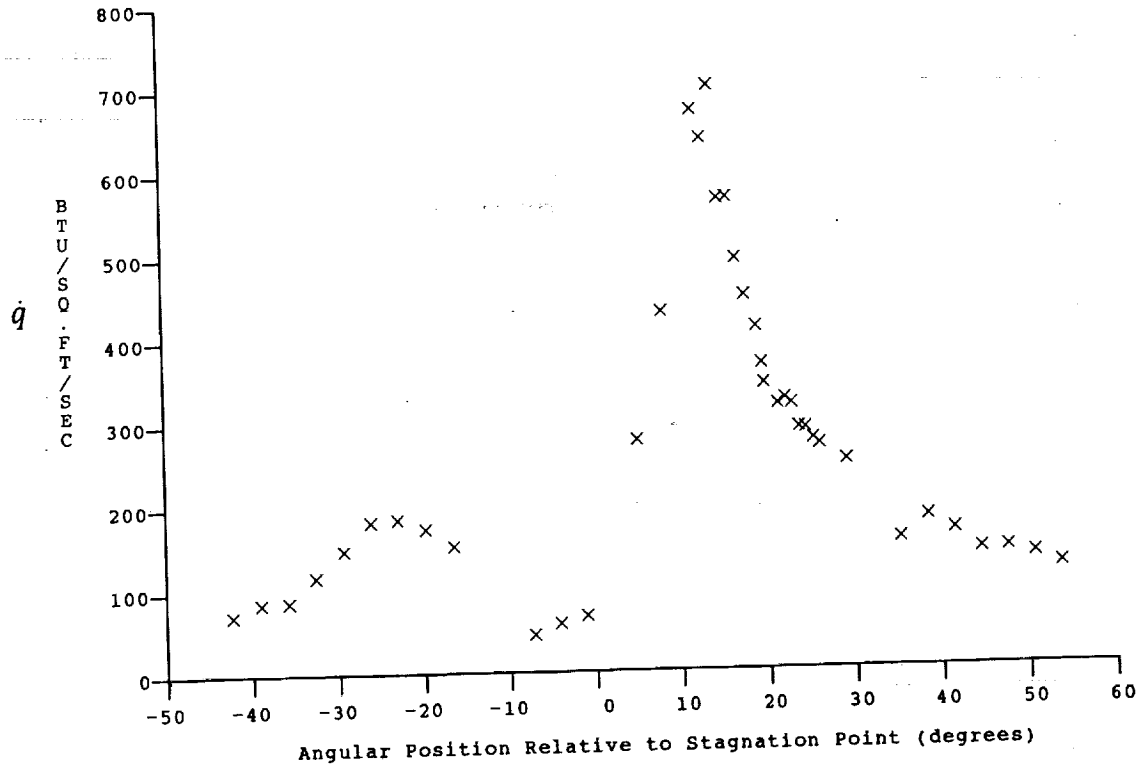

HEAT TRANSFER vs Gauge Position
Run 12

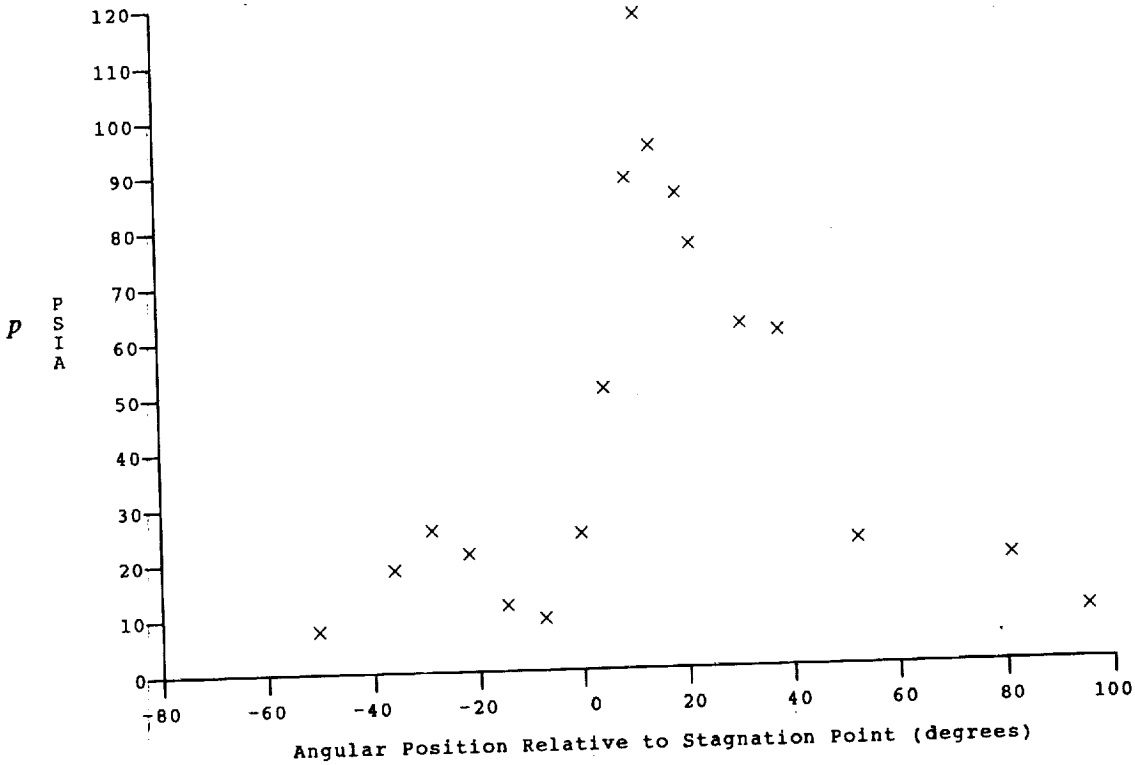

PRESSURE vs Gauge Position
Run 12

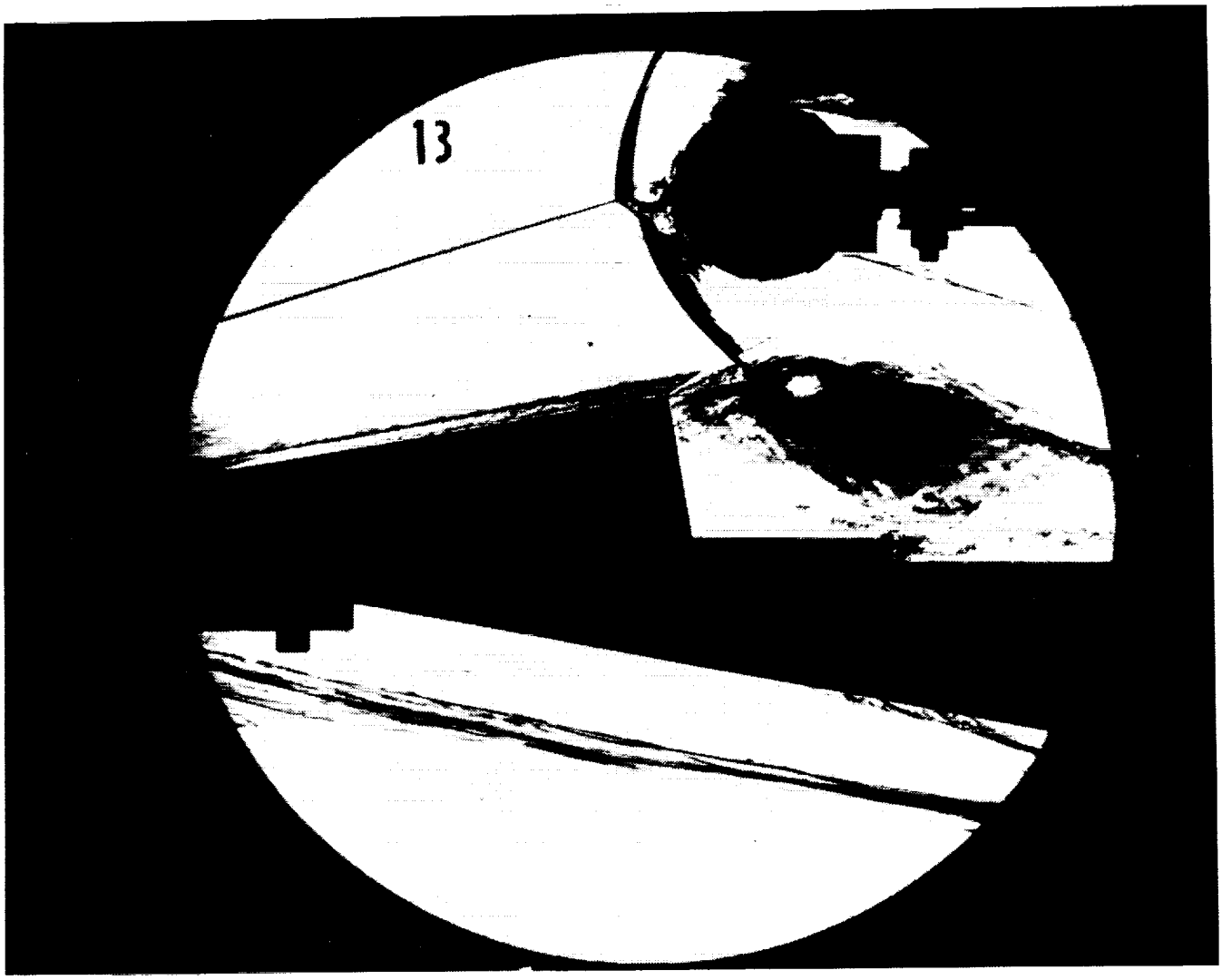

Test Conditions for Run 13 :

Po	= 1.402E+03	PSIA	Reservoir Total Pressure
Ho	= 1.435E+07	(Ft/sec)²	Reservoir Total Enthalpy
To	= 2.243E+03	°R	Reservoir Total Temperature
M	= 6.355E+00		Freestream Mach Number
U	= 5.057E+03	Ft/sec	Freestream Velocity
T	= 2.633E+02	°R	Freestream Temperature
P	= 5.916E-01	PSIA	Freestream Static Pressure
Rho	= 1.886E-04	Slugs/Ft3	Freestream Density
Mu	= 2.148E-07	Slugs/Ft-sec	Freestream Viscosity
Re	= 4.440E+06	1/Ft	Freestream Reynolds Number
Po'	= 3.123E+01	PSIA	Pitot Pressure
Q	= 1.674E+01	PSIA	Dynamic Pressure (½·Rho·U²/144)
Mi	= 2.909E+00		Shock Tube Incident Shock Mach Number
Hw	= 3.183E+06	(Ft/sec)²	Wall Enthalpy (Cp·Tw)
CPf	= 5.973E-02	1/PSIA	Pressure to CP factor (1/Q)
CHf	= 7.305E-05	Ft²-s/BTU	Heat Rate to CH factor (778/(Rho·U·(Ho-Hw))
QoFR	= 5.012E+01	BTU/Ft²-s	Fay-Riddell Heat Transfer to 3" Diam Sphere

Model Configuration Parameter	Value
Stagnation Position (gauge label)	P18
Vertical Distance (inches)	3.34
Horizontal Distance (inches)	0.06
Plate Angle (degrees)	10.00
Plate Length (inches)	26.50
Sweep Angle (degrees)	0.00

Run 13

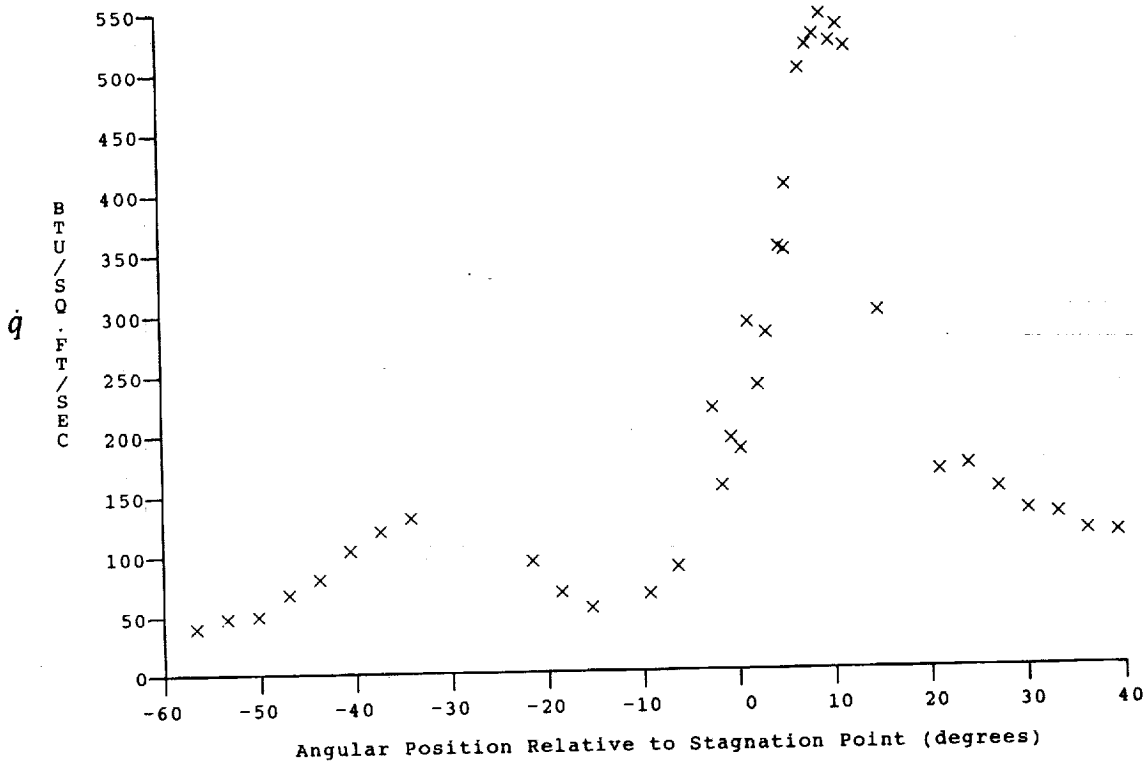

HEAT TRANSFER vs Gauge Position
Run 13

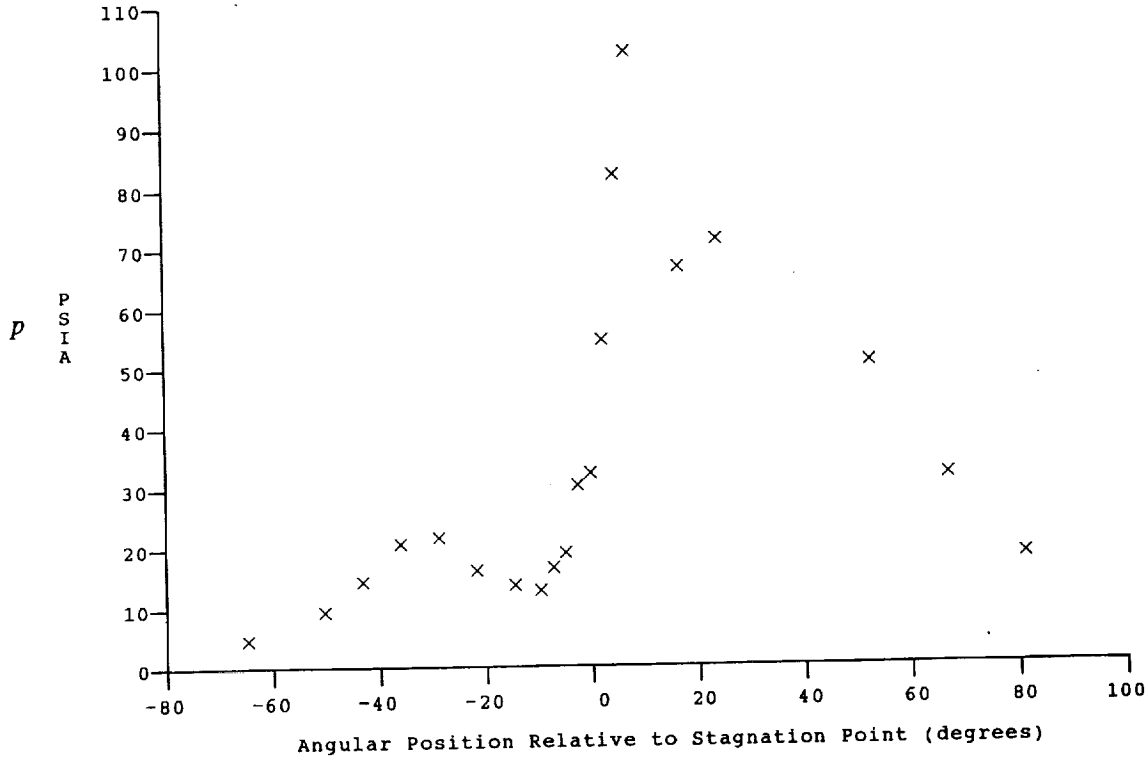

PRESSURE vs Gauge Position
Run 13

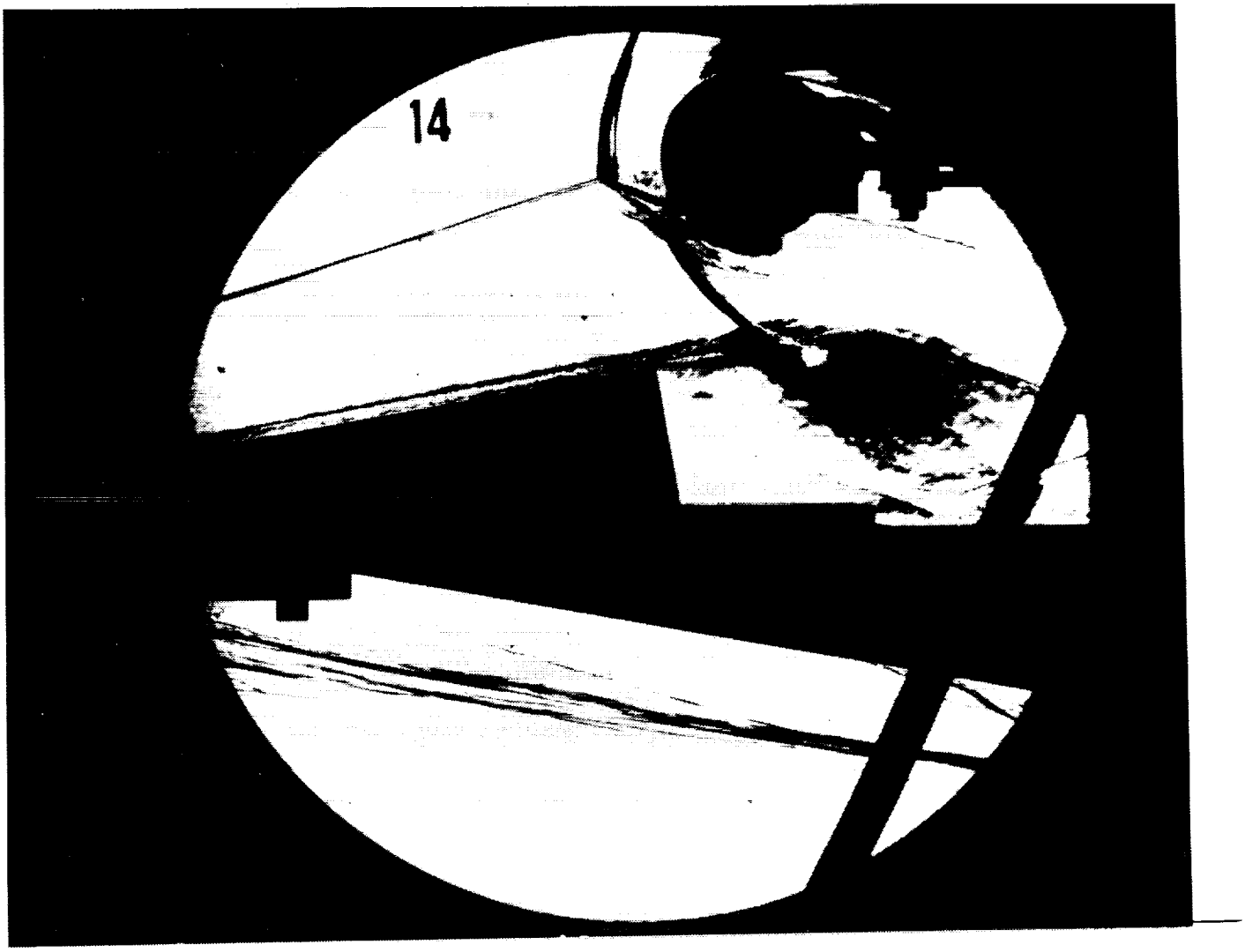

Test Conditions for Run 14 :

Po	= 1.436E-03	PSIA	Reservoir Total Pressure
Ho	= 1.407E+07	$(Ft/sec)^2$	Reservoir Total Enthalpy
To	= 2.201E+03	°R	Reservoir Total Temperature
M	= 6.357E-00		Freestream Mach Number
U	= 5.007E+03	Ft/sec	Freestream Velocity
T	= 2.580E+02	°R	Freestream Temperature
P	= 6.083E-01	PSIA	Freestream Static Pressure
Rho	= 1.979E-04	Slugs/Ft3	Freestream Density
Mu	= 2.108E-07	Slugs/Ft-sec	Freestream Viscosity
Re	= 4.700E+06	1/Ft	Freestream Reynolds Number
Po'	= 3.213E+01	PSIA	Pitot Pressure
Q	= 1.723E+01	PSIA	Dynamic Pressure (½·Rho·U^2/144)
Mi	= 2.909E+00		Shock Tube Incident Shock Mach Number
Hw	= 3.183E+06	$(Ft/sec)^2$	Wall Enthalpy (Cp·Tw)
CPf	= 5.805E-02	1/PSIA	Pressure to CP factor (1/Q)
CHf	= 7.211E-05	Ft^2-s/BTU	Heat Rate to CH factor (778/(Rho·U·(Ho-Hw))
QoFR	= 4.948E+01	BTU/Ft^2-s	Fay-Riddell Heat Transfer to 3" Diam Sphere

Model Configuration Parameter	Value
Stagnation Position (gauge label)	P23
Vertical Distance (inches)	3.55
Horizontal Distance (inches)	0.09
Plate Angle (degrees)	10.00
Plate Length (inches)	26.50
Sweep Angle (degrees)	0.00

Run 14

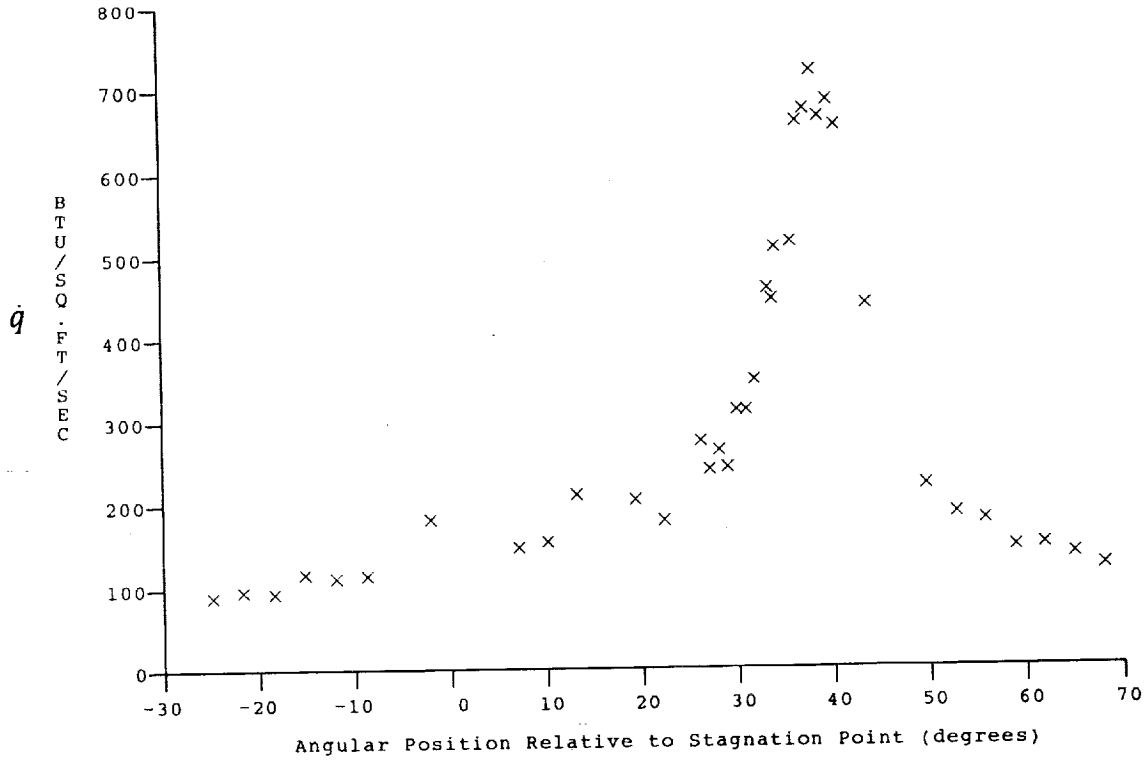

HEAT TRANSFER vs Gauge Position
Run 14

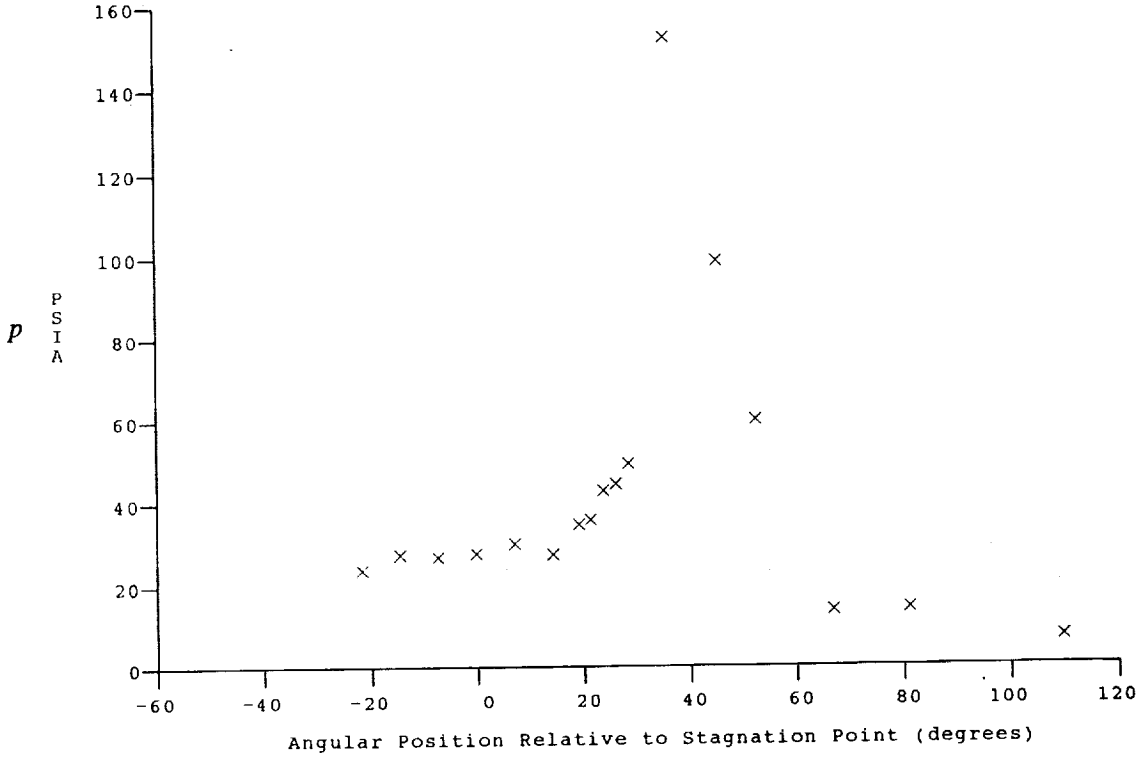

PRESSURE vs Gauge Position
Run 14

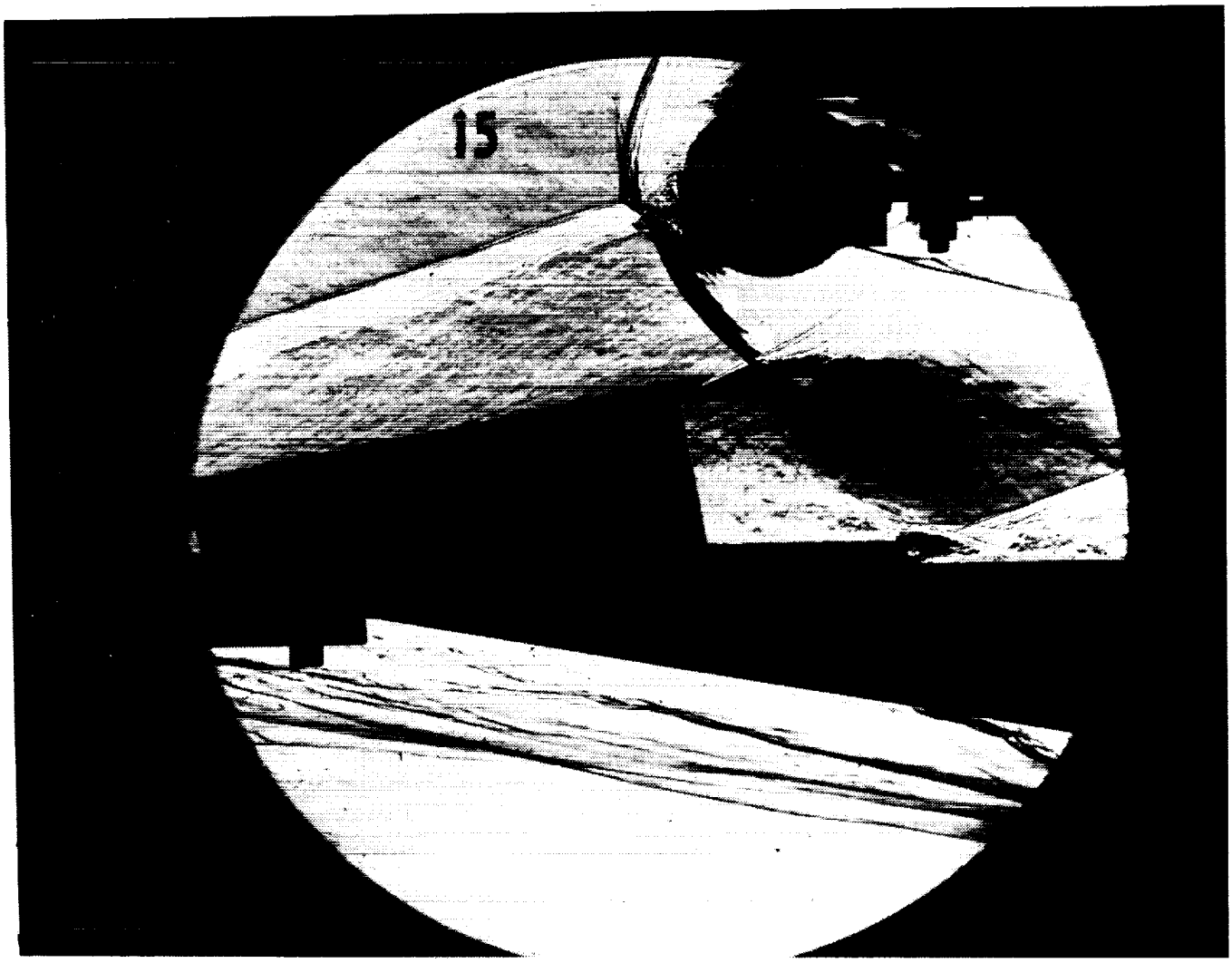

Test Conditions for Run 15 :

Po	= 6.650E+02 PSIA	Reservoir Total Pressure	
Ho	= 1.336E+07 (Ft/sec)²	Reservoir Total Enthalpy	
To	= 2.100E+03 °R	Reservoir Total Temperature	
M	= 6.325E+00	Freestream Mach Number	
U	= 4.875E-03 Ft/sec	Freestream Velocity	
T	= 2.470E+02 °R	Freestream Temperature	
P	= 2.895E-01 PSIA	Freestream Static Pressure	
Rho	= 9.834E-05 Slugs/Ft3	Freestream Density	
Mu	= 2.026E-07 Slugs/Ft-sec	Freestream Viscosity	
Re	= 2.366E+06 1/Ft	Freestream Reynolds Number	
Po'	= 1.512E+01 PSIA	Pitot Pressure	
Q	= 8.116E+00 PSIA	Dynamic Pressure (½·Rho·U²/144)	
Mi	= 2.820E+00	Shock Tube Incident Shock Mach Number	
Hw	= 3.183E+06 (Ft/sec)²	Wall Enthalpy (Cp·Tw)	
CPf	= 1.232E-01 1/PSIA	Pressure to CP factor (1/Q)	
CHf	= 1.595E-04 Ft²-s/BTU	Heat Rate to CH factor (778/(Rho·U·(Ho-Hw))	
QoFR	= 3.159E+01 BTU/Ft²-s	Fay-Riddell Heat Transfer to 3" Diam Sphere	

Model Configuration Parameter	Value
Stagnation Position (gauge label)	P23
Vertical Distance (inches)	3.55
Horizontal Distance (inches)	0.09
Plate Angle (degrees)	10.00
Plate Length (inches)	26.50
Sweep Angle (degrees)	0.00

Run 15

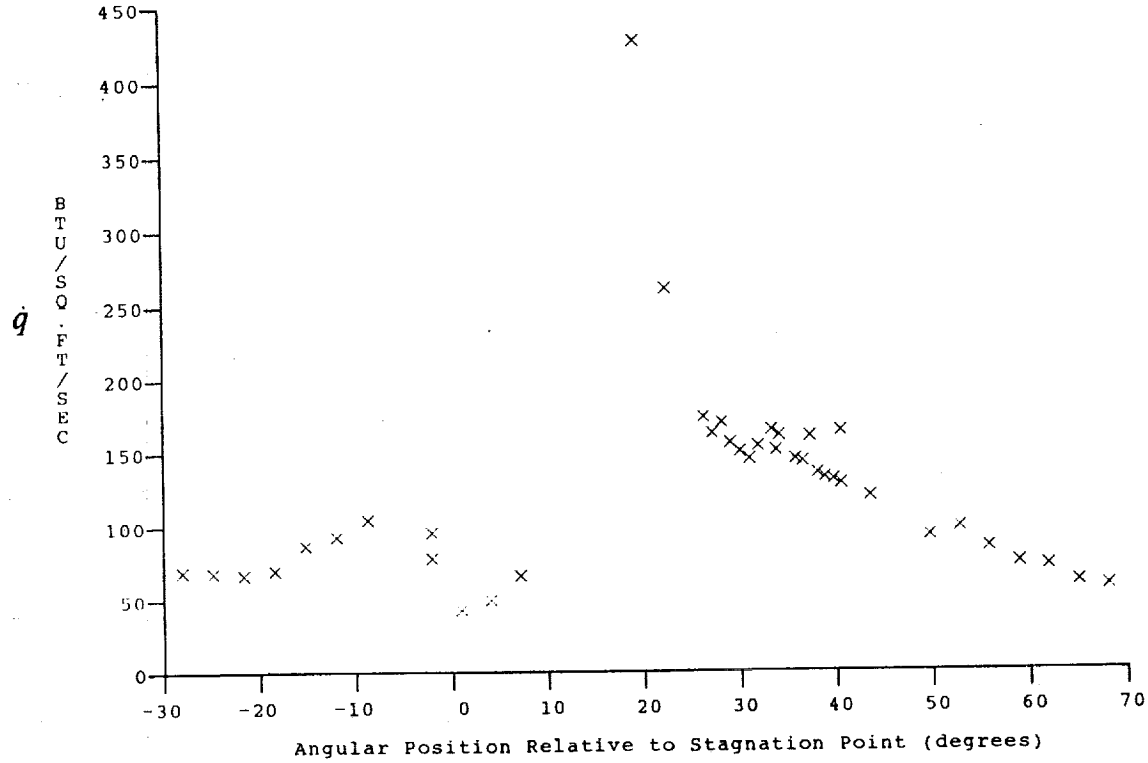

HEAT TRANSFER vs Gauge Position
Run 15

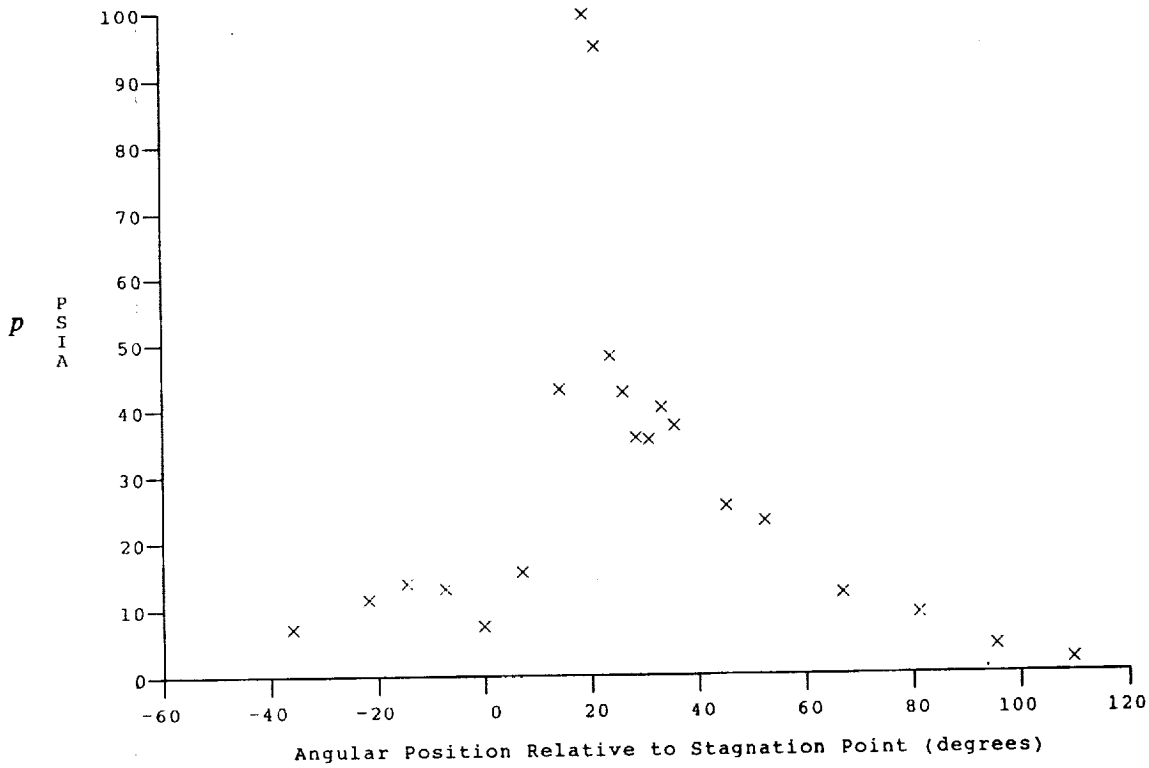

PRESSURE vs Gauge Position
Run 15

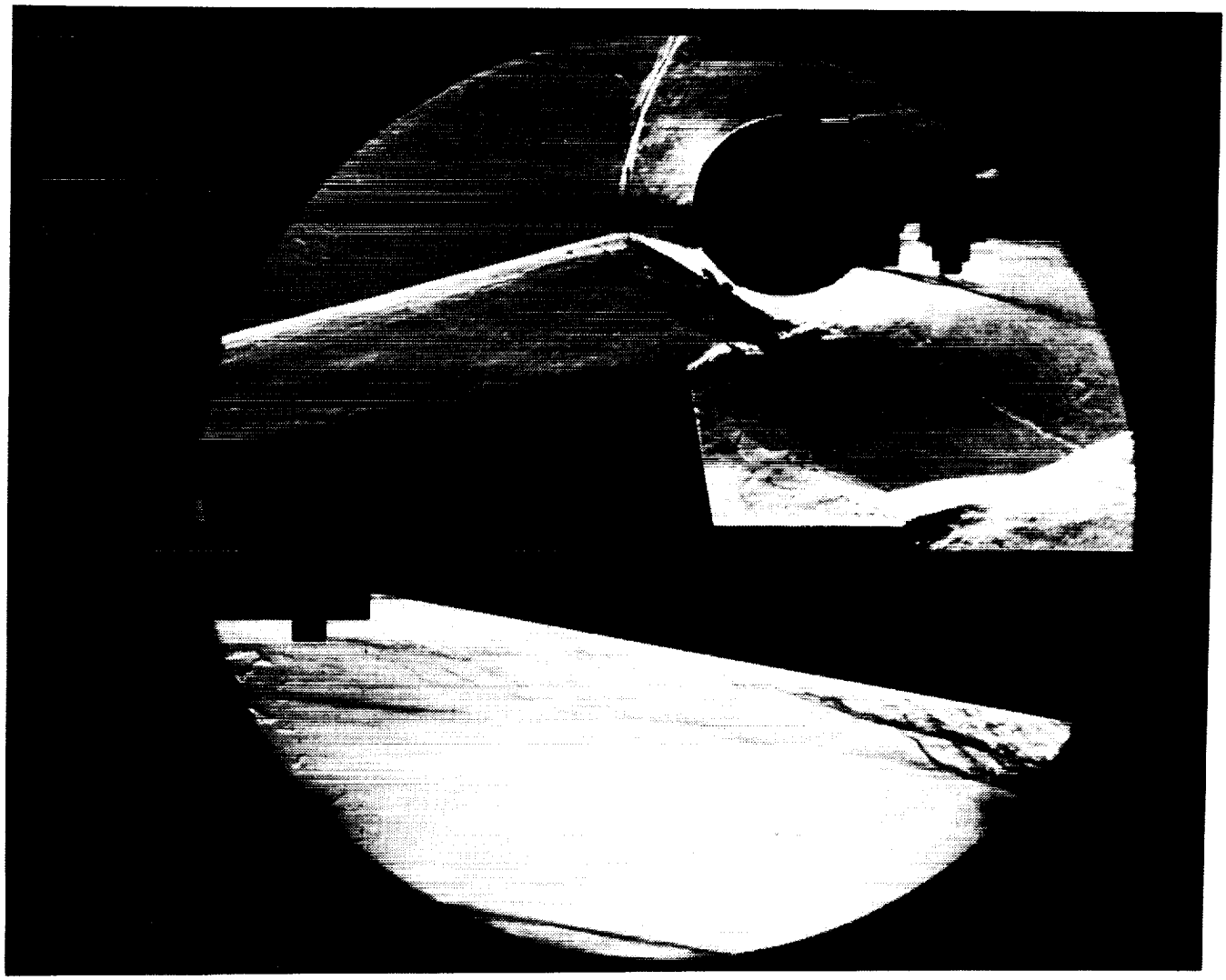

Test Conditions for Run 16 :

Po	= 1.363E-03 PSIA	Reservoir Total Pressure
Ho	= 1.876E-07 (Ft/sec)²	Reservoir Total Enthalpy
To	= 2.846E-03 °R	Reservoir Total Temperature
M	= 8.020E+00	Freestream Mach Number
U	= 5.904E+03 Ft/sec	Freestream Velocity
T	= 2.253E-02 °R	Freestream Temperature
P	= 1.204E-01 PSIA	Freestream Static Pressure
Rho	= 4.485E-05 Slugs/Ft3	Freestream Density
Mu	= 1.860E-07 Slugs/Ft-sec	Freestream Viscosity
Re	= 1.424E+06 1/Ft	Freestream Reynolds Number
Po'	= 1.006E+01 PSIA	Pitot Pressure
Q	= 5.428E+00 PSIA	Dynamic Pressure (½·Rho·U²/144)
Mi	= 3.447E+00	Shock Tube Incident Shock Mach Number
Hw	= 3.183E+06 (Ft/sec)²	Wall Enthalpy (Cp·Tw)
CPf	= 1.842E-01 1/PSIA	Pressure to CP factor (1/Q)
CHf	= 1.886E-04 Ft²-s/BTU	Heat Rate to CH factor (778/(Rho·U·(Ho-Hw))
QoFR	= 4.051E+01 BTU/Ft²-s	Fay-Riddell Heat Transfer to 3" Diam Sphere

Model Configuration Parameter	Value
Stagnation Position (gauge label)	P23
Vertical Distance (inches)	2.95
Horizontal Distance (inches)	0.06
Plate Angle (degrees)	10.00
Plate Length (inches)	26.50
Sweep Angle (degrees)	0.00

Run 16

ORIGINAL PAGE
BLACK AND WHITE PHOTOGRAPH

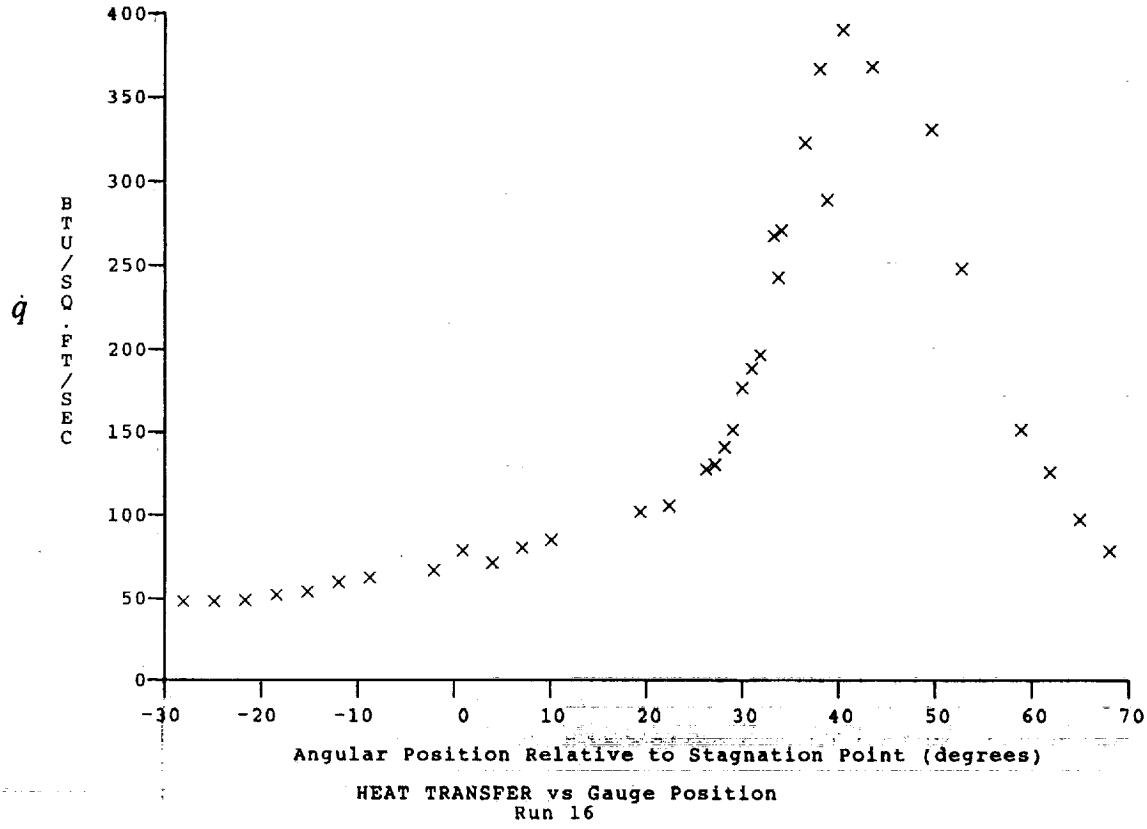

HEAT TRANSFER vs Gauge Position
Run 16

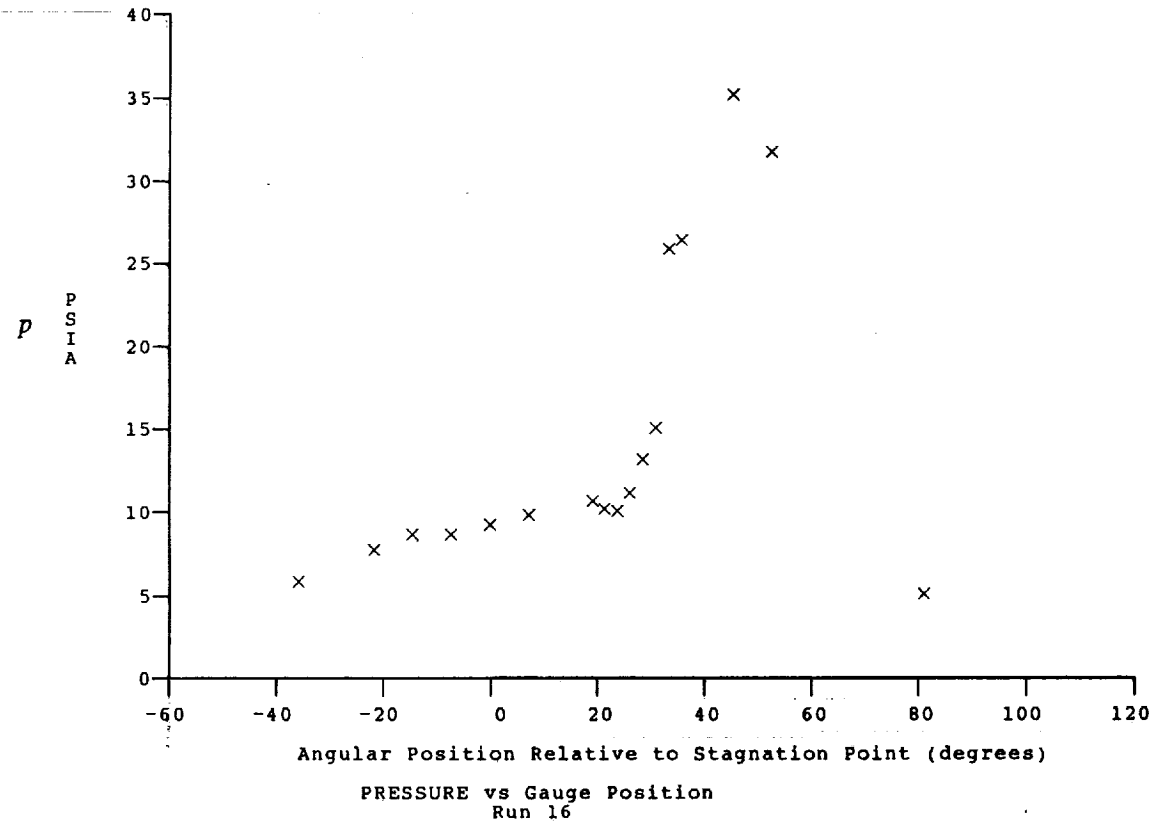

PRESSURE vs Gauge Position
Run 16

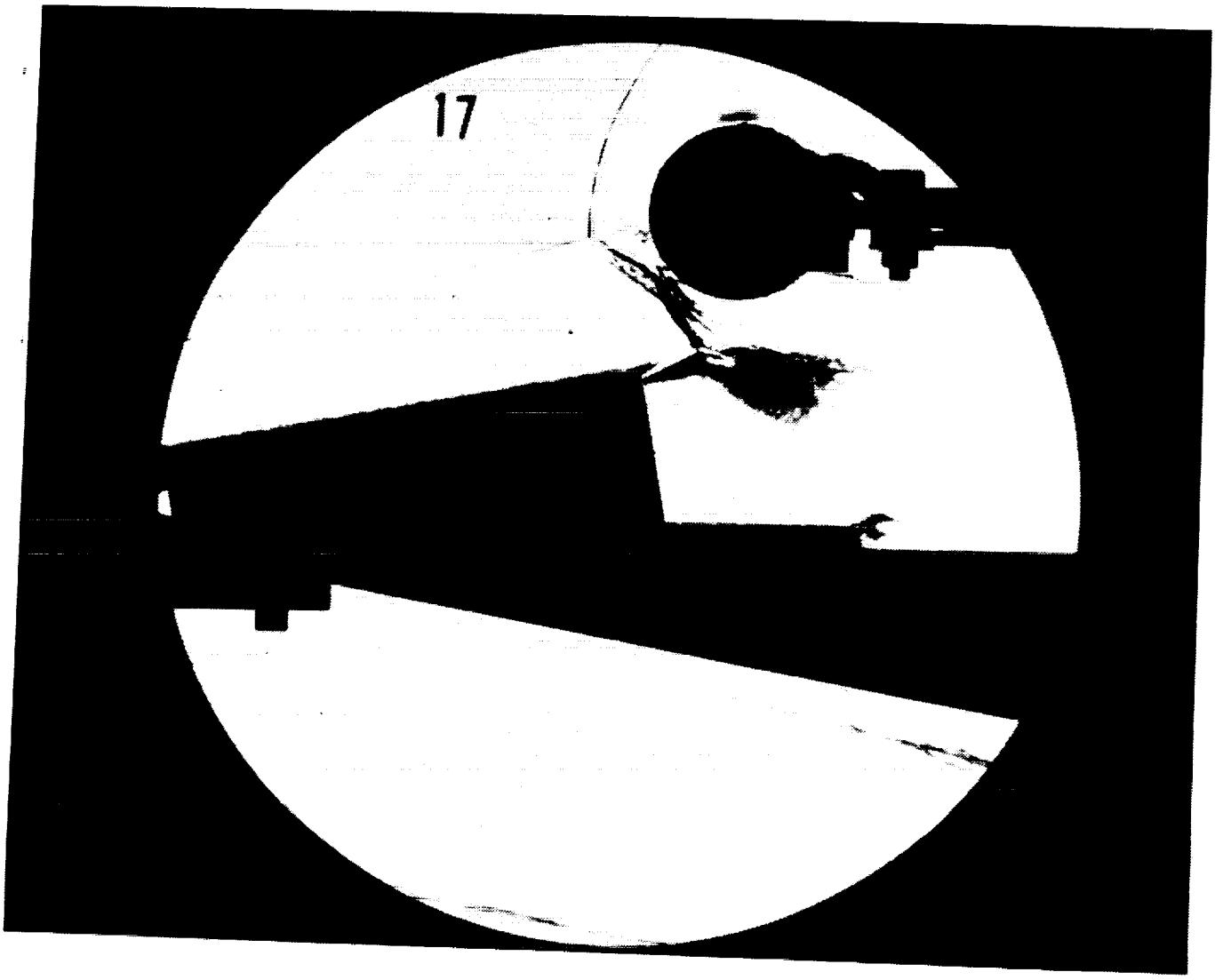

Test Conditions for Run 17 :

Po	= 1.366E+03 PSIA	Reservoir Total Pressure
Ho	= 1.846E+07 (Ft/sec)²	Reservoir Total Enthalpy
To	= 2.809E+03 °R	Reservoir Total Temperature
M	= 8.055E+00	Freestream Mach Number
U	= 5.858E+03 Ft/sec	Freestream Velocity
T	= 2.199E+02 °R	Freestream Temperature
P	= 1.180E-01 PSIA	Freestream Static Pressure
Rho	= 4.504E-05 Slugs/Ft3	Freestream Density
Mu	= 1.818E-07 Slugs/Ft-sec	Freestream Viscosity
Re	= 1.452E+06 1/Ft	Freestream Reynolds Number
Po'	= 9.948E+00 PSIA	Pitot Pressure
Q	= 5.366E+00 PSIA	Dynamic Pressure (½·Rho·U²/144)
Mi	= 3.372E+00	Shock Tube Incident Shock Mach Number
Hw	= 3.183E+06 (Ft/sec)²	Wall Enthalpy (Cp·Tw)
CPf	= 1.863E-01 1/PSIA	Pressure to CP factor (1/Q)
CHf	= 1.930E-04 Ft²-s/BTU	Heat Rate to CH factor (778/(Rho·U·(Ho-Hw))
QoFR	= 3.945E-01 BTU/Ft²-s	Fay-Riddell Heat Transfer to 3" Diam Sphere

Model Configuration Parameter	Value
Stagnation Position (gauge label)	P23
Vertical Distance (inches)	2.95
Horizontal Distance (inches)	0.06
Plate Angle (degrees)	10.00
Plate Length (inches)	26.50
Sweep Angle (degrees)	0.00

Run 17

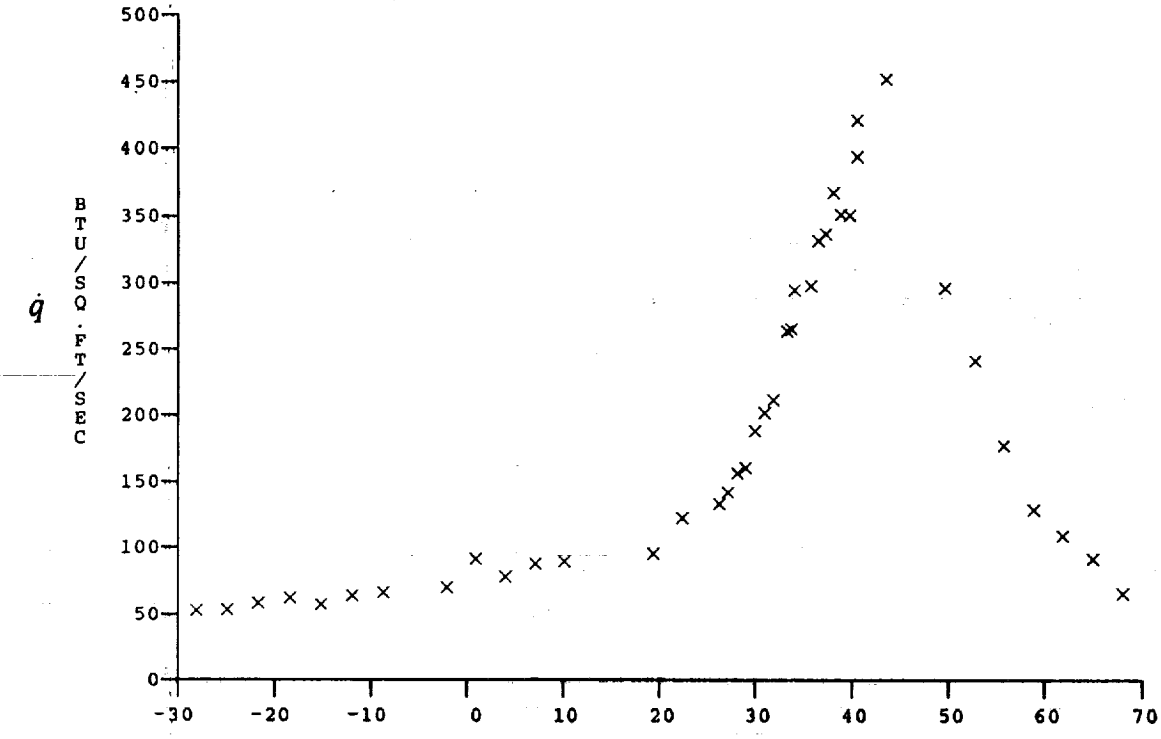

HEAT TRANSFER vs Gauge Position
Run 17

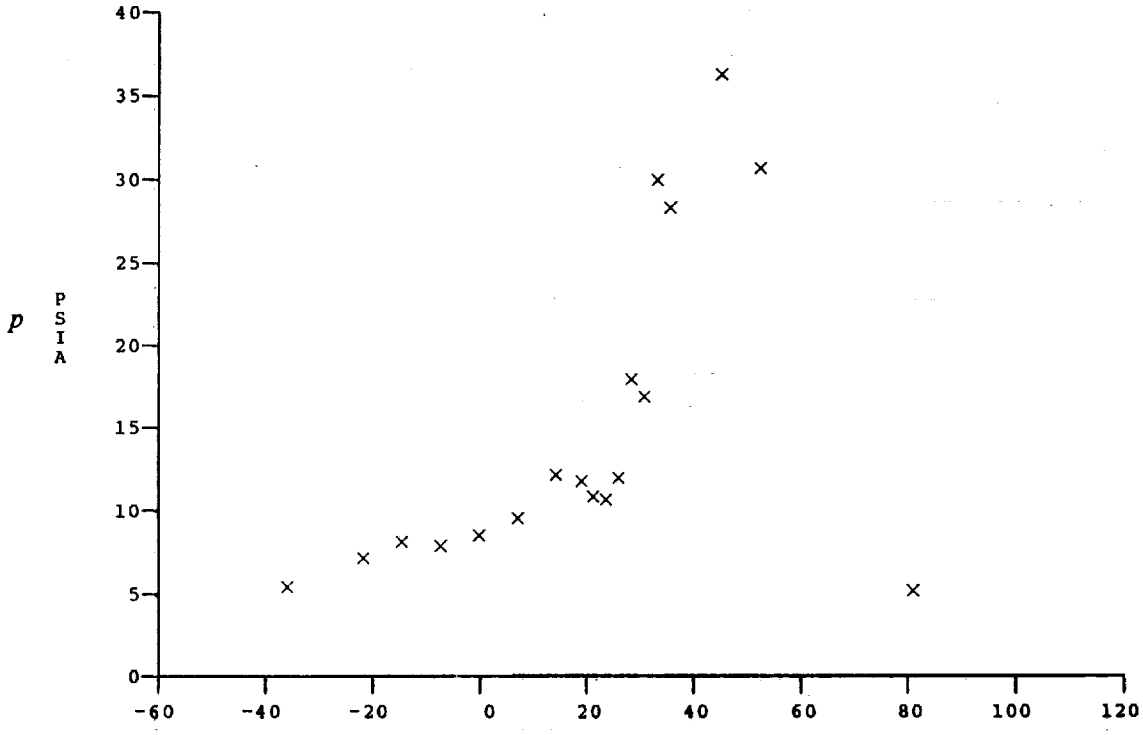

PRESSURE vs Gauge Position
Run 17

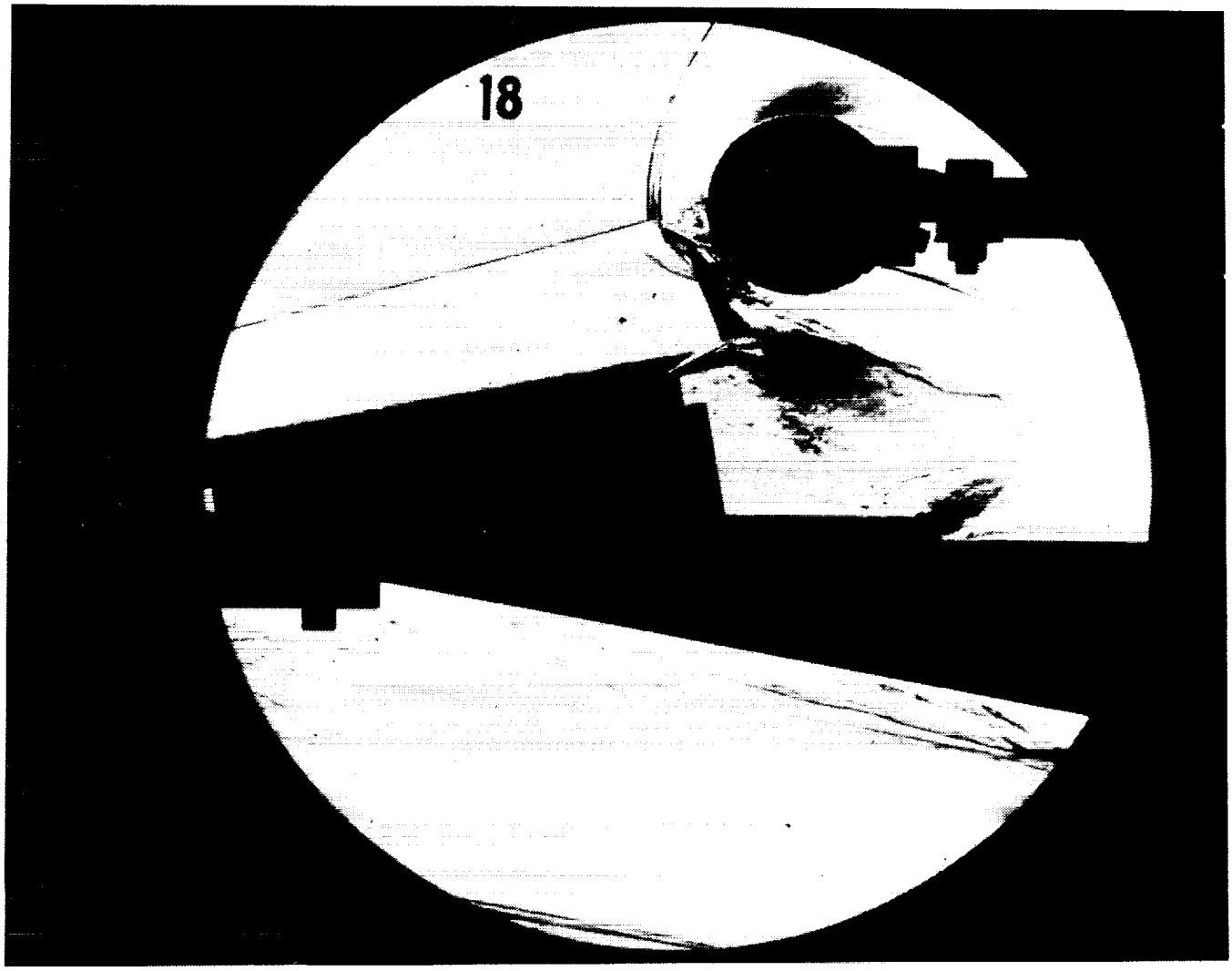

Test Conditions for Run 18 :

Po	= 1.442E+03	PSIA	Reservoir Total Pressure
Ho	= 1.856E+07	(Ft/sec)²	Reservoir Total Enthalpy
To	= 2.817E-03	°R	Reservoir Total Temperature
M	= 8.029E+00		Freestream Mach Number
U	= 5.873E-03	Ft/sec	Freestream Velocity
T	= 2.224E-02	°R	Freestream Temperature
P	= 1.271E-01	PSIA	Freestream Static Pressure
Rho	= 4.797E-05	Slugs/Ft3	Freestream Density
Mu	= 1.838E-07	Slugs/Ft-sec	Freestream Viscosity
Re	= 1.533E+06	1/Ft	Freestream Reynolds Number
Po'	= 1.065E+01	PSIA	Pitot Pressure
Q	= 5.744E+00	PSIA	Dynamic Pressure (½·Rho·U²/144)
Mi	= 3.446E+00		Shock Tube Incident Shock Mach Number
Hw	= 3.183E+06	(Ft/sec)²	Wall Enthalpy (Cp·Tw)
CPf	= 1.741E-01	1/PSIA	Pressure to CP factor (1/Q)
CHf	= 1.796E-04	Ft²-s/BTU	Heat Rate to CH factor (778/(Rho·U·(Ho-Hw))
QoFR	= 4.111E+01	BTU/Ft²-s	Fay-Riddell Heat Transfer to 3" Diam Sphere

Model Configuration Parameter	Value
Stagnation Position (gauge label)	P21
Vertical Distance (inches)	2.86
Horizontal Distance (inches)	0.50
Plate Angle (degrees)	10.00
Plate Length (inches)	26.50
Sweep Angle (degrees)	0.00

Run 18

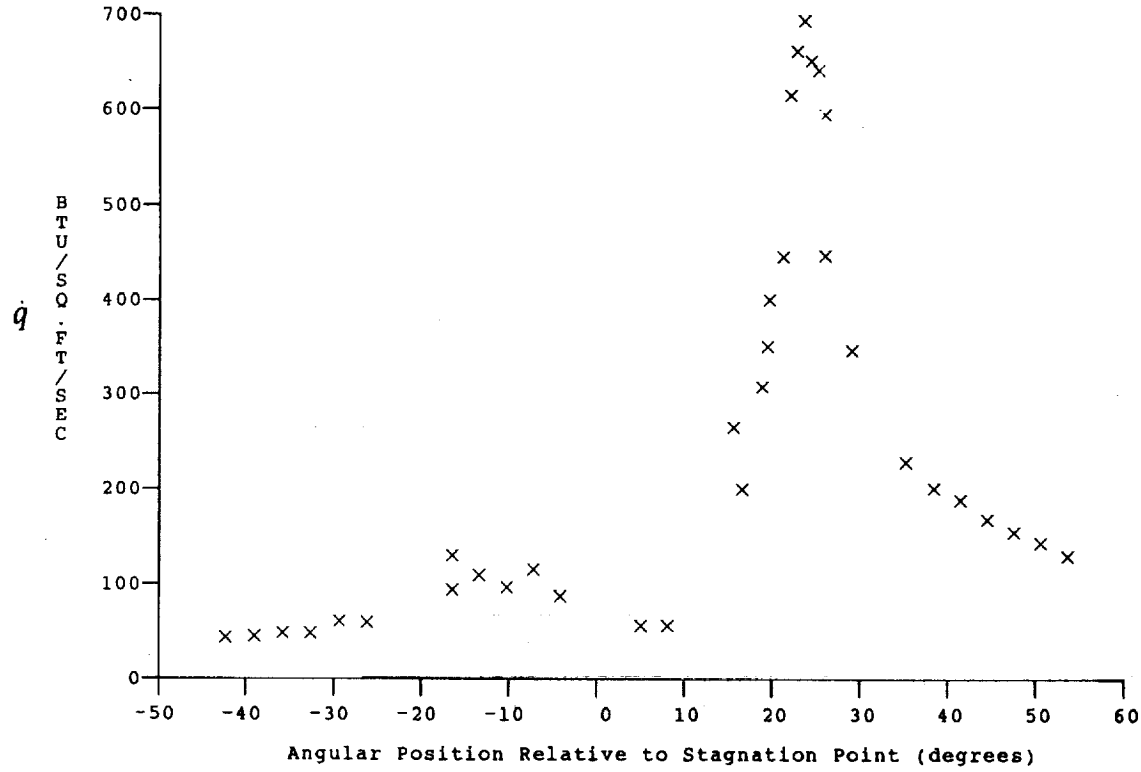

HEAT TRANSFER vs Gauge Position
Run 18

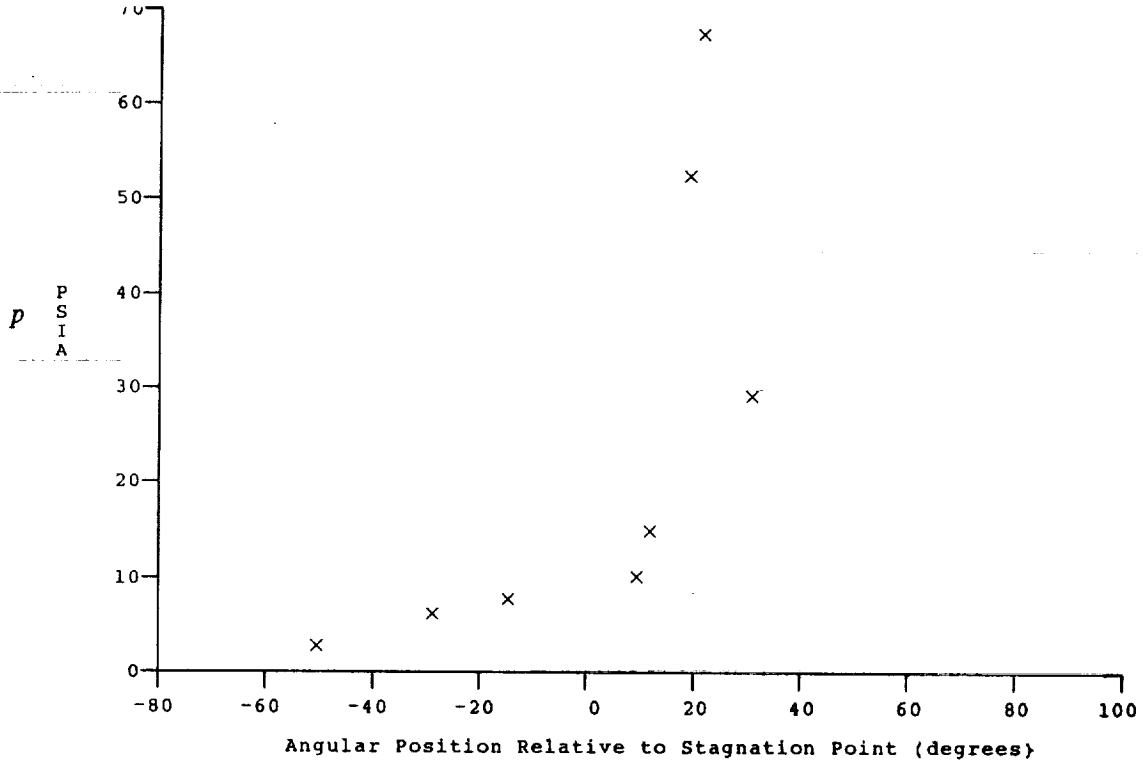

PRESSURE vs Gauge Position
Run 18

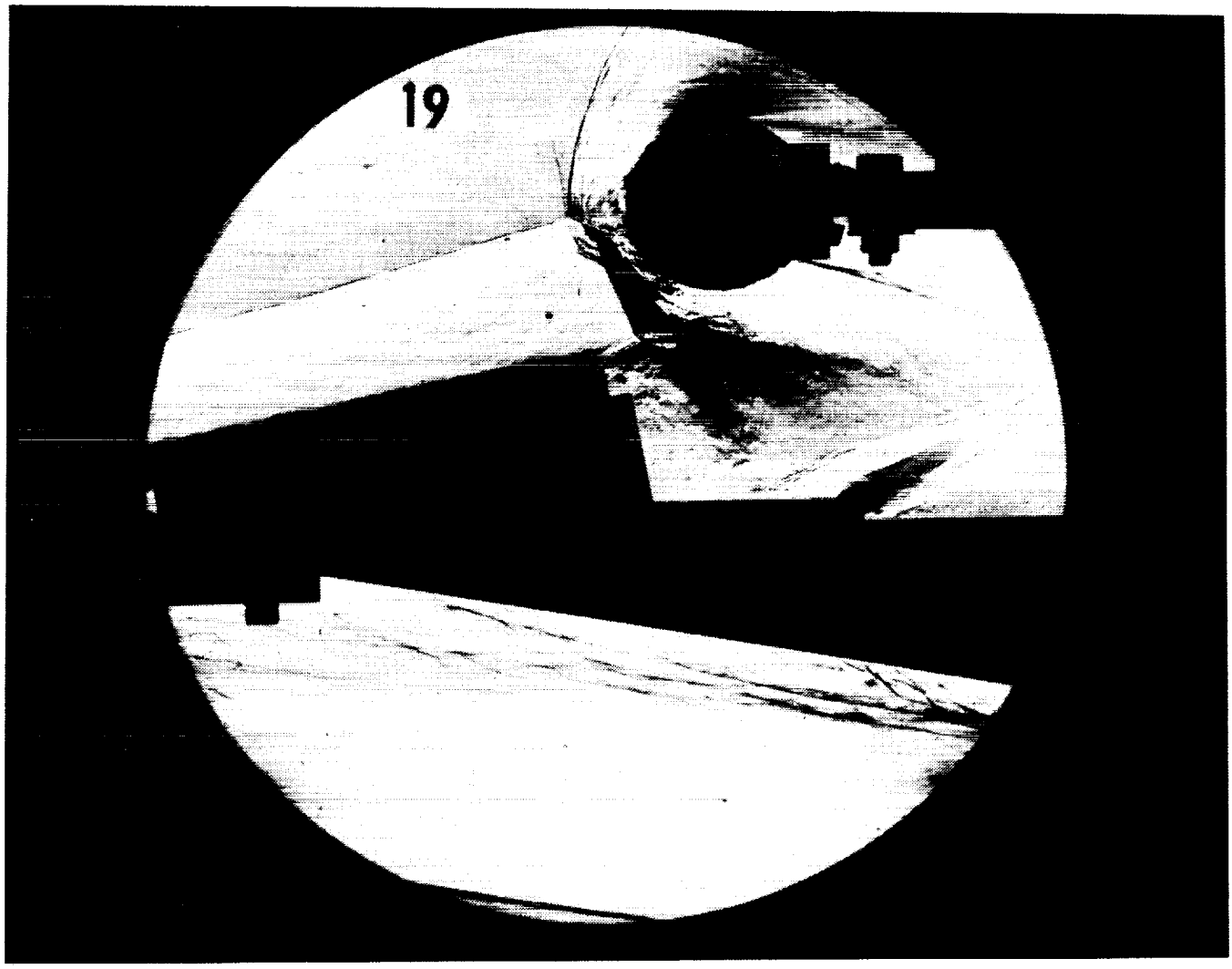

Test Conditions for Run 19 :

Po	= 1.434E-03 PSIA	Reservoir Total Pressure	
Ho	= 1.863E+07 (Ft/sec)²	Reservoir Total Enthalpy	
To	= 2.827E-03 °R	Reservoir Total Temperature	
M	= 8.027E+00	Freestream Mach Number	
U	= 5.883E-03 Ft/sec	Freestream Velocity	
T	= 2.234E+02 °R	Freestream Temperature	
P	= 1.265E-01 PSIA	Freestream Static Pressure	
Rho	= 4.753E-05 Slugs/Ft3	Freestream Density	
Mu	= 1.845E-07 Slugs/Ft-sec	Freestream Viscosity	
Re	= 1.516E+06 1/Ft	Freestream Reynolds Number	
Po'	= 1.059E+01 PSIA	Pitot Pressure	
Q	= 5.712E+00 PSIA	Dynamic Pressure (½·Rho·U²/144)	
Mi	= 3.449E+00	Shock Tube Incident Shock Mach Number	
Hw	= 3.183E+06 (Ft/sec)²	Wall Enthalpy (Cp·Tw)	
CPf	= 1.751E-01 1/PSIA	Pressure to CP factor (1/Q)	
CHf	= 1.801E-04 Ft²-s/BTU	Heat Rate to CH factor (778/(Rho·U·(Ho-Hw))	
QoFR	= 1.119E+01 BTU/Ft²-s	Fay-Riddell Heat Transfer to 3" Diam Sphere	

Model Configuration Parameter	Value
Stagnation Position (gauge label)	P21
Vertical Distance (inches)	2.78
Horizontal Distance (inches)	0.50
Plate Angle (degrees)	10.00
Plate Length (inches)	26.50
Sweep Angle (degrees)	0.00

Run 19

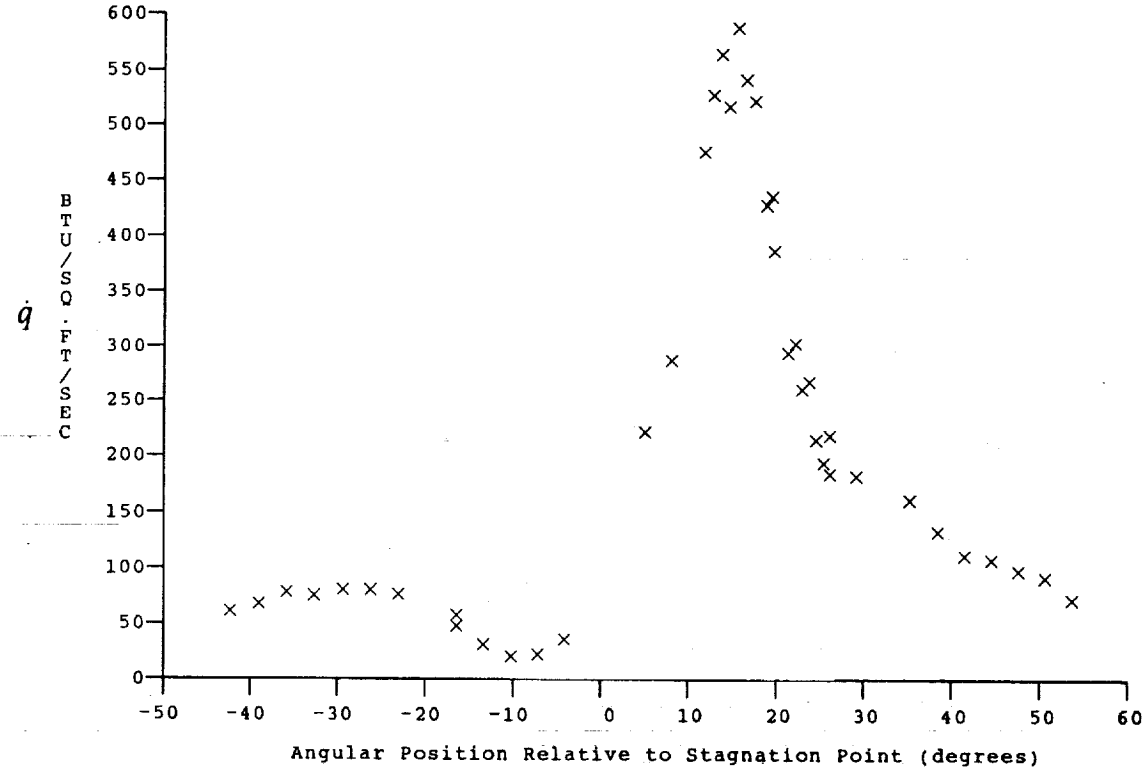

HEAT TRANSFER vs Gauge Position
Run 19

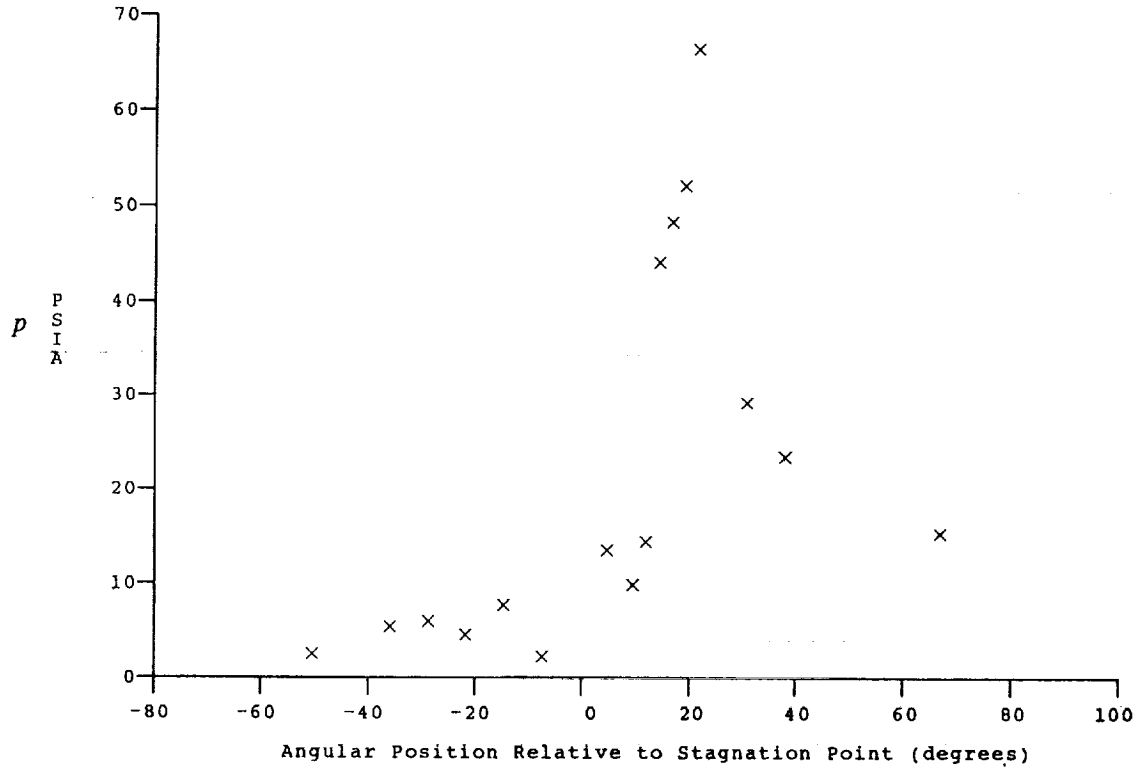

PRESSURE vs Gauge Position
Run 19

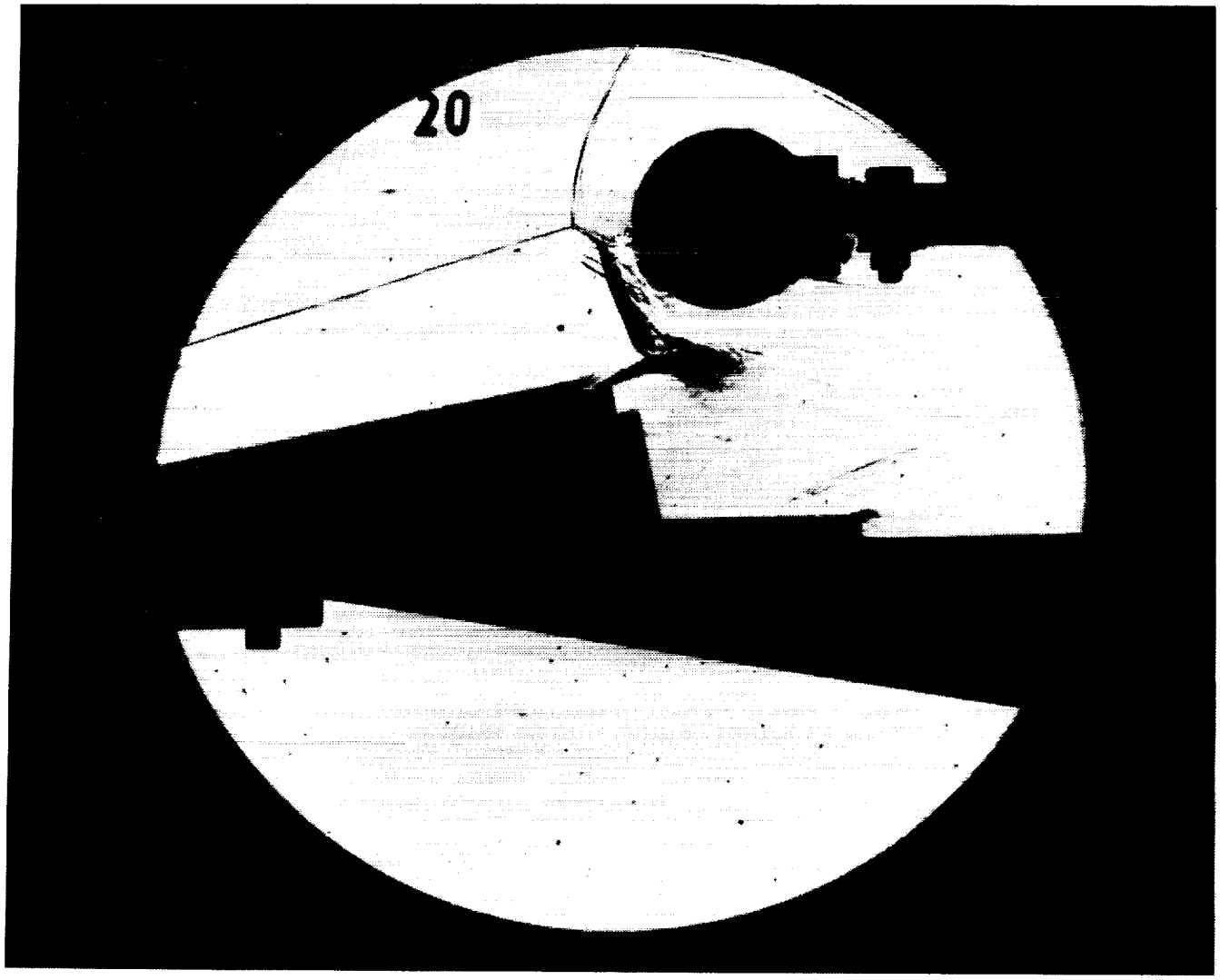

Test Conditions for Run 20 :

Po	= 7.097E+02 PSIA	Reservoir Total Pressure	
Ho	= 1.867E-07 (Ft/sec)²	Reservoir Total Enthalpy	
To	= 2.837E+03 °R	Reservoir Total Temperature	
M	= 7.944E+00	Freestream Mach Number	
U	= 5.885E+03 Ft/sec	Freestream Velocity	
T	= 2.282E+02 °R	Freestream Temperature	
P	= 6.607E-02 PSIA	Freestream Static Pressure	
Rho	= 2.430E-05 Slugs/Ft3	Freestream Density	
Mu	= 1.882E-07 Slugs/Ft-sec	Freestream Viscosity	
Re	= 7.598E+05 1/Ft	Freestream Reynolds Number	
Po'	= 5.417E+00 PSIA	Pitot Pressure	
Q	= 2.922E+00 PSIA	Dynamic Pressure (½·Rho·U²/144)	
Mi	= 3.451E+00	Shock Tube Incident Shock Mach Number	
Hw	= 3.183E+06 (Ft/sec)²	Wall Enthalpy (Cp·Tw)	
CPf	= 3.423E-01 1/PSIA	Pressure to CP factor (1/Q)	
CHf	= 3.514E-04 Ft²-s/BTU	Heat Rate to CH factor (778/(Rho·U·(Ho-Hw))	
QoFR	= 2.953E+01 BTU/Ft²-s	Fay-Riddell Heat Transfer to 3" Diam Sphere	

Model Configuration Parameter	Value
Stagnation Position (gauge label)	P21
Vertical Distance (inches)	2.78
Horizontal Distance (inches)	0.50
Plate Angle (degrees)	10.00
Plate Length (inches)	26.50
Sweep Angle (degrees)	0.00

Run 20

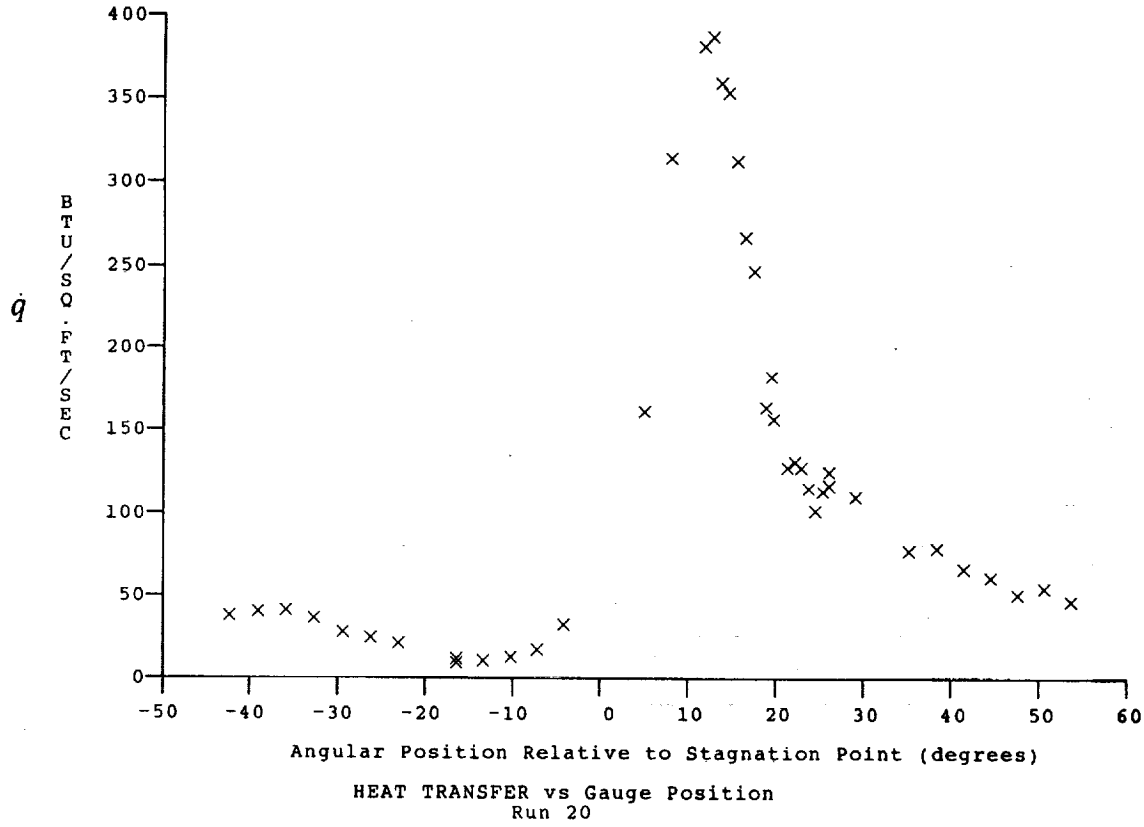

HEAT TRANSFER vs Gauge Position
Run 20

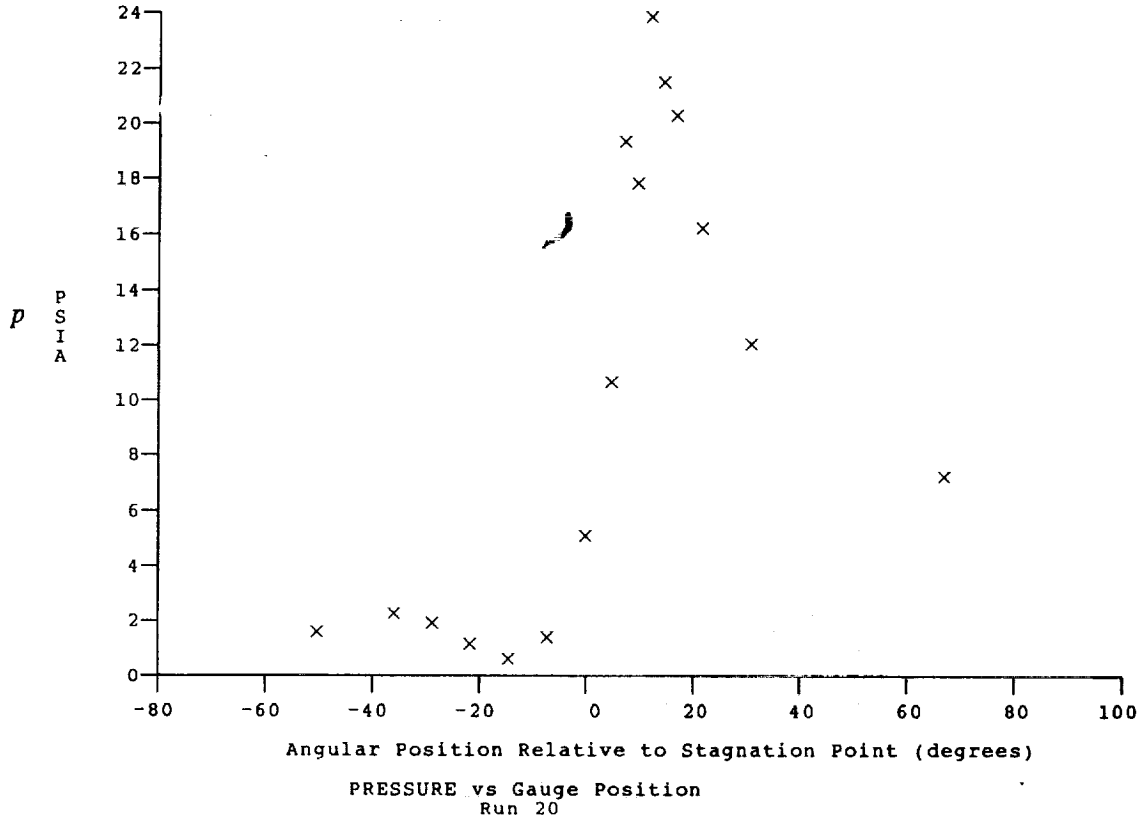

PRESSURE vs Gauge Position
Run 20

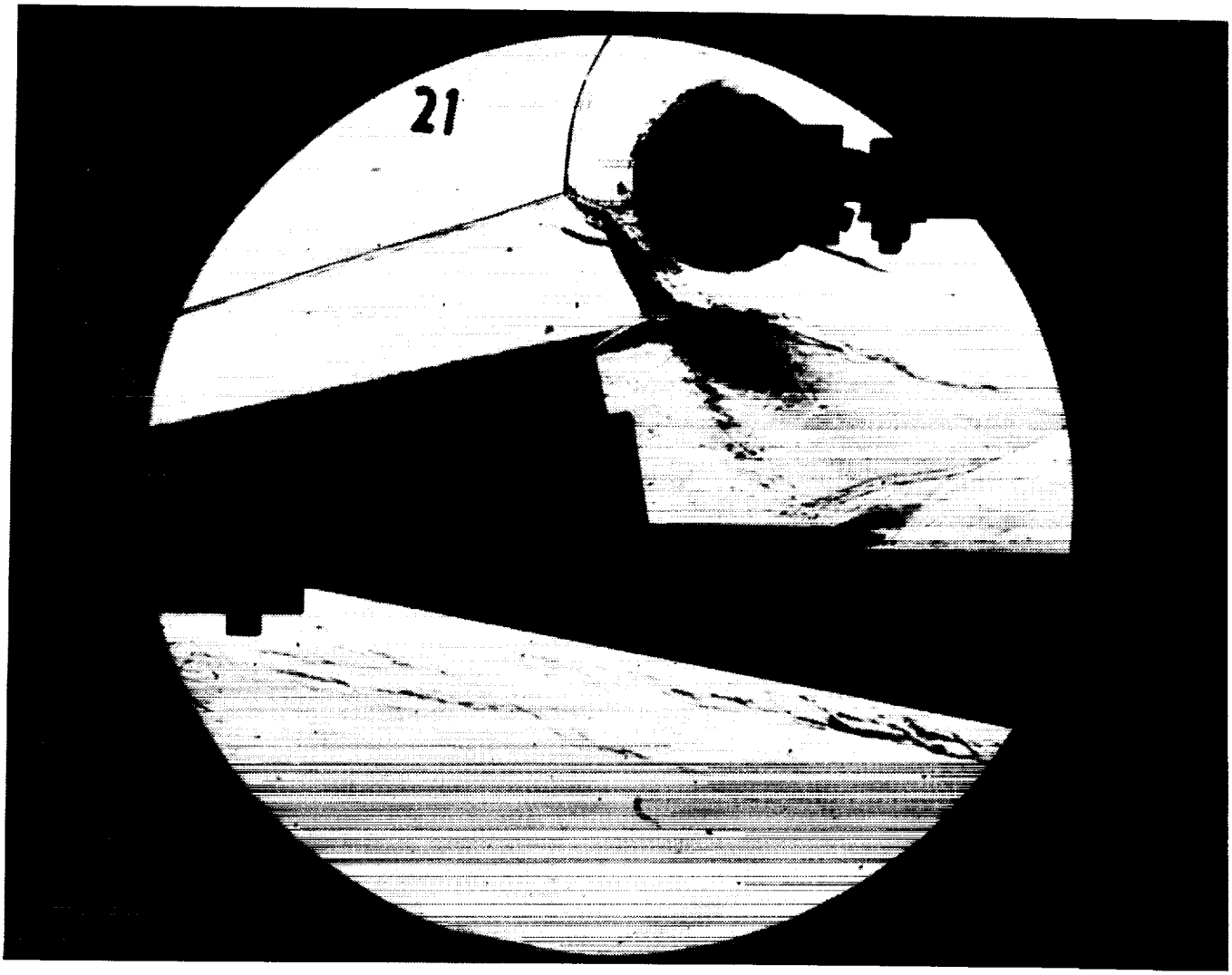

Test Conditions for Run 21 :

Po	= 1.446E+03 PSIA	Reservoir Total Pressure	
Ho	= 1.836E+07 (Ft/sec)²	Reservoir Total Enthalpy	
To	= 2.790E+03 °R	Reservoir Total Temperature	
M	= 8.035E-00	Freestream Mach Number	
U	= 5.841E+03 Ft/sec	Freestream Velocity	
T	= 2.198E+02 °R	Freestream Temperature	
P	= 1.274E-01 PSIA	Freestream Static Pressure	
Rho	= 4.866E-05 Slugs/Ft3	Freestream Density	
Mu	= 1.817E-07 Slugs/Ft-sec	Freestream Viscosity	
Re	= 1.565E+06 1/Ft	Freestream Reynolds Number	
Po'	= 1.069E-01 PSIA	Pitot Pressure	
Q	= 5.765E+00 PSIA	Dynamic Pressure (½·Rho·U²/144)	
Mi	= 3.435E+00	Shock Tube Incident Shock Mach Number	
Hw	= 3.183E+06 (Ft/sec)²	Wall Enthalpy (Cp·Tw)	
CPf	= 1.735E-01 1/PSIA	Pressure to CP factor (1/Q)	
CHf	= 1.803E-04 Ft²-s/BTU	Heat Rate to CH factor (778/(Rho·U·(Ho-Hw))	
QoFR	= 4.061E-01 BTU/Ft²-s	Fay-Riddell Heat Transfer to 3" Diam Sphere	

Model Configuration Parameter	Value
Stagnation Position (gauge label)	P21
Vertical Distance (inches)	2.89
Horizontal Distance (inches)	0.59
Plate Angle (degrees)	12.50
Plate Length (inches)	26.50
Sweep Angle (degrees)	0.00

Run 21

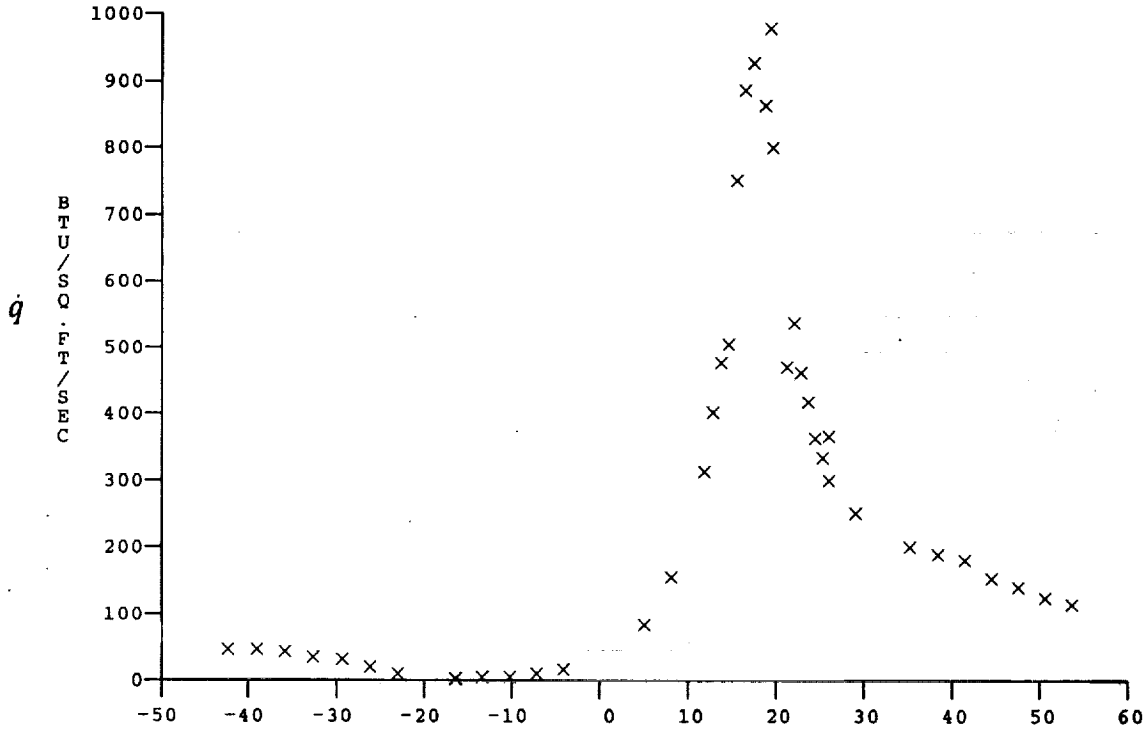

HEAT TRANSFER vs Gauge Position
Run 21

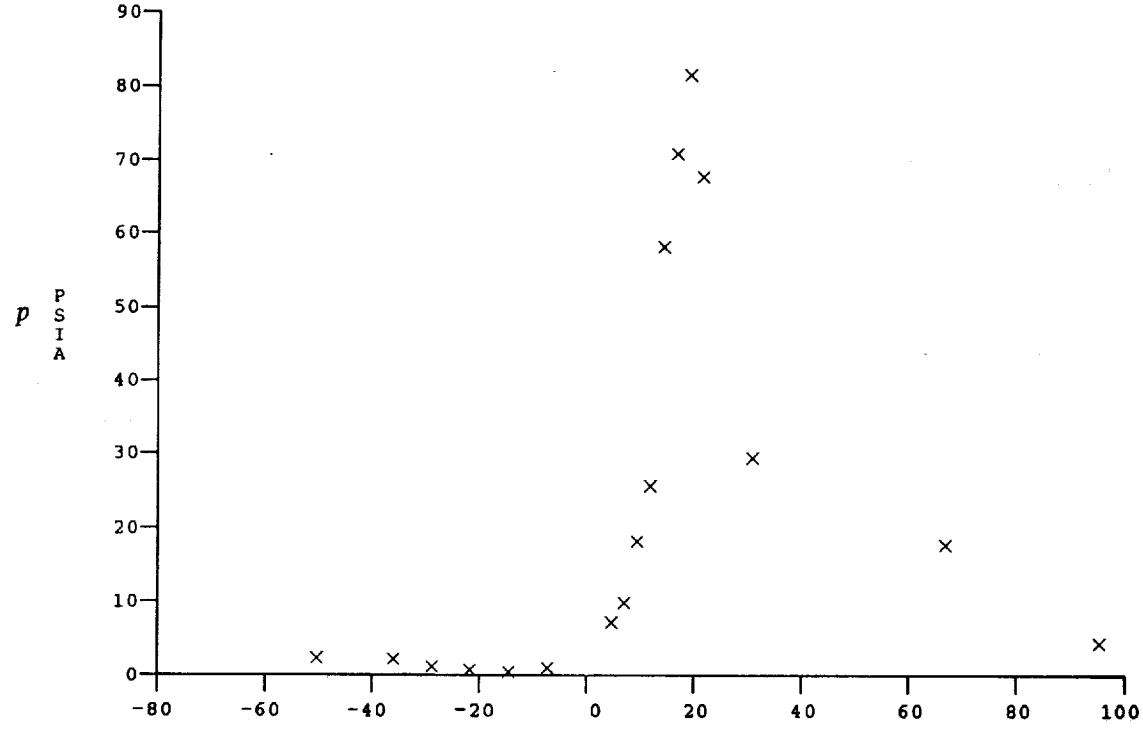

PRESSURE vs Gauge Position
Run 21

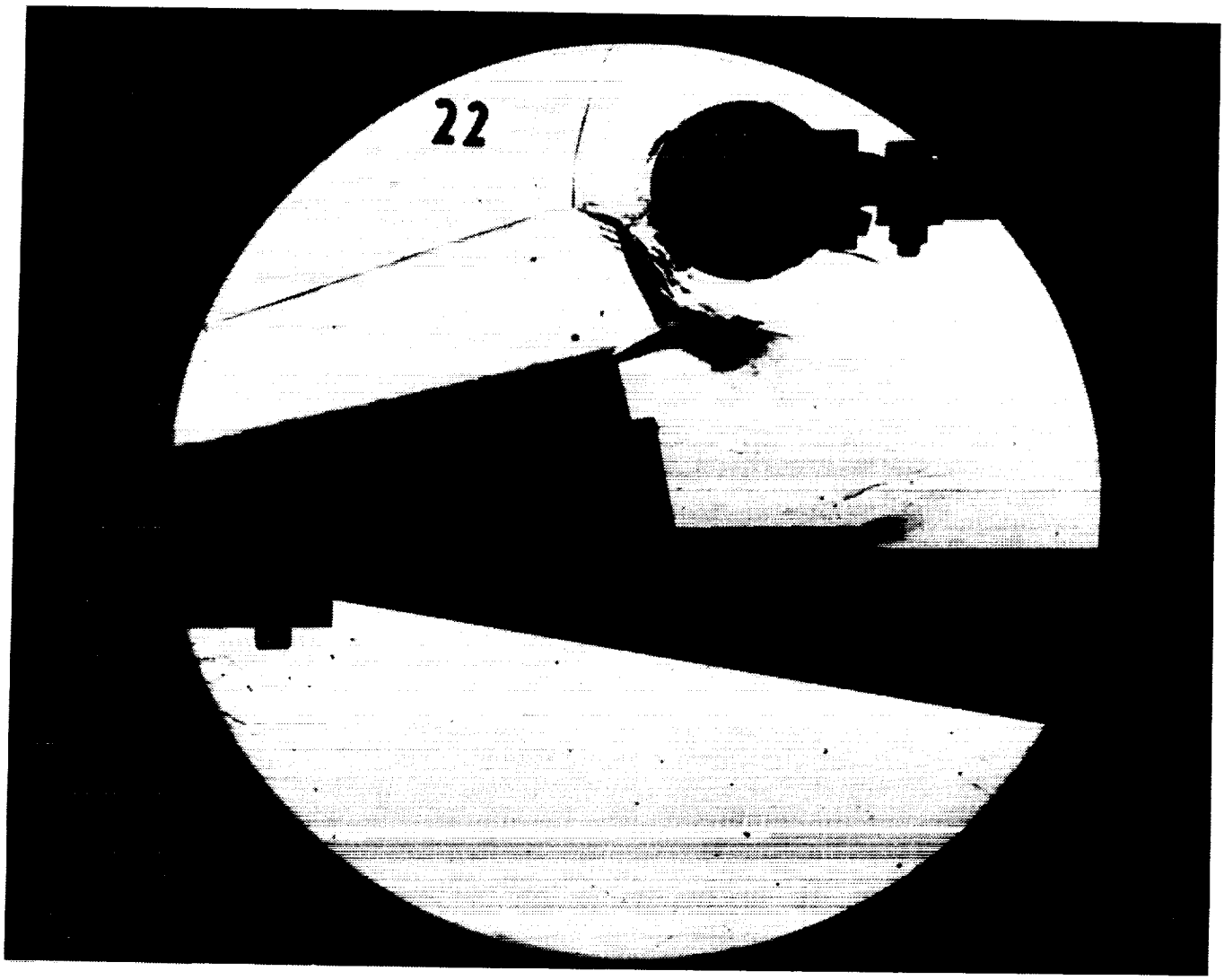

Test Conditions for Run 22 :

Po	= 6.902E+02	PSIA	Reservoir Total Pressure
Ho	= 1.826E-07	(Ft/sec)²	Reservoir Total Enthalpy
To	= 2.781E-03	°R	Reservoir Total Temperature
M	= 7.954E+00		Freestream Mach Number
U	= 5.821E-03	Ft/sec	Freestream Velocity
T	= 2.227E-02	°R	Freestream Temperature
P	= 6.422E-02	PSIA	Freestream Static Pressure
Rho	= 2.420E-05	Slugs/Ft3	Freestream Density
Mu	= 1.840E-07	Slugs/Ft-sec	Freestream Viscosity
Re	= 7.657E+05	1/Ft	Freestream Reynolds Number
Po'	= 5.276E+00	PSIA	Pitot Pressure
Q	= 2.847E+00	PSIA	Dynamic Pressure (½·Rho·U²/144)
Mi	= 3.424E+00		Shock Tube Incident Shock Mach Number
Hw	= 3.183E+06	(Ft/sec)²	Wall Enthalpy (Cp·Tw)
CPf	= 3.513E-01	1/PSIA	Pressure to CP factor (1/Q)
CHf	= 3.664E-04	Ft²-s/BTU	Heat Rate to CH factor (778/(Rho·U·(Ho-Hw))
QoFR	= 2.833E+01	BTU/Ft²-s	Fay-Riddell Heat Transfer to 3" Diam Sphere

Model Configuration Parameter	Value
Stagnation Position (gauge label)	P21
Vertical Distance (inches)	2.89
Horizontal Distance (inches)	0.59
Plate Angle (degrees)	12.50
Plate Length (inches)	26.50
Sweep Angle (degrees)	0.00

Run 22

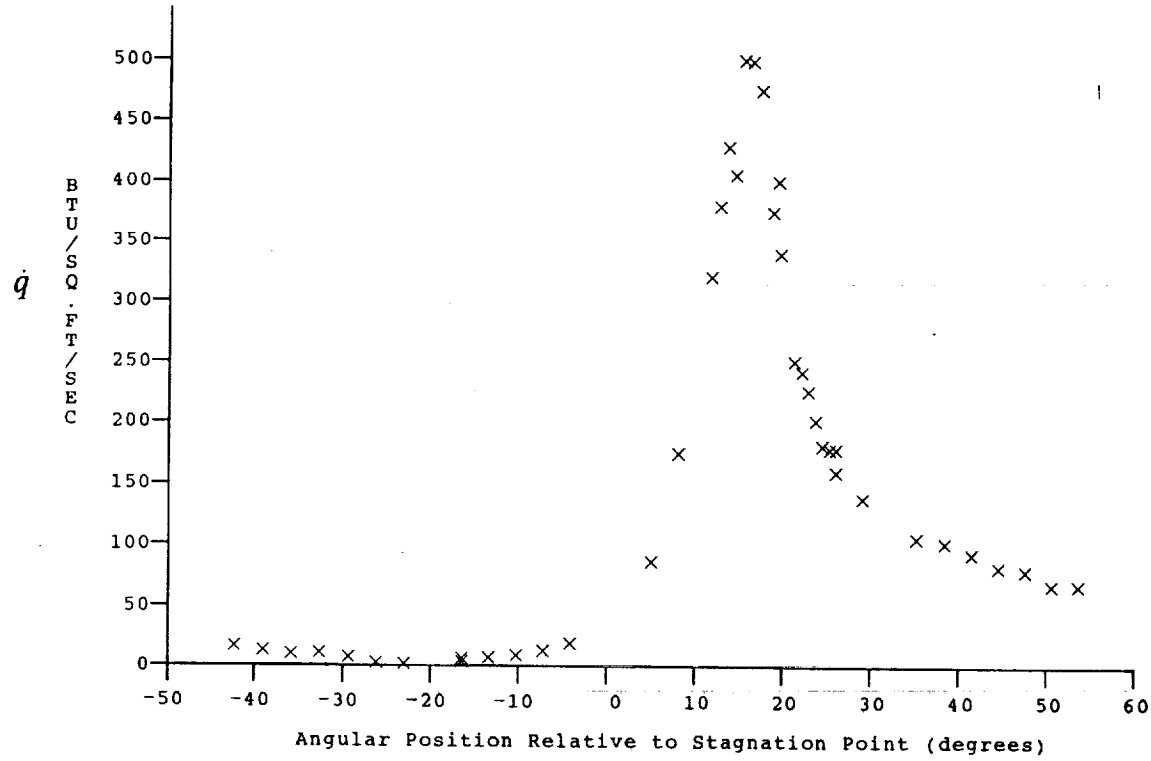

HEAT TRANSFER vs Gauge Position
Run 22

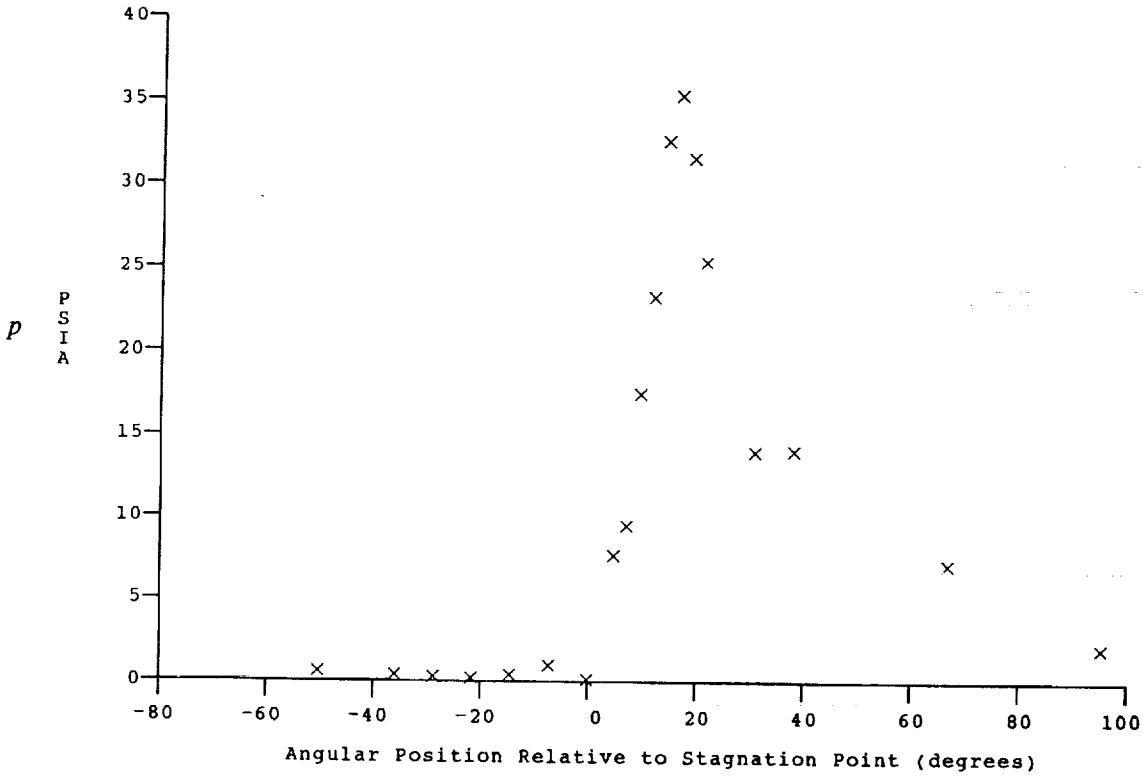

Figure PRESSURE vs Gauge Position
Run 22

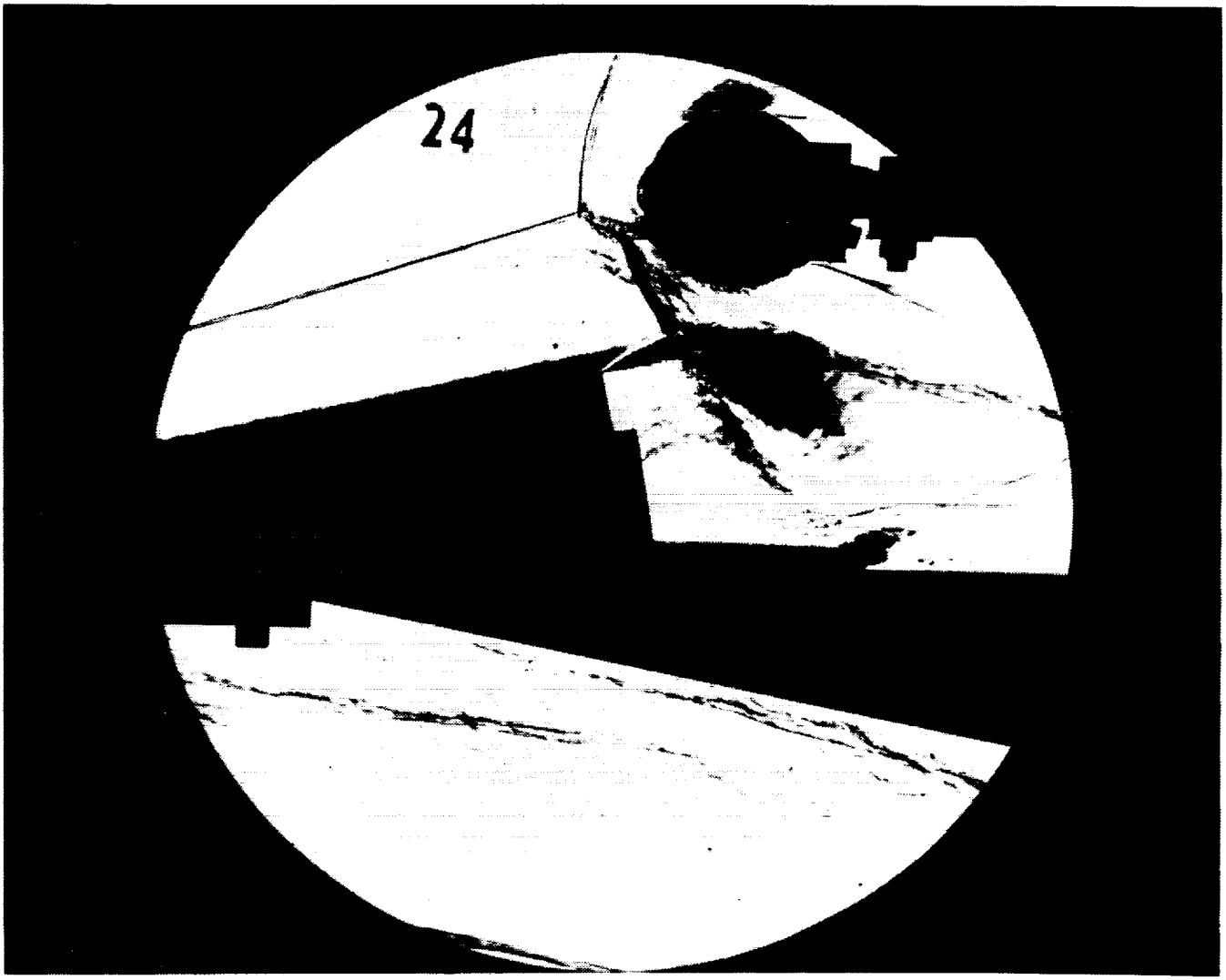

Test Conditions for Run 24 :

Po	= 4.211E+03 PSIA	Reservoir Total Pressure	
Ho	= 2.043E-07 (Ft/sec)²	Reservoir Total Enthalpy	
To	= 3.042E+03 °R	Reservoir Total Temperature	
M	= 8.144E-00	Freestream Mach Number	
U	= 6.167E+03 Ft/sec	Freestream Velocity	
T	= 2.384E+02 °R	Freestream Temperature	
P	= 3.422E-01 PSIA	Freestream Static Pressure	
Rho	= 1.205E-04 Slugs/Ft3	Freestream Density	
Mu	= 1.961E-07 Slugs/Ft-sec	Freestream Viscosity	
Re	= 3.788E+06 1/Ft	Freestream Reynolds Number	
Po'	= 2.953E+01 PSIA	Pitot Pressure	
Q	= 1.590E+01 PSIA	Dynamic Pressure (½·Rho·U²/144)	
Mi	= 3.621E+00	Shock Tube Incident Shock Mach Number	
Hw	= 3.183E-06 (Ft/sec)²	Wall Enthalpy (Cp·Tw)	
CPf	= 6.288E-02 1/PSIA	Pressure to CP factor (1/Q)	
CHf	= 6.074E-05 Ft²-s/BTU	Heat Rate to CH factor (778/(Rho·U·(Ho-Hw))	
QoFR	= 7.721E+01 BTU/Ft²-s	Fay-Riddell Heat Transfer to 3" Diam Sphere	

Model Configuration Parameter	Value
Stagnation Position (gauge label)	P21
Vertical Distance (inches)	2.89
Horizontal Distance (inches)	0.59
Plate Angle (degrees)	12.50
Plate Length (inches)	26.50
Sweep Angle (degrees)	0.00

Run 24

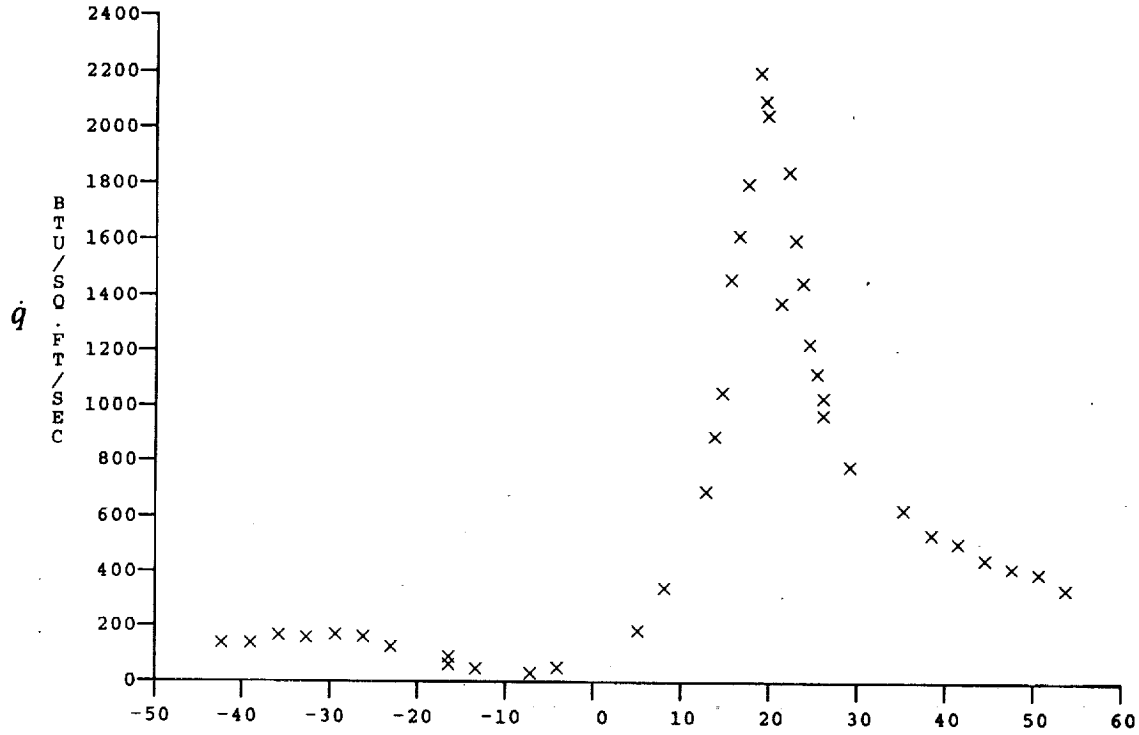

HEAT TRANSFER vs Gauge Position
Run 24

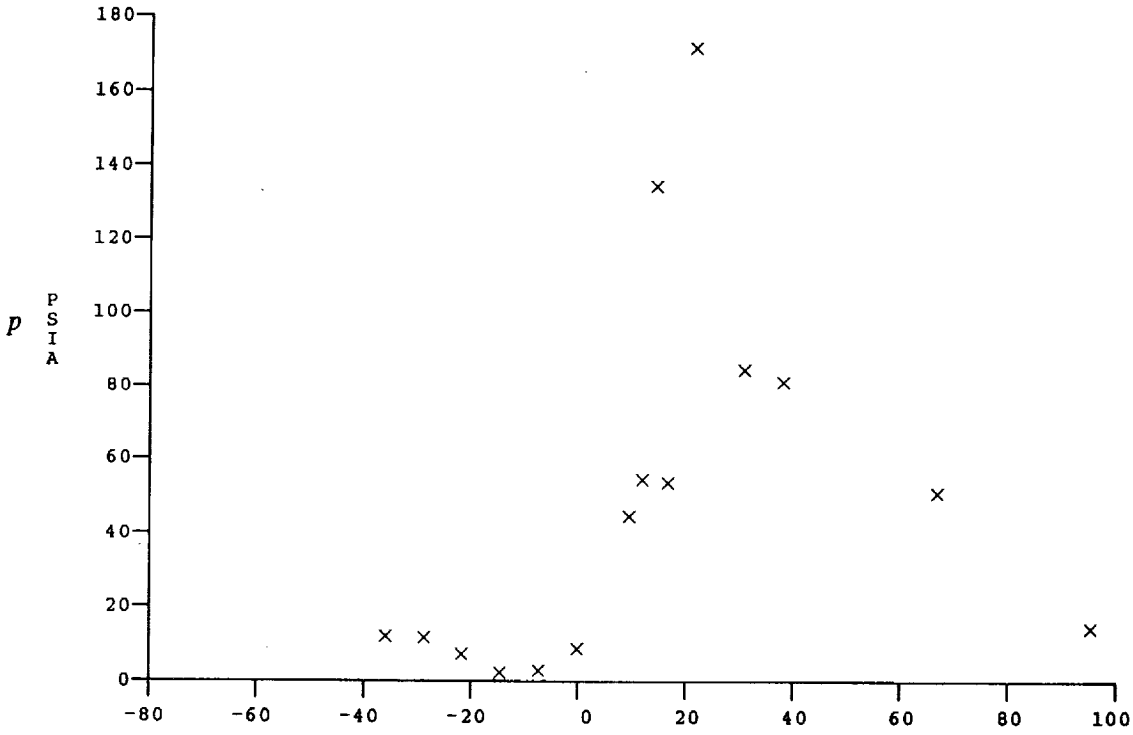

PRESSURE vs Gauge Position
Run 24

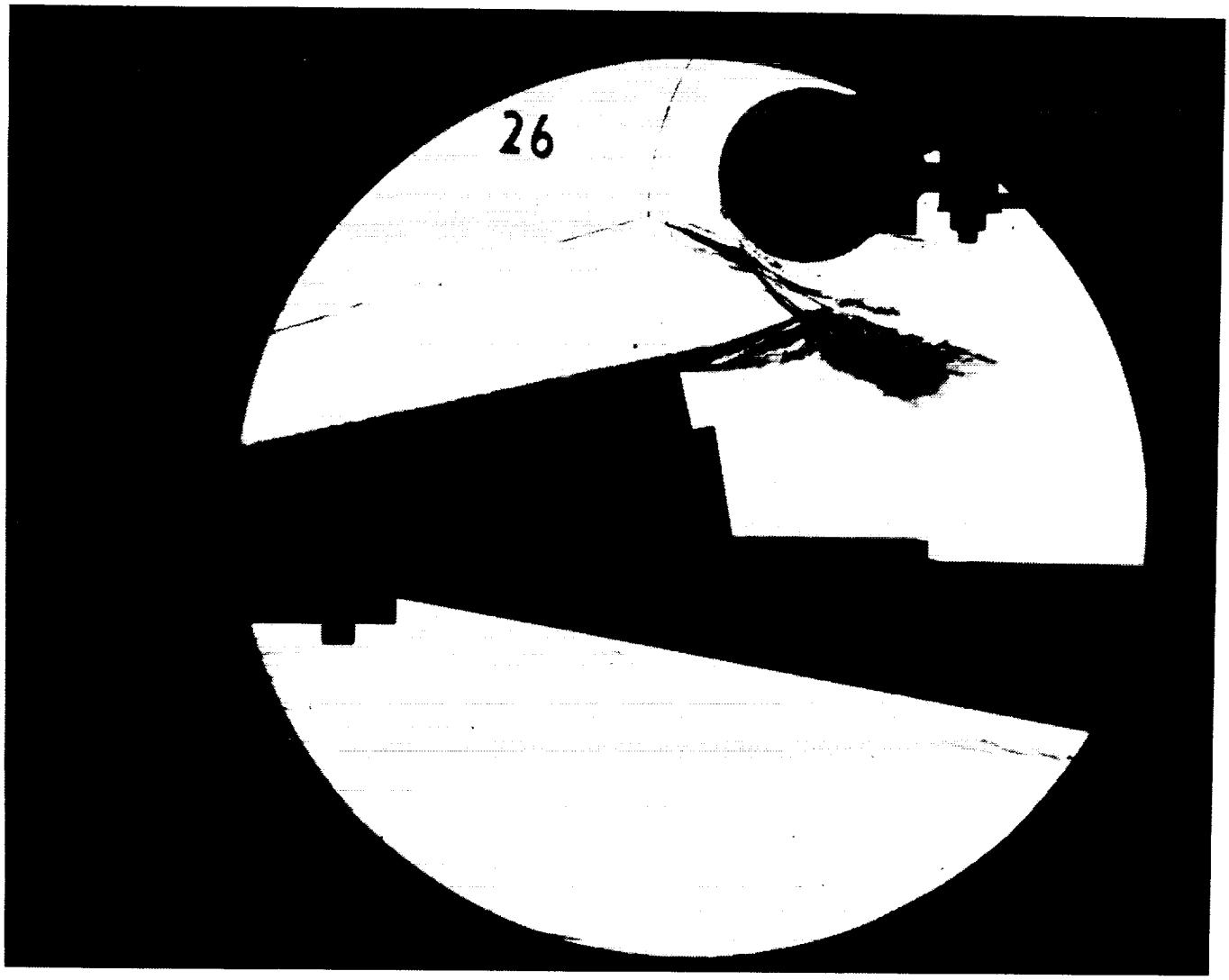

Test Conditions for Run 26 :

Po	= 1.430E-03 PSIA	Reservoir Total Pressure	
Ho	= 1.881E-07 (Ft/sec)²	Reservoir Total Enthalpy	
To	= 2.853E-03 °R	Reservoir Total Temperature	
M	= 8.034E-00	Freestream Mach Number	
U	= 5.911E-03 Ft/sec	Freestream Velocity	
T	= 2.251E-02 °R	Freestream Temperature	
P	= 1.250E-01 PSIA	Freestream Static Pressure	
Rho	= 4.661E-05 Slugs/Ft3	Freestream Density	
Mu	= 1.859E-07 Slugs/Ft-sec	Freestream Viscosity	
Re	= 1.483E+06 1/Ft	Freestream Reynolds Number	
Po'	= 1.049E+01 PSIA	Pitot Pressure	
Q	= 5.656E+00 PSIA	Dynamic Pressure (½·Rho·U²/144)	
Mi	= 3.433E+00	Shock Tube Incident Shock Mach Number	
Hw	= 3.183E+06 (Ft/sec)²	Wall Enthalpy (Cp·Tw)	
CPf	= 1.768E-01 1/PSIA	Pressure to CP factor (1/Q)	
CHf	= 1.807E-04 Ft²-s/BTU	Heat Rate to CH factor (778/(Rho·U·(Ho-Hw))	
QoFR	= 4.148E+01 BTU/Ft²-s	Fay-Riddell Heat Transfer to 3" Diam Sphere	

Model Configuration Parameter	Value
Stagnation Position (gauge label)	HT39
Vertical Distance (inches)	3.36
Horizontal Distance (inches)	0.63
Plate Angle (degrees)	12.50
Plate Length (inches)	26.50
Sweep Angle (degrees)	0.00

Run 26

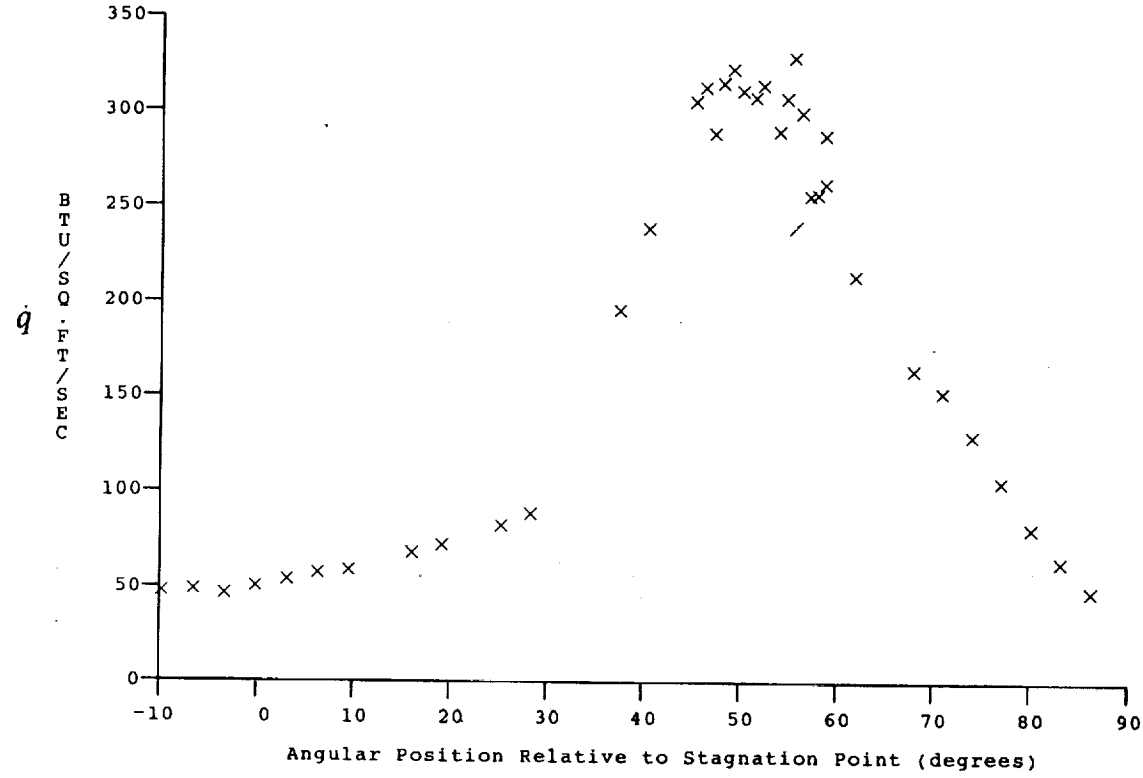

HEAT TRANSFER vs Gauge Position
Run 26

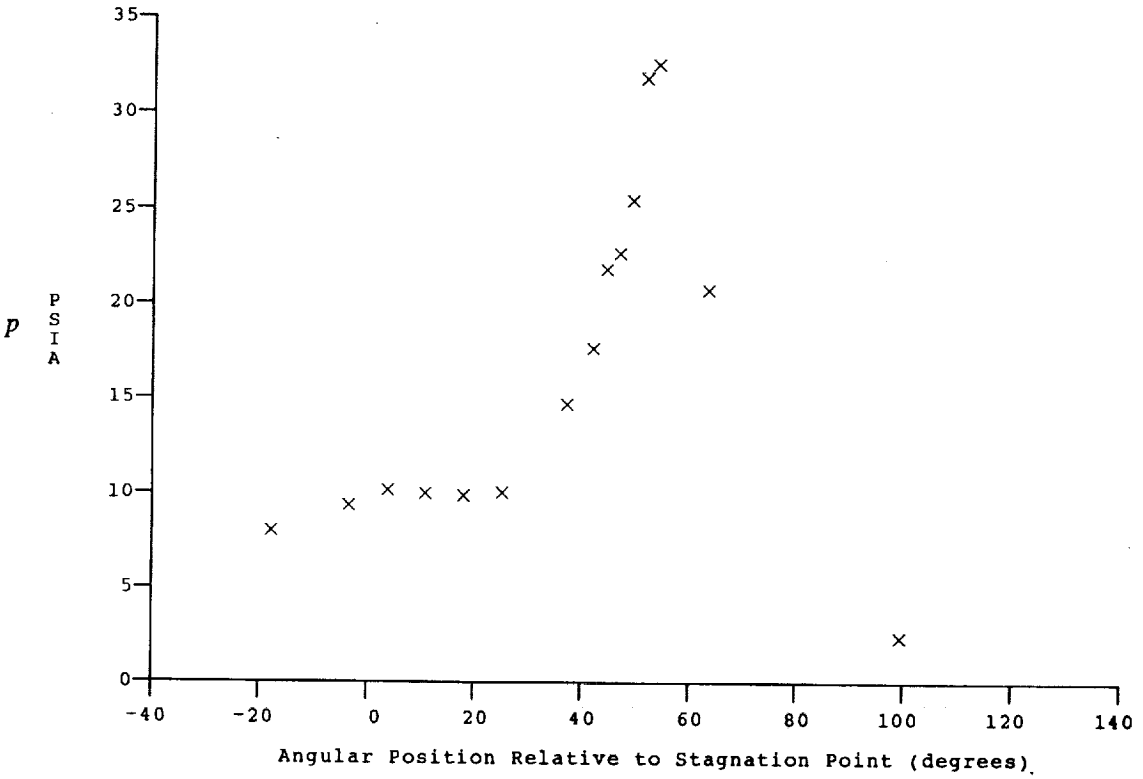

PRESSURE vs Gauge Position
Run 26

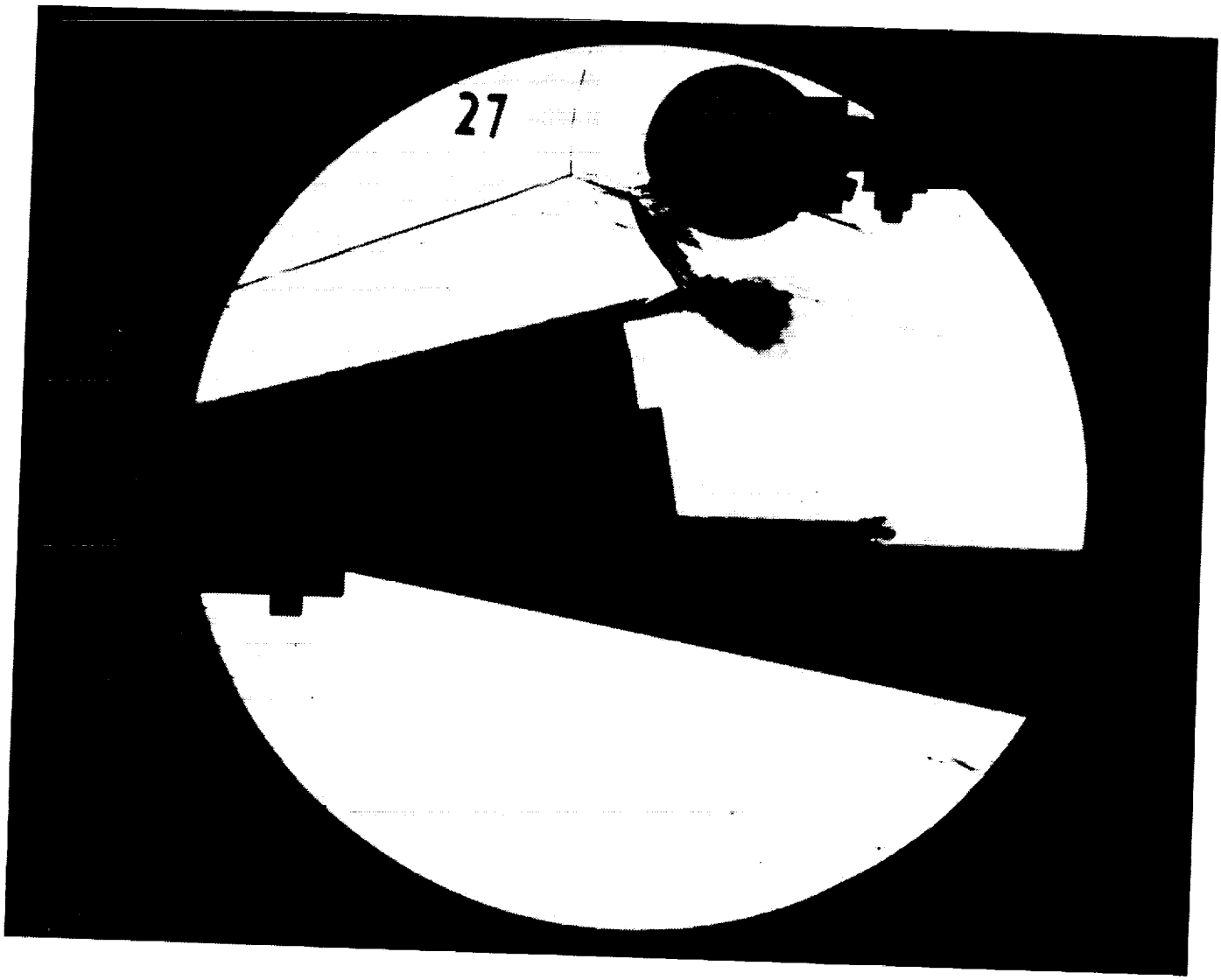

Test Conditions for Run 27 :

Po	= 1.404E-03	PSIA	Reservoir Total Pressure
Ho	= 1.866E-07	(Ft/sec)²	Reservoir Total Enthalpy
To	= 2.833E+03	°R	Reservoir Total Temperature
M	= 8.032E+00		Freestream Mach Number
U	= 5.888E+03	Ft/sec	Freestream Velocity
T	= 2.235E+02	°R	Freestream Temperature
P	= 1.233E-01	PSIA	Freestream Static Pressure
Rho	= 4.628E-05	Slugs/Ft3	Freestream Density
Mu	= 1.846E-07	Slugs/Ft-sec	Freestream Viscosity
Re	= 1.476E+06	1/Ft	Freestream Reynolds Number
Po'	= 1.033E+01	PSIA	Pitot Pressure
Q	= 5.571E+00	PSIA	Dynamic Pressure (½·Rho·U²/144)
Mi	= 3.432E+00		Shock Tube Incident Shock Mach Number
Hw	= 3.183E+06	(Ft/sec)²	Wall Enthalpy (Cp·Tw)
CPf	= 1.795E-01	1/PSIA	Pressure to CP factor (1/Q)
CHf	= 1.845E-04	Ft²-s/BTU	Heat Rate to CH factor (778/(Rho·U·(Ho-Hw))
QoFR	= 4.076E-01	BTU/Ft²-s	Fay-Riddell Heat Transfer to 3" Diam Sphere

Model Configuration Parameter	Value
Stagnation Position (gauge label)	P21
Vertical Distance (inches)	2.95
Horizontal Distance (inches)	0.31
Plate Angle (degrees)	15.00
Plate Length (inches)	26.50
Sweep Angle (degrees)	0.00

Run 27

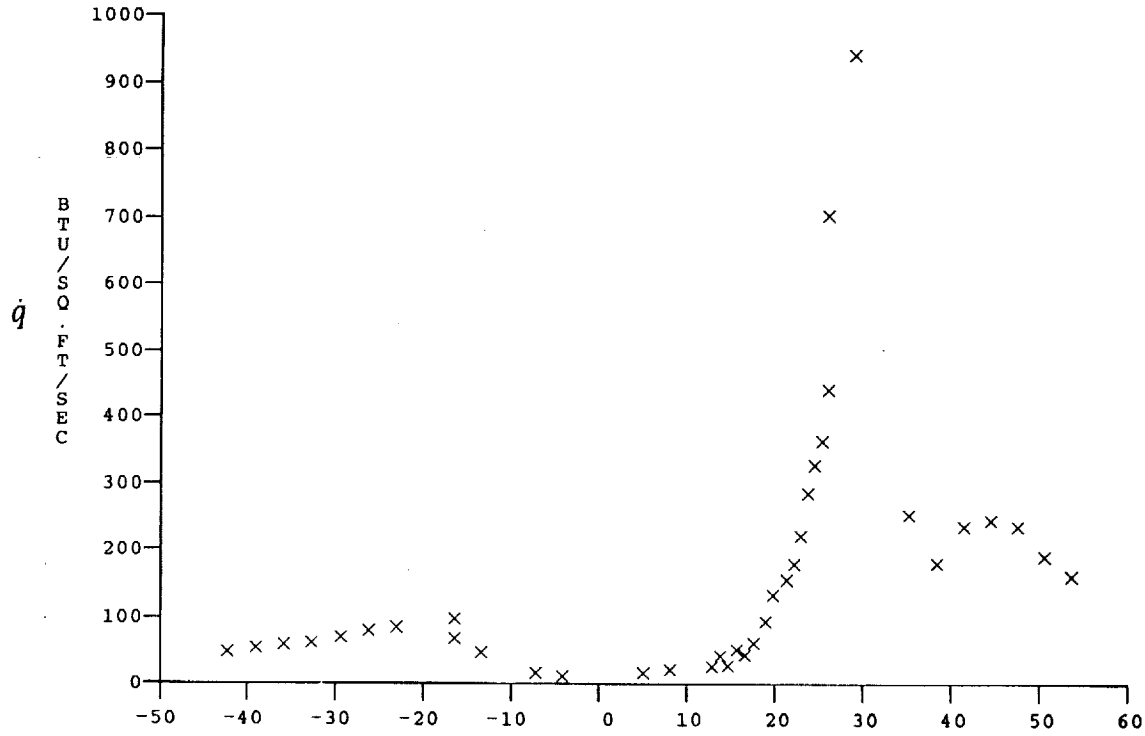

HEAT TRANSFER vs Gauge Position
Run 27

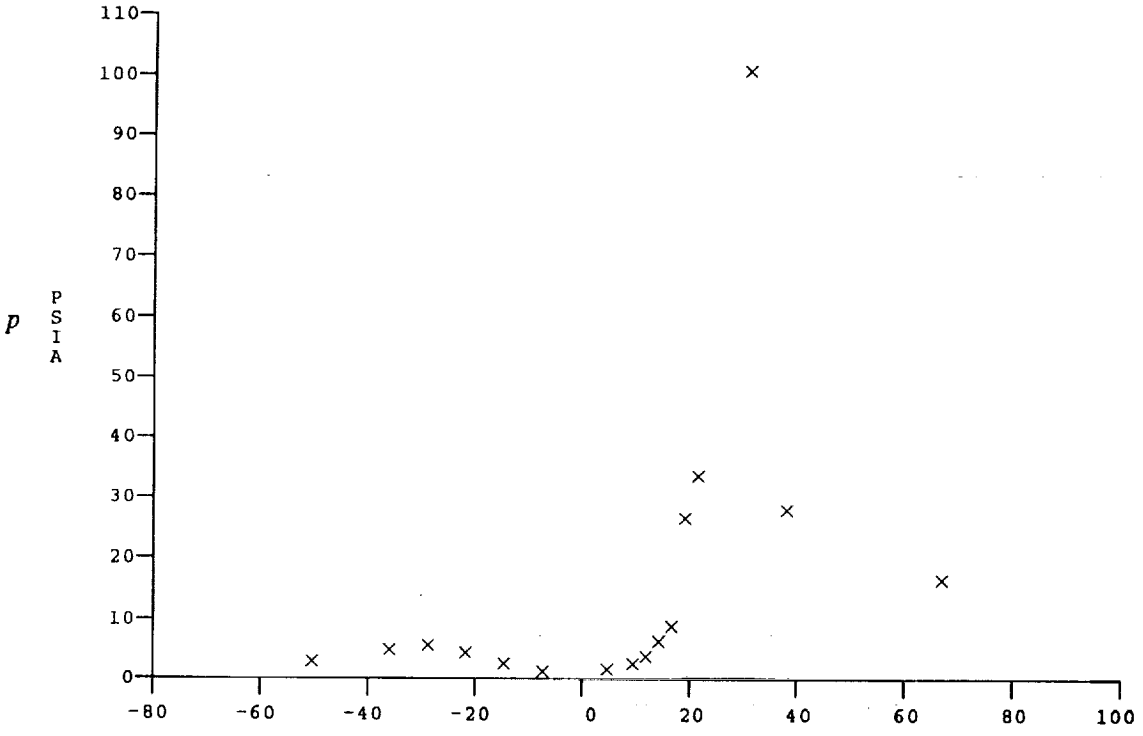

PRESSURE vs Gauge Position
Run 27

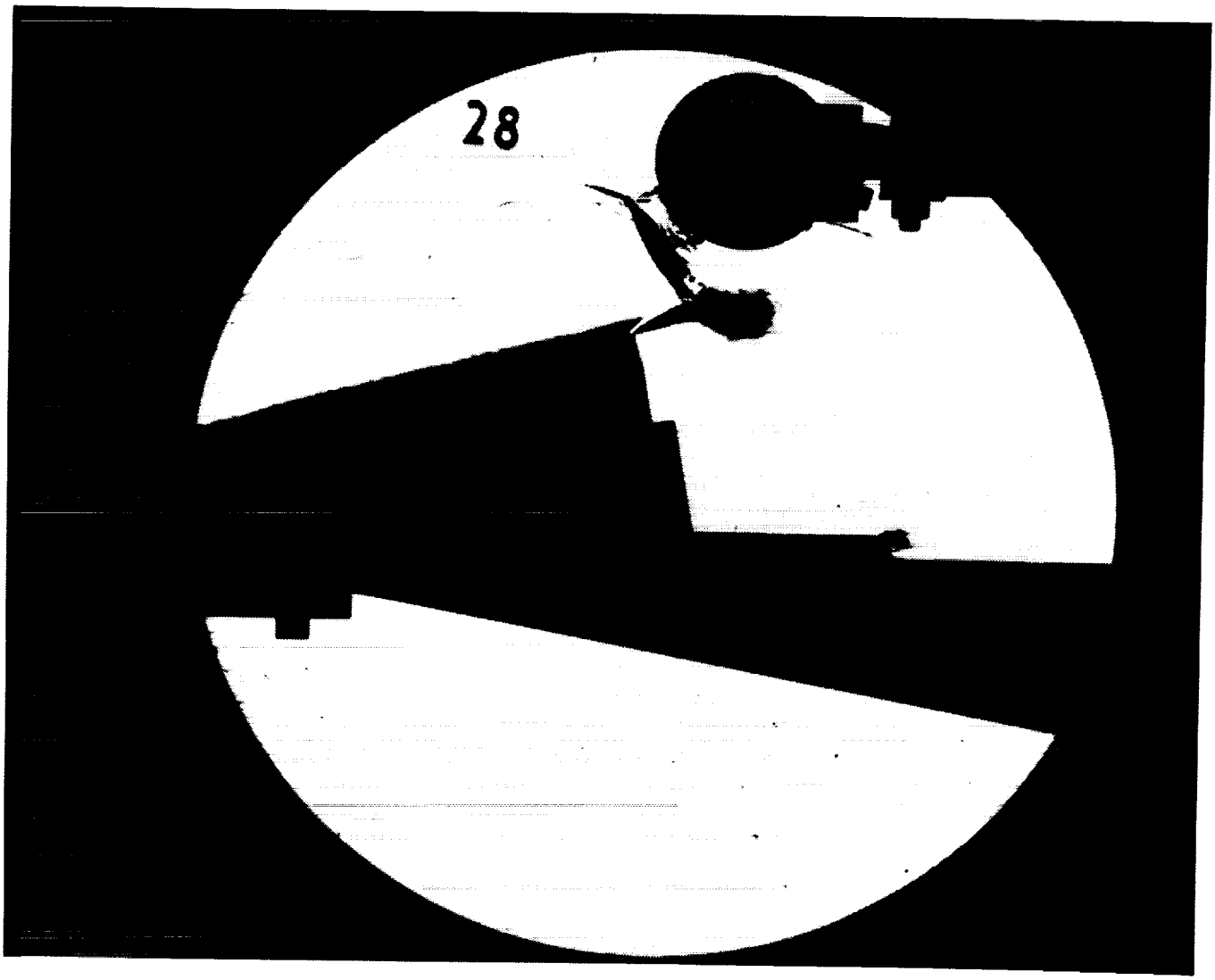

Test Conditions for Run 28 :

Po	= 6.986E-02 PSIA	Reservoir Total Pressure	
Ho	= 1.909E-07 (Ft/sec)²	Reservoir Total Enthalpy	
To	= 2.896E-03 °R	Reservoir Total Temperature	
M	= 7.935E-00	Freestream Mach Number	
U	= 5.950E-03 Ft/sec	Freestream Velocity	
T	= 2.338E-02 °R	Freestream Temperature	
P	= 6.500E-02 PSIA	Freestream Static Pressure	
Rho	= 2.333E-05 Slugs/Ft3	Freestream Density	
Mu	= 1.926E-07 Slugs/Ft-sec	Freestream Viscosity	
Re	= 7.208E-05 1/Ft	Freestream Reynolds Number	
Po'	= 5.319E+00 PSIA	Pitot Pressure	
Q	= 2.868E-00 PSIA	Dynamic Pressure (½·Rho·U²/144)	
Mi	= 3.468E+00	Shock Tube Incident Shock Mach Number	
Hw	= 3.183E+06 (Ft/sec)²	Wall Enthalpy (Cp·Tw)	
CPf	= 3.487E-01 1/PSIA	Pressure to CP factor (1/Q)	
CHf	= 3.524E-04 Ft²-s/BTU	Heat Rate to CH factor (778/(Rho·U·(Ho-Hw))	
QoFR	= 3.011E+01 BTU/Ft²-s	Fay-Riddell Heat Transfer to 3" Diam Sphere	

Model Configuration Parameter	Value
Stagnation Position (gauge label)	P21
Vertical Distance (inches)	2.95
Horizontal Distance (inches)	0.31
Plate Angle (degrees)	15.00
Plate Length (inches)	26.50
Sweep Angle (degrees)	0.00

Run 28

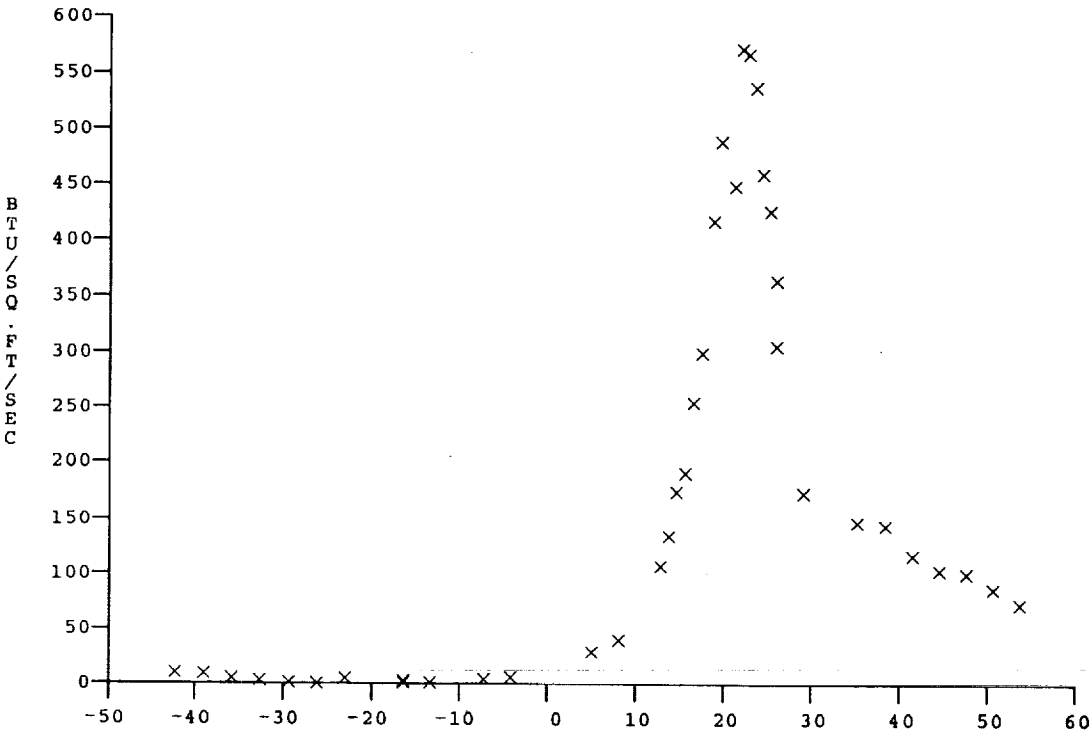

$\dot{q}$

HEAT TRANSFER vs Gauge Position
Run 28

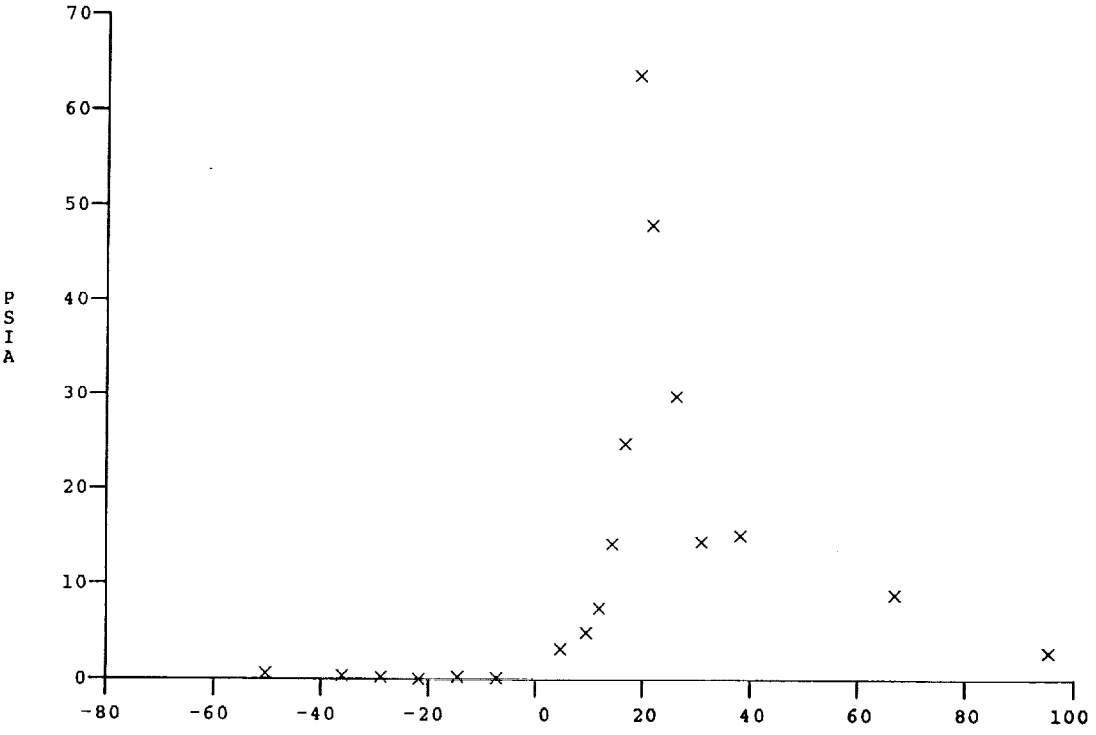

p

PRESSURE vs Gauge Position
Run 28

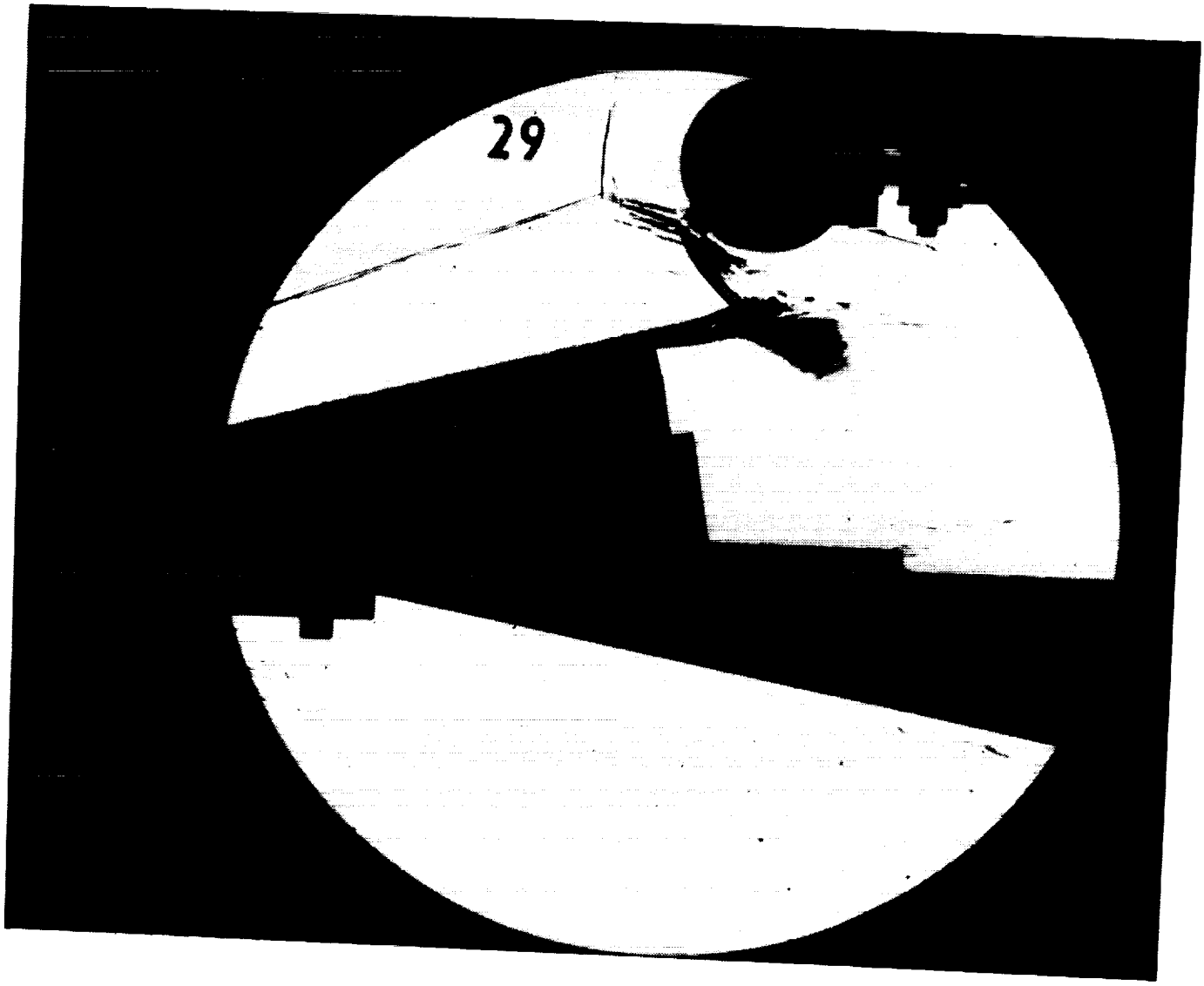

Test Conditions for Run 29 :

Po	= 1.433E+03	PSIA	Reservoir Total Pressure
Ho	= 1.858E+07	(Ft/sec)²	Reservoir Total Enthalpy
To	= 2.820E+03	°R	Reservoir Total Temperature
M	= 8.029E+00		Freestream Mach Number
U	= 5.875E+03	Ft/sec	Freestream Velocity
T	= 2.227E+02	°R	Freestream Temperature
P	= 1.263E-01	PSIA	Freestream Static Pressure
Rho	= 4.759E-05	Slugs/Ft3	Freestream Density
Mu	= 1.839E-07	Slugs/Ft-sec	Freestream Viscosity
Re	= 1.520E+06	1/Ft	Freestream Reynolds Number
Po'	= 1.058E+01	PSIA	Pitot Pressure
Q	= 5.704E+00	PSIA	Dynamic Pressure (½·Rho·U²/144)
Mi	= 3.444E+00		Shock Tube Incident Shock Mach Number
Hw	= 3.183E+06	(Ft/sec)²	Wall Enthalpy (Cp·Tw)
CPf	= 1.753E-01	1/PSIA	Pressure to CP factor (1/Q)
CHf	= 1.807E-04	Ft²-s/BTU	Heat Rate to CH factor (778/(Rho·U·(Ho-Hw))
QoFR	= 4.102E-01	BTU/Ft²-s	Fay-Riddell Heat Transfer to 3" Diam Sphere

Model Configuration Parameter	Value
Stagnation Position (gauge label)	P23
Vertical Distance (inches)	3.19
Horizontal Distance (inches)	0.31
Plate Angle (degrees)	15.00
Plate Length (inches)	26.50
Sweep Angle (degrees)	0.00

Run 29

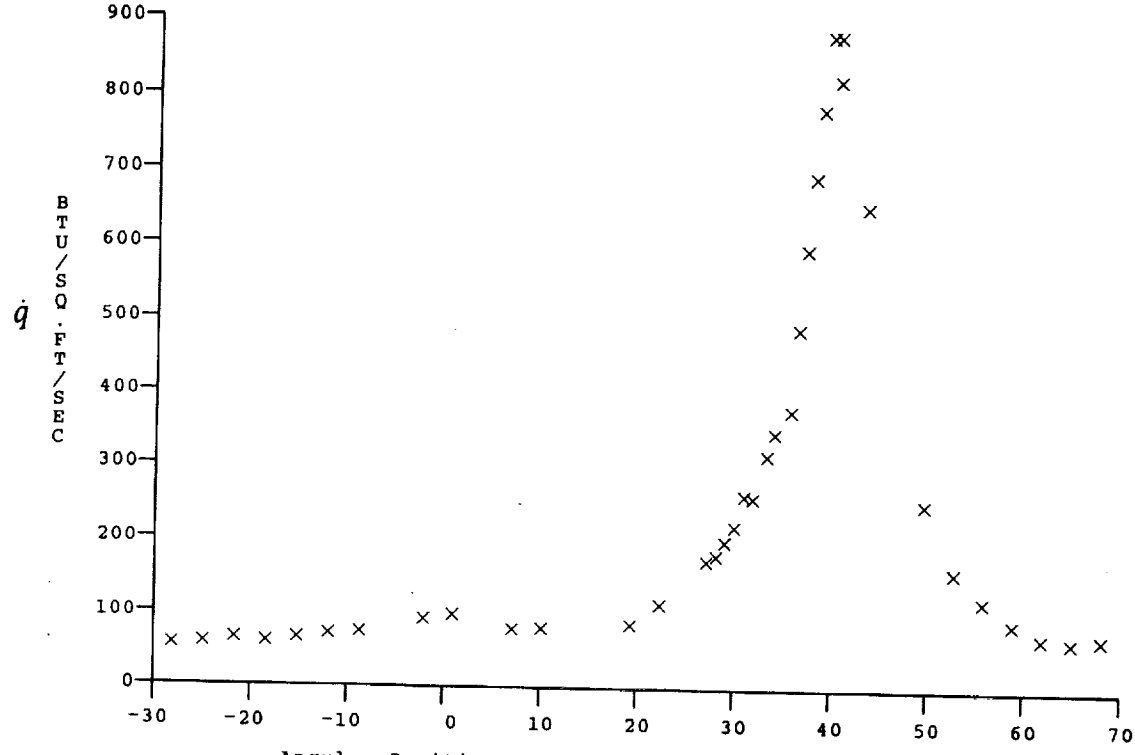

HEAT TRANSFER vs Gauge Position
Run 29

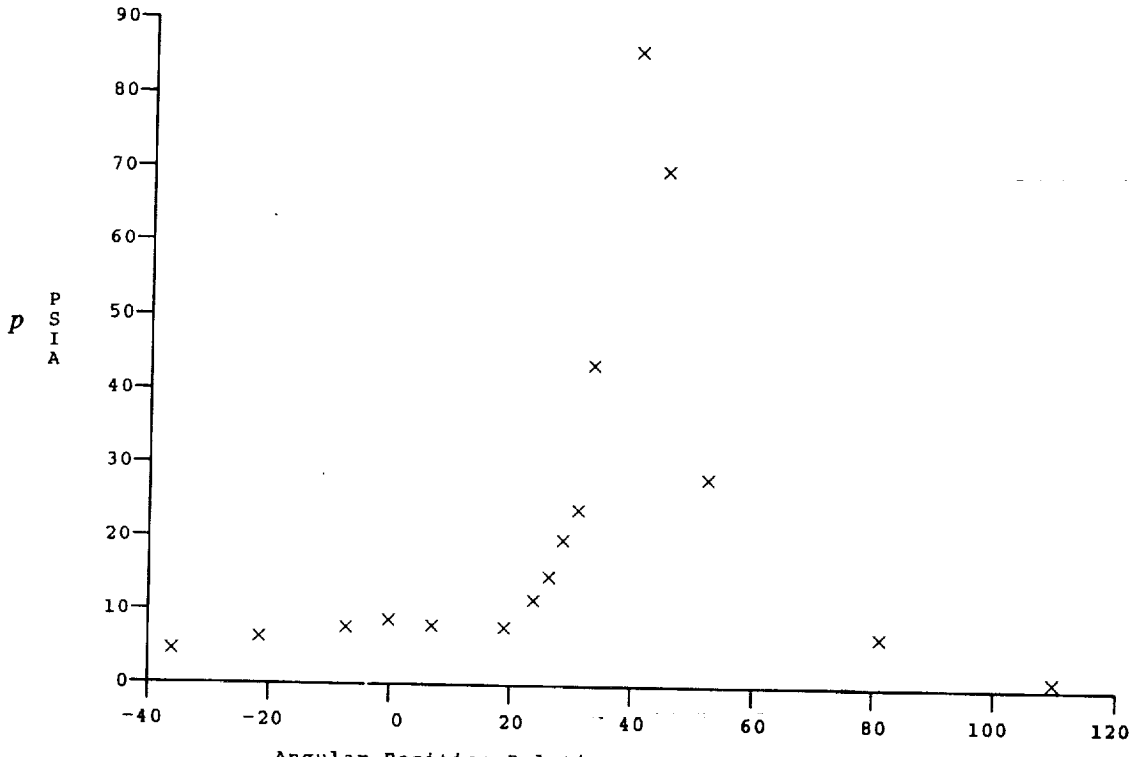

PRESSURE vs Gauge Position
Run 29

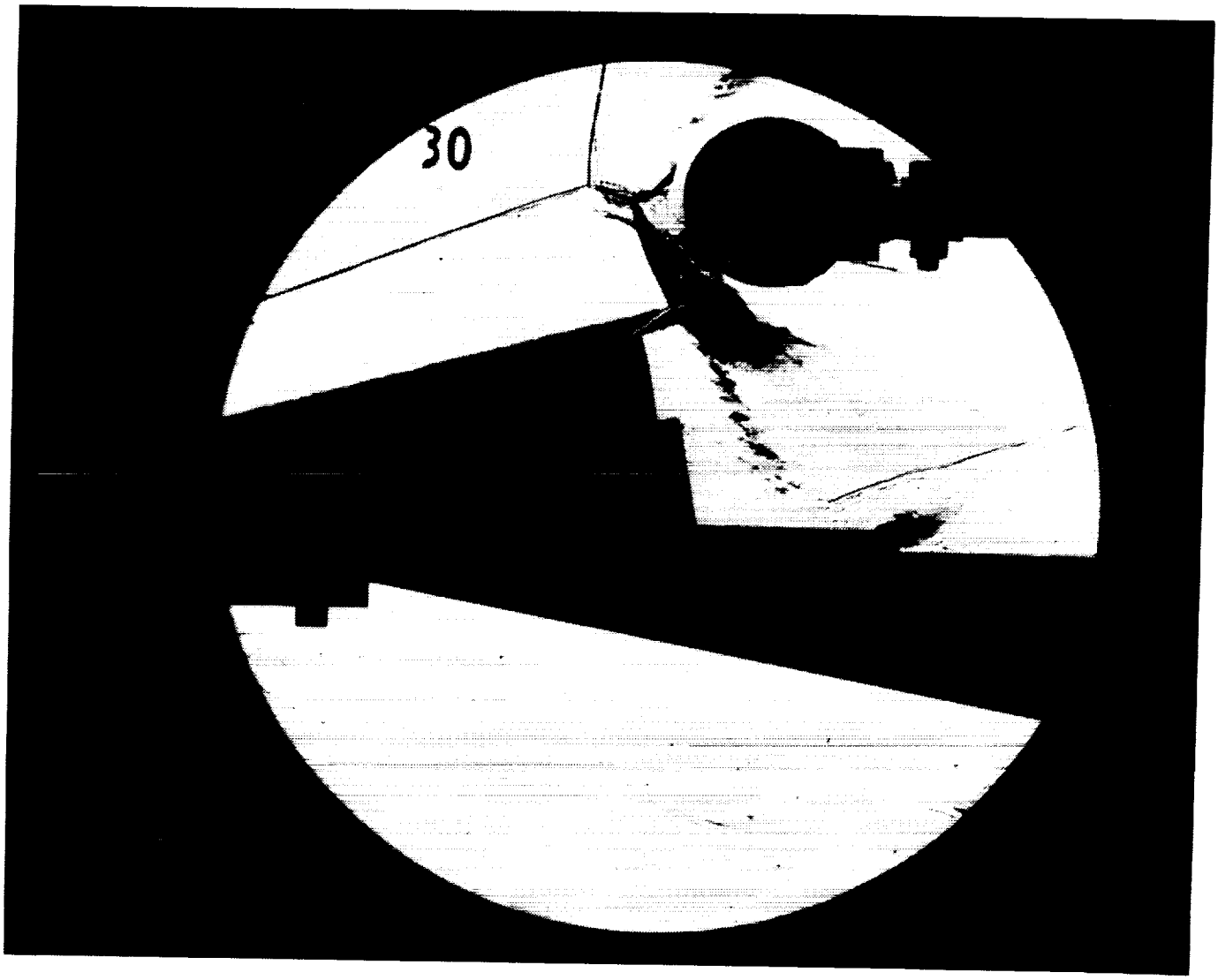

Test Conditions for Run 30 :

Po	= 1.430E+03 PSIA	Reservoir Total Pressure
Ho	= 1.630E+07 (Ft/sec)²	Reservoir Total Enthalpy
To	= 2.513E+03 °R	Reservoir Total Temperature
M	= 8.155E-00	Freestream Mach Number
U	= 5.509E+03 Ft/sec	Freestream Velocity
T	= 1.898E+02 °R	Freestream Temperature
P	= 1.191E-01 PSIA	Freestream Static Pressure
Rho	= 5.264E-05 Slugs/Ft3	Freestream Density
Mu	= 1.581E-07 Slugs/Ft-sec	Freestream Viscosity
Re	= 1.835E+06 1/Ft	Freestream Reynolds Number
Po'	= 1.027E+01 PSIA	Pitot Pressure
Q	= 5.548E+00 PSIA	Dynamic Pressure (½·Rho·U²/144)
Mi	= 3.171E+00	Shock Tube Incident Shock Mach Number
Hw	= 3.183E+06 (Ft/sec)²	Wall Enthalpy (Cp·Tw)
CPf	= 1.802E-01 1/PSIA	Pressure to CP factor (1/Q)
CHf	= 2.045E-04 Ft²-s/BTU	Heat Rate to CH factor (778/(Rho·U·(Ho-Hw))
QoFR	= 3.412E+01 BTU/Ft²-s	Fay-Riddell Heat Transfer to 3" Diam Sphere

Model Configuration Parameter	Value
Stagnation Position (gauge label)	P11
Vertical Distance (inches)	2.31
Horizontal Distance (inches)	0.75
Plate Angle (degrees)	15.00
Plate Length (inches)	26.50
Sweep Angle (degrees)	0.00

Run 30

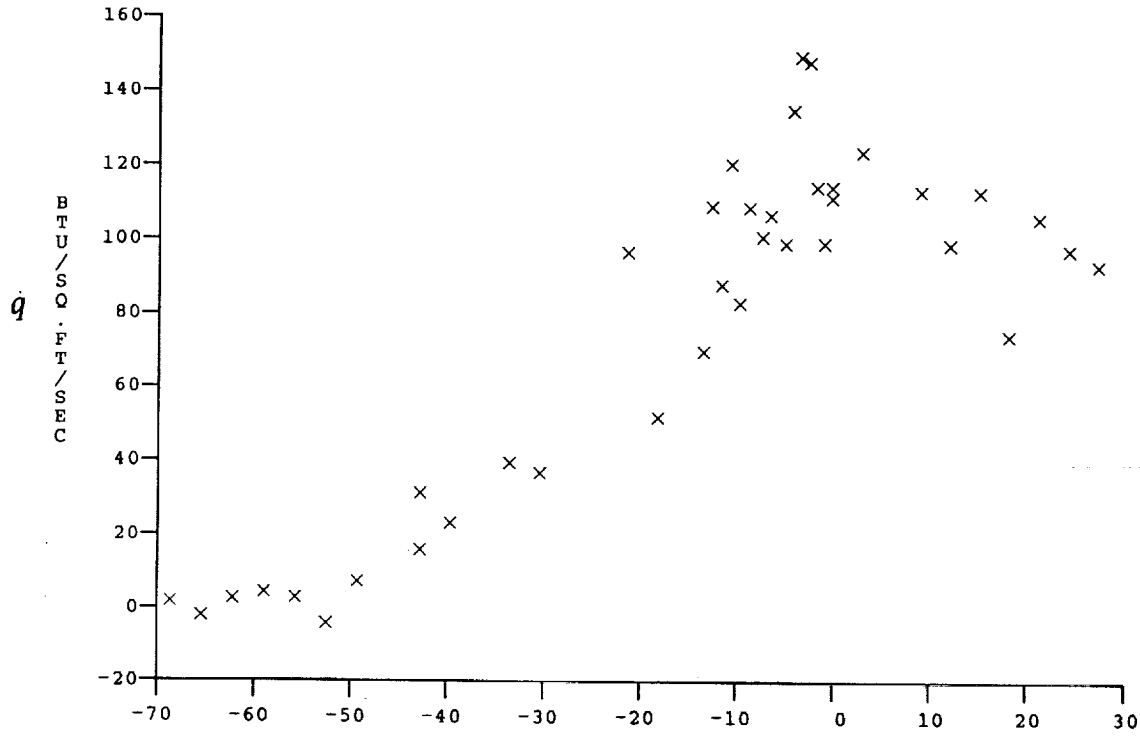

HEAT TRANSFER vs Gauge Position
Run 30

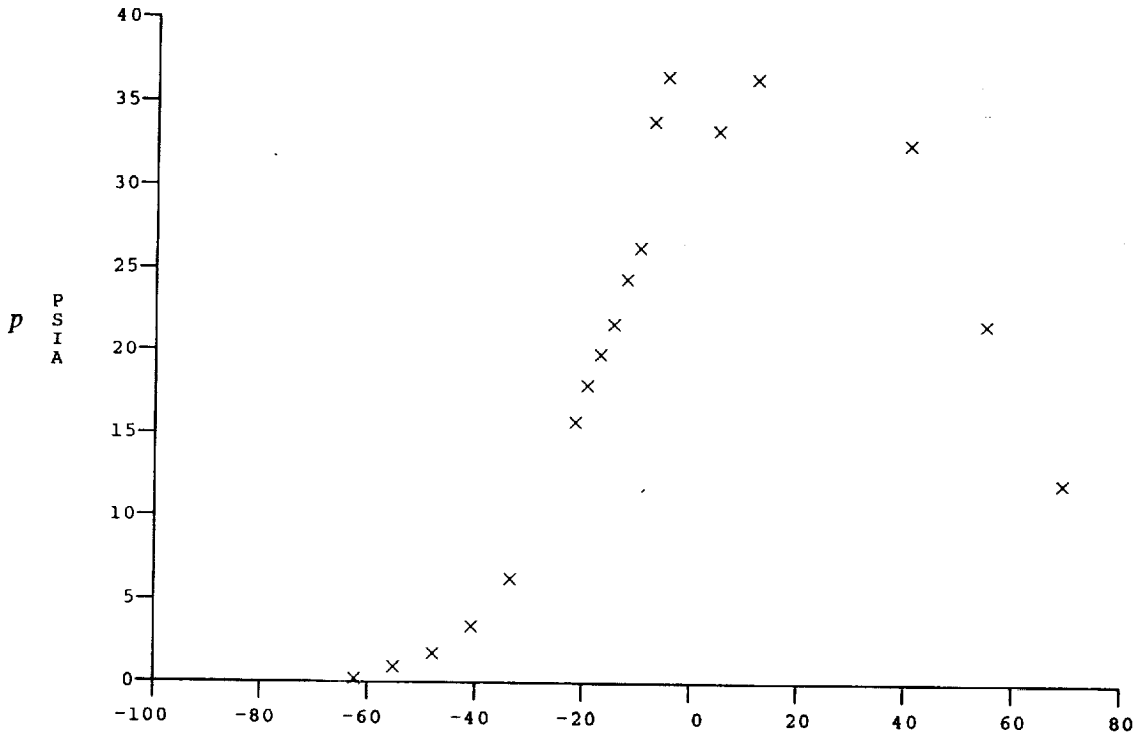

PRESSURE vs Gauge Position
Run 30

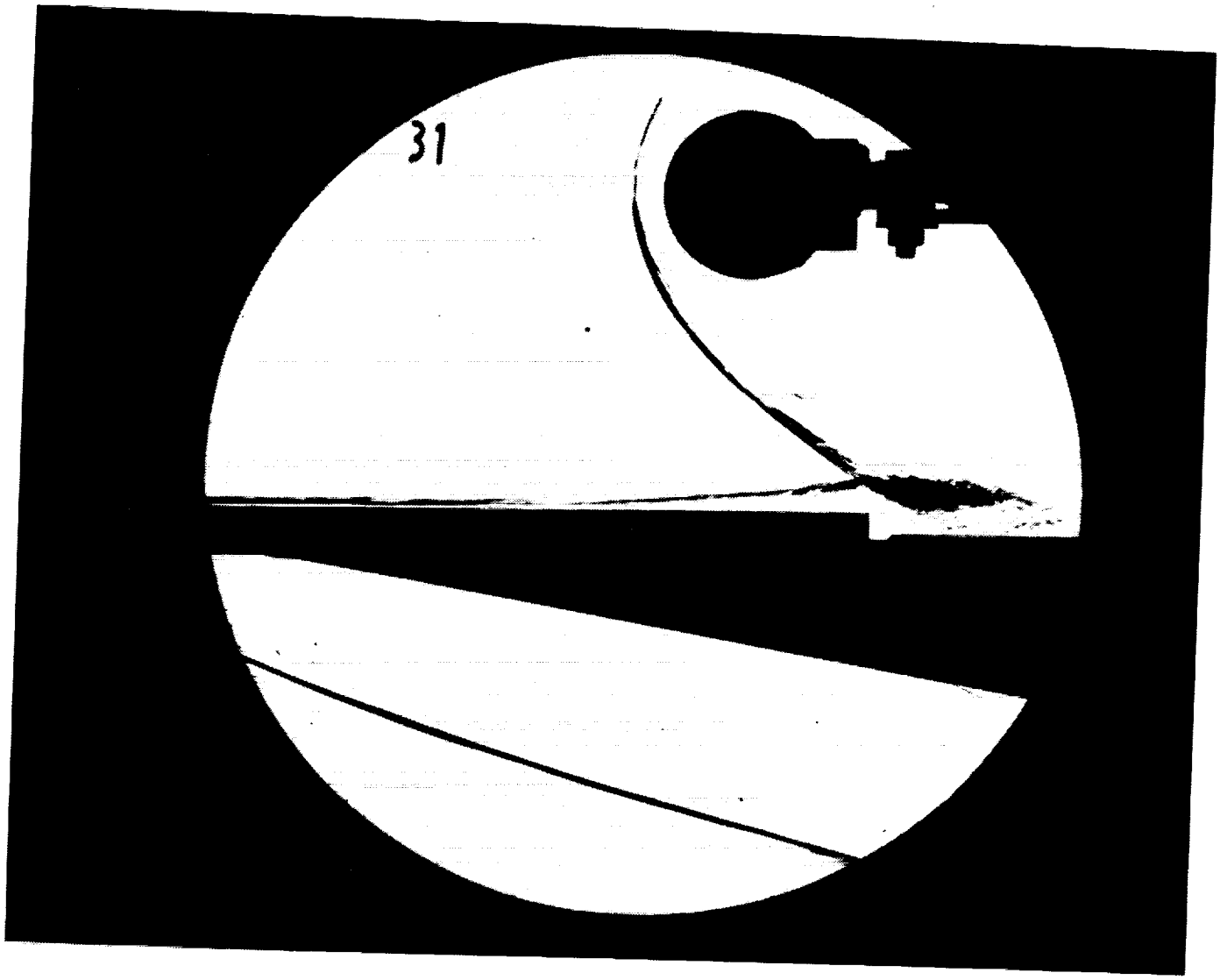

Test Conditions for Run 31 :

Po	= 1.440E+03	PSIA	Reservoir Total Pressure
Ho	= 1.878E+07	(Ft/sec)²	Reservoir Total Enthalpy
To	= 2.849E+03	°R	Reservoir Total Temperature
M	= 8.033E+00		Freestream Mach Number
U	= 5.907E+03	Ft/sec	Freestream Velocity
T	= 2.248E+02	°R	Freestream Temperature
P	= 1.260E-01	PSIA	Freestream Static Pressure
Rho	= 4.704E-05	Slugs/Ft3	Freestream Density
Mu	= 1.856E-07	Slugs/Ft-sec	Freestream Viscosity
Re	= 1.497E+06	1/Ft	Freestream Reynolds Number
Po'	= 1.057E+01	PSIA	Pitot Pressure
Q	= 5.699E+00	PSIA	Dynamic Pressure (½·Rho·U²/144)
Mi	= 3.436E+00		Shock Tube Incident Shock Mach Number
Hw	= 3.183E+06	(Ft/sec)²	Wall Enthalpy (Cp·Tw)
CPf	= 1.755E-01	1/PSIA	Pressure to CP factor (1/Q)
CHf	= 1.796E-04	Ft²-s/BTU	Heat Rate to CH factor (778/(Rho·U·(Ho-Hw))
QoFR	= 4.156E+01	BTU/Ft²-s	Fay-Riddell Heat Transfer to 3" Diam Sphere

Model Configuration Parameter	Value
Stagnation Position (gauge label)	P18
Sweep Angle (degrees)	0.00

Run 31

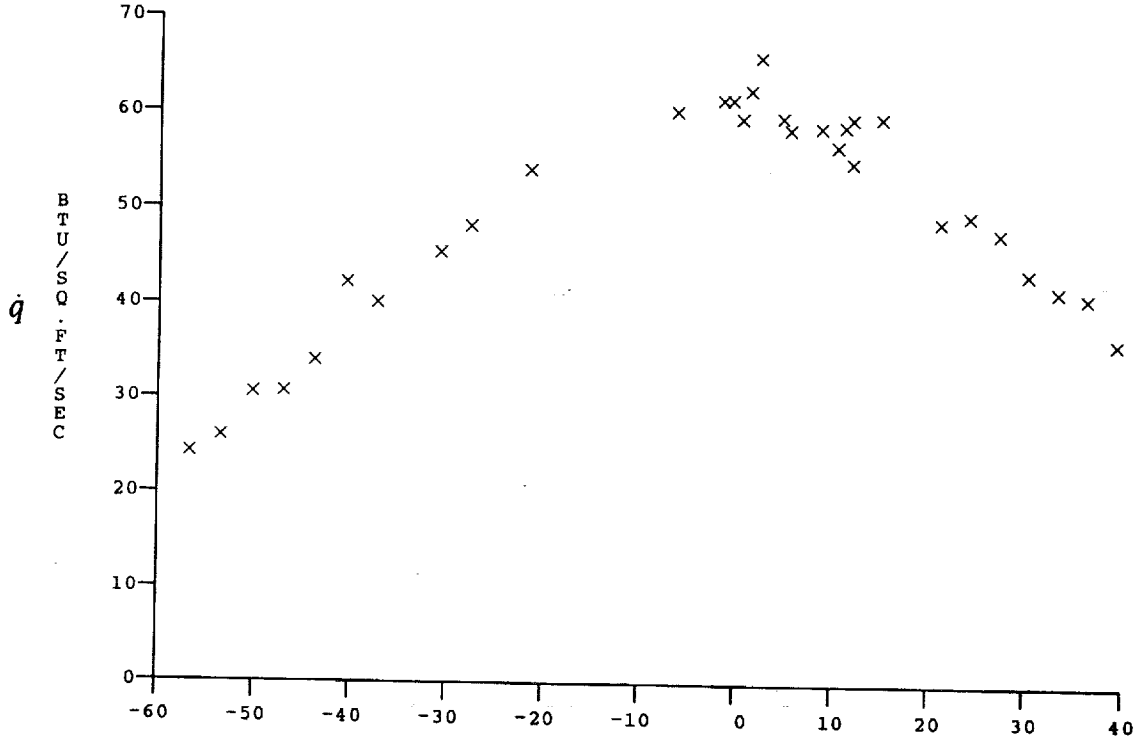

HEAT TRANSFER vs Gauge Position
Run 31

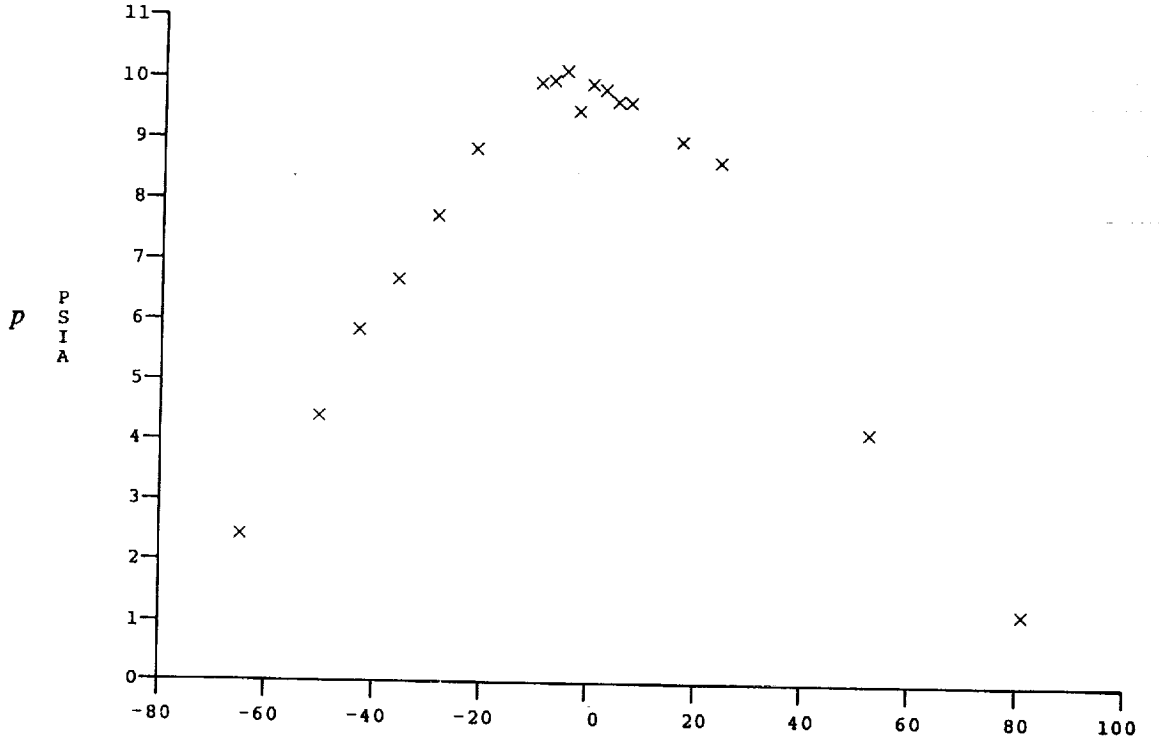

PRESSURE vs Gauge Position
Run 31

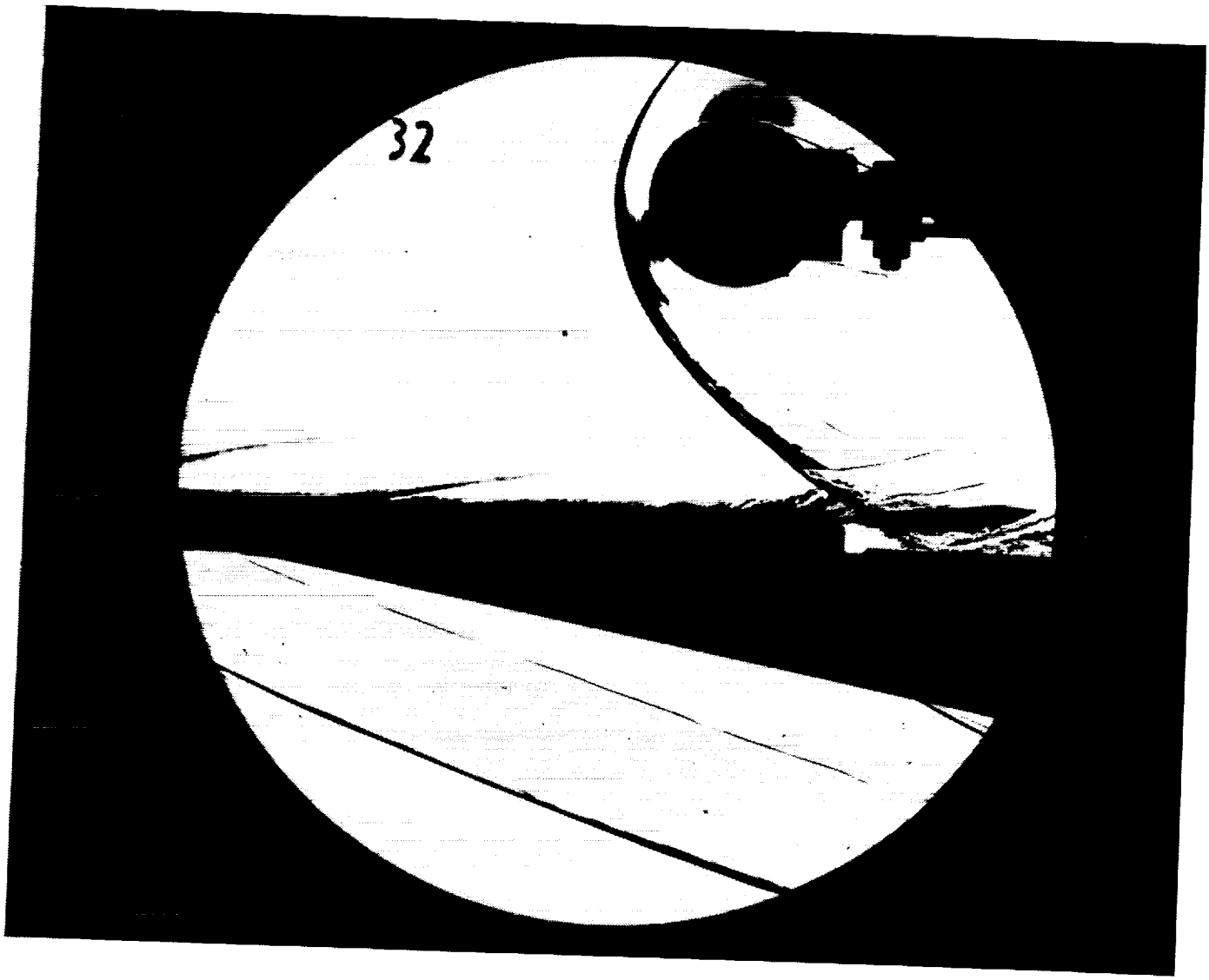

Test Conditions for Run 32 :

Po	= 1.396E+03 PSIA	Reservoir Total Pressure
Ho	= 1.319E+07 (Ft/sec)²	Reservoir Total Enthalpy
To	= 2.078E-03 °R	Reservoir Total Temperature
M	= 6.384E+00	Freestream Mach Number
U	= 4.850E+03 Ft/sec	Freestream Velocity
T	= 2.400E+02 °R	Freestream Temperature
p	= 5.852E-01 PSIA	Freestream Static Pressure
Rho	= 2.046E-04 Slugs/Ft3	Freestream Density
Mu	= 1.973E-07 Slugs/Ft-sec	Freestream Viscosity
Re	= 5.031E+06 1/Ft	Freestream Reynolds Number
Po'	= 3.114E+01 PSIA	Pitot Pressure
Q	= 1.671E+01 PSIA	Dynamic Pressure (½·Rho·U²/144)
Mi	= 2.777E+00	Shock Tube Incident Shock Mach Number
Hw	= 3.183E+06 (Ft/sec)²	Wall Enthalpy (Cp·Tw)
CPf	= 5.983E-02 1/PSIA	Pressure to CP factor (1/Q)
CHf	= 7.832E-05 Ft²-s/BTU	Heat Rate to CH factor (778/(Rho·U·(Ho-Hw))
QoFR	= 4.457E+01 BTU/Ft²-s	Fay-Riddell Heat Transfer to 3" Diam Sphere

Model Configuration Parameter	Value
Stagnation Position (gauge label)	P18
Sweep Angle (degrees)	0.00

Run 32

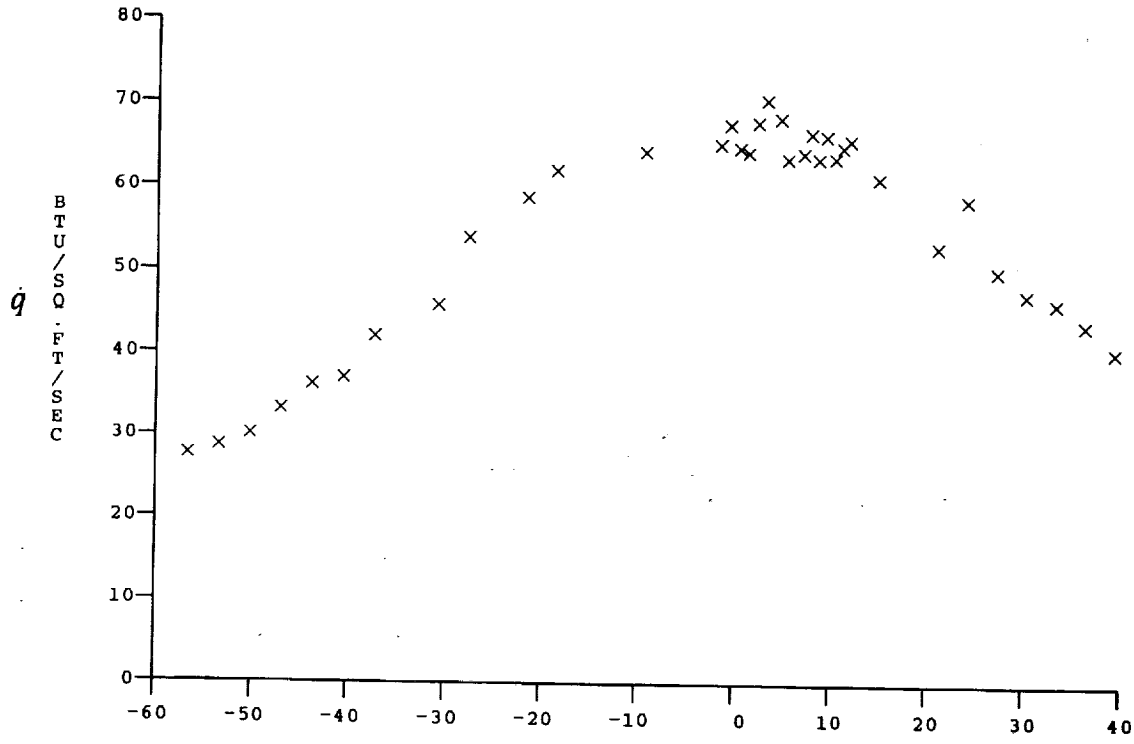

HEAT TRANSFER vs Gauge Position
Run 32

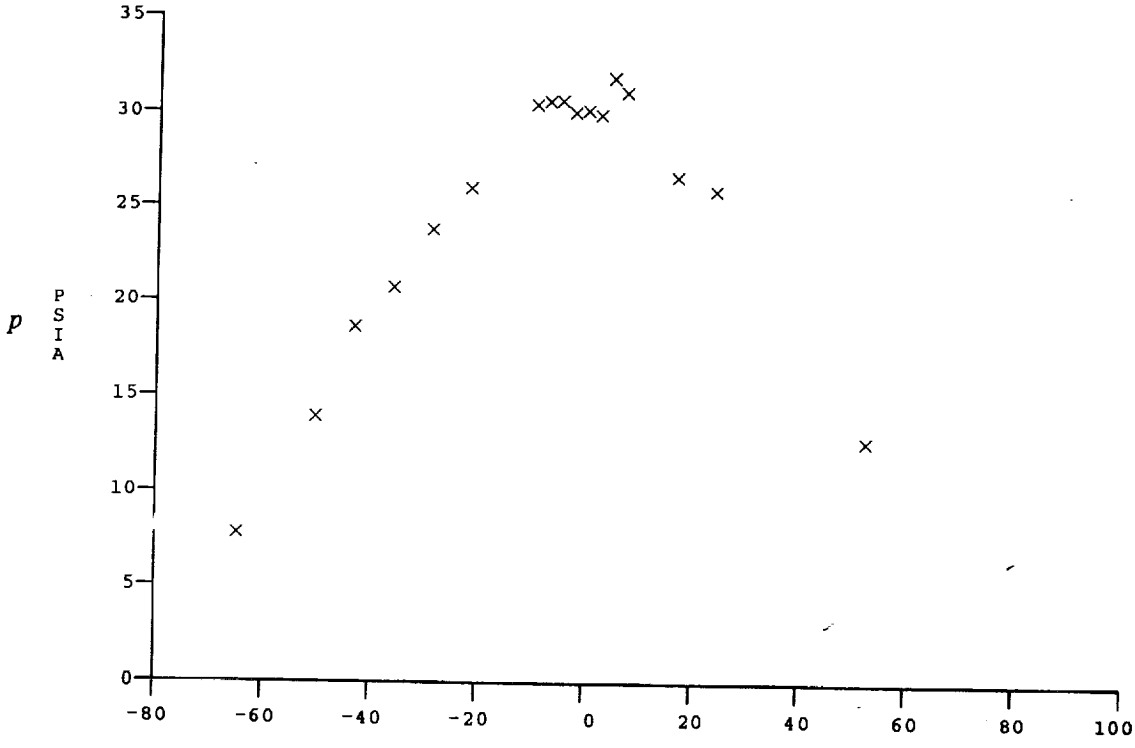

PRESSURE vs Gauge Position
Run 32

Test Conditions

Mi	= 3.2709	
Po	= 7.5213X10+3	PSIA
Ho	= 1.7244X10+7	(Ft/sec)^2
To	= 2.5807X10+3	Degrees R
M	=11.0020	
U	= 5.7580X10+3	Ft/sec
T	= 1.1390X10+2	Degrees R
P	= 9.5955X10-2	PSIA
Q	= 8.1389	PSIA
Rho	= 7.0700X10-5	Slugs/Ft^3
Mu	= 9.5786X10-8	Slugs/Ft-sec
Re	= 4.2500X10+6	1/Ft
Po'	= 1.5072X10+1	PSIA

Model Configuration Parameter	Value
Stagnation Position (gauge label)	P21.5
Vertical Distance (inches)	2.00
Horizontal Distance (inches)	0.44
Plate Angle (degrees)	10.00
Plate Length (inches)	26.50
Sweep Angle (degrees)	0.00

Run 33

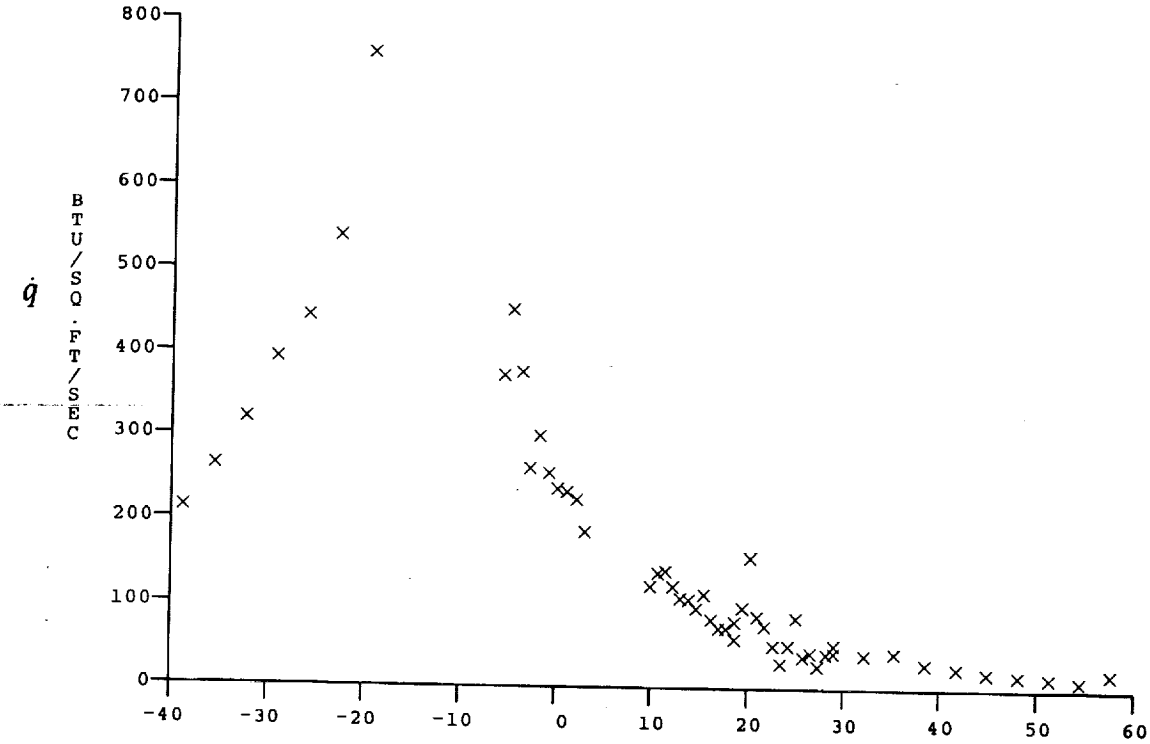

HEAT TRANSFER vs Gauge Position
Run 33

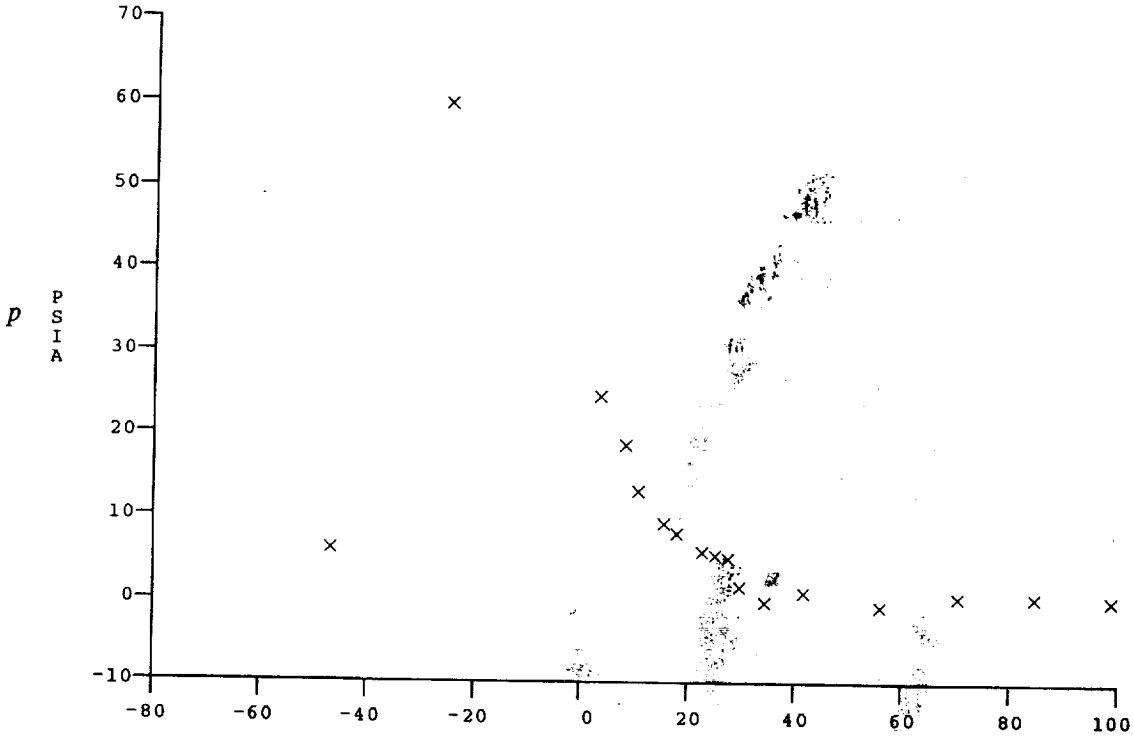

PRESSURE vs Gauge Position
Run 33

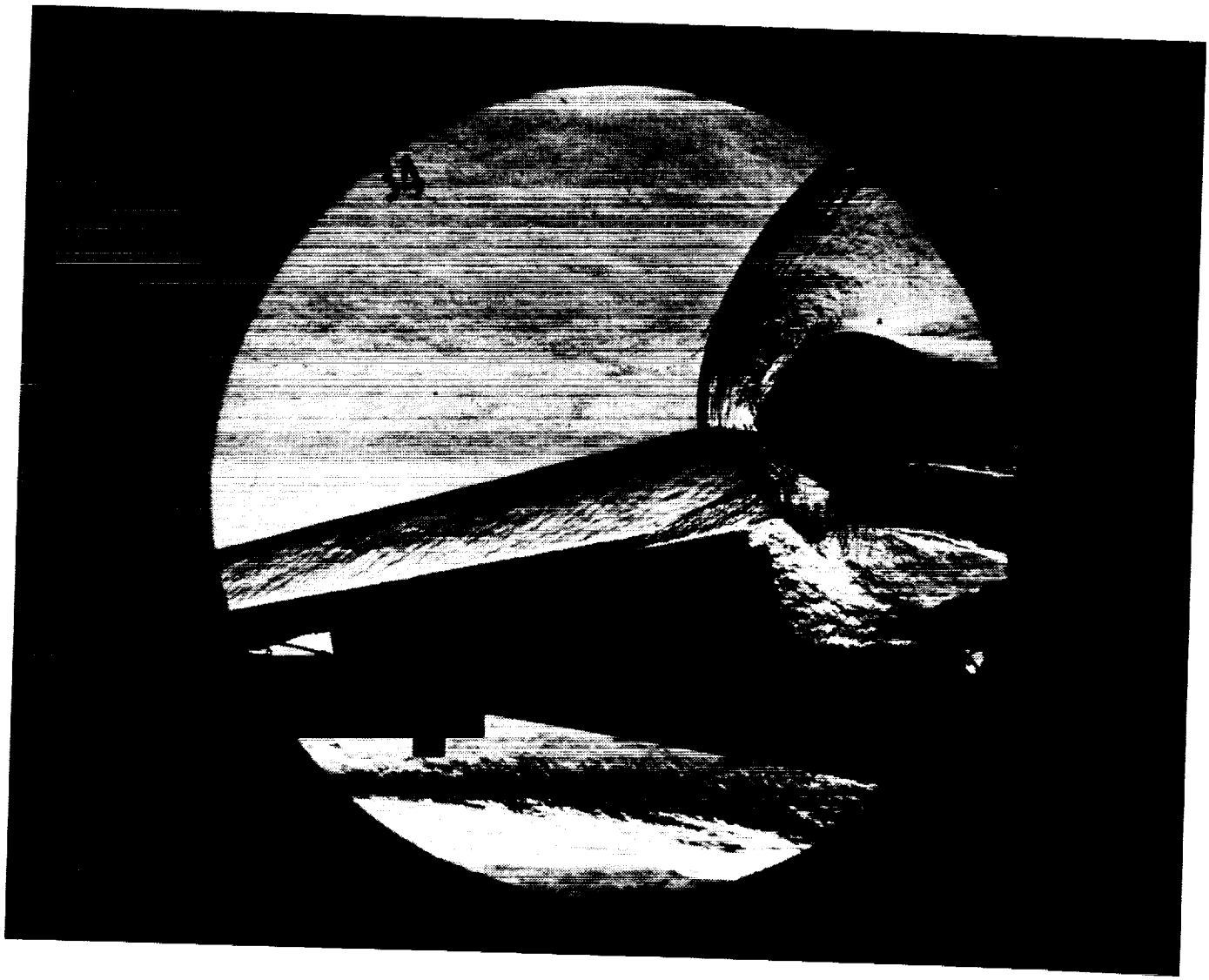

Test Conditions for Run 34 :

Po	= 7.660E+03 PSIA	Reservoir Total Pressure
Ho	= 1.703E-07 (Ft/sec)²	Reservoir Total Enthalpy
To	= 2.552E+03 °R	Reservoir Total Temperature
M	= 1.101E-01	Freestream Mach Number
U	= 5.722E+03 Ft/sec	Freestream Velocity
T	= 1.123E+02 °R	Freestream Temperature
P	= 9.796E-02 PSIA	Freestream Static Pressure
Rho	= 7.319E-05 Slugs/Ft3	Freestream Density
Mu	= 9.446E-08 Slugs/Ft-sec	Freestream Viscosity
Re	= 4.434E+06 1/Ft	Freestream Reynolds Number
Po'	= 1.541E+01 PSIA	Pitot Pressure
Q	= 8.321E+00 PSIA	Dynamic Pressure (½·Rho·U²/144)
Mi	= 3.264E+00	Shock Tube Incident Shock Mach Number
Hw	= 3.183E+06 (Ft/sec)²	Wall Enthalpy (Cp·Tw)
CPf	= 1.202E-01 1/PSIA	Pressure to CP factor (1/Q)
CHf	= 1.342E-04 Ft²-s/BTU	Heat Rate to CH factor (778/(Rho·U·(Ho-Hw))
QoFR	= 4.448E+01 BTU/Ft²-s	Fay-Riddell Heat Transfer to 3" Diam Sphere

Model Configuration Parameter	Value
Stagnation Position (gauge label)	P21.5
Vertical Distance (inches)	2.25
Horizontal Distance (inches)	0.44
Plate Angle (degrees)	10.00
Plate Length (inches)	26.50
Sweep Angle (degrees)	0.00

Run 34

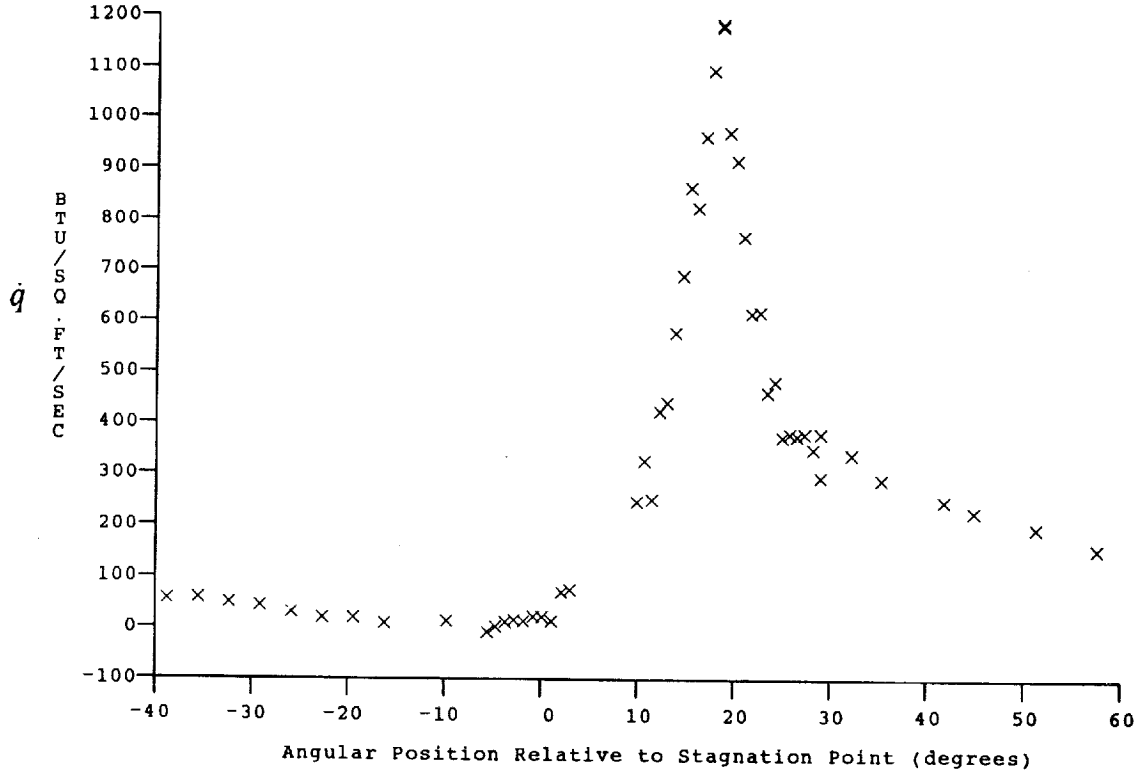

HEAT TRANSFER vs Gauge Position
Run 34

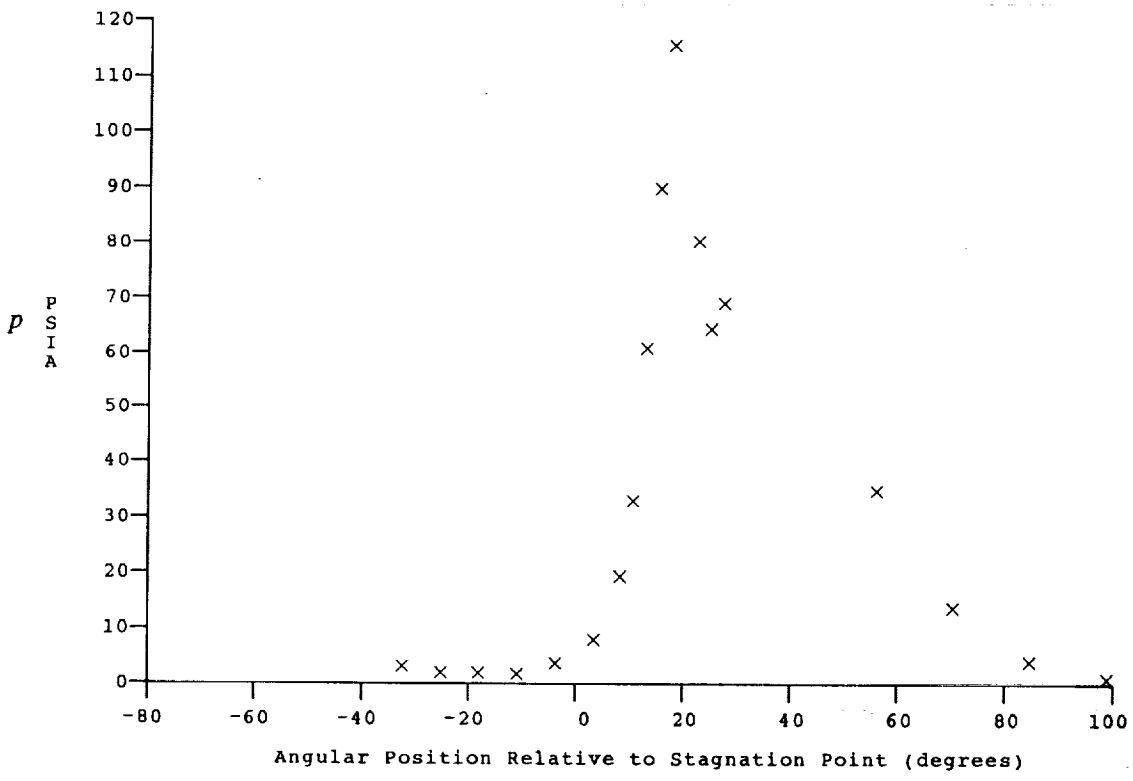

PRESSURE vs Gauge Position
Run 34

Test Conditions for Run 35 :

Po	= 7.816E+03	PSIA
Ho	= 1.703E+07	(Ft/sec)²
To	= 2.553E+03	°R
M	= 1.102E+01	
U	= 5.723E+03	Ft/sec
T	= 1.121E+02	°R
P	= 9.950E-02	PSIA
Rho	= 7.450E-05	Slugs/Ft3
Mu	= 9.427E-08	Slugs/Ft-sec
Re	= 4.522E+06	1/Ft
Po'	= 1.568E+01	PSIA
Q	= 8.471E+00	PSIA
Mi	= 3.251E+00	
Hw	= 3.183E+06	(Ft/sec)²
CPf	= 1.181E-01	1/PSIA
CHf	= 1.318E-04	Ft²-s/BTU
QoFR	= 4.488E+01	BTU/Ft²-s

Reservoir Total Pressure
Reservoir Total Enthalpy
Reservoir Total Temperature
Freestream Mach Number
Freestream Velocity
Freestream Temperature
Freestream Static Pressure
Freestream Density
Freestream Viscosity
Freestream Reynolds Number
Pitot Pressure
Dynamic Pressure (½·Rho·U²/144)
Shock Tube Incident Shock Mach Number
Wall Enthalpy (Cp·Tw)
Pressure to CP factor (1/Q)
Heat Rate to CH factor (778/(Rho·U·(Ho-Hw))
Fay-Riddell Heat Transfer to 3" Diam Sphere

Model Configuration Parameter	Value
Stagnation Position (gauge label)	P21.5
Vertical Distance (inches)	2.72
Horizontal Distance (inches)	1.81
Plate Angle (degrees)	10.00
Plate Length (inches)	26.50
Sweep Angle (degrees)	0.00

Run 35

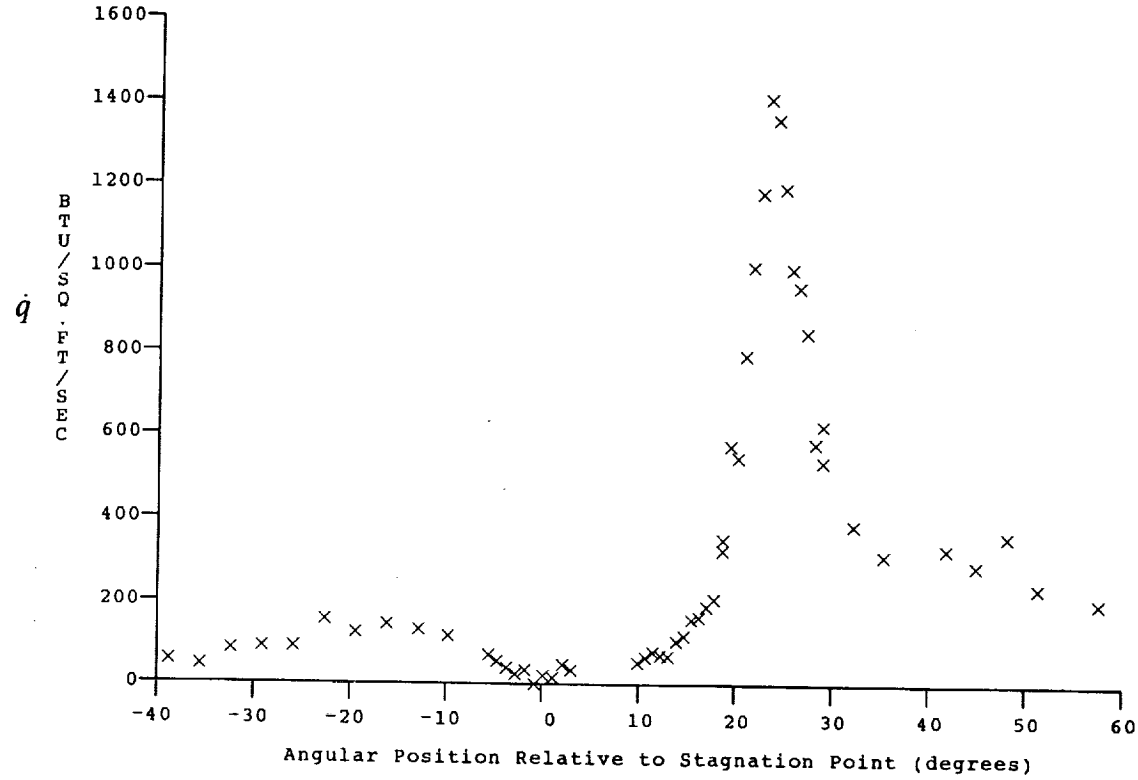

HEAT TRANSFER vs Gauge Position
Run 35

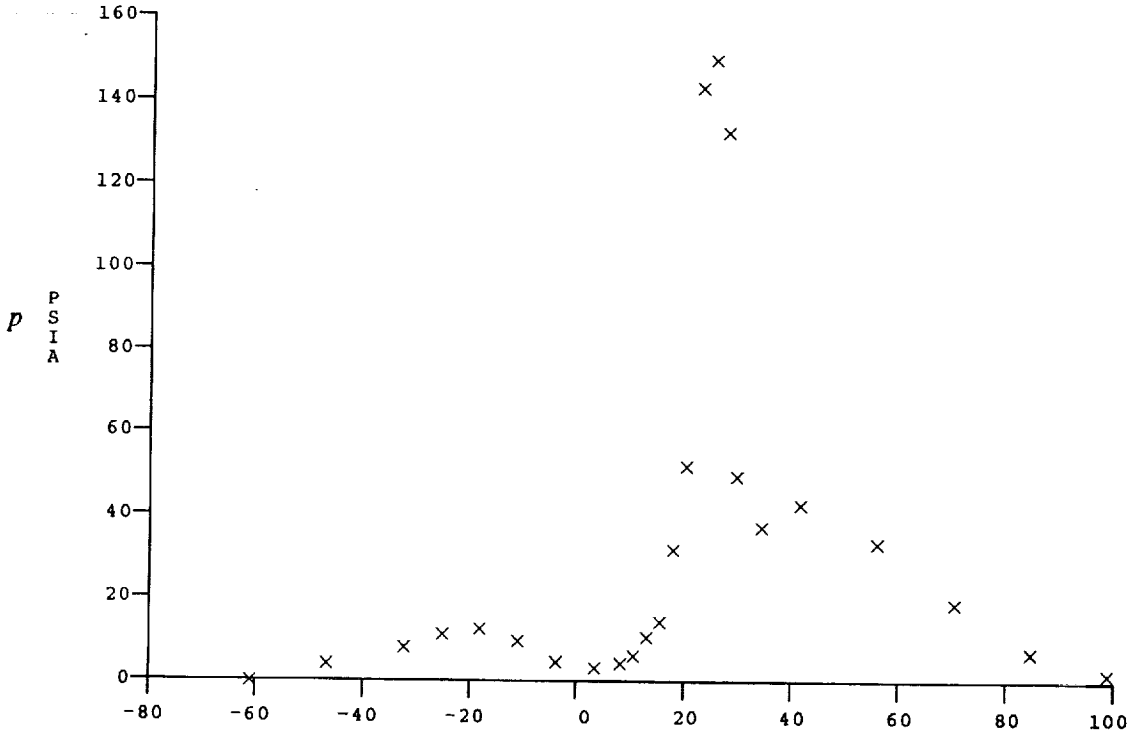

PRESSURE vs Gauge Position
Run 35

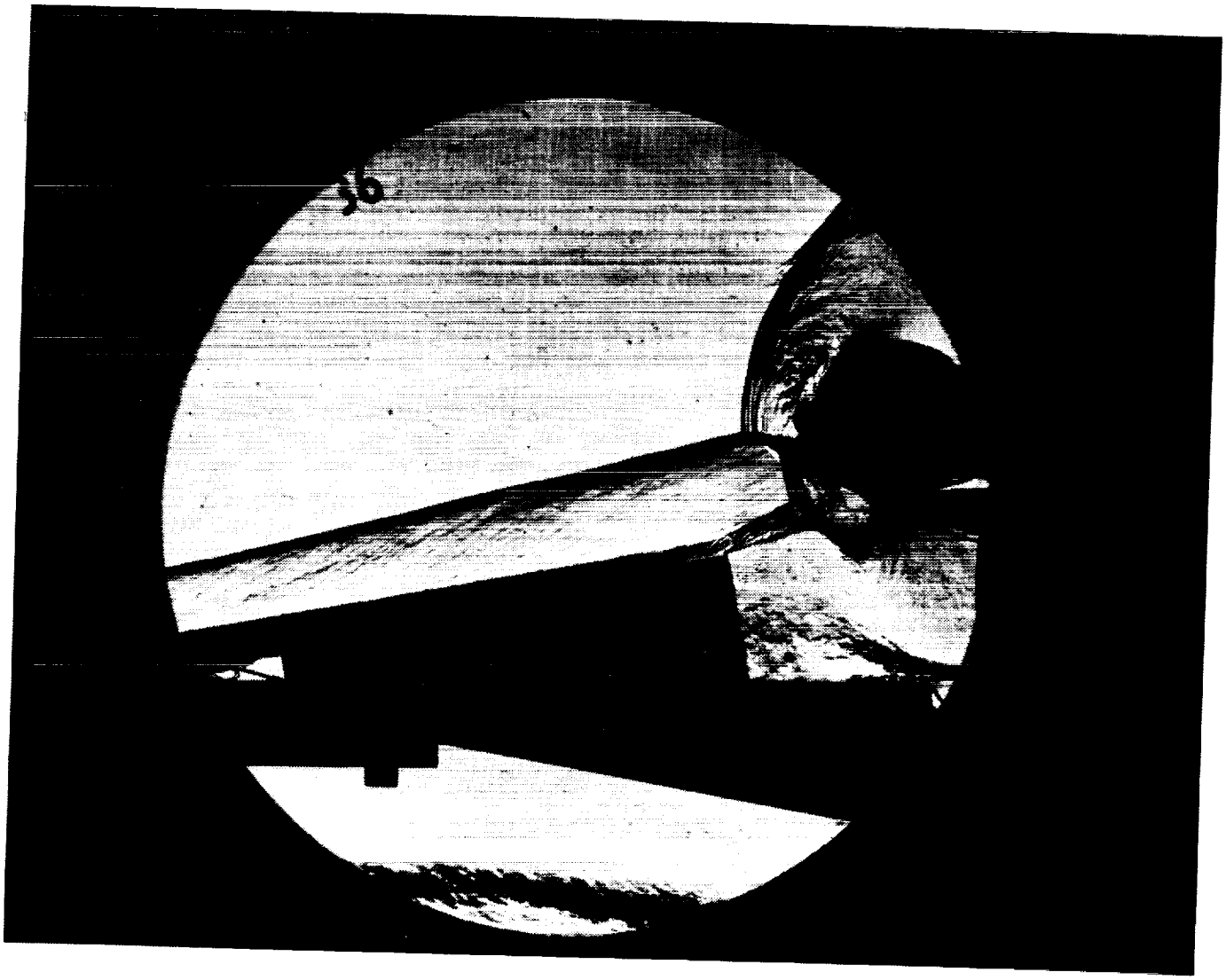

Test Conditions for Run 36 :

Po	= 7.560E+03	PSIA	Reservoir Total Pressure
Ho	= 1.716E+07	(Ft/sec)²	Reservoir Total Enthalpy
To	= 2.570E+03	°R	Reservoir Total Temperature
M	= 1.101E+01		Freestream Mach Number
U	= 5.744E-03	Ft/sec	Freestream Velocity
T	= 1.133E-02	°R	Freestream Temperature
P	= 9.647E-02	PSIA	Freestream Static Pressure
Rho	= 7.147E-05	Slugs/Ft3	Freestream Density
Mu	= 9.526E-08	Slugs/Ft-sec	Freestream Viscosity
Re	= 4.310E+06	1/Ft	Freestream Reynolds Number
Po'	= 1.516E+01	PSIA	Pitot Pressure
Q	= 8.189E+00	PSIA	Dynamic Pressure (½·Rho·U²/144)
Mi	= 3.265E+00		Shock Tube Incident Shock Mach Number
Hw	= 3.183E+06	(Ft/sec)²	Wall Enthalpy (Cp·Tw)
CPf	= 1.221E-01	1/PSIA	Pressure to CP factor (1/Q)
CHf	= 1.356E-04	Ft²-s/BTU	Heat Rate to CH factor (778/(Rho·U·(Ho-Hw))
QoFR	= 4.457E+01	BTU/Ft²-s	Fay-Riddell Heat Transfer to 3" Diam Sphere

Model Configuration Parameter	Value
Stagnation Position (gauge label)	P21.5
Vertical Distance (inches)	2.41
Horizontal Distance (inches)	1.50
Plate Angle (degrees)	10.00
Plate Length (inches)	26.50
Sweep Angle (degrees)	0.00

Run 36

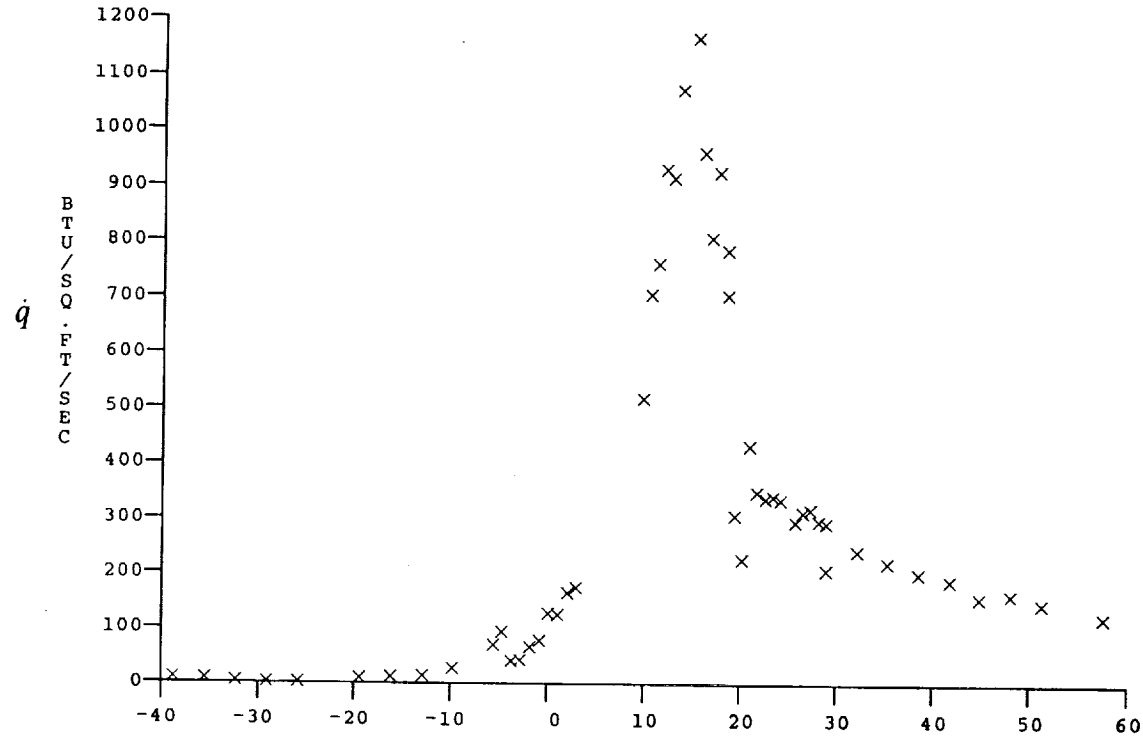

HEAT TRANSFER vs Gauge Position
Run 36

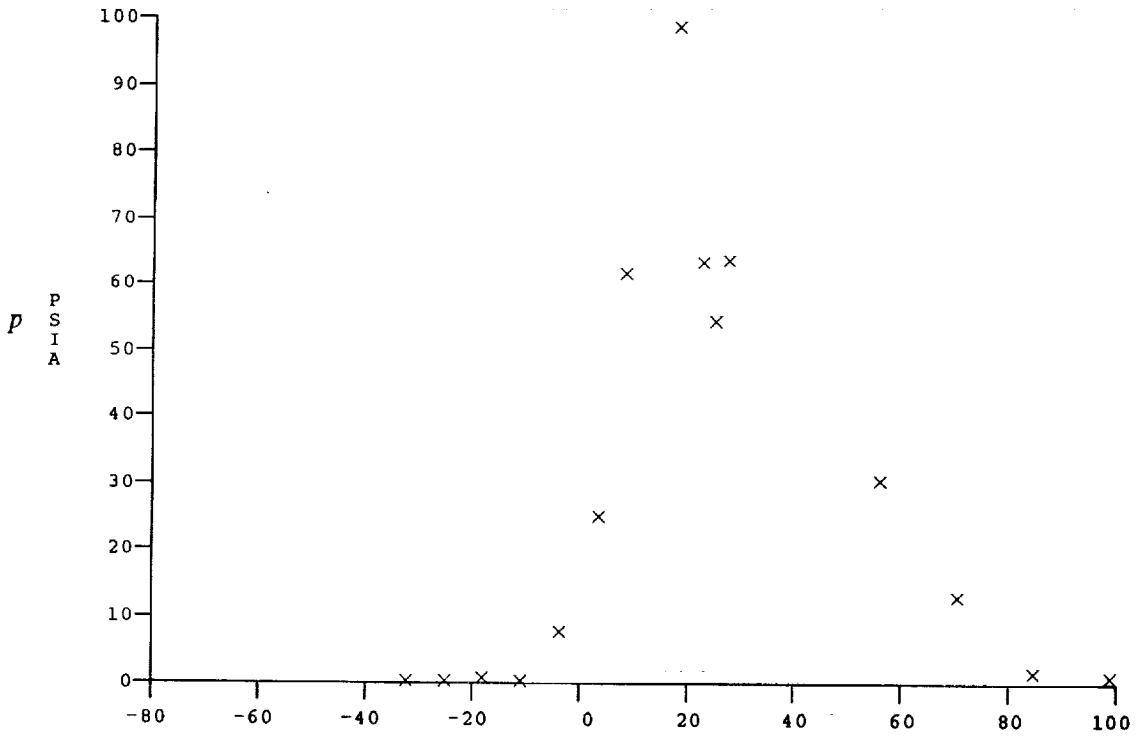

PRESSURE vs Gauge Position
Run 36

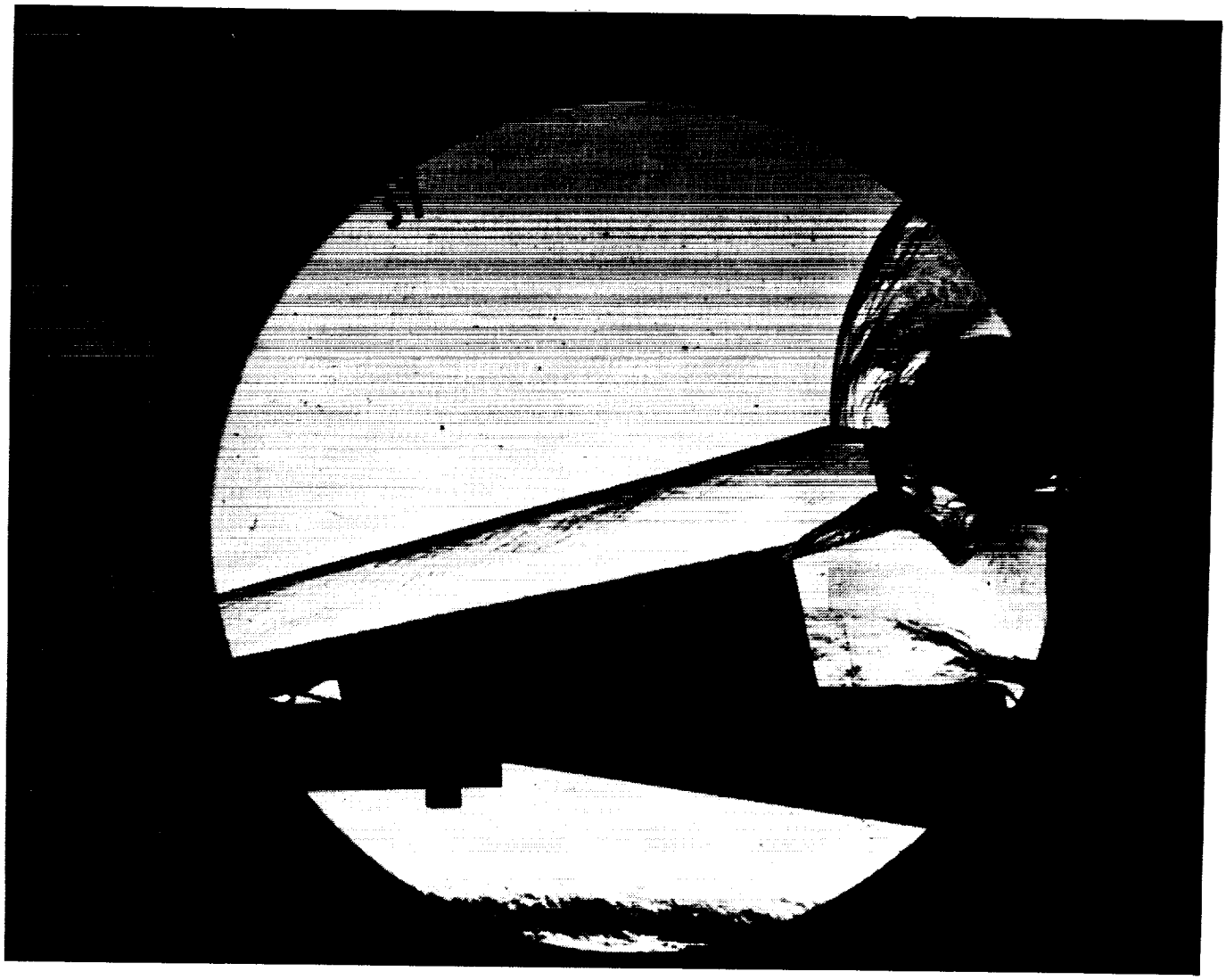

Test Conditions for Run 37 :

Po	= 7.555E+03	PSIA	Reservoir Total Pressure
Ho	= 1.740E-07	(Ft/sec)²	Reservoir Total Enthalpy
To	= 2.602E+03	°R	Reservoir Total Temperature
M	= 1.100E+01		Freestream Mach Number
U	= 5.783E+03	Ft/sec	Freestream Velocity
T	= 1.149E+02	°R	Freestream Temperature
P	= 9.600E-02	PSIA	Freestream Static Pressure
Rho	= 7.014E-05	Slugs/Ft3	Freestream Density
Mu	= 9.659E-08	Slugs/Ft-sec	Freestream Viscosity
Re	= 4.200E+06	1/Ft	Freestream Reynolds Number
Po'	= 1.509E+01	PSIA	Pitot Pressure
Q	= 8.145E-00	PSIA	Dynamic Pressure (½·Rho·U²/144)
Mi	= 3.270E-00		Shock Tube Incident Shock Mach Number
Hw	= 3.183E+06	(Ft/sec)²	Wall Enthalpy (Cp·Tw)
CPf	= 1.228E-01	1/PSIA	Pressure to CP factor (1/Q)
CHf	= 1.350E-04	Ft²-s/BTU	Heat Rate to CH factor (778/(Rho·U·(Ho-Hw))
QoFR	= 4.524E+01	BTU/Ft²-s	Fay-Riddell Heat Transfer to 3" Diam Sphere

Model Configuration Parameter	Value
Stagnation Position (gauge label)	P21.5
Vertical Distance (inches)	2.41
Horizontal Distance (inches)	2.10
Plate Angle (degrees)	10.00
Plate Length (inches)	26.50
Sweep Angle (degrees)	0.00

Run 37

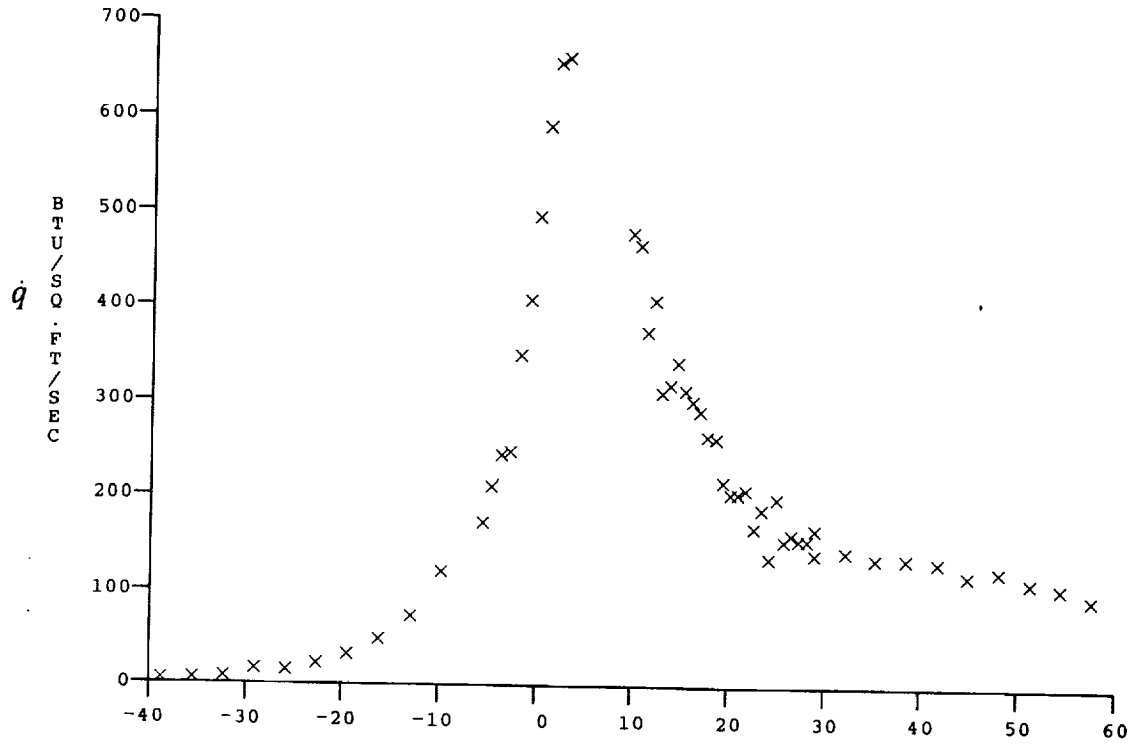

HEAT TRANSFER vs Gauge Position
Run 37

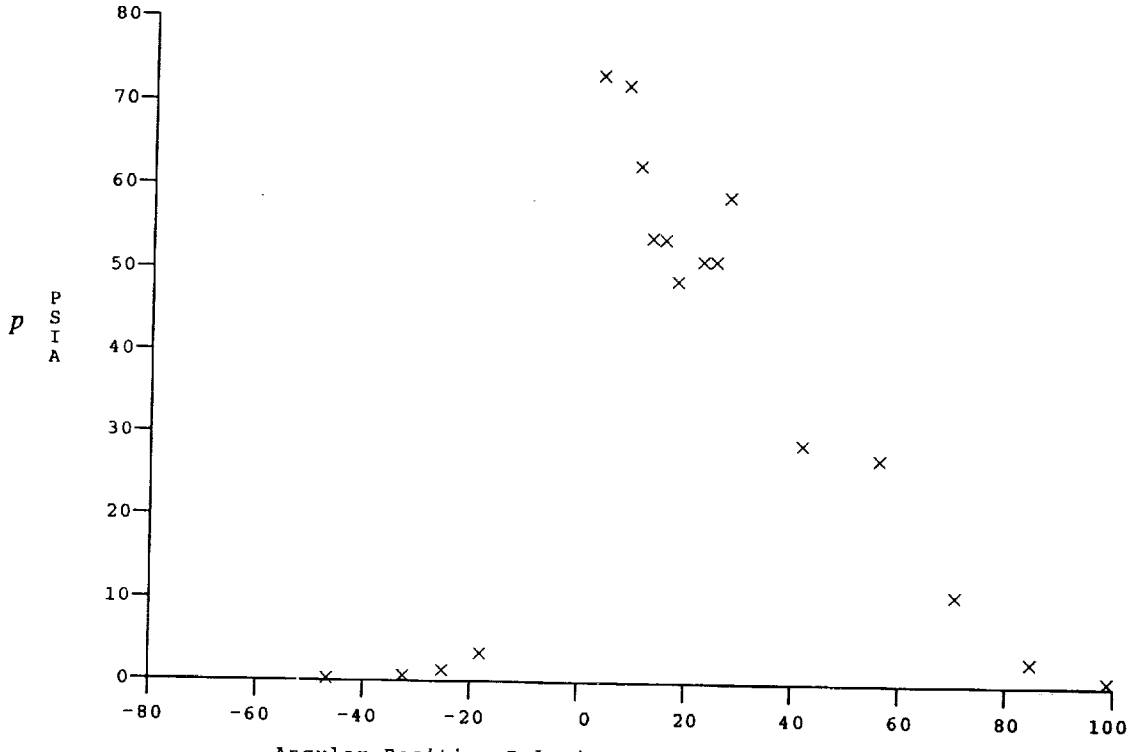

PRESSURE vs Gauge Position
Run 37

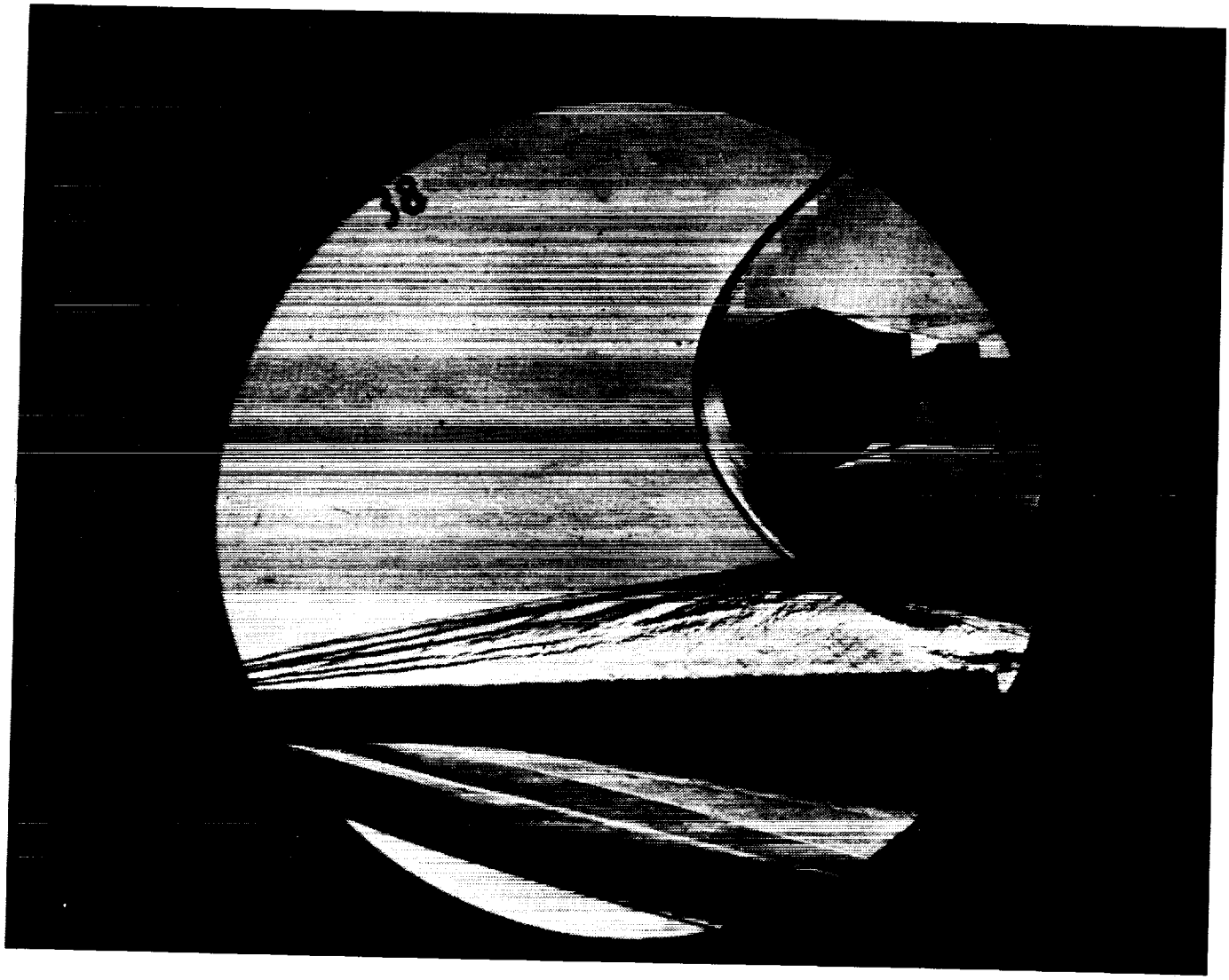

Test Conditions for Run 38 :

Po	= 7.646E-03	PSIA	Reservoir Total Pressure
Ho	= 1.731E+07	$(Ft/sec)^2$	Reservoir Total Enthalpy
To	= 2.589E-03	°R	Reservoir Total Temperature
M	= 1.100E-01		Freestream Mach Number
U	= 5.769E-03	Ft/sec	Freestream Velocity
T	= 1.143E-02	°R	Freestream Temperature
P	= 9.746E-02	PSIA	Freestream Static Pressure
Rho	= 7.156E-05	Slugs/Ft3	Freestream Density
Mu	= 9.612E-08	Slugs/Ft-sec	Freestream Viscosity
Re	= 4.296E+06	1/Ft	Freestream Reynolds Number
Po'	= 1.532E+01	PSIA	Pitot Pressure
Q	= 8.270E+00	PSIA	Dynamic Pressure (½·Rho·U^2/144)
Mi	= 3.278E+00		Shock Tube Incident Shock Mach Number
Hw	= 3.183E+06	$(Ft/sec)^2$	Wall Enthalpy (Cp·Tw)
CPf	= 1.209E-01	1/PSIA	Pressure to CP factor (1/Q)
CHf	= 1.334E-04	Ft^2-s/BTU	Heat Rate to CH factor (778/(Rho·U·(Ho-Hw))
QoFR	= 4.530E+01	BTU/Ft^2-s	Fay-Riddell Heat Transfer to 3" Diam Sphere

Model Configuration Parameter	Value
Stagnation Position (gauge label)	P18
Sweep Angle (degrees)	0.00

Run 38

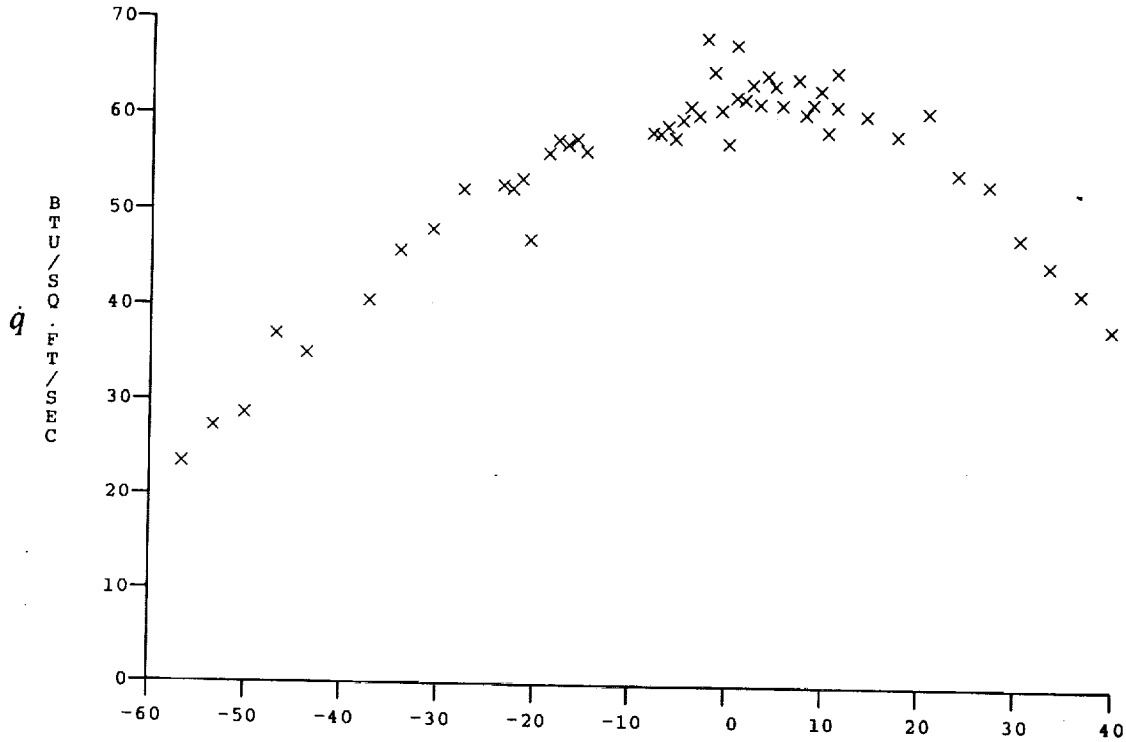

HEAT TRANSFER vs Gauge Position
Run 38

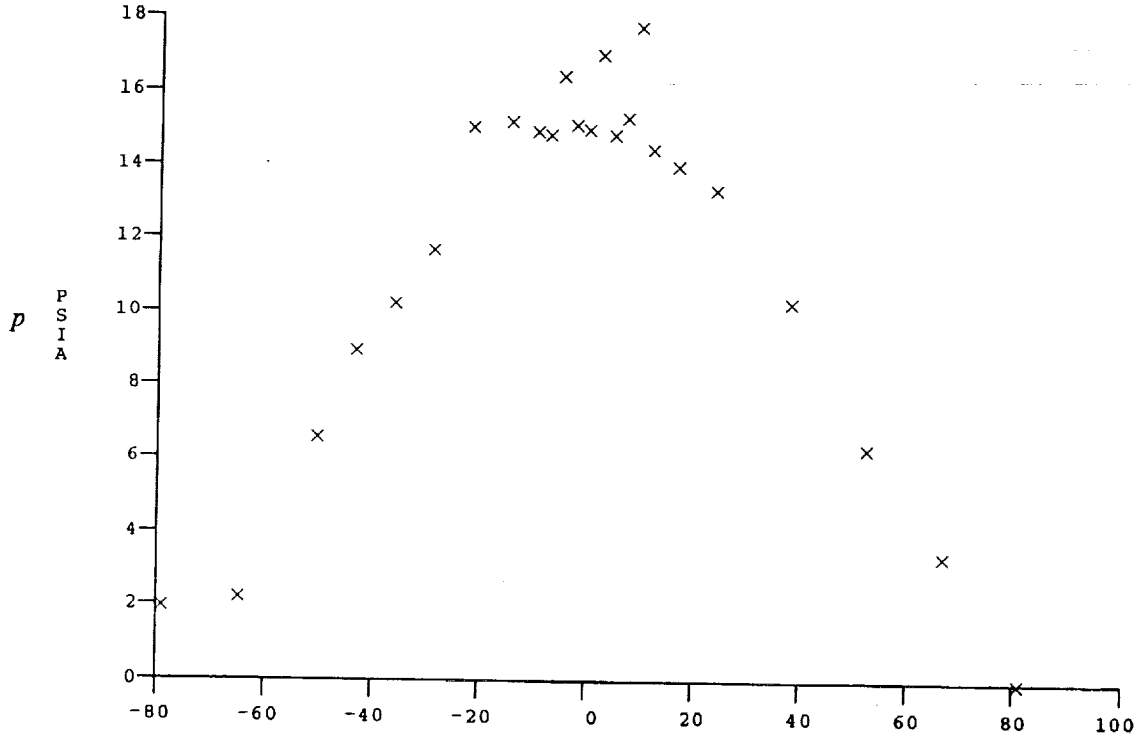

PRESSURE vs Gauge Position
Run 38

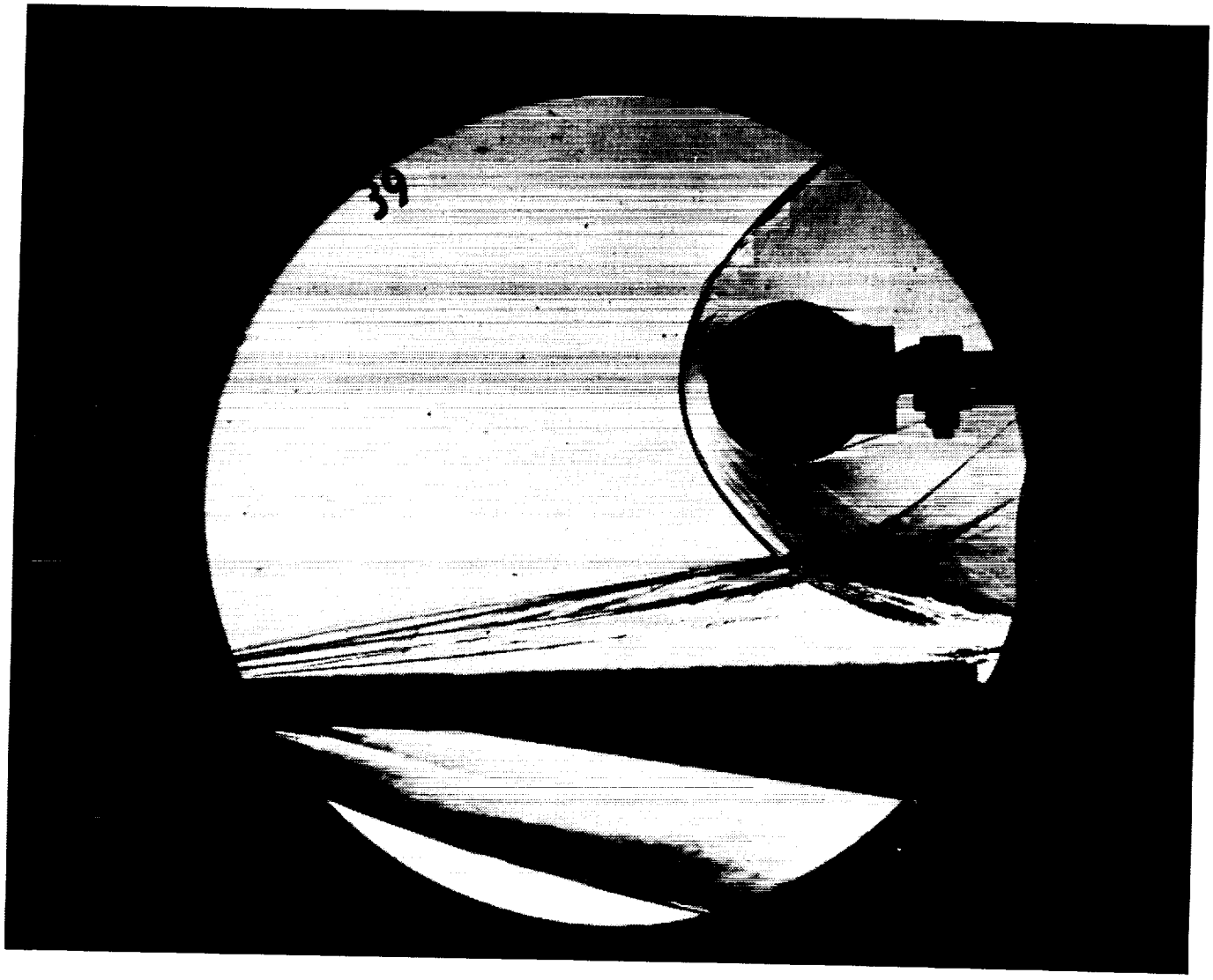

Test Conditions for Run 39 :

Po	= 1.895E+04 PSIA	Reservoir Total Pressure	
Ho	= 2.201E+07 (Ft/sec)²	Reservoir Total Enthalpy	
To	= 3.163E-03 °R	Reservoir Total Temperature	
M	= 1.297E+01	Freestream Mach Number	
U	= 6.542E+03 Ft/sec	Freestream Velocity	
T	= 1.058E+02 °R	Freestream Temperature	
P	= 8.081E-02 PSIA	Freestream Static Pressure	
Rho	= 6.408E-05 Slugs/Ft3	Freestream Density	
Mu	= 8.902E-08 Slugs/Ft-sec	Freestream Viscosity	
Re	= 4.709E+06 1/Ft	Freestream Reynolds Number	
Po'	= 1.770E+01 PSIA	Pitot Pressure	
Q	= 9.522E+00 PSIA	Dynamic Pressure (½·Rho·U²/144)	
Mi	= 3.753E+00	Shock Tube Incident Shock Mach Number	
Hw	= 3.183E+06 (Ft/sec)²	Wall Enthalpy (Cp·Tw)	
CPf	= 1.050E-01 1/PSIA	Pressure to CP factor (1/Q)	
CHf	= 9.857E-05 Ft²-s/BTU	Heat Rate to CH factor (778/(Rho·U·(Ho-Hw))	
QoFR	= 6.592E+01 BTU/Ft²-s	Fay-Riddell Heat Transfer to 3" Diam Sphere	

Model Configuration Parameter	Value
Stagnation Position (gauge label)	P18
Sweep Angle (degrees)	0.00

Run 39

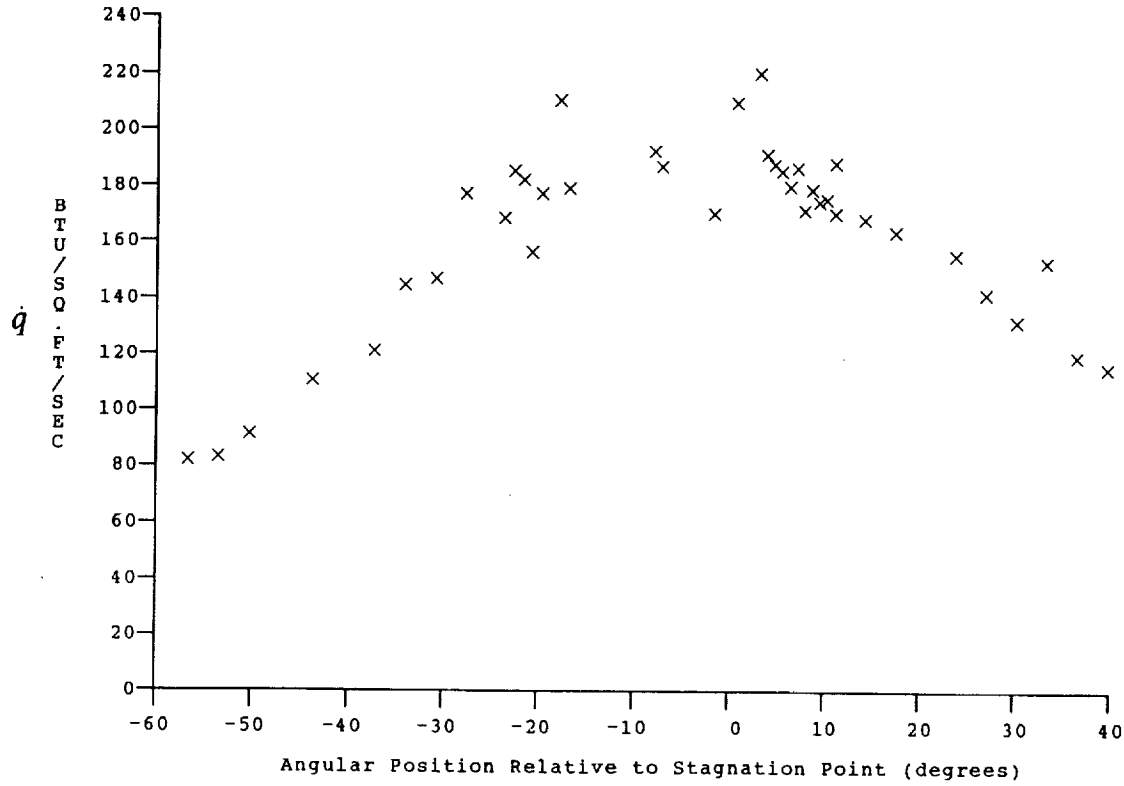

HEAT TRANSFER vs Gauge Position
Run 39

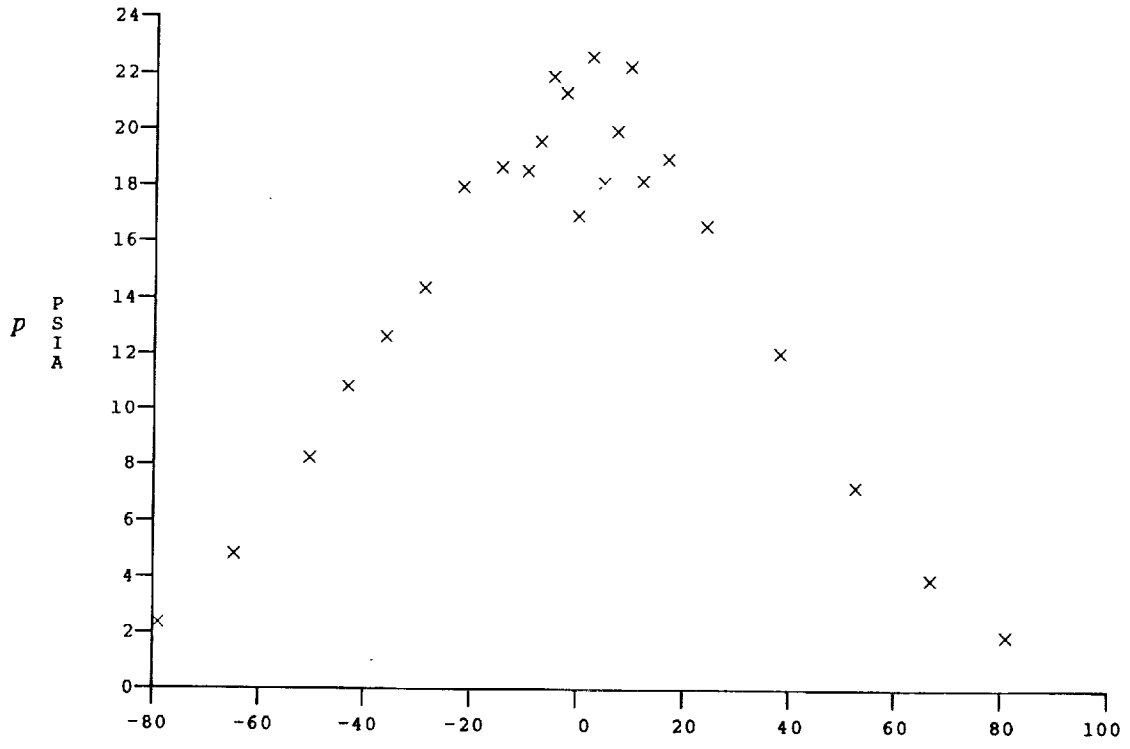

PRESSURE vs Gauge Position
Run 39

Test Conditions

Mi	= 4.3690	
Po	= 1.7470X10+4	PSIA
Ho	= 2.9031X10+7	(Ft/sec)^2
To	= 4.0161X10+3	Degrees R
M	=16.5000	
U	= 7.5546X10+3	Ft/sec
T	= 8.7169X10+1	Degrees R
P	= 1.1773X10-2	PSIA
Q	= 2.2462	PSIA
Rho	= 1.1335X10-5	Slugs/Ft^3
Mu	= 7.3329X10-8	Slugs/Ft-sec
Re	= 1.1677X10+6	1/Ft
Po'	= 4.1990	PSIA

Model Configuration Parameter	Value
Stagnation Position (gauge label)	P18
Sweep Angle (degrees)	0.00

Run 40

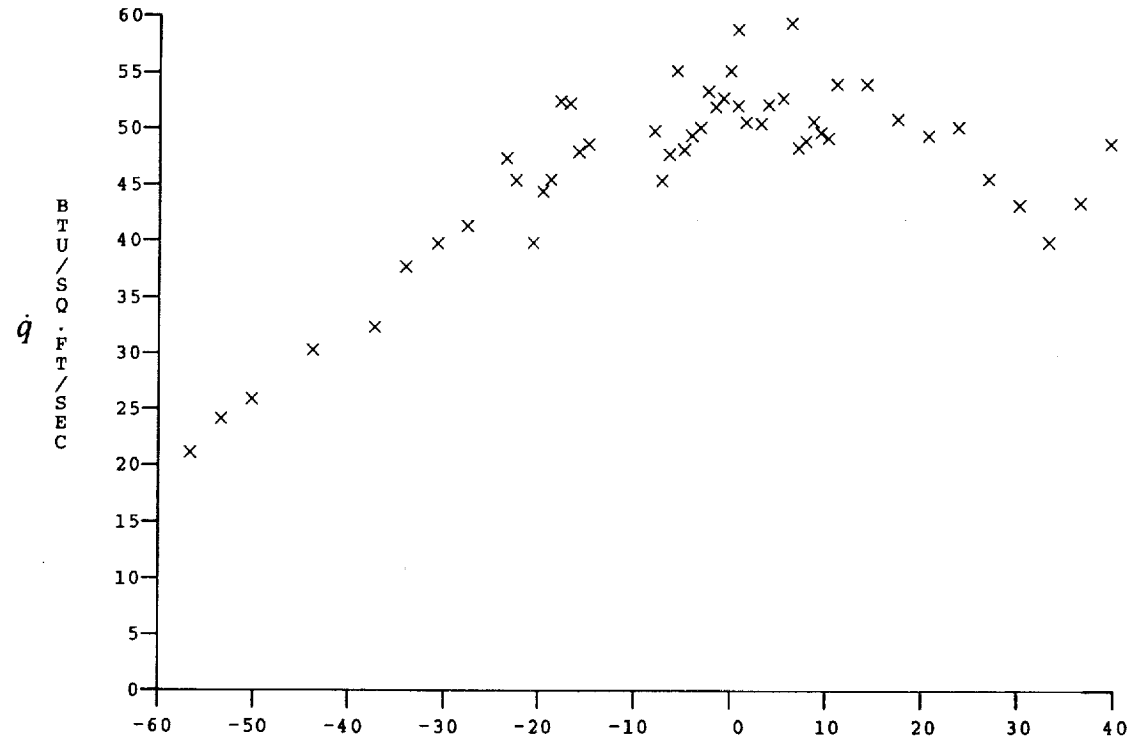

HEAT TRANSFER vs Gauge Position
Run 40

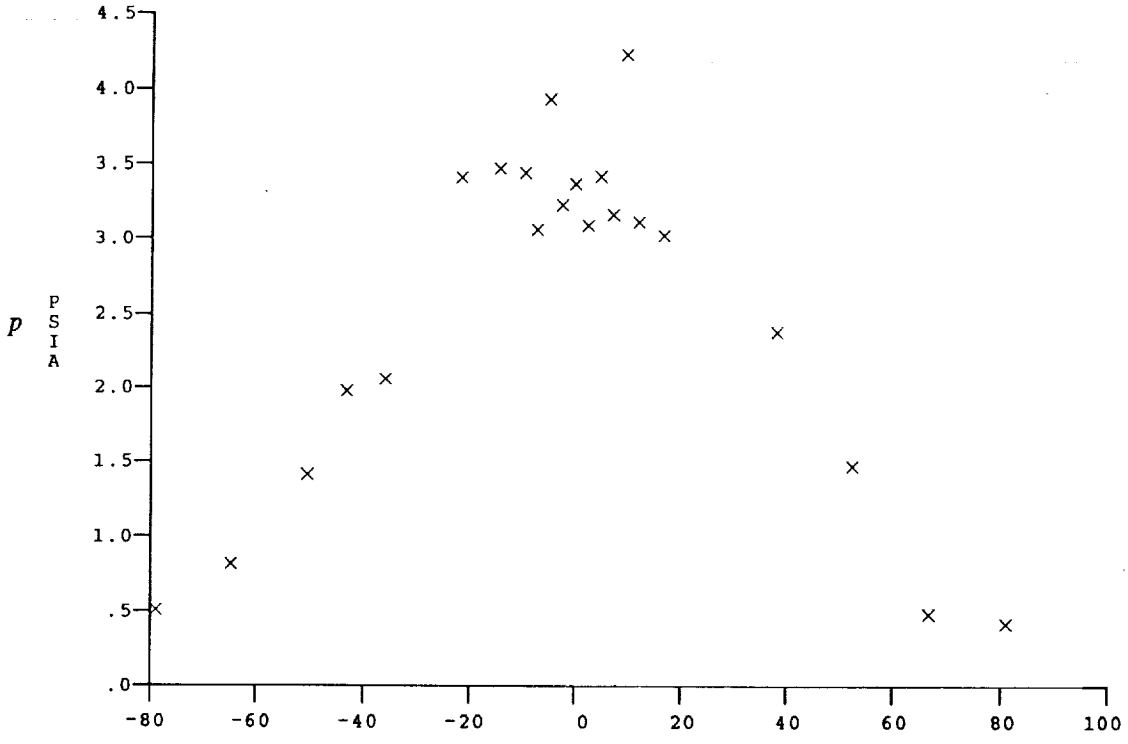

PRESSURE vs Gauge Position
Run 40

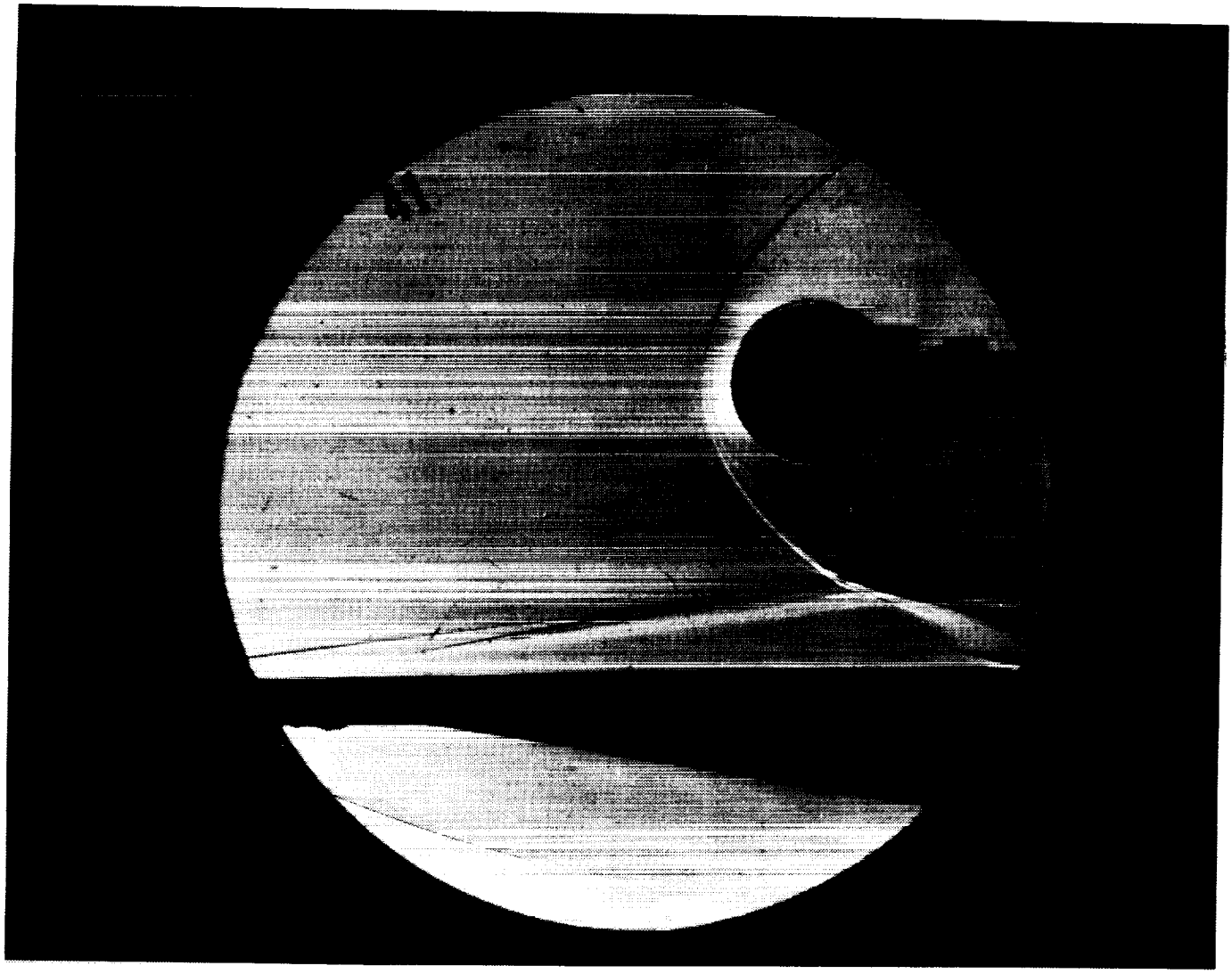

Test Conditions for Run 41 :

Po	= 1.776E+04 PSIA	Reservoir Total Pressure	
Ho	= 4.006E+07 (Ft/sec)²	Reservoir Total Enthalpy	
To	= 5.303E+03 °R	Reservoir Total Temperature	
M	= 1.914E+01	Freestream Mach Number	
U	= 8.895E+03 Ft/sec	Freestream Velocity	
T	= 8.980E+01 °R	Freestream Temperature	
P	= 3.335E-03 PSIA	Freestream Static Pressure	
Rho	= 3.117E-06 Slugs/Ft3	Freestream Density	
Mu	= 7.555E-08 Slugs/Ft-sec	Freestream Viscosity	
Re	= 3.669E+05 1/Ft	Freestream Reynolds Number	
Po'	= 1.612E+00 PSIA	Pitot Pressure	
Q	= 8.561E-01 PSIA	Dynamic Pressure (½·Rho·U²/144)	
Mi	= 5.179E+00	Shock Tube Incident Shock Mach Number	
Hw	= 3.183E-06 (Ft/sec)²	Wall Enthalpy (Cp·Tw)	
CPf	= 1.168E-00 1/PSIA	Pressure to CP factor (1/Q)	
CHf	= 7.612E-04 Ft²-s/BTU	Heat Rate to CH factor (778/(Rho·U·(Ho-Hw))	
QoFR	= 1.004E+01 BTU/Ft²-s	Fay-Riddell Heat Transfer to 3" Diam Sphere	

Model Configuration Parameter	Value
Stagnation Position (gauge label)	P18
Sweep Angle (degrees)	0.00

Run 41

C-3

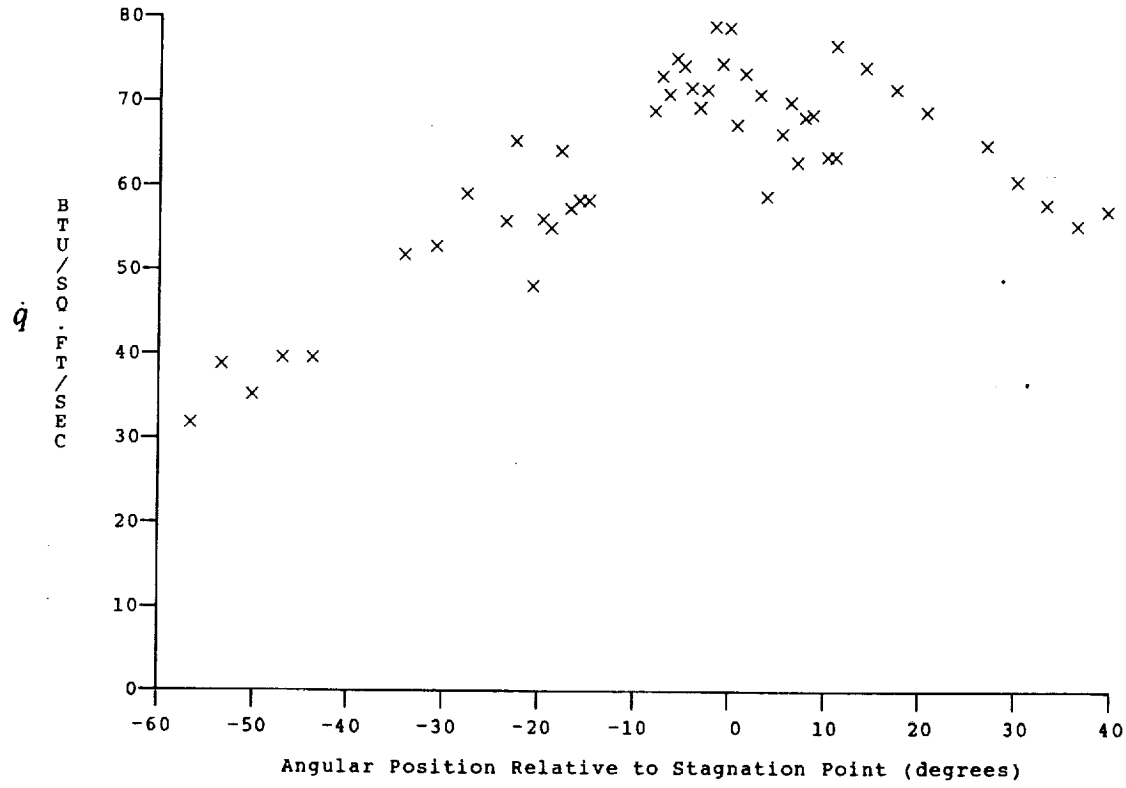

HEAT TRANSFER vs Gauge Position
Run 41

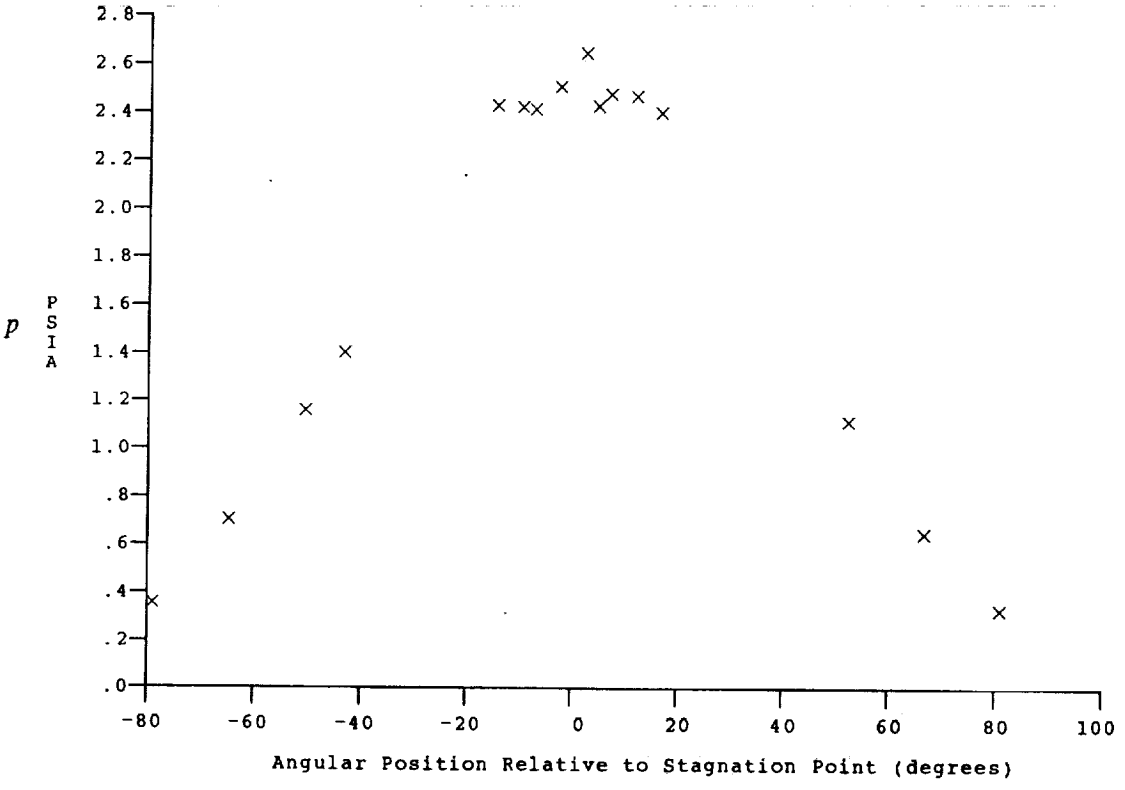

PRESSURE vs Gauge Position
Run 41

Test Conditions for Run 42 :

Po	= 1.748E+04	PSIA
Ho	= 3.114E+07	(Ft/sec)²
To	= 4.253E+03	°R
M	= 1.631E-01	
U	= 7.823E+03	Ft/sec
T	= 9.569E+01	°R
P	= 1.212E-02	PSIA
Rho	= 1.063E-05	Slugs/Ft3
Mu	= 8.051E-08	Slugs/Ft-sec
Re	= 1.033E+06	1/Ft
Po'	= 4.230E+00	PSIA
Q	= 2.259E+00	PSIA
Mi	= 4.567E+00	
Hw	= 3.183E+06	(Ft/sec)²
CPf	= 4.426E-01	1/PSIA
CHf	= 3.346E-04	Ft²-s/BTU
QoFR	= 4.870E+01	BTU/Ft²-s

Reservoir Total Pressure
Reservoir Total Enthalpy
Reservoir Total Temperature
Freestream Mach Number
Freestream Velocity
Freestream Temperature
Freestream Static Pressure
Freestream Density
Freestream Viscosity
Freestream Reynolds Number
Pitot Pressure
Dynamic Pressure (½·Rho·U²/144)
Shock Tube Incident Shock Mach Number
Wall Enthalpy (Cp·Tw)
Pressure to CP factor (1/Q)
Heat Rate to CH factor (778/(Rho·U·(Ho-Hw))
Fay-Riddell Heat Transfer to 3" Diam Sphere

Model Configuration Parameter	Value
Stagnation Position (gauge label)	P21.5
Vertical Distance (inches)	2.94
Horizontal Distance (inches)	0.16
Plate Angle (degrees)	10.00
Plate Length (inches)	48.00
Sweep Angle (degrees)	0.00

Run 42

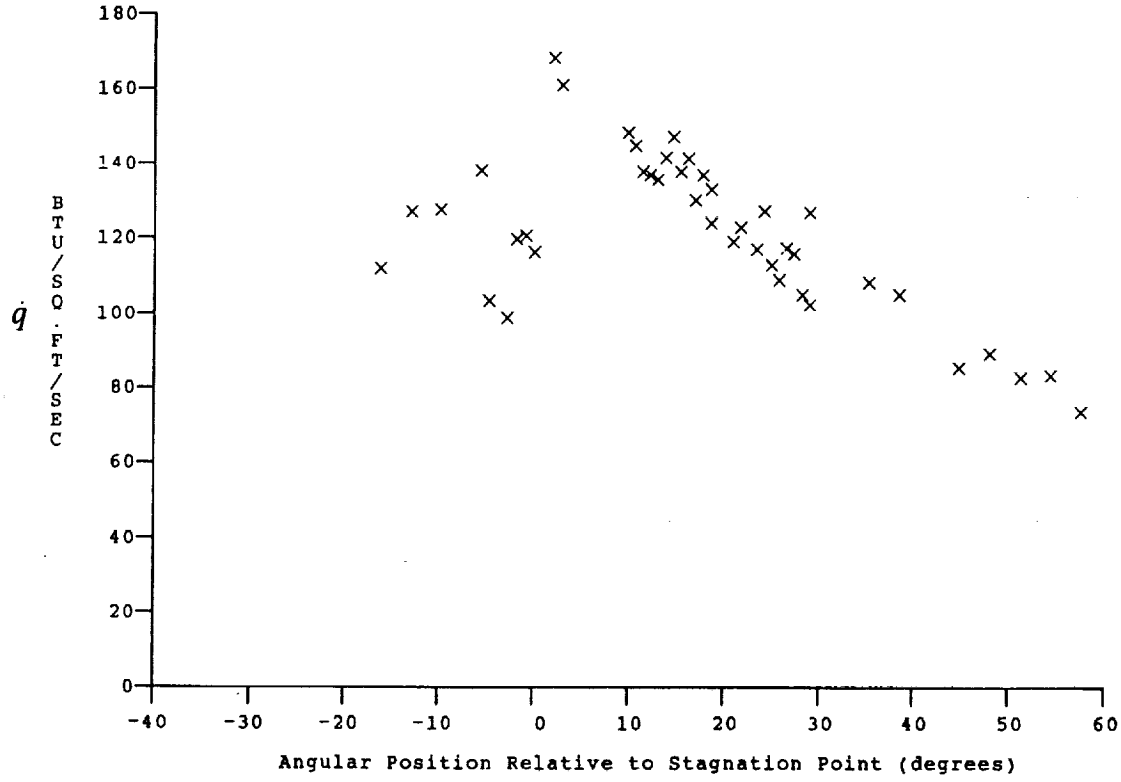

HEAT TRANSFER vs Gauge Position
Run 42

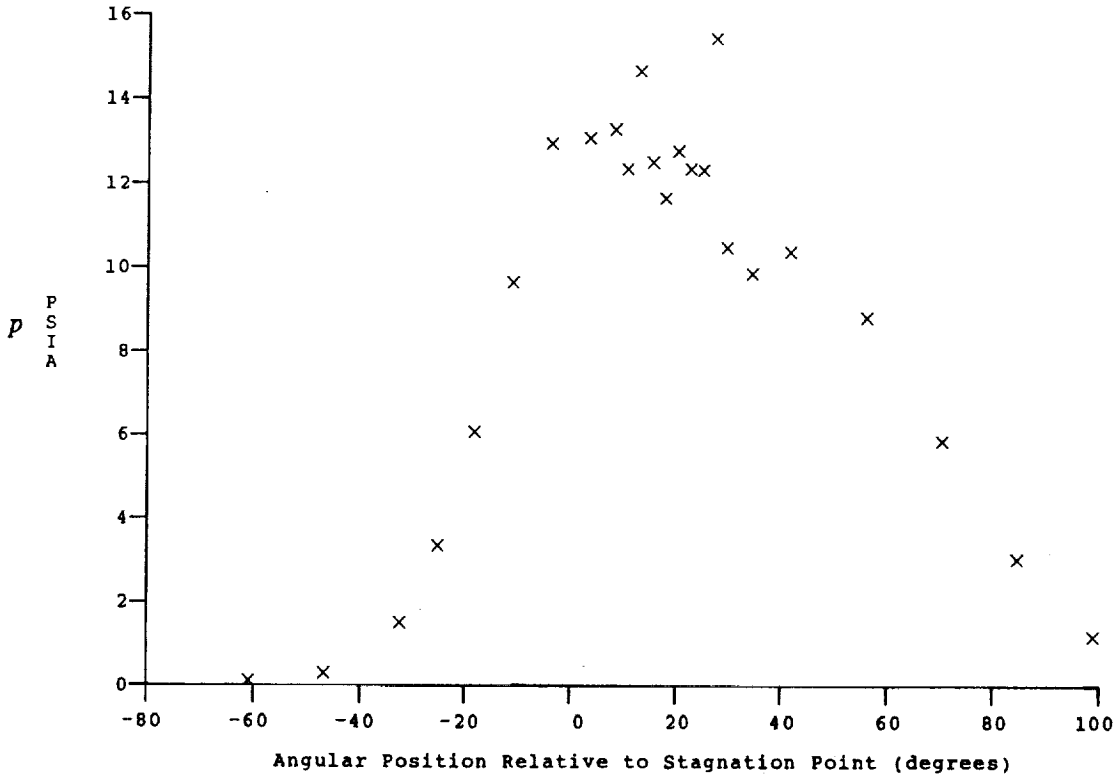

PRESSURE vs Gauge Position
Run 42

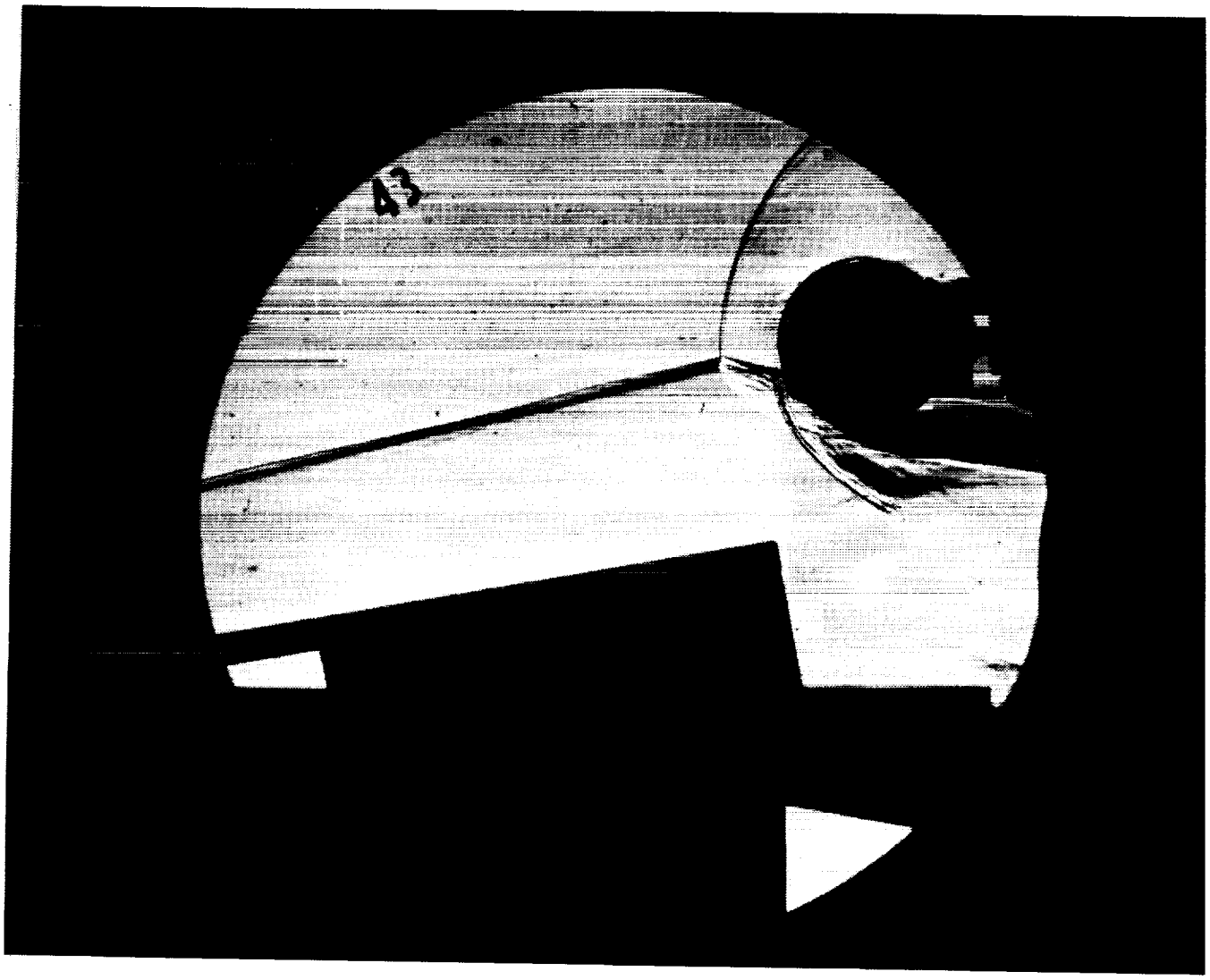

Test Conditions for Run 43 :

Po	= 1.717E+04 PSIA	Reservoir Total Pressure	
Ho	= 3.071E+07 (Ft/sec)²	Reservoir Total Enthalpy	
To	= 4.204E+03 °R	Reservoir Total Temperature	
M	= 1.633E+01	Freestream Mach Number	
U	= 7.768E+03 Ft/sec	Freestream Velocity	
T	= 9.408E+01 °R	Freestream Temperature	
P	= 1.189E-02 PSIA	Freestream Static Pressure	
Rho	= 1.061E-05 Slugs/Ft3	Freestream Density	
Mu	= 7.915E-08 Slugs/Ft-sec	Freestream Viscosity	
Re	= 1.041E+06 1/Ft	Freestream Reynolds Number	
Po'	= 4.159E+00 PSIA	Pitot Pressure	
Q	= 2.222E+00 PSIA	Dynamic Pressure (½·Rho·U²/144)	
Mi	= 4.527E+00	Shock Tube Incident Shock Mach Number	
Hw	= 3.183E+06 (Ft/sec)²	Wall Enthalpy (Cp·Tw)	
CPf	= 4.501E-01 1/PSIA	Pressure to CP factor (1/Q)	
CHf	= 3.432E-04 Ft²-s/BTU	Heat Rate to CH factor (778/(Rho·U·(Ho-Hw))	
QoFR	= 4.751E+01 BTU/Ft²-s	Fay-Riddell Heat Transfer to 3" Diam Sphere	

Model Configuration Parameter	Value
Stagnation Position (gauge label)	P23
Vertical Distance (inches)	3.63
Horizontal Distance (inches)	0.09
Plate Angle (degrees)	10.00
Plate Length (inches)	48.00
Sweep Angle (degrees)	0.00

Run 43

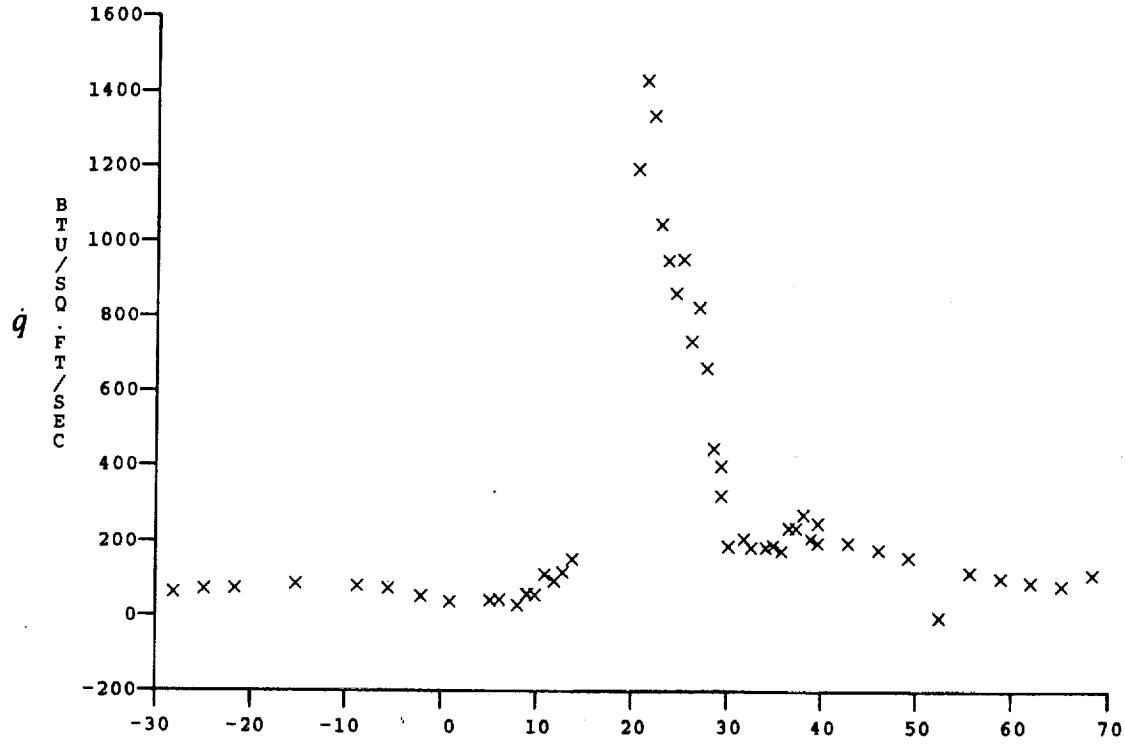

HEAT TRANSFER vs Gauge Position
Run 43

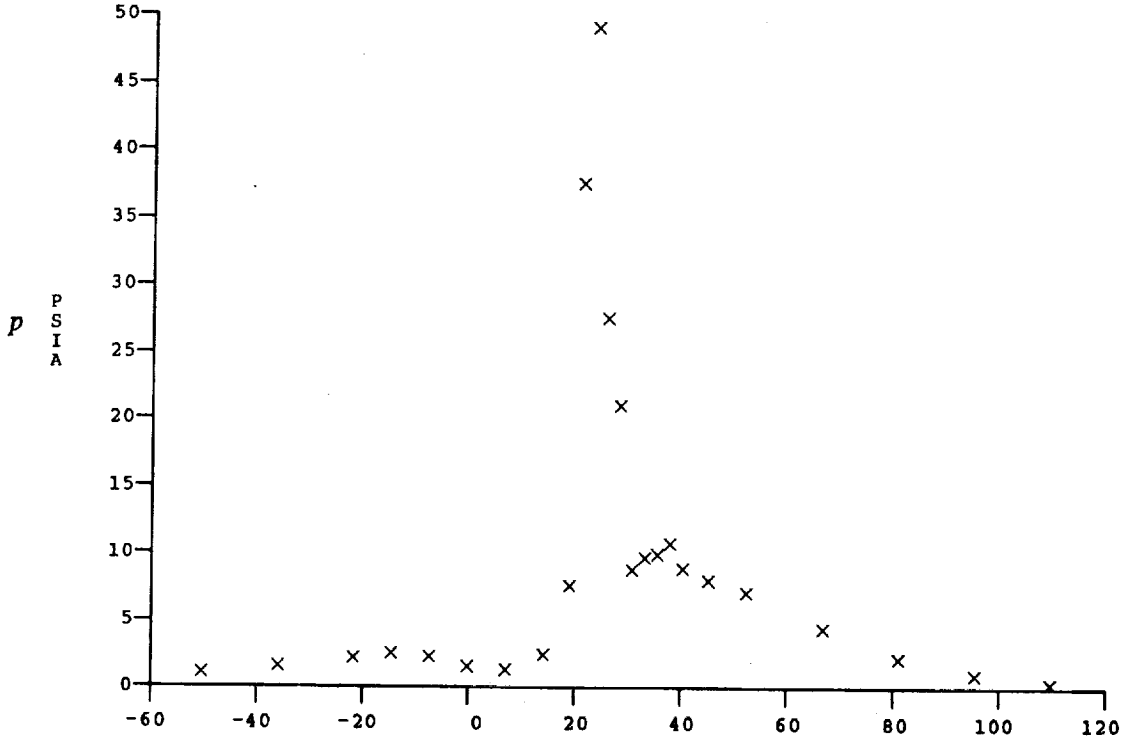

PRESSURE vs Gauge Position
Run 43

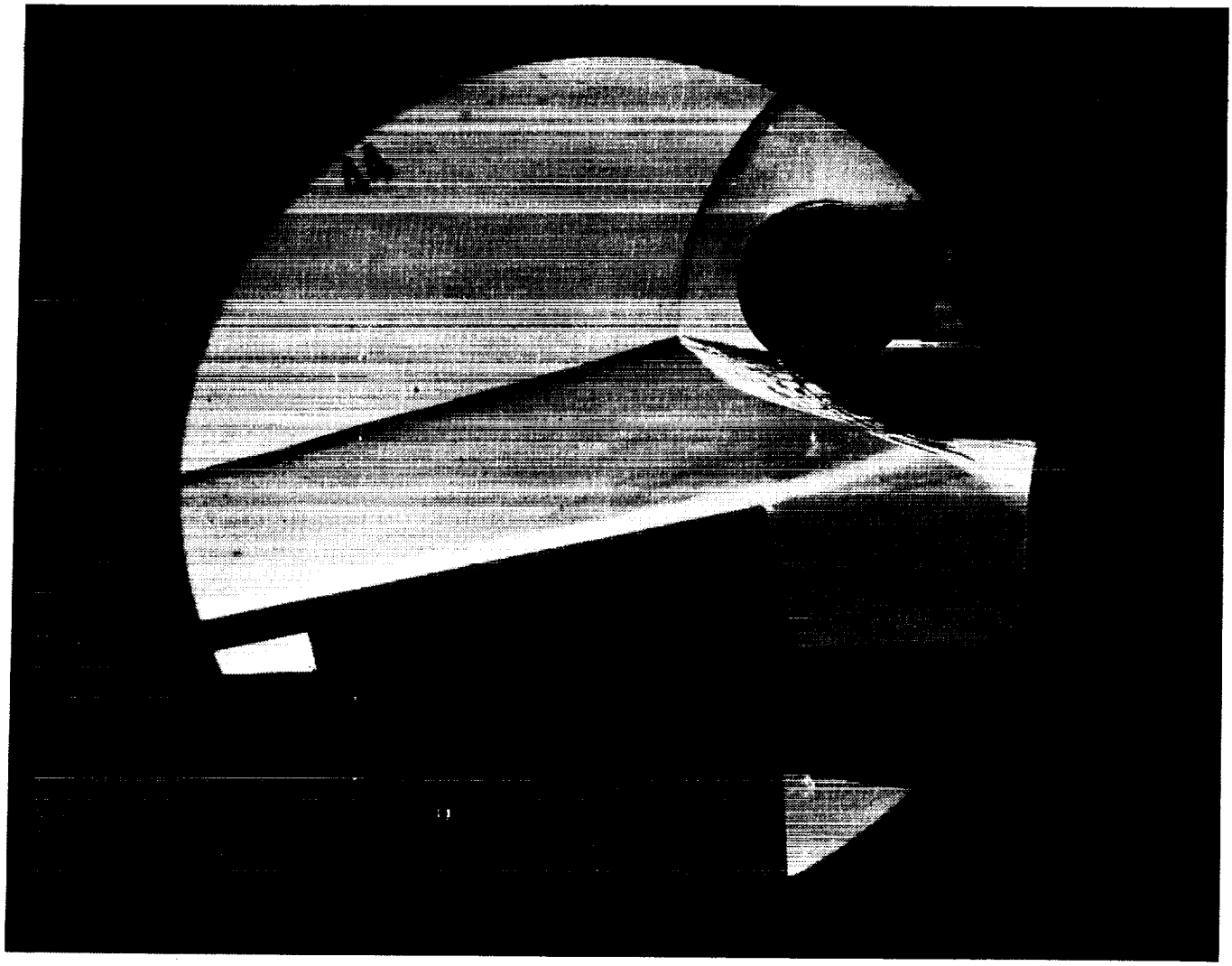

Test Conditions for Run 44 :

Po	= 1.698E+04	PSIA	Reservoir Total Pressure
Ho	= 3.202E-07	(Ft/sec)²	Reservoir Total Enthalpy
To	= 4.359E-03	°R	Reservoir Total Temperature
M	= 1.627E-01		Freestream Mach Number
U	= 7.932E+03	Ft/sec	Freestream Velocity
T	= 9.880E+01	°R	Freestream Temperature
P	= 1.165E-02	PSIA	Freestream Static Pressure
Rho	= 9.895E-06	Slugs/Ft3	Freestream Density
Mu	= 8.312E-08	Slugs/Ft-sec	Freestream Viscosity
Re	= 9.443E+05	1/Ft	Freestream Reynolds Number
Po'	= 4.050E+00	PSIA	Pitot Pressure
Q	= 2.162E+00	PSIA	Dynamic Pressure (½·Rho·U²/144)
Mi	= 4.576E+00		Shock Tube Incident Shock Mach Number
Hw	= 3.183E+06	(Ft/sec)²	Wall Enthalpy (Cp·Tw)
CPf	= 4.626E-01	1/PSIA	Pressure to CP factor (1/Q)
CHf	= 3.437E-04	Ft²-s/BTU	Heat Rate to CH factor (778/(Rho·U·(Ho-Hw))
QoFR	= 4.923E+01	BTU/Ft²-s	Fay-Riddell Heat Transfer to 3" Diam Sphere

Model Configuration Parameter	Value
Stagnation Position (gauge label)	P25
Vertical Distance (inches)	3.94
Horizontal Distance (inches)	-0.25
Plate Angle (degrees)	10.00
Plate Length (inches)	48.00
Sweep Angle (degrees)	0.00

Run 44

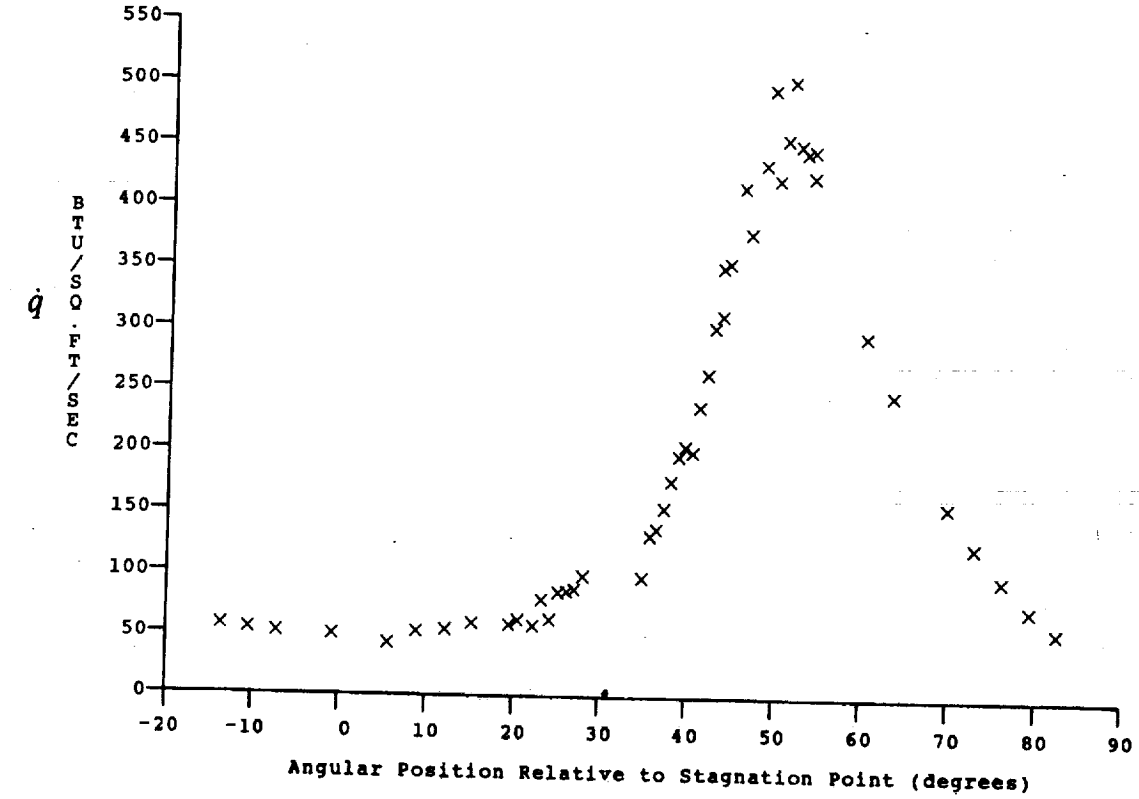

HEAT TRANSFER vs Gauge Position
Run 44

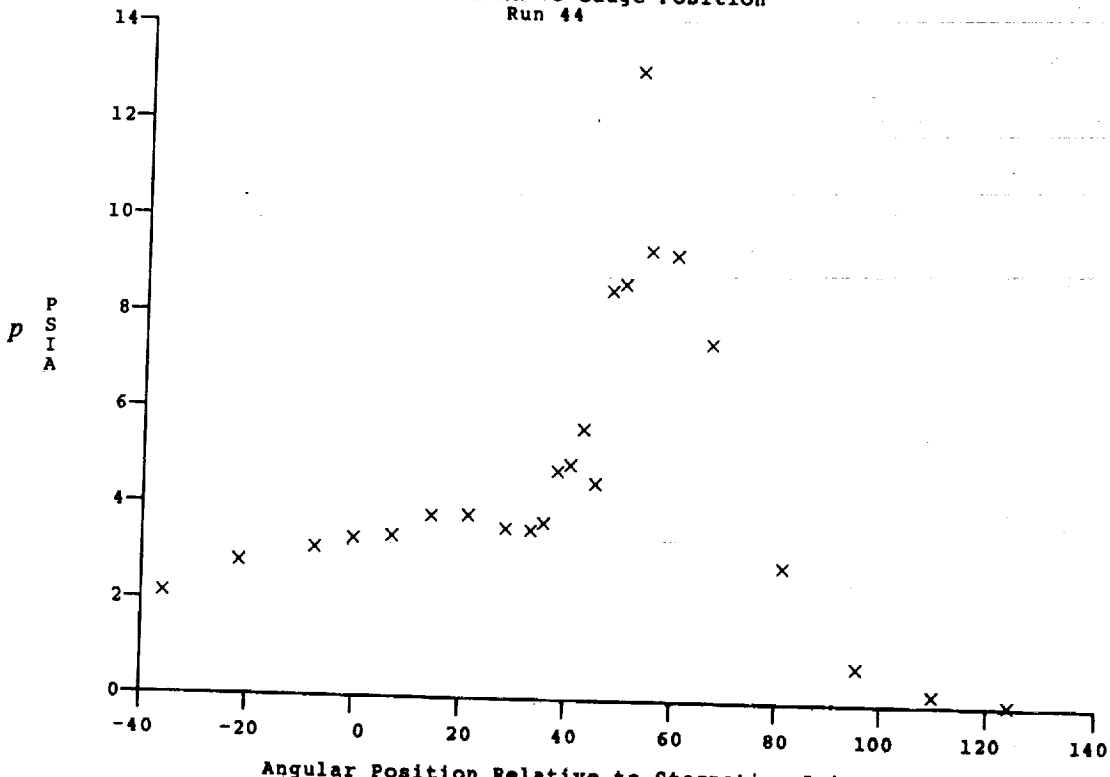

PRESSURE vs Gauge Position
Run 44

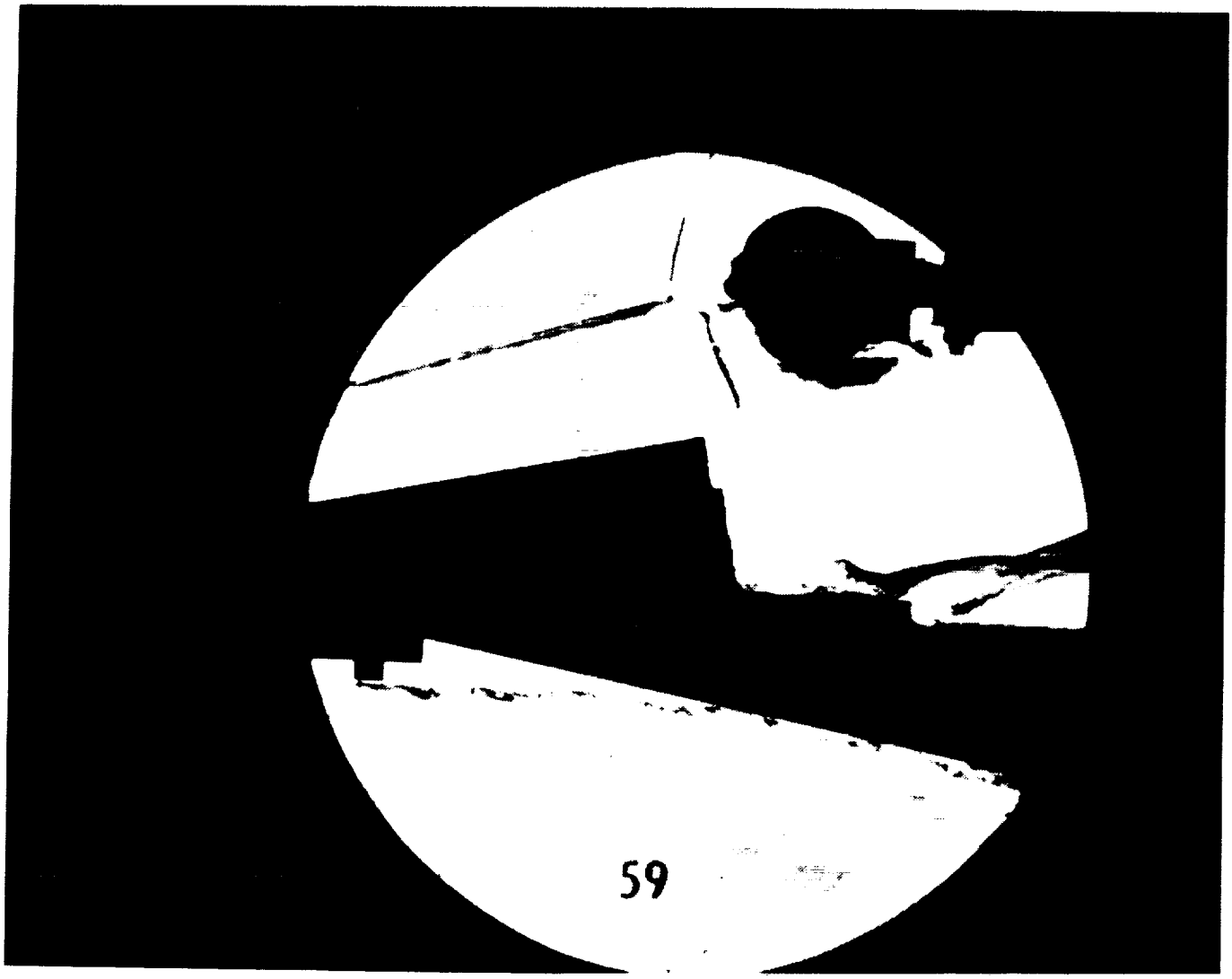

Test Conditions for Run 59 :

Po	= 1.352E+03 PSIA	Reservoir Total Pressure	
Ho	= 1.855E+07 (Ft/sec)²	Reservoir Total Enthalpy	
To	= 2.819E+03 °R	Reservoir Total Temperature	
M	= 8.036E+00	Freestream Mach Number	
U	= 5.872E-03 Ft/sec	Freestream Velocity	
T	= 2.220E-02 °R	Freestream Temperature	
P	= 1.185E-01 PSIA	Freestream Static Pressure	
Rho	= 4.478E-05 Slugs/Ft3	Freestream Density	
Mu	= 1.834E-07 Slugs/Ft-sec	Freestream Viscosity	
Re	= 1.433E+06 1/Ft	Freestream Reynolds Number	
Po'	= 9.939E+00 PSIA	Pitot Pressure	
Q	= 5.361E+00 PSIA	Dynamic Pressure (½·Rho·U²/144)	
Mi	= 3.412E+00	Shock Tube Incident Shock Mach Number	
Hw	= 3.183E+06 (Ft/sec)²	Wall Enthalpy (Cp·Tw)	
CPf	= 1.865E-01 1/PSIA	Pressure to CP factor (1/Q)	
CHf	= 1.925E-04 Ft²-s/BTU	Heat Rate to CH factor (778/(Rho·U·(Ho-Hw))	
QoFR	= 3.969E-01 BTU/Ft²-s	Fay-Riddell Heat Transfer to 3" Diam Sphere	

Model Configuration Parameter	Value
Stagnation Position (gauge label)	P21
Vertical Distance (inches)	2.83
Horizontal Distance (inches)	2.76
Plate Angle (degrees)	12.50
Plate Length (inches)	26.50
Sweep Angle (degrees)	0.00

Run 59

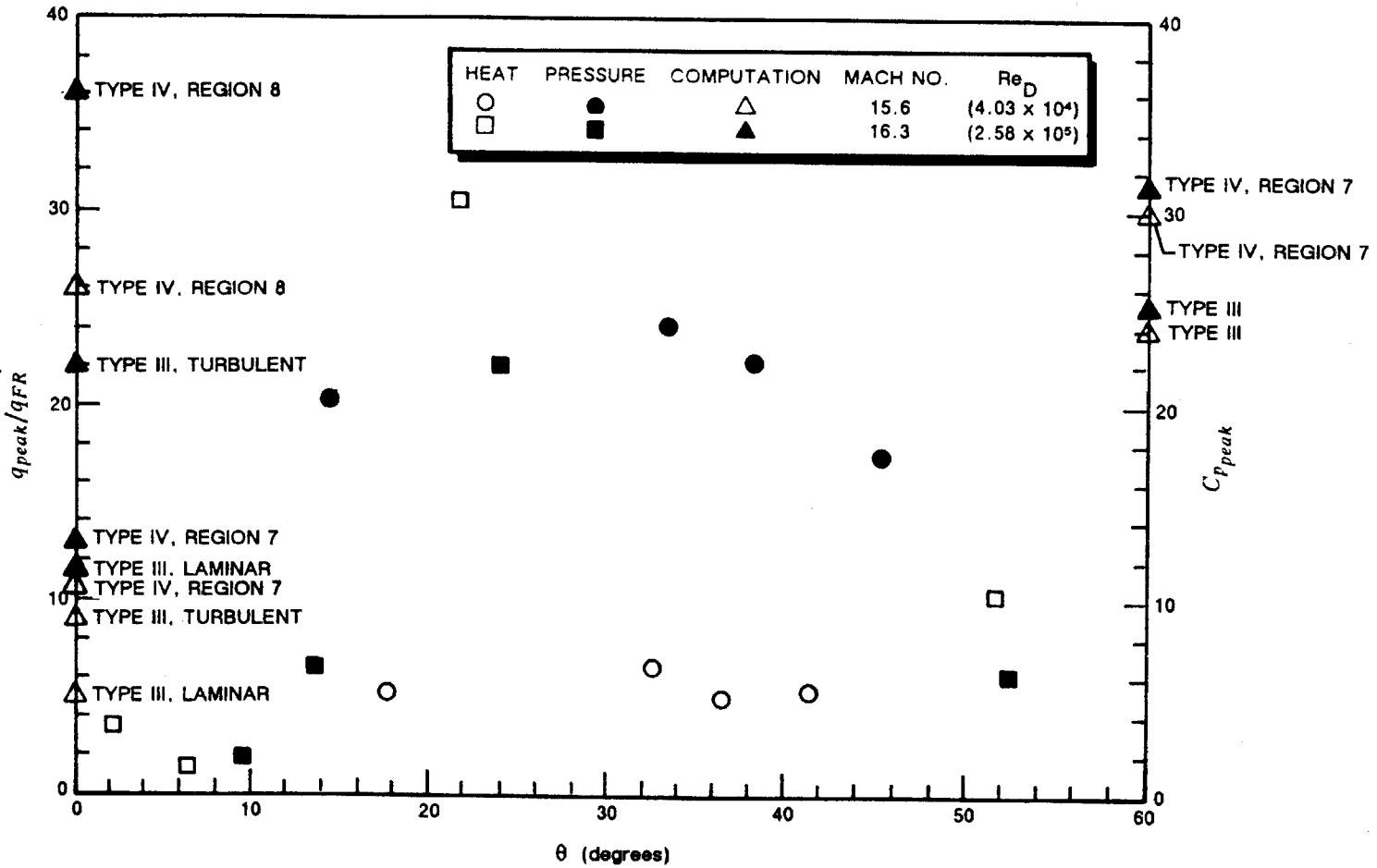

Figure 32c VARIATIONS OF PEAK HEATING AND PRESSURE WITH ANGULAR POSITION OF THE INTERACTION REGION FOR MACH 15.6 AND 16.3

Test Conditions for Run 60 :

Po	= 1.335E+03 PSIA	Reservoir Total Pressure
Ho	= 1.831E+07 (Ft/sec)²	Reservoir Total Enthalpy
To	= 2.785E+03 °R	Reservoir Total Temperature
M	= 8.039E-00	Freestream Mach Number
U	= 5.832E+03 Ft/sec	Freestream Velocity
T	= 2.189E+02 °R	Freestream Temperature
P	= 1.172E-01 PSIA	Freestream Static Pressure
Rho	= 4.493E-05 Slugs/Ft3	Freestream Density
Mu	= 1.810E-07 Slugs/Ft-sec	Freestream Viscosity
Re	= 1.448E+06 1/Ft	Freestream Reynolds Number
Po'	= 9.837E+00 PSIA	Pitot Pressure
Q	= 5.307E+00 PSIA	Dynamic Pressure (½·Rho·U²/144)
Mi	= 3.401E+00	Shock Tube Incident Shock Mach Number
Hw	= 3.183E+06 (Ft/sec)²	Wall Enthalpy (Cp·Tw)
CPf	= 1.884E-01 1/PSIA	Pressure to CP factor (1/Q)
CHf	= 1.963E-04 Ft²-s/BTU	Heat Rate to CH factor (778/(Rho·U·(Ho-Hw))
QoFR	= 3.881E+01 BTU/Ft²-s	Fay-Riddell Heat Transfer to 3" Diam Sphere

Model Configuration Parameter	Value
Stagnation Position (gauge label)	P21
Vertical Distance (inches)	3.19
Horizontal Distance (inches)	1.81
Plate Angle (degrees)	12.50
Plate Length (inches)	26.50
Sweep Angle (degrees)	0.00

Run 60

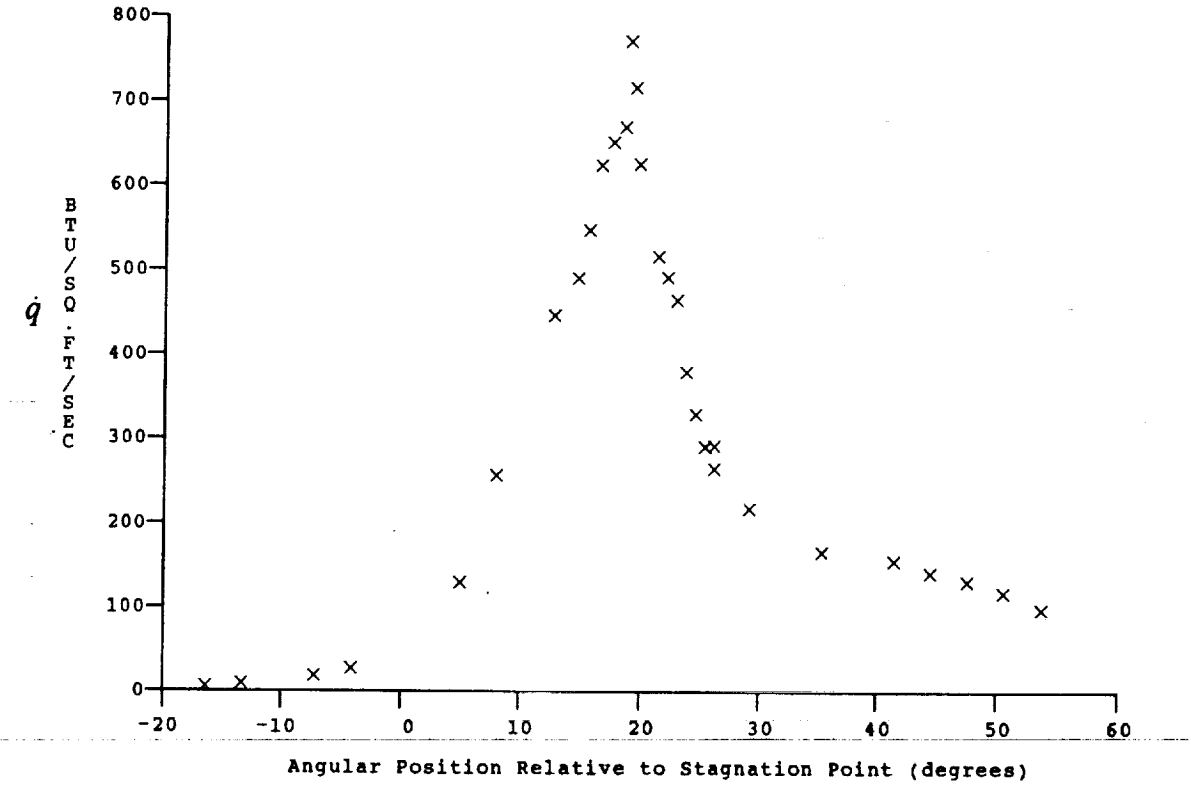

HEAT TRANSFER vs Gauge Position
Run 60

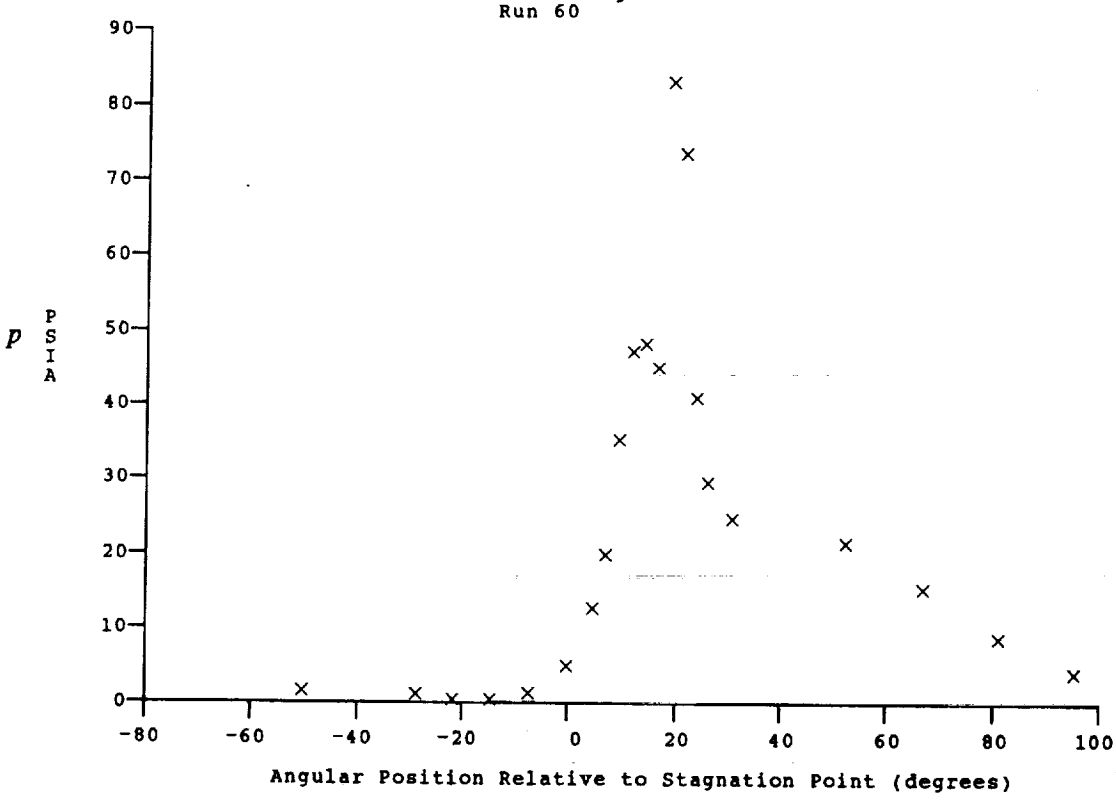

PRESSURE vs Gauge Position
Run 60

Test Conditions for Run 61 :

Po	= 1.341E+03	PSIA	Reservoir Total Pressure
Ho	= 1.826E-07	(Ft/sec)²	Reservoir Total Enthalpy
To	= 2.780E+03	°R	Reservoir Total Temperature
M	= 8.049E+00		Freestream Mach Number
U	= 5.826E+03	Ft/sec	Freestream Velocity
T	= 2.178E+02	°R	Freestream Temperature
P	= 1.169E-01	PSIA	Freestream Static Pressure
Rho	= 4.503E-05	Slugs/Ft3	Freestream Density
Mu	= 1.802E-07	Slugs/Ft-sec	Freestream Viscosity
Re	= 1.456E+06	1/Ft	Freestream Reynolds Number
Po'	= 9.836E+00	PSIA	Pitot Pressure
Q	= 5.307E+00	PSIA	Dynamic Pressure (½·Rho·U²/144)
Mi	= 3.381E+00		Shock Tube Incident Shock Mach Number
Hw	= 3.183E+06	(Ft/sec)²	Wall Enthalpy (Cp·Tw)
CPf	= 1.884E-01	1/PSIA	Pressure to CP factor (1/Q)
CHf	= 1.967E-04	Ft²-s/BTU	Heat Rate to CH factor (778/(Rho·U·(Ho-Hw))
QoFR	= 3.869E+01	BTU/Ft²-s	Fay-Riddell Heat Transfer to 3" Diam Sphere

Model Configuration Parameter	Value
Stagnation Position (gauge label)	P23
Vertical Distance (inches)	3.08
Horizontal Distance (inches)	0.35
Plate Angle (degrees)	12.50
Plate Length (inches)	26.50
Sweep Angle (degrees)	0.00

Run 61

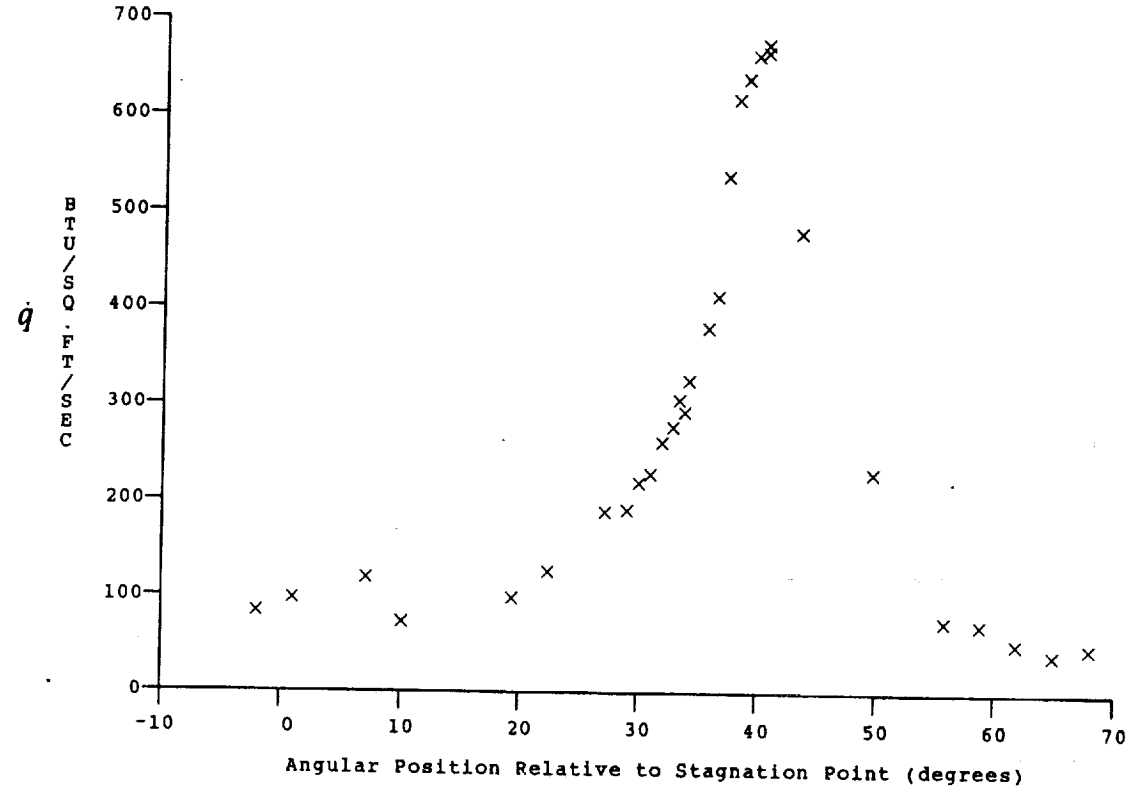

HEAT TRANSFER vs Gauge Position
Run 61

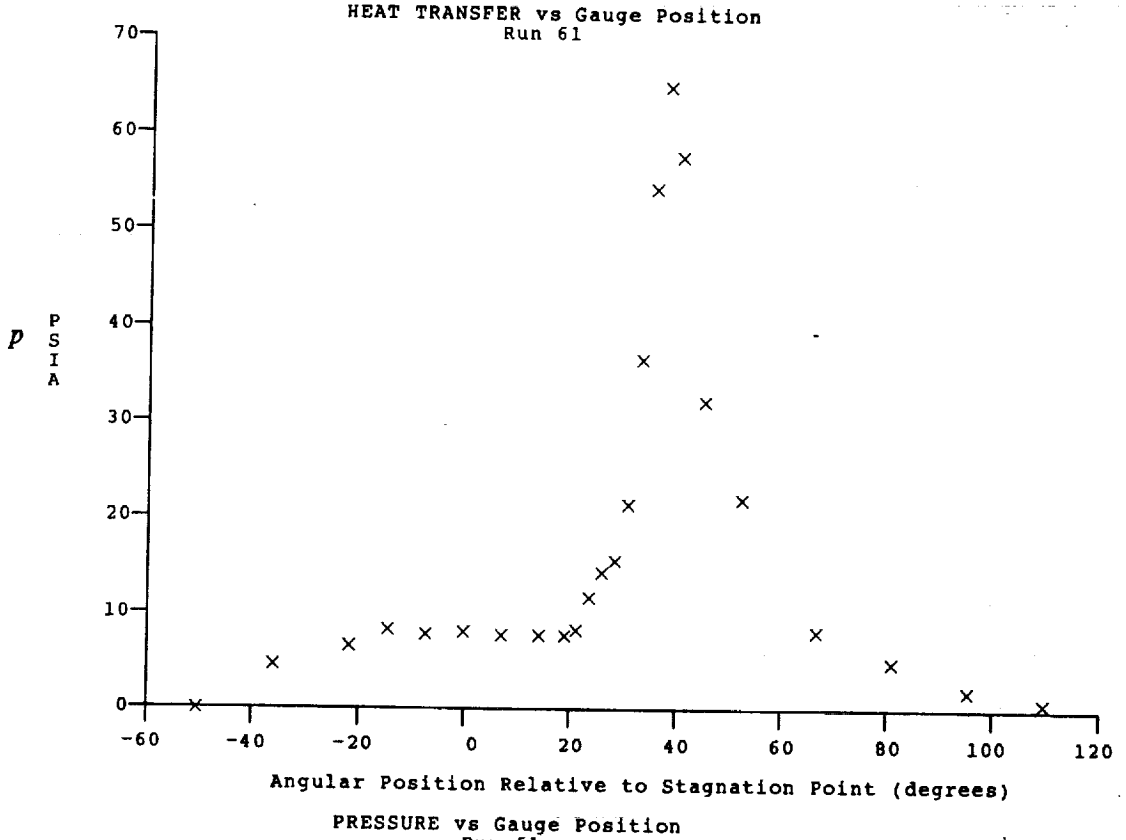

PRESSURE vs Gauge Position
Run 61

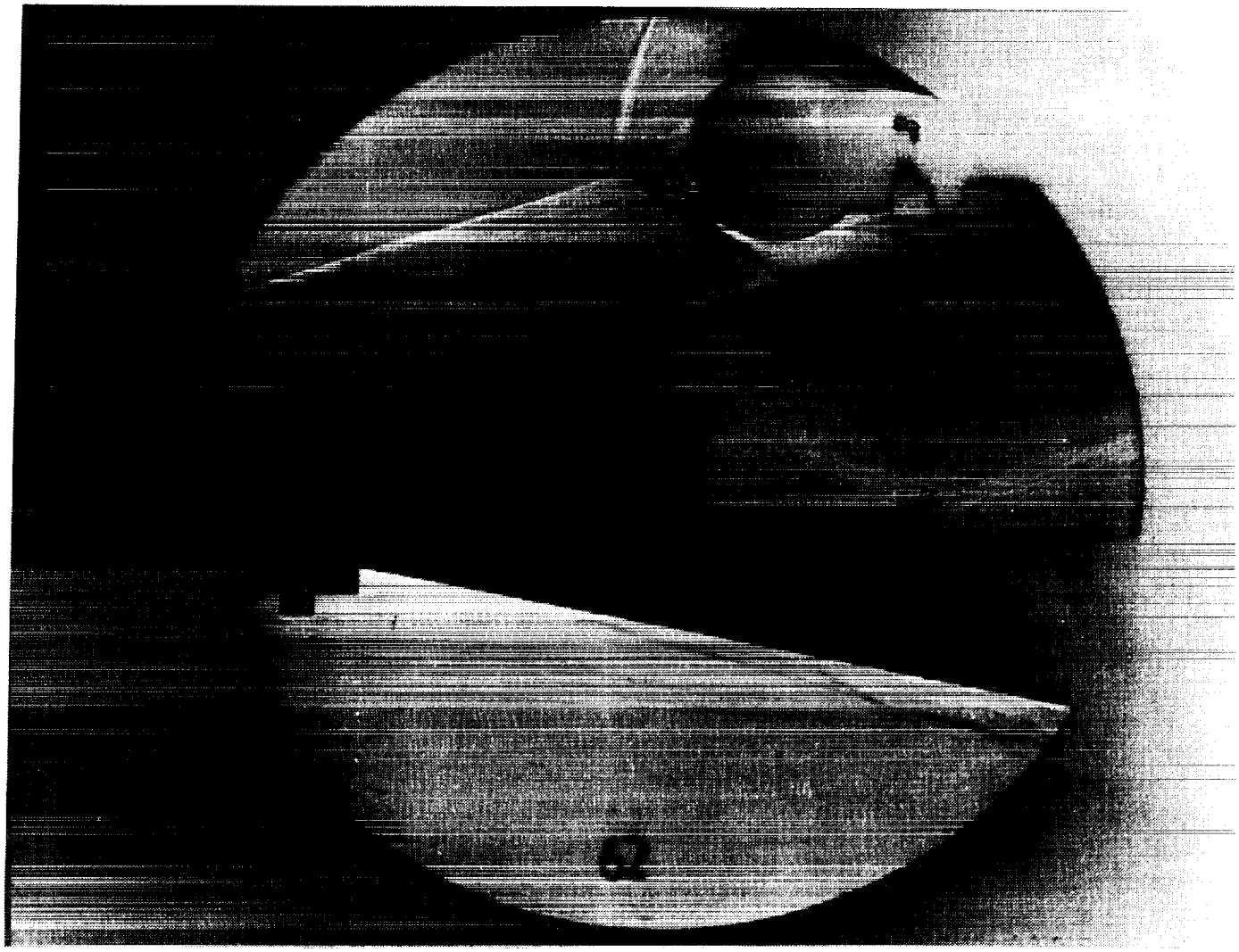

Test Conditions for Run 62 :

Po	= 5.681E+02 PSIA	Reservoir Total Pressure
Ho	= 1.646E+07 (Ft/sec)²	Reservoir Total Enthalpy
To	= 2.539E+03 °R	Reservoir Total Temperature
M	= 8.046E-00	Freestream Mach Number
U	= 5.531E+03 Ft/sec	Freestream Velocity
T	= 1.965E+02 °R	Freestream Temperature
P	= 5.053E-02 PSIA	Freestream Static Pressure
Rho	= 2.158E-05 Slugs/Ft3	Freestream Density
Mu	= 1.634E-07 Slugs/Ft-sec	Freestream Viscosity
Re	= 7.302E+05 1/Ft	Freestream Reynolds Number
Po'	= 4.211E+00 PSIA	Pitot Pressure
Q	= 2.292E+00 PSIA	Dynamic Pressure (½·Rho·U²/144)
Mi	= 3.185E+00	Shock Tube Incident Shock Mach Number
Hw	= 3.183E+06 (Ft/sec)²	Wall Enthalpy (Cp·Tw)
CPf	= 4.363E-01 1/PSIA	Pressure to CP factor (1/Q)
CHf	= 4.909E-04 Ft²-s/BTU	Heat Rate to CH factor (778/(Rho·U·(Ho-Hw))
QoFR	= 2.222E+01 BTU/Ft²-s	Fay-Riddell Heat Transfer to 3" Diam Sphere

Model Configuration Parameter	Value
Stagnation Position (gauge label)	P24
Vertical Distance (inches)	3.08
Horizontal Distance (inches)	0.35
Plate Angle (degrees)	12.50
Plate Length (inches)	26.50
Sweep Angle (degrees)	0.00

Run 62

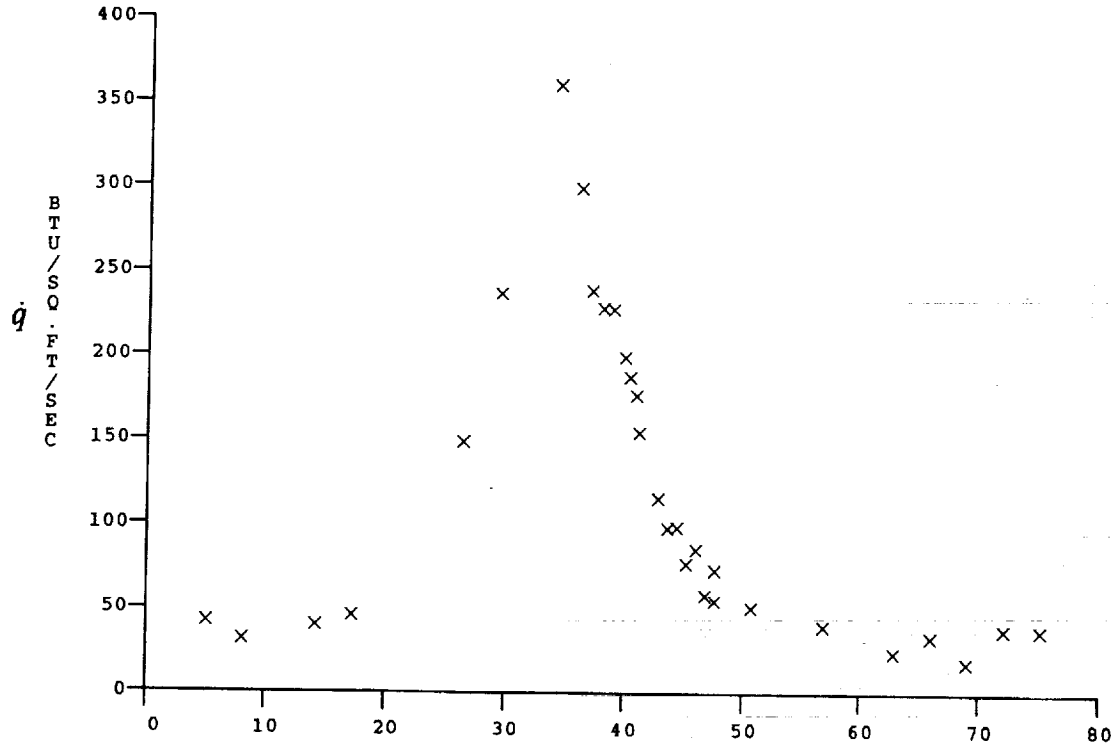

HEAT TRANSFER vs Gauge Position
Run 62

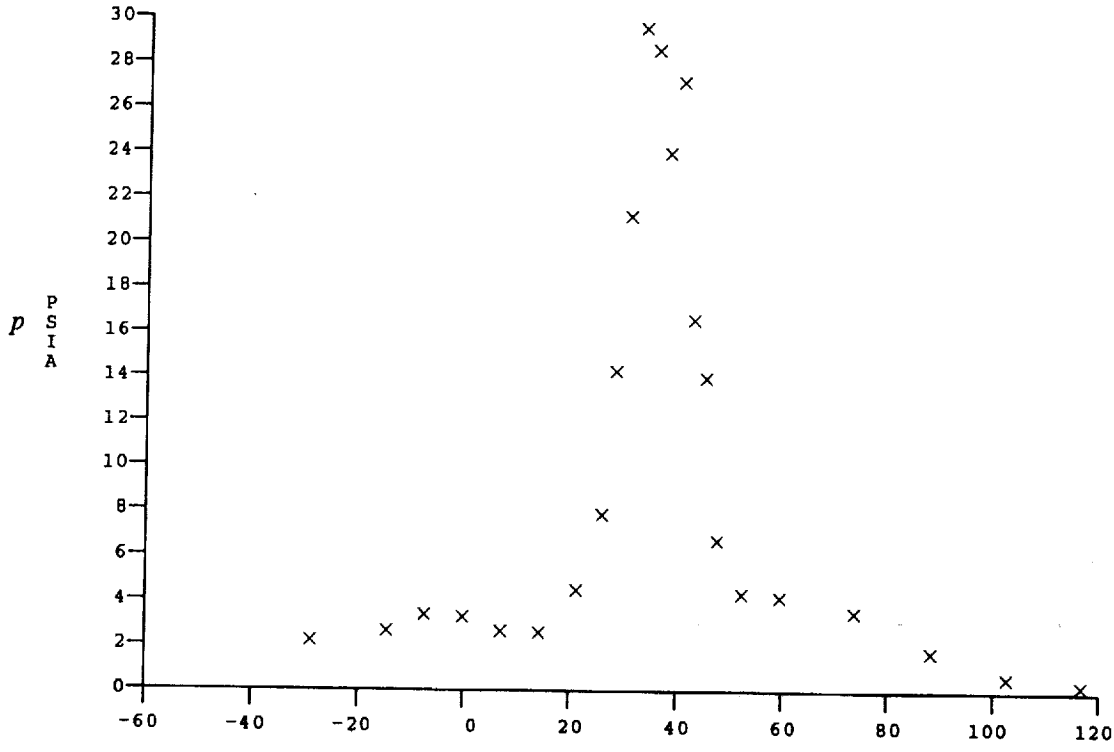

PRESSURE vs Gauge Position
Run 62

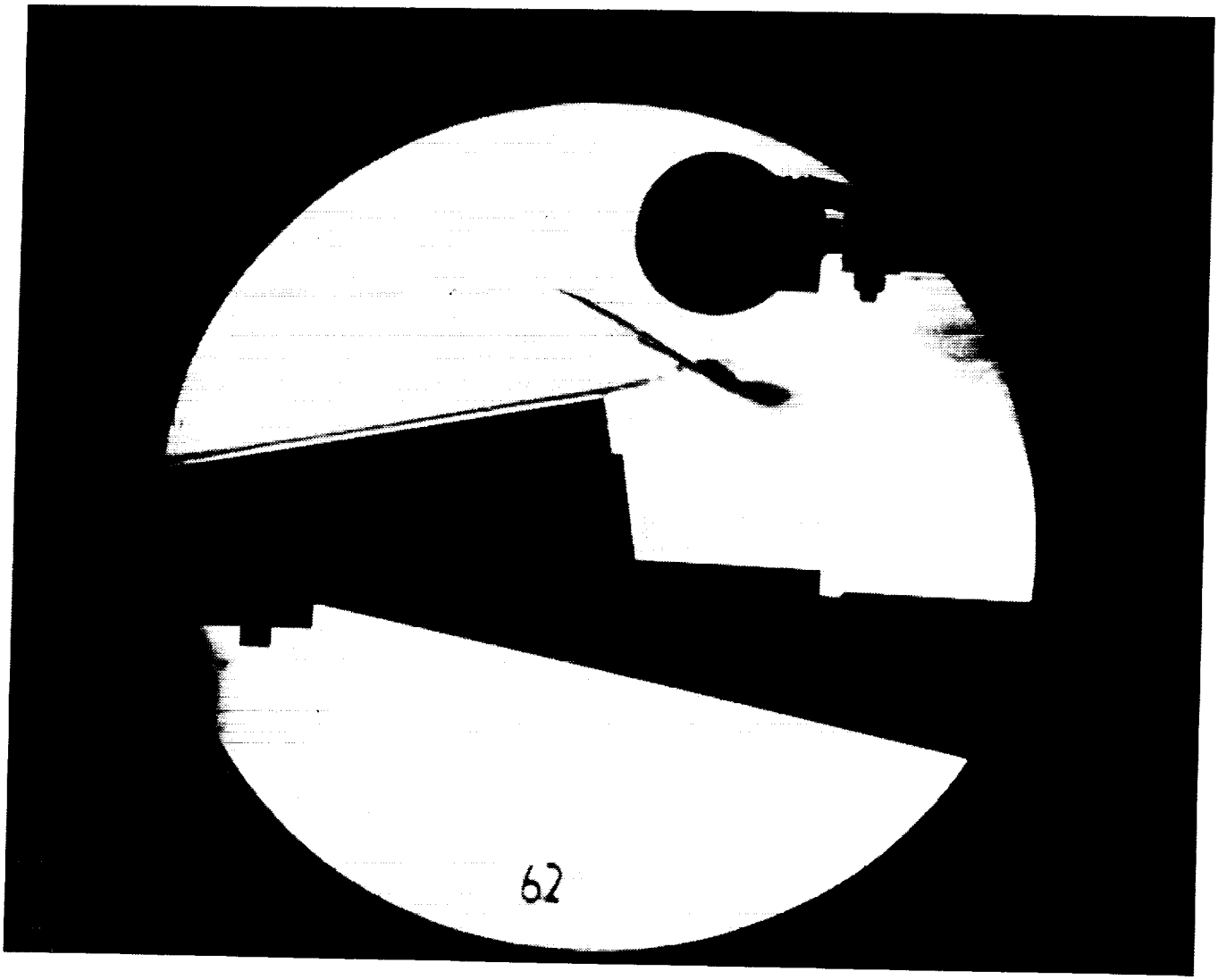

Test Conditions for Run 63 :

Po	= 4.500E+02 PSIA	Reservoir Total Pressure
Ho	= 2.245E+07 (Ft/sec)²	Reservoir Total Enthalpy
To	= 3.343E+03 °R	Reservoir Total Temperature
M	= 7.749E+00	Freestream Mach Number
U	= 6.441E+03 Ft/sec	Freestream Velocity
T	= 2.873E+02 °R	Freestream Temperature
P	= 4.549E-02 PSIA	Freestream Static Pressure
Rho	= 1.329E-05 Slugs/Ft3	Freestream Density
Mu	= 2.323E-07 Slugs/Ft-sec	Freestream Viscosity
Re	= 3.685E+05 1/Ft	Freestream Reynolds Number
Po'	= 3.561E+00 PSIA	Pitot Pressure
Q	= 1.914E+00 PSIA	Dynamic Pressure (½·Rho·U²/144)
Mi	= 3.787E+00	Shock Tube Incident Shock Mach Number
Hw	= 3.183E+06 (Ft/sec)²	Wall Enthalpy (Cp·Tw)
CPf	= 5.224E-01 1/PSIA	Pressure to CP factor (1/Q)
CHf	= 4.718E-04 Ft²-s/BTU	Heat Rate to CH factor (778/(Rho·U·(Ho-Hw))
QoFR	= 3.015E+01 BTU/Ft²-s	Fay-Riddell Heat Transfer to 3" Diam Sphere

Model Configuration Parameter	Value
Stagnation Position (gauge label)	P24
Vertical Distance (inches)	3.08
Horizontal Distance (inches)	0.35
Plate Angle (degrees)	12.50
Plate Length (inches)	26.50
Sweep Angle (degrees)	0.00

Run 63

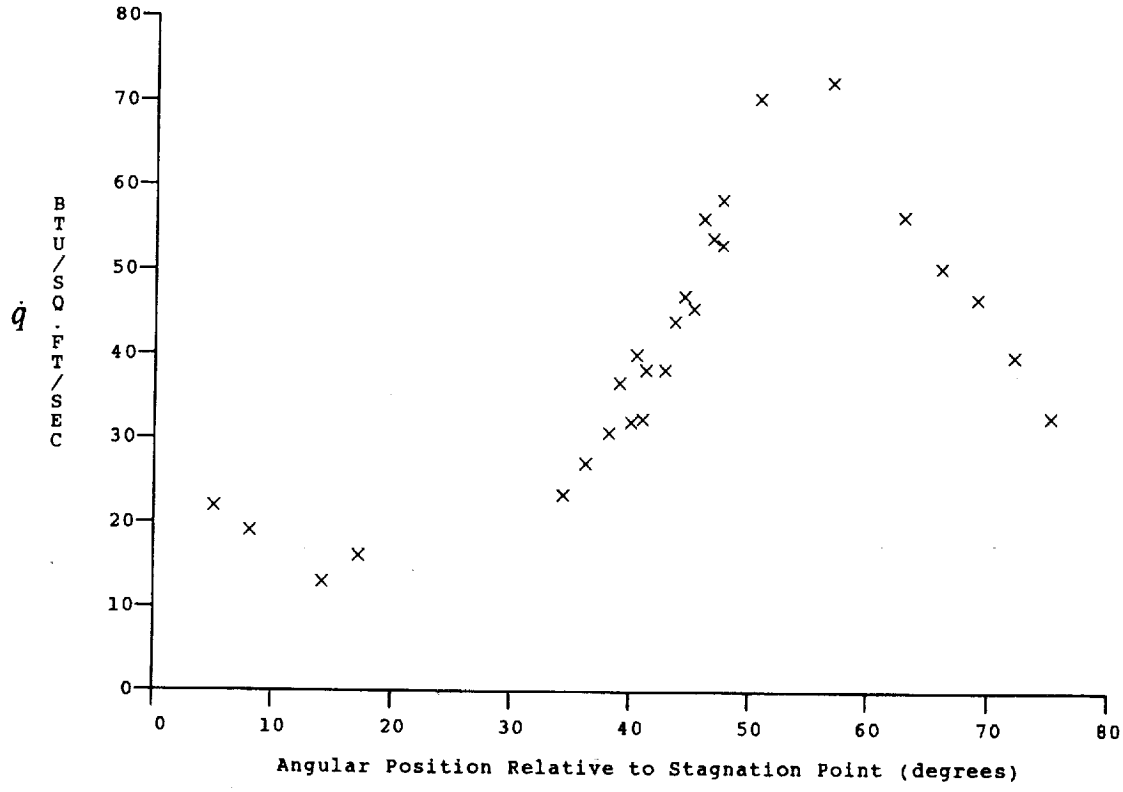

HEAT TRANSFER vs Gauge Position
Run 63

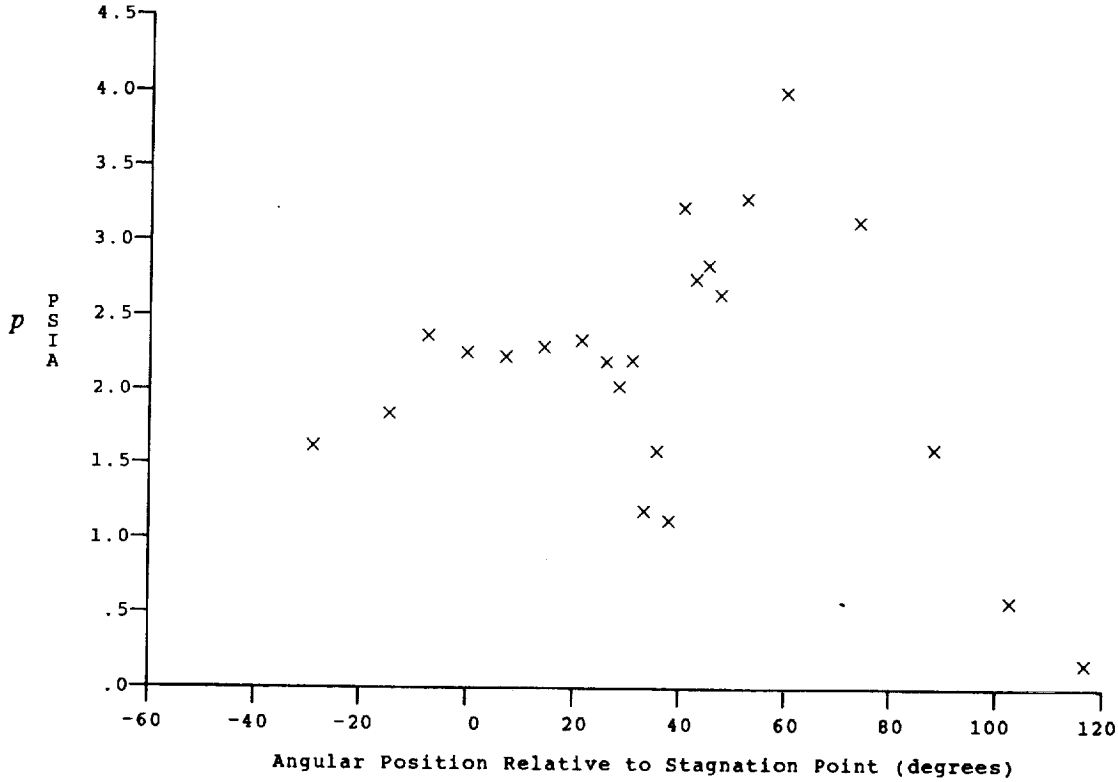

PRESSURE vs Gauge Position
Run 63

Test Conditions

Mi	= 3.4570	
Po	= 1.8100X10+3	PSIA
Ho	= 1.9321X10+7	(Ft/sec)^2
To	= 2.9223X10+3	Degrees R
M	= 8.0620	
U	= 5.9932X10+3	Ft/sec
T	= 2.2980X10+2	Degrees R
P	= 1.5471X10-1	PSIA
Q	= 7.0463	PSIA
Rho	= 5.6499X10-5	Slugs/Ft^3
Mu	= 1.8946X10-7	Slugs/Ft-sec
Re	= 1.7873X10+6	1/Ft
Po'	= 1.3072X10+1	PSIA

Model Configuration Parameter	Value
Stagnation Position (gauge label)	P24
Vertical Distance (inches)	3.08
Horizontal Distance (inches)	0.35
Plate Angle (degrees)	12.50
Plate Length (inches)	26.50
Sweep Angle (degrees)	0.00

Run 64

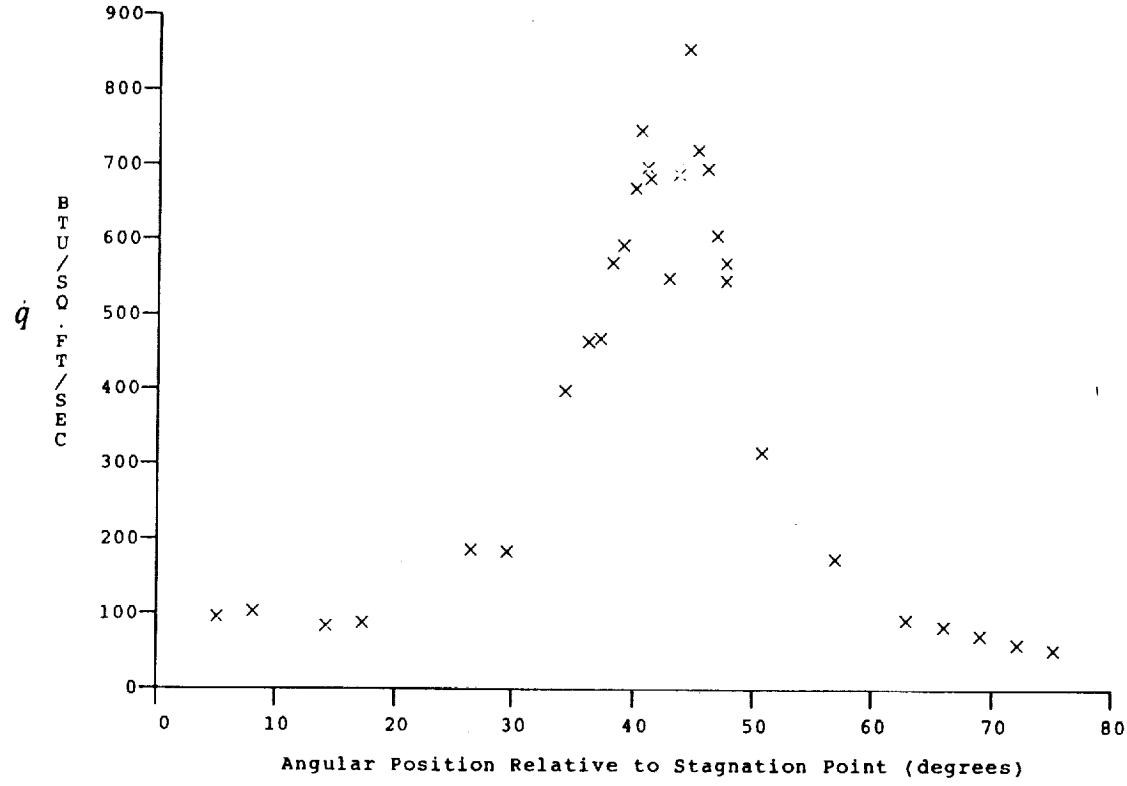

HEAT TRANSFER vs Gauge Position
Run 64

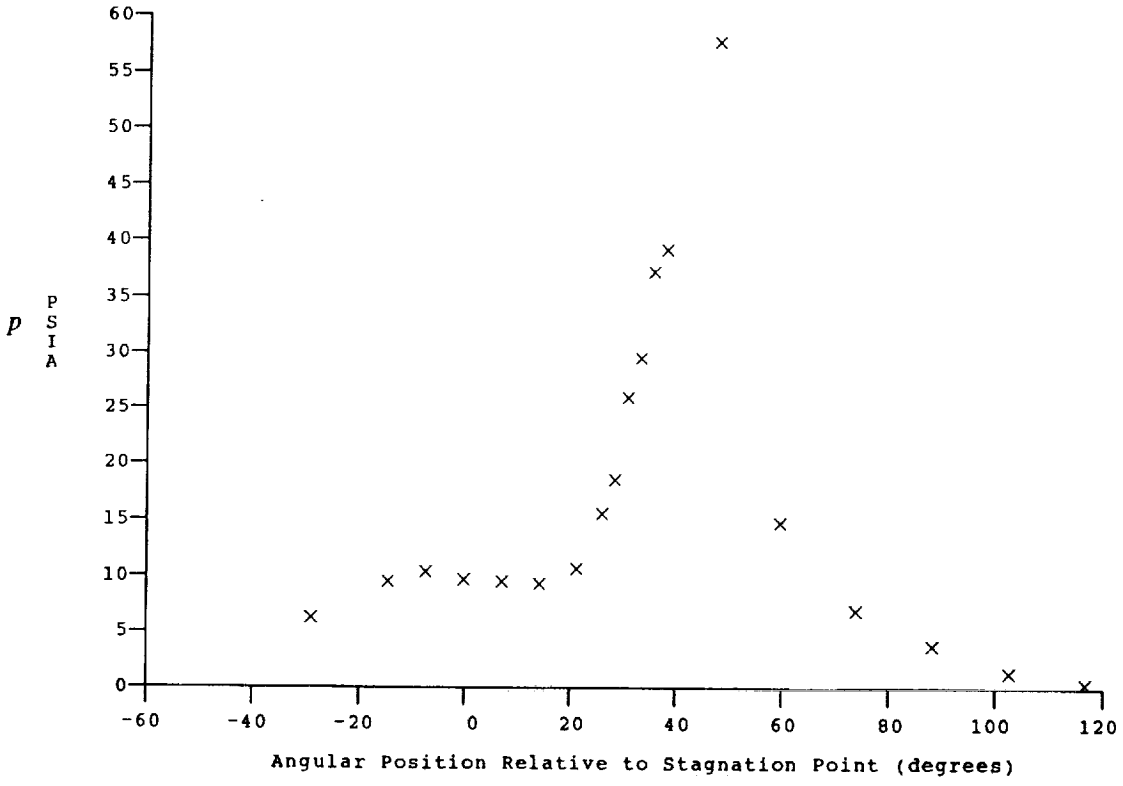

PRESSURE vs Gauge Position
Run 64

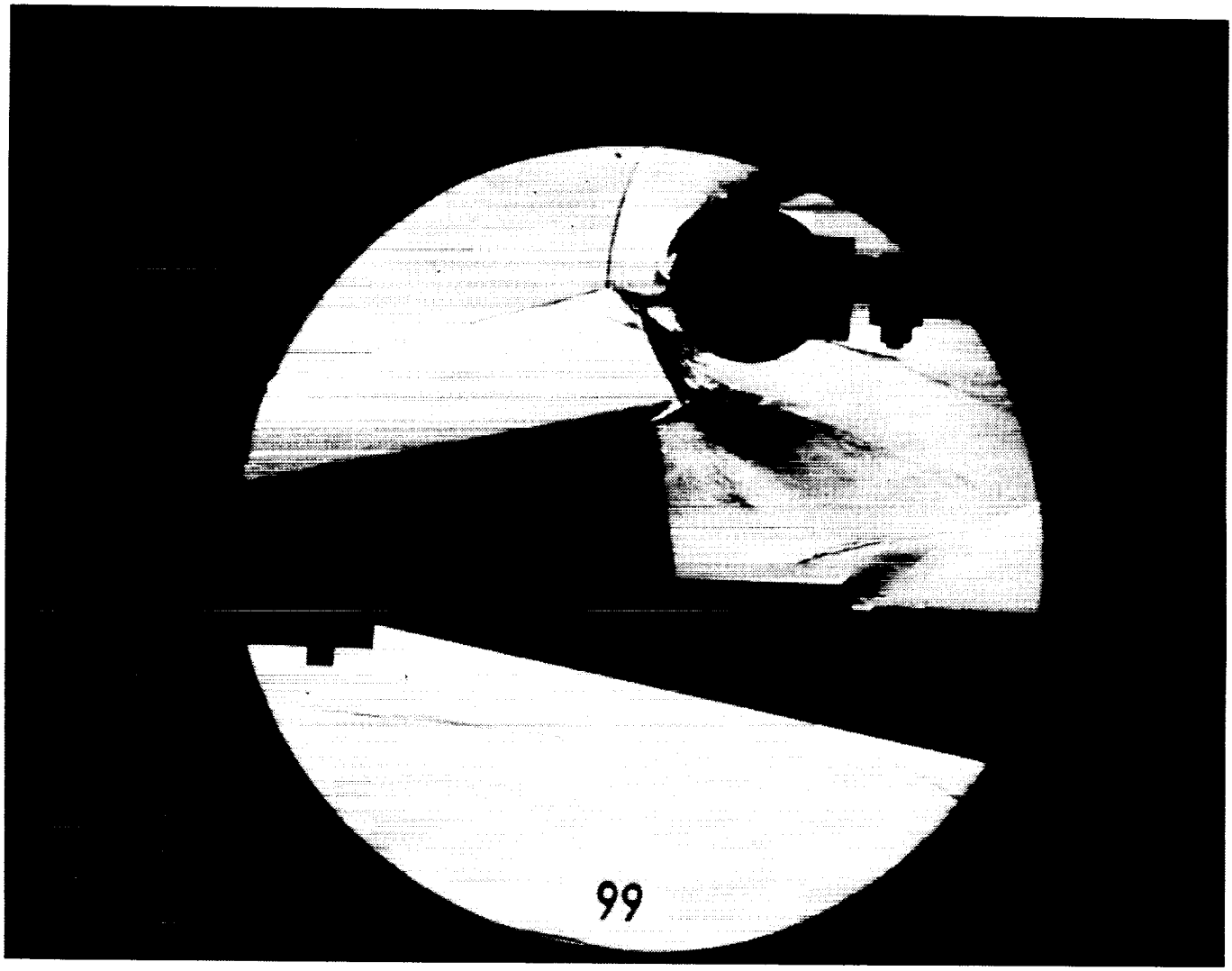

Test Conditions for Run 99 :

Po	= 1.307E-03 PSIA	Reservoir Total Pressure	
Ho	= 1.336E+07 (Ft/sec)²	Reservoir Total Enthalpy	
To	= 2.100E-03 °R	Reservoir Total Temperature	
M	= 8.295E-00	Freestream Mach Number	
U	= 4.994E+03 Ft/sec	Freestream Velocity	
T	= 1.507E-02 °R	Freestream Temperature	
P	= 1.028E-01 PSIA	Freestream Static Pressure	
Rho	= 5.721E-05 Slugs/Ft3	Freestream Density	
Mu	= 1.264E-07 Slugs/Ft-sec	Freestream Viscosity	
Re	= 2.261E+06 1/Ft	Freestream Reynolds Number	
Po'	= 9.142E+00 PSIA	Pitot Pressure	
Q	= 4.955E+00 PSIA	Dynamic Pressure (½·Rho·U²/144)	
Mi	= 2.838E+00	Shock Tube Incident Shock Mach Number	
Hw	= 3.183E+06 (Ft/sec)²	Wall Enthalpy (Cp·Tw)	
CPf	= 2.018E-01 1/PSIA	Pressure to CP factor (1/Q)	
CHf	= 2.675E-04 Ft²-s/BTU	Heat Rate to CH factor (778/(Rho·U·(Ho-Hw))	
QoFR	= 2.463E+01 BTU/Ft²-s	Fay-Riddell Heat Transfer to 3" Diam Sphere	

Model Configuration Parameter	Value
Stagnation Position (gauge label)	P21
Vertical Distance (inches)	2.79
Horizontal Distance (inches)	0.22
Plate Angle (degrees)	12.50
Plate Length (inches)	26.50
Sweep Angle (degrees)	0.00

Run 99

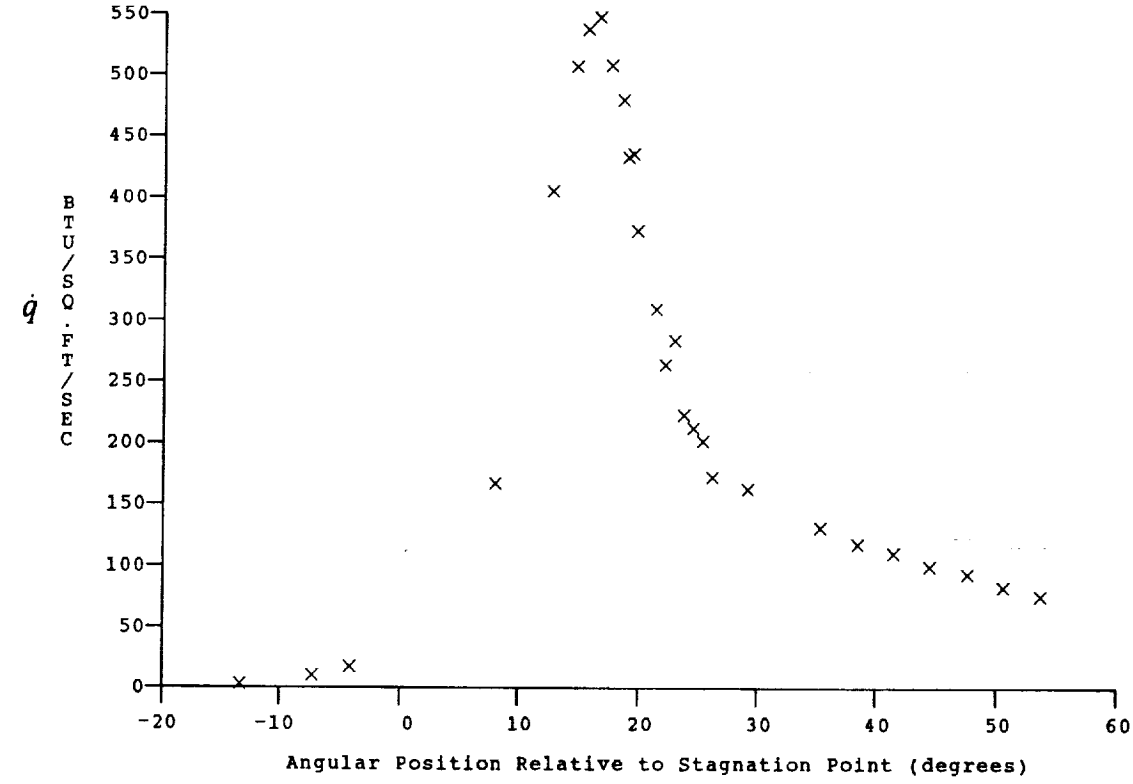

HEAT TRANSFER vs Gauge Position
Run 99

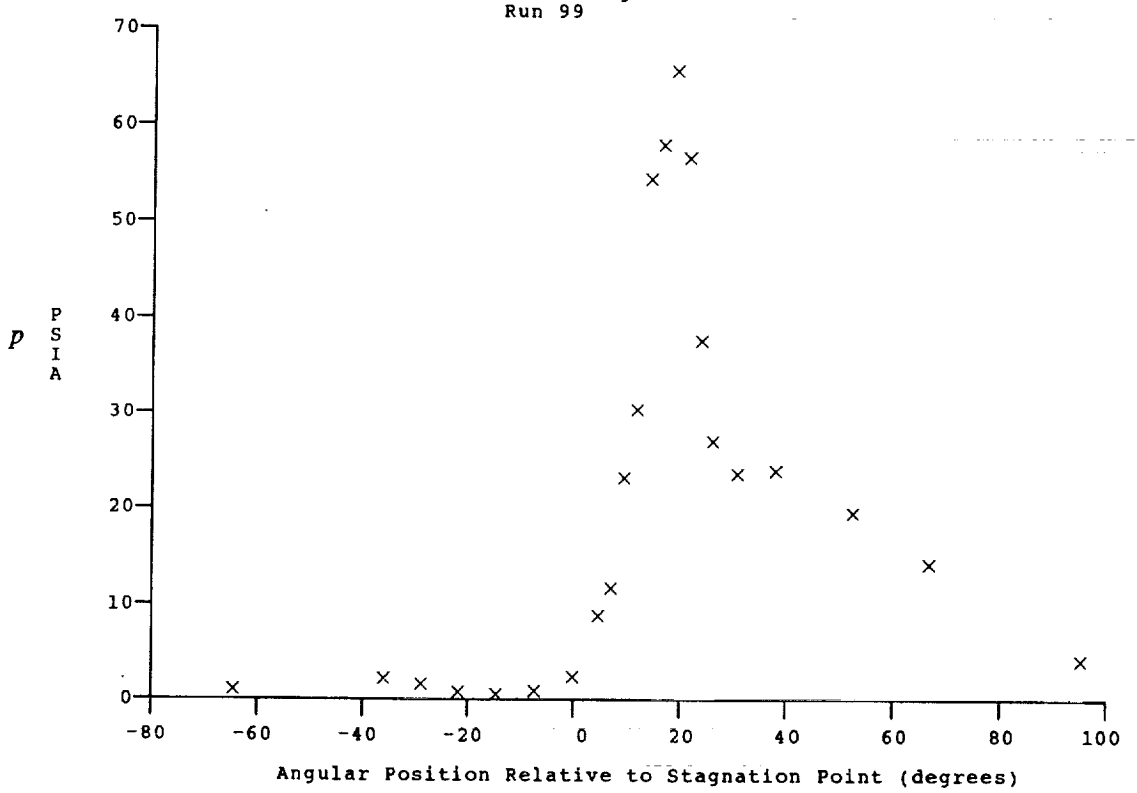

PRESSURE vs Gauge Position
Run 99

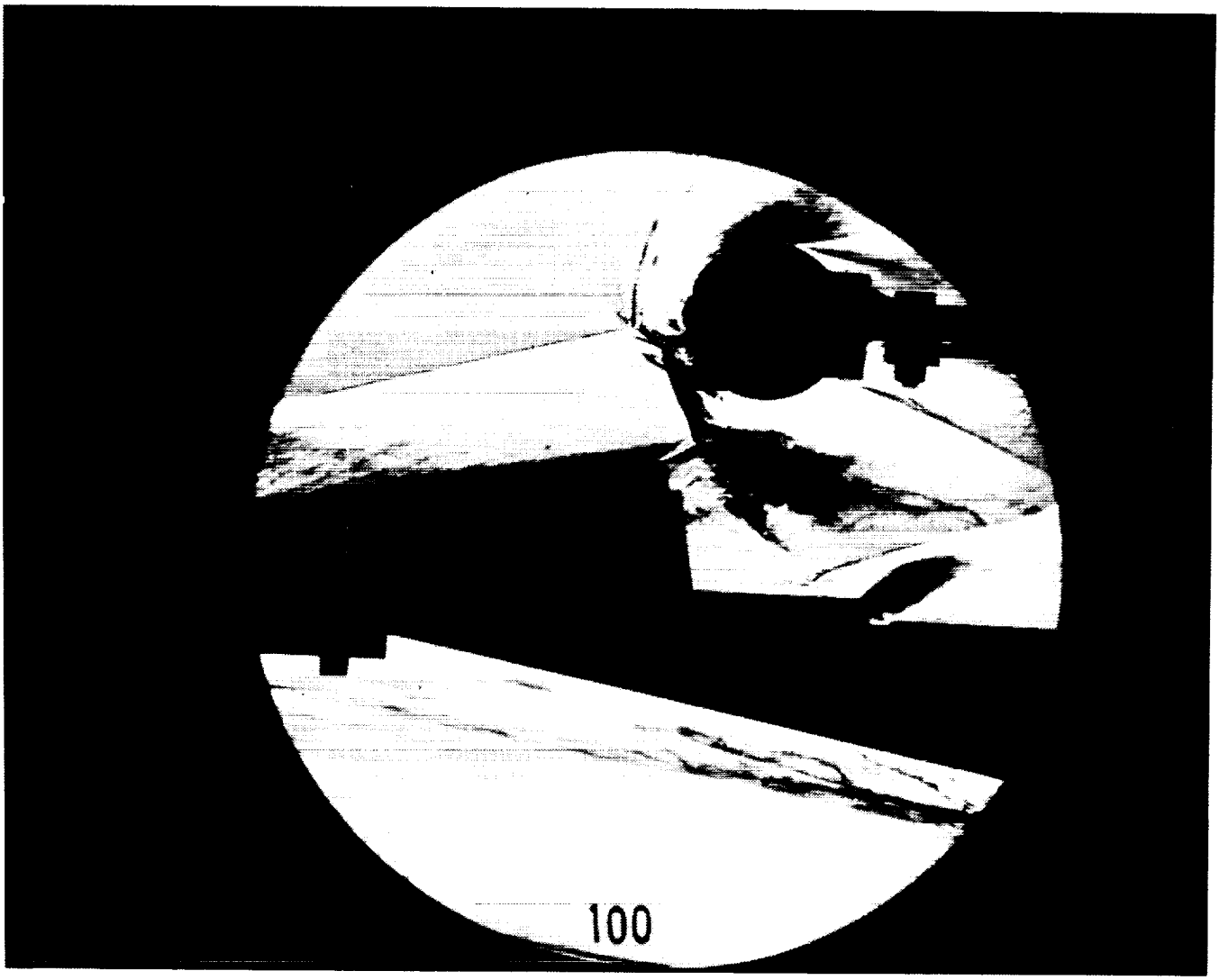

Test Conditions for Run 100 :

Po	= 1.286E+03 PSIA	Reservoir Total Pressure
Ho	= 1.334E+07 (Ft/sec)²	Reservoir Total Enthalpy
To	= 2.097E+03 °R	Reservoir Total Temperature
M	= 8.294E+00	Freestream Mach Number
U	= 4.990E+03 Ft/sec	Freestream Velocity
T	= 1.506E+02 °R	Freestream Temperature
P	= 1.012E-01 PSIA	Freestream Static Pressure
Rho	= 5.642E-05 Slugs/Ft3	Freestream Density
Mu	= 1.262E-07 Slugs/Ft-sec	Freestream Viscosity
Re	= 2.231E+06 1/Ft	Freestream Reynolds Number
Po'	= 9.002E+00 PSIA	Pitot Pressure
Q	= 4.879E+00 PSIA	Dynamic Pressure (½·Rho·U²/144)
Mi	= 2.837E+00	Shock Tube Incident Shock Mach Number
Hw	= 3.183E+06 (Ft/sec)²	Wall Enthalpy (Cp·Tw)
CPf	= 2.050E-01 1/PSIA	Pressure to CP factor (1/Q)
CHf	= 2.719E-04 Ft²-s/BTU	Heat Rate to CH factor (778/(Rho·U·(Ho-Hw))
QoFR	= 2.439E+01 BTU/Ft²-s	Fay-Riddell Heat Transfer to 3" Diam Sphere

Model Configuration Parameter	Value
Stagnation Position (gauge label)	P21
Vertical Distance (inches)	2.79
Horizontal Distance (inches)	0.22
Plate Angle (degrees)	10.00
Plate Length (inches)	26.50
Sweep Angle (degrees)	0.00

Run 100

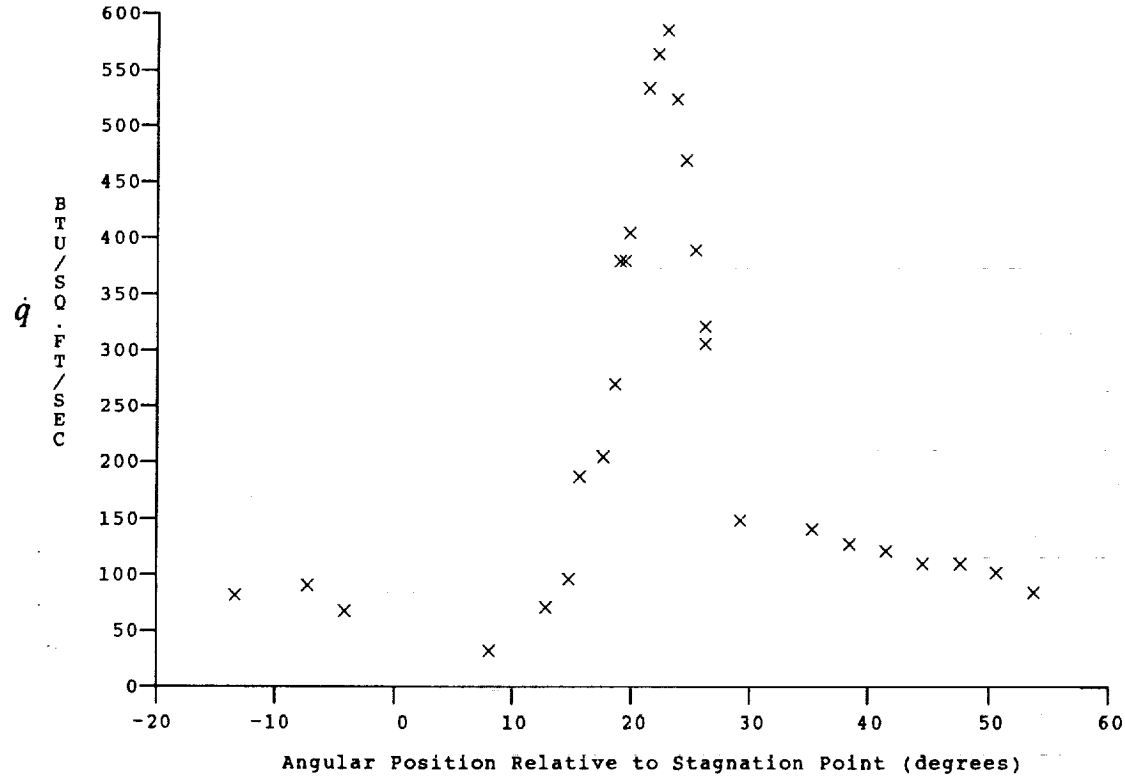

HEAT TRANSFER vs Gauge Position
Run 100

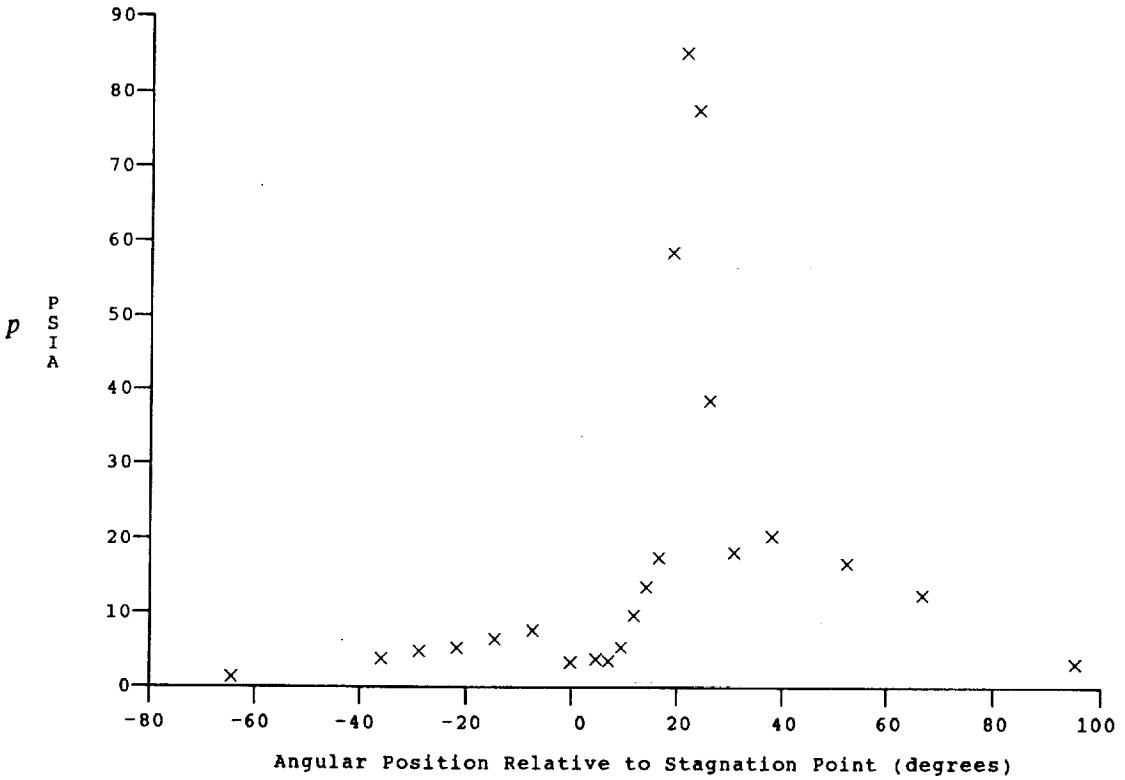

PRESSURE vs Gauge Position
Run 100

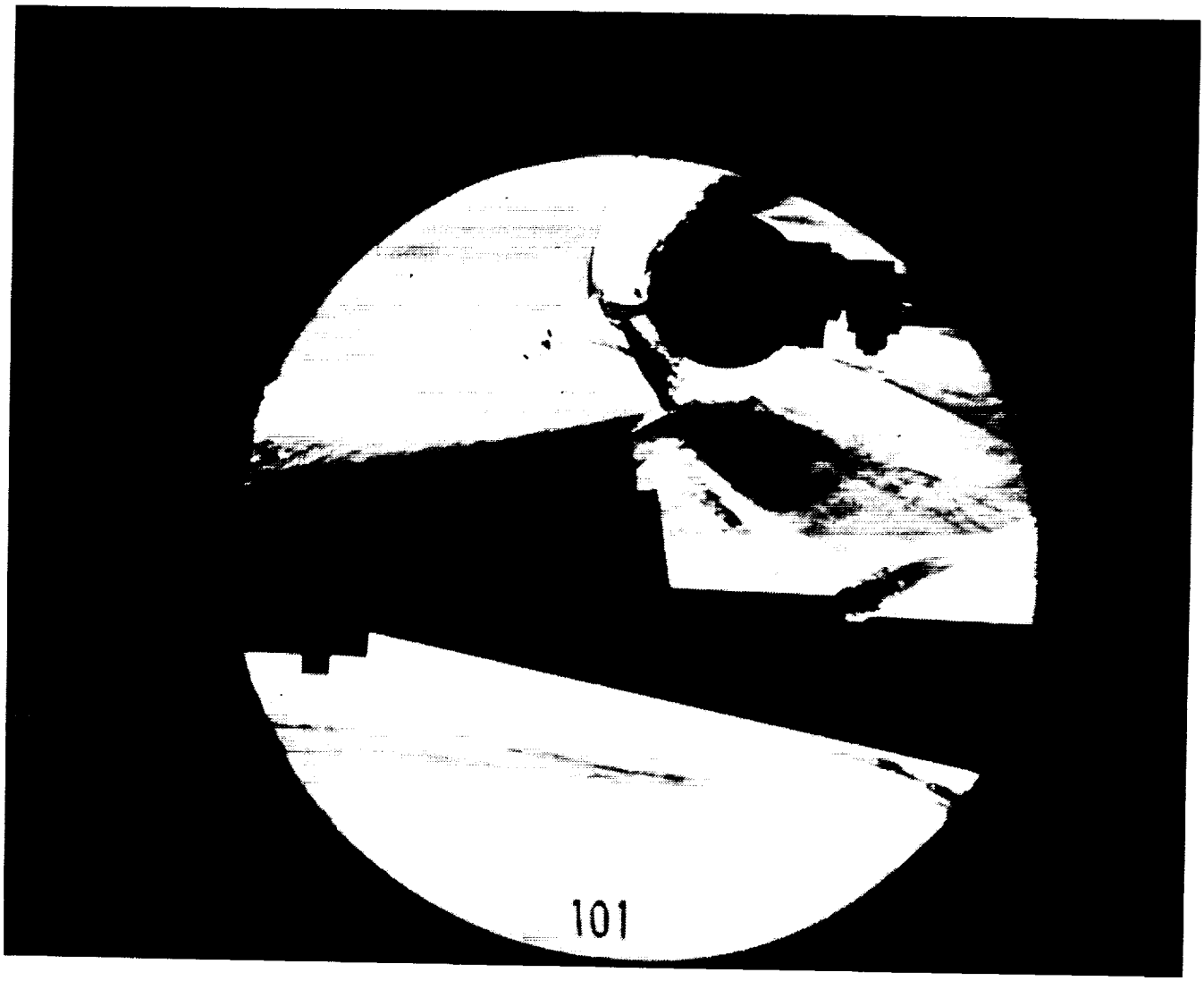

Test Conditions for Run 101 :

Po	= 1.377E-03 PSIA	Reservoir Total Pressure	
Ho	= 1.312E+07 (Ft/sec)²	Reservoir Total Enthalpy	
To	= 2.064E+03 °R	Reservoir Total Temperature	
M	= 8.307E-00	Freestream Mach Number	
U	= 4.949E-03 Ft/sec	Freestream Velocity	
T	= 1.476E-02 °R	Freestream Temperature	
P	= 1.079E-01 PSIA	Freestream Static Pressure	
Rho	= 6.135E-05 Slugs/Ft3	Freestream Density	
Mu	= 1.238E-07 Slugs/Ft-sec	Freestream Viscosity	
Re	= 2.453E+06 1/Ft	Freestream Reynolds Number	
Po'	= 9.624E+00 PSIA	Pitot Pressure	
Q	= 5.217E+00 PSIA	Dynamic Pressure (½·Rho·U²/144)	
Mi	= 2.828E+00	Shock Tube Incident Shock Mach Number	
Hw	= 3.183E+06 (Ft/sec)²	Wall Enthalpy (Cp·Tw)	
CPf	= 1.917E-01 1/PSIA	Pressure to CP factor (1/Q)	
CHf	= 2.579E-04 Ft²-s/BTU	Heat Rate to CH factor (778/(Rho·U·(Ho-Hw))	
QoFR	= 2.463E+01 BTU/Ft²-s	Fay-Riddell Heat Transfer to 3" Diam Sphere	

Model Configuration Parameter	Value
Stagnation Position (gauge label)	P22
Vertical Distance (inches)	2.89
Horizontal Distance (inches)	0.22
Plate Angle (degrees)	12.50
Plate Length (inches)	26.50
Sweep Angle (degrees)	0.00

Run 101

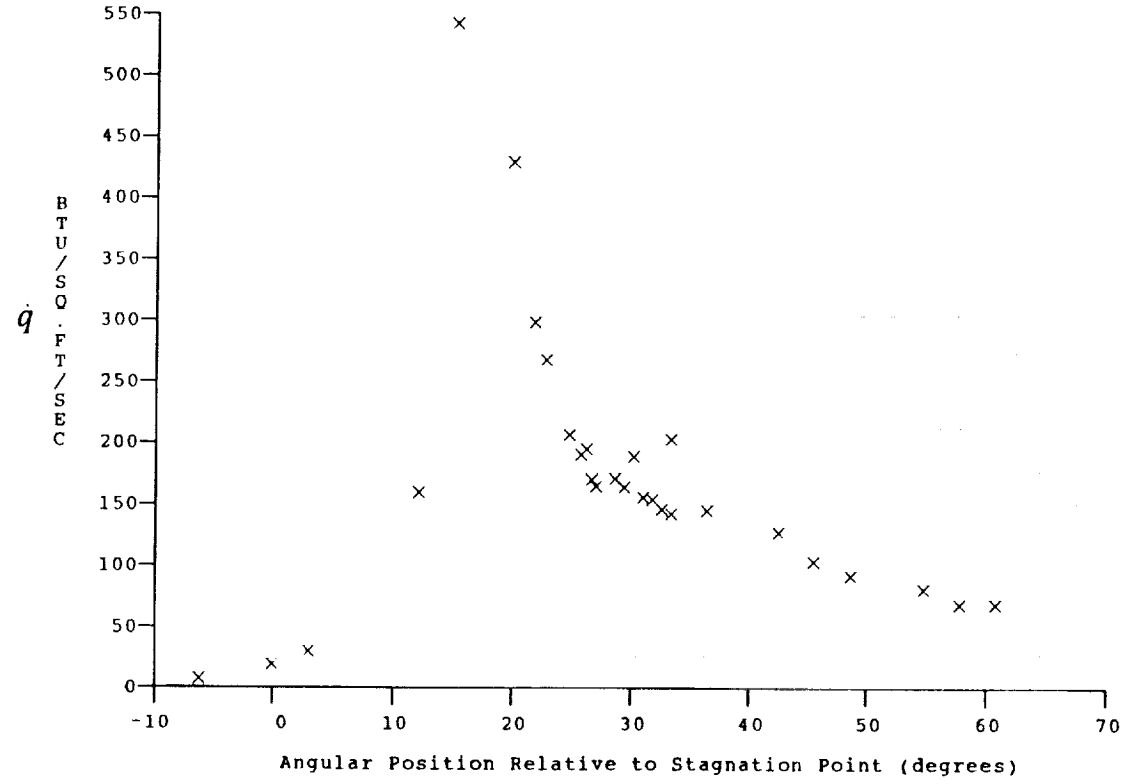

HEAT TRANSFER vs Gauge Position
Run 101

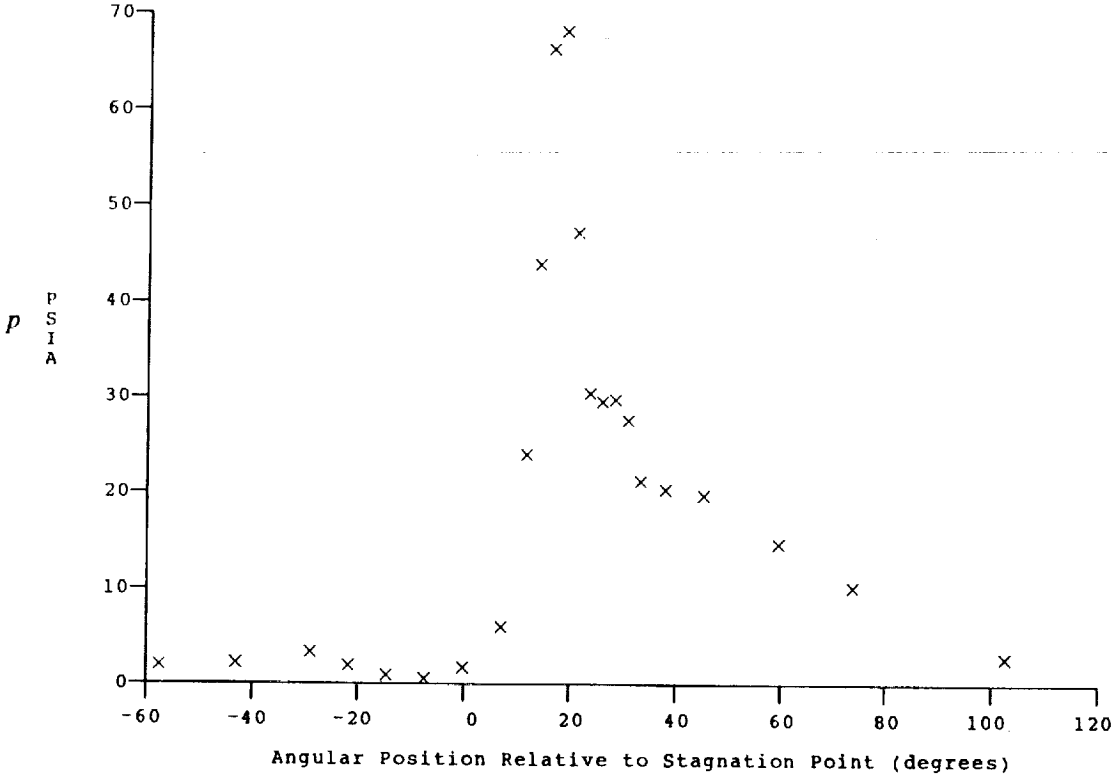

PRESSURE vs Gauge Position
Run 101

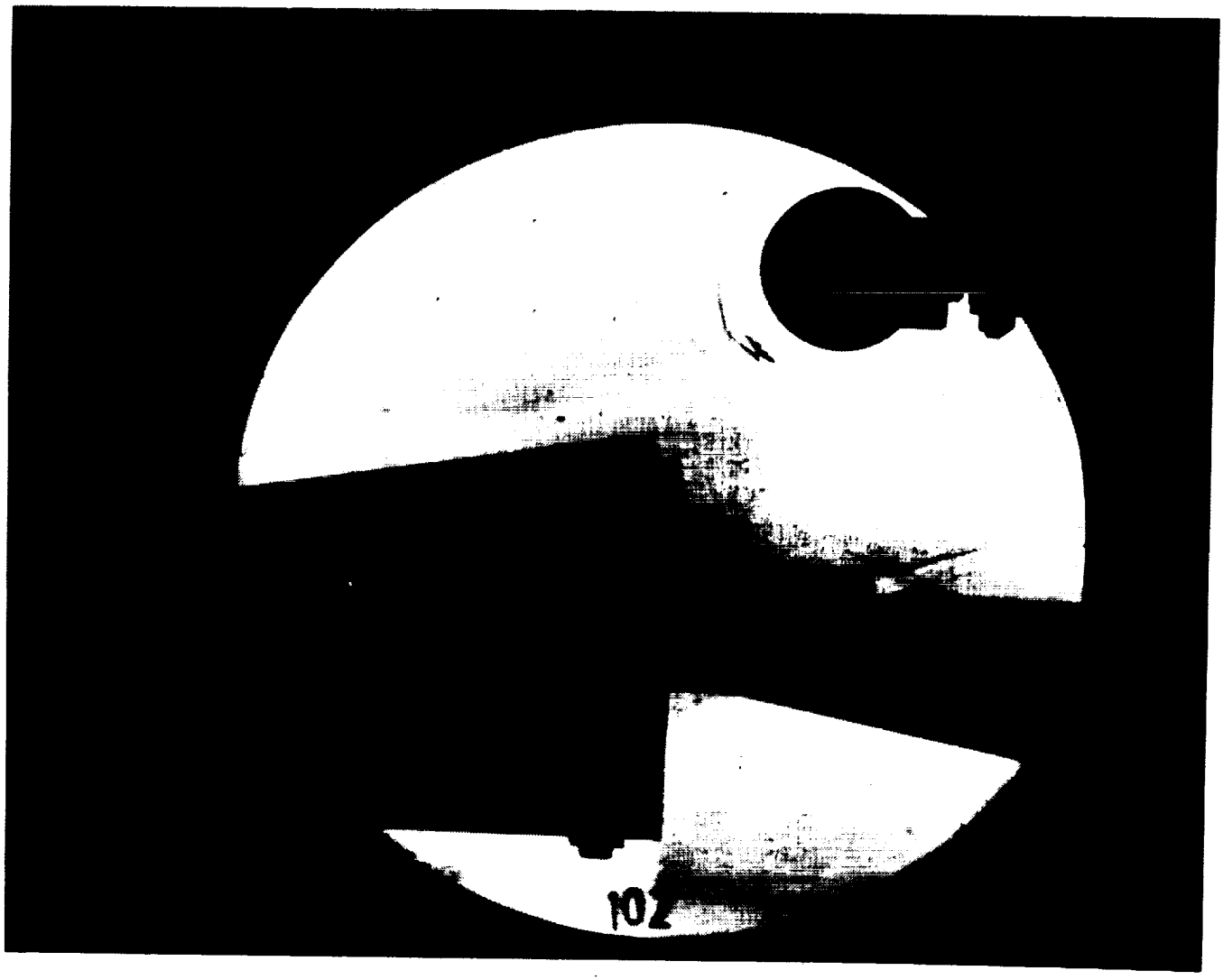

Test Conditions for Run 102 :

Po	= 5.730E+02	PSIA	Reservoir Total Pressure
Ho	= 1.882E+07	(Ft/sec)²	Reservoir Total Enthalpy
To	= 2.857E+03	°R	Reservoir Total Temperature
M	= 1.170E+01		Freestream Mach Number
U	= 6.029E+03	Ft/sec	Freestream Velocity
T	= 1.103E+02	°R	Freestream Temperature
P	= 4.081E-03	PSIA	Freestream Static Pressure
Rho	= 3.104E-06	Slugs/Ft3	Freestream Density
Mu	= 9.281E-08	Slugs/Ft-sec	Freestream Viscosity
Re	= 2.016E+05	1/Ft	Freestream Reynolds Number
Po'	= 7.263E-01	PSIA	Pitot Pressure
Q	= 3.917E-01	PSIA	Dynamic Pressure (½·Rho·U²/144)
Mi	= 3.493E+00		Shock Tube Incident Shock Mach Number
Hw	= 3.183E+06	(Ft/sec)²	Wall Enthalpy (Cp·Tw)
CPf	= 2.553E+00	1/PSIA	Pressure to CP factor (1/Q)
CHf	= 2.660E-03	Ft²-s/BTU	Heat Rate to CH factor (778/(Rho·U·(Ho-Hw))
QoFR	= 1.095E-01	BTU/Ft²-s	Fay Riddell Heat Transfer to 3" Diam Sphere

Model Configuration Parameter	Value
Stagnation Position (gauge label)	P22
Vertical Distance (inches)	3.35
Horizontal Distance (inches)	1.86
Plate Angle (degrees)	10.00
Plate Length (inches)	46.25
Sweep Angle (degrees)	0.00

Run 102

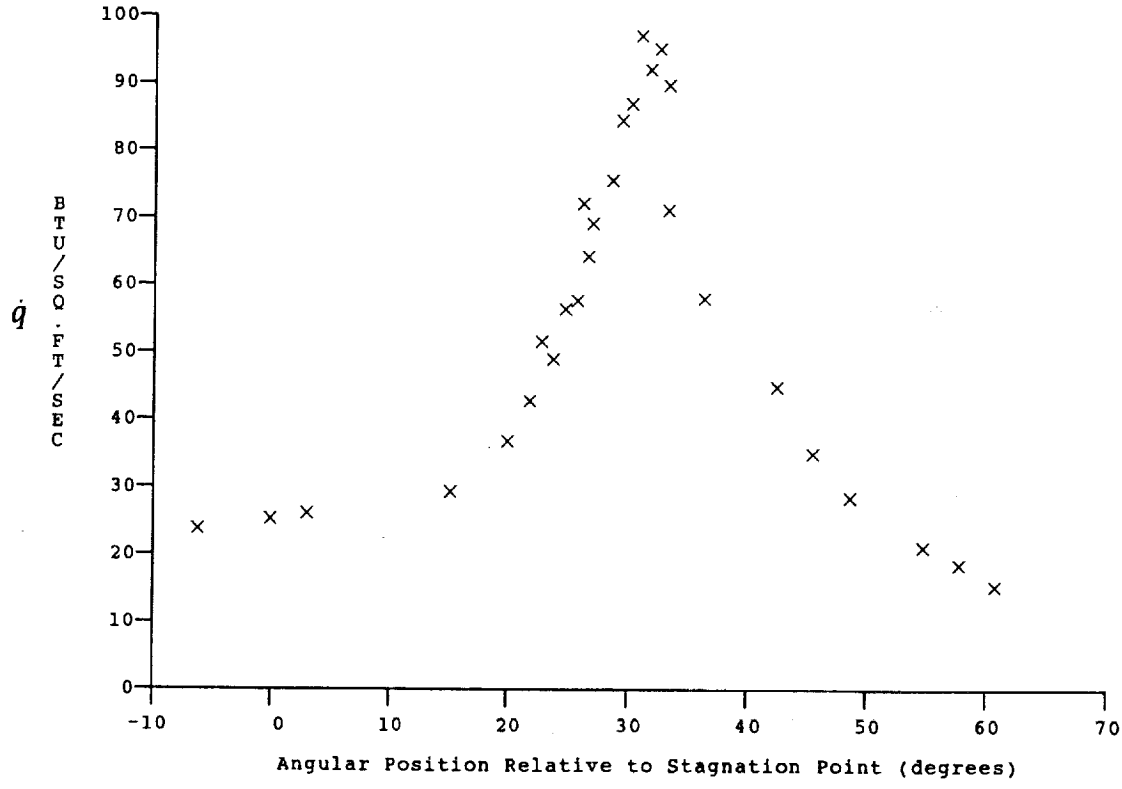

HEAT TRANSFER vs Gauge Position
Run 102

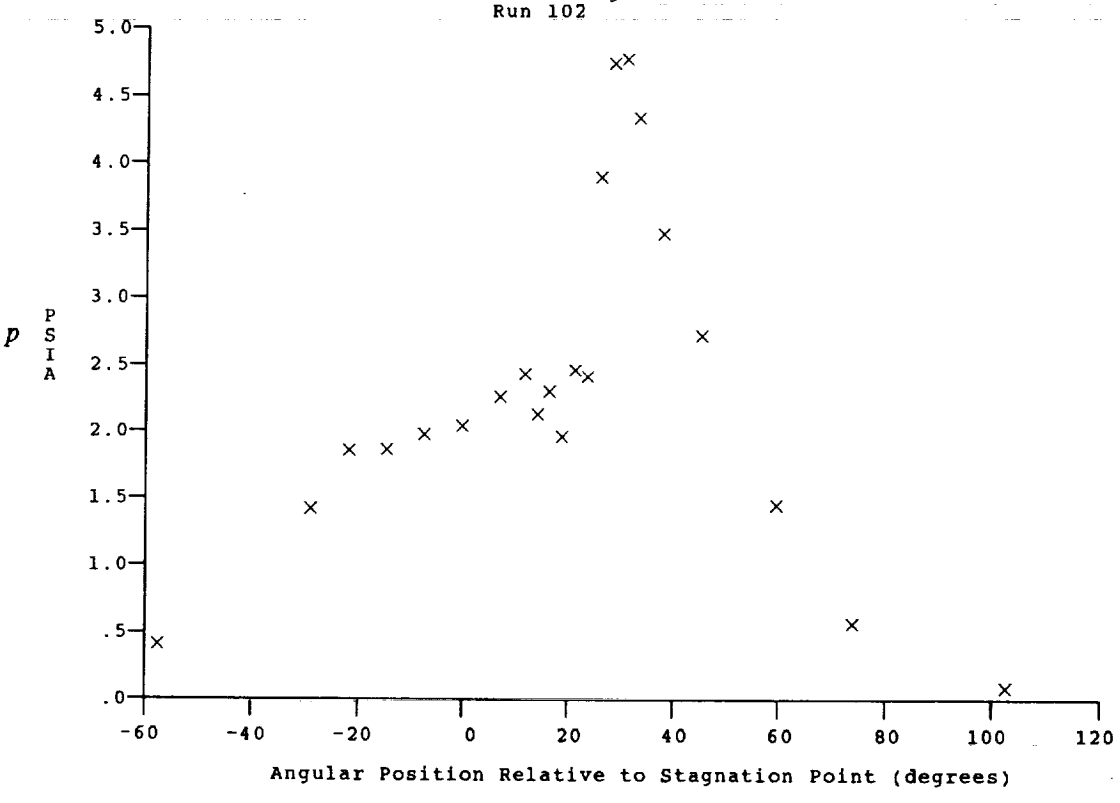

PRESSURE vs Gauge Position
Run 102

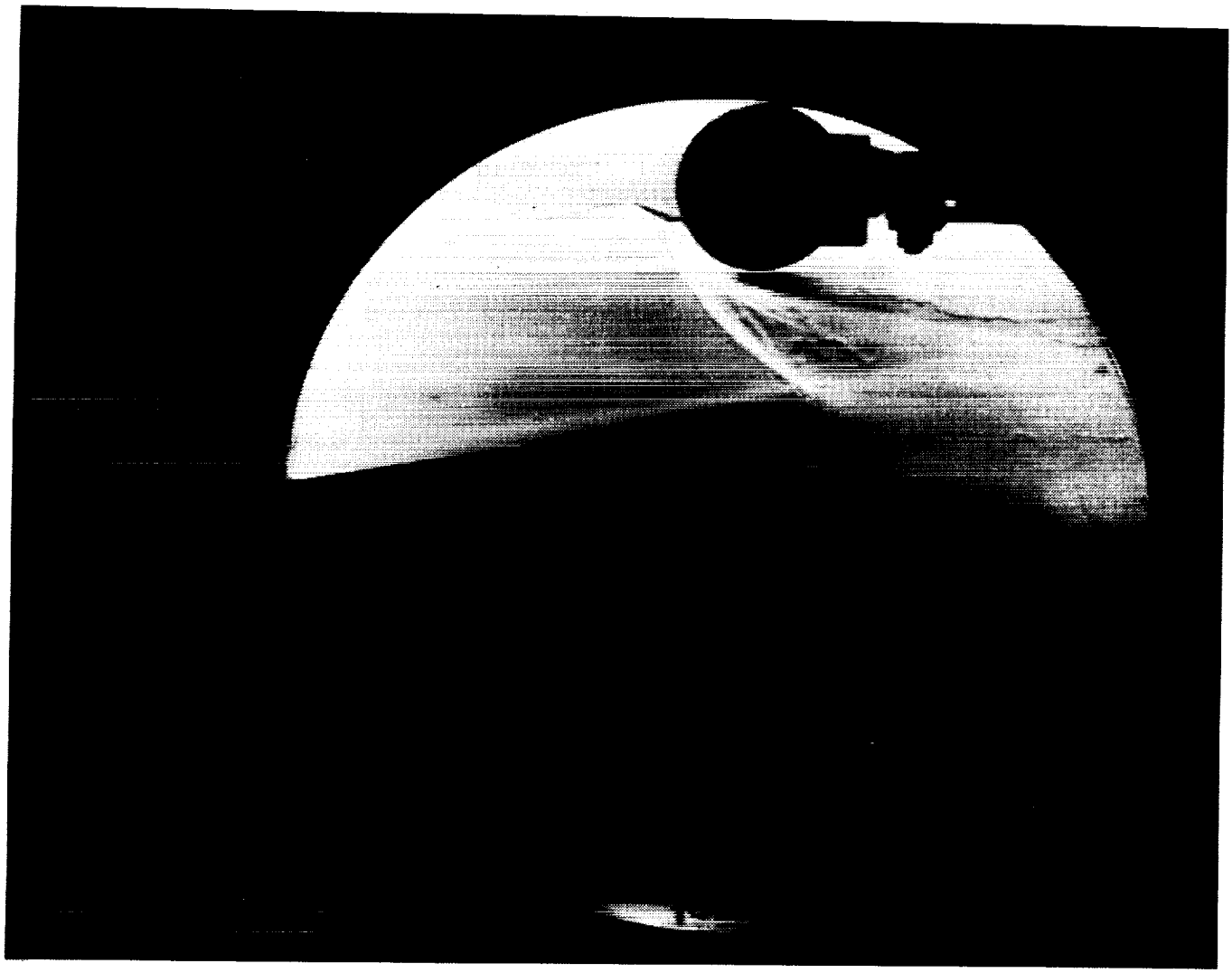

Test Conditions for Run 103 :

Po	= 5.950E+02 PSIA	Reservoir Total Pressure
Ho	= 1.926E+07 (Ft/sec)²	Reservoir Total Enthalpy
To	= 2.912E+03 °R	Reservoir Total Temperature
M	= 1.163E+01	Freestream Mach Number
U	= 6.099E+03 Ft/sec	Freestream Velocity
T	= 1.143E+02 °R	Freestream Temperature
P	= 4.386E-03 PSIA	Freestream Static Pressure
Rho	= 3.219E-06 Slugs/Ft3	Freestream Density
Mu	= 9.615E-08 Slugs/Ft-sec	Freestream Viscosity
Re	= 2.042E+05 1/Ft	Freestream Reynolds Number
Po'	= 7.713E-01 PSIA	Pitot Pressure
Q	= 4.158E-01 PSIA	Dynamic Pressure (½·Rho·U²/144)
Mi	= 3.598E+00	Shock Tube Incident Shock Mach Number
Hw	= 3.183E+06 (Ft/sec)²	Wall Enthalpy (Cp·Tw)
CPf	= 2.405E+00 1/PSIA	Pressure to CP factor (1/Q)
CHf	= 2.464E-03 Ft²-s/BTU	Heat Rate to CH factor (778/(Rho·U·(Ho-Hw))
QoFR	= 1.162E+01 BTU/Ft²-s	Fay-Riddell Heat Transfer to 3" Diam Sphere

Model Configuration Parameter	Value
Stagnation Position (gauge label)	P22
Vertical Distance (inches)	4.15
Horizontal Distance (inches)	-1.40
Plate Angle (degrees)	10.00
Plate Length (inches)	46.25
Sweep Angle (degrees)	0.00

Run 103

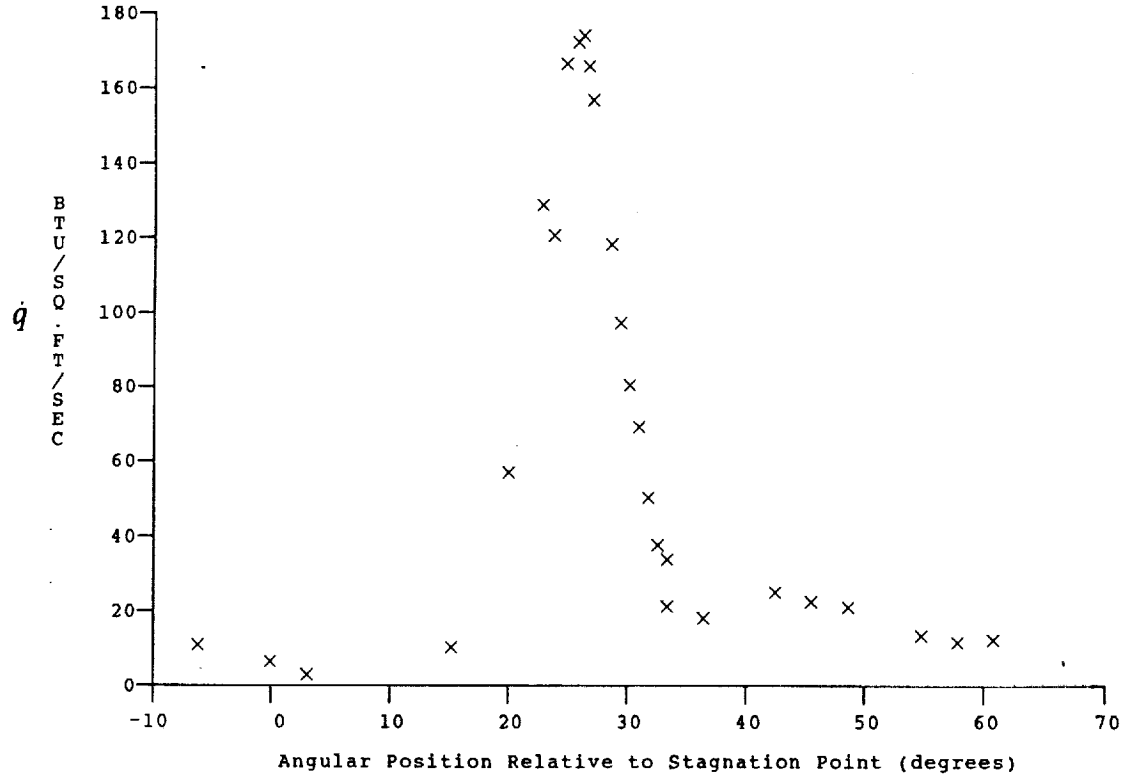

HEAT TRANSFER vs Gauge Position
Run 103

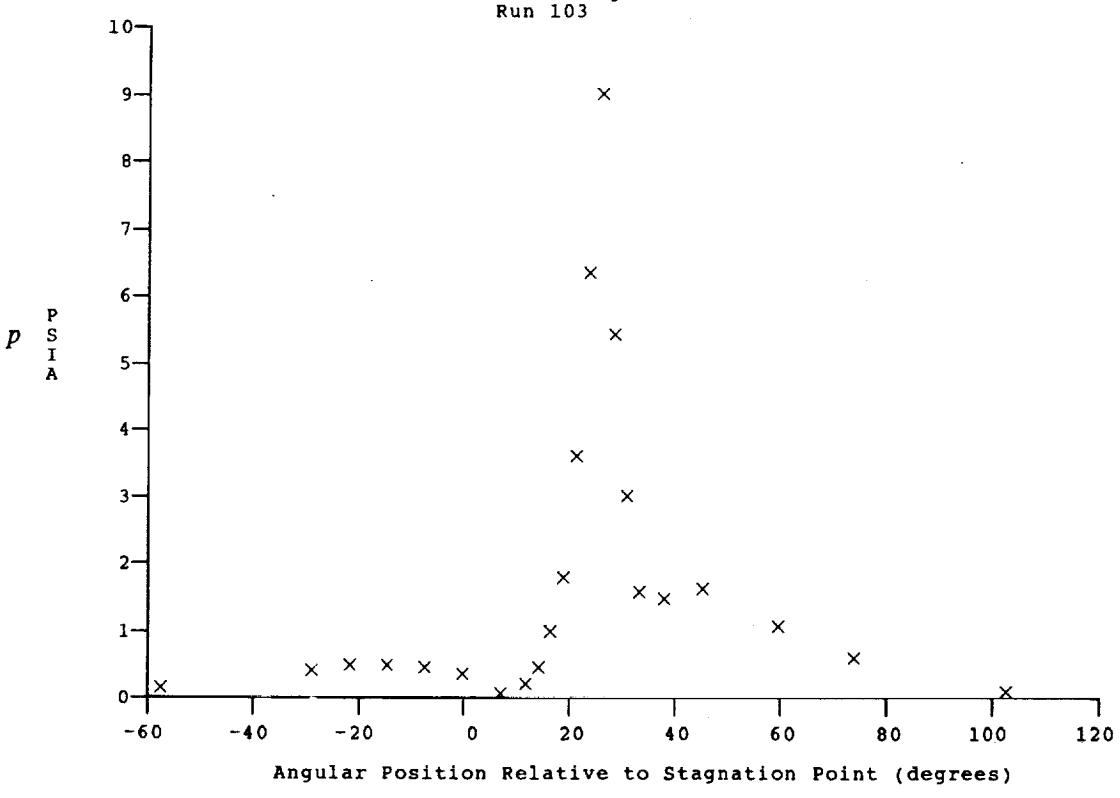

PRESSURE vs Gauge Position
Run 103

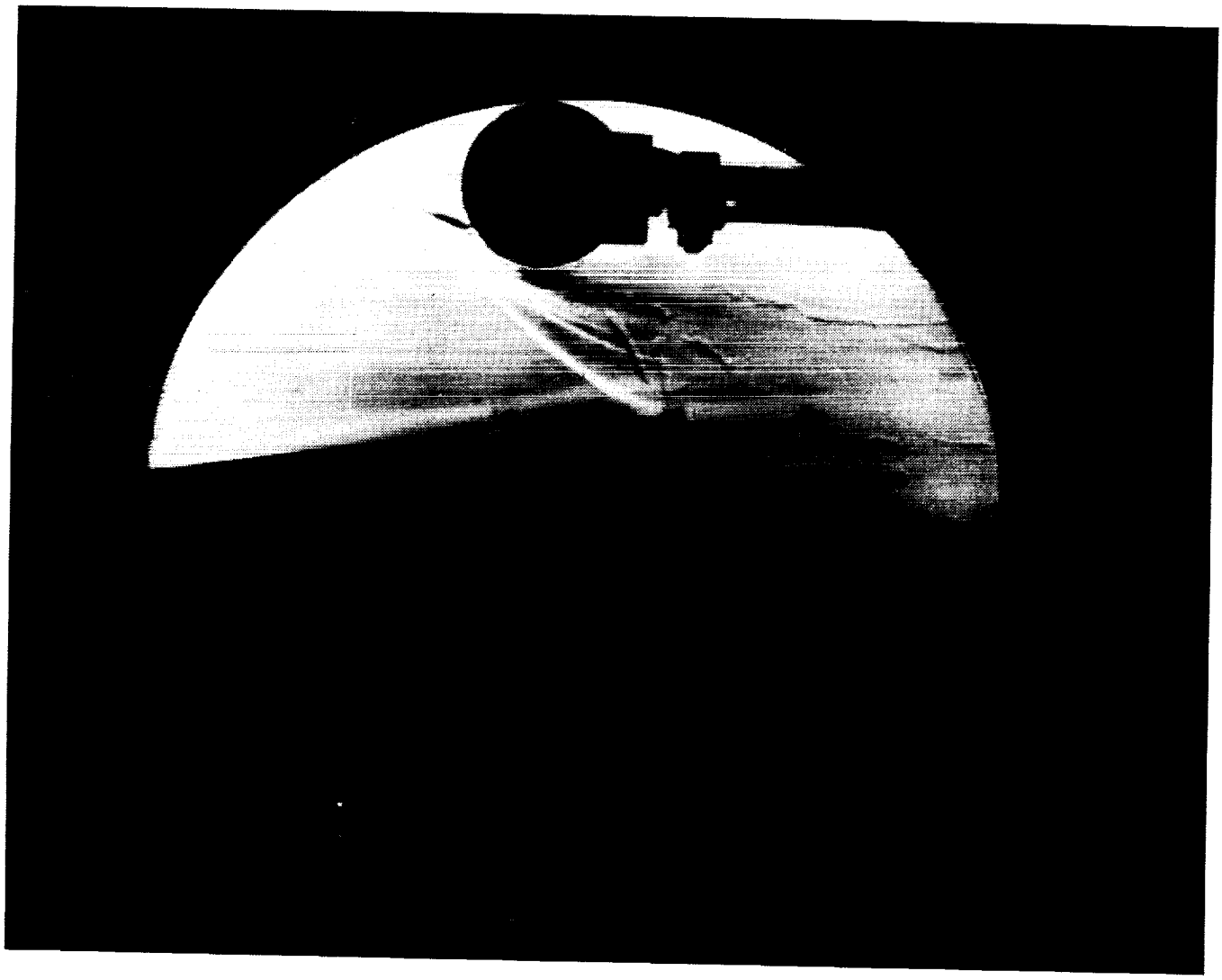

Test Conditions for Run 104 :

Po	= 5.660E+02 PSIA	Reservoir Total Pressure
Ho	= 2.066E+07 (Ft/sec)²	Reservoir Total Enthalpy
To	= 3.101E+03 °R	Reservoir Total Temperature
M	= 1.155E+01	Freestream Mach Number
U	= 6.314E+03 Ft/sec	Freestream Velocity
T	= 1.243E+02 °R	Freestream Temperature
P	= 4.257E-03 PSIA	Freestream Static Pressure
Rho	= 2.875E-06 Slugs/Ft3	Freestream Density
Mu	= 1.044E-07 Slugs/Ft-sec	Freestream Viscosity
Re	= 1.738E+05 1/Ft	Freestream Reynolds Number
Po'	= 7.390E-01 PSIA	Pitot Pressure
Q	= 3.979E-01 PSIA	Dynamic Pressure (½·Rho·U²/144)
Mi	= 3.682E+00	Shock Tube Incident Shock Mach Number
Hw	= 3.183E+06 (Ft/sec)²	Wall Enthalpy (Cp·Tw)
CPf	= 2.513E+00 1/PSIA	Pressure to CP factor (1/Q)
CHf	= 2.453E-03 Ft²-s/BTU	Heat Rate to CH factor (778/(Rho·U·(Ho-Hw))
QoFR	= 1.242E+01 BTU/Ft²-s	Fay Riddell Heat Transfer to 3" Diam Sphere

Model Configuration Parameter	Value
Stagnation Position (gauge label)	P22
Vertical Distance (inches)	4.52
Horizontal Distance (inches)	-0.62
Plate Angle (degrees)	10.00
Plate Length (inches)	44.00
Sweep Angle (degrees)	0.00

Run 104

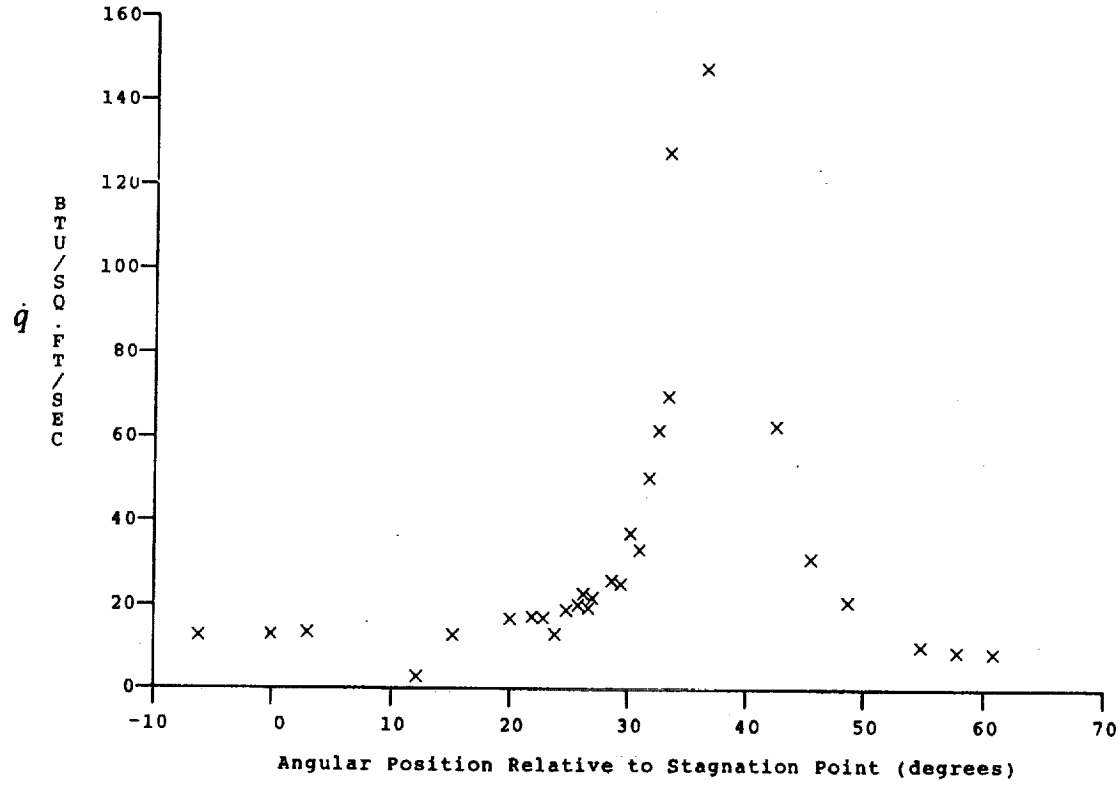

HEAT TRANSFER vs Gauge Position
Run 104

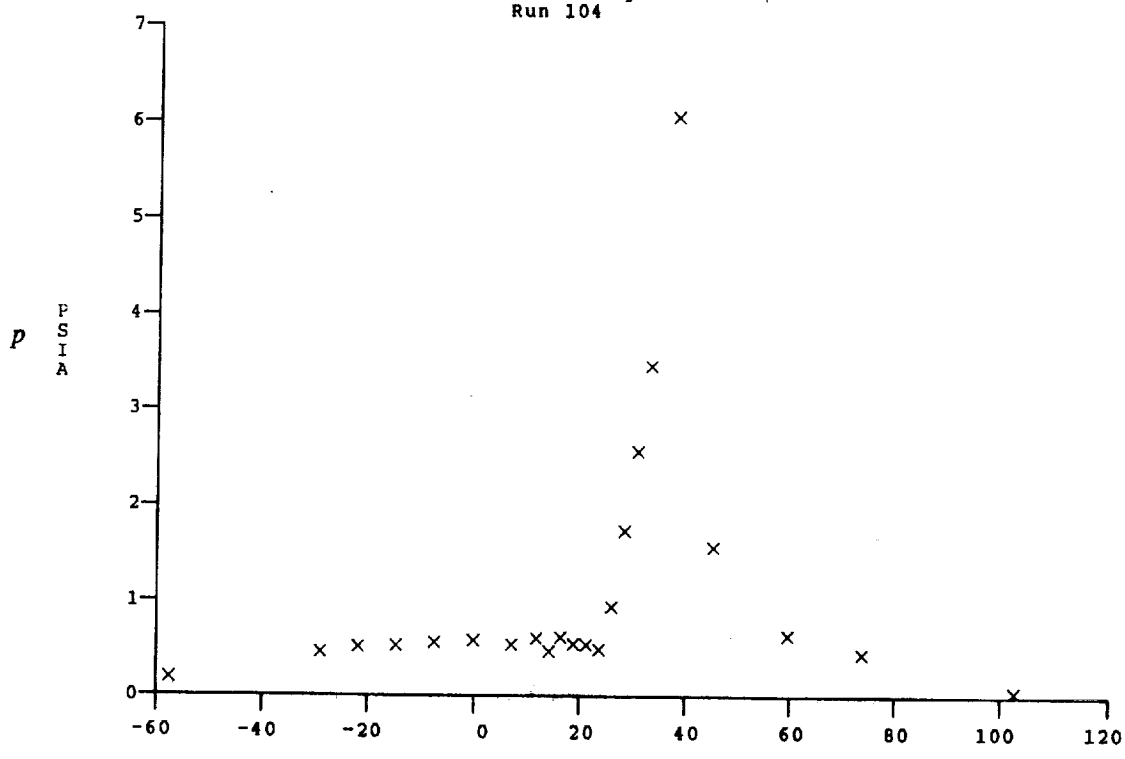

PRESSURE vs Gauge Position
Run 104

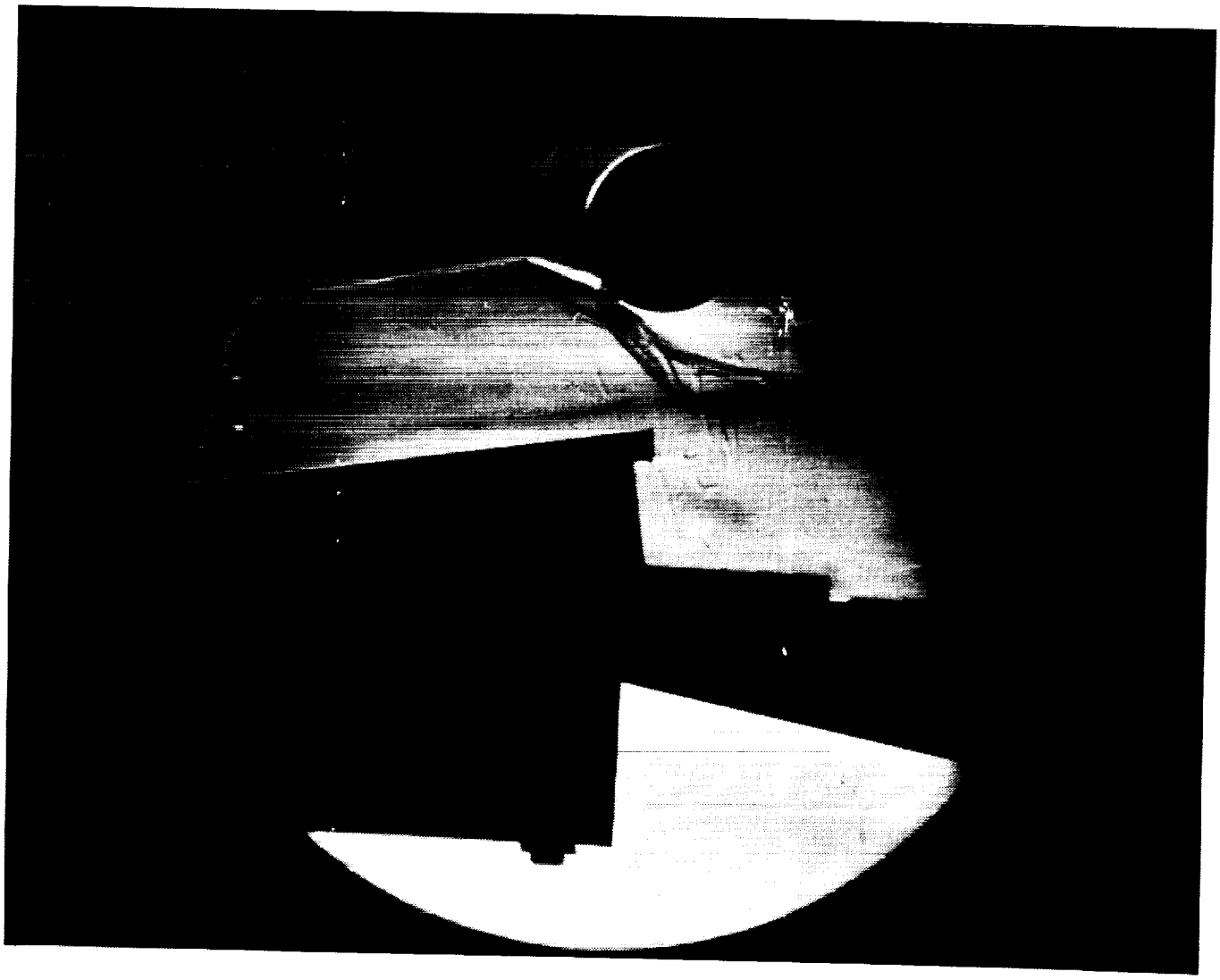

Test Conditions for Run 106 :

Po	= 1.429E-03 PSIA	Reservoir Total Pressure	
Ho	= 2.220E-07 (Ft/sec)²	Reservoir Total Enthalpy	
To	= 3.296E+03 °R	Reservoir Total Temperature	
M	= 1.562E-01	Freestream Mach Number	
U	= 6.600E-03 Ft/sec	Freestream Velocity	
T	= 7.421E-01 °R	Freestream Temperature	
P	= 1.360E-03 PSIA	Freestream Static Pressure	
Rho	= 1.538E-06 Slugs/Ft3	Freestream Density	
Mu	= 6.240E-08 Slugs/Ft-sec	Freestream Viscosity	
Re	= 1.627E+05 1/Ft	Freestream Reynolds Number	
Po'	= 4.327E-01 PSIA	Pitot Pressure	
Q	= 2.327E-01 PSIA	Dynamic Pressure (½·Rho·U²/144)	
Mi	= 3.839E+00	Shock Tube Incident Shock Mach Number	
Hw	= 3.183E+06 (Ft/sec)²	Wall Enthalpy (Cp·Tw)	
CPf	= 4.298E+00 1/PSIA	Pressure to CP factor (1/Q)	
CHf	= 4.029E-03 Ft²-s/BTU	Heat Rate to CH factor (778/(Rho·U·(Ho-Hw))	
QoFR	= 1.039E+01 BTU/Ft²-s	Fay-Riddell Heat Transfer to 3" Diam Sphere	

Model Configuration Parameter	Value
Stagnation Position (gauge label)	P24
Vertical Distance (inches)	3.69
Horizontal Distance (inches)	-1.40
Plate Angle (degrees)	10.00
Plate Length (inches)	46.25
Sweep Angle (degrees)	0.00

Run 106

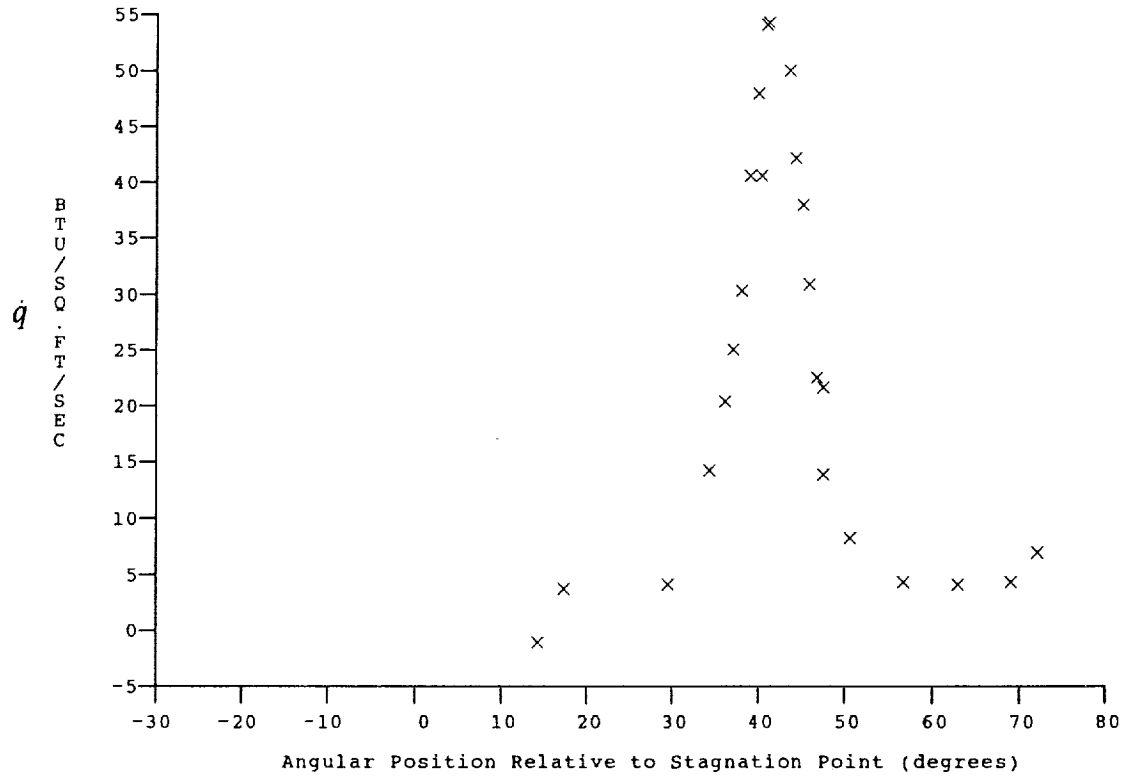

HEAT TRANSFER vs Gauge Position
Run 106

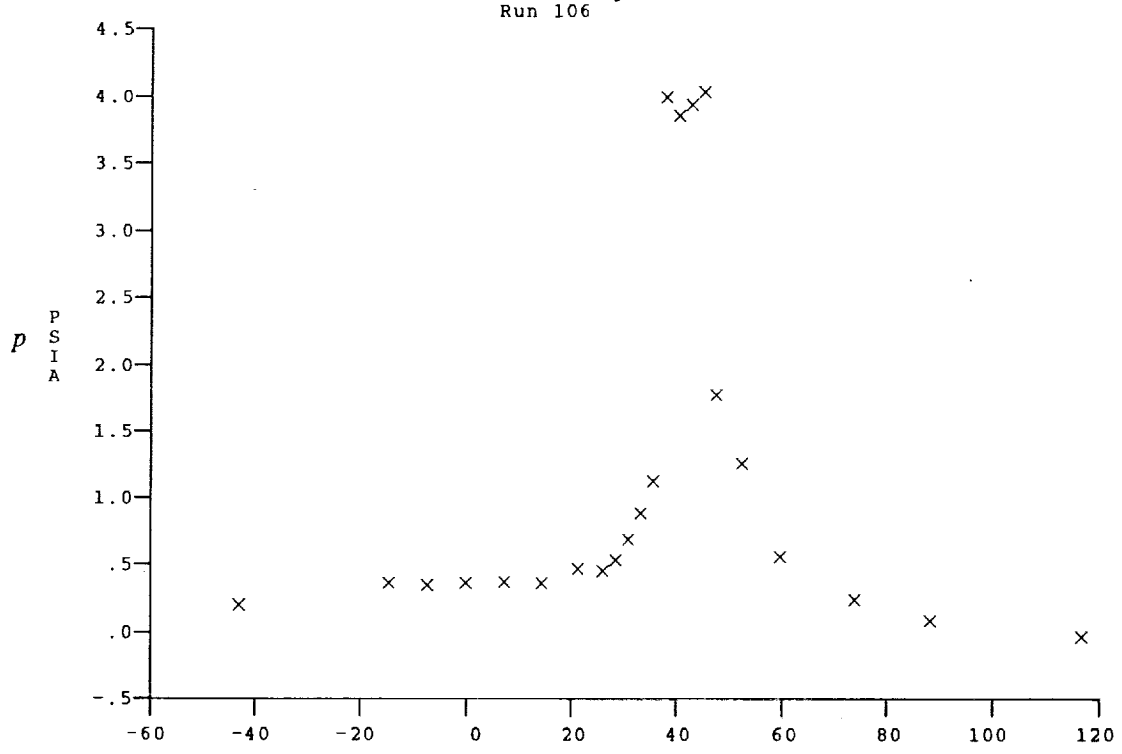

PRESSURE vs Gauge Position
Run 106

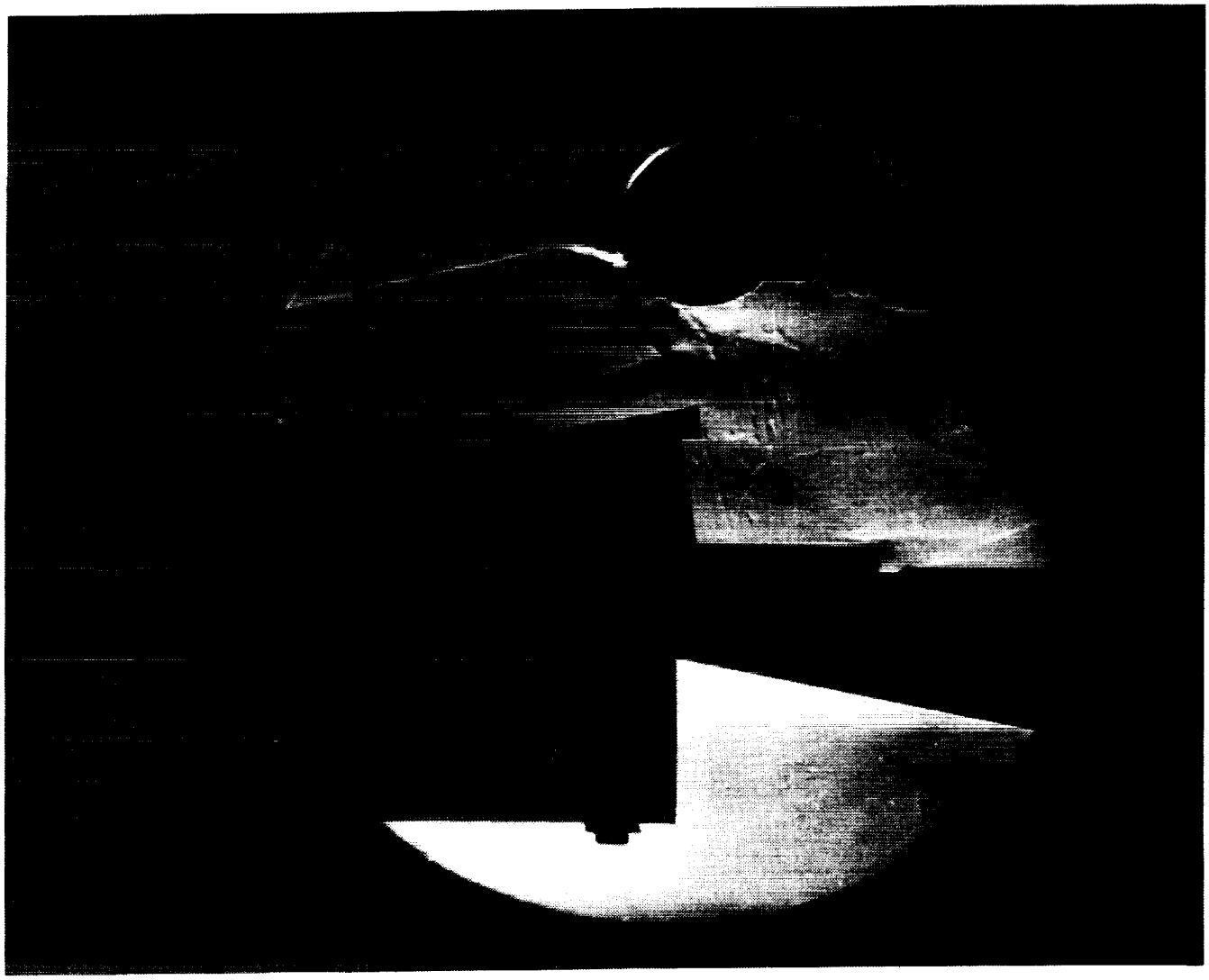

Test Conditions for Run 107 :

Po	= 1.410E+03 PSIA	Reservoir Total Pressure	
Ho	= 2.219E+07 (Ft/sec)²	Reservoir Total Enthalpy	
To	= 3.294E+03 °R	Reservoir Total Temperature	
M	= 1.561E+01	Freestream Mach Number	
U	= 6.598E+03 Ft/sec	Freestream Velocity	
T	= 7.431E+01 °R	Freestream Temperature	
P	= 1.351E-03 PSIA	Freestream Static Pressure	
Rho	= 1.526E-06 Slugs/Ft3	Freestream Density	
Mu	= 6.248E-08 Slugs/Ft-sec	Freestream Viscosity	
Re	= 1.612E+05 1/Ft	Freestream Reynolds Number	
Po'	= 4.291E-01 PSIA	Pitot Pressure	
Q	= 2.307E-01 PSIA	Dynamic Pressure (½·Rho·U²/144)	
Mi	= 3.846E+00	Shock Tube Incident Shock Mach Number	
Hw	= 3.183E+06 (Ft/sec)²	Wall Enthalpy (Cp·Tw)	
CPf	= 4.334E+00 1/PSIA	Pressure to CP factor (1/Q)	
CHf	= 4.064E-03 Ft²-s/BTU	Heat Rate to CH factor (778/(Rho·U·(Ho-Hw))	
QoFR	= 1.034E+01 BTU/Ft²-s	Fay-Riddell Heat Transfer to 3" Diam Sphere	

Model Configuration Parameter	Value
Stagnation Position (gauge label)	P22
Vertical Distance (inches)	3.39
Horizontal Distance (inches)	-1.40
Plate Angle (degrees)	10.00
Plate Length (inches)	46.25
Sweep Angle (degrees)	0.00

Run 107

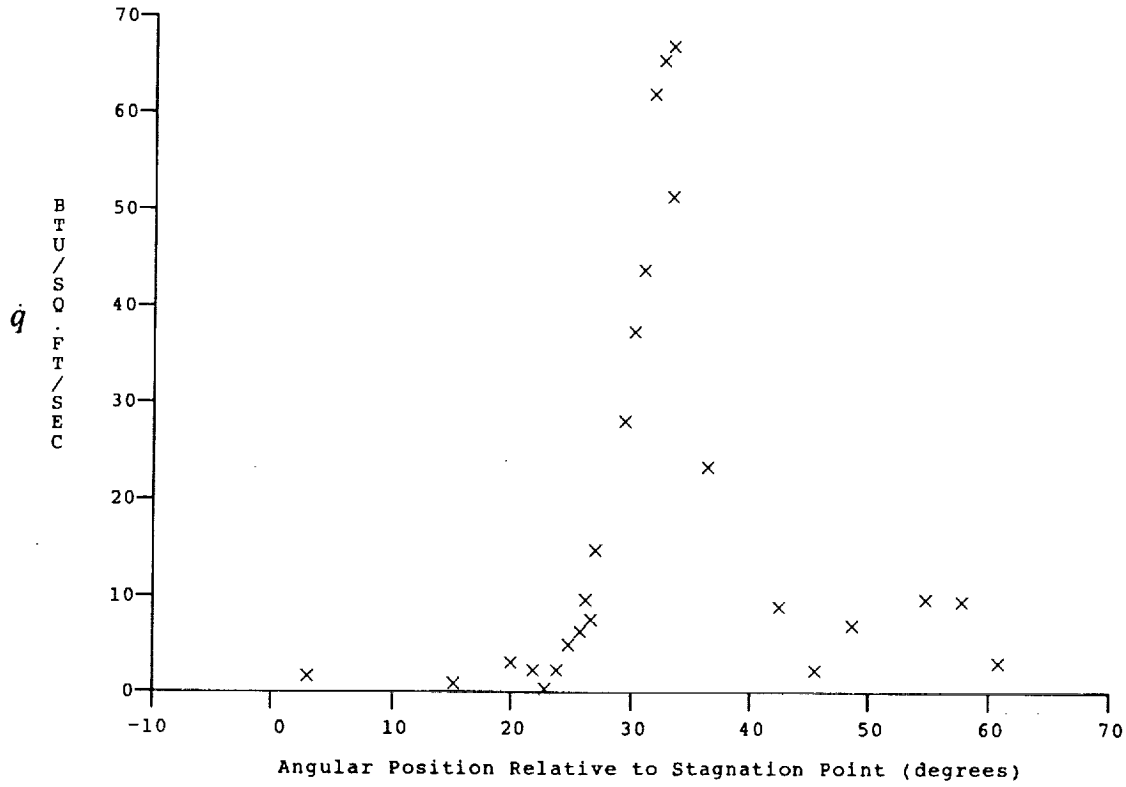

HEAT TRANSFER vs Gauge Position
Run 107

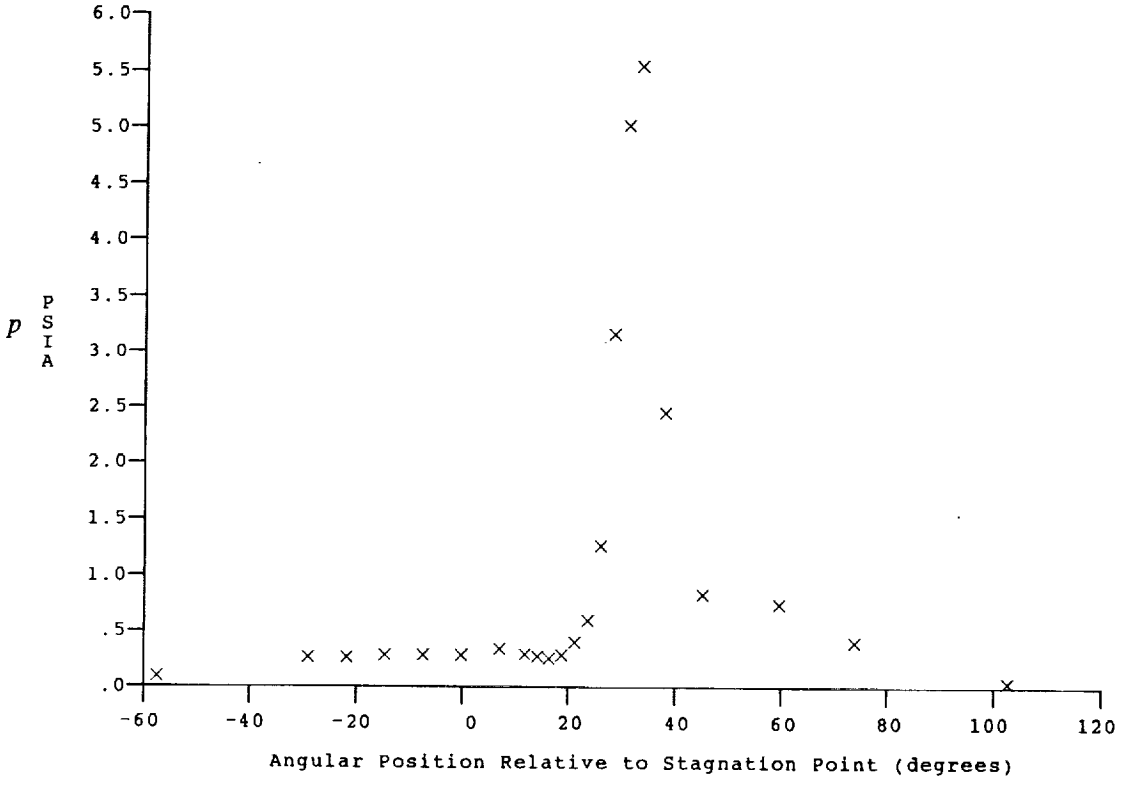

PRESSURE vs Gauge Position
Run 107

Test Conditions

Mi	= 3.8831	
Po	= 1.4150X10+3	PSIA
Ho	= 2.2648X10+7	(Ft/sec)^2
To	= 3.3531X10+3	Degrees R
M	=15.5770	
U	= 6.6654X10+3	Ft/sec
T	= 7.6136X10+1	Degrees R
P	= 1.3633X10-3	PSIA
Q	= 2.3181X10-1	PSIA
Rho	= 1.5027X10-6	Slugs/Ft^3
Mu	= 6.4024X10-8	Slugs/Ft-sec
Re	= 1.5644X10+5	1/Ft
Po'	= 4.3124X10-1	PSIA

Model Configuration Parameter	Value
Stagnation Position (gauge label)	P22
Vertical Distance (inches)	3.30
Horizontal Distance (inches)	-1.40
Plate Angle (degrees)	10.00
Plate Length (inches)	46.25
Sweep Angle (degrees)	0.00

Run 108

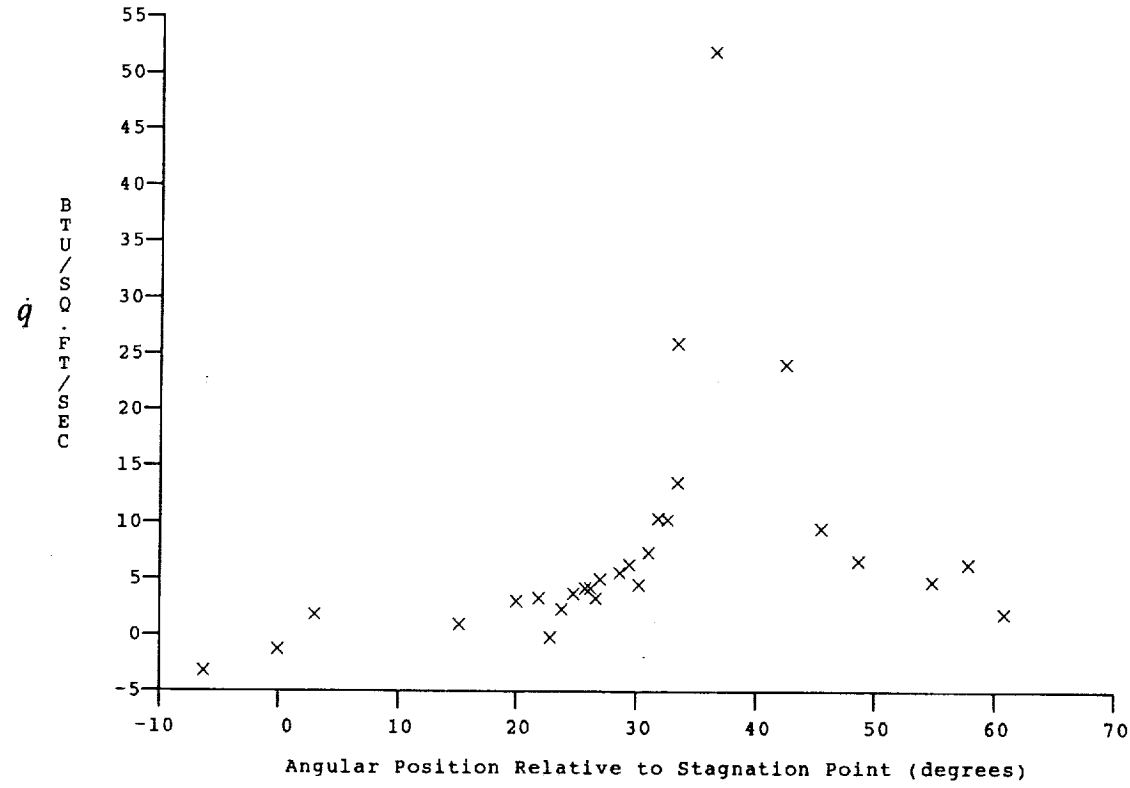

HEAT TRANSFER vs Gauge Position
Run 108

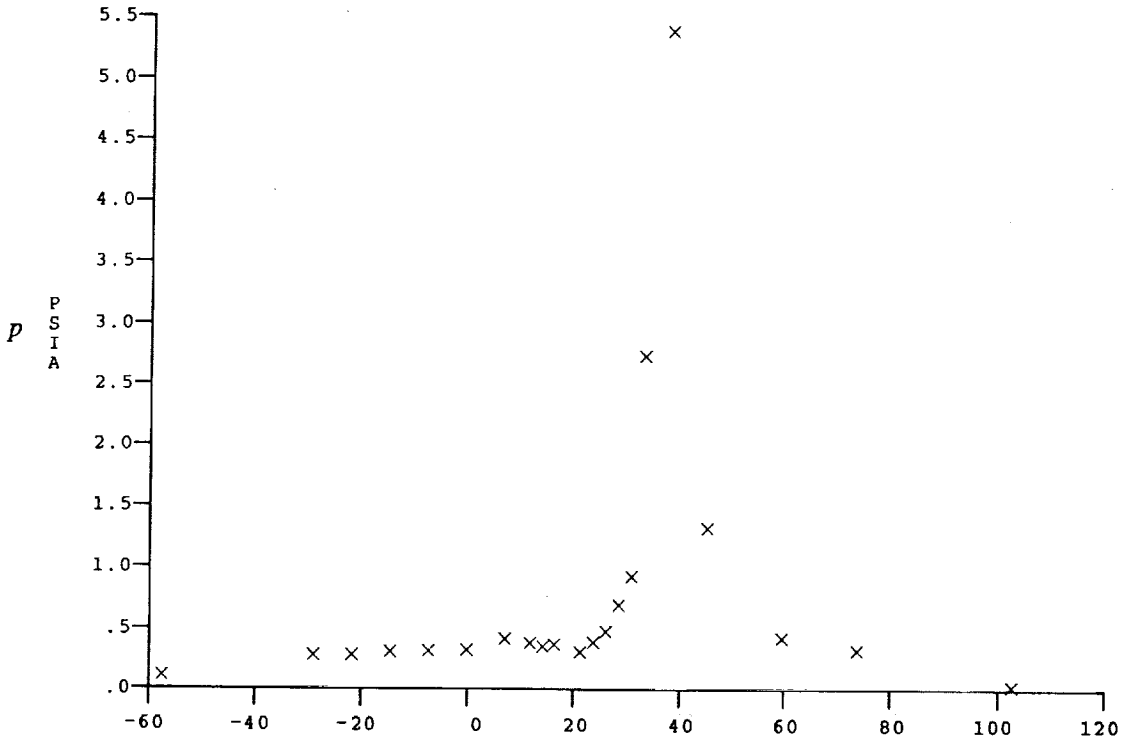

PRESSURE vs Gauge Position
Run 108

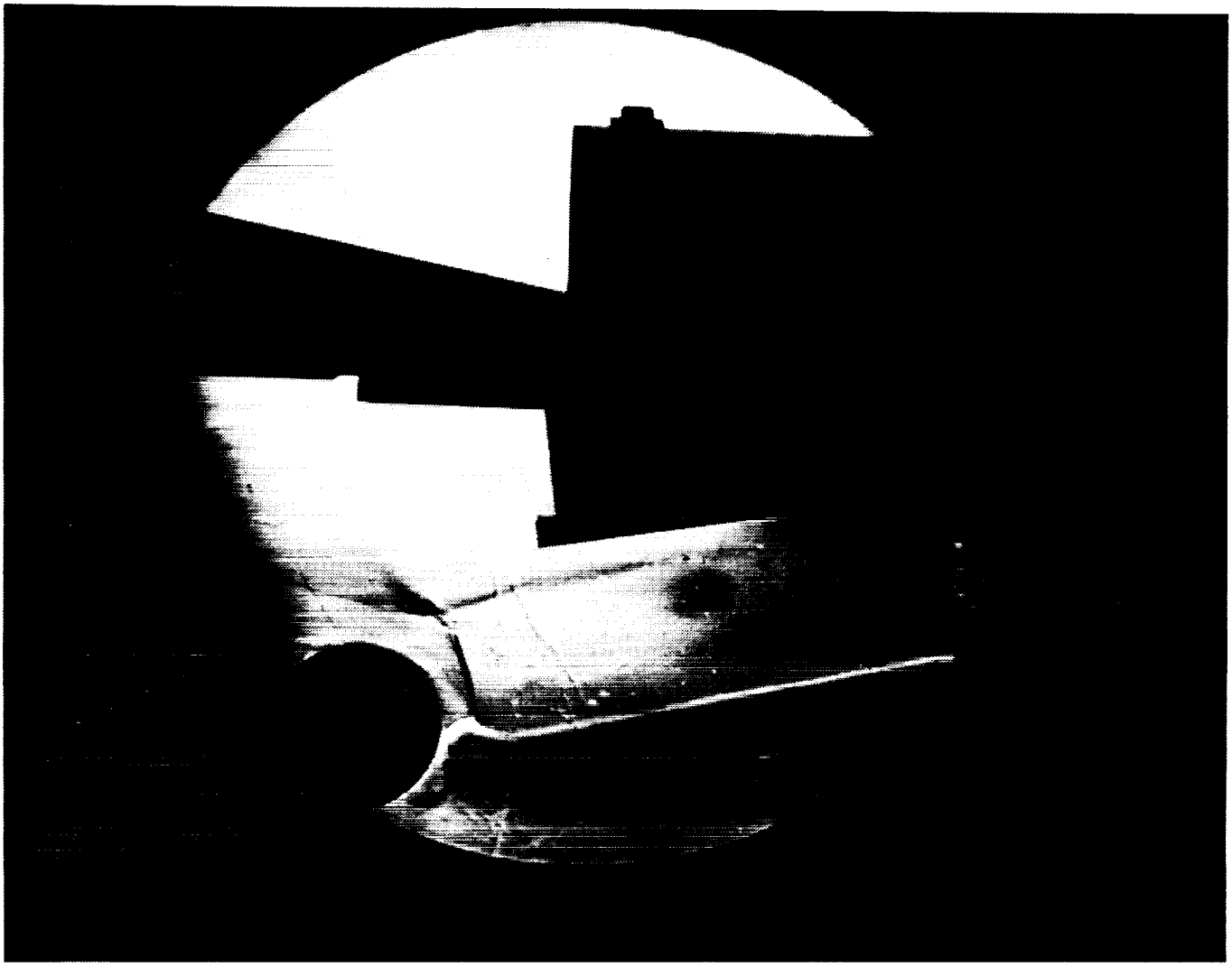

Test Conditions for Run 109 :

Po	= 4.263E-03 PSIA	Reservoir Total Pressure
Ho	= 2.730E+07 (Ft/sec)²	Reservoir Total Enthalpy
To	= 3.925E+03 °R	Reservoir Total Temperature
M	= 1.886E+01	Freestream Mach Number
U	= 7.341E+03 Ft/sec	Freestream Velocity
T	= 6.300E+01 °R	Freestream Temperature
P	= 1.048E-03 PSIA	Freestream Static Pressure
Rho	= 1.397E-06 Slugs/Ft3	Freestream Density
Mu	= 5.294E-08 Slugs/Ft-sec	Freestream Viscosity
Re	= 1.937E+05 1/Ft	Freestream Reynolds Number
Po'	= 4.879E-01 PSIA	Pitot Pressure
Q	= 2.613E-01 PSIA	Dynamic Pressure (½·Rho·U²/144)
Mi	= 4.251E+00	Shock Tube Incident Shock Mach Number
Hw	= 3.183E+06 (Ft/sec)²	Wall Enthalpy (Cp·Tw)
CPf	= 3.827E+00 1/PSIA	Pressure to CP factor (1/Q)
CHf	= 3.147E-03 Ft²-s/BTU	Heat Rate to CH factor (778/(Rho·U·(Ho-Hw))
QoFR	= 1.416E-01 BTU/Ft²-s	Fay-Riddell Heat Transfer to 3" Diam Sphere

Model Configuration Parameter	Value
Stagnation Position (gauge label)	P22
Vertical Distance (inches)	3.42
Horizontal Distance (inches)	1.60
Plate Angle (degrees)	10.00
Plate Length (inches)	46.25
Sweep Angle (degrees)	0.00

Run 109

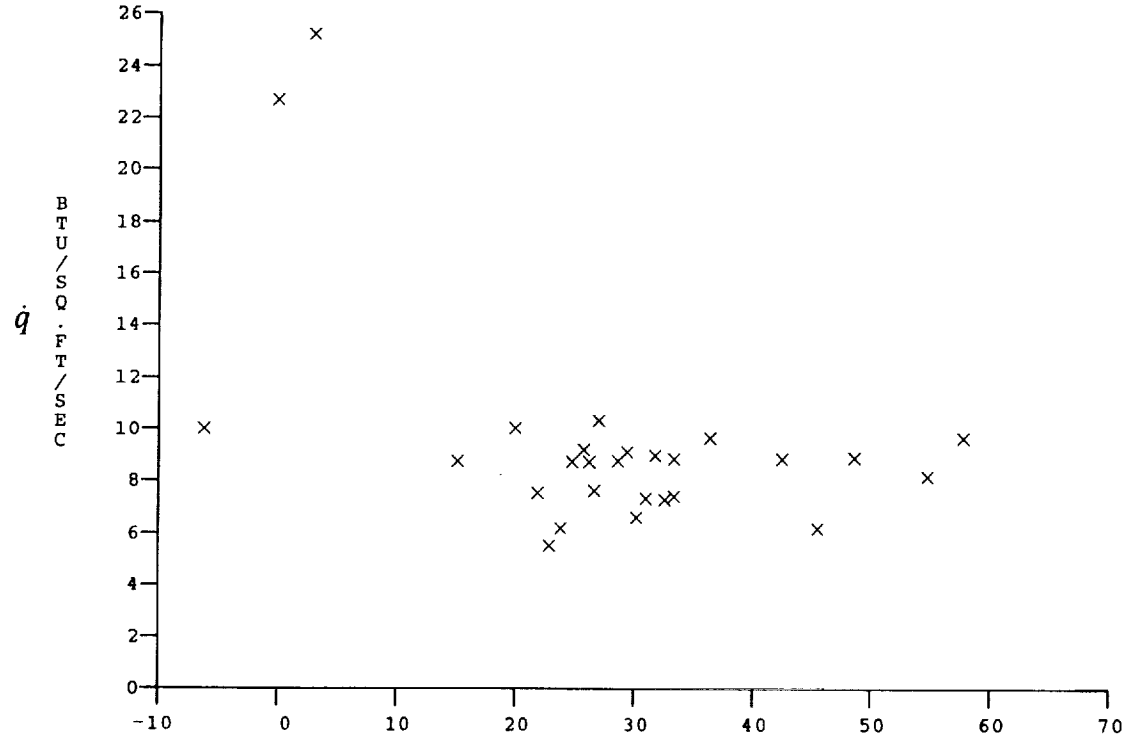

HEAT TRANSFER vs Gauge Position
Run 109

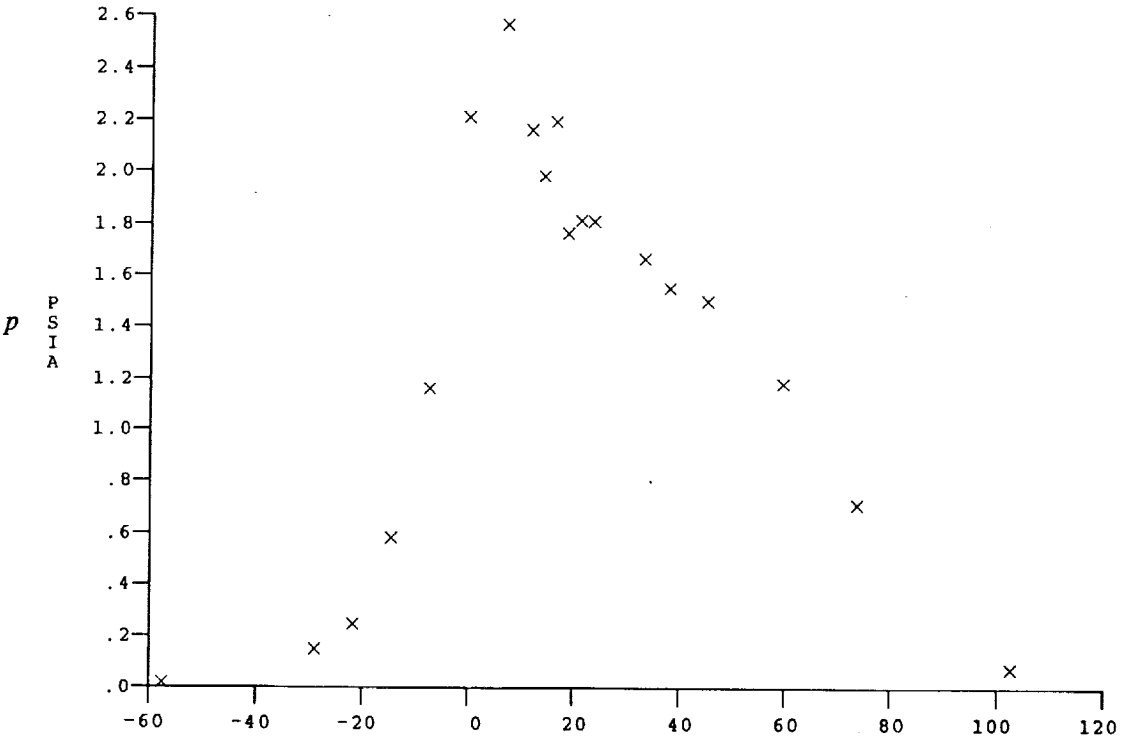

PRESSURE vs Gauge Position
Run 109

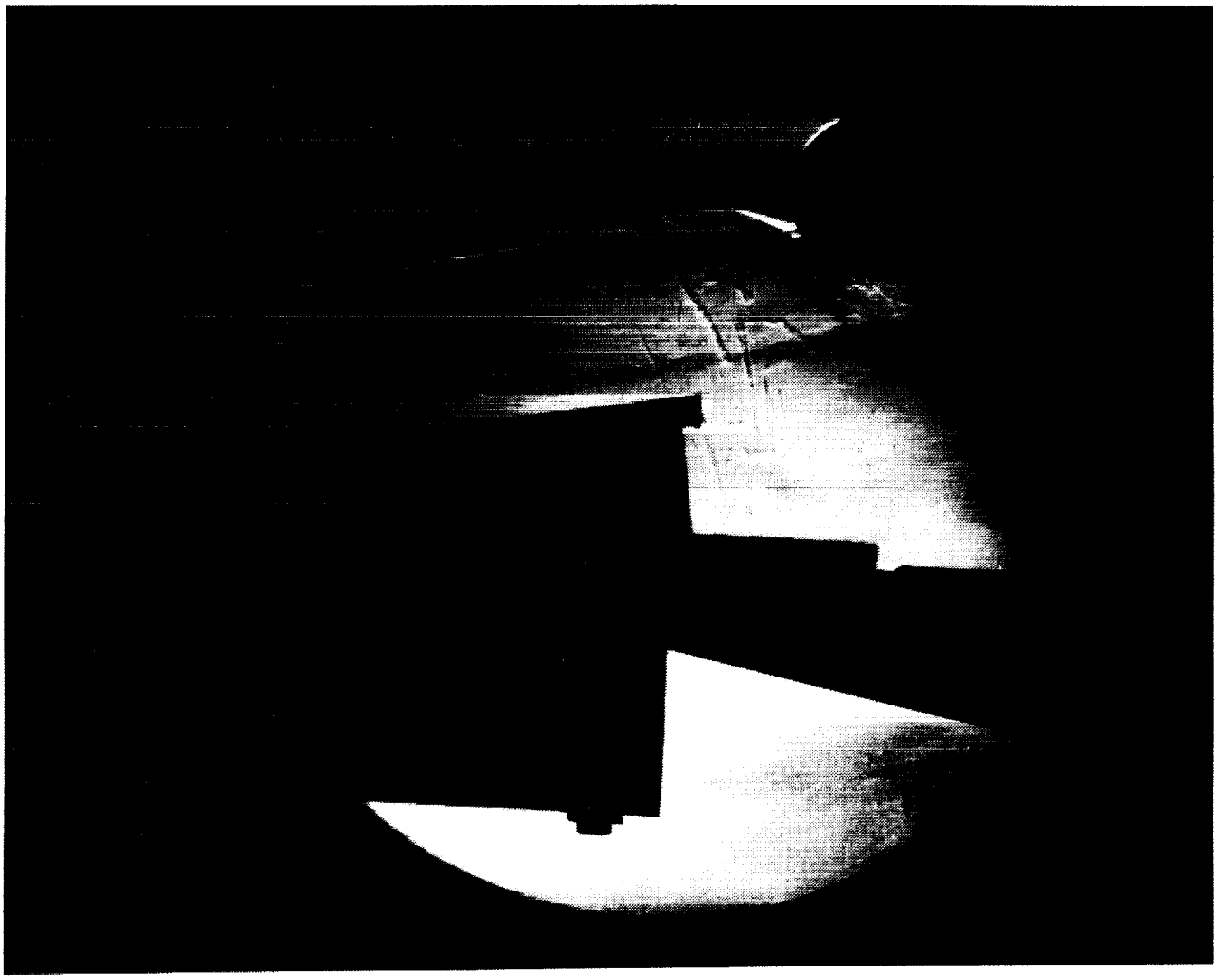

Test Conditions for Run 110 :

Po	= 4.314E-03 PSIA	Reservoir Total Pressure
Ho	= 2.846E-07 (Ft/sec)²	Reservoir Total Enthalpy
To	= 4.070E-03 °R	Reservoir Total Temperature
M	= 1.880E-01	Freestream Mach Number
U	= 7.495E-03 Ft/sec	Freestream Velocity
T	= 6.611E-01 °R	Freestream Temperature
P	= 1.060E-03 PSIA	Freestream Static Pressure
Rho	= 1.345E-06 Slugs/Ft3	Freestream Density
Mu	= 5.556E-08 Slugs/Ft-sec	Freestream Viscosity
Re	= 1.814E+05 1/Ft	Freestream Reynolds Number
Po'	= 4.903E-01 PSIA	Pitot Pressure
Q	= 2.624E-01 PSIA	Dynamic Pressure (½·Rho·U²/144)
Mi	= 4.313E+00	Shock Tube Incident Shock Mach Number
Hw	= 3.183E+06 (Ft/sec)²	Wall Enthalpy (Cp·Tw)
CPf	= 3.811E+00 1/PSIA	Pressure to CP factor (1/Q)
CHf	= 3.053E-03 Ft²-s/BTU	Heat Rate to CH factor (778/(Rho·U·(Ho-Hw))
QoFR	= 1.492E+01 BTU/Ft²-s	Fay-Riddell Heat Transfer to 3" Diam Sphere

Model Configuration Parameter	Value
Stagnation Position (gauge label)	P22
Vertical Distance (inches)	3.85
Horizontal Distance (inches)	1.54
Plate Angle (degrees)	10.00
Plate Length (inches)	46.25
Sweep Angle (degrees)	0.00

Run 110

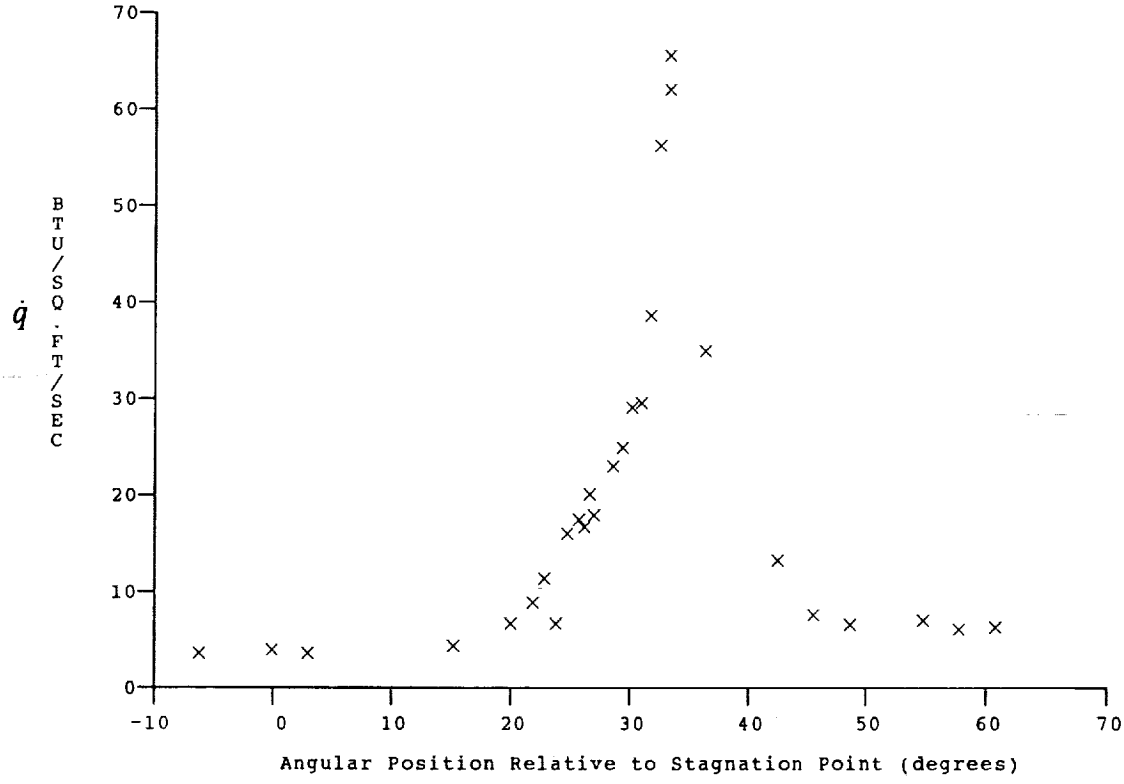

HEAT TRANSFER vs Gauge Position
Run 110

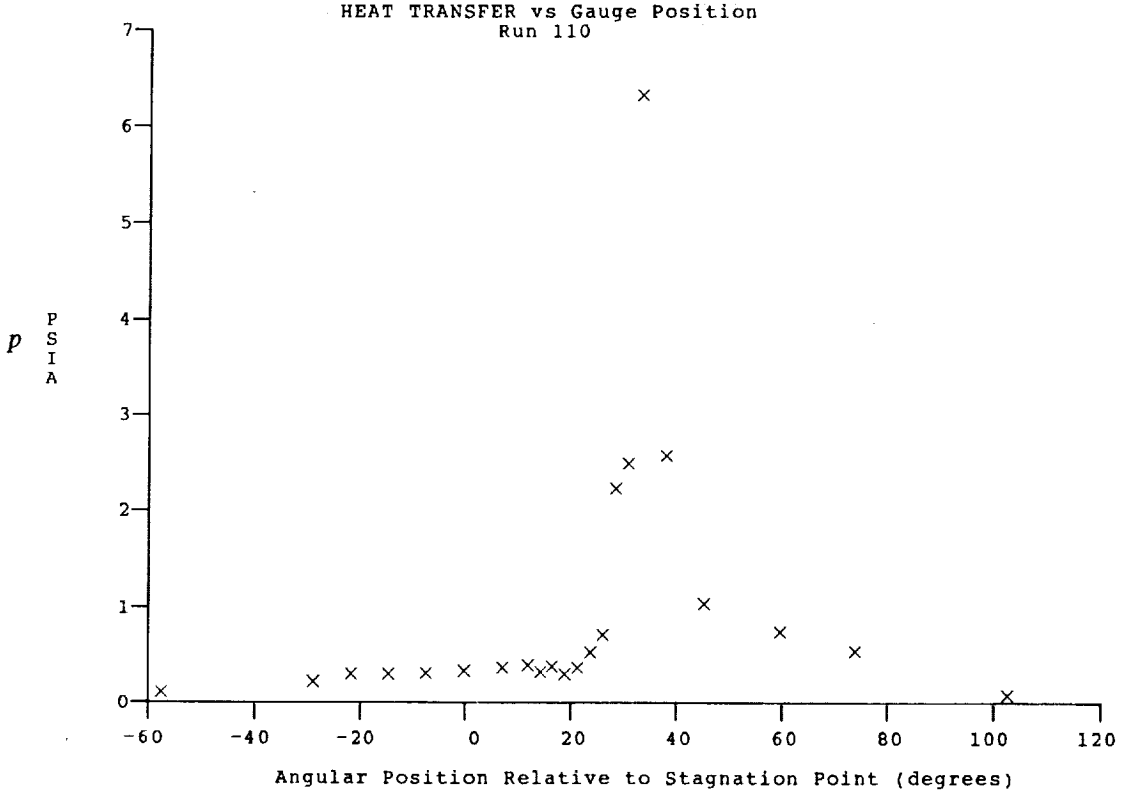

PRESSURE vs Gauge Position
Run 110

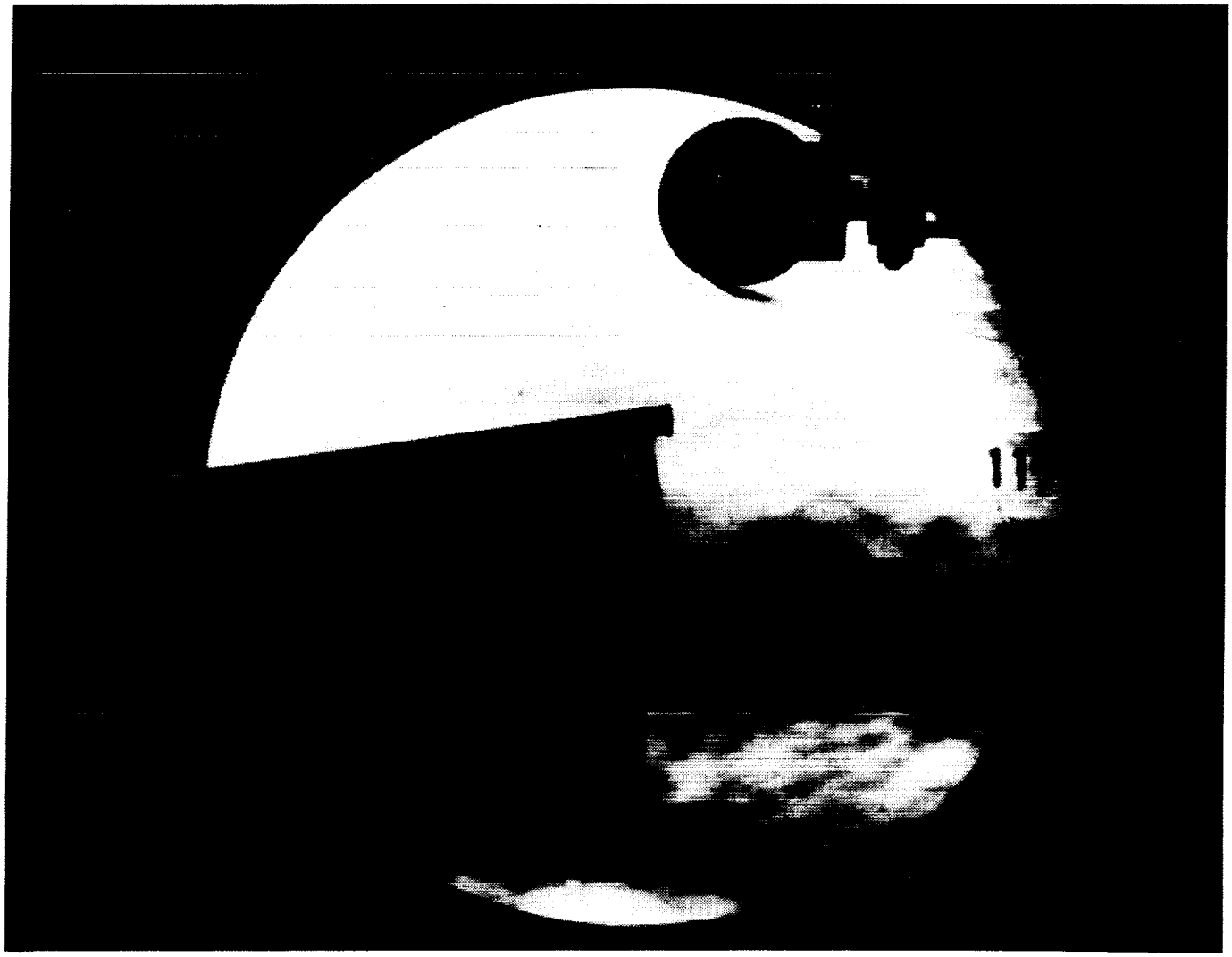

Test Conditions for Run 112 :

Po	= 4.028E-03 PSIA	Reservoir Total Pressure
Ho	= 2.709E-07 (Ft/sec)²	Reservoir Total Enthalpy
To	= 3.901E+03 °R	Reservoir Total Temperature
M	= 1.884E+01	Freestream Mach Number
U	= 7.313E+03 Ft/sec	Freestream Velocity
T	= 6.265E+01 °R	Freestream Temperature
P	= 9.993E-04 PSIA	Freestream Static Pressure
Rho	= 1.339E-06 Slugs/Ft3	Freestream Density
Mu	= 5.264E-08 Slugs/Ft-sec	Freestream Viscosity
Re	= 1.860E+05 1/Ft	Freestream Reynolds Number
Po'	= 4.641E-01 PSIA	Pitot Pressure
Q	= 2.486E-01 PSIA	Dynamic Pressure (½·Rho·U²/144)
Mi	= 4.221E+00	Shock Tube Incident Shock Mach Number
Hw	= 3.183E+06 (Ft/sec)²	Wall Enthalpy (Cp·Tw)
CPf	= 4.022E+00 1/PSIA	Pressure to CP factor (1/Q)
CHf	= 3.324E-03 Ft²-s/BTU	Heat Rate to CH factor (778/(Rho·U·(Ho-Hw))
QoFR	= 1.369E+01 BTU/Ft²-s	Fay-Riddell Heat Transfer to 3" Diam Sphere

Model Configuration Parameter	Value
Stagnation Position (gauge label)	P24
Vertical Distance (inches)	3.75
Horizontal Distance (inches)	-0.34
Plate Angle (degrees)	10.00
Plate Length (inches)	46.25
Sweep Angle (degrees)	0.00

Run 112

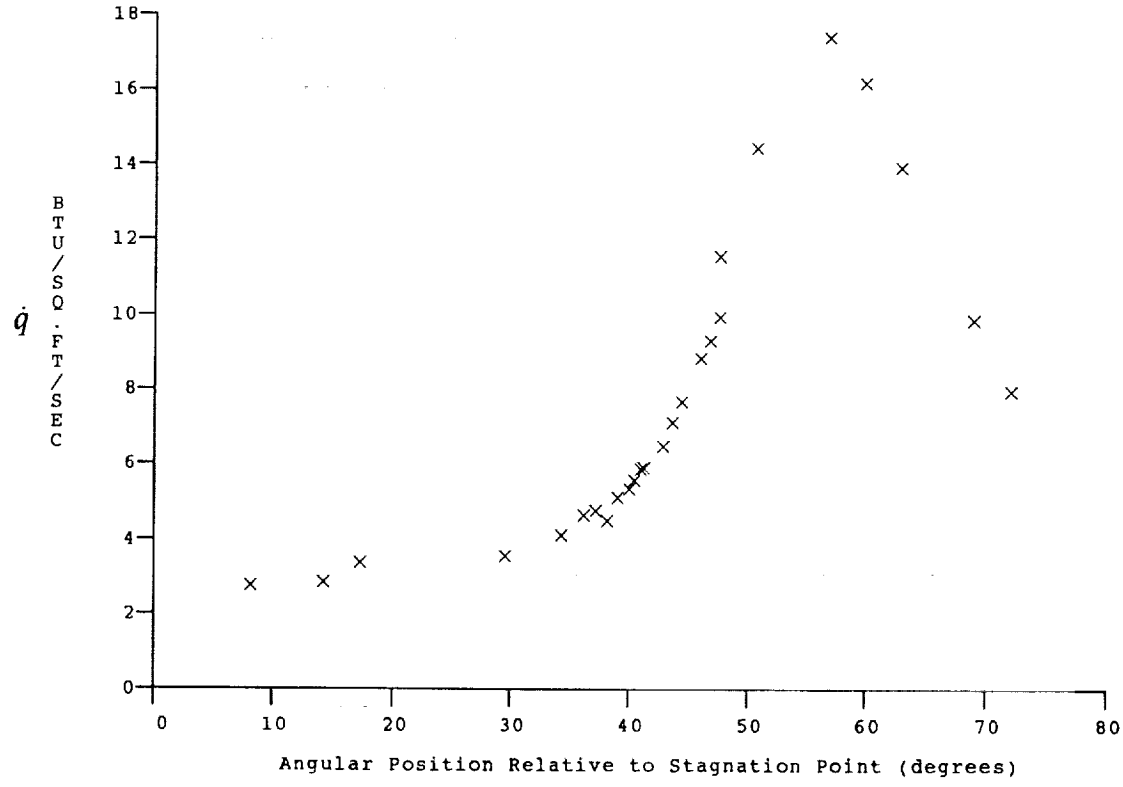

HEAT TRANSFER vs Gauge Position
Run 112

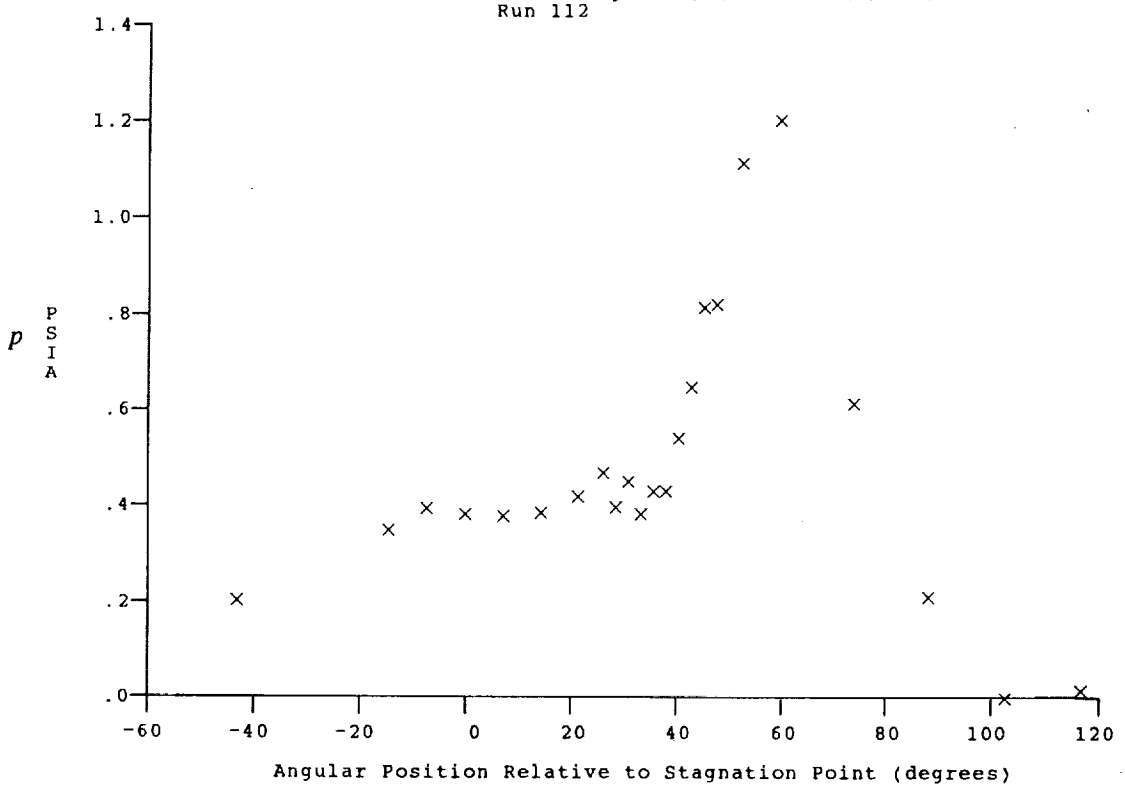

PRESSURE vs Gauge Position
Run 112

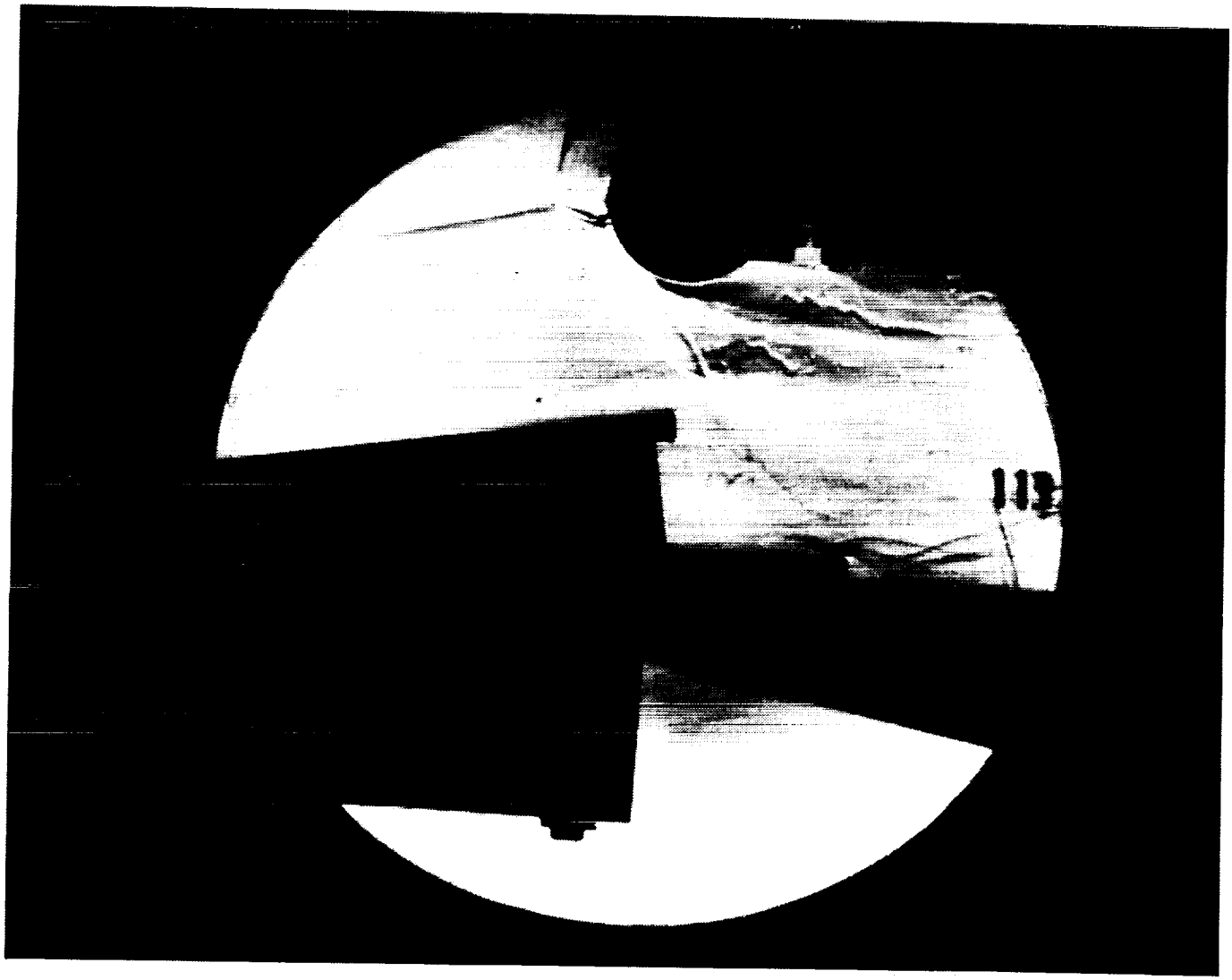

Test Conditions for Run 113 :

Po	= 6.070E-02	PSIA	Reservoir Total Pressure
Ho	= 1.986E-07	(Ft/sec)²	Reservoir Total Enthalpy
To	= 2.996E+03	°R	Reservoir Total Temperature
M	= 1.163E+01		Freestream Mach Number
U	= 6.192E-03	Ft/sec	Freestream Velocity
T	= 1.178E+02	°R	Freestream Temperature
P	= 4.422E-03	PSIA	Freestream Static Pressure
Rho	= 3.150E-06	Slugs/Ft3	Freestream Density
Mu	= 9.907E-08	Slugs/Ft-sec	Freestream Viscosity
Re	= 1.969E+05	1/Ft	Freestream Reynolds Number
Po'	= 7.783E-01	PSIA	Pitot Pressure
Q	= 4.193E-01	PSIA	Dynamic Pressure (½·Rho·U²/144)
Mi	= 3.603E+00		Shock Tube Incident Shock Mach Number
Hw	= 3.183E+06	(Ft/sec)²	Wall Enthalpy (Cp·Tw)
CPf	= 2.385E+00	1/PSIA	Pressure to CP factor (1/Q)
CHf	= 2.392E-03	Ft²-s/BTU	Heat Rate to CH factor (778/(Rho·U·(Ho-Hw))
QoFR	= 1.213E+01	BTU/Ft²-s	Fay-Riddell Heat Transfer to 3" Diam Sphere

Model Configuration Parameter	Value
Stagnation Position (gauge label)	P21
Vertical Distance (inches)	3.94
Horizontal Distance (inches)	-1.40
Plate Angle (degrees)	10.00
Plate Length (inches)	46.25
Sweep Angle (degrees)	0.00

Run 113

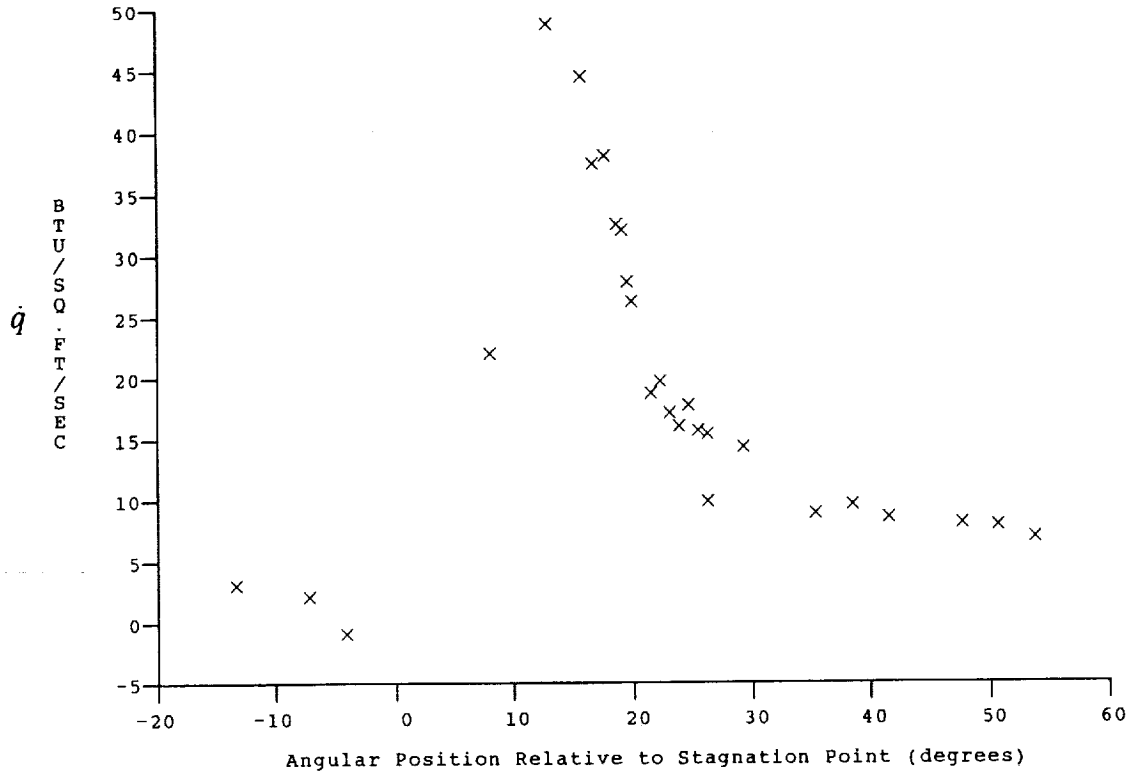

HEAT TRANSFER vs Gauge Position
Run 113

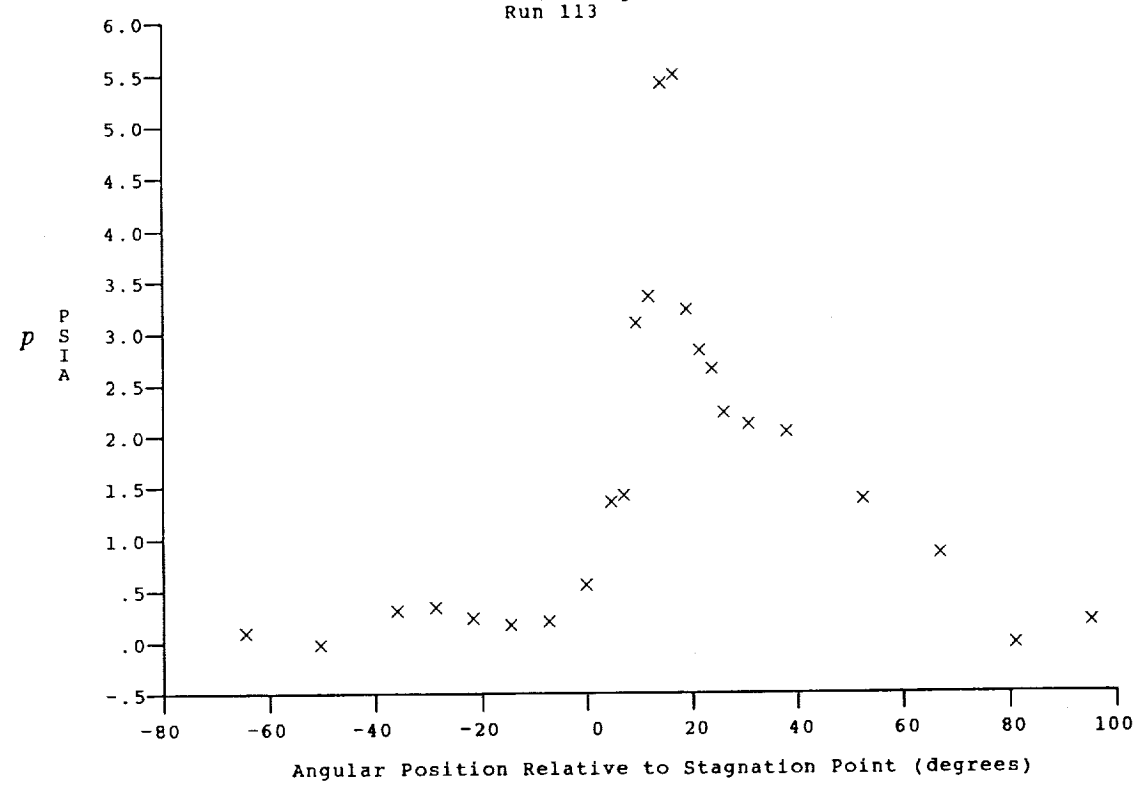

PRESSURE vs Gauge Position
Run 113

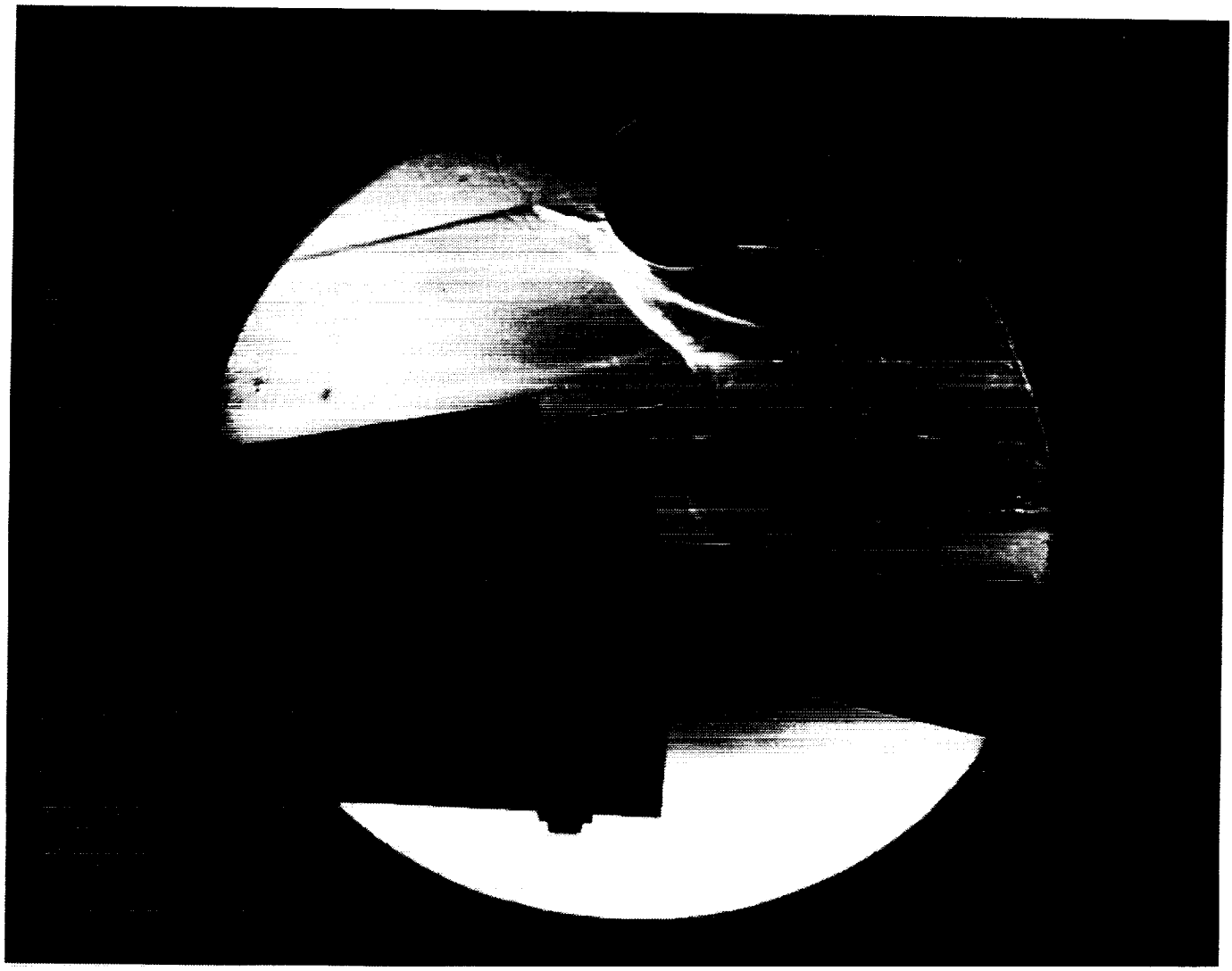

Test Conditions for Run 114 :

Po	= 1.370E+03 PSIA	Reservoir Total Pressure
Ho	= 2.155E+07 (Ft/sec)²	Reservoir Total Enthalpy
To	= 3.213E+03 °R	Reservoir Total Temperature
M	= 1.567E+01	Freestream Mach Number
U	= 6.503E+03 Ft/sec	Freestream Velocity
T	= 7.165E+01 °R	Freestream Temperature
P	= 1.296E-03 PSIA	Freestream Static Pressure
Rho	= 1.518E-06 Slugs/Ft3	Freestream Density
Mu	= 6.024E-08 Slugs/Ft-sec	Freestream Viscosity
Re	= 1.639E+05 1/Ft	Freestream Reynolds Number
Po'	= 4.144E-01 PSIA	Pitot Pressure
Q	= 2.229E-01 PSIA	Dynamic Pressure (½·Rho·U²/144)
Mi	= 3.767E+00	Shock Tube Incident Shock Mach Number
Hw	= 3.183E+06 (Ft/sec)²	Wall Enthalpy (Cp·Tw)
CPf	= 4.485E+00 1/PSIA	Pressure to CP factor (1/Q)
CHf	= 4.289E-03 Ft²-s/BTU	Heat Rate to CH factor (778/(Rho·U·(Ho-Hw))
QoFR	= 9.806E+00 BTU/Ft²-s	Fay-Riddell Heat Transfer to 3" Diam Sphere

Model Configuration Parameter	Value
Stagnation Position (gauge label)	P22
Vertical Distance (inches)	3.99
Horizontal Distance (inches)	1.10
Plate Angle (degrees)	12.50
Plate Length (inches)	44.00
Sweep Angle (degrees)	0.00

Run 114

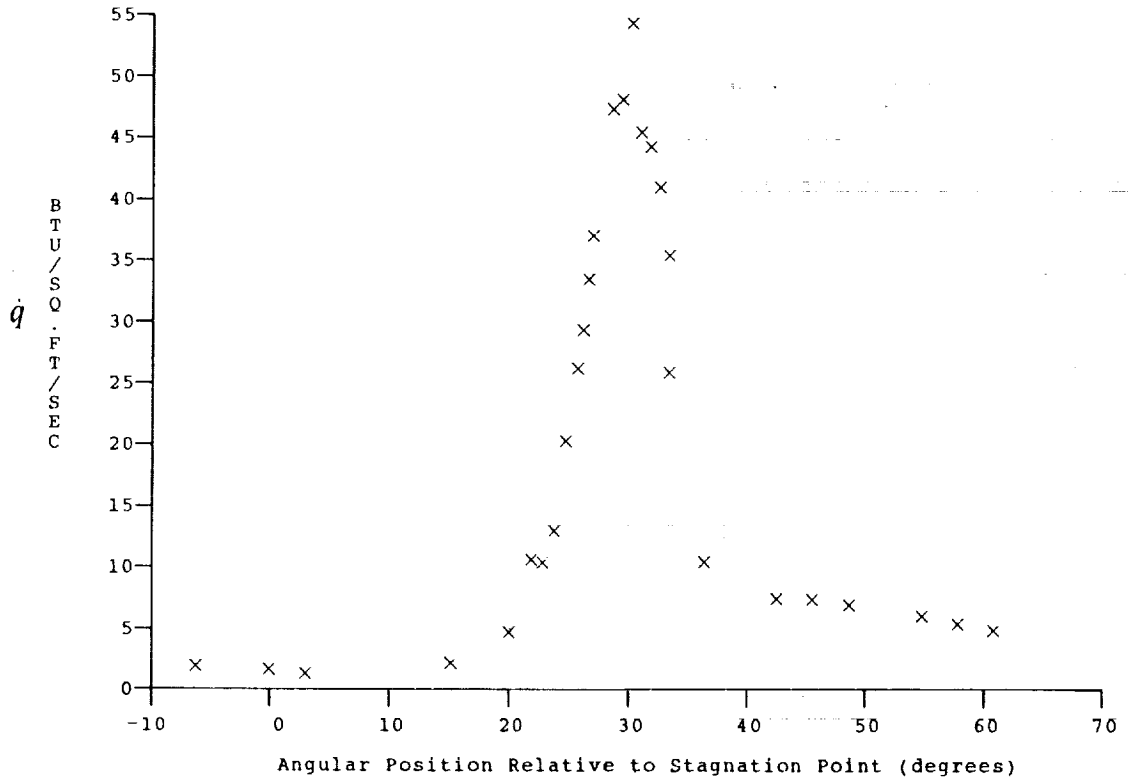

HEAT TRANSFER vs Gauge Position
Run 114

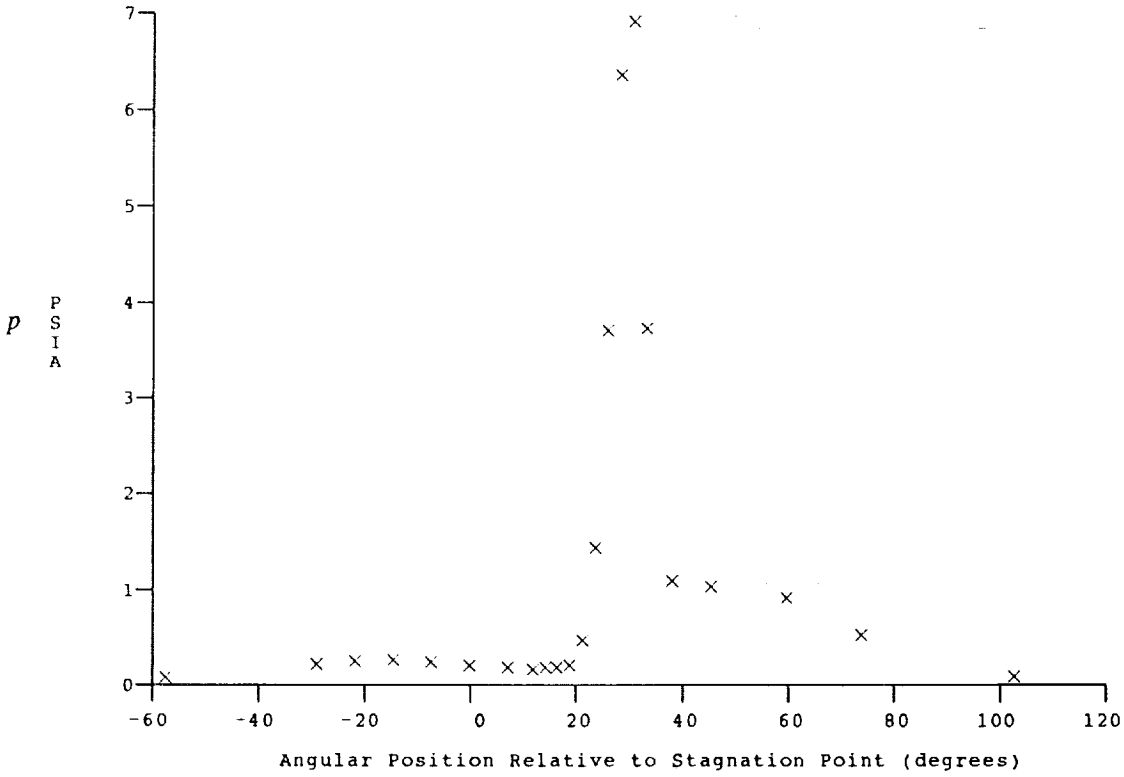

PRESSURE vs Gauge Position
Run 114

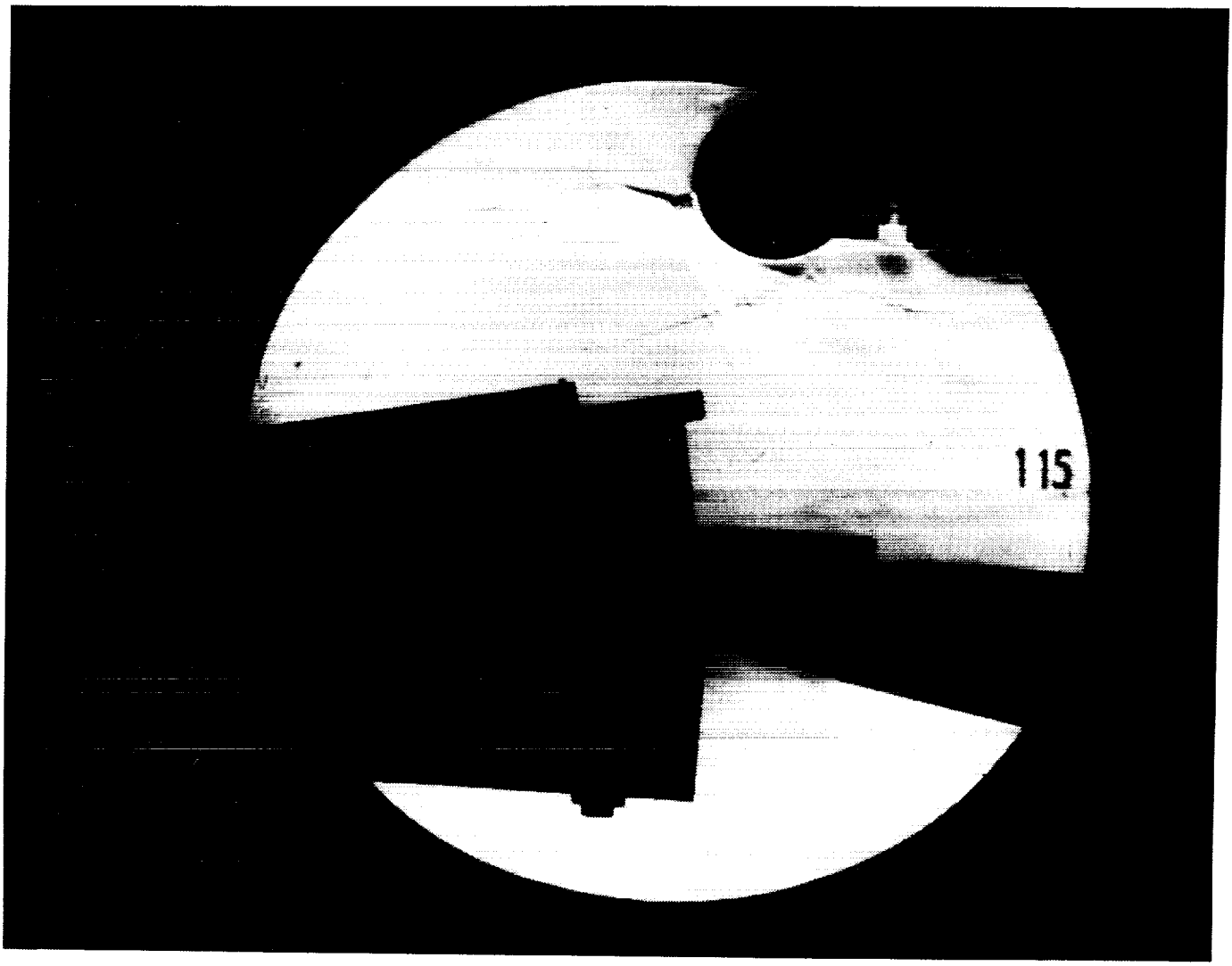

Test Conditions for Run 115 :

Po	= 1.408E+03 PSIA	Reservoir Total Pressure
Ho	= 2.126E+07 (Ft/sec)²	Reservoir Total Enthalpy
To	= 3.173E+03 °R	Reservoir Total Temperature
M	= 1.568E+01	Freestream Mach Number
U	= 6.459E-03 Ft/sec	Freestream Velocity
T	= 7.056E+01 °R	Freestream Temperature
P	= 1.332E-03 PSIA	Freestream Static Pressure
Rho	= 1.584E-06 Slugs/Ft3	Freestream Density
Mu	= 5.932E-08 Slugs/Ft-sec	Freestream Viscosity
Re	= 1.725E+05 1/Ft	Freestream Reynolds Number
Po'	= 4.265E-01 PSIA	Pitot Pressure
Q	= 2.295E-01 PSIA	Dynamic Pressure (½·Rho·U²/144)
Mi	= 3.769E+00	Shock Tube Incident Shock Mach Number
Hw	= 3.183E+06 (Ft/sec)²	Wall Enthalpy (Cp·Tw)
CPf	= 4.357E+00 1/PSIA	Pressure to CP factor (1/Q)
CHf	= 4.205E-03 Ft²-s/BTU	Heat Rate to CH factor (778/(Rho·U·(Ho-Hw))
QoFR	= 9.781E+00 BTU/Ft²-s	Fay-Riddell Heat Transfer to 3" Diam Sphere

Model Configuration Parameter	Value
Stagnation Position (gauge label)	P21
Vertical Distance (inches)	3.93
Horizontal Distance (inches)	2.10
Plate Angle (degrees)	12.50
Plate Length (inches)	44.00
Sweep Angle (degrees)	0.00

Run 115

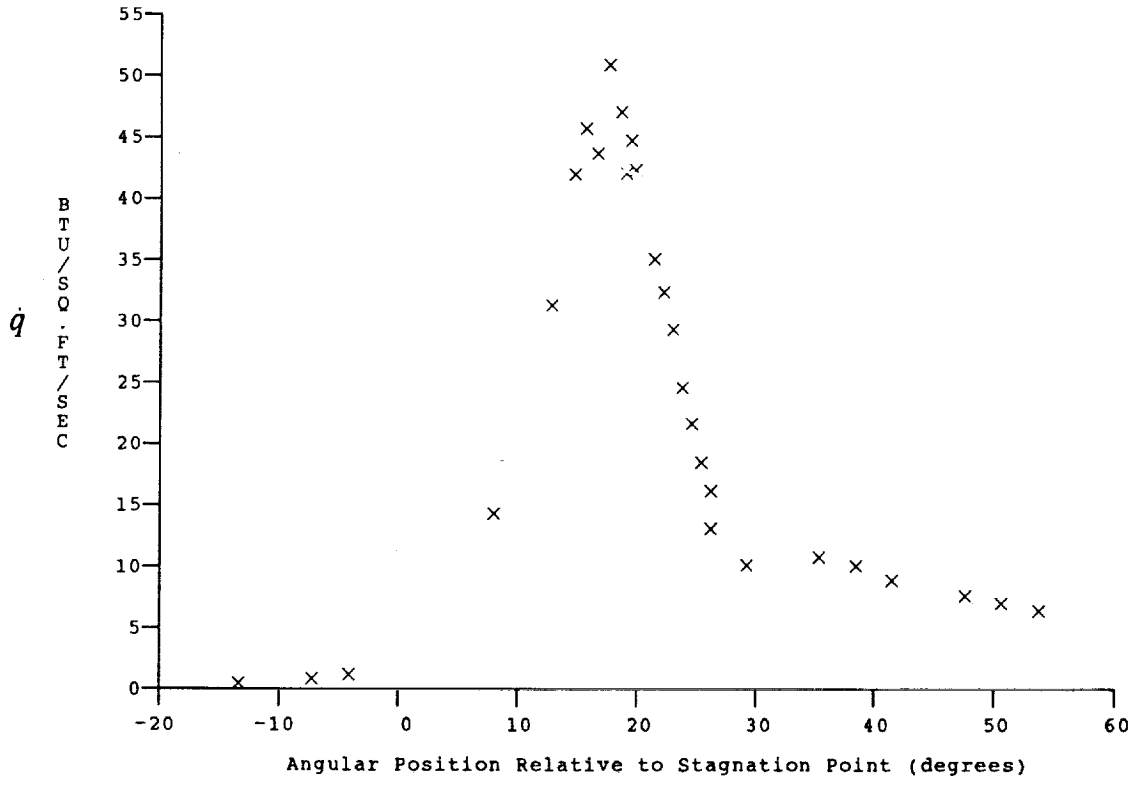

HEAT TRANSFER vs Gauge Position
Run 115

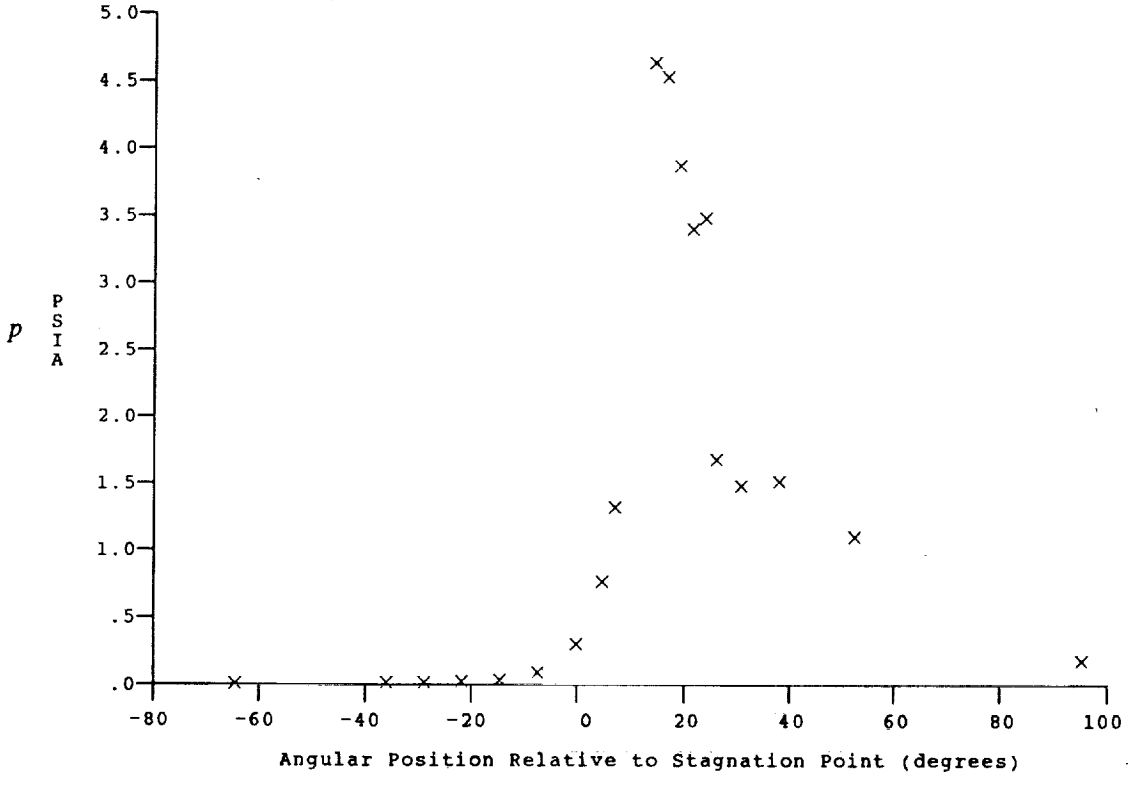

PRESSURE vs Gauge Position
Run 115

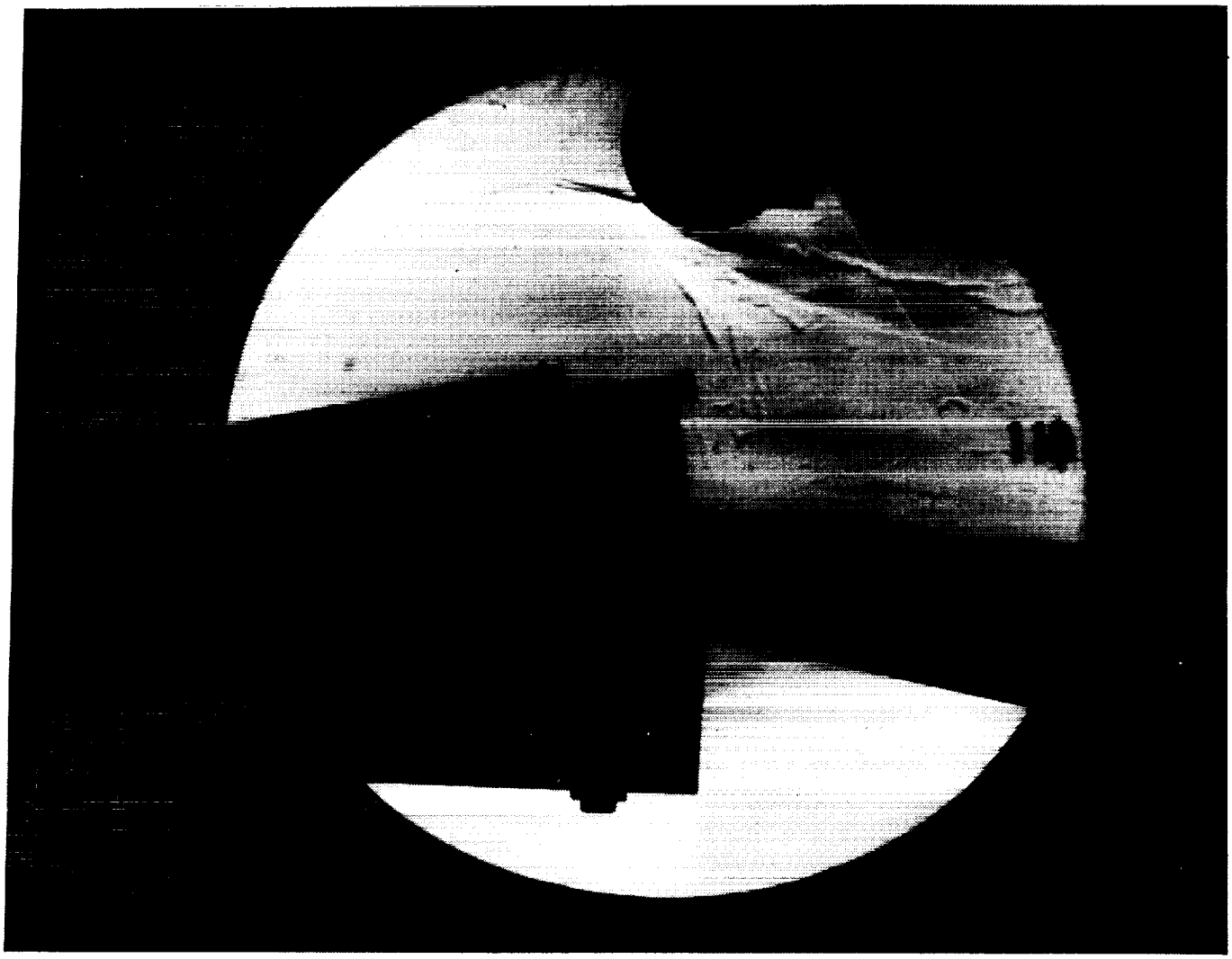

Test Conditions for Run 116 :

Po	= 4.184E+03	PSIA	Reservoir Total Pressure
Ho	= 2.564E+07	(Ft/sec)²	Reservoir Total Enthalpy
To	= 3.713E+03	°R	Reservoir Total Temperature
M	= 1.892E+01		Freestream Mach Number
U	= 7.115E+03	Ft/sec	Freestream Velocity
T	= 5.881E+01	°R	Freestream Temperature
P	= 1.041E-03	PSIA	Freestream Static Pressure
Rho	= 1.485E-06	Slugs/Ft3	Freestream Density
Mu	= 4.940E-08	Slugs/Ft-sec	Freestream Viscosity
Re	= 2.140E+05	1/Ft	Freestream Reynolds Number
Po'	= 4.870E-01	PSIA	Pitot Pressure
Q	= 2.612E-01	PSIA	Dynamic Pressure (½·Rho·U²/144)
Mi	= 4.185E+00		Shock Tube Incident Shock Mach Number
Hw	= 3.183E+06	(Ft/sec)²	Wall Enthalpy (Cp·Tw)
CPf	= 3.829E+00	1/PSIA	Pressure to CP factor (1/Q)
CHf	= 3.277E-03	Ft²-s/BTU	Heat Rate to CH factor (778/(Rho·U·(Ho-Hw))
QoFR	= 1.313E+01	BTU/Ft²-s	Fay-Riddell Heat Transfer to 3" Diam Sphere

Model Configuration Parameter	Value
Stagnation Position (gauge label)	P21
Vertical Distance (inches)	3.99
Horizontal Distance (inches)	1.10
Plate Angle (degrees)	12.50
Plate Length (inches)	44.00
Sweep Angle (degrees)	0.00

Run 116

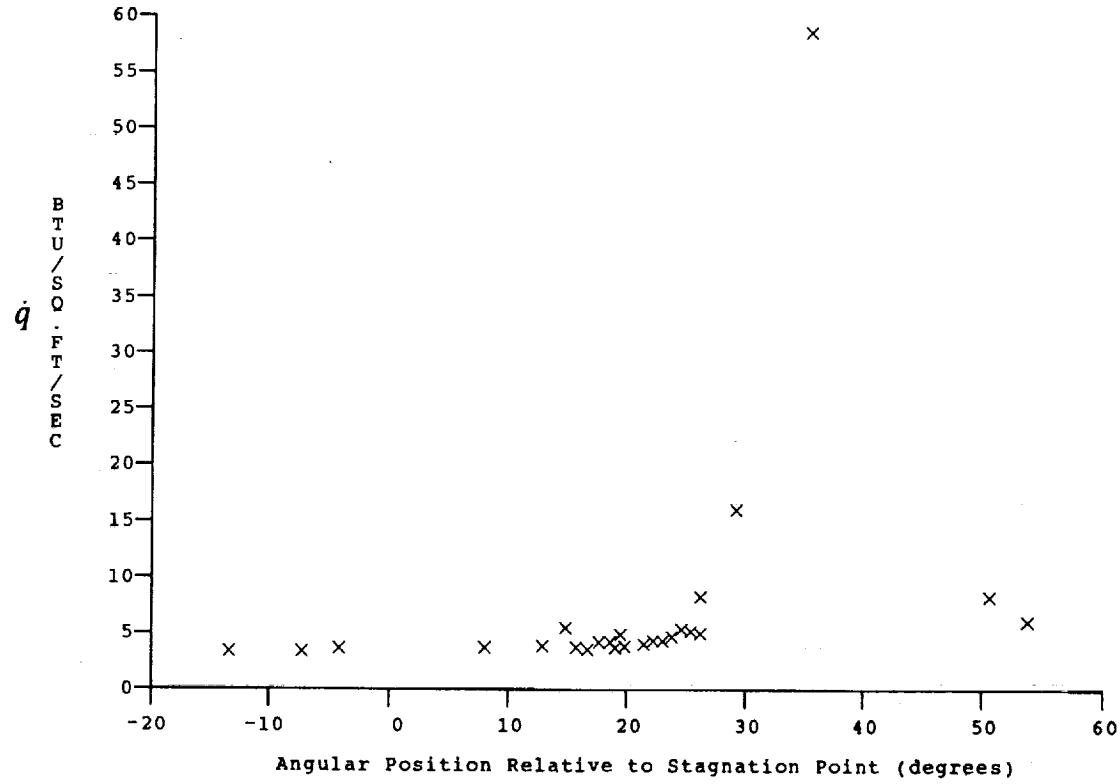

HEAT TRANSFER vs Gauge Position
Run 116

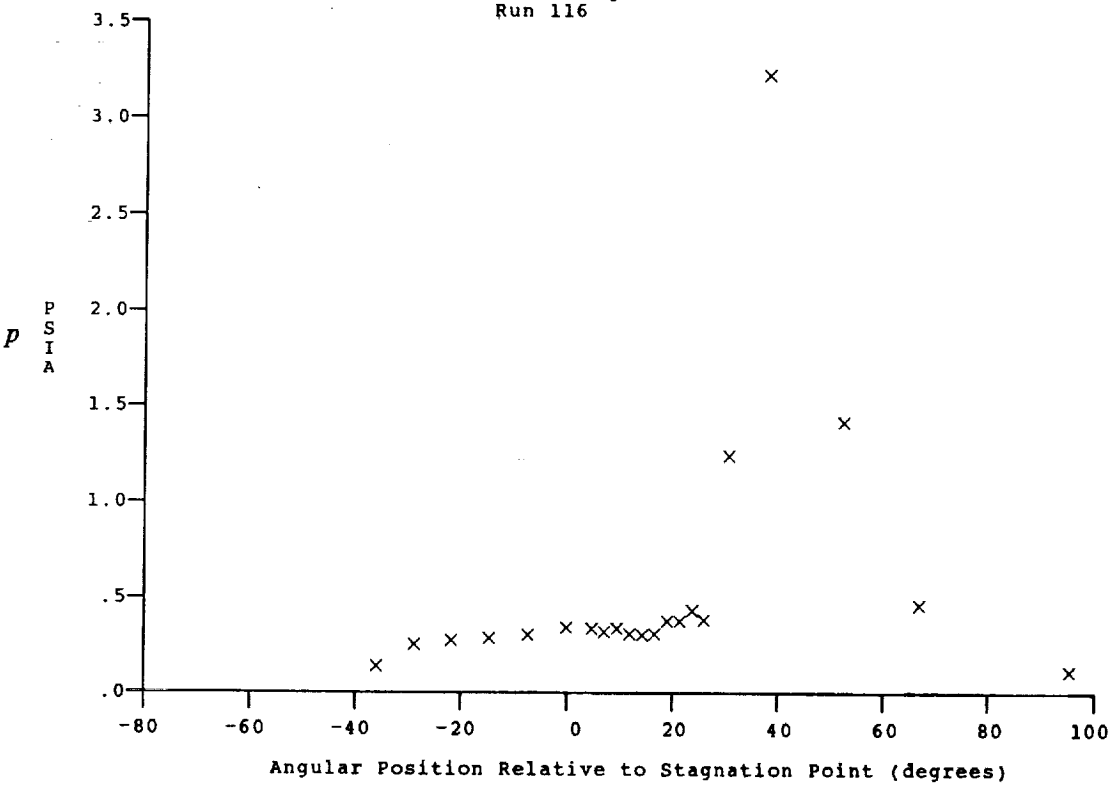

PRESSURE vs Gauge Position
Run 116

Gauge Label	Angle (deg)	(PSIA)	T Surf (DegR)	Gauge Label	Angle (deg)	(PSIA)	T Surf (DegR)	Gauge Label	Angle (deg)	(PSIA)	T Surf (DegR)
P 30	-78.76	Null		P 20	-9.53	2.755(1)		P 16	9.57	Null	
P 28	-64.44	Null		P 15	-7.14	2.665(1)		P 10	16.73	2.768(1)	
P 26	-50.11	1.234(1)		P 19	-4.76	2.602(1)		P 9	23.89	2.615(1)	
P 25	-42.95	1.650(1)		P 14	-2.37	2.970(1)		P 7	38.22	1.434(1)	
P 24	-35.79	Null		P 18	.02	2.909(1)		P 5	52.54	1.337(1)	
P 23	-28.63	2.201(1)		P 13	2.41	2.677(1)		P 3	66.86	7.731(0)	
P 22	-21.47	2.475(1)		P 17	4.79	2.809(1)					
P 21	-14.30	Null		P 12	7.18	2.803(1)					

Gauge Label	Angle (deg)	(BTU/Ft2-Sec)	T Surf (DegR)	Gauge Label	Angle (deg)	(BTU/Ft2-Sec)	T Surf (DegR)	Gauge Label	Angle (deg)	(BTU/Ft2-Sec)	T Surf (DegR)
HT 42	-56.55	2.831(1)	561.58	HT 25	-9.24	6.386(1)	601.49	HT 6	7.97	Null	Null
HT 41	-53.33	3.372(1)	566.90	HT 24	-6.19	6.981(1)	604.18	HT 5	8.77	7.032(1)	604.60
HT 40	-50.11	3.463(1)	568.98	HT 63	-2.37	6.938(1)	608.21	HT 4	9.57	7.111(1)	605.31
HT 39	-46.89	3.619(1)	570.71	HT 64	-1.41	6.799(1)	606.41	HT 3	10.37	6.492(1)	601.39
HT 38	-43.67	3.895(1)	573.96	HT 65	-.46	6.729(1)	607.97	HT 2	11.17	6.895(1)	603.64
HT 37	-40.45	4.225(1)	578.22	HT 66	.50	6.247(1)	605.39	HT 1	11.97	6.872(1)	603.34
HT 36	-37.24	4.681(1)	582.31	HT 67	1.45	6.670(1)	608.02	HT 61	15.02	6.467(1)	605.03
HT 35	-34.02	5.304(1)	587.76	HT 68	2.41	6.853(1)	609.12	HT 60	18.08	5.931(1)	601.39
HT 32	-30.63	Null	Null	HT 69	3.36	6.813(1)	607.38	HT 59	21.13	5.618(1)	594.33
HT 33	-27.58	Null	Null	HT 70	4.32	Null	Null	HT 58	24.19	5.887(1)	598.68
HT 30	-24.52	Null	Null	HT 10	4.77	6.939(1)	605.75	HT 57	27.25	5.855(1)	594.60
HT 29	-21.47	5.909(1)	595.74	HT 71	5.27	6.873(1)	607.75	HT 56	30.30	5.307(1)	589.98
HT 28	-18.41	5.858(1)	596.15	HT 9	5.58	7.583(1)	609.91	HT 55	33.36	5.375(1)	588.34
HT 27	-15.36	6.575(1)	604.51	HT 8	6.38	Null	Null	HT 54	36.41	4.663(1)	583.23
HT 26	-12.30	Null	Null	HT 7	7.18	6.424(1)	602.38	HT 53	39.47	4.748(1)	583.13

Run 9 Reduced Data Tabulation

Gauge Label	Angle (deg)	(PSIA)	T Surf (DegR)	Gauge Label	Angle (deg)	(PSIA)	T Surf (DegR)	Gauge Label	Angle (deg)	(PSIA)	T Surf (DegR)
P 30	-78.76	Null		P 20	-9.53	2.141(1)		P 11	11.96	Null	
P 28	-64.44	4.665(0)		P 15	-7.14	Null		P 10	16.73	6.804(1)	
P 26	-50.11	9.926(0)		P 19	-4.76	3.645(1)		P 9	23.89	6.822(1)	
P 25	-42.95	1.219(1)		P 14	-2.37	4.233(1)		P 7	38.22	Null	
P 24	-35.79	1.257(1)		P 18	.02	5.369(1)		P 5	52.54	4.851(1)	
P 23	-28.63	1.000(1)		P 13	2.41	6.583(1)		P 3	66.86	3.179(1)	
P 22	-21.47	9.459(0)		P 17	4.79	8.203(1)		P 1	81.19	1.847(1)	
P 21	-14.30	Null		P 12	7.18	8.513(1)					

Gauge Label	Angle (deg)	(BTU/Ft2-Sec)	T Surf (DegR)	Gauge Label	Angle (deg)	(BTU/Ft2-Sec)	T Surf (DegR)	Gauge Label	Angle (deg)	(BTU/Ft2-Sec)	T Surf (DegR)
HT 42	-56.55	5.244(1)	586.94	HT 25	-9.24	1.096(2)	681.89	HT 6	7.97	3.215(2)	713.15
HT 41	-53.33	6.084(1)	590.07	HT 24	-6.19	1.346(2)	705.54	HT 5	8.77	3.484(2)	730.10
HT 40	-50.11	6.027(1)	582.77	HT 63	-2.37	Null	Null	HT 4	9.57	3.710(2)	730.67
HT 39	-46.89	7.160(1)	591.20	HT 64	-1.41	2.081(2)	723.95	HT 3	10.37	2.982(2)	704.81
HT 38	-43.67	6.467(1)	596.35	HT 65	-.46	2.502(2)	746.08	HT 2	11.17	3.153(2)	710.95
HT 37	-40.45	7.195(1)	592.45	HT 66	.50	1.931(2)	713.61	HT 1	11.97	2.518(2)	704.97
HT 36	-37.24	5.012(1)	593.82	HT 67	1.45	2.856(2)	747.50	HT 61	15.02	2.063(2)	702.34
HT 35	-34.02	9.761(1)	610.18	HT 68	2.41	2.778(2)	742.48	HT 60	18.08	Null	Null
HT 32	-30.63	6.544(1)	622.38	HT 69	3.36	2.689(2)	740.51	HT 59	21.13	1.544(2)	652.66
HT 33	-27.58	Null	Null	HT 70	4.32	Null	Null	HT 58	24.19	1.211(2)	673.68
HT 30	-24.52	Null	Null	HT 10	4.77	3.415(2)	741.86	HT 57	27.25	9.111(1)	664.63
HT 29	-21.47	6.585(1)	622.24	HT 71	5.27	3.382(2)	742.87	HT 56	30.30	1.094(2)	655.67
HT 28	-18.41	4.536(1)	613.28	HT 9	5.58	3.788(2)	747.60	HT 55	33.36	1.028(2)	651.56
HT 27	-15.36	6.305(1)	623.52	HT 8	6.38	3.939(2)	746.38	HT 54	36.41	1.127(2)	660.62
HT 26	-12.30	Null	Null	HT 7	7.18	3.624(2)	734.52	HT 53	39.47	8.481(1)	638.12

Run 10 Reduced Data Tabulation

Gauge Label	Angle (deg)	(PSIA)	T Surf (DegR)	Gauge Label	Angle (deg)	(PSIA)	T Surf (DegR)	Gauge Label	Angle (deg)	(PSIA)	T Surf (DegR)
P 30	-78.76	Null		P 20	-9.53	2.802(1)		P 11	11.96	Null	
P 28	-64.44	5.635(0)		P 15	-7.14	Null		P 10	16.73	Null	
P 26	-50.11	1.103(1)		P 19	-4.76	2.534(1)		P 9	23.89	4.536(1)	
P 25	-42.95	1.454(1)		P 14	-2.37	2.481(1)		P 7	38.22	1.237(2)	
P 24	-35.79	1.647(1)		P 18	.02	2.689(1)		P 5	52.54	Null	
P 23	-28.63	1.940(1)		P 13	2.41	2.648(1)		P 3	66.86	3.090(1)	
P 22	-21.47	2.262(1)		P 17	4.79	3.151(1)		P 1	81.19	1.463(1)	
P 21	-14.30	Null		P 12	7.18	3.270(1)					

Gauge Label	Angle (deg)	(BTU/Ft2-Sec)	T Surf (DegR)	Gauge Label	Angle (deg)	(BTU/Ft2-Sec)	T Surf (DegR)	Gauge Label	Angle (deg)	(BTU/Ft2-Sec)	T Surf (DegR)
HT 42	-56.55	5.051(1)	589.19	HT 25	-9.24	1.553(2)	660.93	HT 6	7.97	1.877(2)	691.39
HT 41	-53.33	5.608(1)	593.72	HT 24	-6.19	1.515(2)	661.75	HT 5	8.77	1.819(2)	683.53
HT 40	-50.11	5.704(1)	594.47	HT 63	-2.37	1.503(2)	678.30	HT 4	9.57	1.705(2)	685.29
HT 39	-46.89	5.950(1)	599.28	HT 64	-1.41	1.504(2)	661.38	HT 3	10.37	1.692(2)	682.42
HT 38	-43.67	6.693(1)	603.54	HT 65	-.46	1.319(2)	663.17	HT 2	11.17	Null	Null
HT 37	-40.45	7.108(1)	609.98	HT 66	.50	1.538(2)	669.77	HT 1	11.97	1.835(2)	687.07
HT 36	-37.24	7.801(1)	616.06	HT 67	1.45	1.472(2)	668.37	HT 61	15.02	1.428(2)	699.30
HT 35	-34.02	7.967(1)	618.87	HT 68	2.41	1.498(2)	669.87	HT 60	18.08	Null	Null
HT 32	-30.63	1.431(2)	658.45	HT 69	3.36	1.477(2)	662.69	HT 59	21.13	1.608(2)	713.87
HT 33	-27.58	Null	Null	HT 70	4.32	Null	Null	HT 58	24.19	2.514(2)	767.92
HT 30	-24.52	Null	Null	HT 10	4.77	1.439(2)	666.64	HT 57	27.25	3.203(2)	827.80
HT 29	-21.47	1.264(2)	643.14	HT 71	5.27	1.504(2)	666.69	HT 56	30.30	5.578(2)	884.40
HT 28	-18.41	1.305(2)	646.50	HT 9	5.58	1.699(2)	676.28	HT 55	33.36	7.251(2)	893.54
HT 27	-15.36	1.363(2)	649.01	HT 8	6.38	1.566(2)	677.75	HT 54	36.41	5.623(2)	855.96
HT 26	-12.30	Null	Null	HT 7	7.18	1.676(2)	679.61	HT 53	39.47	3.110(2)	812.51

Run 11 Reduced Data Tabulation

Gauge Label	Angle (deg)	(PSIA)	T Surf (DegR)	Gauge Label	Angle (deg)	(PSIA)	T Surf (DegR)	Gauge Label	Angle (deg)	(PSIA)	T Surf (DegR)
P 30	-64.44	Null		P 20	4.79	5.088(1)		P 11	26.28	Null	
P 28	-50.11	7.921(0)		P 15	7.18	Null		P 10	31.05	6.188(1)	
P 26	-35.79	1.863(1)		P 19	9.57	8.874(1)		P 9	38.22	6.063(1)	
P 25	-28.63	2.565(1)		P 14	11.96	1.182(2)		P 7	52.54	2.270(1)	
P 24	-21.47	2.140(1)		P 18	14.34	9.448(1)		P 5	66.86	Null	
P 23	-14.30	1.204(1)		P 13	16.73	Null		P 3	81.19	1.936(1)	
P 22	-7.14	9.379(0)		P 17	19.12	8.576(1)		P 1	95.51	9.710(0)	
P 21	.02	2.477(1)		P 12	21.51	7.649(1)					

Gauge Label	Angle (deg)	(BTU/Ft2-Sec)	T Surf (DegR)	Gauge Label	Angle (deg)	(BTU/Ft2-Sec)	T Surf (DegR)	Gauge Label	Angle (deg)	(BTU/Ft2-Sec)	T Surf (DegR)
HT 42	-42.23	7.261(1)	637.17	HT 25	5.08	2.783(2)	854.34	HT 6	22.30	3.259(2)	772.17
HT 41	-39.01	8.703(1)	646.01	HT 24	8.14	4.314(2)	900.58	HT 5	23.09	3.195(2)	769.10
HT 40	-35.79	8.804(1)	641.14	HT 63	11.96	6.720(2)	911.95	HT 4	23.89	2.911(2)	755.46
HT 39	-32.57	1.180(2)	658.59	HT 64	12.91	6.386(2)	887.61	HT 3	24.69	2.894(2)	756.66
HT 38	-29.35	1.492(2)	664.61	HT 65	13.87	7.009(2)	895.59	HT 2	25.49	2.761(2)	744.94
HT 37	-26.13	1.822(2)	680.70	HT 66	14.82	5.649(2)	847.21	HT 1	26.29	2.693(2)	743.36
HT 36	-22.91	1.856(2)	677.15	HT 67	15.78	5.665(2)	848.70	HT 61	29.35	2.510(2)	738.07
HT 35	-19.69	1.732(2)	668.85	HT 68	16.73	4.942(2)	824.29	HT 60	32.40	Null	Null
HT 32	-16.31	1.526(2)	681.76	HT 69	17.69	4.498(2)	813.64	HT 59	35.46	1.548(2)	689.89
HT 33	-13.25	Null	Null	HT 70	18.64	Null	Null	HT 58	38.51	1.816(2)	712.84
HT 30	-10.20	Null	Null	HT 10	19.10	4.119(2)	797.82	HT 57	41.57	1.645(2)	697.78
HT 29	-7.14	4.554(1)	668.54	HT 71	19.60	3.675(2)	786.41	HT 56	44.63	1.413(2)	685.88
HT 28	-4.09	5.960(1)	700.90	HT 9	19.90	3.435(2)	783.17	HT 55	47.68	1.421(2)	683.81
HT 27	-1.03	6.787(1)	730.01	HT 8	20.70	Null	Null	HT 54	50.74	1.343(2)	678.77
HT 26	2.02	Null	Null	HT 7	21.51	3.199(2)	761.49	HT 53	53.79	1.222(2)	674.02

Run 12 Reduced Data Tabulation

Gauge Label	Angle (deg)	(PSIA)	T Surf (DegR)	Gauge Label	Angle (deg)	(PSIA)	T Surf (DegR)	Gauge Label	Angle (deg)	(PSIA)	T Surf (DegR)
P 30	-78.76	Null		P 20	-9.53	1.298(1)		P 11	11.96	Null	
P 28	-64.44	4.991(0)		P 15	-7.14	1.667(1)		P 10	16.73	6.707(1)	
P 26	-50.11	9.571(0)		P 19	-4.76	1.927(1)		P 9	23.89	7.169(1)	
P 25	-42.95	1.455(1)		P 14	-2.37	3.055(1)		P 7	38.22	Null	
P 24	-35.79	2.076(1)		P 18	.02	3.240(1)		P 5	52.54	5.096(1)	
P 23	-28.63	2.188(1)		P 13	2.41	5.481(1)		P 3	66.86	3.189(1)	
P 22	-21.47	1.638(1)		P 17	4.79	8.261(1)		P 1	81.19	1.843(1)	
P 21	-14.30	1.378(1)		P 12	7.18	1.028(2)					

Gauge Label	Angle (deg)	(BTU/Ft2-Sec)	T Surf (DegR)	Gauge Label	Angle (deg)	(BTU/Ft2-Sec)	T Surf (DegR)	Gauge Label	Angle (deg)	(BTU/Ft2-Sec)	T Surf (DegR)
HT 42	-56.55	4.113(1)	592.18	HT 25	-9.24	6.601(1)	671.83	HT 6	7.97	5.196(2)	835.70
HT 41	-53.33	4.903(1)	600.53	HT 24	-6.19	8.836(1)	680.42	HT 5	8.77	5.278(2)	831.80
HT 40	-50.11	5.091(1)	595.95	HT 63	-2.37	2.194(2)	786.83	HT 4	9.57	5.448(2)	832.54
HT 39	-46.89	6.821(1)	611.77	HT 64	-1.41	1.549(2)	732.26	HT 3	10.37	5.229(2)	817.24
HT 38	-43.67	8.126(1)	618.84	HT 65	-.46	1.948(2)	753.99	HT 2	11.17	5.360(2)	820.12
HT 37	-40.45	1.042(2)	629.22	HT 66	.50	1.858(2)	747.56	HT 1	11.97	5.179(2)	805.81
HT 36	-37.24	1.207(2)	634.48	HT 67	1.45	2.912(2)	796.01	HT 61	15.02	2.994(2)	741.27
HT 35	-34.02	1.310(2)	638.68	HT 68	2.41	2.381(2)	780.31	HT 60	18.08	Null	Null
HT 32	-30.63	Null	Null	HT 69	3.36	2.820(2)	788.83	HT 59	21.13	1.655(2)	684.04
HT 33	-27.58	Null	Null	HT 70	4.32	Null	Null	HT 58	24.19	1.701(2)	690.68
HT 30	-24.52	Null	Null	HT 10	4.77	3.531(2)	802.83	HT 57	27.25	1.511(2)	680.60
HT 29	-21.47	9.475(1)	627.99	HT 71	5.27	3.500(2)	810.36	HT 56	30.30	1.318(2)	667.73
HT 28	-18.41	6.808(1)	625.07	HT 9	5.58	4.050(2)	817.16	HT 55	33.36	1.279(2)	666.86
HT 27	-15.36	5.511(1)	627.69	HT 8	6.38	Null	Null	HT 54	36.41	1.138(2)	657.19
HT 26	-12.30	Null	Null	HT 7	7.18	5.002(2)	851.68	HT 53	39.47	1.123(2)	654.77

Run 13 Reduced Data Tabulation

Gauge Label	Angle (deg)	(PSIA)	T Surf (DegR)	Gauge Label	Angle (deg)	(PSIA)	T Surf (DegR)	Gauge Label	Angle (deg)	(PSIA)	T Surf (DegR)
P 30	-50.11	Null		P 20	19.12	3.502(1)		P 11	40.60	Null	
P 28	-35.79	Null		P 15	21.51	3.600(1)		P 10	45.38	9.918(1)	
P 26	-21.47	2.397(1)		P 19	23.89	4.315(1)		P 9	52.54	6.023(1)	
P 25	-14.30	2.759(1)		P 14	26.28	4.469(1)		P 7	66.86	1.391(1)	
P 24	-7.14	2.713(1)		P 18	28.67	4.946(1)		P 5	81.19	1.432(1)	
P 23	.02	2.791(1)		P 13	31.05	Null		P 3	95.51	Null	
P 22	7.18	3.019(1)		P 17	33.44	Null		P 1	109.84	7.307(0)	
P 21	14.34	2.775(1)		P 12	35.83	1.528(2)					

Gauge Label	Angle (deg)	(BTU/Ft2-Sec)	T Surf (DegR)	Gauge Label	Angle (deg)	(BTU/Ft2-Sec)	T Surf (DegR)	Gauge Label	Angle (deg)	(BTU/Ft2-Sec)	T Surf (DegR)
HT 42	-27.91	Null	Null	HT 25	19.40	2.048(2)	737.99	HT 6	36.62	6.601(2)	903.53
HT 41	-24.69	9.033(1)	630.76	HT 24	22.46	1.807(2)	749.36	HT 5	37.42	6.745(2)	911.86
HT 40	-21.47	9.655(1)	634.90	HT 63	26.28	2.755(2)	827.05	HT 4	38.22	7.196(2)	905.99
HT 39	-18.25	9.434(1)	635.99	HT 64	27.23	2.400(2)	814.44	HT 3	39.01	6.658(2)	889.26
HT 38	-15.03	1.180(2)	656.78	HT 65	28.19	2.631(2)	833.30	HT 2	39.81	6.849(2)	892.24
HT 37	-11.81	1.124(2)	651.27	HT 66	29.14	2.428(2)	822.56	HT 1	40.62	6.549(2)	882.42
HT 36	-8.59	1.148(2)	658.26	HT 67	30.10	3.126(2)	859.66	HT 61	43.67	4.400(2)	838.52
HT 35	-5.37	Null	Null	HT 68	31.05	3.126(2)	869.14	HT 60	46.73	Null	Null
HT 32	-1.99	1.827(2)	704.61	HT 69	32.01	3.497(2)	866.32	HT 59	49.78	2.207(2)	742.38
HT 33	1.07	Null	Null	HT 70	32.96	Null	Null	HT 58	52.84	1.872(2)	740.56
HT 30	4.13	Null	Null	HT 10	33.42	4.604(2)	882.62	HT 57	55.89	1.791(2)	719.21
HT 29	7.18	1.492(2)	674.75	HT 71	33.92	4.463(2)	882.67	HT 56	58.95	1.460(2)	695.64
HT 28	10.24	1.557(2)	679.89	HT 9	34.22	5.089(2)	897.35	HT 55	62.01	1.496(2)	683.47
HT 27	13.29	2.108(2)	693.52	HT 8	35.03	Null	Null	HT 54	65.06	1.367(2)	669.25
HT 26	16.35	Null	Null	HT 7	35.83	5.163(2)	861.55	HT 53	68.12	1.226(2)	656.41

Run 14 Reduced Data Tabulation

Gauge Label	Angle (deg)	(PSIA)	T Surf (DegR)	Gauge Label	Angle (deg)	(PSIA)	T Surf (DegR)	Gauge Label	Angle (deg)	(PSIA)	T Surf (DegR)
P 30	-50.11	Null		P 20	19.12	9.988(1)		P 11	40.60	Null	
P 28	-35.79	7.297(0)		P 15	21.51	9.500(1)		P 10	45.38	2.546(1)	
P 26	-21.47	1.165(1)		P 19	23.89	4.820(1)		P 9	52.54	2.320(1)	
P 25	-14.30	1.414(1)		P 14	26.28	4.274(1)		P 7	66.86	1.235(1)	
P 24	-7.14	1.322(1)		P 18	28.67	3.583(1)		P 5	81.19	9.164(0)	
P 23	.02	7.508(0)		P 13	31.05	3.555(1)		P 3	95.51	4.246(0)	
P 22	7.18	1.564(1)		P 17	33.44	4.041(1)		P 1	109.84	2.184(0)	
P 21	14.34	4.321(1)		P 12	35.83	3.756(1)					

Gauge Label	Angle (deg)	(BTU/Ft2-Sec)	T Surf (DegR)	Gauge Label	Angle (deg)	(BTU/Ft2-Sec)	T Surf (DegR)	Gauge Label	Angle (deg)	(BTU/Ft2-Sec)	T Surf (DegR)
HT 42	-27.91	7.012(1)	604.69	HT 26	16.35	Null	Null	HT 6	36.62	1.449(2)	655.45
HT 41	-24.69	6.906(1)	610.72	HT 25	19.40	4.280(2)	754.70	HT 5	37.42	1.614(2)	661.90
HT 40	-21.47	6.738(1)	613.66	HT 24	22.46	2.616(2)	696.83	HT 4	38.22	1.367(2)	652.09
HT 39	-18.25	7.077(1)	618.92	HT 63	26.28	1.746(2)	679.34	HT 3	39.01	1.332(2)	643.42
HT 38	-15.03	8.707(1)	624.10	HT 64	27.23	1.638(2)	667.06	HT 2	39.81	1.321(2)	646.06
HT 37	-11.81	9.351(1)	617.09	HT 65	28.19	1.708(2)	674.45	HT 62	40.62	1.648(2)	668.55
HT 36	-8.59	1.053(2)	608.53	HT 66	29.14	1.570(2)	666.04	HT 1	40.62	1.295(2)	645.86
HT 35	-5.37	Null	Null	HT 67	30.10	1.514(2)	663.92	HT 61	43.67	1.204(2)	644.18
HT 34	-1.99	7.887(1)	591.85	HT 68	31.05	1.463(2)	657.25	HT 59	49.78	9.324(1)	612.10
HT 32	-1.99	9.618(1)	610.95	HT 69	32.01	1.547(2)	661.59	HT 58	52.84	9.922(1)	621.58
HT 31	1.07	4.328(1)	604.09	HT 70	32.96	Null	Null	HT 57	55.89	8.554(1)	612.12
HT 30	4.13	5.015(1)	625.27	HT 10	33.42	1.654(2)	664.38	HT 56	58.95	7.485(1)	602.85
HT 29	7.18	6.681(1)	675.69	HT 71	33.92	1.516(2)	657.63	HT 55	62.01	7.255(1)	600.29
HT 28	10.24	Null	Null	HT 9	34.22	1.617(2)	657.19	HT 54	65.06	6.210(1)	592.05
HT 27	13.29	Null	Null	HT 7	35.83	1.462(2)	653.09	HT 53	68.12	5.897(1)	585.74

Run 15 Reduced Data Tabulation

Gauge Label	Angle (deg)	(PSIA)	T Surf (DegR)	Gauge Label	Angle (deg)	(PSIA)	T Surf (DegR)	Gauge Label	Angle (deg)	(PSIA)	T Surf (DegR)
P 30	-50.11	Null		P 20	19.12	1.069(1)		P 11	40.60	Null	
P 28	-35.79	5.897(0)		P 15	21.51	1.023(1)		P 10	45.38	3.535(1)	
P 26	-21.47	7.786(0)		P 19	23.89	1.011(1)		P 9	52.54	3.192(1)	
P 25	-14.30	8.702(0)		P 14	26.28	1.122(1)		P 7	66.86	Null	
P 24	-7.14	8.666(0)		P 18	28.67	1.323(1)		P 5	81.19	5.202(0)	
P 23	.02	9.261(0)		P 13	31.05	1.515(1)		P 3	95.51	Null	
P 22	7.18	9.844(0)		P 17	33.44	2.597(1)		P 1	109.84	Null	
P 21	14.34	Null		P 12	35.83	2.650(1)					

Gauge Label	Angle (deg)	(BTU/Ft2-Sec)	T Surf (DegR)	Gauge Label	Angle (deg)	(BTU/Ft2-Sec)	T Surf (DegR)	Gauge Label	Angle (deg)	(BTU/Ft2-Sec)	T Surf (DegR)
HT 42	-27.91	4.877(1)	580.18	HT 26	16.35	Null	Null	HT 6	36.62	3.237(2)	776.53
HT 41	-24.69	4.835(1)	580.46	HT 25	19.40	1.025(2)	624.21	HT 5	37.42	Null	Null
HT 40	-21.47	4.928(1)	580.69	HT 24	22.46	1.063(2)	629.02	HT 4	38.22	3.676(2)	801.02
HT 39	-18.25	5.216(1)	583.47	HT 63	26.28	1.284(2)	650.25	HT 3	39.01	2.896(2)	790.38
HT 38	-15.03	5.427(1)	585.66	HT 64	27.23	1.310(2)	650.52	HT 2	39.81	Null	Null
HT 37	-11.81	6.040(1)	589.10	HT 65	28.19	1.416(2)	661.18	HT 62	40.62	3.912(2)	820.32
HT 36	-8.59	6.252(1)	592.51	HT 66	29.14	1.519(2)	666.74	HT 1	40.62	Null	Null
HT 35	-5.37	Null	Null	HT 67	30.10	1.773(2)	685.82	HT 61	43.67	3.690(2)	843.89
HT 34	-1.99	6.721(1)	597.53	HT 68	31.05	1.888(2)	691.24	HT 59	49.78	3.312(2)	789.53
HT 32	-1.99	Null	Null	HT 69	32.01	1.973(2)	699.07	HT 58	52.84	2.487(2)	746.71
HT 31	1.07	7.898(1)	608.83	HT 70	32.96	Null	Null	HT 57	55.89	Null	Null
HT 30	4.13	7.179(1)	603.24	HT 10	33.42	2.681(2)	739.03	HT 56	58.95	1.520(2)	673.92
HT 29	7.18	8.107(1)	610.43	HT 71	33.92	2.436(2)	726.80	HT 55	62.01	1.265(2)	653.40
HT 28	10.24	8.576(1)	612.53	HT 9	34.22	2.714(2)	743.47	HT 54	65.06	9.811(1)	630.93
HT 27	13.29	Null	Null	HT 7	35.83	Null	Null	HT 53	68.12	7.878(1)	612.40

Run 16 Reduced Data Tabulation

Gauge Label	Angle (deg)	(PSIA)	T Surf (DegR)	Gauge Label	Angle (deg)	(PSIA)	T Surf (DegR)	Gauge Label	Angle (deg)	(PSIA)	T Surf (DegR)
P 30	-50.11	Null		P 20	19.12	1.183(1)		P 11	40.60	Null	
P 28	-35.79	5.430(0)		P 15	21.51	1.089(1)		P 10	45.38	3.640(1)	
P 26	-21.47	7.185(0)		P 19	23.89	1.068(1)		P 9	52.54	3.078(1)	
P 25	-14.30	8.171(0)		P 14	26.28	1.199(1)		P 7	66.86	Null	
P 24	-7.14	7.883(0)		P 18	28.67	1.804(1)		P 5	81.19	5.234(0)	
P 23	.02	8.540(0)		P 13	31.05	1.694(1)		P 3	95.51	Null	
P 22	7.18	9.617(0)		P 17	33.44	3.005(1)		P 1	109.84	Null	
P 21	14.34	1.219(1)		P 12	35.83	2.836(1)					

Gauge Label	Angle (deg)	(BTU/Ft2-Sec)	T Surf (DegR)	Gauge Label	Angle (deg)	(BTU/Ft2-Sec)	T Surf (DegR)	Gauge Label	Angle (deg)	(BTU/Ft2-Sec)	T Surf (DegR)
HT 42	-27.91	5.302(1)	592.52	HT 26	16.35	Null	Null	HT 6	36.62	3.324(2)	782.50
HT 41	-24.69	5.384(1)	593.79	HT 25	19.40	9.633(1)	629.19	HT 5	37.42	3.373(2)	785.00
HT 40	-21.47	5.925(1)	598.95	HT 24	22.46	1.231(2)	644.00	HT 4	38.22	3.682(2)	795.04
HT 39	-18.25	6.327(1)	599.54	HT 63	26.28	1.341(2)	662.11	HT 3	39.01	3.518(2)	787.57
HT 38	-15.03	5.834(1)	597.84	HT 64	27.23	1.423(2)	664.13	HT 2	39.81	3.510(2)	783.81
HT 37	-11.81	6.472(1)	600.15	HT 65	28.19	1.577(2)	672.56	HT 62	40.62	4.216(2)	802.55
HT 36	-8.59	6.704(1)	604.98	HT 66	29.14	1.613(2)	675.40	HT 1	40.62	3.947(2)	798.61
HT 35	-5.37	Null	Null	HT 67	30.10	1.886(2)	691.06	HT 61	43.67	4.521(2)	825.77
HT 34	-1.99	7.083(1)	607.20	HT 68	31.05	2.030(2)	697.18	HT 59	49.78	2.970(2)	772.17
HT 32	-1.99	Null	Null	HT 69	32.01	2.125(2)	705.47	HT 58	52.84	2.416(2)	751.37
HT 31	1.07	9.246(1)	615.33	HT 70	32.96	Null	Null	HT 57	55.89	1.788(2)	716.89
HT 30	4.13	7.890(1)	611.24	HT 10	33.42	2.649(2)	739.81	HT 56	58.95	1.299(2)	675.42
HT 29	7.18	8.923(1)	618.02	HT 71	33.92	2.664(2)	727.19	HT 55	62.01	1.099(2)	655.68
HT 28	10.24	9.066(1)	619.27	HT 9	34.22	2.951(2)	753.85	HT 54	65.06	9.289(1)	640.11
HT 27	13.29	Null	Null	HT 7	35.83	2.984(2)	758.16	HT 53	68.12	6.704(1)	618.88

Run 17 Reduced Data Tabulation

Gauge Label	Angle (deg)	(PSIA)	T Surf (DegR)	Gauge Label	Angle (deg)	(PSIA)	T Surf (DegR)	Gauge Label	Angle (deg)	(PSIA)	T Surf (DegR)
P 30	-64.44	Null		P 21	.02	Null		P 12	21.51	6.775(1)	
P 28	-50.11	2.853(0)		P 19	9.57	1.030(1)		P 10	31.05	2.938(1)	
P 25	-28.63	6.260(0)		P 14	11.96	1.514(1)		P 7	52.54	Null	
P 23	-14.30	7.876(0)		P 17	19.12	5.280(1)		P 3	81.19	Null	

Gauge Label	Angle (deg)	(BTU/Ft2-Sec)	T Surf (DegR)	Gauge Label	Angle (deg)	(BTU/Ft2-Sec)	T Surf (DegR)	Gauge Label	Angle (deg)	(BTU/Ft2-Sec)	T Surf (DegR)
HT 42	-42.23	4.484(1)	582.04	HT 26	2.02	Null	Null	HT 6	22.30	6.159(2)	885.39
HT 41	-39.01	4.601(1)	587.52	HT 25	5.08	5.716(1)	632.81	HT 5	23.09	6.633(2)	878.85
HT 40	-35.79	4.929(1)	593.91	HT 24	8.14	5.772(1)	690.74	HT 4	23.89	6.954(2)	873.76
HT 39	-32.57	4.922(1)	598.77	HT 63	11.96	Null	Null	HT 3	24.69	6.533(2)	850.63
HT 38	-29.35	6.205(1)	610.69	HT 64	12.91	Null	Null	HT 2	25.49	6.423(2)	838.18
HT 37	-26.13	6.108(1)	615.92	HT 65	13.87	Null	Null	HT 62	26.29	4.477(2)	817.26
HT 36	-22.91	Null	Null	HT 66	14.82	Null	Null	HT 1	26.29	5.953(2)	831.22
HT 35	-19.69	Null	Null	HT 67	15.78	2.659(2)	863.89	HT 61	29.35	3.473(2)	761.34
HT 34	-16.31	9.506(1)	614.06	HT 68	16.73	2.012(2)	874.01	HT 59	35.46	2.291(2)	696.25
HT 32	-16.31	1.299(2)	640.84	HT 69	17.69	Null	Null	HT 58	38.51	2.016(2)	693.18
HT 31	-13.25	1.096(2)	605.87	HT 70	18.64	Null	Null	HT 57	41.57	1.897(2)	681.96
HT 30	-10.20	9.715(1)	592.24	HT 10	19.10	3.086(2)	854.10	HT 56	44.63	1.691(2)	664.83
HT 29	-7.14	1.154(2)	597.20	HT 71	19.60	3.523(2)	880.09	HT 55	47.68	1.558(2)	657.16
HT 28	-4.09	8.779(1)	587.45	HT 9	19.90	4.014(2)	883.55	HT 54	50.74	1.446(2)	648.75
HT 27	-1.03	Null	Null	HT 7	21.51	4.469(2)	850.38	HT 53	53.79	1.305(2)	638.94

Run 18 Reduced Data Tabulation

Gauge Label	Angle (deg)	(PSIA)	T Surf (DegR)	Gauge Label	Angle (deg)	(PSIA)	T Surf (DegR)	Gauge Label	Angle (deg)	(PSIA)	T Surf (DegR)
P 30	-64.44	Null		P 20	4.79	1.360(1)		P 11	26.28	Null	
P 28	-50.11	2.707(0)		P 15	7.18	Null		P 10	31.05	2.938(1)	
P 26	-35.79	5.553(0)		P 19	9.57	1.000(1)		P 9	38.22	2.356(1)	
P 25	-28.63	6.056(0)		P 14	11.96	1.457(1)		P 7	52.54	Null	
P 24	-21.47	4.716(0)		P 18	14.34	4.438(1)		P 5	66.86	1.542(1)	
P 23	-14.30	7.747(0)		P 13	16.73	4.849(1)		P 3	81.19	Null	
P 22	-7.14	2.411(0)		P 17	19.12	5.241(1)		P 1	95.51	Null	
P 21	.02	Null		P 12	21.51	6.679(1)					

Gauge Label	Angle (deg)	(BTU/Ft2-Sec)	T Surf (DegR)	Gauge Label	Angle (deg)	(BTU/Ft2-Sec)	T Surf (DegR)	Gauge Label	Angle (deg)	(BTU/Ft2-Sec)	T Surf (DegR)
HT 42	-42.23	6.194(1)	592.57	HT 26	2.02	Null	Null	HT 6	22.30	3.040(2)	749.78
HT 41	-39.01	6.879(1)	596.53	HT 25	5.08	2.229(2)	803.00	HT 5	23.09	2.616(2)	735.67
HT 40	-35.79	7.948(1)	603.87	HT 24	8.14	2.888(2)	825.02	HT 4	23.89	2.690(2)	736.35
HT 39	-32.57	7.646(1)	597.72	HT 63	11.96	4.767(2)	888.38	HT 3	24.69	2.165(2)	711.64
HT 38	-29.35	8.156(1)	595.09	HT 64	12.91	5.281(2)	888.03	HT 2	25.49	1.956(2)	704.16
HT 37	-26.13	8.147(1)	591.40	HT 65	13.87	5.650(2)	888.42	HT 62	26.29	2.200(2)	714.82
HT 36	-22.91	7.800(1)	589.02	HT 66	14.82	5.178(2)	859.29	HT 1	26.29	1.856(2)	698.73
HT 35	-19.69	Null	Null	HT 67	15.78	5.883(2)	879.85	HT 61	29.35	1.840(2)	688.25
HT 34	-16.31	4.916(1)	571.31	HT 68	16.73	5.416(2)	850.21	HT 59	35.46	1.621(2)	662.51
HT 32	-16.31	5.860(1)	585.42	HT 69	17.69	5.221(2)	842.40	HT 58	38.51	1.346(2)	659.80
HT 31	-13.25	3.236(1)	569.15	HT 70	18.64	Null	Null	HT 57	41.57	1.128(2)	642.49
HT 30	-10.20	2.236(1)	568.76	HT 10	19.10	4.288(2)	794.86	HT 56	44.63	1.085(2)	633.36
HT 29	-7.14	2.412(1)	578.05	HT 71	19.60	4.369(2)	795.53	HT 55	47.68	9.918(1)	624.08
HT 28	-4.09	3.709(1)	591.65	HT 9	19.90	3.882(2)	786.35	HT 54	50.74	9.323(1)	620.96
HT 27	-1.03	Null	Null	HT 7	21.51	2.955(2)	745.23	HT 53	53.79	7.404(1)	611.08

Run 19 Reduced Data Tabulation

Gauge Label	Angle (deg)	(PSIA)	T Surf (DegR)	Gauge Label	Angle (deg)	(PSIA)	T Surf (DegR)	Gauge Label	Angle (deg)	(PSIA)	T Surf (DegR)
P 30	-64.44	Null		P 20	4.79	1.074(1)		P 11	26.28	Null	
P 28	-50.11	1.643(0)		P 15	7.18	1.947(1)		P 10	31.05	1.215(1)	
P 26	-35.79	2.326(0)		P 19	9.57	1.792(1)		P 9	38.22	Null	
P 25	-28.63	1.968(0)		P 14	11.96	2.399(1)		P 7	52.54	Null	
P 24	-21.47	1.230(0)		P 18	14.34	2.161(1)		P 5	66.86	7.329(0)	
P 23	-14.30	6.696(-1)		P 13	16.73	2.041(1)		P 3	81.19	Null	
P 22	-7.14	1.474(0)		P 17	19.12	Null		P 1	95.51	Null	
P 21	.02	5.186(0)		P 12	21.51	1.633(1)					

Gauge Label	Angle (deg)	(BTU/Ft2-Sec)	T Surf (DegR)	Gauge Label	Angle (deg)	(BTU/Ft2-Sec)	T Surf (DegR)	Gauge Label	Angle (deg)	(BTU/Ft2-Sec)	T Surf (DegR)
HT 42	-42.23	3.779(1)	561.76	HT 26	2.02	Null	Null	HT 6	22.30	1.311(2)	646.59
HT 41	-39.01	4.080(1)	562.46	HT 25	5.08	1.618(2)	707.39	HT 5	23.09	1.276(2)	642.70
HT 40	-35.79	4.118(1)	562.40	HT 24	8.14	3.150(2)	771.45	HT 4	23.89	1.153(2)	641.01
HT 39	-32.57	3.703(1)	557.34	HT 63	11.96	3.818(2)	784.25	HT 3	24.69	1.019(2)	642.78
HT 38	-29.35	2.848(1)	555.47	HT 64	12.91	3.878(2)	772.43	HT 2	25.49	1.137(2)	631.37
HT 37	-26.13	2.509(1)	553.16	HT 65	13.87	3.602(2)	763.84	HT 62	26.29	1.166(2)	632.87
HT 36	-22.91	2.165(1)	551.56	HT 66	14.82	3.542(2)	753.17	HT 1	26.29	1.250(2)	635.92
HT 35	-19.69	Null	Null	HT 67	15.78	3.131(2)	737.60	HT 61	29.35	1.099(2)	633.28
HT 34	-16.31	1.278(1)	550.32	HT 68	16.73	2.675(2)	707.42	HT 59	35.46	7.794(1)	605.52
HT 32	-16.31	9.775(0)	552.75	HT 69	17.69	2.473(2)	704.10	HT 58	38.51	7.904(1)	613.77
HT 31	-13.25	1.165(1)	554.03	HT 70	18.64	Null	Null	HT 57	41.57	6.694(1)	601.60
HT 30	-10.20	1.347(1)	556.30	HT 10	19.10	1.642(2)	669.01	HT 56	44.63	6.121(1)	593.70
HT 29	-7.14	1.780(1)	566.29	HT 71	19.60	1.830(2)	674.41	HT 55	47.68	5.105(1)	590.30
HT 28	-4.09	3.280(1)	582.48	HT 9	19.90	1.571(2)	669.18	HT 54	50.74	5.477(1)	590.31
HT 27	-1.03	Null	Null	HT 7	21.51	1.275(2)	641.21	HT 53	53.79	4.715(1)	583.23

Run 20 Reduced Data Tabulation

Gauge Label	Angle (deg)	(PSIA)	T Surf (DegR)	Gauge Label	Angle (deg)	(PSIA)	T Surf (DegR)	Gauge Label	Angle (deg)	(PSIA)	T Surf (DegR)
P 30	-64.44	Null		P 20	4.79	7.434(0)		P 11	26.28	Null	
P 28	-50.11	2.615(0)		P 15	7.18	1.002(1)		P 10	31.05	2.961(1)	
P 26	-35.79	2.435(0)		P 19	9.57	1.842(1)		P 9	38.22	Null	
P 25	-28.63	1.421(0)		P 14	11.96	2.588(1)		P 7	52.54	Null	
P 24	-21.47	9.149(-1)		P 18	14.34	5.852(1)		P 5	66.86	1.794(1)	
P 23	-14.30	6.076(-1)		P 13	16.73	7.113(1)		P 3	81.19	Null	
P 22	-7.14	1.182(0)		P 17	19.12	8.189(1)		P 1	95.51	4.549(0)	
P 21	.02	Null		P 12	21.51	6.804(1)					

Gauge Label	Angle (deg)	(BTU/Ft2-Sec)	T Surf (DegR)	Gauge Label	Angle (deg)	(BTU/Ft2-Sec)	T Surf (DegR)	Gauge Label	Angle (deg)	(BTU/Ft2-Sec)	T Surf (DegR)
HT 42	-42.23	4.734(1)	574.90	HT 26	2.02	Null	Null	HT 6	22.30	5.388(2)	925.44
HT 41	-39.01	4.754(1)	572.61	HT 25	5.08	8.494(1)	638.32	HT 5	23.09	4.637(2)	900.86
HT 40	-35.79	4.456(1)	569.68	HT 24	8.14	1.576(2)	720.17	HT 4	23.89	4.203(2)	872.83
HT 39	-32.57	3.645(1)	562.53	HT 63	11.96	3.149(2)	855.84	HT 3	24.69	3.658(2)	833.87
HT 38	-29.35	3.324(1)	558.70	HT 64	12.91	4.044(2)	889.34	HT 2	25.49	3.359(2)	816.69
HT 37	-26.13	2.212(1)	551.57	HT 65	13.87	4.782(2)	926.67	HT 62	26.29	3.681(2)	816.70
HT 36	-22.91	1.206(1)	546.44	HT 66	14.82	5.059(2)	928.74	HT 1	26.29	3.008(2)	797.47
HT 35	-19.69	Null	Null	HT 67	15.78	7.520(2)	1010.80	HT 61	29.35	2.523(2)	751.49
HT 34	-16.31	4.829(0)	540.02	HT 68	16.73	8.877(2)	1045.30	HT 59	35.46	2.027(2)	715.92
HT 32	-16.31	5.056(0)	544.72	HT 69	17.69	9.279(2)	1050.70	HT 58	38.51	1.906(2)	709.41
HT 31	-13.25	7.189(0)	543.63	HT 70	18.64	Null	Null	HT 57	41.57	1.826(2)	697.84
HT 30	-10.20	7.006(0)	546.35	HT 10	19.10	8.643(2)	1030.50	HT 56	44.63	1.546(2)	676.77
HT 29	-7.14	1.185(1)	553.90	HT 71	19.60	9.797(2)	1060.40	HT 55	47.68	1.426(2)	669.85
HT 28	-4.09	1.929(1)	558.58	HT 9	19.90	8.003(2)	1012.90	HT 54	50.74	1.268(2)	657.67
HT 27	-1.03	Null	Null	HT 7	21.51	4.730(2)	915.40	HT 53	53.79	1.167(2)	648.00

Run 21 Reduced Data Tabulation

Gauge Label	Angle (deg)	(PSIA)	T Surf (DegR)	Gauge Label	Angle (deg)	(PSIA)	T Surf (DegR)	Gauge Label	Angle (deg)	(PSIA)	T Surf (DegR)
P 30	-64.44	Null		P 20	4.79	7.709(0)		P 11	26.28	Null	
P 28	-50.11	6.933(-1)		P 15	7.18	9.500(0)		P 10	31.05	1.406(1)	
P 26	-35.79	4.562(-1)		P 19	9.57	1.759(1)		P 9	38.22	1.415(1)	
P 25	-28.63	3.686(-1)		P 14	11.96	2.340(1)		P 7	52.54	Null	
P 24	-21.47	2.856(-1)		P 18	14.34	3.272(1)		P 5	66.86	7.172(0)	
P 23	-14.30	4.991(-1)		P 13	16.73	3.548(1)		P 3	81.19	Null	
P 22	-7.14	1.084(0)		P 17	19.12	3.172(1)		P 1	95.51	2.165(0)	
P 21	.02	1.965(-1)		P 12	21.51	2.555(1)					

Gauge Label	Angle (deg)	(BTU/Ft2-Sec)	T Surf (DegR)	Gauge Label	Angle (deg)	(BTU/Ft2-Sec)	T Surf (DegR)	Gauge Label	Angle (deg)	(BTU/Ft2-Sec)	T Surf (DegR)
HT 42	-42.23	1.705(1)	542.12	HT 26	2.02	Null	Null	HT 6	22.30	2.431(2)	714.31
HT 41	-39.01	1.390(1)	539.62	HT 25	5.08	8.745(1)	687.76	HT 5	23.09	2.263(2)	705.17
HT 40	-35.79	1.135(1)	538.67	HT 24	8.14	1.753(2)	760.52	HT 4	23.89	2.029(2)	692.50
HT 39	-32.57	1.186(1)	541.47	HT 63	11.96	3.218(2)	827.16	HT 3	24.69	1.819(2)	681.68
HT 38	-29.35	8.883(0)	541.18	HT 64	12.91	3.808(2)	834.68	HT 2	25.49	1.792(2)	679.66
HT 37	-26.13	4.372(0)	535.90	HT 65	13.87	4.301(2)	847.00	HT 62	26.29	1.795(2)	679.86
HT 36	-22.91	3.428(0)	536.57	HT 66	14.82	4.065(2)	824.17	HT 1	26.29	1.607(2)	670.57
HT 35	-19.69	Null	Null	HT 67	15.78	5.017(2)	853.80	HT 61	29.35	1.389(2)	661.38
HT 34	-16.31	5.150(0)	540.02	HT 68	16.73	5.007(2)	842.29	HT 59	35.46	1.063(2)	630.82
HT 32	-16.31	7.510(0)	545.53	HT 69	17.69	4.765(2)	824.45	HT 58	38.51	1.023(2)	625.60
HT 31	-13.25	8.667(0)	545.80	HT 70	18.64	Null	Null	HT 57	41.57	9.348(1)	621.53
HT 30	-10.20	9.854(0)	549.71	HT 10	19.10	3.747(2)	773.73	HT 56	44.63	8.248(1)	611.54
HT 29	-7.14	1.368(1)	559.08	HT 71	19.60	4.008(2)	788.66	HT 55	47.68	8.002(1)	608.64
HT 28	-4.09	2.004(1)	573.04	HT 9	19.90	3.407(2)	758.35	HT 54	50.74	6.803(1)	600.27
HT 27	-1.03	Null	Null	HT 7	21.51	2.521(2)	716.41	HT 53	53.79	6.838(1)	595.48

Run 22 Reduced Data Tabulation

Gauge Label	Angle (deg)	(PSIA)	T Surf (DegR)	Gauge Label	Angle (deg)	(PSIA)	T Surf (DegR)	Gauge Label	Angle (deg)	(PSIA)	T Surf (DegR)
P 30	-64.44	Null		P 15	7.18	Null		P 10	31.05	8.508(1)	
P 28	-50.11	Null		P 19	9.57	4.485(1)		P 9	38.22	8.195(1)	
P 26	-35.79	1.250(1)		P 14	11.96	5.488(1)		P 7	52.54	Null	
P 25	-28.63	1.207(1)		P 18	14.34	1.351(2)		P 5	66.86	5.151(1)	
P 24	-21.47	7.746(0)		P 13	16.73	5.409(1)		P 3	81.19	Null	
P 23	-14.30	2.850(0)		P 17	19.12	Null		P 1	95.51	1.479(1)	
P 22	-7.14	3.384(0)		P 12	21.51	1.722(2)					
P 21	.02	9.287(0)		P 11	26.28	Null					

Gauge Label	Angle (deg)	(BTU/Ft2-Sec)	T Surf (DegR)	Gauge Label	Angle (deg)	(BTU/Ft2-Sec)	T Surf (DegR)	Gauge Label	Angle (deg)	(BTU/Ft2-Sec)	T Surf (DegR)
HT 42	-42.23	1.405(2)	638.46	HT 26	2.02	Null	Null	HT 6	22.30	1.849(3)	1210.90
HT 41	-39.01	1.430(2)	640.71	HT 25	5.08	1.893(2)	747.77	HT 5	23.09	1.606(3)	1161.20
HT 40	-35.79	1.708(2)	658.17	HT 24	8.14	3.451(2)	874.20	HT 4	23.89	1.454(3)	1125.90
HT 39	-32.57	1.612(2)	644.63	HT 63	11.96	Null	Null	HT 3	24.69	1.232(3)	1064.00
HT 38	-29.35	1.747(2)	646.99	HT 64	12.91	6.979(2)	1061.00	HT 2	25.49	1.128(3)	1026.70
HT 37	-26.13	1.659(2)	641.05	HT 65	13.87	8.973(2)	1129.70	HT 62	26.29	1.035(3)	1020.30
HT 36	-22.91	1.308(2)	620.58	HT 66	14.82	1.054(3)	1174.10	HT 1	26.29	9.738(2)	993.09
HT 35	-19.69	Null	Null	HT 67	15.78	1.467(3)	1271.50	HT 61	29.35	7.862(2)	950.24
HT 34	-16.31	7.024(1)	586.35	HT 68	16.73	1.622(3)	1274.30	HT 59	35.46	6.284(2)	891.62
HT 32	-16.31	9.389(1)	606.77	HT 69	17.69	1.806(3)	1288.50	HT 58	38.51	5.397(2)	862.05
HT 31	-13.25	5.319(1)	590.70	HT 70	18.64	Null	Null	HT 57	41.57	5.089(2)	847.81
HT 30	-10.20	Null	Null	HT 10	19.10	2.204(3)	1319.40	HT 56	44.63	4.495(2)	825.26
HT 29	-7.14	3.684(1)	587.69	HT 71	19.60	2.102(3)	1309.20	HT 55	47.68	4.214(2)	811.63
HT 28	-4.09	5.572(1)	604.16	HT 9	19.90	2.051(3)	1283.40	HT 54	50.74	3.994(2)	794.01
HT 27	-1.03	Null	Null	HT 7	21.51	1.379(3)	1111.00	HT 53	53.79	3.402(2)	771.62

Run 24 Reduced Data Tabulation

Gauge Label	Angle (deg)	(PSIA)	T Surf (DegR)	Gauge Label	Angle (deg)	(PSIA)	T Surf (DegR)	Gauge Label	Angle (deg)	(PSIA)	T Surf (DegR)
P 30	-31.86	Null		P 21	32.60	Null		P 12	54.09	3.271(1)	
P 28	-17.53	8.044(0)		P 20	37.38	1.478(1)		P 11	58.86	Null	
P 26	-3.21	9.446(0)		P 19	42.15	1.773(1)		P 10	63.64	2.089(1)	
P 25	3.95	1.023(1)		P 14	44.54	2.195(1)		P 7	85.12	Null	
P 24	11.12	1.004(1)		P 18	46.93	2.278(1)		P 5	99.45	2.490(0)	
P 23	18.28	9.928(0)		P 13	49.31	2.559(1)		P 3	113.77	Null	
P 22	25.44	1.009(1)		P 17	51.70	3.195(1)		P 1	128.09	Null	

Gauge Label	Angle (deg)	(BTU/Ft2-Sec)	T Surf (DegR)	Gauge Label	Angle (deg)	(BTU/Ft2-Sec)	T Surf (DegR)	Gauge Label	Angle (deg)	(BTU/Ft2-Sec)	T Surf (DegR)
HT 42	-9.65	4.829(1)	587.09	HT 26	34.61	Null	Null	HT 6	54.88	3.074(2)	778.23
HT 41	-6.43	4.901(1)	588.64	HT 25	37.66	1.959(2)	710.69	HT 5	55.68	3.290(2)	780.87
HT 40	-3.21	4.687(1)	584.91	HT 24	40.72	2.391(2)	728.44	HT 4	56.47	3.000(2)	766.74
HT 39	.01	5.116(1)	588.19	HT 63	44.54	Null	Null	HT 3	57.27	2.562(2)	750.91
HT 38	3.23	5.419(1)	589.58	HT 64	45.49	3.061(2)	769.70	HT 2	58.07	2.568(2)	741.85
HT 37	6.45	5.755(1)	595.49	HT 65	46.45	3.135(2)	772.92	HT 62	58.87	2.882(2)	761.26
HT 36	9.67	5.961(1)	596.47	HT 66	47.40	2.895(2)	772.20	HT 1	58.87	2.627(2)	742.51
HT 35	12.89	Null	Null	HT 67	48.36	3.154(2)	785.42	HT 61	61.93	2.144(2)	722.36
HT 34	16.27	6.878(1)	602.68	HT 68	49.31	3.230(2)	784.94	HT 59	68.04	1.645(2)	676.02
HT 32	16.27	Null	Null	HT 69	50.27	3.118(2)	778.91	HT 58	71.10	1.530(2)	664.65
HT 31	19.33	7.239(1)	605.93	HT 70	51.22	Null	Null	HT 57	74.15	1.294(2)	647.63
HT 30	22.38	Null	Null	HT 10	51.68	3.082(2)	776.83	HT 56	77.21	1.056(2)	628.11
HT 29	25.44	8.278(1)	615.77	HT 71	52.18	Null	Null	HT 55	80.26	8.184(1)	609.02
HT 28	28.50	8.926(1)	620.95	HT 9	52.48	3.147(2)	778.20	HT 54	83.32	6.428(1)	597.13
HT 27	31.55	Null	Null	HT 7	54.09	2.906(2)	766.78	HT 53	86.38	4.848(1)	582.09

Run 26 Reduced Data Tabulation

Gauge Label	Angle (deg)	(PSIA)	T Surf (DegR)	Gauge Label	Angle (deg)	(PSIA)	T Surf (DegR)	Gauge Label	Angle (deg)	(PSIA)	T Surf (DegR)
P 30	-64.44	Null		P 20	4.79	1.840(0)		P 11	26.28	Null	
P 28	-50.11	3.166(0)		P 15	7.18	Null		P 10	31.05	1.014(2)	
P 26	-35.79	5.088(0)		P 19	9.57	2.741(0)		P 9	38.22	2.821(1)	
P 25	-28.63	5.858(0)		P 14	11.96	3.965(0)		P 7	52.54	Null	
P 24	-21.47	4.589(0)		P 18	14.34	6.567(0)		P 5	66.86	1.668(1)	
P 23	-14.30	2.801(0)		P 13	16.73	8.995(0)		P 3	81.19	Null	
P 22	-7.14	1.476(0)		P 17	19.12	2.672(1)		P 1	95.51	Null	
P 21	.02	Null		P 12	21.51	3.381(1)					

Gauge Label	Angle (deg)	(BTU/Ft2-Sec)	T Surf (DegR)	Gauge Label	Angle (deg)	(BTU/Ft2-Sec)	T Surf (DegR)	Gauge Label	Angle (deg)	(BTU/Ft2-Sec)	T Surf (DegR)
HT 42	-42.23	5.005(1)	589.33	HT 26	2.02	Null	Null	HT 6	22.30	1.812(2)	844.26
HT 41	-39.01	5.568(1)	592.51	HT 25	5.08	1.869(1)	562.15	HT 5	23.09	2.241(2)	870.27
HT 40	-35.79	6.112(1)	595.76	HT 24	8.14	2.322(1)	569.41	HT 4	23.89	2.891(2)	927.28
HT 39	-32.57	6.362(1)	595.35	HT 63	11.96	Null	Null	HT 3	24.69	3.288(2)	943.48
HT 38	-29.35	7.258(1)	598.62	HT 64	12.91	2.889(1)	586.10	HT 2	25.49	3.653(2)	982.68
HT 37	-26.13	8.197(1)	599.63	HT 65	13.87	4.515(1)	615.32	HT 62	26.29	7.043(2)	1059.90
HT 36	-22.91	8.709(1)	599.26	HT 66	14.82	2.978(1)	613.35	HT 1	26.29	4.437(2)	1019.10
HT 35	-19.69	Null	Null	HT 67	15.78	5.415(1)	626.31	HT 61	29.35	9.439(2)	1011.20
HT 34	-16.31	7.093(1)	582.06	HT 68	16.73	4.686(1)	633.69	HT 59	35.46	2.566(2)	752.36
HT 32	-16.31	9.974(1)	600.02	HT 69	17.69	6.397(1)	652.69	HT 58	38.51	1.829(2)	753.36
HT 31	-13.25	4.996(1)	569.00	HT 70	18.64	Null	Null	HT 57	41.57	2.384(2)	768.92
HT 30	-10.20	Null	Null	HT 10	19.10	9.737(1)	698.08	HT 56	44.63	2.485(2)	750.33
HT 29	-7.14	1.922(1)	554.39	HT 71	19.60	Null	Null	HT 55	47.68	2.385(2)	732.30
HT 28	-4.09	1.342(1)	550.58	HT 9	19.90	1.361(2)	742.04	HT 54	50.74	1.925(2)	708.78
HT 27	-1.03	Null	Null	HT 7	21.51	1.591(2)	780.55	HT 53	53.79	1.635(2)	693.21

Run 27 Reduced Data Tabulation

Gauge Label	Angle (deg)	(PSIA)	T Surf (DegR)	Gauge Label	Angle (deg)	(PSIA)	T Surf (DegR)	Gauge Label	Angle (deg)	(PSIA)	T Surf (DegR)
P 30	-64.44	Null		P 20	4.79	3.321(0)		P 11	26.28	2.996(1)	
P 28	-50.11	7.445(-1)		P 15	7.18	Null		P 10	31.05	1.451(1)	
P 26	-35.79	5.077(-1)		P 19	9.57	5.010(0)		P 9	38.22	1.521(1)	
P 25	-28.63	4.425(-1)		P 14	11.96	7.555(0)		P 7	52.54	Null	
P 24	-21.47	1.472(-1)		P 18	14.34	1.424(1)		P 5	66.86	8.930(0)	
P 23	-14.30	4.023(-1)		P 13	16.73	2.484(1)		P 3	81.19	Null	
P 22	-7.14	2.912(-1)		P 17	19.12	6.396(1)		P 1	95.51	3.047(0)	
P 21	.02	Null		P 12	21.51	4.822(1)					

Gauge Label	Angle (deg)	(BTU/Ft2-Sec)	T Surf (DegR)	Gauge Label	Angle (deg)	(BTU/Ft2-Sec)	T Surf (DegR)	Gauge Label	Angle (deg)	(BTU/Ft2-Sec)	T Surf (DegR)
HT 42	-42.23	1.109(1)	554.21	HT 26	2.02	Null	Null	HT 6	22.30	5.723(2)	942.06
HT 41	-39.01	9.904(0)	553.36	HT 25	5.08	3.032(1)	573.35	HT 5	23.09	5.670(2)	954.73
HT 40	-35.79	6.019(0)	550.45	HT 24	8.14	4.125(1)	583.77	HT 4	23.89	5.371(2)	950.86
HT 39	-32.57	4.483(0)	548.09	HT 63	11.96	Null	Null	HT 3	24.69	4.601(2)	918.55
HT 38	-29.35	2.442(0)	545.80	HT 64	12.91	1.075(2)	643.16	HT 2	25.49	4.265(2)	907.77
HT 37	-26.13	1.365(0)	543.77	HT 65	13.87	1.349(2)	676.28	HT 62	26.29	3.056(2)	829.84
HT 36	-22.91	6.458(0)	549.64	HT 66	14.82	1.753(2)	695.18	HT 1	26.29	3.647(2)	875.66
HT 35	-19.69	Null	Null	HT 67	15.78	1.918(2)	717.30	HT 61	29.35	1.742(2)	725.80
HT 34	-16.31	2.159(0)	543.49	HT 68	16.73	2.554(2)	746.09	HT 59	35.46	1.475(2)	683.71
HT 32	-16.31	4.543(0)	550.17	HT 69	17.69	3.000(2)	777.23	HT 58	38.51	1.449(2)	685.95
HT 31	-13.25	2.315(0)	543.73	HT 70	18.64	Null	Null	HT 57	41.57	1.174(2)	671.15
HT 30	-10.20	Null	Null	HT 10	19.10	4.185(2)	848.58	HT 56	44.63	1.039(2)	651.71
HT 29	-7.14	4.915(0)	547.10	HT 71	19.60	Null	Null	HT 55	47.68	1.013(2)	644.31
HT 28	-4.09	7.419(0)	547.54	HT 9	19.90	4.889(2)	883.24	HT 54	50.74	8.703(1)	634.98
HT 27	-1.03	Null	Null	HT 7	21.51	4.492(2)	884.01	HT 53	53.79	7.333(1)	624.17

Run 28 Reduced Data Tabulation

Gauge Label	Angle (deg)	(PSIA)	T Surf (DegR)	Gauge Label	Angle (deg)	(PSIA)	T Surf (DegR)	Gauge Label	Angle (deg)	(PSIA)	T Surf (DegR)
P 28	-35.79	4.800(0)		P 15	21.51	Null		P 10	45.38	7.012(1)	
P 26	-21.47	6.510(0)		P 19	23.89	1.175(1)		P 9	52.54	2.843(1)	
P 24	-7.14	7.758(0)		P 14	26.28	1.497(1)		P 7	66.86	Null	
P 23	.02	8.840(0)		P 18	28.67	1.997(1)		P 5	81.19	6.888(0)	
P 22	7.18	8.107(0)		P 13	31.05	2.403(1)		P 3	95.51	Null	
P 21	14.34	Null		P 17	33.44	4.387(1)		P 1	109.84	1.262(0)	
P 20	19.12	8.042(0)		P 11	40.60	8.633(1)					

Gauge Label	Angle (deg)	(BTU/Ft2-Sec)	T Surf (DegR)	Gauge Label	Angle (deg)	(BTU/Ft2-Sec)	T Surf (DegR)	Gauge Label	Angle (deg)	(BTU/Ft2-Sec)	T Surf (DegR)
HT 42	-27.91	5.838(1)	586.73	HT 26	16.35	Null	Null	HT 6	36.62	4.914(2)	869.12
HT 41	-24.69	6.145(1)	589.79	HT 25	19.40	8.790(1)	614.49	HT 5	37.42	5.974(2)	899.19
HT 40	-21.47	6.611(1)	591.39	HT 24	22.46	1.163(2)	636.47	HT 4	38.22	6.938(2)	935.70
HT 39	-18.25	6.292(1)	591.11	HT 63	26.28	Null	Null	HT 3	39.01	7.846(2)	946.65
HT 38	-15.03	6.833(1)	593.66	HT 64	27.23	1.753(2)	680.63	HT 2	39.81	8.825(2)	984.19
HT 37	-11.81	7.451(1)	599.46	HT 65	28.19	1.824(2)	690.45	HT 62	40.62	8.240(2)	975.18
HT 36	-8.59	7.610(1)	602.25	HT 66	29.14	2.014(2)	700.67	HT 1	40.62	8.828(2)	980.29
HT 35	-5.37	Null	Null	HT 67	30.10	2.215(2)	719.71	HT 61	43.67	6.545(2)	936.10
HT 34	-1.99	9.512(1)	612.92	HT 68	31.05	2.641(2)	734.50	HT 59	49.78	2.543(2)	751.84
HT 32	-1.99	Null	Null	HT 69	32.01	2.616(2)	746.20	HT 58	52.84	1.621(2)	691.40
HT 31	1.07	1.005(2)	617.98	HT 70	32.96	Null	Null	HT 57	55.89	1.237(2)	660.35
HT 30	4.13	Null	Null	HT 10	33.42	3.183(2)	784.75	HT 56	58.95	9.221(1)	634.07
HT 29	7.18	8.111(1)	607.18	HT 71	33.92	Null	Null	HT 55	62.01	7.446(1)	619.49
HT 28	10.24	8.232(1)	613.63	HT 9	34.22	3.495(2)	802.19	HT 54	65.06	6.962(1)	611.27
HT 27	13.29	Null	Null	HT 7	35.83	3.802(2)	809.83	HT 53	68.12	7.385(1)	606.55

Run 29 Reduced Data Tabulation

Gauge Label	Angle (deg)	(PSIA)	T Surf (DegR)	Gauge Label	Angle (deg)	(PSIA)	T Surf (DegR)	Gauge Label	Angle (deg)	(PSIA)	T Surf (DegR)
P 30	-90.72	Null		P 20	-21.49	1.583(1)		P 11	.00	Null	
P 28	-76.39	Null		P 15	-19.10	1.804(1)		P 10	4.77	3.353(1)	
P 26	-62.07	3.003(-1)		P 19	-16.71	1.994(1)		P 9	11.94	3.656(1)	
P 25	-54.91	1.040(0)		P 14	-14.32	2.185(1)		P 7	26.26	Null	
P 24	-47.75	1.825(0)		P 18	-11.94	2.457(1)		P 5	40.58	3.273(1)	
P 23	-40.58	3.512(0)		P 13	-9.55	2.647(1)		P 3	54.91	2.188(1)	
P 22	-33.42	6.318(0)		P 17	-7.16	3.405(1)		P 1	69.23	1.223(1)	
P 21	-26.26	Null		P 12	-4.77	3.669(1)					

Gauge Label	Angle (deg)	(BTU/Ft2-Sec)	T Surf (DegR)	Gauge Label	Angle (deg)	(BTU/Ft2-Sec)	T Surf (DegR)	Gauge Label	Angle (deg)	(BTU/Ft2-Sec)	T Surf (DegR)
HT 42	-68.51	2.036(0)	534.84	HT 26	-24.26	Null	Null	HT 6	-3.98	1.349(2)	668.00
HT 41	-65.29	-1.718(0)	536.84	HT 25	-21.20	9.696(1)	632.14	HT 5	-3.19	1.496(2)	645.33
HT 40	-62.07	3.051(0)	538.01	HT 24	-18.14	5.212(1)	596.71	HT 4	-2.39	1.480(2)	656.40
HT 39	-58.85	4.669(0)	539.11	HT 63	-14.32	Null	Null	HT 3	-1.59	1.146(2)	643.91
HT 38	-55.63	3.374(0)	540.32	HT 64	-13.37	6.991(1)	612.09	HT 2	-.79	9.934(1)	638.37
HT 37	-52.41	-3.877(0)	536.12	HT 65	-12.41	1.093(2)	641.34	HT 62	.01	1.114(2)	650.64
HT 36	-49.19	7.530(0)	546.07	HT 66	-11.46	8.811(1)	631.89	HT 1	.01	1.144(2)	645.43
HT 35	-45.97	Null	Null	HT 67	-10.50	1.206(2)	635.33	HT 61	3.07	1.237(2)	677.36
HT 34	-42.59	1.626(1)	552.38	HT 68	-9.55	8.310(1)	633.60	HT 59	9.18	1.133(2)	657.63
HT 32	-42.59	3.154(1)	563.62	HT 69	-8.59	1.089(2)	630.91	HT 58	12.23	9.903(1)	660.70
HT 31	-39.53	2.335(1)	562.44	HT 70	-7.64	Null	Null	HT 57	15.29	1.132(2)	661.52
HT 30	-36.48	Null	Null	HT 10	-7.18	1.010(2)	628.42	HT 56	18.35	7.451(1)	617.68
HT 29	-33.42	3.996(1)	570.76	HT 71	-6.68	Null	Null	HT 55	21.40	1.059(2)	651.02
HT 28	-30.37	3.719(1)	577.69	HT 9	-6.38	1.067(2)	641.29	HT 54	24.46	9.743(1)	648.00
HT 27	-27.31	Null	Null	HT 7	-4.77	9.925(1)	640.28	HT 53	27.51	9.336(1)	646.96

Run 30 Reduced Data Tabulation

Gauge Label	Angle (deg)	(PSIA)	T Surf (DegR)	Gauge Label	Angle (deg)	(PSIA)	T Surf (DegR)	Gauge Label	Angle (deg)	(PSIA)	T Surf (DegR)
P 30	-78.76	Null		P 20	-9.53	9.990(0)		P 11	11.96	Null	
P 28	-64.44	2.448(0)		P 15	-7.14	1.002(1)		P 10	16.73	9.050(0)	
P 26	-50.11	4.432(0)		P 19	-4.76	1.018(1)		P 9	23.89	8.697(0)	
P 25	-42.95	5.871(0)		P 14	-2.37	9.531(0)		P 7	38.22	Null	
P 24	-35.79	6.710(0)		P 18	.02	9.967(0)		P 5	52.54	4.204(0)	
P 23	-28.63	7.774(0)		P 13	2.41	9.873(0)		P 3	66.86	Null	
P 22	-21.47	8.884(0)		P 17	4.79	9.689(0)		P 1	81.19	1.220(0)	
P 21	-14.30	Null		P 12	7.18	9.666(0)					

Gauge Label	Angle (deg)	(BTU/Ft2-Sec)	T Surf (DegR)	Gauge Label	Angle (deg)	(BTU/Ft2-Sec)	T Surf (DegR)	Gauge Label	Angle (deg)	(BTU/Ft2-Sec)	T Surf (DegR)
HT 42	-56.55	2.430(1)	556.55	HT 26	-12.30	Null	Null	HT 6	7.97	Null	Null
HT 41	-53.33	2.603(1)	557.93	HT 25	-9.24	Null	Null	HT 5	8.77	5.878(1)	586.33
HT 40	-50.11	3.063(1)	562.08	HT 24	-6.19	6.040(1)	587.55	HT 4	9.57	Null	Null
HT 39	-46.89	3.082(1)	562.51	HT 63	-2.37	Null	Null	HT 3	10.37	5.682(1)	584.15
HT 38	-43.67	3.409(1)	564.74	HT 64	-1.41	6.166(1)	587.81	HT 2	11.17	5.893(1)	586.84
HT 37	-40.45	4.239(1)	570.24	HT 65	-.46	6.160(1)	588.58	HT 62	11.97	5.967(1)	587.88
HT 36	-37.24	4.026(1)	570.84	HT 66	.50	5.973(1)	587.28	HT 1	11.97	5.519(1)	583.97
HT 35	-34.02	Null	Null	HT 67	1.45	6.266(1)	591.58	HT 61	15.02	5.976(1)	589.43
HT 34	-30.63	4.554(1)	575.21	HT 68	2.41	6.617(1)	592.31	HT 59	21.13	4.895(1)	579.34
HT 32	-30.63	Null	Null	HT 69	3.36	Null	Null	HT 58	24.19	4.970(1)	579.92
HT 31	-27.58	4.832(1)	577.43	HT 70	4.32	Null	Null	HT 57	27.25	4.789(1)	577.57
HT 30	-24.52	Null	Null	HT 10	4.77	5.982(1)	587.02	HT 56	30.30	4.361(1)	574.11
HT 29	-21.47	5.425(1)	582.82	HT 71	5.27	Null	Null	HT 55	33.36	4.183(1)	572.25
HT 28	-18.41	Null	Null	HT 9	5.58	5.859(1)	585.99	HT 54	36.41	4.112(1)	571.31
HT 27	-15.36	Null	Null	HT 7	7.18	Null	Null	HT 53	39.47	3.634(1)	566.72

Run 31 Reduced Data Tabulation

Gauge Label	Angle (deg)	(PSIA)	T Surf (DegR)	Gauge Label	Angle (deg)	(PSIA)	T Surf (DegR)	Gauge Label	Angle (deg)	(PSIA)	T Surf (DegR)
P 30	-78.76	Null		P 20	-9.53	3.060(1)		P 11	11.96	Null	
P 28	-64.44	7.853(0)		P 15	-7.14	3.078(1)		P 10	16.73	2.677(1)	
P 26	-50.11	1.397(1)		P 19	-4.76	3.082(1)		P 9	23.89	2.602(1)	
P 25	-42.95	1.872(1)		P 14	-2.37	3.021(1)		P 7	38.22	Null	
P 24	-35.79	2.079(1)		P 18	.02	3.030(1)		P 5	52.54	1.279(1)	
P 23	-28.63	2.389(1)		P 13	2.41	3.007(1)		P 3	66.86	Null	
P 22	-21.47	2.607(1)		P 17	4.79	3.201(1)		P 1	81.19	Null	
P 21	-14.30	Null		P 12	7.18	3.125(1)					

Gauge Label	Angle (deg)	(BTU/Ft2-Sec)	T Surf (DegR)	Gauge Label	Angle (deg)	(BTU/Ft2-Sec)	T Surf (DegR)	Gauge Label	Angle (deg)	(BTU/Ft2-Sec)	T Surf (DegR)
HT 42	-56.55	2.780(1)	565.58	HT 26	-12.30	Null	Null	HT 6	7.97	6.673(1)	611.65
HT 41	-53.33	2.887(1)	566.96	HT 25	-9.24	6.440(1)	606.39	HT 5	8.77	6.374(1)	610.89
HT 40	-50.11	3.029(1)	569.32	HT 24	-6.19	Null	Null	HT 4	9.57	6.641(1)	609.34
HT 39	-46.89	3.332(1)	572.26	HT 63	-2.37	Null	Null	HT 3	10.37	6.381(1)	606.49
HT 38	-43.67	3.630(1)	575.08	HT 64	-1.41	6.538(1)	606.54	HT 2	11.17	6.512(1)	607.45
HT 37	-40.45	3.712(1)	576.64	HT 65	-.46	6.771(1)	609.97	HT 62	11.97	Null	Null
HT 36	-37.24	4.222(1)	581.95	HT 66	.50	6.494(1)	605.79	HT 1	11.97	6.589(1)	606.43
HT 35	-34.02	Null	Null	HT 67	1.45	6.441(1)	608.88	HT 61	15.02	6.133(1)	607.02
HT 34	-30.63	4.599(1)	585.65	HT 68	2.41	6.799(1)	608.49	HT 59	21.13	5.310(1)	596.73
HT 32	-30.63	Null	Null	HT 69	3.36	7.075(1)	614.77	HT 58	24.19	5.877(1)	600.77
HT 31	-27.58	5.399(1)	594.75	HT 70	4.32	Null	Null	HT 57	27.25	5.033(1)	593.78
HT 30	-24.52	Null	Null	HT 10	4.77	6.846(1)	616.93	HT 56	30.30	4.758(1)	588.33
HT 29	-21.47	5.881(1)	600.31	HT 71	5.27	Null	Null	HT 55	33.36	4.650(1)	587.57
HT 28	-18.41	6.217(1)	601.34	HT 9	5.58	6.369(1)	612.91	HT 54	36.41	4.389(1)	582.52
HT 27	-15.36	Null	Null	HT 7	7.18	6.432(1)	610.74	HT 53	39.47	4.062(1)	580.64

Run 32 Reduced Data Tabulation

Gauge Label	Angle (deg)	(PSIA)	T Surf (DegR)	Gauge Label	Angle (deg)	(PSIA)	T Surf (DegR)	Gauge Label	Angle (deg)	(PSIA)	T Surf (DegR)
P 30	-60.85	Null		P 20	8.38	1.880(1)		P 16	27.48	5.122(0)	
P 28	-46.52	6.207(0)		P 15	10.77	1.324(1)		P 11	29.87	1.782(0)	
P 26	-32.20	Null		P 19	13.16	Null		P 10	34.64	1.533(-2)	
P 25	-25.04	6.001(1)		P 14	15.55	9.358(0)		P 9	41.81	1.105(0)	
P 24	-17.88	Null		P 18	17.93	8.159(0)		P 7	56.13	-6.014(-1)	
P 23	-10.71	Null		P 13	20.32	Null		P 5	70.45	5.758(-1)	
P 22	-3.55	Null		P 17	22.71	5.907(0)		P 3	84.78	6.607(-1)	
P 21	3.61	2.465(1)		P 12	25.10	5.501(0)		P 1	99.10	1.574(-1)	

Gauge Label	Angle (deg)	(BTU/Ft2-Sec)	T Surf (DegR)	Gauge Label	Angle (deg)	(BTU/Ft2-Sec)	T Surf (DegR)	Gauge Label	Angle (deg)	(BTU/Ft2-Sec)	T Surf (DegR)
HT 42	-38.64	2.138(2)	697.98	HT 81	3.13	1.867(2)	676.83	HT 107	23.50	3.136(1)	608.12
HT 41	-35.42	2.651(2)	726.37	HT 11	9.98	1.224(2)	630.86	HT 108	24.30	5.316(1)	617.33
HT 40	-32.20	3.207(2)	752.06	HT 12	10.78	1.386(2)	644.26	HT 109	25.09	8.704(1)	628.17
HT 39	-28.98	3.947(2)	785.01	HT 13	11.57	1.411(2)	624.79	HT 110	25.89	3.951(1)	595.79
HT 38	-25.76	4.451(2)	794.54	HT 14	12.37	1.234(2)	633.52	HT 111	26.68	4.546(1)	592.55
HT 37	-22.54	5.400(2)	817.51	HT 15	13.16	1.084(2)	616.01	HT 112	27.48	2.922(1)	587.31
HT 36	-19.32	7.618(2)	882.37	HT 16	13.96	1.074(2)	617.08	HT 113	28.27	4.422(1)	594.43
HT 35	-16.10	Null	Null	HT 17	14.75	9.651(1)	624.78	HT 43	29.07	5.463(1)	579.64
HT 34	-12.72	Null	Null	HT 18	15.55	1.143(2)	630.21	HT 114	29.07	4.480(1)	593.63
HT 33	-9.66	Null	Null	HT 19	16.34	8.353(1)	622.57	HT 44	32.25	4.271(1)	565.15
HT 72	-5.46	3.744(2)	795.20	HT 20	17.14	7.311(1)	616.30	HT 45	35.44	4.471(1)	561.34
HT 73	-4.51	4.539(2)	813.24	HT 21	17.93	7.409(1)	617.65	HT 46	38.62	3.138(1)	554.04
HT 74	-3.55	3.773(2)	780.87	HT 22	18.72	8.106(1)	627.56	HT 47	41.81	2.655(1)	550.22
HT 75	-2.60	2.625(2)	746.77	HT 101	18.72	6.044(1)	611.59	HT 48	44.99	2.117(1)	546.64
HT 76	-1.64	3.017(2)	756.03	HT 102	19.52	9.883(1)	630.83	HT 49	48.18	1.835(1)	544.23
HT 77	-.69	2.567(2)	742.14	HT 103	20.31	1.585(2)	664.79	HT 50	51.36	1.613(1)	542.36
HT 78	.27	2.384(2)	722.79	HT 104	21.11	8.823(1)	630.26	HT 51	54.55	1.240(1)	539.67
HT 79	1.22	2.343(2)	728.47	HT 105	21.90	7.576(1)	640.00	HT 52	57.73	2.196(1)	546.50
HT 80	2.18	2.261(2)	722.16	HT 106	22.71	5.229(1)	617.64				

Run 33 Reduced Data Tabulation

Gauge Label	Angle (deg)	(PSIA)	T Surf (DegR)	Gauge Label	Angle (deg)	(PSIA)	T Surf (DegR)	Gauge Label	Angle (deg)	(PSIA)	T Surf (DegR)
P 30	-60.85	Null		P 20	8.38	1.969(1)		P 16	27.48	6.954(1)	
P 28	-46.52	Null		P 15	10.77	3.320(1)		P 11	29.87	Null	
P 26	-32.20	3.334(0)		P 19	13.16	6.134(1)		P 10	34.64	Null	
P 25	-25.04	2.192(0)		P 14	15.55	9.046(1)		P 9	41.81	Null	
P 24	-17.88	2.244(0)		P 18	17.93	1.162(2)		P 7	56.13	3.521(1)	
P 23	-10.71	1.995(0)		P 13	20.32	Null		P 5	70.45	1.408(1)	
P 22	-3.55	4.013(0)		P 17	22.71	8.090(1)		P 3	84.78	4.308(0)	
P 21	3.61	8.359(0)		P 12	25.10	6.493(1)		P 1	99.10	1.199(0)	

Gauge Label	Angle (deg)	(BTU/Ft2-Sec)	T Surf (DegR)	Gauge Label	Angle (deg)	(BTU/Ft2-Sec)	T Surf (DegR)	Gauge Label	Angle (deg)	(BTU/Ft2-Sec)	T Surf (DegR)
HT 42	-38.64	5.687(1)	572.54	HT 81	3.13	7.703(1)	618.64	HT 107	23.50	4.613(2)	820.54
HT 41	-35.42	6.004(1)	574.70	HT 11	9.98	2.477(2)	698.54	HT 108	24.30	4.829(2)	824.25
HT 40	-32.20	5.124(1)	571.51	HT 12	10.78	3.270(2)	742.11	HT 109	25.09	3.749(2)	786.23
HT 39	-28.98	4.428(1)	570.52	HT 13	11.57	2.510(2)	735.72	HT 110	25.89	3.802(2)	793.58
HT 38	-25.76	3.301(1)	564.38	HT 14	12.37	4.259(2)	775.35	HT 111	26.68	3.769(2)	809.58
HT 37	-22.54	2.104(1)	559.71	HT 15	13.16	4.412(2)	777.22	HT 112	27.48	3.803(2)	814.99
HT 36	-19.32	2.084(1)	559.89	HT 16	13.96	5.787(2)	811.83	HT 113	28.27	3.512(2)	802.93
HT 35	-16.10	1.062(1)	556.71	HT 17	14.75	6.925(2)	833.94	HT 43	29.07	3.798(2)	802.34
HT 34	-12.72	Null	Null	HT 18	15.55	8.652(2)	867.44	HT 114	29.07	2.973(2)	787.03
HT 33	-9.66	1.602(1)	557.89	HT 19	16.34	8.254(2)	866.69	HT 44	32.25	3.402(2)	801.05
HT 72	-5.46	-6.121(0)	558.90	HT 20	17.14	9.646(2)	878.02	HT 45	35.44	2.922(2)	768.54
HT 73	-4.51	4.338(0)	566.29	HT 21	17.93	1.096(3)	920.44	HT 46	38.62	Null	Null
HT 74	-3.55	1.272(1)	561.96	HT 22	18.72	1.187(3)	957.51	HT 47	41.81	2.491(2)	736.76
HT 75	-2.60	1.724(1)	558.45	HT 101	18.72	1.182(3)	945.86	HT 48	44.99	2.283(2)	726.00
HT 76	-1.64	1.447(1)	565.43	HT 102	19.52	9.726(2)	910.97	HT 49	48.18	Null	Null
HT 77	-.69	2.261(1)	570.19	HT 103	20.31	9.175(2)	880.36	HT 50	51.36	1.971(2)	705.76
HT 78	.27	2.309(1)	575.09	HT 104	21.11	7.667(2)	882.80	HT 51	54.55	Null	Null
HT 79	1.22	1.446(1)	580.04	HT 105	21.90	6.183(2)	846.57	HT 52	57.73	1.578(2)	678.29
HT 80	2.18	7.196(1)	615.37	HT 106	22.71	6.203(2)	836.48				

Run 34 Reduced Data Tabulation

Gauge Label	Angle (deg)	(PSIA)	T Surf (DegR)	Gauge Label	Angle (deg)	(PSIA)	T Surf (DegR)	Gauge Label	Angle (deg)	(PSIA)	T Surf (DegR)
P 30	-60.85	2.244(-2)		P 20	8.38	4.661(0)		P 16	27.48	1.332(2)	
P 28	-46.52	4.327(0)		P 15	10.77	6.476(0)		P 11	29.87	4.949(1)	
P 26	-32.20	8.238(0)		P 19	13.16	1.079(1)		P 10	34.64	3.727(1)	
P 25	-25.04	1.126(1)		P 14	15.55	1.441(1)		P 9	41.81	4.267(1)	
P 24	-17.88	1.253(1)		P 18	17.93	3.200(1)		P 7	56.13	3.345(1)	
P 23	-10.71	9.883(0)		P 13	20.32	5.197(1)		P 5	70.45	1.887(1)	
P 22	-3.55	4.736(0)		P 17	22.71	1.436(2)		P 3	84.78	7.272(0)	
P 21	3.61	3.426(0)		P 12	25.10	1.505(2)		P 1	99.10	2.286(0)	

Gauge Label	Angle (deg)	(BTU/Ft2-Sec)	T Surf (DegR)	Gauge Label	Angle (deg)	(BTU/Ft2-Sec)	T Surf (DegR)	Gauge Label	Angle (deg)	(BTU/Ft2-Sec)	T Surf (DegR)
HT 42	-38.64	5.760(1)	581.62	HT 81	3.13	3.694(1)	577.96	HT 107	23.50	1.413(3)	1047.90
HT 41	-35.42	4.816(1)	571.91	HT 11	9.98	5.716(1)	584.79	HT 108	24.30	1.362(3)	1059.60
HT 40	-32.20	8.681(1)	601.63	HT 12	10.78	6.802(1)	599.02	HT 109	25.09	1.195(3)	1032.40
HT 39	-28.98	9.155(1)	601.74	HT 13	11.57	8.068(1)	599.04	HT 110	25.89	1.003(3)	999.02
HT 38	-25.76	9.296(1)	604.88	HT 14	12.37	7.484(1)	606.63	HT 111	26.68	9.596(2)	1025.40
HT 37	-22.54	1.562(2)	648.39	HT 15	13.16	7.069(1)	602.83	HT 112	27.48	8.497(2)	988.68
HT 36	-19.32	1.271(2)	622.71	HT 16	13.96	1.080(2)	607.29	HT 113	28.27	5.803(2)	908.43
HT 35	-16.10	1.461(2)	634.20	HT 17	14.75	1.203(2)	622.48	HT 43	29.07	6.251(2)	894.75
HT 34	-12.72	1.336(2)	630.04	HT 18	15.55	1.602(2)	626.42	HT 114	29.07	5.371(2)	886.28
HT 33	-9.66	1.172(2)	624.09	HT 19	16.34	1.646(2)	646.15	HT 44	32.25	3.855(2)	806.23
HT 72	-5.46	7.395(1)	616.39	HT 20	17.14	1.900(2)	661.78	HT 45	35.44	3.140(2)	780.79
HT 73	-4.51	5.864(1)	598.36	HT 21	17.93	2.083(2)	665.84	HT 46	38.62	Null	Null
HT 74	-3.55	4.178(1)	583.55	HT 22	18.72	3.266(2)	727.57	HT 47	41.81	3.287(2)	761.20
HT 75	-2.60	2.786(1)	578.08	HT 101	18.72	3.536(2)	737.14	HT 48	44.99	2.901(2)	753.66
HT 76	-1.64	3.664(1)	582.35	HT 102	19.52	5.761(2)	800.02	HT 49	48.18	3.614(2)	791.04
HT 77	-.69	4.301(0)	577.24	HT 103	20.31	5.486(2)	814.26	HT 50	51.36	2.375(2)	718.20
HT 78	.27	2.433(1)	571.52	HT 104	21.11	7.942(2)	895.05	HT 51	54.55	Null	Null
HT 79	1.22	1.873(1)	563.45	HT 105	21.90	1.009(3)	957.53	HT 52	57.73	2.012(2)	696.86
HT 80	2.18	4.944(1)	594.63	HT 106	22.71	1.184(3)	993.53				

Run 35 Reduced Data Tabulation

Gauge Label	Angle (deg)	(PSIA)	T Surf (DegR)	Gauge Label	Angle (deg)	(PSIA)	T Surf (DegR)	Gauge Label	Angle (deg)	(PSIA)	T Surf (DegR)
P 30	-60.85	Null		P 20	8.38	6.200(1)		P 16	27.48	6.417(1)	
P 28	-46.52	Null		P 15	10.77	Null		P 11	29.87	Null	
P 26	-32.20	5.487(-1)		P 19	13.16	Null		P 10	34.64	Null	
P 25	-25.04	5.678(-1)		P 14	15.55	Null		P 9	41.81	Null	
P 24	-17.88	9.910(-1)		P 18	17.93	9.921(1)		P 7	56.13	3.073(1)	
P 23	-10.71	5.911(-1)		P 13	20.32	Null		P 5	70.45	1.333(1)	
P 22	-3.55	7.837(0)		P 17	22.71	6.378(1)		P 3	84.78	1.845(0)	
P 21	3.61	2.524(1)		P 12	25.10	5.482(1)		P 1	99.10	1.163(0)	

Gauge Label	Angle (deg)	(BTU/Ft2-Sec)	T Surf (DegR)	Gauge Label	Angle (deg)	(BTU/Ft2-Sec)	T Surf (DegR)	Gauge Label	Angle (deg)	(BTU/Ft2-Sec)	T Surf (DegR)
HT 42	-38.64	1.314(1)	545.63	HT 81	3.13	1.772(2)	732.61	HT 107	23.50	3.426(2)	733.54
HT 41	-35.42	1.014(1)	545.10	HT 11	9.98	5.202(2)	881.35	HT 108	24.30	3.372(2)	722.12
HT 40	-32.20	6.705(0)	543.68	HT 12	10.78	7.066(2)	914.67	HT 109	25.09	Null	Null
HT 39	-28.98	4.232(0)	540.91	HT 13	11.57	7.621(2)	920.52	HT 110	25.89	2.960(2)	694.70
HT 38	-25.76	4.785(0)	544.09	HT 14	12.37	9.325(2)	948.98	HT 111	26.68	3.135(2)	721.94
HT 37	-22.54	Null	Null	HT 15	13.16	9.166(2)	917.80	HT 112	27.48	3.189(2)	714.40
HT 36	-19.32	1.361(1)	549.98	HT 16	13.96	1.074(3)	946.15	HT 113	28.27	2.969(2)	706.90
HT 35	-16.10	1.495(1)	554.57	HT 17	14.75	Null	Null	HT 43	29.07	2.939(2)	732.12
HT 34	-12.72	1.749(1)	557.85	HT 18	15.55	1.168(3)	938.02	HT 114	29.07	2.082(2)	684.25
HT 33	-9.66	3.081(1)	567.25	HT 19	16.34	9.601(2)	894.45	HT 44	32.25	2.421(2)	714.24
HT 72	-5.46	7.409(1)	612.33	HT 20	17.14	8.087(2)	853.23	HT 45	35.44	2.216(2)	704.71
HT 73	-4.51	9.628(1)	645.47	HT 21	17.93	9.264(2)	872.93	HT 46	38.62	2.029(2)	698.79
HT 74	-3.55	4.470(1)	596.02	HT 22	18.72	7.855(2)	842.97	HT 47	41.81	1.907(2)	688.46
HT 75	-2.60	4.575(1)	596.62	HT 101	18.72	7.052(2)	812.71	HT 48	44.99	1.591(2)	668.64
HT 76	-1.64	7.013(1)	615.02	HT 102	19.52	3.082(2)	677.81	HT 49	48.18	1.650(2)	670.14
HT 77	-.69	8.056(1)	636.56	HT 103	20.31	2.277(2)	671.56	HT 50	51.36	1.494(2)	659.94
HT 78	.27	1.292(2)	664.45	HT 104	21.11	4.335(2)	737.03	HT 51	54.55	Null	Null
HT 79	1.22	1.281(2)	679.19	HT 105	21.90	3.506(2)	727.76	HT 52	57.73	1.242(2)	646.61
HT 80	2.18	1.662(2)	705.49	HT 106	22.71	3.390(2)	725.75				

Run 36 Reduced Data Tabulation

Gauge Label	Angle (deg)	(PSIA)	T Surf (DegR)	Gauge Label	Angle (deg)	(PSIA)	T Surf (DegR)	Gauge Label	Angle (deg)	(PSIA)	T Surf (DegR)
P 30	-60.85	Null		P 20	8.38	7.239(1)		P 16	27.48	5.906(1)	
P 28	-46.52	4.398(-1)		P 15	10.77	6.282(1)		P 11	29.87	Null	
P 26	-32.20	8.251(-1)		P 19	13.16	5.422(1)		P 10	34.64	Null	
P 25	-25.04	1.548(0)		P 14	15.55	5.405(1)		P 9	41.81	2.902(1)	
P 24	-17.88	3.616(0)		P 18	17.93	4.897(1)		P 7	56.13	2.739(1)	
P 23	-10.71	Null		P 13	20.32	Null		P 5	70.45	1.098(1)	
P 22	-3.55	Null		P 17	22.71	5.140(1)		P 3	84.78	3.080(0)	
P 21	3.61	7.359(1)		P 12	25.10	5.149(1)		P 1	99.10	8.445(-1)	

Gauge Label	Angle (deg)	(BTU/Ft2-Sec)	T Surf (DegR)	Gauge Label	Angle (deg)	(BTU/Ft2-Sec)	T Surf (DegR)	Gauge Label	Angle (deg)	(BTU/Ft2-Sec)	T Surf (DegR)
HT 42	-38.64	5.858(0)	543.46	HT 81	3.13	6.627(2)	826.88	HT 107	23.50	1.887(2)	682.46
HT 41	-35.42	7.864(0)	545.80	HT 11	9.98	4.792(2)	784.44	HT 108	24.30	1.369(2)	663.22
HT 40	-32.20	9.400(0)	547.30	HT 12	10.78	4.676(2)	785.52	HT 109	25.09	1.993(2)	675.68
HT 39	-28.98	1.727(1)	557.83	HT 13	11.57	3.747(2)	751.30	HT 110	25.89	1.557(2)	665.70
HT 38	-25.76	1.634(1)	553.70	HT 14	12.37	4.078(2)	754.41	HT 111	26.68	1.626(2)	687.05
HT 37	-22.54	2.325(1)	559.83	HT 15	13.16	3.115(2)	712.20	HT 112	27.48	1.563(2)	683.10
HT 36	-19.32	3.323(1)	566.58	HT 16	13.96	3.191(2)	716.73	HT 113	28.27	1.565(2)	680.05
HT 35	-16.10	4.914(1)	578.02	HT 17	14.75	3.428(2)	711.04	HT 43	29.07	1.678(2)	700.75
HT 34	-12.72	7.406(1)	594.26	HT 18	15.55	3.141(2)	712.27	HT 114	29.07	1.422(2)	680.97
HT 33	-9.66	1.217(2)	621.52	HT 19	16.34	3.017(2)	707.81	HT 44	32.25	1.436(2)	712.98
HT 72	-5.46	1.732(2)	652.79	HT 20	17.14	2.914(2)	706.72	HT 45	35.44	1.377(2)	721.56
HT 73	-4.51	2.109(2)	671.96	HT 21	17.93	2.647(2)	694.06	HT 46	38.62	1.372(2)	718.15
HT 74	-3.55	2.442(2)	688.57	HT 22	18.72	2.626(2)	700.16	HT 47	41.81	1.335(2)	703.77
HT 75	-2.60	2.472(2)	687.53	HT 101	18.72	2.618(2)	688.20	HT 48	44.99	1.205(2)	670.97
HT 76	-1.64	3.497(2)	730.98	HT 102	19.52	2.169(2)	674.01	HT 49	48.18	1.249(2)	655.55
HT 77	-.69	4.083(2)	751.74	HT 103	20.31	2.047(2)	673.90	HT 50	51.36	1.128(2)	635.31
HT 78	.27	4.973(2)	782.30	HT 104	21.11	2.043(2)	671.75	HT 51	54.55	1.074(2)	623.64
HT 79	1.22	5.912(2)	802.87	HT 105	21.90	2.089(2)	671.30	HT 52	57.73	9.655(1)	609.62
HT 80	2.18	6.577(2)	824.44	HT 106	22.71	1.691(2)	664.56				

Run 37 Reduced Data Tabulation

Gauge Label	Angle	(PSIA)	T Surf (DegR)	Gauge Label	Angle (deg)	(PSIA)	T Surf (DegR)	Gauge Label	Angle (deg)	(PSIA)	T Surf (DegR)
P 30	-78.76	1.989(0)		P 20	-9.53	1.498(1)		P 16	9.57	1.780(1)	
P 28	-64.44	2.253(0)		P 15	-7.14	1.489(1)		P 11	11.96	1.449(1)	
P 26	-50.11	6.604(0)		P 19	-4.76	1.646(1)		P 10	16.73	1.403(1)	
P 25	-42.95	8.960(0)		P 14	-2.37	1.514(1)		P 9	23.89	1.340(1)	
P 24	-35.79	1.025(1)		P 18	.02	1.503(1)		P 7	38.22	1.032(1)	
P 23	-28.63	1.174(1)		P 13	2.41	1.705(1)		P 5	52.54	6.341(0)	
P 22	-21.47	1.507(1)		P 17	4.79	1.487(1)		P 3	66.86	3.407(0)	
P 21	-14.30	1.523(1)		P 12	7.18	1.536(1)		P 1	81.19	3.365(-3)	

Gauge Label	Angle (deg)	(BTU/Ft2-Sec)	T Surf (DegR)	Gauge Label	Angle (deg)	(BTU/Ft2-Sec)	T Surf (DegR)	Gauge Label	Angle (deg)	(BTU/Ft2-Sec)	T Surf (DegR)
HT 42	-56.55	2.353(1)	548.35	HT 81	-14.78	5.650(1)	573.28	HT 107	5.59	6.156(1)	577.87
HT 41	-53.33	2.738(1)	551.15	HT 11	-7.93	5.857(1)	575.04	HT 108	6.38	Null	Null
HT 40	-50.11	2.875(1)	552.14	HT 12	-7.14	5.849(1)	575.97	HT 109	7.18	6.421(1)	577.64
HT 39	-46.89	3.718(1)	558.49	HT 13	-6.34	5.927(1)	575.16	HT 110	7.97	6.060(1)	575.69
HT 38	-43.67	3.511(1)	556.69	HT 14	-5.55	5.804(1)	575.60	HT 111	8.77	6.168(1)	577.31
HT 37	-40.45	Null	Null	HT 15	-4.75	5.997(1)	575.32	HT 112	9.56	6.313(1)	578.23
HT 36	-37.24	4.069(1)	560.21	HT 16	-3.96	6.130(1)	576.03	HT 113	10.36	5.882(1)	575.16
HT 35	-34.02	4.595(1)	563.95	HT 17	-3.16	6.033(1)	575.07	HT 43	11.15	6.492(1)	579.24
HT 34	-30.63	4.816(1)	565.67	HT 18	-2.37	6.851(1)	578.35	HT 114	11.15	6.144(1)	577.31
HT 33	-27.58	5.246(1)	568.83	HT 19	-1.57	6.490(1)	576.92	HT 44	14.34	6.049(1)	575.88
HT 72	-23.38	5.286(1)	568.50	HT 20	-.78	6.091(1)	574.82	HT 45	17.52	5.849(1)	574.28
HT 73	-22.42	5.256(1)	569.56	HT 21	.02	5.753(1)	576.04	HT 46	20.71	6.079(1)	574.05
HT 74	-21.47	5.356(1)	570.11	HT 22	.81	6.781(1)	578.65	HT 47	23.89	5.441(1)	571.62
HT 75	-20.51	4.718(1)	565.36	HT 101	.81	6.233(1)	578.33	HT 48	27.08	5.328(1)	570.19
HT 76	-19.56	Null	Null	HT 102	1.60	6.208(1)	577.98	HT 49	30.26	4.779(1)	567.52
HT 77	-18.60	5.634(1)	571.19	HT 103	2.40	6.368(1)	576.57	HT 50	33.45	4.494(1)	565.63
HT 78	-17.65	5.761(1)	572.60	HT 104	3.19	6.160(1)	577.72	HT 51	36.63	4.201(1)	563.48
HT 79	-16.69	5.718(1)	573.01	HT 105	3.99	6.458(1)	578.20	HT 52	39.82	3.831(1)	561.43
HT 80	-15.74	5.781(1)	572.47	HT 106	4.79	6.355(1)	579.16				

Run 38 Reduced Data Tabulation

Gauge Label	Angle (deg)	(PSIA)	T Surf (DegR)	Gauge Label	Angle (deg)	(PSIA)	T Surf (DegR)	Gauge Label	Angle (deg)	(PSIA)	T Surf (DegR)
P 30	-78.76	2.381(0)		P 20	-9.53	1.858(1)		P 16	9.57	2.230(1)	
P 28	-64.44	4.858(0)		P 15	-7.14	1.966(1)		P 11	11.96	1.825(1)	
P 26	-50.11	8.310(0)		P 19	-4.76	2.196(1)		P 10	16.73	1.901(1)	
P 25	-42.95	1.087(1)		P 14	-2.37	2.138(1)		P 9	23.89	1.663(1)	
P 24	-35.79	1.267(1)		P 18	.02	1.699(1)		P 7	38.22	1.212(1)	
P 23	-28.63	1.441(1)		P 13	2.41	2.266(1)		P 5	52.54	7.285(0)	
P 22	-21.47	1.800(1)		P 17	4.79	1.815(1)		P 3	66.86	4.014(0)	
P 21	-14.30	1.870(1)		P 12	7.18	2.001(1)		P 1	81.19	1.973(0)	

Gauge Label	Angle (deg)	(BTU/Ft2-Sec)	T Surf (DegR)	Gauge Label	Angle (deg)	(BTU/Ft2-Sec)	T Surf (DegR)	Gauge Label	Angle (deg)	(BTU/Ft2-Sec)	T Surf (DegR)
HT 42	-56.55	8.270(1)	572.92	HT 81	-14.78	Null	Null	HT 107	5.59	1.857(2)	635.86
HT 41	-53.33	8.385(1)	574.64	HT 11	-7.93	1.925(2)	633.42	HT 108	6.38	1.800(2)	634.44
HT 40	-50.11	9.180(1)	577.94	HT 12	-7.14	1.873(2)	631.71	HT 109	7.18	1.867(2)	637.70
HT 39	-46.89	Null	Null	HT 13	-6.34	Null	Null	HT 110	7.97	1.715(2)	625.96
HT 38	-43.67	1.111(2)	588.67	HT 14	-5.55	Null	Null	HT 111	8.77	1.790(2)	630.86
HT 37	-40.45	Null	Null	HT 15	-4.75	Null	Null	HT 112	9.56	1.746(2)	627.57
HT 36	-37.24	1.215(2)	596.16	HT 16	-3.96	Null	Null	HT 113	10.36	1.755(2)	628.69
HT 35	-34.02	1.449(2)	604.07	HT 17	-3.16	Null	Null	HT 43	11.15	1.882(2)	634.16
HT 34	-30.63	1.474(2)	606.71	HT 18	-2.37	Null	Null	HT 114	11.15	1.703(2)	627.06
HT 33	-27.58	1.774(2)	620.86	HT 19	-1.57	1,703(2)	627.28	HT 44	14.34	1.686(2)	628.72
HT 72	-23.38	1.690(2)	613.47	HT 20	-.78	Null	Null	HT 45	17.52	1.638(2)	625.24
HT 73	-22.42	1.857(2)	621.90	HT 21	.02	Null	Null	HT 46	20.71	Null	Null
HT 74	-21.47	1.822(2)	621.84	HT 22	.81	Null	Null	HT 47	23.89	1.557(2)	620.64
HT 75	-20.51	1.566(2)	610.30	HT 101	.81	2.096(2)	644.45	HT 48	27.08	1.419(2)	615.06
HT 76	-19.56	1.773(2)	622.68	HT 102	1.60	Null	Null	HT 49	30.26	1.320(2)	610.23
HT 77	-18.60	Null	Null	HT 103	2.40	Null	Null	HT 50	33.45	1.531(2)	621.57
HT 78	-17.65	2.104(2)	640.23	HT 104	3.19	2.203(2)	652.23	HT 51	36.63	1.196(2)	602.06
HT 79	-16.69	1.793(2)	628.58	HT 105	3.99	1.913(2)	636.81	HT 52	39.82	1.152(2)	599.72
HT 80	-15.74	Null	Null	HT 106	4.79	1.880(2)	635.88				

Run 39 Reduced Data Tabulation

Gauge Label	Angle (deg)	(PSIA)	T Surf (DegR)	Gauge Label	Angle (deg)	(PSIA)	T Surf (DegR)	Gauge Label	Angle (deg)	(PSIA)	T Surf (DegR)
P 30	-78.76	5.191(-1)		P 20	-9.53	3.452(0)		P 16	9.57	4.241(0)	
P 28	-64.44	8.214(-1)		P 15	-7.14	3.073(0)		P 11	11.96	3.119(0)	
P 26	-50.11	1.420(0)		P 19	-4.76	3.938(0)		P 10	16.73	3.036(0)	
P 25	-42.95	1.990(0)		P 14	-2.37	3.238(0)		P 9	23.89	Null	
P 24	-35.79	2.064(0)		P 18	.02	3.379(0)		P 7	38.22	2.390(0)	
P 23	-28.63	Null		P 13	2.41	3.095(0)		P 5	52.54	1.480(0)	
P 22	-21.47	3.424(0)		P 17	4.79	3.428(0)		P 3	66.86	4.970(-1)	
P 21	-14.30	3.477(0)		P 12	7.18	3.171(0)		P 1	81.19	4.304(-1)	

Gauge Label	Angle (deg)	(BTU/Ft2-Sec)	T Surf (DegR)	Gauge Label	Angle (deg)	(BTU/Ft2-Sec)	T Surf (DegR)	Gauge Label	Angle (deg)	(BTU/Ft2-Sec)	T Surf (DegR)
HT 42	-56.55	2.118(1)	549.57	HT 81	-14.78	4.876(1)	571.52	HT 107	5.59	5.284(1)	572.48
HT 41	-53.33	2.421(1)	552.10	HT 11	-7.93	4.989(1)	572.16	HT 108	6.38	5.960(1)	575.53
HT 40	-50.11	2.598(1)	553.55	HT 12	-7.14	4.555(1)	571.08	HT 109	7.18	4.848(1)	570.75
HT 39	-46.89	Null	Null	HT 13	-6.34	4.787(1)	571.49	HT 110	7.97	4.905(1)	570.52
HT 38	-43.67	3.034(1)	557.10	HT 14	-5.55	5.523(1)	574.59	HT 111	8.77	5.075(1)	572.82
HT 37	-40.45	Null	Null	HT 15	-4.75	4.820(1)	569.70	HT 112	9.56	4.979(1)	570.54
HT 36	-37.24	3.242(1)	560.93	HT 16	-3.96	4.947(1)	570.96	HT 113	10.36	4.937(1)	571.05
HT 35	-34.02	3.780(1)	563.16	HT 17	-3.16	5.016(1)	570.17	HT 43	11.15	5.408(1)	575.83
HT 34	-30.63	3.982(1)	564.82	HT 18	-2.37	5.345(1)	572.55	HT 114	11.15	Null	Null
HT 33	-27.58	4.143(1)	565.60	HT 19	-1.57	5.207(1)	571.67	HT 44	14.34	5.405(1)	575.18
HT 72	-23.38	4.744(1)	568.92	HT 20	-.78	5.283(1)	571.25	HT 45	17.52	5.099(1)	573.11
HT 73	-22.42	4.554(1)	568.55	HT 21	.02	5.524(1)	572.61	HT 46	20.71	4.947(1)	572.22
HT 74	-21.47	Null	Null	HT 22	.81	5.901(1)	576.65	HT 47	23.89	5.034(1)	573.66
HT 75	-20.51	3.997(1)	563.77	HT 101	.81	5.211(1)	573.32	HT 48	27.08	4.570(1)	569.07
HT 76	-19.56	4.458(1)	568.13	HT 102	1.60	5.067(1)	571.81	HT 49	30.26	4.333(1)	567.86
HT 77	-18.60	4.564(1)	567.86	HT 103	2.40	Null	Null	HT 50	33.45	4.005(1)	564.96
HT 78	-17.65	5.258(1)	571.84	HT 104	3.19	5.059(1)	571.63	HT 51	36.63	4.359(1)	568.52
HT 79	-16.69	5.234(1)	575.31	HT 105	3.99	5.220(1)	571.95	HT 52	39.82	4.883(1)	567.82
HT 80	-15.74	4.801(1)	569.35	HT 106	4.79	Null	Null				

Run 40 Reduced Data Tabulation

Gauge Label	Angle (deg)	(PSIA)	T Surf (DegR)	Gauge Label	Angle (deg)	(PSIA)	T Surf (DegR)	Gauge Label	Angle (deg)	(PSIA)	T Surf (DegR)
P 30	-78.76	3.554(-1)		P 20	-9.53	2.433(0)		P 16	9.57	Null	
P 28	-64.44	7.097(-1)		P 15	-7.14	2.424(0)		P 11	11.96	2.479(0)	
P 26	-50.11	1.164(0)		P 19	-4.76	Null		P 10	16.73	2.410(0)	
P 25	-42.95	1.410(0)		P 14	-2.37	2.520(0)		P 9	23.89	Null	
P 24	-35.79	Null		P 18	.02	Null		P 7	38.22	Null	
P 23	-28.63	Null		P 13	2.41	2.655(0)		P 5	52.54	1.123(0)	
P 22	-21.47	Null		P 17	4.79	2.437(0)		P 3	66.86	6.542(-1)	
P 21	-14.30	2.438(0)		P 12	7.18	2.487(0)		P 1	81.19	3.347(-1)	

Gauge Label	Angle (deg)	(BTU/Ft2-Sec)	T Surf (DegR)	Gauge Label	Angle (deg)	(BTU/Ft2-Sec)	T Surf (DegR)	Gauge Label	Angle (deg)	(BTU/Ft2-Sec)	T Surf (DegR)
HT 42	-56.55	3.198(1)	559.23	HT 81	-14.78	5.848(1)	582.99	HT 107	5.59	6.641(1)	586.67
HT 41	-53.33	3.894(1)	563.46	HT 11	-7.93	6.907(1)	587.28	HT 108	6.38	7.012(1)	588.97
HT 40	-50.11	3.527(1)	562.67	HT 12	-7.14	7.327(1)	591.57	HT 109	7.18	6.308(1)	585.14
HT 39	-46.89	3.979(1)	566.14	HT 13	-6.34	7.104(1)	588.07	HT 110	7.97	6.840(1)	588.56
HT 38	-43.67	3.980(1)	566.95	HT 14	-5.55	7.542(1)	588.54	HT 111	8.77	6.856(1)	589.35
HT 37	-40.45	Null	Null	HT 15	-4.75	7.448(1)	589.23	HT 112	9.56	Null	Null
HT 36	-37.24	Null	Null	HT 16	-3.96	7.192(1)	588.75	HT 113	10.36	6.366(1)	587.15
HT 35	-34.02	5.192(1)	576.04	HT 17	-3.16	6.956(1)	586.22	HT 43	11.15	7.691(1)	593.28
HT 34	-30.63	5.300(1)	577.57	HT 18	-2.37	7.167(1)	589.05	HT 114	11.15	6.364(1)	589.01
HT 33	-27.58	5.926(1)	581.57	HT 19	-1.57	7.918(1)	592.62	HT 44	14.34	7.433(1)	592.34
HT 72	-23.38	5.603(1)	578.53	HT 20	-.78	7.472(1)	589.34	HT 45	17.52	7.175(1)	590.97
HT 73	-22.42	6.553(1)	583.87	HT 21	.02	7.898(1)	590.64	HT 46	20.71	6.901(1)	588.71
HT 74	-21.47	Null	Null	HT 22	.81	6.746(1)	588.66	HT 47	23.89	Null	Null
HT 75	-20.51	4.838(1)	572.36	HT 101	.81	Null	Null	HT 48	27.08	6.508(1)	586.69
HT 76	-19.56	5.626(1)	579.06	HT 102	1.60	7.360(1)	591.38	HT 49	30.26	6.079(1)	582.54
HT 77	-18.60	5.519(1)	578.66	HT 103	2.40	Null	Null	HT 50	33.45	5.812(1)	581.12
HT 78	-17.65	6.427(1)	584.54	HT 104	3.19	7.107(1)	586.98	HT 51	36.63	5.558(1)	579.06
HT 79	-16.69	5.754(1)	581.44	HT 105	3.99	5.902(1)	582.77	HT 52	39.82	5.725(1)	578.10
HT 80	-15.74	5.849(1)	581.45	HT 106	4.79	Null	Null				

Run 41 Reduced Data Tabulation

Gauge Label	Angle (deg)	(PSIA)	T Surf (DegR)	Gauge Label	Angle (deg)	(PSIA)	T Surf (DegR)	Gauge Label	Angle (deg)	(PSIA)	T Surf (DegR)
P 30	-60.85	1.475(-1)		P 20	8.38	1.333(1)		P 16	27.48	1.549(1)	
P 28	-46.52	3.363(-1)		P 15	10.77	1.239(1)		P 11	29.87	1.053(1)	
P 26	-32.20	1.526(0)		P 19	13.16	1.471(1)		P 10	34.64	9.912(0)	
P 25	-25.04	3.373(0)		P 14	15.55	1.256(1)		P 9	41.81	1.042(1)	
P 24	-17.88	6.088(0)		P 18	17.93	1.168(1)		P 7	56.13	8.852(0)	
P 23	-10.71	9.698(0)		P 13	20.32	1.280(1)		P 5	70.45	5.886(0)	
P 22	-3.55	1.300(1)		P 17	22.71	1.241(1)		P 3	84.78	3.062(0)	
P 21	3.61	1.311(1)		P 12	25.10	1.238(1)		P 1	99.10	1.206(0)	

Gauge Label	Angle (deg)	(BTU/Ft2-Sec)	T Surf (DegR)	Gauge Label	Angle (deg)	(BTU/Ft2-Sec)	T Surf (DegR)	Gauge Label	Angle (deg)	(BTU/Ft2-Sec)	T Surf (DegR)
HT 42	-38.64	Null	Null	HT 81	3.13	1.615(2)	656.67	HT 107	23.50	1.175(2)	658.90
HT 41	-35.42	Null	Null	HT 11	9.98	1.488(2)	669.21	HT 108	24.30	1.277(2)	669.06
HT 40	-32.20	Null	Null	HT 12	10.78	1.452(2)	685.14	HT 109	25.09	1.133(2)	653.51
HT 39	-28.98	Null	Null	HT 13	11.57	1.384(2)	667.78	HT 110	25.89	1.092(2)	651.31
HT 38	-25.76	Null	Null	HT 14	12.37	1.375(2)	666.70	HT 111	26.68	1.177(2)	659.00
HT 37	-22.54	Null	Null	HT 15	13.16	1.362(2)	663.34	HT 112	27.48	1.163(2)	661.07
HT 36	-19.32	Null	Null	HT 16	13.96	1.421(2)	675.19	HT 113	28.27	1.055(2)	650.64
HT 35	-16.10	1.123(2)	650.66	HT 17	14.75	1.477(2)	665.66	HT 43	29.07	1.274(2)	672.25
HT 34	-12.72	1.275(2)	666.94	HT 18	15.55	1.381(2)	668.86	HT 114	29.07	1.028(2)	648.03
HT 33	-9.66	1.281(2)	672.41	HT 19	16.34	1.418(2)	668.25	HT 44	32.25	Null	Null
HT 72	-5.46	1.385(2)	666.46	HT 20	17.14	1.306(2)	663.32	HT 45	35.44	1.086(2)	649.39
HT 73	-4.51	1.037(2)	662.08	HT 21	17.93	1.374(2)	671.03	HT 46	38.62	1.056(2)	648.15
HT 74	-3.55	Null	Null	HT 22	18.72	1.337(2)	671.25	HT 47	41.81	Null	Null
HT 75	-2.60	9.893(1)	638.98	HT 101	18.72	1.244(2)	665.01	HT 48	44.99	8.586(1)	631.81
HT 76	-1.64	1.200(2)	655.12	HT 102	19.52	Null	Null	HT 49	48.18	8.979(1)	635.31
HT 77	-.69	1.209(2)	652.20	HT 103	20.31	Null	Null	HT 50	51.36	8.326(1)	626.78
HT 78	.27	1.167(2)	637.63	HT 104	21.11	1.195(2)	656.82	HT 51	54.55	8.385(1)	629.14
HT 79	1.22	Null	Null	HT 105	21.90	1.234(2)	657.45	HT 52	57.73	7.418(1)	619.12
HT 80	2.18	1.688(2)	676.68	HT 106	22.71	Null	Null				

Run 42 Reduced Data Tabulation

Gauge Label	Angle (deg)	(PSIA)	T Surf (DegR)	Gauge Label	Angle (deg)	(PSIA)	T Surf (DegR)	Gauge Label	Angle (deg)	(PSIA)	T Surf (DegR)
P 30	-50.11	1.147(0)		P 20	19.12	7.678(0)		P 16	38.22	1.084(1)	
P 28	-35.79	1.669(0)		P 15	21.51	3.767(1)		P 11	40.60	8.952(0)	
P 26	-21.47	2.327(0)		P 19	23.89	4.926(1)		P 10	45.38	8.109(0)	
P 25	-14.30	2.619(0)		P 14	26.28	2.766(1)		P 9	52.54	7.161(0)	
P 24	-7.14	2.367(0)		P 18	28.67	2.108(1)		P 7	66.86	4.534(0)	
P 23	.02	1.659(0)		P 13	31.05	8.908(0)		P 5	81.19	2.296(0)	
P 22	7.18	1.404(0)		P 17	33.44	9.831(0)		P 3	95.51	1.098(0)	
P 21	14.34	2.578(0)		P 12	35.83	1.002(1)		P 1	109.84	4.387(-1)	

Gauge Label	Angle (deg)	(BTU/Ft2-Sec)	T Surf (DegR)	Gauge Label	Angle (deg)	(BTU/Ft2-Sec)	T Surf (DegR)	Gauge Label	Angle (deg)	(BTU/Ft2-Sec)	T Surf (DegR)
HT 42	-27.91	6.587(1)	592.46	HT 81	13.87	1.548(2)	703.07	HT 107	34.24	1.877(2)	751.39
HT 41	-24.69	7.270(1)	599.16	HT 11	20.72	1.196(3)	1066.60	HT 108	35.03	1.947(2)	744.30
HT 40	-21.47	7.632(1)	602.79	HT 12	21.51	1.436(3)	1107.40	HT 109	35.83	1.787(2)	729.01
HT 39	-18.25	Null	Null	HT 13	22.31	1.341(3)	1099.70	HT 110	36.62	2.394(2)	728.14
HT 38	-15.03	8.837(1)	609.88	HT 14	23.10	1.050(3)	1054.80	HT 111	37.41	2.392(2)	749.88
HT 37	-11.81	Null	Null	HT 15	23.90	9.540(2)	1049.10	HT 112	38.21	2.749(2)	749.07
HT 36	-8.59	8.345(1)	608.89	HT 16	24.69	8.656(2)	1036.20	HT 113	39.00	2.098(2)	726.49
HT 35	-5.37	7.600(1)	603.54	HT 17	25.49	9.573(2)	1032.30	HT 43	39.80	2.510(2)	742.73
HT 34	-1.99	5.701(1)	596.40	HT 18	26.28	7.394(2)	997.07	HT 114	39.80	2.005(2)	712.57
HT 33	1.07	4.210(1)	594.90	HT 19	27.07	8.298(2)	988.80	HT 44	42.99	1.996(2)	709.76
HT 72	5.27	4.463(1)	595.73	HT 20	27.87	6.667(2)	929.26	HT 45	46.17	1.808(2)	699.87
HT 73	6.23	4.637(1)	594.60	HT 21	28.66	4.522(2)	905.64	HT 46	49.35	1.605(2)	683.68
HT 74	7.18	Null	Null	HT 22	29.46	4.056(2)	877.99	HT 47	52.54	-3.125(-1)	554.94
HT 75	8.14	3.221(1)	582.06	HT 101	29.46	3.251(2)	859.68	HT 48	55.73	1.217(2)	652.98
HT 76	9.09	6.082(1)	599.58	HT 102	30.25	1.919(2)	810.23	HT 49	58.91	1.072(2)	638.50
HT 77	10.05	5.874(1)	608.63	HT 103	31.05	Null	Null	HT 50	62.09	9.333(1)	626.96
HT 78	11.00	1.145(2)	637.89	HT 104	31.84	2.105(2)	770.03	HT 51	65.28	8.596(1)	618.61
HT 79	11.96	9.615(1)	636.53	HT 105	32.64	1.883(2)	740.26	HT 52	68.46	1.137(2)	647.34
HT 80	12.91	1.211(2)	673.64	HT 106	33.44	Null	Null				

Run 43 Reduced Data Tabulation

Gauge Label	Angle (deg)	(PSIA)	T Surf (DegR)	Gauge Label	Angle (deg)	(PSIA)	T Surf (DegR)	Gauge Label	Angle (deg)	(PSIA)	T Surf (DegR)
P 30	-35.79	2.162(0)		P 20	33.44	3.536(0)		P 16	52.54	1.317(1)	
P 28	-21.47	2.819(0)		P 15	35.83	3.694(0)		P 11	54.93	9.432(0)	
P 26	-7.14	3.099(0)		P 19	38.22	4.784(0)		P 10	59.70	9.333(0)	
P 25	.02	3.320(0)		P 14	40.60	4.933(0)		P 9	66.86	7.529(0)	
P 24	7.18	3.386(0)		P 18	42.99	5.689(0)		P 7	81.19	2.867(0)	
P 23	14.34	3.818(0)		P 13	45.38	4.544(0)		P 5	95.51	8.033(-1)	
P 22	21.51	3.842(0)		P 17	47.77	8.589(0)		P 3	109.84	2.719(-1)	
P 21	28.67	3.563(0)		P 12	50.15	8.723(0)		P 1	124.16	8.957(-2)	

Gauge Label	Angle (deg)	(BTU/Ft2-Sec)	T Surf (DegR)	Gauge Label	Angle (deg)	(BTU/Ft2-Sec)	T Surf (DegR)	Gauge Label	Angle (deg)	(BTU/Ft2-Sec)	T Surf (DegR)
HT 42	-13.58	5.795(1)	595.17	HT 81	28.19	9.939(1)	627.44	HT 107	48.56	4.365(2)	820.77
HT 41	-10.36	5.481(1)	595.61	HT 11	35.04	9.879(1)	647.54	HT 108	49.35	4.973(2)	852.87
HT 40	-7.14	5.233(1)	594.18	HT 12	35.84	1.332(2)	667.51	HT 109	50.15	4.243(2)	827.26
HT 39	-3.92	Null	Null	HT 13	36.63	1.381(2)	682.61	HT 110	50.94	4.572(2)	828.14
HT 38	-.70	5.039(1)	595.14	HT 14	37.43	1.549(2)	683.75	HT 111	51.74	5.047(2)	858.95
HT 37	2.52	Null	Null	HT 15	38.22	1.777(2)	689.18	HT 112	52.53	4.533(2)	843.37
HT 36	5.73	4.365(1)	596.38	HT 16	39.01	1.978(2)	702.07	HT 113	53.33	4.463(2)	832.43
HT 35	8.95	5.311(1)	599.86	HT 17	39.81	2.059(2)	703.67	HT 43	54.13	4.488(2)	843.67
HT 34	12.34	5.489(1)	600.17	HT 18	40.60	2.018(2)	715.82	HT 114	54.13	4.272(2)	817.46
HT 33	15.39	6.023(1)	609.16	HT 19	41.40	2.387(2)	731.31	HT 44	57.31	Null	Null
HT 72	19.60	5.969(1)	603.57	HT 20	42.19	2.650(2)	727.18	HT 45	60.50	2.971(2)	774.33
HT 73	20.55	6.308(1)	603.64	HT 21	42.99	3.035(2)	757.05	HT 46	63.68	2.489(2)	743.14
HT 74	21.51	Null	Null	HT 22	43.78	3.136(2)	768.94	HT 47	66.86	Null	Null
HT 75	22.46	5.886(1)	594.42	HT 101	43.78	3.529(2)	774.81	HT 48	70.05	1.576(2)	679.49
HT 76	23.41	7.977(1)	605.65	HT 102	44.58	3.562(2)	783.91	HT 49	73.24	1.254(2)	653.82
HT 77	24.37	6.413(1)	604.13	HT 103	45.37	Null	Null	HT 50	76.42	9.911(1)	631.74
HT 78	25.32	8.642(1)	614.62	HT 104	46.17	4.184(2)	808.07	HT 51	79.60	7.500(1)	613.70
HT 79	26.28	8.756(1)	618.66	HT 105	46.96	3.810(2)	797.96	HT 52	82.79	5.721(1)	597.54
HT 80	27.23	8.925(1)	623.45	HT 106	47.77	Null	Null				

Run 44 Reduced Data Tabulation

Gauge Label	Angle (deg)	(PSIA)	T Surf (DegR)	Gauge Label	Angle (deg)	(PSIA)	T Surf (DegR)	Gauge Label	Angle (deg)	(PSIA)	T Surf (DegR)
P 30	-64.44	Null		P 20	4.79	5.263(0)		P 16	23.89	6.013(1)	
P 28	-50.11	2.982(0)		P 15	7.18	7.079(0)		P 11	26.28	3.191(1)	
P 26	-35.79	4.887(0)		P 19	9.57	1.330(1)		P 10	31.05	2.530(1)	
P 25	-28.63	4.450(0)		P 14	11.96	1.780(1)		P 9	38.22	2.583(1)	
P 24	-21.47	2.423(0)		P 18	14.34	3.120(1)		P 7	52.54	2.174(1)	
P 23	-14.30	1.251(0)		P 13	16.73	4.977(1)		P 5	66.86	1.615(1)	
P 22	-7.14	9.331(-1)		P 17	19.12	1.058(2)		P 3	81.19	9.587(0)	
P 21	.02	2.339(0)		P 12	21.51	8.751(1)		P 1	95.51	4.313(0)	

Gauge Label	Angle (deg)	(BTU/Ft2-Sec)	T Surf (DegR)	Gauge Label	Angle (deg)	(BTU/Ft2-Sec)	T Surf (DegR)	Gauge Label	Angle (deg)	(BTU/Ft2-Sec)	T Surf (DegR)
HT 32	-16.31	1.646(1)	556.59	HT 69	17.69	6.041(2)	939.79	HT 1	26.29	3.418(2)	787.25
HT 31	-13.25	8.262(0)	553.09	HT 70	18.64	6.976(2)	952.99	HT 62	26.29	3.636(2)	793.81
HT 29	-7.14	8.074(0)	557.10	HT 10	19.10	8.441(2)	982.67	HT 61	29.35	2.278(2)	729.24
HT 28	-4.09	1.214(1)	560.29	HT 71	19.60	8.164(2)	970.58	HT 59	35.46	2.163(2)	713.88
HT 25	5.08	4.938(1)	645.53	HT 9	19.90	8.131(2)	950.51	HT 58	38.51	1.842(2)	691.67
HT 24	8.14	7.789(1)	710.50	HT 7	21.51	5.593(2)	897.48	HT 57	41.57	1.676(2)	688.30
HT 64	12.91	2.087(2)	836.80	HT 6	22.30	6.604(2)	921.67	HT 56	44.63	1.501(2)	672.37
HT 65	13.87	Null	Null	HT 5	23.09	6.838(2)	920.78	HT 55	47.68	1.526(2)	673.81
HT 66	14.82	3.277(2)	879.51	HT 4	23.89	5.250(2)	866.73	HT 54	50.74	1.325(2)	656.69
HT 67	15.78	4.317(2)	910.72	HT 3	24.69	4.661(2)	841.31	HT 53	53.79	1.206(2)	644.60
HT 68	16.73	5.040(2)	922.51	HT 2	25.49	3.732(2)	802.54				

Run 59 Reduced Data Tabulation

Gauge Label	Angle (deg)	(PSIA)	T Surf (DegR)	Gauge Label	Angle (deg)	(PSIA)	T Surf (DegR)	Gauge Label	Angle (deg)	(PSIA)	T Surf (DegR)
P 30	-64.44	Null		P 20	4.79	1.294(1)		P 16	23.89	4.125(1)	
P 28	-50.11	1.780(0)		P 15	7.18	2.017(1)		P 11	26.28	2.975(1)	
P 26	-35.79	Null		P 19	9.57	3.549(1)		P 10	31.05	2.489(1)	
P 25	-28.63	1.382(0)		P 14	11.96	4.750(1)		P 9	38.22	Null	
P 24	-21.47	5.966(-1)		P 18	14.34	4.848(1)		P 7	52.54	2.169(1)	
P 23	-14.30	6.702(-1)		P 13	16.73	4.535(1)		P 5	66.86	1.560(1)	
P 22	-7.14	1.561(0)		P 17	19.12	8.355(1)		P 3	81.19	8.943(0)	
P 21	.02	5.219(0)		P 12	21.51	7.391(1)		P 1	95.51	4.326(0)	

Gauge Label	Angle (deg)	(BTU/Ft2-Sec)	T Surf (DegR)	Gauge Label	Angle (deg)	(BTU/Ft2-Sec)	T Surf (DegR)	Gauge Label	Angle (deg)	(BTU/Ft2-Sec)	T Surf (DegR)
HT 32	-16.31	7.111(0)	547.82	HT 69	17.69	6.535(2)	950.39	HT 1	26.29	2.662(2)	746.48
HT 31	-13.25	1.077(1)	552.12	HT 70	18.64	6.714(2)	929.90	HT 62	26.29	2.938(2)	779.43
HT 29	-7.14	1.977(1)	566.82	HT 10	19.10	7.733(2)	934.46	HT 61	29.35	2.194(2)	724.22
HT 28	-4.09	2.914(1)	580.14	HT 71	19.60	7.185(2)	922.67	HT 59	35.46	1.675(2)	702.27
HT 25	5.08	1.302(2)	733.74	HT 9	19.90	6.274(2)	880.66	HT 58	38.51	Null	Null
HT 24	8.14	2.584(2)	838.91	HT 7	21.51	5.189(2)	840.31	HT 57	41.57	1.565(2)	672.87
HT 64	12.91	4.483(2)	963.58	HT 6	22.30	4.933(2)	831.93	HT 56	44.63	1.424(2)	668.37
HT 65	13.87	Null	Null	HT 5	23.09	4.670(2)	836.68	HT 55	47.68	1.316(2)	660.10
HT 66	14.82	4.929(2)	964.43	HT 4	23.89	3.813(2)	799.00	HT 54	50.74	1.192(2)	650.09
HT 67	15.78	5.490(2)	946.61	HT 3	24.69	3.314(2)	774.59	HT 53	53.79	9.902(1)	638.18
HT 68	16.73	6.266(2)	967.58	HT 2	25.49	2.917(2)	752.24				

Run 60 Reduced Data Tabulation

Gauge Label	Angle (deg)	(PSIA)	T Surf (DegR)	Gauge Label	Angle (deg)	(PSIA)	T Surf (DegR)	Gauge Label	Angle (deg)	(PSIA)	T Surf (DegR)
P 30	-50.11	5.802(-4)		P 20	19.12	7.804(0)		P 16	38.22	6.504(1)	
P 28	-35.79	4.714(0)		P 15	21.51	8.379(0)		P 11	40.60	5.778(1)	
P 26	-21.47	6.624(0)		P 19	23.89	1.182(1)		P 10	45.38	3.229(1)	
P 25	-14.30	8.340(0)		P 14	26.28	1.440(1)		P 9	52.54	2.199(1)	
P 24	-7.14	7.901(0)		P 18	28.67	1.569(1)		P 7	66.86	8.277(0)	
P 23	.02	8.149(0)		P 13	31.05	2.143(1)		P 5	81.19	5.038(0)	
P 22	7.18	7.810(0)		P 17	33.44	3.669(1)		P 3	95.51	2.099(0)	
P 21	14.34	7.836(0)		P 12	35.83	5.450(1)		P 1	109.84	8.285(-1)	

Gauge Label	Angle (deg)	(BTU/Ft2-Sec)	T Surf (DegR)	Gauge Label	Angle (deg)	(BTU/Ft2-Sec)	T Surf (DegR)	Gauge Label	Angle (deg)	(BTU/Ft2-Sec)	T Surf (DegR)
HT 32	-1.99	8.512(1)	602.67	HT 69	32.01	2.620(2)	715.40	HT 1	40.62	6.751(2)	885.75
HT 31	1.07	9.818(1)	607.30	HT 70	32.96	2.778(2)	725.93	HT 62	40.62	6.671(2)	883.17
HT 29	7.18	1.199(2)	626.77	HT 10	33.42	3.063(2)	750.49	HT 61	43.67	4.811(2)	867.94
HT 28	10.24	7.489(1)	607.91	HT 71	33.92	2.937(2)	737.40	HT 59	49.78	2.303(2)	748.37
HT 25	19.40	9.927(1)	621.11	HT 9	34.22	3.275(2)	749.39	HT 58	52.84	Null	Null
HT 24	22.46	1.271(2)	632.00	HT 7	35.83	3.820(2)	780.78	HT 57	55.89	7.635(1)	653.34
HT 64	27.23	1.896(2)	671.48	HT 6	36.62	4.151(2)	783.48	HT 56	58.95	7.305(1)	628.14
HT 65	28.19	Null	Null	HT 5	37.42	5.391(2)	837.75	HT 55	62.01	5.444(1)	613.05
HT 66	29.14	1.923(2)	684.72	HT 4	38.22	6.184(2)	842.55	HT 54	65.06	4.301(1)	590.88
HT 67	30.10	2.207(2)	681.59	HT 3	39.01	6.397(2)	860.97	HT 53	68.12	4.935(1)	592.53
HT 68	31.05	2.289(2)	702.02	HT 2	39.81	6.640(2)	867.08				

Run 61 Reduced Data Tabulation

Gauge Label	Angle (deg)	(PSIA)	T Surf (DegR)	Gauge Label	Angle (deg)	(PSIA)	T Surf (DegR)	Gauge Label	Angle (deg)	(PSIA)	T Surf (DegR)
? 30	-42.97	Null		P 20	26.26	7.933(0)		P 16	45.36	1.408(1)	
? 28	-28.65	2.248(0)		P 15	28.65	1.438(1)		P 11	47.75	6.808(0)	
? 26	-14.32	2.721(0)		P 19	31.04	2.128(1)		P 10	52.52	4.410(0)	
? 25	-7.16	3.428(0)		P 14	33.42	2.969(1)		P 9	59.68	4.292(0)	
? 24	.00	3.336(0)		P 18	35.81	2.873(1)		P 7	74.01	3.569(0)	
? 23	7.16	2.711(0)		P 13	38.20	2.412(1)		P 5	88.33	1.843(0)	
? 22	14.32	2.674(0)		P 17	40.58	2.729(1)		P 3	102.65	7.158(-1)	
? 21	21.49	4.543(0)		P 12	42.97	1.673(1)		P 1	116.98	3.635(-1)	

Gauge Label	Angle (deg)	(BTU/Ft2-Sec)	T Surf (DegR)	Gauge Label	Angle (deg)	(BTU/Ft2-Sec)	T Surf (DegR)	Gauge Label	Angle (deg)	(BTU/Ft2-Sec)	T Surf (DegR)
HT 32	5.16	4.279(1)	565.75	HT 69	39.15	2.286(2)	748.41	HT 1	47.76	5.541(1)	606.15
HT 31	8.21	3.231(1)	563.97	HT 70	40.11	2.000(2)	734.68	HT 62	47.76	7.373(1)	611.91
HT 29	14.32	4.068(1)	566.03	HT 10	40.57	1.884(2)	723.27	HT 61	50.81	5.151(1)	589.31
HT 28	17.38	4.638(1)	574.66	HT 71	41.06	1.770(2)	722.86	HT 59	56.93	4.071(1)	576.28
HT 25	26.55	1.492(2)	647.14	HT 9	41.37	1.550(2)	696.85	HT 58	59.98	Null	Null
HT 24	29.60	2.379(2)	700.67	HT 7	42.97	1.159(2)	673.27	HT 57	63.04	2.530(1)	563.66
HT 64	34.38	3.616(2)	785.69	HT 6	43.76	9.871(1)	656.67	HT 56	66.09	3.420(1)	566.50
HT 65	35.33	Null	Null	HT 5	44.56	9.918(1)	659.06	HT 55	69.15	1.900(1)	555.57
HT 66	36.29	3.001(2)	779.74	HT 4	45.36	7.800(1)	630.59	HT 54	72.20	3.888(1)	554.97
HT 67	37.24	2.398(2)	744.04	HT 3	46.16	8.611(1)	635.06	HT 53	75.26	3.799(1)	554.20
HT 68	38.20	2.294(2)	739.87	HT 2	46.96	5.908(1)	614.73				

Run 62 Reduced Data Tabulation

Gauge Label	Angle (deg)	(PSIA)	T Surf (DegR)	Gauge Label	Angle (deg)	(PSIA)	T Surf (DegR)	Gauge Label	Angle (deg)	(PSIA)	T Surf (DegR)
? 30	-42.97	Null		P 20	26.26	2.209(0)		P 16	45.36	2.852(0)	
? 28	-28.65	1.626(0)		P 15	28.65	2.039(0)		P 11	47.75	2.656(0)	
? 26	-14.32	1.848(0)		P 19	31.04	2.210(0)		P 10	52.52	3.300(0)	
? 25	-7.16	2.372(0)		P 14	33.42	1.197(0)		P 9	59.68	4.004(0)	
? 24	.00	2.261(0)		P 18	35.81	1.599(0)		P 7	74.01	3.143(0)	
? 23	7.16	2.236(0)		P 13	38.20	1.129(0)		P 5	88.33	1.615(0)	
? 22	14.32	2.299(0)		P 17	40.58	3.236(0)		P 3	102.65	5.870(-1)	
? 21	21.49	2.345(0)		P 12	42.97	2.752(0)		P 1	116.98	1.805(-1)	

Gauge Label	Angle (deg)	(BTU/Ft2-Sec)	T Surf (DegR)	Gauge Label	Angle (deg)	(BTU/Ft2-Sec)	T Surf (DegR)	Gauge Label	Angle (deg)	(BTU/Ft2-Sec)	T Surf (DegR)
HT 32	5.16	2.210(1)	554.07	HT 69	39.15	3.683(1)	559.86	HT 1	47.76	5.860(1)	572.14
HT 31	8.21	1.918(1)	553.01	HT 70	40.11	3.225(1)	557.87	HT 62	47.76	5.332(1)	571.57
HT 29	14.32	1.301(1)	551.24	HT 10	40.57	4.022(1)	561.37	HT 61	50.81	7.064(1)	582.21
HT 28	17.38	1.620(1)	552.35	HT 71	41.06	3.258(1)	559.05	HT 59	56.93	7.264(1)	585.49
HT 25	26.55	Null	Null	HT 9	41.37	3.850(1)	558.01	HT 58	59.98	Null	Null
HT 24	29.60	Null	Null	HT 7	42.97	3.845(1)	561.89	HT 57	63.04	5.666(1)	580.38
HT 64	34.38	2.348(1)	555.70	HT 6	43.76	4.422(1)	564.27	HT 56	66.09	5.049(1)	578.05
HT 65	35.33	Null	Null	HT 5	44.56	4.720(1)	568.09	HT 55	69.15	4.688(1)	574.81
HT 66	36.29	2.720(1)	555.73	HT 4	45.36	4.577(1)	565.65	HT 54	72.20	4.018(1)	569.41
HT 67	37.24	Null	Null	HT 3	46.16	5.644(1)	570.95	HT 53	75.26	3.281(1)	563.18
HT 68	38.20	3.096(1)	555.73	HT 2	46.96	5.399(1)	569.56				

Run 63 Reduced Data Tabulation

Gauge Label	Angle (deg)	(PSIA)	T Surf (DegR)	Gauge Label	Angle (deg)	(PSIA)	T Surf (DegR)	Gauge Label	Angle (deg)	(PSIA)	T Surf (DegR)
P 30	-42.97	Null		P 20	26.26	1.561(1)		P 16	45.36	Null	
P 28	-28.65	6.366(0)		P 15	28.65	1.865(1)		P 11	47.75	5.790(1)	
P 26	-14.32	9.644(0)		P 19	31.04	2.612(1)		P 10	52.52	Null	
P 25	-7.16	1.050(1)		P 14	33.42	2.975(1)		P 9	59.68	1.485(1)	
P 24	.00	9.850(0)		P 18	35.81	3.740(1)		P 7	74.01	7.059(0)	
P 23	7.16	9.597(0)		P 13	38.20	3.933(1)		P 5	88.33	3.983(0)	
P 22	14.32	9.377(0)		P 17	40.58	Null		P 3	102.65	1.553(0)	
P 21	21.49	1.076(1)		P 12	42.97	Null		P 1	116.98	5.336(-1)	

Gauge Label	Angle (deg)	(BTU/Ft2-Sec)	T Surf (DegR)	Gauge Label	Angle (deg)	(BTU/Ft2-Sec)	T Surf (DegR)	Gauge Label	Angle (deg)	(BTU/Ft2-Sec)	T Surf (DegR)
HT 32	5.16	9.797(1)	617.48	HT 69	39.15	5.955(2)	884.92	HT 1	47.76	5.722(2)	870.56
HT 31	8.21	1.042(2)	619.87	HT 70	40.11	6.716(2)	908.52	HT 62	47.76	5.487(2)	856.61
HT 29	14.32	8.612(1)	609.31	HT 10	40.57	7.490(2)	932.44	HT 61	50.81	3.176(2)	757.67
HT 28	17.38	8.981(1)	616.48	HT 71	41.06	6.994(2)	924.26	HT 59	56.93	1.767(2)	676.01
HT 25	26.55	1.876(2)	679.24	HT 9	41.37	6.841(2)	903.21	HT 58	59.98	Null	Null
HT 24	29.60	1.846(2)	616.07	HT 7	42.97	5.503(2)	907.75	HT 57	63.04	9.503(1)	621.19
HT 64	34.38	4.005(2)	803.41	HT 6	43.76	6.897(2)	923.04	HT 56	66.09	8.517(1)	614.47
HT 65	35.33	Null	Null	HT 5	44.56	8.566(2)	963.16	HT 55	69.15	7.422(1)	605.64
HT 66	36.29	4.660(2)	830.78	HT 4	45.36	7.224(2)	920.78	HT 54	72.20	6.266(1)	598.29
HT 67	37.24	4.705(2)	819.99	HT 3	46.16	6.974(2)	908.37	HT 53	75.26	5.449(1)	588.93
HT 68	38.20	5.711(2)	873.27	HT 2	46.96	6.079(2)	883.38				

Run 64 Reduced Data Tabulation

Gauge Label	Angle (deg)	(PSIA)	T Surf (DegR)	Gauge Label	Angle (deg)	(PSIA)	T Surf (DegR)	Gauge Label	Angle (deg)	(PSIA)	T Surf (DegR)
P 30	-64.44	1.208(0)		P 20	4.79	8.914(0)		P 16	23.89	3.774(1)	
P 28	-50.11	Null		P 15	7.18	1.176(1)		P 11	26.28	2.720(1)	
P 26	-35.79	2.364(0)		P 19	9.57	2.332(1)		P 10	31.05	2.368(1)	
P 25	-28.63	1.790(0)		P 14	11.96	3.049(1)		P 9	38.22	2.412(1)	
P 24	-21.47	9.123(-1)		P 18	14.34	5.455(1)		P 7	52.54	1.966(1)	
P 23	-14.30	7.113(-1)		P 13	16.73	5.813(1)		P 5	66.86	1.433(1)	
P 22	-7.14	1.091(0)		P 17	19.12	6.583(1)		P 3	81.19	Null	
P 21	.02	2.512(0)		P 12	21.51	5.673(1)		P 1	95.51	4.314(0)	

Gauge Label	Angle (deg)	(BTU/Ft2-Sec)	T Surf (DegR)	Gauge Label	Angle (deg)	(BTU/Ft2-Sec)	T Surf (DegR)	Gauge Label	Angle (deg)	(BTU/Ft2-Sec)	T Surf (DegR)
HT 32	-16.31	Null	Null	HT 69	17.69	5.092(2)	884.18	HT 1	26.29	1.729(2)	705.82
HT 31	-13.25	4.251(0)	543.23	HT 70	18.64	4.805(2)	866.61	HT 62	26.29	Null	Null
HT 29	-7.14	1.135(1)	558.16	HT 10	19.10	4.340(2)	849.70	HT 61	29.35	1.631(2)	690.04
HT 28	-4.09	1.871(1)	572.43	HT 71	19.60	4.373(2)	843.84	HT 59	35.46	1.317(2)	664.79
HT 25	5.08	Null	Null	HT 9	19.90	3.739(2)	814.78	HT 58	38.51	1.185(2)	650.37
HT 24	8.14	1.681(2)	793.12	HT 7	21.51	3.110(2)	776.94	HT 57	41.57	1.115(2)	644.85
HT 64	12.91	4.063(2)	892.95	HT 6	22.30	2.649(2)	760.70	HT 56	44.63	1.007(2)	640.03
HT 65	13.87	Null	Null	HT 5	23.09	2.853(2)	774.14	HT 55	47.68	9.397(1)	634.35
HT 66	14.82	5.085(2)	907.63	HT 4	23.89	2.242(2)	736.49	HT 54	50.74	8.389(1)	626.02
HT 67	15.78	5.387(2)	912.79	HT 3	24.69	2.130(2)	727.13	HT 53	53.79	7.624(1)	614.26
HT 68	16.73	5.484(2)	900.65	HT 2	25.49	2.027(2)	718.91				

Run 99 Reduced Data Tabulation

Gauge Label	Angle (deg)	(PSIA)	T Surf (DegR)	Gauge Label	Angle (deg)	(PSIA)	T Surf (DegR)	Gauge Label	Angle (deg)	(PSIA)	T Surf (DegR)
P 30	-64.44	1.598(0)		P 20	4.79	3.956(0)		P 16	23.89	7.771(1)	
P 28	-50.11	Null		P 15	7.18	3.793(0)		P 11	26.28	3.870(1)	
P 26	-35.79	4.063(0)		P 19	9.57	5.641(0)		P 10	31.05	1.837(1)	
P 25	-28.63	5.030(0)		P 14	11.96	9.836(0)		P 9	38.22	2.055(1)	
P 24	-21.47	5.504(0)		P 18	14.34	1.364(1)		P 7	52.54	1.684(1)	
P 23	-14.30	6.655(0)		P 13	16.73	1.771(1)		P 5	66.86	1.267(1)	
P 22	-7.14	7.816(0)		P 17	19.12	5.879(1)		P 3	81.19	Null	
P 21	.02	3.579(0)		P 12	21.51	8.538(1)		P 1	95.51	3.376(0)	

Gauge Label	Angle (deg)	(BTU/Ft2-Sec)	T Surf (DegR)	Gauge Label	Angle (deg)	(BTU/Ft2-Sec)	T Surf (DegR)	Gauge Label	Angle (deg)	(BTU/Ft2-Sec)	T Surf (DegR)
HT 32	-16.31	Null	Null	HT 69	17.69	2.064(2)	777.00	HT 1	26.29	3.224(2)	751.92
HT 31	-13.25	8.252(1)	600.70	HT 70	18.64	2.703(2)	791.42	HT 62	26.29	3.073(2)	758.42
HT 29	-7.14	9.116(1)	595.97	HT 10	19.10	3.813(2)	827.94	HT 61	29.35	1.501(2)	675.18
HT 28	-4.09	6.902(1)	586.49	HT 71	19.60	3.805(2)	840.40	HT 59	35.46	1.415(2)	668.11
HT 25	5.08	Null	Null	HT 9	19.90	4.065(2)	827.49	HT 58	38.51	1.288(2)	645.08
HT 24	8.14	3.349(1)	671.50	HT 7	21.51	5.355(2)	851.76	HT 57	41.57	1.221(2)	641.01
HT 64	12.91	7.198(1)	729.96	HT 6	22.30	5.653(2)	850.16	HT 56	44.63	1.105(2)	637.91
HT 65	13.87	Null	Null	HT 5	23.09	5.872(2)	867.11	HT 55	47.68	1.109(2)	633.11
HT 66	14.82	9.753(1)	741.90	HT 4	23.89	5.253(2)	836.21	HT 54	50.74	1.029(2)	624.58
HT 67	15.78	1.887(2)	829.61	HT 3	24.69	4.712(2)	808.25	HT 53	53.79	8.507(1)	612.24
HT 68	16.73	Null	Null	HT 2	25.49	3.908(2)	777.10				

Run 100 Reduced Data Tabulation

Gauge Label	Angle (deg)	(PSIA)	T Surf (DegR)	Gauge Label	Angle (deg)	(PSIA)	T Surf (DegR)	Gauge Label	Angle (deg)	(PSIA)	T Surf (DegR)
P 30	-57.30	2.142(0)		P 20	11.94	2.406(1)		P 16	31.04	2.770(1)	
P 28	-42.97	2.312(0)		P 15	14.32	4.410(1)		P 11	33.42	2.138(1)	
P 26	-28.65	3.417(0)		P 19	16.71	6.655(1)		P 10	38.20	2.048(1)	
P 25	-21.49	2.102(0)		P 14	19.10	6.831(1)		P 9	45.36	1.990(1)	
P 24	-14.32	1.120(0)		P 18	21.49	4.742(1)		P 7	59.68	1.481(1)	
P 23	-7.16	7.404(-1)		P 13	23.87	3.056(1)		P 5	74.01	1.035(1)	
P 22	.00	1.920(0)		P 17	26.26	2.969(1)		P 3	88.33	Null	
P 21	7.16	6.107(0)		P 12	28.65	2.985(1)		P 1	102.65	2.934(0)	

Gauge Label	Angle (deg)	(BTU/Ft2-Sec)	T Surf (DegR)	Gauge Label	Angle (deg)	(BTU/Ft2-Sec)	T Surf (DegR)	Gauge Label	Angle (deg)	(BTU/Ft2-Sec)	T Surf (DegR)
HT 32	-9.17	Null	Null	HT 69	24.83	2.082(2)	697.43	HT 1	33.43	1.435(2)	652.36
HT 31	-6.11	8.320(0)	545.73	HT 70	25.78	1.918(2)	689.65	HT 62	33.43	2.041(2)	693.31
HT 29	.00	1.995(1)	562.36	HT 10	26.24	1.959(2)	691.23	HT 61	36.49	1.466(2)	657.17
HT 28	3.06	3.046(1)	585.73	HT 71	26.74	1.709(2)	679.74	HT 59	42.60	1.281(2)	637.06
HT 25	12.22	1.607(2)	737.48	HT 9	27.04	1.662(2)	676.24	HT 58	45.66	1.042(2)	619.58
HT 24	15.28	5.444(2)	887.83	HT 7	28.65	1.726(2)	671.66	HT 57	48.71	9.234(1)	615.61
HT 64	20.05	4.310(2)	809.23	HT 6	29.44	1.648(2)	667.89	HT 56	51.77	Null	Null
HT 65	21.01	Null	Null	HT 5	30.24	1.900(2)	690.32	HT 55	54.82	8.165(1)	604.72
HT 66	21.96	2.997(2)	749.17	HT 4	31.04	1.565(2)	664.10	HT 54	57.88	6.928(1)	589.58
HT 67	22.92	2.696(2)	737.07	HT 3	31.83	1.554(2)	662.64	HT 53	60.94	6.900(1)	585.94
HT 68	23.87	Null	Null	HT 2	32.63	1.474(2)	653.93				

Run 101 Reduced Data Tabulation

Gauge Label	Angle (deg)	(PSIA)	T Surf (DegR)	Gauge Label	Angle (deg)	(PSIA)	T Surf (DegR)	Gauge Label	Angle (deg)	(PSIA)	T Surf (DegR)
P 30	-57.30	4.205(-1)		P 20	11.94	2.446(0)		P 16	31.04	4.792(0)	
P 28	-42.97	Null		P 15	14.32	2.141(0)		P 11	33.42	4.351(0)	
P 26	-28.65	1.425(0)		P 19	16.71	2.317(0)		P 10	38.20	3.491(0)	
P 25	-21.49	1.863(0)		P 14	19.10	1.971(0)		P 9	45.36	2.736(0)	
P 24	-14.32	1.871(0)		P 18	21.49	2.479(0)		P 7	59.68	1.457(0)	
P 23	-7.16	1.991(0)		P 13	23.87	2.430(0)		P 5	74.01	5.808(-1)	
P 22	.00	2.054(0)		P 17	26.26	3.911(0)		P 3	88.33	Null	
P 21	7.16	2.269(0)		P 12	28.65	4.763(0)		P 1	102.65	1.045(-1)	

Gauge Label	Angle (deg)	(BTU/Ft2-Sec)	T Surf (DegR)	Gauge Label	Angle (deg)	(BTU/Ft2-Sec)	T Surf (DegR)	Gauge Label	Angle (deg)	(BTU/Ft2-Sec)	T Surf (DegR)
HT 32	-9.17	Null	Null	HT 69	24.83	5.669(1)	562.29	HT 1	33.43	9.003(1)	572.22
HT 31	-6.11	2.393(1)	551.24	HT 70	25.78	5.798(1)	562.69	HT 62	33.43	7.150(1)	568.96
HT 29	.00	2.539(1)	551.88	HT 10	26.24	7.244(1)	566.96	HT 61	36.49	5.833(1)	567.78
HT 28	3.06	2.633(1)	552.58	HT 71	26.74	6.463(1)	564.72	HT 59	42.60	4.512(1)	564.85
HT 25	12.22	Null	Null	HT 9	27.04	6.949(1)	564.05	HT 58	45.66	3.518(1)	560.78
HT 24	15.28	2.953(1)	552.18	HT 7	28.65	7.592(1)	567.01	HT 57	48.71	2.865(1)	558.63
HT 64	20.05	3.707(1)	557.40	HT 6	29.44	8.481(1)	568.22	HT 56	51.77	Null	Null
HT 65	21.01	Null	Null	HT 5	30.24	8.732(1)	571.74	HT 55	54.82	2.145(1)	554.06
HT 66	21.96	4.296(1)	558.07	HT 4	31.04	9.735(1)	576.30	HT 54	57.88	1.872(1)	551.34
HT 67	22.92	5.173(1)	561.39	HT 3	31.83	9.221(1)	572.93	HT 53	60.94	1.545(1)	547.50
HT 68	23.87	4.912(1)	557.37	HT 2	32.63	9.532(1)	572.29				

Run 102 Reduced Data Tabulation

Gauge Label	Angle (deg)	(PSIA)	T Surf (DegR)	Gauge Label	Angle (deg)	(PSIA)	T Surf (DegR)	Gauge Label	Angle (deg)	(PSIA)	T Surf (DegR)
P 30	-57.30	1.670(-1)		P 20	11.94	2.340(-1)		P 16	31.04	3.030(0)	
P 28	-42.97	Null		P 15	14.32	4.795(-1)		P 11	33.42	1.596(0)	
P 26	-28.65	4.381(-1)		P 19	16.71	1.019(0)		P 10	38.20	1.509(0)	
P 25	-21.49	5.153(-1)		P 14	19.10	1.808(0)		P 9	45.36	1.650(0)	
P 24	-14.32	5.114(-1)		P 18	21.49	3.634(0)		P 7	59.68	1.093(0)	
P 23	-7.16	4.871(-1)		P 13	23.87	6.380(0)		P 5	74.01	6.194(-1)	
P 22	.00	3.869(-1)		P 17	26.26	9.051(0)		P 3	88.33	Null	
P 21	7.16	8.460(-2)		P 12	28.65	5.476(0)		P 1	102.65	1.193(-1)	

Gauge Label	Angle (deg)	(BTU/Ft2-Sec)	T Surf (DegR)	Gauge Label	Angle (deg)	(BTU/Ft2-Sec)	T Surf (DegR)	Gauge Label	Angle (deg)	(BTU/Ft2-Sec)	T Surf (DegR)
HT 32	-9.17	Null	Null	HT 69	24.83	1.670(2)	610.98	HT 1	33.43	3.442(1)	552.42
HT 31	-6.11	1.140(1)	527.48	HT 70	25.78	1.728(2)	607.15	HT 62	33.43	2.189(1)	547.08
HT 29	.00	6.967(0)	527.30	HT 10	26.24	1.747(2)	605.79	HT 61	36.49	1.856(1)	544.47
HT 28	3.06	3.402(0)	528.24	HT 71	26.74	1.663(2)	600.04	HT 59	42.60	2.566(1)	543.06
HT 25	12.22	Null	Null	HT 9	27.04	1.573(2)	593.98	HT 58	45.66	2.306(1)	539.82
HT 24	15.28	1.081(1)	559.85	HT 7	28.65	1.187(2)	576.58	HT 57	48.71	2.160(1)	538.63
HT 64	20.05	5.745(1)	587.25	HT 6	29.44	9.753(1)	569.40	HT 56	51.77	Null	Null
HT 65	21.01	Null	Null	HT 5	30.24	8.087(1)	566.27	HT 55	54.82	1.381(1)	534.77
HT 66	21.96	Null	Null	HT 4	31.04	6.987(1)	560.72	HT 54	57.88	1.201(1)	533.09
HT 67	22.92	1.292(2)	607.30	HT 3	31.83	5.075(1)	554.61	HT 53	60.94	1.276(1)	531.30
HT 68	23.87	1.210(2)	593.51	HT 2	32.63	3.815(1)	551.87				

Run 103 Reduced Data Tabulation

Gauge Label	Angle (deg)	(PSIA)	T Surf (DegR)	Gauge Label	Angle (deg)	(PSIA)	T Surf (DegR)	Gauge Label	Angle (deg)	(PSIA)	T Surf (DegR)
P 30	-57.30	1.978(-1)		P 20	11.94	6.186(-1)		P 16	31.04	2.582(0)	
P 28	-42.97	Null		P 15	14.32	4.832(-1)		P 11	33.42	3.481(0)	
P 26	-28.65	4.680(-1)		P 19	16.71	6.293(-1)		P 10	38.20	6.079(0)	
P 25	-21.49	5.280(-1)		P 14	19.10	5.588(-1)		P 9	45.36	1.581(0)	
P 24	-14.32	5.426(-1)		P 18	21.49	5.520(-1)		P 7	59.68	6.565(-1)	
P 23	-7.16	5.703(-1)		P 13	23.87	5.014(-1)		P 5	74.01	4.557(-1)	
P 22	.00	5.954(-1)		P 17	26.26	9.531(-1)		P 3	88.33	Null	
P 21	7.16	5.496(-1)		P 12	28.65	1.750(0)		P 1	102.65	5.736(-2)	

Gauge Label	Angle (deg)	(BTU/Ft2-Sec)	T Surf (DegR)	Gauge Label	Angle (deg)	(BTU/Ft2-Sec)	T Surf (DegR)	Gauge Label	Angle (deg)	(BTU/Ft2-Sec)	T Surf (DegR)
HT 32	-9.17	Null	Null	HT 69	24.83	1.913(1)	546.43	HT 1	33.43	7.023(1)	595.09
HT 31	-6.11	1.292(1)	539.21	HT 70	25.78	2.031(1)	548.22	HT 62	33.43	1.282(2)	609.79
HT 29	.00	1.324(1)	539.36	HT 10	26.24	2.297(1)	553.16	HT 61	36.49	1.482(2)	617.92
HT 28	3.06	1.364(1)	539.11	HT 71	26.74	1.955(1)	550.09	HT 59	42.60	6.298(1)	581.07
HT 25	12.22	3.285(0)	530.86	HT 9	27.04	2.210(1)	556.04	HT 58	45.66	3.145(1)	559.34
HT 24	15.28	1.325(1)	537.52	HT 7	28.65	2.612(1)	562.91	HT 57	48.71	2.108(1)	549.68
HT 64	20.05	1.711(1)	541.69	HT 6	29.44	2.540(1)	564.52	HT 56	51.77	Null	Null
HT 65	21.01	Null	Null	HT 5	30.24	3.725(1)	575.12	HT 55	54.82	1.059(1)	541.39
HT 66	21.96	1.768(1)	542.32	HT 4	31.04	3.342(1)	576.05	HT 54	57.88	9.171(0)	539.43
HT 67	22.92	1.730(1)	543.64	HT 3	31.83	5.055(1)	582.41	HT 53	60.94	8.870(0)	537.98
HT 68	23.87	1.331(1)	541.01	HT 2	32.63	6.193(1)	588.96				

Run 104 Reduced Data Tabulation

Gauge Label	Angle (deg)	(PSIA)	T Surf (DegR)	Gauge Label	Angle (deg)	(PSIA)	T Surf (DegR)	Gauge Label	Angle (deg)	(PSIA)	T Surf (DegR)
P 30	-42.97	2.083(-1)		P 20	26.26	4.645(-1)		P 16	45.36	4.046(0)	
P 28	-28.65	Null		P 15	28.65	5.444(-1)		P 11	47.75	1.791(0)	
P 26	-14.32	3.707(-1)		P 19	31.04	7.012(-1)		P 10	52.52	1.265(0)	
P 25	-7.16	3.605(-1)		P 14	33.42	8.904(-1)		P 9	59.68	5.655(-1)	
P 24	.00	3.766(-1)		P 18	35.81	1.139(0)		P 7	74.01	2.504(-1)	
P 23	7.16	3.798(-1)		P 13	38.20	4.007(0)		P 5	88.33	9.609(-2)	
P 22	14.32	3.770(-1)		P 17	40.58	3.873(0)		P 3	102.65	Null	
P 21	21.49	4.806(-1)		P 12	42.97	3.949(0)		P 1	116.98	-2.643(-2)	

Gauge Label	Angle (deg)	(BTU/Ft2-Sec)	T Surf (DegR)	Gauge Label	Angle (deg)	(BTU/Ft2-Sec)	T Surf (DegR)	Gauge Label	Angle (deg)	(BTU/Ft2-Sec)	T Surf (DegR)
HT 42	-20.76	Null	Null	HT 64	34.38	1.435(1)	549.78	HT 6	43.76	5.005(1)	557.60
HT 41	-17.54	Null	Null	HT 66	36.29	2.053(1)	549.90	HT 5	44.56	4.223(1)	554.72
HT 40	-14.32	Null	Null	HT 67	37.24	2.519(1)	549.88	HT 4	45.36	3.803(1)	554.74
HT 39	-11.10	Null	Null	HT 68	38.20	3.051(1)	551.20	HT 3	46.16	3.101(1)	553.59
HT 37	-4.66	Null	Null	HT 69	39.15	4.069(1)	557.19	HT 2	46.96	2.268(1)	550.40
HT 36	-1.45	Null	Null	HT 70	40.11	4.799(1)	558.50	HT 62	47.76	1.401(1)	545.27
HT 35	1.77	Null	Null	HT 10	40.57	4.067(1)	558.65	HT 1	47.76	2.180(1)	549.45
HT 34	5.16	Null	Null	HT 106	40.58	Null	Null	HT 61	50.81	8.300(0)	540.25
HT 32	5.16	Null	Null	HT 71	41.06	5.414(1)	558.96	HT 59	56.93	4.385(0)	533.34
HT 31	8.21	Null	Null	HT 9	41.37	5.438(1)	562.83	HT 58	59.98	Null	Null
HT 33	8.21	Null	Null	HT 107	41.38	Null	Null	HT 57	63.04	4.201(0)	532.52
HT 29	14.32	-9.195(-1)	526.40	HT 108	42.17	Null	Null	HT 55	69.15	4.408(0)	531.41
HT 28	17.38	3.819(0)	529.85	HT 109	42.97	Null	Null	HT 54	72.20	7.011(0)	533.58
HT 24	29.60	4.241(0)	537.63	HT 7	42.97	Null	Null	HT 53	75.26	Null	Null

Run 106 Reduced Data Tabulation

Gauge Label	Angle (deg)	(PSIA)	T Surf (DegR)	Gauge Label	Angle (deg)	(PSIA)	T Surf (DegR)	Gauge Label	Angle (deg)	(PSIA)	T Surf (DegR)
? 30	-57.30	9.928(-2)		P 20	11.94	3.085(-1)		P 16	31.04	5.034(0)	
? 28	-42.97	Null		P 15	14.32	2.901(-1)		P 11	33.42	5.560(0)	
? 26	-28.65	2.774(-1)		P 19	16.71	2.712(-1)		P 10	38.20	2.463(0)	
? 25	-21.49	2.820(-1)		P 14	19.10	2.931(-1)		P 9	45.36	8.414(-1)	
? 24	-14.32	2.999(-1)		P 18	21.49	4.129(-1)		P 7	59.68	7.526(-1)	
? 23	-7.16	2.963(-1)		P 13	23.87	6.131(-1)		P 5	74.01	4.182(-1)	
? 22	.00	2.932(-1)		P 17	26.26	1.277(0)		P 3	88.33	Null	
? 21	7.16	3.555(-1)		P 12	28.65	3.180(0)		P 1	102.65	5.299(-2)	

Gauge Label	Angle (deg)	(BTU/Ft2-Sec)	T Surf (DegR)	Gauge Label	Angle (deg)	(BTU/Ft2-Sec)	T Surf (DegR)	Gauge Label	Angle (deg)	(BTU/Ft2-Sec)	T Surf (DegR)
HT 31	-6.11	Null	Null	HT 10	26.24	9.756(0)	538.28	HT 1	33.43	6.713(1)	561.13
HT 29	.00	Null	Null	HT 71	26.74	7.630(0)	538.21	HT 61	36.49	2.352(1)	543.30
HT 28	3.06	1.747(0)	527.39	HT 9	27.04	1.483(1)	542.45	HT 59	42.60	9.025(0)	534.20
HT 24	15.28	1.089(0)	527.09	HT 7	28.65	Null	Null	HT 58	45.66	2.438(0)	530.62
HT 64	20.05	3.228(0)	530.60	HT 6	29.44	2.811(1)	551.75	HT 57	48.71	7.084(0)	533.60
HT 66	21.96	2.463(0)	529.85	HT 5	30.24	3.754(1)	555.22	HT 55	54.82	9.846(0)	532.84
HT 67	22.92	4.667(-1)	529.23	HT 4	31.04	4.384(1)	559.04	HT 54	57.88	9.576(0)	533.73
HT 68	23.87	2.462(0)	531.15	HT 3	31.83	6.208(1)	564.35	HT 53	60.94	3.224(0)	527.57
HT 69	24.83	5.081(0)	535.18	HT 2	32.63	6.562(1)	561.20				
HT 70	25.78	6.380(0)	536.98	HT 62	33.43	5.149(1)	556.66				

Run 107 Reduced Data Tabulation

Gauge Label	Angle (deg)	(PSIA)	T Surf (DegR)	Gauge Label	Angle (deg)	(PSIA)	T Surf (DegR)	Gauge Label	Angle (deg)	(PSIA)	T Surf (DegR)
P 30	-57.30	1.234(-1)		P 20	11.94	3.868(-1)		P 16	31.04	9.363(-1)	
P 28	-42.97	Null		P 15	14.32	3.642(-1)		P 11	33.42	2.746(0)	
P 26	-28.65	2.874(-1)		P 19	16.71	3.830(-1)		P 10	38.20	5.402(0)	
P 25	-21.49	2.875(-1)		P 14	19.10	Null		P 9	45.36	1.327(0)	
P 24	-14.32	3.168(-1)		P 18	21.49	3.162(-1)		P 7	59.68	4.357(-1)	
P 23	-7.16	3.251(-1)		P 13	23.87	3.942(-1)		P 5	74.01	3.375(-1)	
P 22	.00	3.378(-1)		P 17	26.26	4.844(-1)		P 3	88.33	Null	
P 21	7.16	4.264(-1)		P 12	28.65	7.026(-1)		P 1	102.65	3.899(-2)	

Gauge Label	Angle (deg)	(BTU/Ft2-Sec)	T Surf (DegR)	Gauge Label	Angle (deg)	(BTU/Ft2-Sec)	T Surf (DegR)	Gauge Label	Angle (deg)	(BTU/Ft2-Sec)	T Surf (DegR)
HT 31	-6.11	-3.077(0)	522.98	HT 10	26.24	4.318(0)	532.19	HT 1	33.43	1.365(1)	545.49
HT 29	.00	-1.106(0)	525.53	HT 71	26.74	3.477(0)	530.99	HT 61	36.49	5.207(1)	568.68
HT 28	3.06	1.967(0)	528.84	HT 9	27.04	5.144(0)	533.88	HT 59	42.60	2.422(1)	549.54
HT 24	15.28	1.063(0)	528.70	HT 7	28.65	5.730(0)	534.21	HT 58	45.66	9.599(0)	538.52
HT 64	20.05	3.165(0)	530.91	HT 6	29.44	6.329(0)	534.50	HT 57	48.71	6.721(0)	537.28
HT 66	21.96	3.428(0)	529.20	HT 5	30.24	4.618(0)	533.57	HT 55	54.82	4.907(0)	532.32
HT 67	22.92	-5.636(-2)	526.86	HT 4	31.04	7.402(0)	537.61	HT 54	57.88	6.484(0)	534.97
HT 68	23.87	2.427(0)	529.50	HT 3	31.83	1.043(1)	541.30	HT 53	60.94	2.071(0)	528.56
HT 69	24.83	3.821(0)	531.39	HT 2	32.63	1.032(1)	541.39				
HT 70	25.78	4.277(0)	531.44	HT 62	33.43	2.610(1)	555.37				

Run 108 Reduced Data Tabulation

Gauge Label	Angle (deg)	(PSIA)	T Surf (DegR)	Gauge Label	Angle (deg)	(PSIA)	T Surf (DegR)	Gauge Label	Angle (deg)	(PSIA)	T Surf (DegR)
P 30	-57.30	2.357(-2)		P 20	11.94	2.168(0)		P 16	31.04	Null	
P 28	-42.97	Null		P 15	14.32	1.988(0)		P 11	33.42	1.672(0)	
P 26	-28.65	1.538(-1)		P 19	16.71	2.201(0)		P 10	38.20	1.559(0)	
P 25	-21.49	2.533(-1)		P 14	19.10	1.768(0)		P 9	45.36	1.507(0)	
P 24	-14.32	5.875(-1)		P 18	21.49	1.819(0)		P 7	59.68	1.187(0)	
P 23	-7.16	1.163(0)		P 13	23.87	1.816(0)		P 5	74.01	7.156(-1)	
P 22	.00	2.217(0)		P 17	26.26	Null		P 3	88.33	Null	
P 21	7.16	2.573(0)		P 12	28.65	Null		P 1	102.65	8.421(-2)	

Gauge Label	Angle (deg)	(BTU/Ft2-Sec)	T Surf (DegR)	Gauge Label	Angle (deg)	(BTU/Ft2-Sec)	T Surf (DegR)	Gauge Label	Angle (deg)	(BTU/Ft2-Sec)	T Surf (DegR)
HT 31	-6.11	1.004(1)	543.53	HT 10	26.24	8.763(0)	544.68	HT 1	33.43	7.454(0)	543.75
HT 29	.00	2.273(1)	551.26	HT 71	26.74	7.667(0)	544.15	HT 61	36.49	9.700(0)	545.57
HT 28	3.06	2.525(1)	553.14	HT 9	27.04	1.036(1)	545.84	HT 59	42.60	8.885(0)	545.01
HT 24	15.28	8.831(0)	545.82	HT 7	28.65	8.794(0)	544.22	HT 58	45.66	6.241(0)	541.84
HT 64	20.05	1.007(1)	546.52	HT 6	29.44	9.172(0)	544.35	HT 57	48.71	8.936(0)	543.96
HT 66	21.96	7.585(0)	543.19	HT 5	30.24	6.656(0)	542.59	HT 55	54.82	8.220(0)	542.54
HT 67	22.92	5.546(0)	542.01	HT 4	31.04	7.378(0)	544.21	HT 54	57.88	9.683(0)	543.54
HT 68	23.87	6.253(0)	541.75	HT 3	31.83	9.039(0)	545.09	HT 53	60.94	Null	Null
HT 69	24.83	8.767(0)	545.41	HT 2	32.63	7.316(0)	543.43				
HT 70	25.78	9.239(0)	545.15	HT 62	33.43	8.884(0)	545.60				

Run 109 Reduced Data Tabulation

Gauge Label	Angle (deg)	(PSIA)	T Surf (DegR)	Gauge Label	Angle (deg)	(PSIA)	T Surf (DegR)	Gauge Label	Angle (deg)	(PSIA)	T Surf (DegR)
P 30	-57.30	1.140(-1)		P 20	11.94	4.091(-1)		P 16	31.04	2.510(0)	
P 28	-42.97	Null		P 15	14.32	3.380(-1)		P 11	33.42	6.353(0)	
P 26	-28.65	2.371(-1)		P 19	16.71	3.945(-1)		P 10	38.20	2.594(0)	
P 25	-21.49	3.108(-1)		P 14	19.10	3.152(-1)		P 9	45.36	1.056(0)	
P 24	-14.32	3.082(-1)		P 18	21.49	3.792(-1)		P 7	59.68	7.529(-1)	
P 23	-7.16	3.283(-1)		P 13	23.87	5.400(-1)		P 5	74.01	5.523(-1)	
P 22	.00	3.445(-1)		P 17	26.26	7.239(-1)		P 3	88.33	Null	
P 21	7.16	3.783(-1)		P 12	28.65	2.243(0)		P 1	102.65	1.011(-1)	

Gauge Label	Angle (deg)	(BTU/Ft2-Sec)	T Surf (DegR)	Gauge Label	Angle (deg)	(BTU/Ft2-Sec)	T Surf (DegR)	Gauge Label	Angle (deg)	(BTU/Ft2-Sec)	T Surf (DegR)
HT 31	-6.11	3.753(0)	543.24	HT 10	26.24	1.682(1)	554.35	HT 1	33.43	6.222(1)	586.02
HT 29	.00	4.027(0)	543.29	HT 71	26.74	2.024(1)	556.25	HT 61	36.49	3.515(1)	586.97
HT 28	3.06	3.720(0)	543.43	HT 9	27.04	1.808(1)	555.81	HT 59	42.60	1.332(1)	563.66
HT 24	15.28	4.476(0)	544.42	HT 7	28.65	2.309(1)	561.21	HT 58	45.66	7.712(0)	554.34
HT 64	20.05	6.821(0)	545.83	HT 6	29.44	2.494(1)	563.16	HT 57	48.71	6.658(0)	548.97
HT 66	21.96	8.971(0)	547.11	HT 5	30.24	2.925(1)	568.95	HT 55	54.82	7.169(0)	546.43
HT 67	22.92	1.145(1)	548.33	HT 4	31.04	2.962(1)	572.72	HT 54	57.88	6.229(0)	545.97
HT 68	23.87	6.828(0)	546.70	HT 3	31.83	3.875(1)	577.90	HT 53	60.94	6.416(0)	545.54
HT 69	24.83	1.612(1)	551.94	HT 2	32.63	5.637(1)	584.12				
HT 70	25.78	1.761(1)	553.74	HT 62	33.43	6.570(1)	598.70				

Run 110 Reduced Data Tabulation

Gauge Label	Angle (deg)	(PSIA)	T Surf (DegR)	Gauge Label	Angle (deg)	(PSIA)	T Surf (DegR)	Gauge Label	Angle (deg)	(PSIA)	T Surf (DegR)
P 30	-42.97	2.036(-1)		P 20	26.26	4.691(-1)		P 16	45.36	8.178(-1)	
P 28	-28.65	Null		P 15	28.65	3.982(-1)		P 11	47.75	8.259(-1)	
P 26	-14.32	3.491(-1)		P 19	31.04	4.518(-1)		P 10	52.52	1.119(0)	
P 25	-7.16	3.951(-1)		P 14	33.42	3.837(-1)		P 9	59.68	1.207(0)	
P 24	.00	3.844(-1)		P 18	35.81	4.311(-1)		P 7	74.01	6.150(-1)	
P 23	7.16	3.781(-1)		P 13	38.20	4.308(-1)		P 5	88.33	2.119(-1)	
P 22	14.32	3.868(-1)		P 17	40.58	5.427(-1)		P 3	102.65	1.374(-3)	
P 21	21.49	4.207(-1)		P 12	42.97	6.498(-1)		P 1	116.98	1.755(-2)	

Gauge Label	Angle (deg)	(BTU/Ft2-Sec)	T Surf (DegR)	Gauge Label	Angle (deg)	(BTU/Ft2-Sec)	T Surf (DegR)	Gauge Label	Angle (deg)	(BTU/Ft2-Sec)	T Surf (DegR)
HT 31	8.21	2.781(0)	539.41	HT 10	40.57	5.611(0)	542.27	HT 1	47.76	9.981(0)	546.75
HT 29	14.32	2.876(0)	539.95	HT 71	41.06	5.902(0)	542.57	HT 61	50.81	1.452(1)	550.42
HT 28	17.38	3.419(0)	541.74	HT 9	41.37	5.930(0)	542.73	HT 59	56.93	1.745(1)	552.01
HT 24	29.60	3.581(0)	540.24	HT 7	42.97	6.508(0)	543.38	HT 58	59.98	1.624(1)	551.05
HT 64	34.38	4.133(0)	540.57	HT 6	43.76	7.162(0)	544.01	HT 57	63.04	1.398(1)	549.00
HT 66	36.29	4.663(0)	540.87	HT 5	44.56	7.724(0)	544.68	HT 55	69.15	9.922(0)	545.18
HT 67	37.24	4.780(0)	541.18	HT 4	45.36	Null	Null	HT 54	72.20	8.016(0)	543.43
HT 68	38.20	4.513(0)	540.81	HT 3	46.16	8.886(0)	545.79	HT 53	75.26	Null	Null
HT 69	39.15	5.127(0)	541.59	HT 2	46.96	9.353(0)	546.14				
HT 70	40.11	5.362(0)	541.78	HT 62	47.76	1.159(1)	548.33				

Run 112 Reduced Data Tabulation

Gauge Label	Angle (deg)	(PSIA)	T Surf (DegR)	Gauge Label	Angle (deg)	(PSIA)	T Surf (DegR)	Gauge Label	Angle (deg)	(PSIA)	T Surf (DegR)
P 30	-64.44	1.051(-1)		P 20	4.79	1.360(0)		P 16	23.89	2.669(0)	
P 28	-50.11	-7.370(-3)		P 15	7.18	1.433(0)		P 11	26.28	2.235(0)	
P 26	-35.79	3.233(-1)		P 19	9.57	3.109(0)		P 10	31.05	2.116(0)	
P 25	-28.63	3.556(-1)		P 14	11.96	3.359(0)		P 9	38.22	2.039(0)	
P 24	-21.47	2.447(-1)		P 18	14.34	5.424(0)		P 7	52.54	1.391(0)	
P 23	-14.30	1.774(-1)		P 13	16.73	5.511(0)		P 5	66.86	8.549(-1)	
P 22	-7.14	2.085(-1)		P 17	19.12	3.239(0)		P 3	81.19	-5.920(-3)	
P 21	.02	5.659(-1)		P 12	21.51	2.844(0)		P 1	95.51	2.034(-1)	

Gauge Label	Angle (deg)	(BTU/Ft2-Sec)	T Surf (DegR)	Gauge Label	Angle (deg)	(BTU/Ft2-Sec)	T Surf (DegR)	Gauge Label	Angle (deg)	(BTU/Ft2-Sec)	T Surf (DegR)
HT 31	-13.25	3.218(0)	529.34	HT 10	19.10	3.208(1)	548.26	HT 1	26.29	9.899(0)	535.98
HT 29	-7.14	2.216(0)	529.91	HT 71	19.60	2.783(1)	546.46	HT 61	29.35	1.439(1)	539.63
HT 28	-4.09	-8.505(-1)	528.98	HT 9	19.90	2.621(1)	546.69	HT 59	35.46	8.932(0)	535.84
HT 24	8.14	2.209(1)	545.10	HT 7	21.51	1.876(1)	542.90	HT 58	38.51	9.605(0)	534.20
HT 64	12.91	4.890(1)	553.16	HT 6	22.30	1.975(1)	543.13	HT 57	41.57	8.516(0)	533.94
HT 66	14.82	Null	Null	HT 5	23.09	1.709(1)	541.87	HT 55	47.68	8.097(0)	533.55
HT 67	15.78	4.460(1)	552.12	HT 4	23.89	1.604(1)	541.17	HT 54	50.74	7.930(0)	533.48
HT 68	16.73	3.751(1)	548.95	HT 3	24.69	1.773(1)	541.97	HT 53	53.79	6.950(0)	532.52
HT 69	17.69	3.811(1)	550.31	HT 2	25.49	1.569(1)	541.21				
HT 70	18.64	3.256(1)	548.58	HT 62	26.29	1.540(1)	541.81				

Run 113 Reduced Data Tabulation

Gauge Label	Angle (deg)	(PSIA)	T Surf (DegR)	Gauge Label	Angle (deg)	(PSIA)	T Surf (DegR)	Gauge Label	Angle (deg)	(PSIA)	T Surf (DegR)
P 30	-57.30	9.126(-2)		P 20	11.94	1.807(-1)		P 16	31.04	6.937(0)	
P 28	-42.97	Null		P 15	14.32	1.971(-1)		P 11	33.42	3.747(0)	
P 26	-28.65	2.290(-1)		P 19	16.71	2.030(-1)		P 10	38.20	1.102(0)	
P 25	-21.49	2.708(-1)		P 14	19.10	2.186(-1)		P 9	45.36	1.046(0)	
P 24	-14.32	2.739(-1)		P 18	21.49	4.887(-1)		P 7	59.68	9.249(-1)	
P 23	-7.16	2.578(-1)		P 13	23.87	1.443(0)		P 5	74.01	5.458(-1)	
P 22	.00	2.186(-1)		P 17	26.26	3.728(0)		P 3	88.33	Null	
P 21	7.16	1.982(-1)		P 12	28.65	6.383(0)		P 1	102.65	1.102(-1)	

Gauge Label	Angle (deg)	(BTU/Ft2-Sec)	T Surf (DegR)	Gauge Label	Angle (deg)	(BTU/Ft2-Sec)	T Surf (DegR)	Gauge Label	Angle (deg)	(BTU/Ft2-Sec)	T Surf (DegR)
HT 31	-6.11	2.055(0)	530.38	HT 10	26.24	2.944(1)	554.50	HT 1	33.43	3.556(1)	562.64
HT 29	.00	1.712(0)	530.37	HT 71	26.74	3.357(1)	556.17	HT 61	36.49	1.050(1)	544.36
HT 28	3.06	1.412(0)	530.30	HT 9	27.04	3.719(1)	559.15	HT 59	42.60	7.529(0)	537.19
HT 24	15.28	2.239(0)	532.18	HT 7	28.65	4.743(1)	565.90	HT 58	45.66	7.499(0)	536.35
HT 64	20.05	4.792(0)	536.54	HT 6	29.44	4.826(1)	568.39	HT 57	48.71	7.023(0)	535.40
HT 66	21.96	1.065(1)	538.91	HT 5	30.24	5.449(1)	577.10	HT 55	54.82	6.108(0)	534.47
HT 67	22.92	1.046(1)	542.07	HT 4	31.04	4.557(1)	568.42	HT 54	57.88	5.465(0)	533.85
HT 68	23.87	1.298(1)	542.87	HT 3	31.83	4.437(1)	567.80	HT 53	60.94	5.005(0)	533.30
HT 69	24.83	2.034(1)	548.29	HT 2	32.63	4.108(1)	565.57				
HT 70	25.78	2.632(1)	551.49	HT 62	33.43	2.594(1)	558.59				

Run 114 Reduced Data Tabulation

Gauge Label	Angle (deg)	(PSIA)	T Surf (DegR)	Gauge Label	Angle (deg)	(PSIA)	T Surf (DegR)	Gauge Label	Angle (deg)	(PSIA)	T Surf (DegR)
P 30	-64.44	2.385(-2)		P 20	4.79	7.802(-1)		P 16	23.89	3.492(0)	
P 28	-50.11	Null		P 15	7.18	1.333(0)		P 11	26.28	1.686(0)	
P 26	-35.79	3.190(-2)		P 19	9.57	Null		P 10	31.05	1.493(0)	
P 25	-28.63	3.015(-2)		P 14	11.96	Null		P 9	38.22	1.525(0)	
P 24	-21.47	3.937(-2)		P 18	14.34	4.646(0)		P 7	52.54	1.106(0)	
P 23	-14.30	4.742(-2)		P 13	16.73	4.542(0)		P 5	66.86	Null	
P 22	-7.14	1.038(-1)		P 17	19.12	3.882(0)		P 3	81.19	Null	
P 21	.02	3.103(-1)		P 12	21.51	3.409(0)		P 1	95.51	1.876(-1)	

Gauge Label	Angle (deg)	(BTU/Ft2-Sec)	T Surf (DegR)	Gauge Label	Angle (deg)	(BTU/Ft2-Sec)	T Surf (DegR)	Gauge Label	Angle (deg)	(BTU/Ft2-Sec)	T Surf (DegR)
HT 31	-13.25	5.729(-1)	525.56	HT 10	19.10	4.219(1)	558.40	HT 1	26.29	1.625(1)	540.47
HT 29	-7.14	9.531(-1)	526.61	HT 71	19.60	4.485(1)	559.31	HT 61	29.35	1.025(1)	537.14
HT 28	-4.09	1.300(0)	527.89	HT 9	19.90	4.247(1)	557.21	HT 59	35.46	1.083(1)	535.44
HT 24	8.14	1.434(1)	551.59	HT 7	21.51	3.520(1)	551.71	HT 58	38.51	1.015(1)	534.61
HT 64	12.91	3.140(1)	562.21	HT 6	22.30	3.253(1)	550.32	HT 57	41.57	8.992(0)	533.63
HT 66	14.82	4.211(1)	564.53	HT 5	23.09	2.948(1)	548.91	HT 55	47.68	7.721(0)	532.36
HT 67	15.78	4.585(1)	564.54	HT 4	23.89	2.471(1)	545.94	HT 54	50.74	7.069(0)	531.65
HT 68	16.73	4.375(1)	559.84	HT 3	24.69	2.173(1)	544.18	HT 53	53.79	6.486(0)	531.09
HT 69	17.69	5.104(1)	563.98	HT 2	25.49	1.854(1)	541.97				
HT 70	18.64	4.714(1)	561.14	HT 62	26.29	1.319(1)	539.27				

Run 115 Reduced Data Tabulation

Gauge Label	Angle (deg)	(PSIA)	T Surf (DegR)	Gauge Label	Angle (deg)	(PSIA)	T Surf (DegR)	Gauge Label	Angle (deg)	(PSIA)	T Surf (DegR)
P 30	-64.44	Null		P 20	4.79	3.451(-1)		P 16	23.89	4.421(-1)	
P 28	-50.11	Null		P 15	7.18	3.261(-1)		P 11	26.28	3.914(-1)	
P 26	-35.79	1.477(-1)		P 19	9.57	3.437(-1)		P 10	31.05	1.249(0)	
P 25	-28.63	2.614(-1)		P 14	11.96	3.164(-1)		P 9	38.22	3.243(0)	
P 24	-21.47	2.807(-1)		P 18	14.34	3.099(-1)		P 7	52.54	1.425(0)	
P 23	-14.30	2.913(-1)		P 13	16.73	3.173(-1)		P 5	66.86	4.716(-1)	
P 22	-7.14	3.117(-1)		P 17	19.12	3.819(-1)		P 3	81.19	Null	
P 21	.02	3.490(-1)		P 12	21.51	3.847(-1)		P 1	95.51	1.229(-1)	

Gauge Label	Angle (deg)	(BTU/Ft2-Sec)	T Surf (DegR)	Gauge Label	Angle (deg)	(BTU/Ft2-Sec)	T Surf (DegR)	Gauge Label	Angle (deg)	(BTU/Ft2-Sec)	T Surf (DegR)
HT 31	-13.25	3.482(0)	528.21	HT 10	19.10	3.823(0)	529.93	HT 1	26.29	5.104(0)	530.53
HT 29	-7.14	3.449(0)	528.33	HT 71	19.60	5.061(0)	530.77	HT 61	29.35	1.616(1)	538.01
HT 28	-4.09	3.790(0)	528.64	HT 9	19.90	3.928(0)	530.01	HT 59	35.46	5.876(1)	558.88
HT 24	8.14	3.855(0)	529.65	HT 7	21.51	4.185(0)	530.09	HT 58	38.51	Null	Null
HT 64	12.91	3.950(0)	529.01	HT 6	22.30	4.419(0)	530.44	HT 57	41.57	Null	Null
HT 66	14.82	5.657(0)	529.72	HT 5	23.09	4.476(0)	530.53	HT 55	47.68	Null	Null
HT 67	15.78	3.875(0)	529.38	HT 4	23.89	4.797(0)	530.76	HT 54	50.74	8.465(0)	548.11
HT 68	16.73	3.611(0)	528.96	HT 3	24.69	5.499(0)	531.25	HT 53	53.79	6.183(0)	539.48
HT 69	17.69	4.351(0)	529.91	HT 2	25.49	5.314(0)	531.11				
HT 70	18.64	4.346(0)	529.84	HT 62	26.29	8.460(0)	533.16				

Run 116 Reduced Data Tabulation

Appendix C
MULTIPLE-SHOCK/SHOCK-INTERACTION STUDY DATA

Test Conditions, Heat Transfer and
Pressure Measurements, Schlieren Photographs,
and Reduced Data Tabulations

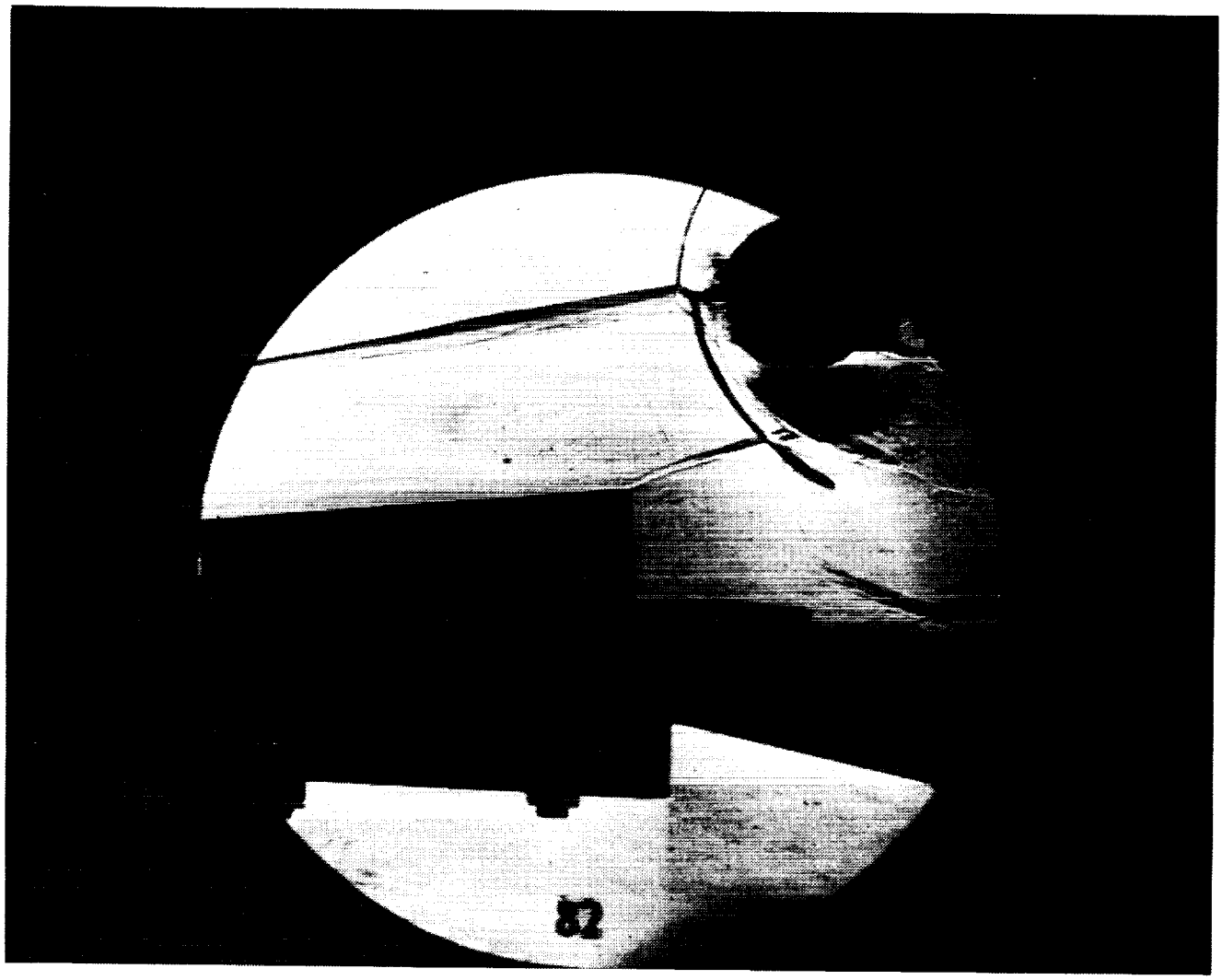

Test Conditions for Run 82 :

Po	= 1.403E+03 PSIA	Reservoir Total Pressure
Ho	= 1.852E+07 (Ft/sec)²	Reservoir Total Enthalpy
To	= 2.814E-03 °R	Reservoir Total Temperature
M	= 8.041E+00	Freestream Mach Number
U	= 5.866E+03 Ft/sec	Freestream Velocity
T	= 2.213E-02 °R	Freestream Temperature
P	= 1.226E-01 PSIA	Freestream Static Pressure
Rho	= 4.648E-05 Slugs/Ft3	Freestream Density
Mu	= 1.829E-07 Slugs/Ft-sec	Freestream Viscosity
Re	= 1.491E+06 1/Ft	Freestream Reynolds Number
Po'	= 1.030E+01 PSIA	Pitot Pressure
Q	= 5.553E+00 PSIA	Dynamic Pressure (½·Rho·U²/144)
Mi	= 3.411E+00	Shock Tube Incident Shock Mach Number
Hw	= 3.183E+06 (Ft/sec)²	Wall Enthalpy (Cp·Tw)
CPf	= 1.801E-01 1/PSIA	Pressure to CP factor (1/Q)
CHf	= 1.861E-04 Ft²-s/BTU	Heat Rate to CH factor (778/(Rho·U·(Ho-Hw))
QoFR	= 4.029E-01 BTU/Ft²-s	Fay-Riddell Heat Transfer to 3" Diam Sphere

Model Configuration Parameter	Value
Stagnation Position (gauge label)	P21
Vertical Distance (inches)	3.90
Horizontal Distance (inches)	1.58
Plate Angle (degrees)	7.50
Plate Length (inches)	36.00
Sweep Angle (degrees)	0.00

Run 82

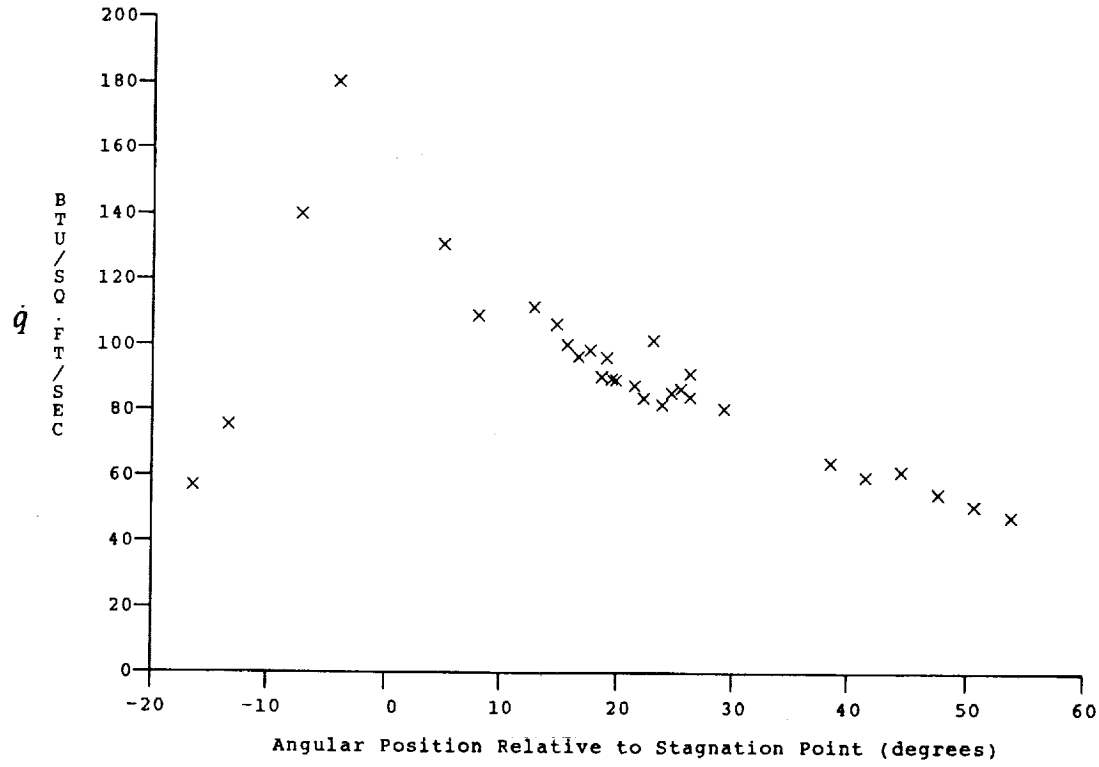

HEAT TRANSFER vs Gauge Position
Run 82

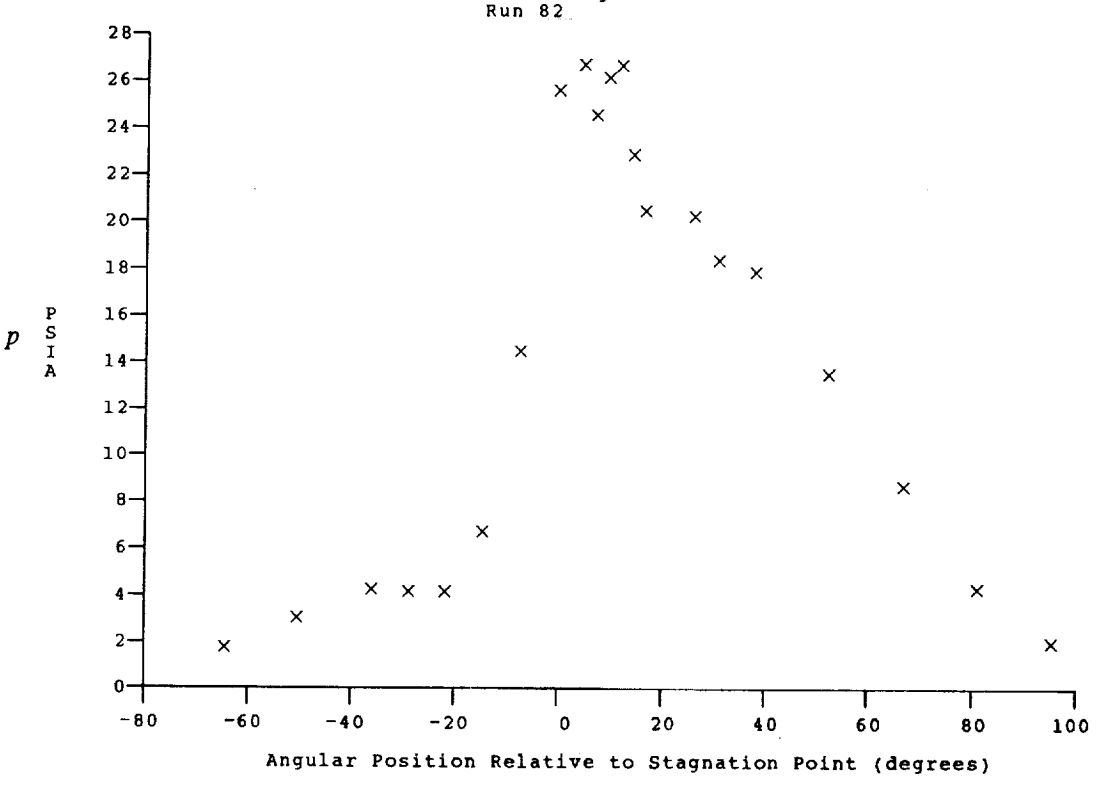

PRESSURE vs Gauge Position
Run 82

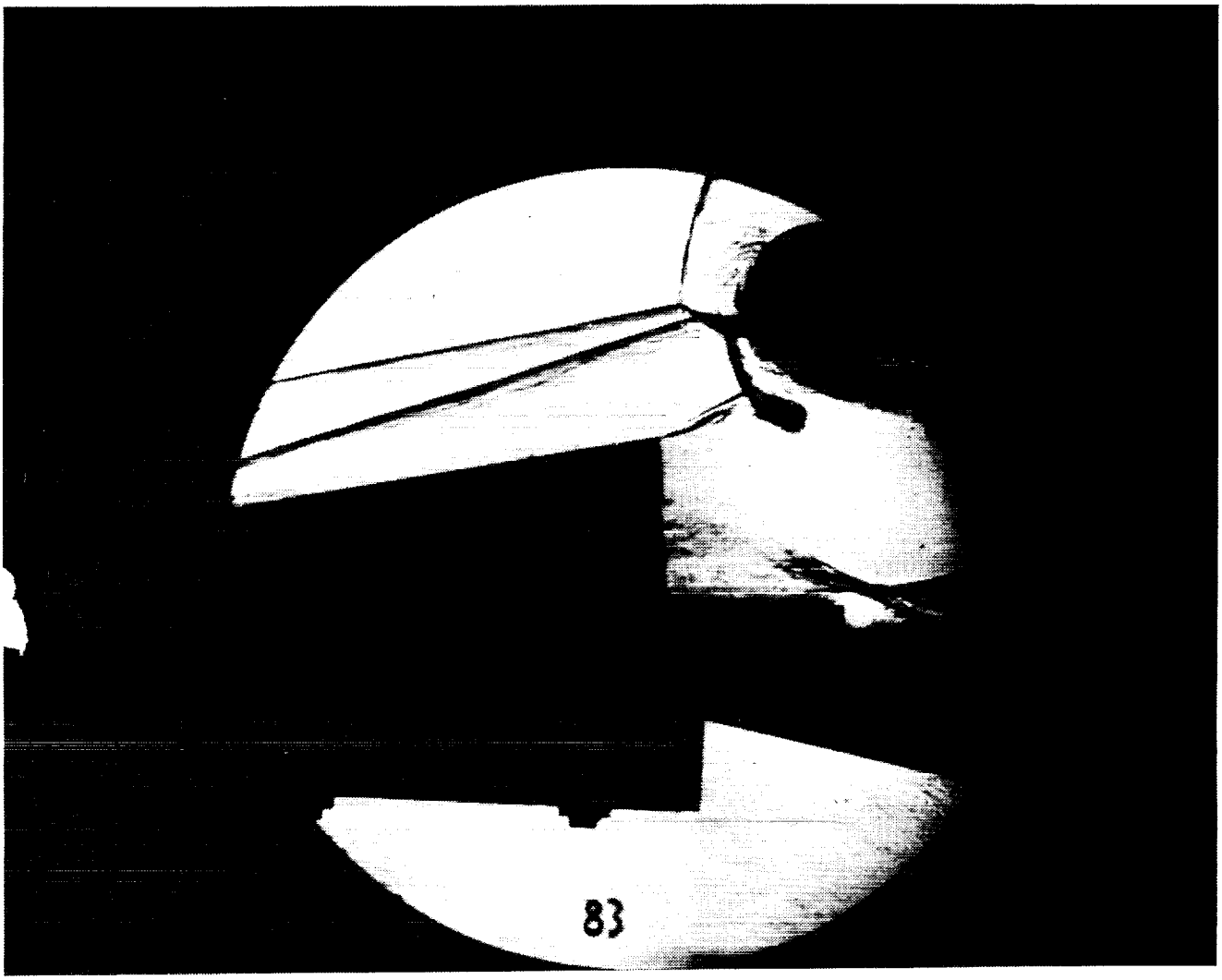

Test Conditions for Run 83 :

Po	= 1.380E-03	PSIA	Reservoir Total Pressure
Ho	= 1.881E+07	(Ft/sec)²	Reservoir Total Enthalpy
To	= 2.856E-03	°R	Reservoir Total Temperature
M	= 8.038E-00		Freestream Mach Number
U	= 5.912E-03	Ft/sec	Freestream Velocity
T	= 2.250E+02	°R	Freestream Temperature
P	= 1.201E-01	PSIA	Freestream Static Pressure
Rho	= 4.482E-05	Slugs/Ft3	Freestream Density
Mu	= 1.857E-07	Slugs/Ft-sec	Freestream Viscosity
Re	= 1.427E+06	1/Ft	Freestream Reynolds Number
Po'	= 1.009E+01	PSIA	Pitot Pressure
Q	= 5.440E+00	PSIA	Dynamic Pressure (½·Rho·U²/144)
Mi	= 3.413E+00		Shock Tube Incident Shock Mach Number
Hw	= 3.183E+06	(Ft/sec)²	Wall Enthalpy (Cp·Tw)
CPf	= 1.838E-01	1/PSIA	Pressure to CP factor (1/Q)
CHf	= 1.879E-04	Ft²-s/BTU	Heat Rate to CH factor (778/(Rho·U·(Ho-Hw))
QoFR	= 4.070E+01	BTU/Ft²-s	Fay-Riddell Heat Transfer to 3" Diam Sphere

Model Configuration Parameter	Value
Stagnation Position (gauge label)	P21
Vertical Distance (inches)	3.97
Horizontal Distance (inches)	1.32
Plate Angle (degrees)	7.50
Plate Length (inches)	36.00
Sweep Angle (degrees)	0.00
BOW to BOP (inches)	0.05
Wedge Angle (degrees)	5.00
Wedge Length (inches)	14.00

Run 83

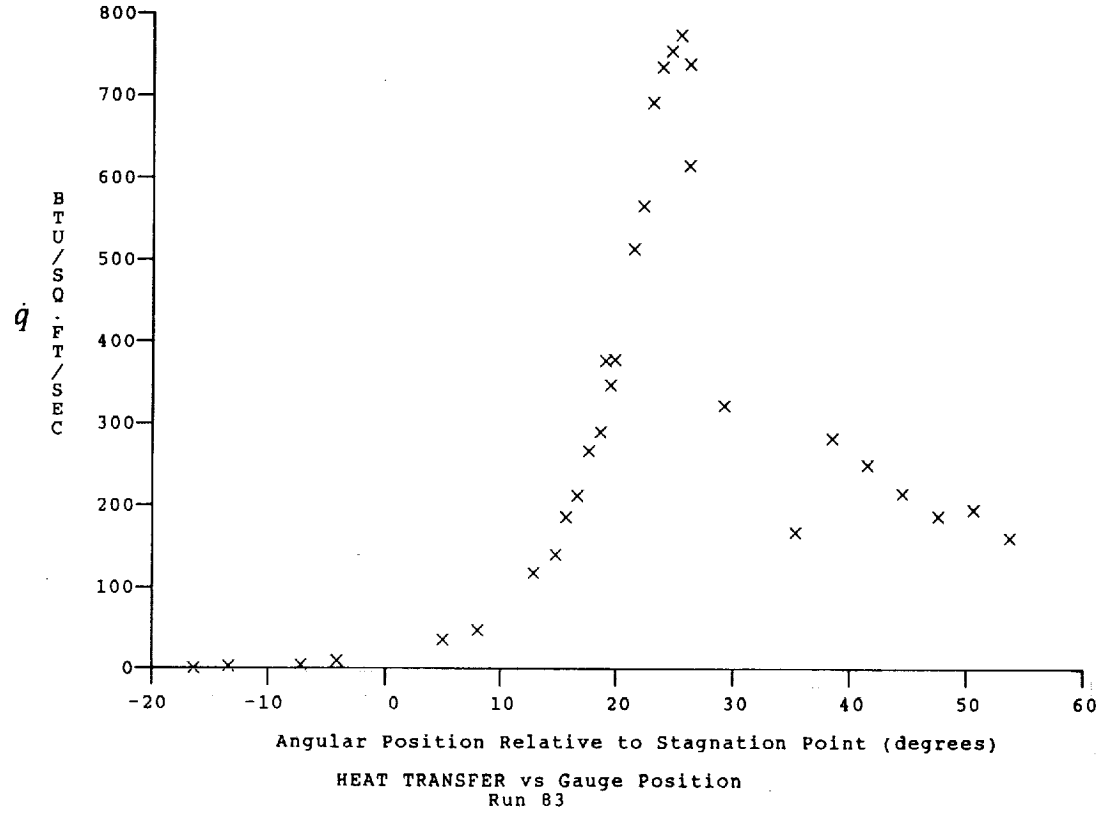

HEAT TRANSFER vs Gauge Position
Run 83

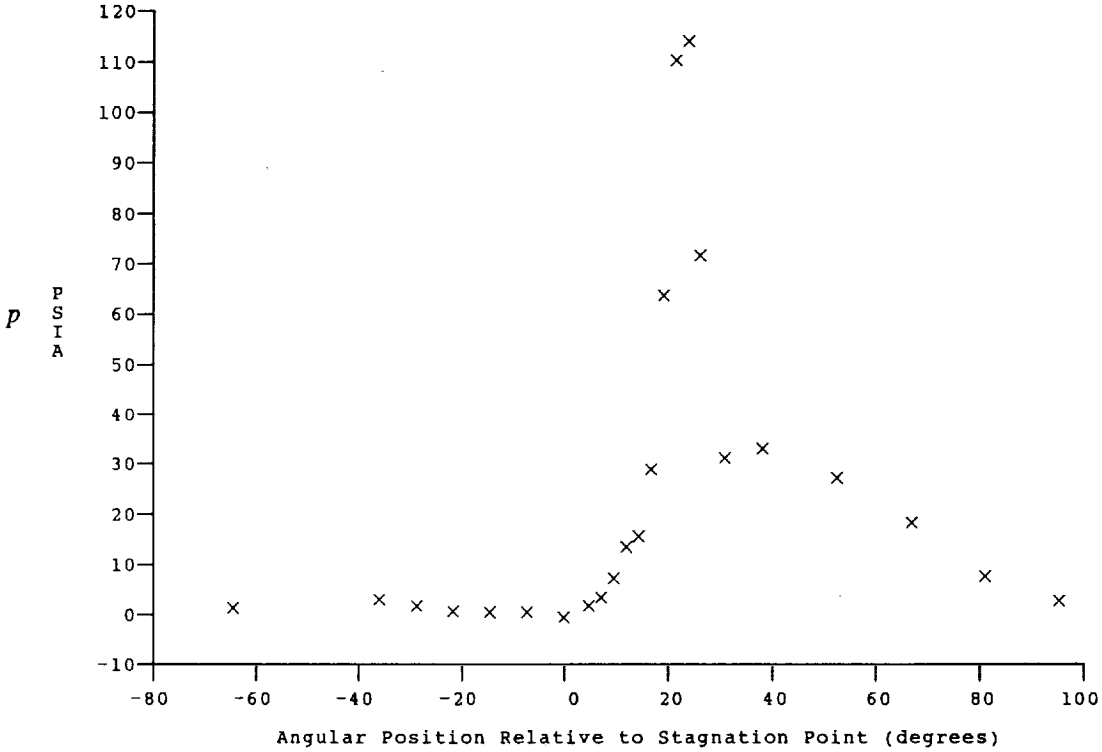

PRESSURE vs Gauge Position
Run 83

Test Conditions

Mi	= 3.4127	
Po	= 1.4010X10+3	PSIA
Ho	= 1.8926X10+7	(Ft/sec)^2
To	= 2.8722X10+3	Degrees R
M	= 8.0403	
U	= 5.9304X10+3	Ft/sec
T	= 2.2623X10+2	Degrees R
P	= 1.2152X10-1	PSIA
Q	= 5.5050	PSIA
Rho	= 4.5080X10-5	Slugs/Ft^3
Mu	= 1.8670X10-7	Slugs/Ft-sec
Re	= 1.4319X10+6	1/Ft
Po'	= 1.0209X10+1	PSIA

Model Configuration Parameter	Value
Stagnation Position (gauge label)	P21
Vertical Distance (inches)	3.97
Horizontal Distance (inches)	1.32
Plate Angle (degrees)	7.50
Plate Length (inches)	36.00
Sweep Angle (degrees)	0.00
BOW to BOP (inches)	1.05
Wedge Angle (degrees)	5.00
Wedge Length (inches)	14.00

Run 84

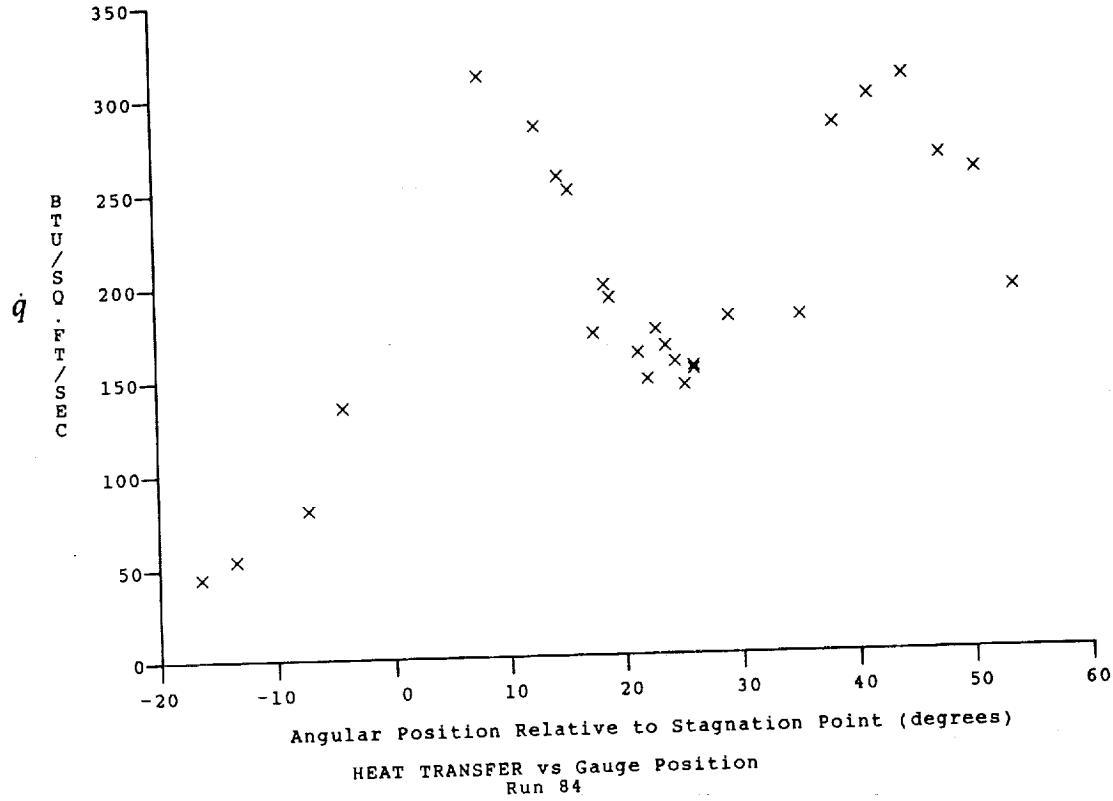

HEAT TRANSFER vs Gauge Position
Run 84

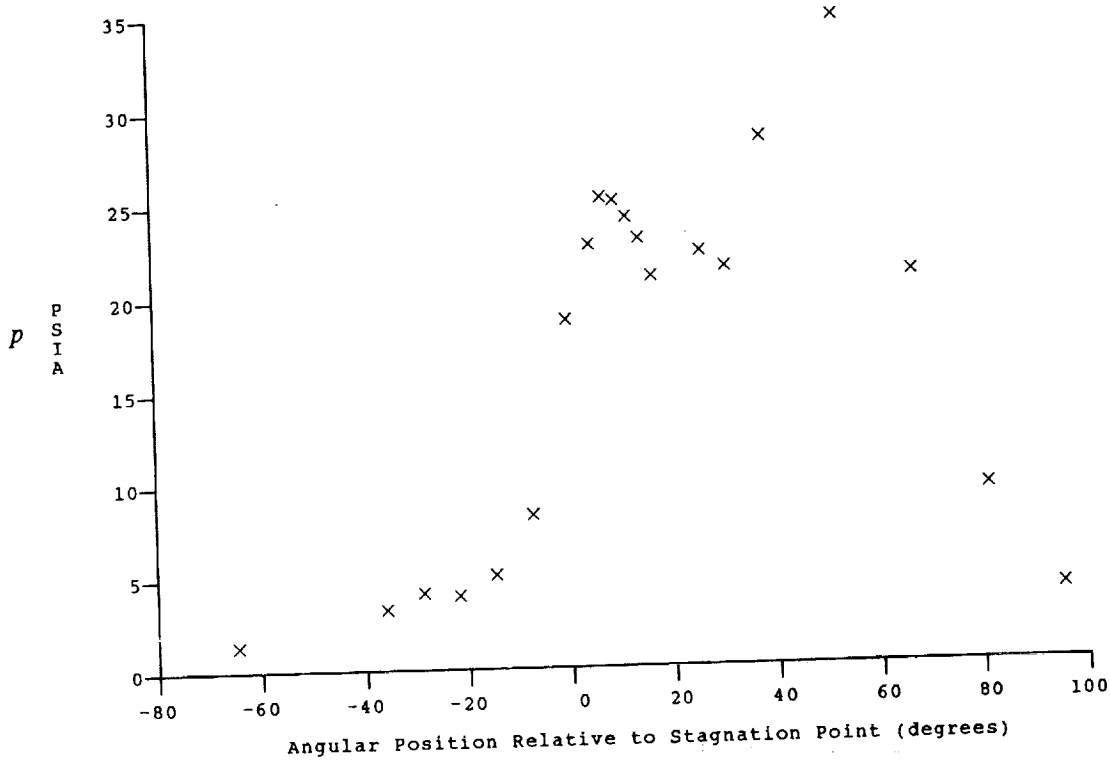

PRESSURE vs Gauge Position
Run 84

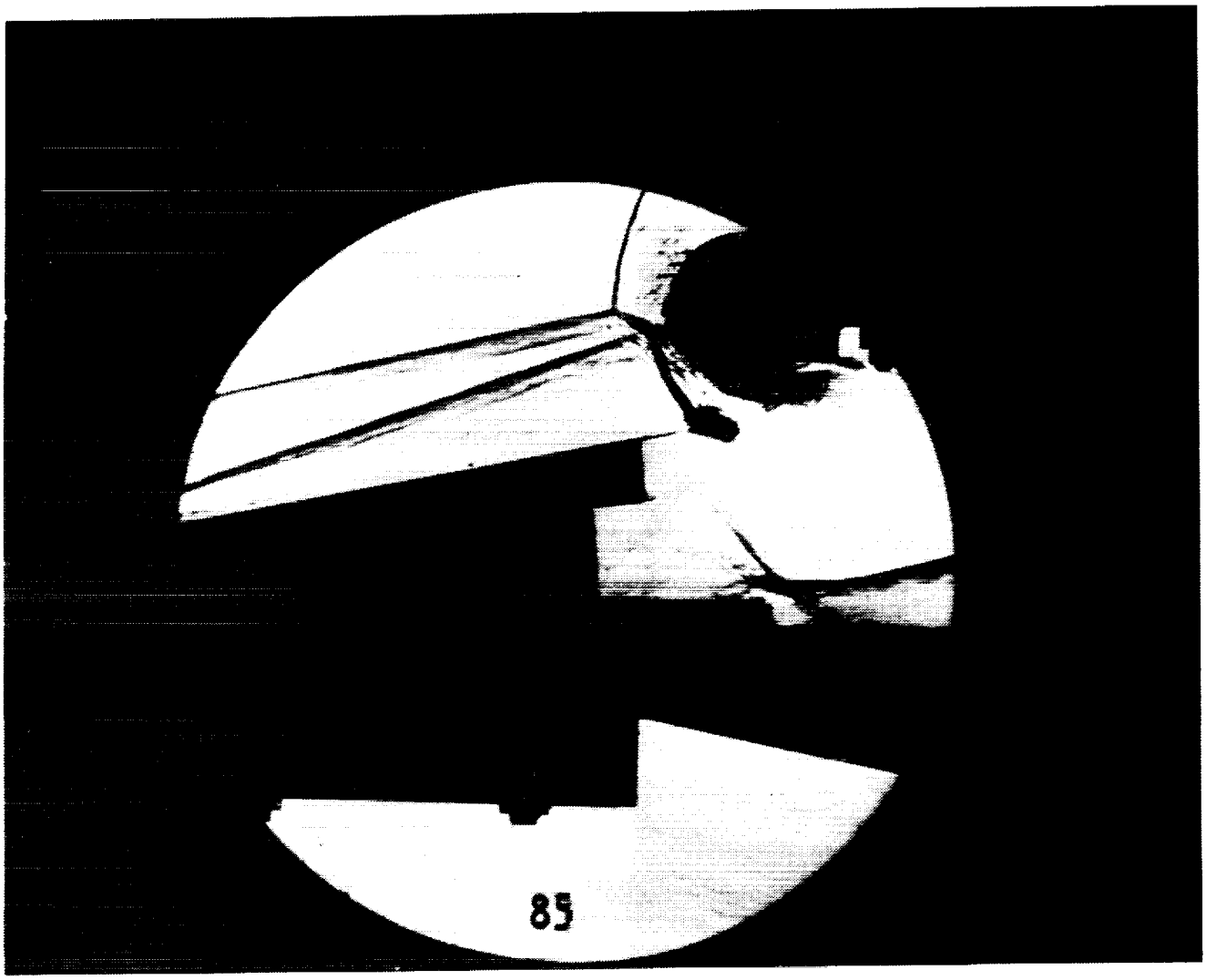

Test Conditions for Run 85 :

Po	= 1.366E-03	PSIA	Reservoir Total Pressure
Ho	= 1.866E-07	(Ft/sec)²	Reservoir Total Enthalpy
To	= 2.835E-03	°R	Reservoir Total Temperature
M	= 8.044E+00		Freestream Mach Number
U	= 5.888E+03	Ft/sec	Freestream Velocity
T	= 2.228E-02	°R	Freestream Temperature
P	= 1.187E-01	PSIA	Freestream Static Pressure
Rho	= 4.472E-05	Slugs/Ft3	Freestream Density
Mu	= 1.841E-07	Slugs/Ft-sec	Freestream Viscosity
Re	= 1.431E+06	1/Ft	Freestream Reynolds Number
Po'	= 9.981E+00	PSIA	Pitot Pressure
Q	= 5.383E+00	PSIA	Dynamic Pressure (½·Rho·U²/144)
Mi	= 3.398E+00		Shock Tube Incident Shock Mach Number
Hw	= 3.183E+06	(Ft/sec)²	Wall Enthalpy (Cp·Tw)
CPf	= 1.858E-01	1/PSIA	Pressure to CP factor (1/Q)
CHf	= 1.910E-04	Ft²-s/BTU	Heat Rate to CH factor (778/(Rho·U·(Ho-Hw))
QoFR	= 4.006E+01	BTU/Ft²-s	Fay-Riddell Heat Transfer to 3" Diam Sphere

Model Configuration Parameter	Value
Stagnation Position (gauge label)	P21
Vertical Distance (inches)	3.97
Horizontal Distance (inches)	1.32
Plate Angle (degrees)	7.50
Plate Length (inches)	36.00
Sweep Angle (degrees)	0.00
BOW to BOP (inches)	1.05
Wedge Angle (degrees)	5.00
Wedge Length (inches)	14.00

Run 85

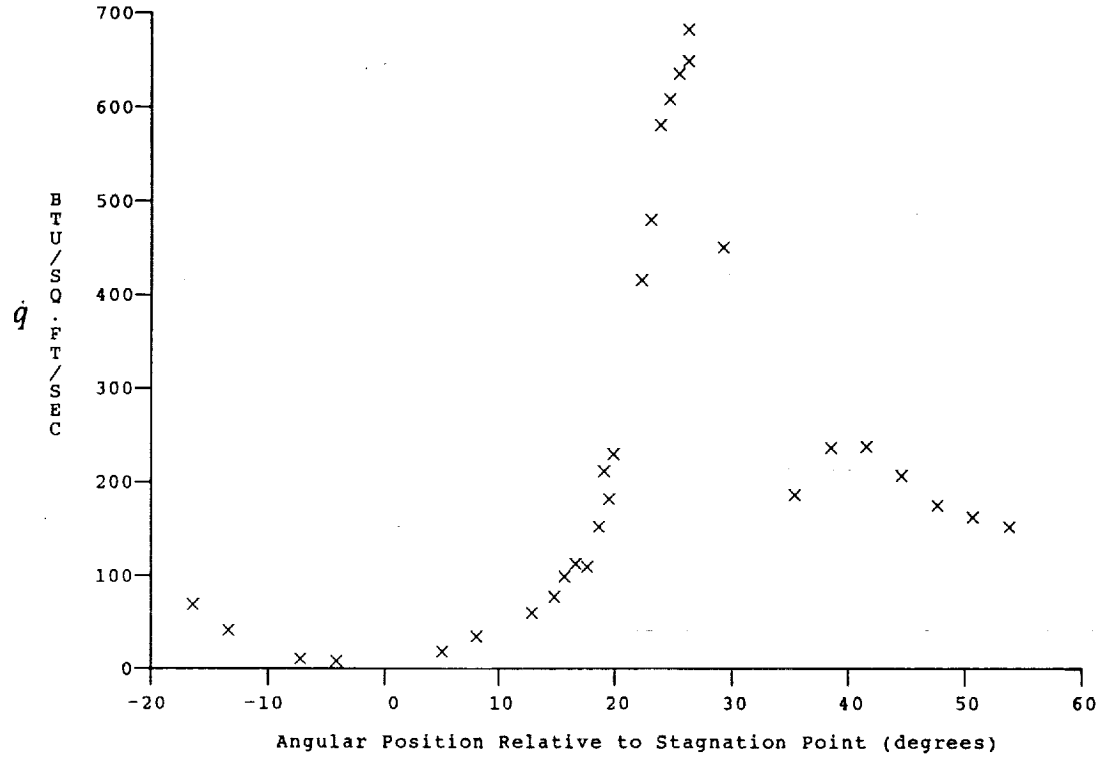

HEAT TRANSFER vs Gauge Position
Run 85

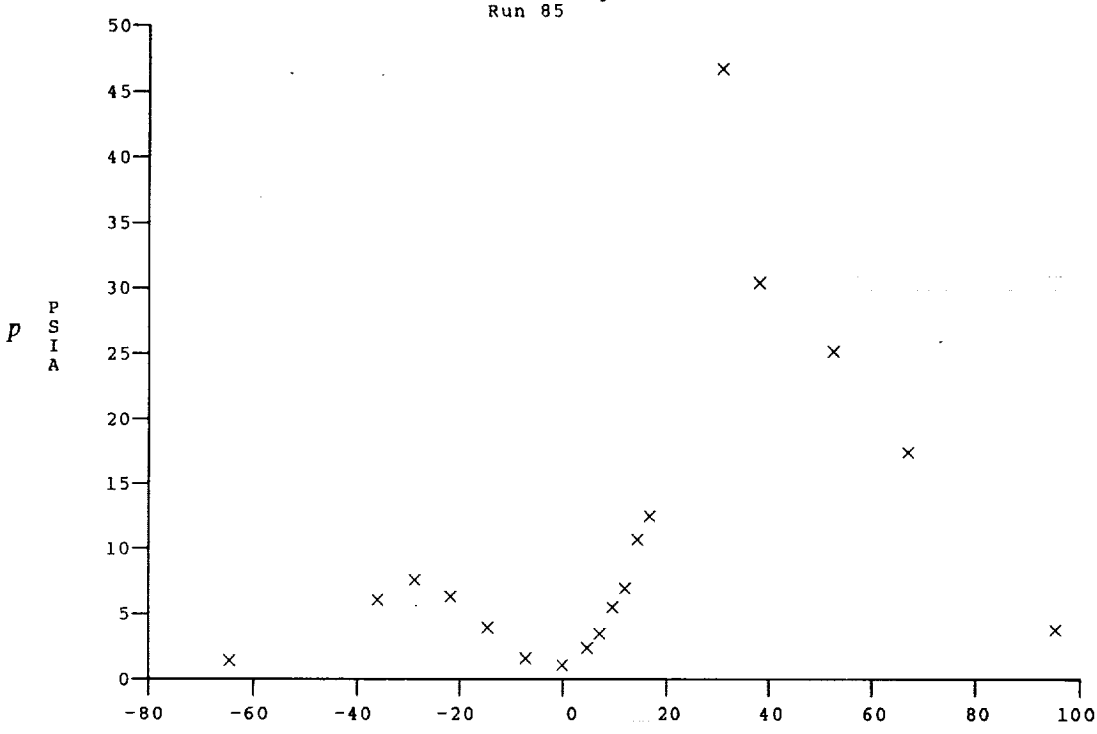

PRESSURE vs Gauge Position
Run 85

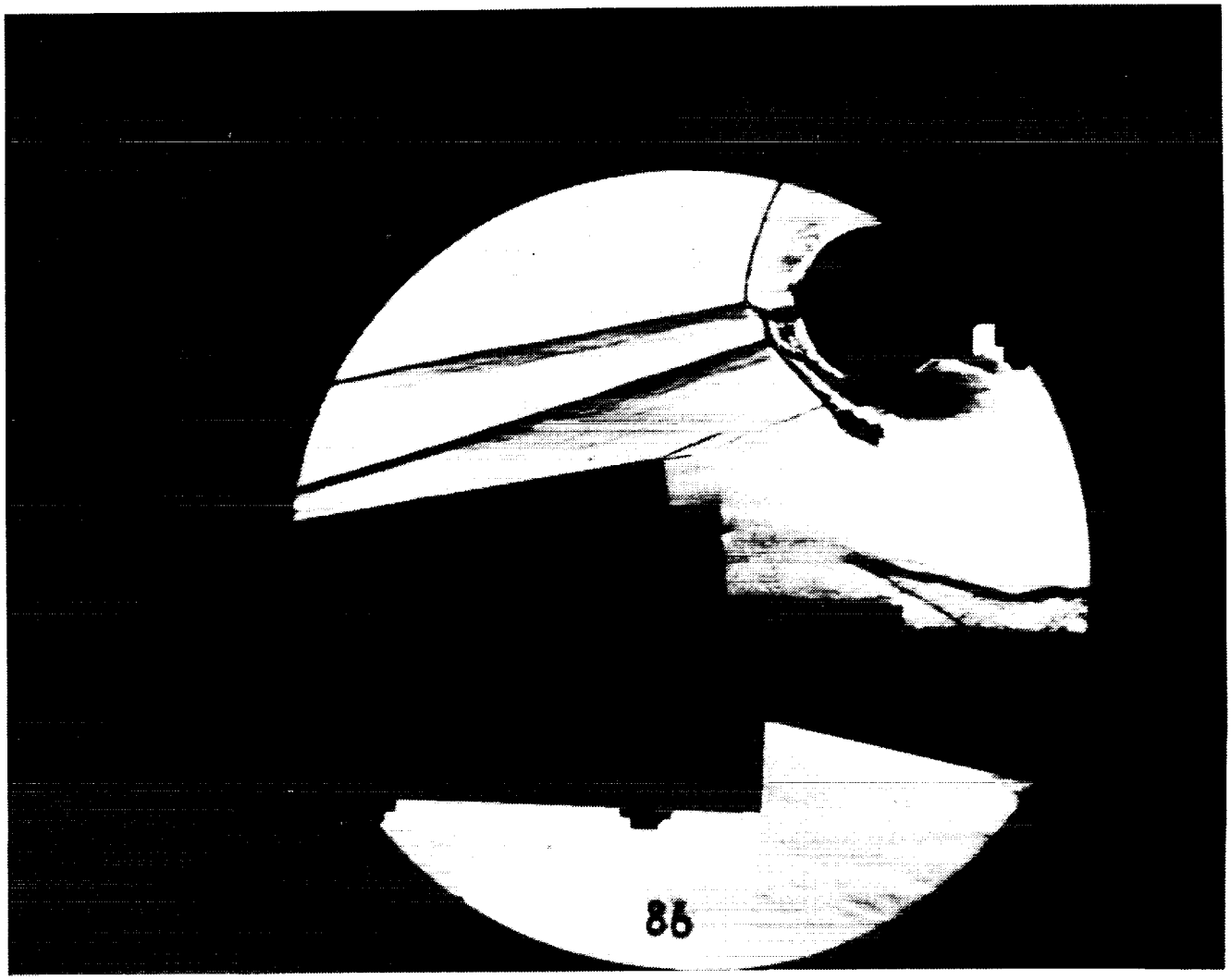

Test Conditions for Run 86 :

Po	= 1.365E+03 PSIA	Reservoir Total Pressure
Ho	= 1.885E-07 (Ft/sec)²	Reservoir Total Enthalpy
To	= 2.861E-03 °R	Reservoir Total Temperature
M	= 8.036E-00	Freestream Mach Number
U	= 5.919E+03 Ft/sec	Freestream Velocity
T	= 2.256E+02 °R	Freestream Temperature
P	= 1.189E-01 PSIA	Freestream Static Pressure
Rho	= 4.425E-05 Slugs/Ft3	Freestream Density
Mu	= 1.862E-07 Slugs/Ft-sec	Freestream Viscosity
Re	= 1.407E+06 1/Ft	Freestream Reynolds Number
Po'	= 9.981E+00 PSIA	Pitot Pressure
Q	= 5.382E+00 PSIA	Dynamic Pressure (½·Rho·U²/144)
Mi	= 3.414E+00	Shock Tube Incident Shock Mach Number
Hw	= 3.183E-06 (Ft/sec)²	Wall Enthalpy (Cp·Tw)
CPf	= 1.858E-01 1/PSIA	Pressure to CP factor (1/Q)
CHf	= 1.896E-04 Ft²-s/BTU	Heat Rate to CH factor (778/(Rho·U·(Ho-Hw))
QofR	= 4.059E+01 BTU/Ft²-s	Fay-Riddell Heat Transfer to 3" Diam Sphere

Model Configuration Parameter	Value
Stagnation Position (gauge label)	P21
Vertical Distance (inches)	3.97
Horizontal Distance (inches)	1.32
Plate Angle (degrees)	7.50
Plate Length (inches)	36.00
Sweep Angle (degrees)	0.00
BOW to BOP (inches)	-1.00
Wedge Angle (degrees)	6.00
Wedge Length (inches)	11.00

Run 86

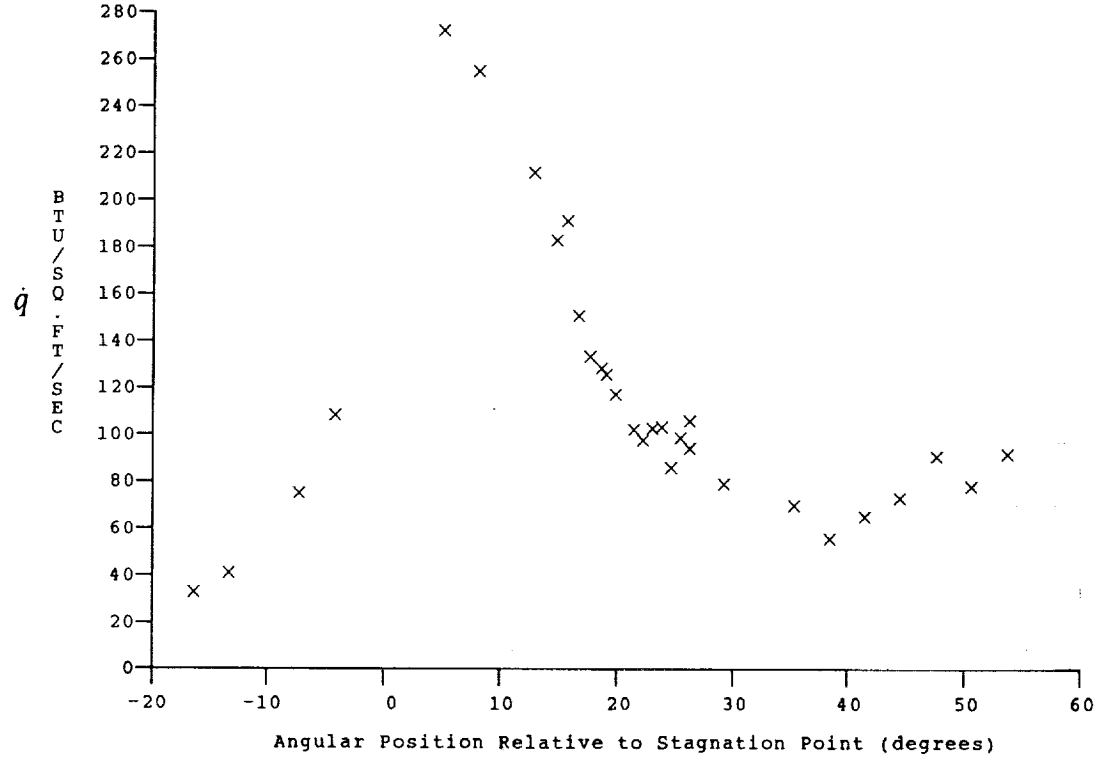

HEAT TRANSFER vs Gauge Position
Run 86

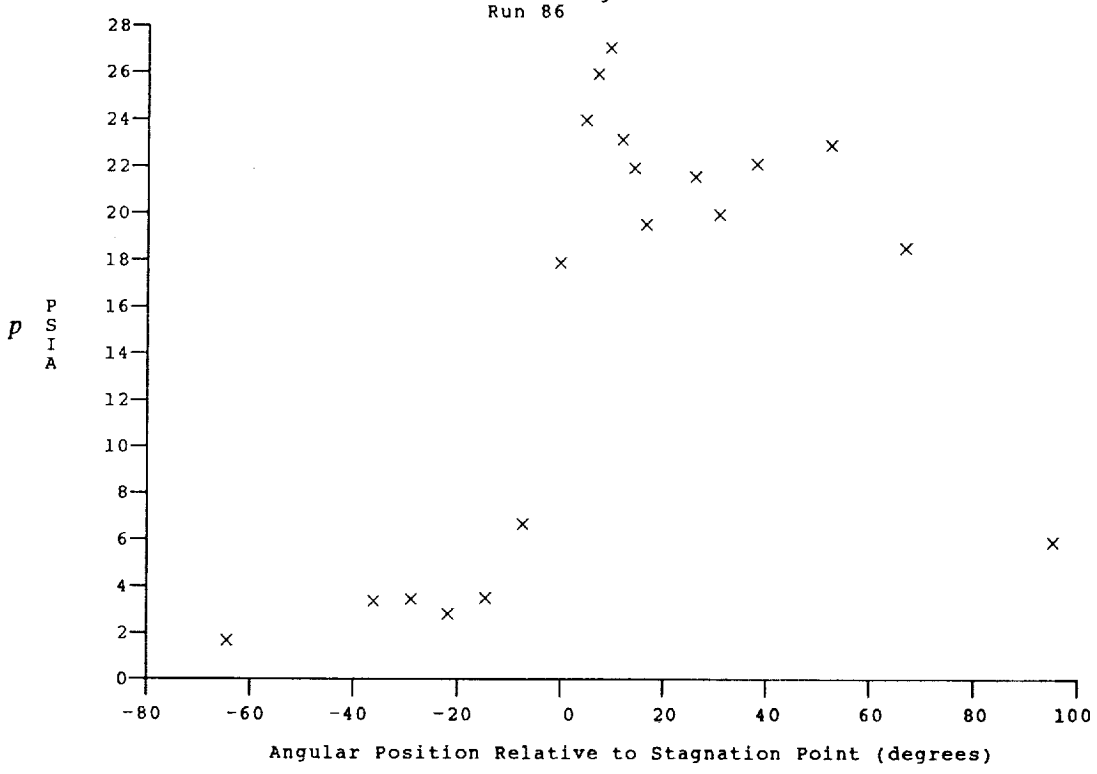

PRESSURE vs Gauge Position
Run 86

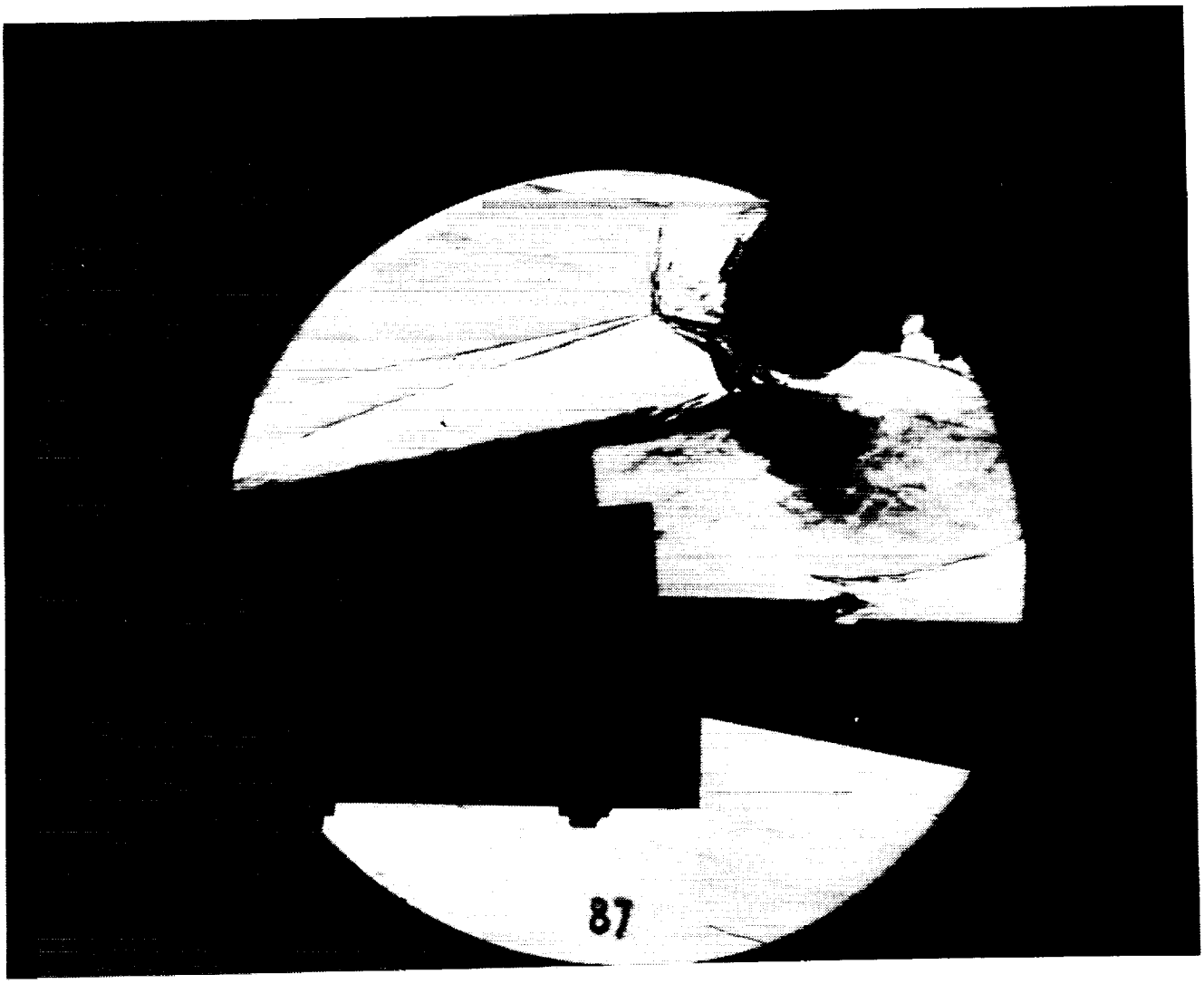

Test Conditions for Run 87 :

Po	= 1.416E+03 PSIA	Reservoir Total Pressure	
Ho	= 1.839E-07 (Ft/sec)²	Reservoir Total Enthalpy	
To	= 2.795E+03 °R	Reservoir Total Temperature	
M	= 8.042E+00	Freestream Mach Number	
U	= 5.845E+03 Ft/sec	Freestream Velocity	
T	= 2.197E-02 °R	Freestream Temperature	
P	= 1.240E-01 PSIA	Freestream Static Pressure	
Rho	= 4.736E-05 Slugs/Ft3	Freestream Density	
Mu	= 1.816E-07 Slugs/Ft-sec	Freestream Viscosity	
Re	= 1.524E+06 1/Ft	Freestream Reynolds Number	
Po'	= 1.041E+01 PSIA	Pitot Pressure	
Q	= 5.618E+00 PSIA	Dynamic Pressure (½·Rho·U²/144)	
Mi	= 3.413E+00	Shock Tube Incident Shock Mach Number	
Hw	= 3.183E+06 (Ft/sec)²	Wall Enthalpy (Cp·Tw)	
CPf	= 1.780E-01 1/PSIA	Pressure to CP factor (1/Q)	
CHf	= 1.849E-04 Ft²-s/BTU	Heat Rate to CH factor (778/(Rho·U·(Ho-Hw))	
QoFR	= 4.016E+01 BTU/Ft²-s	Fay-Riddell Heat Transfer to 3" Diam Sphere	

Model Configuration Parameter	Value
Stagnation Position (gauge label)	P21
Vertical Distance (inches)	3.97
Horizontal Distance (inches)	1.32
Plate Angle (degrees)	7.50
Plate Length (inches)	36.00
Sweep Angle (degrees)	0.00
BOW to BOP (inches)	-1.00
Wedge Angle (degrees)	5.00
Wedge Length (inches)	14.00

Run 87

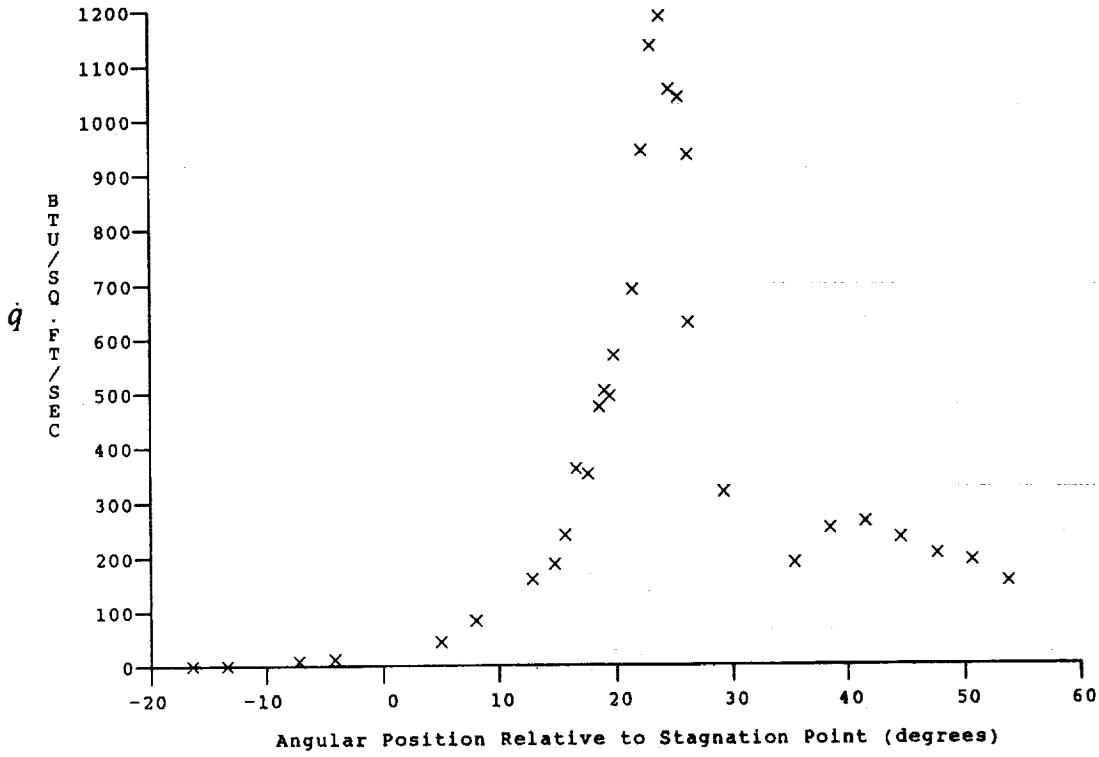

HEAT TRANSFER vs Gauge Position
Run 87

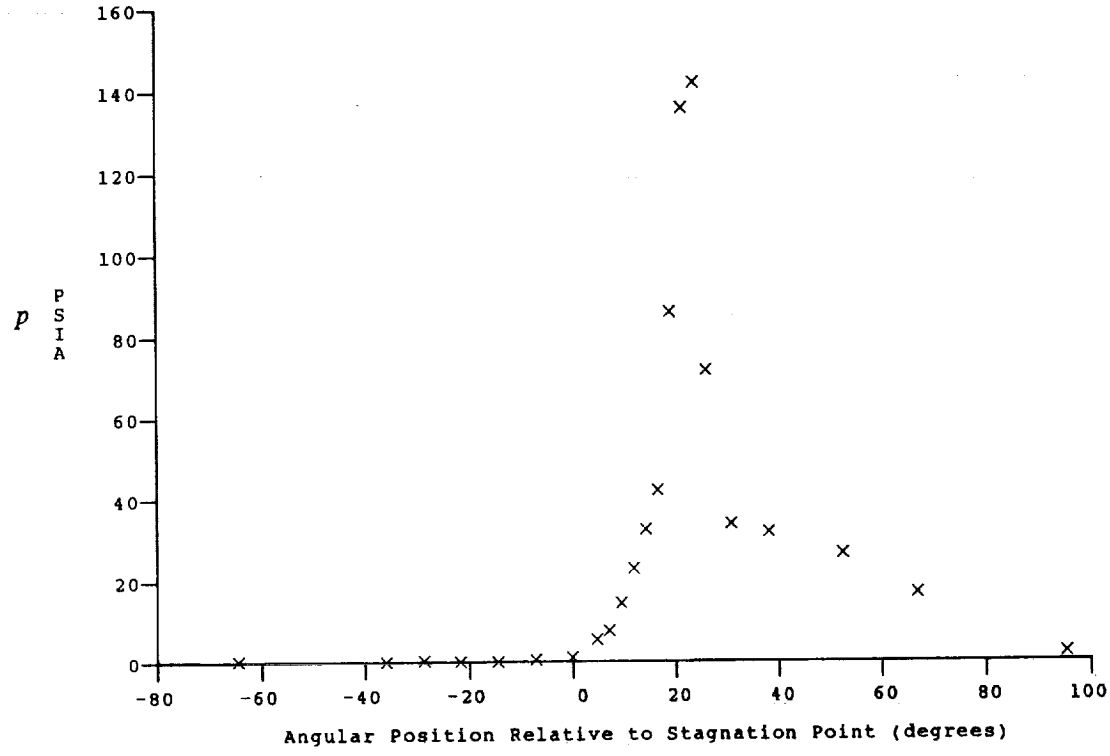

PRESSURE vs Gauge Position
Run 87

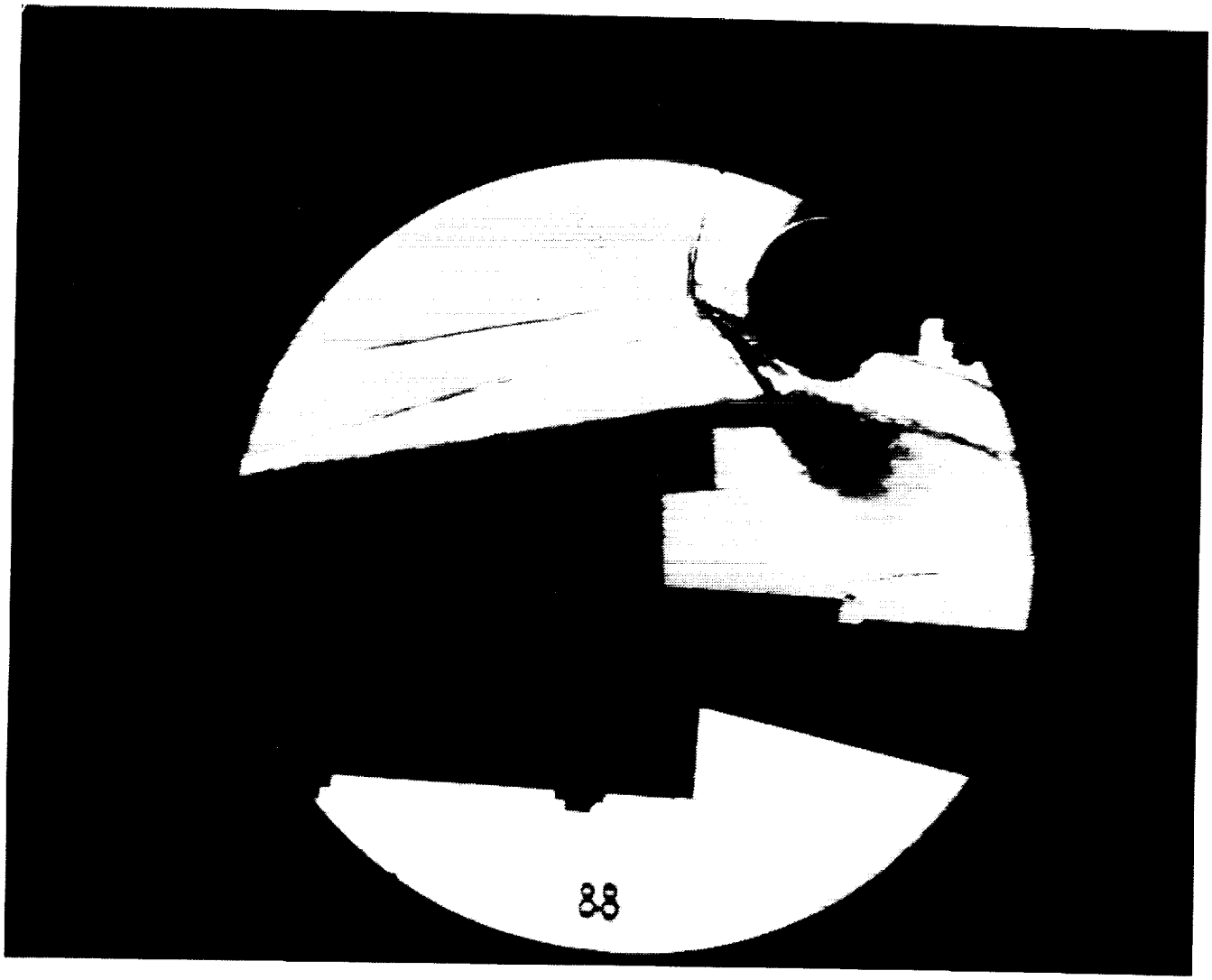

Test Conditions for Run 88 :

Po	= 1.782E-03	PSIA	Reservoir Total Pressure
Ho	= 1.967E-07	(Ft/sec)²	Reservoir Total Enthalpy
To	= 2.969E-03	°R	Reservoir Total Temperature
M	= 8.045E+00		Freestream Mach Number
U	= 6.046E+03	Ft/sec	Freestream Velocity
T	= 2.349E+02	°R	Freestream Temperature
P	= 1.532E-01	PSIA	Freestream Static Pressure
Rho	= 5.475E-05	Slugs/Ft3	Freestream Density
Mu	= 1.933E-07	Slugs/Ft-sec	Freestream Viscosity
Re	= 1.712E+06	1/Ft	Freestream Reynolds Number
Po'	= 1.290E+01	PSIA	Pitot Pressure
Q	= 6.950E+00	PSIA	Dynamic Pressure (½·Rho·U²/144)
Mi	= 3.487E+00		Shock Tube Incident Shock Mach Number
Hw	= 3.183E+06	(Ft/sec)²	Wall Enthalpy (Cp·Tw)
CPf	= 1.439E-01	1/PSIA	Pressure to CP factor (1/Q)
CHf	= 1.425E-04	Ft²-s/BTU	Heat Rate to CH factor (778/(Rho·U·(Ho-Hw))
QoFR	= 4.869E+01	BTU/Ft²-s	Fay-Riddell Heat Transfer to 3" Diam Sphere

Model Configuration Parameter	Value
Stagnation Position (gauge label)	P21
Vertical Distance (inches)	3.97
Horizontal Distance (inches)	1.32
Plate Angle (degrees)	7.50
Plate Length (inches)	36.00
Sweep Angle (degrees)	0.00
BOW to BOP (inches)	1.05
Wedge Angle (degrees)	5.00
Wedge Length (inches)	14.00

Run 88

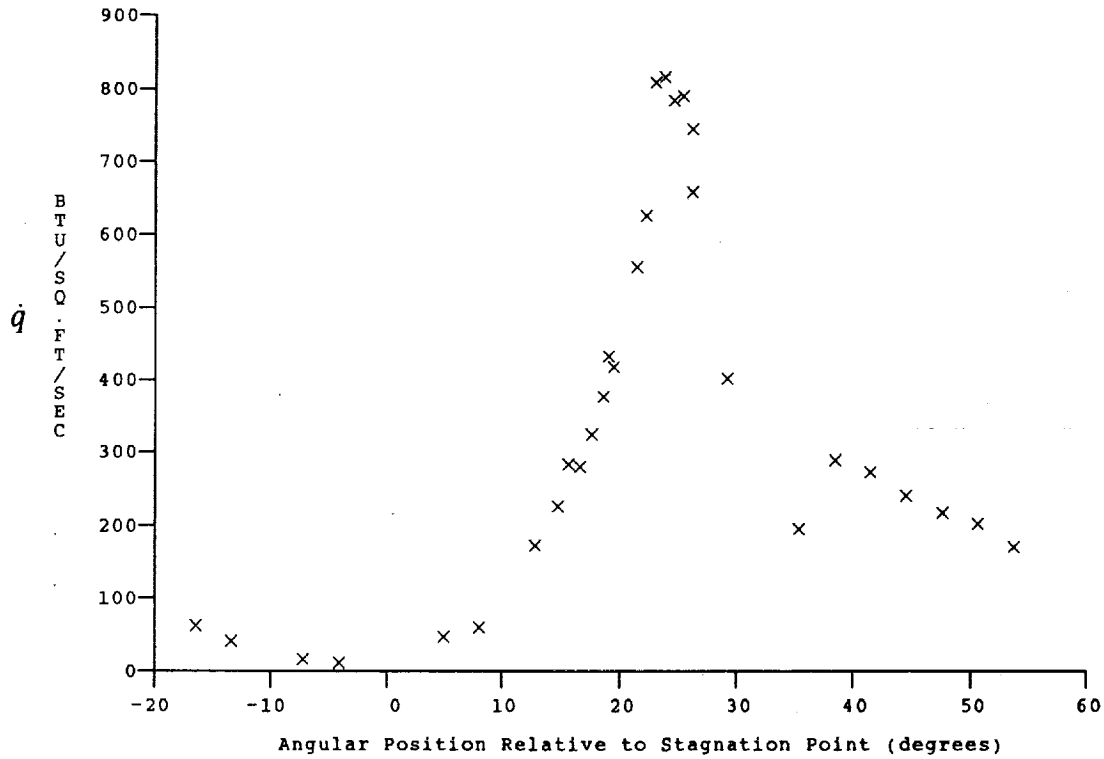

HEAT TRANSFER vs Gauge Position
Run 88

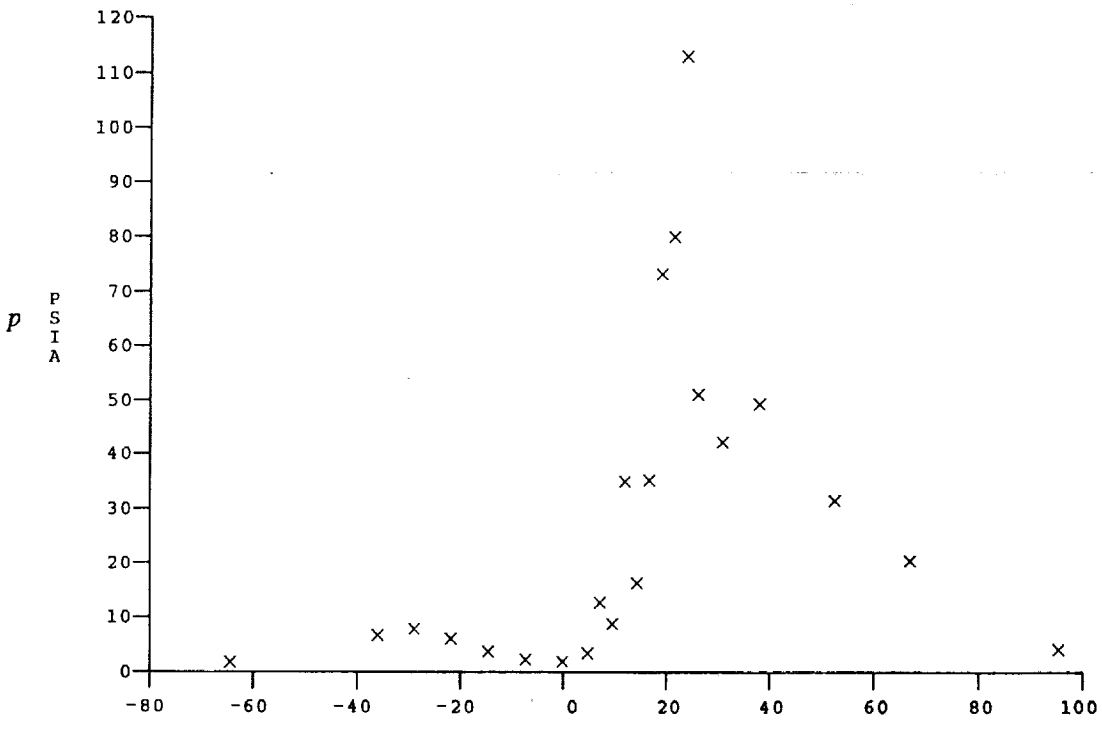

PRESSURE vs Gauge Position
Run 88

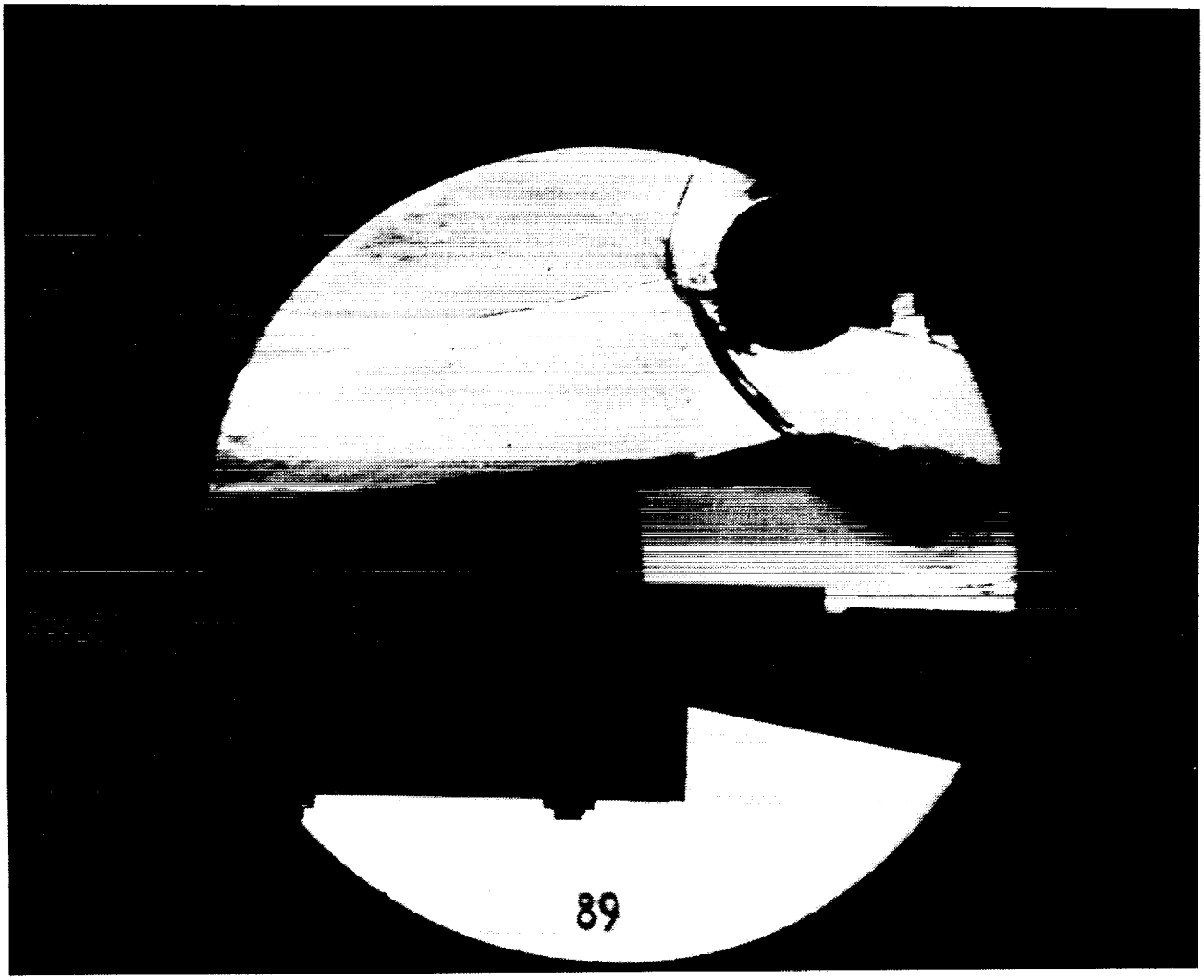

Test Conditions for Run 89 :

Po	= 1.383E+03 PSIA	Reservoir Total Pressure	
Ho	= 1.858E+07 (Ft/sec)²	Reservoir Total Enthalpy	
To	= 2.823E+03 °R	Reservoir Total Temperature	
M	= 8.040E+00	Freestream Mach Number	
U	= 5.876E-03 Ft/sec	Freestream Velocity	
T	= 2.221E+02 °R	Freestream Temperature	
P	= 1.208E-01 PSIA	Freestream Static Pressure	
Rho	= 4.562E-05 Slugs/Ft3	Freestream Density	
Mu	= 1.835E-07 Slugs/Ft-sec	Freestream Viscosity	
Re	= 1.461E+06 1/Ft	Freestream Reynolds Number	
Po'	= 1.014E+01 PSIA	Pitot Pressure	
Q	= 5.470E+00 PSIA	Dynamic Pressure (½·Rho·U²/144)	
Mi	= 3.409E+00	Shock Tube Incident Shock Mach Number	
Hw	= 3.183E+06 (Ft/sec)²	Wall Enthalpy (Cp·Tw)	
CPf	= 1.828E-01 1/PSIA	Pressure to CP factor (1/Q)	
CHf	= 1.885E-04 Ft²-s/BTU	Heat Rate to CH factor (778/(Rho·U·(Ho-Hw))	
QoFR	= 4.017E+01 BTU/Ft²-s	Fay-Riddell Heat Transfer to 3" Diam Sphere	

Model Configuration Parameter	Value
Stagnation Position (gauge label)	P21
Vertical Distance (inches)	4.12
Horizontal Distance (inches)	1.32
Plate Angle (degrees)	7.50
Plate Length (inches)	36.00
Sweep Angle (degrees)	0.00

Run 89

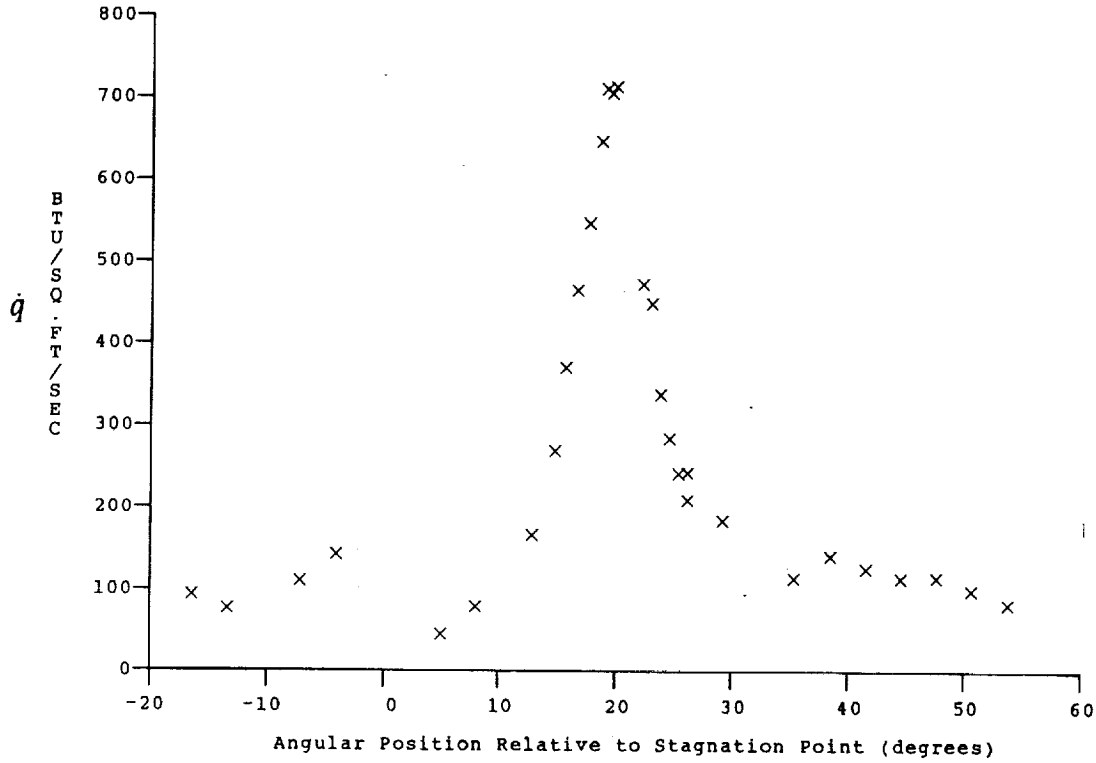

HEAT TRANSFER vs Gauge Position
Run 89

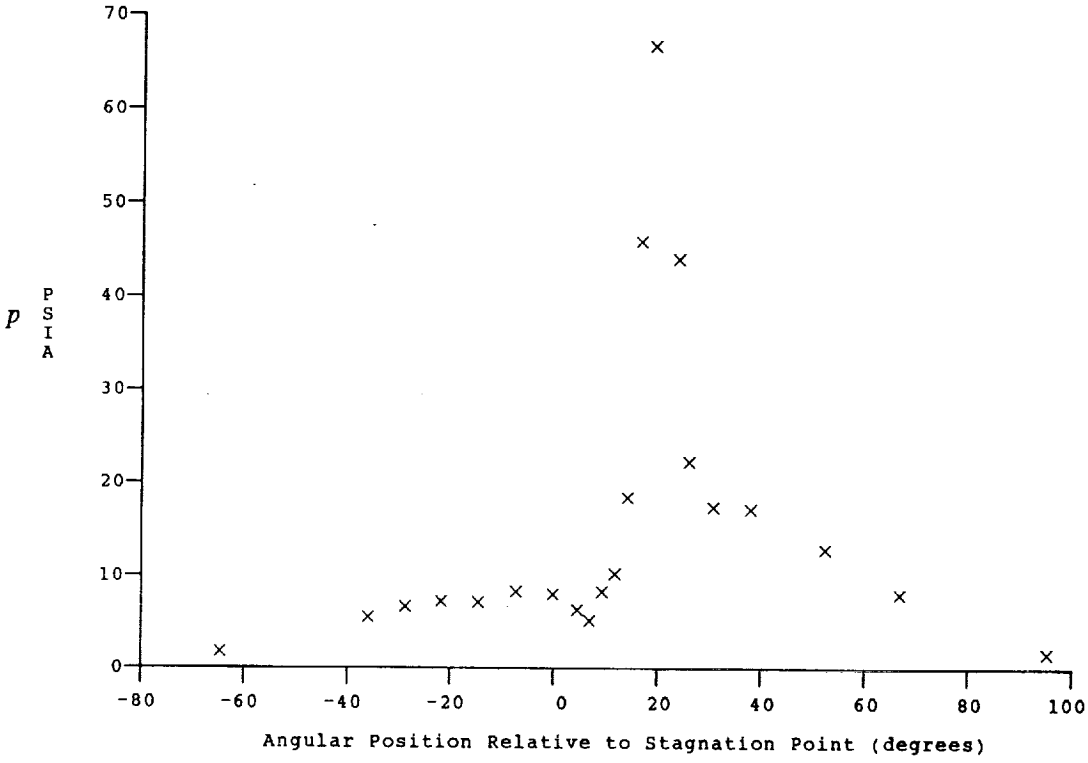

PRESSURE vs Gauge Position
Run 89

Test Conditions

Mi	= 3.4194	
Po	= 1.3940X10+3	PSIA
Ho	= 1.8741X10+7	(Ft/sec)^2
To	= 2.8453X10+3	Degrees R
M	= 8.0365	
U	= 5.9013X10+3	Ft/sec
T	= 2.2422X10+2	Degrees R
P	= 1.2171X10-1	PSIA
Q	= 5.5082	PSIA
Rho	= 4.5553X10-5	Slugs/Ft^3
Mu	= 1.8515X10-7	Slugs/Ft-sec
Re	= 1.4519X10+6	1/Ft
Po'	= 1.0213X10+1	PSIA

Model Configuration Parameter	Value
Stagnation Position (gauge label)	P21
Vertical Distance (inches)	4.00
Horizontal Distance (inches)	1.32
Plate Angle (degrees)	7.50
Plate Length (inches)	36.00
Sweep Angle (degrees)	0.00
BOW to BOP (inches)	-1.44
Wedge Angle (degrees)	6.00
Wedge Length (inches)	11.00

Run 90

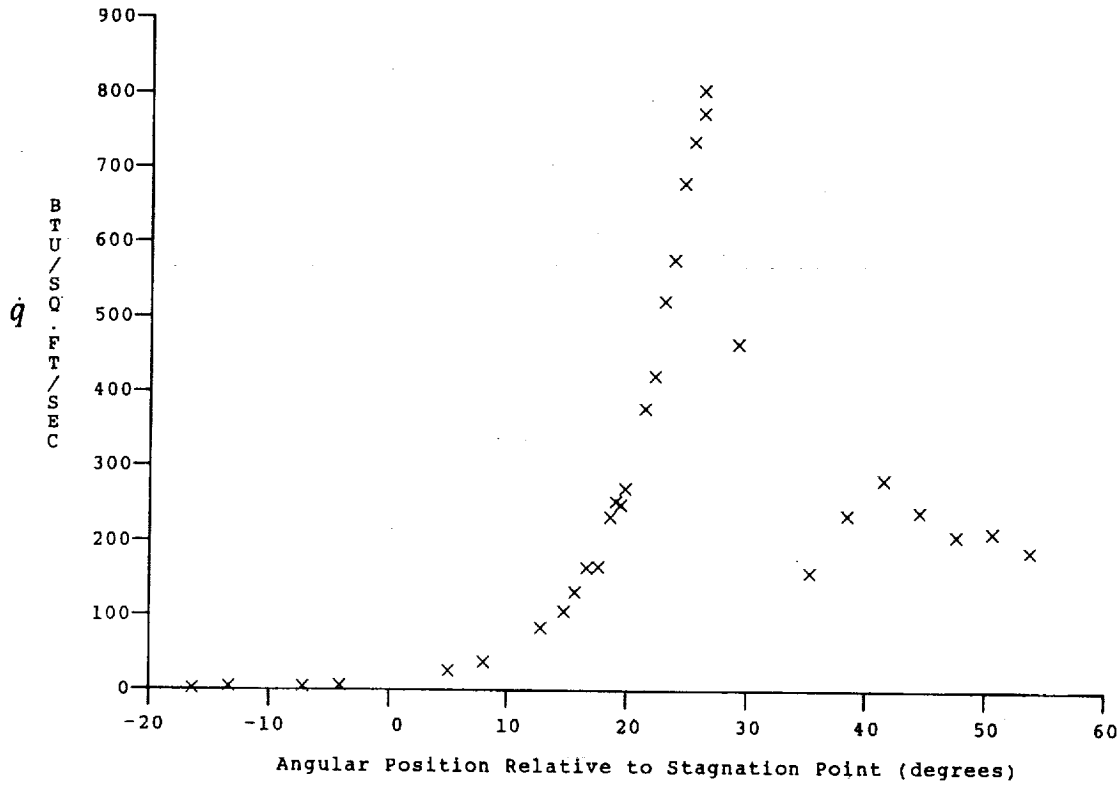

HEAT TRANSFER vs Gauge Position
Run 90

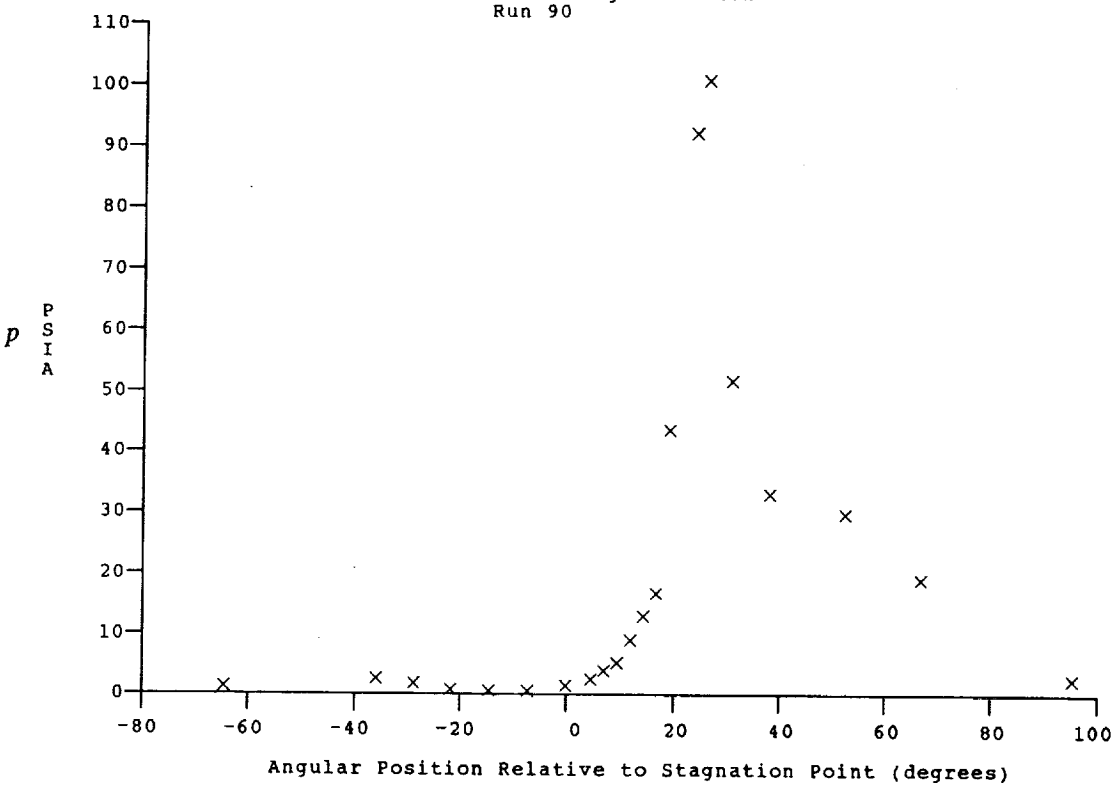

PRESSURE vs Gauge Position
Run 90

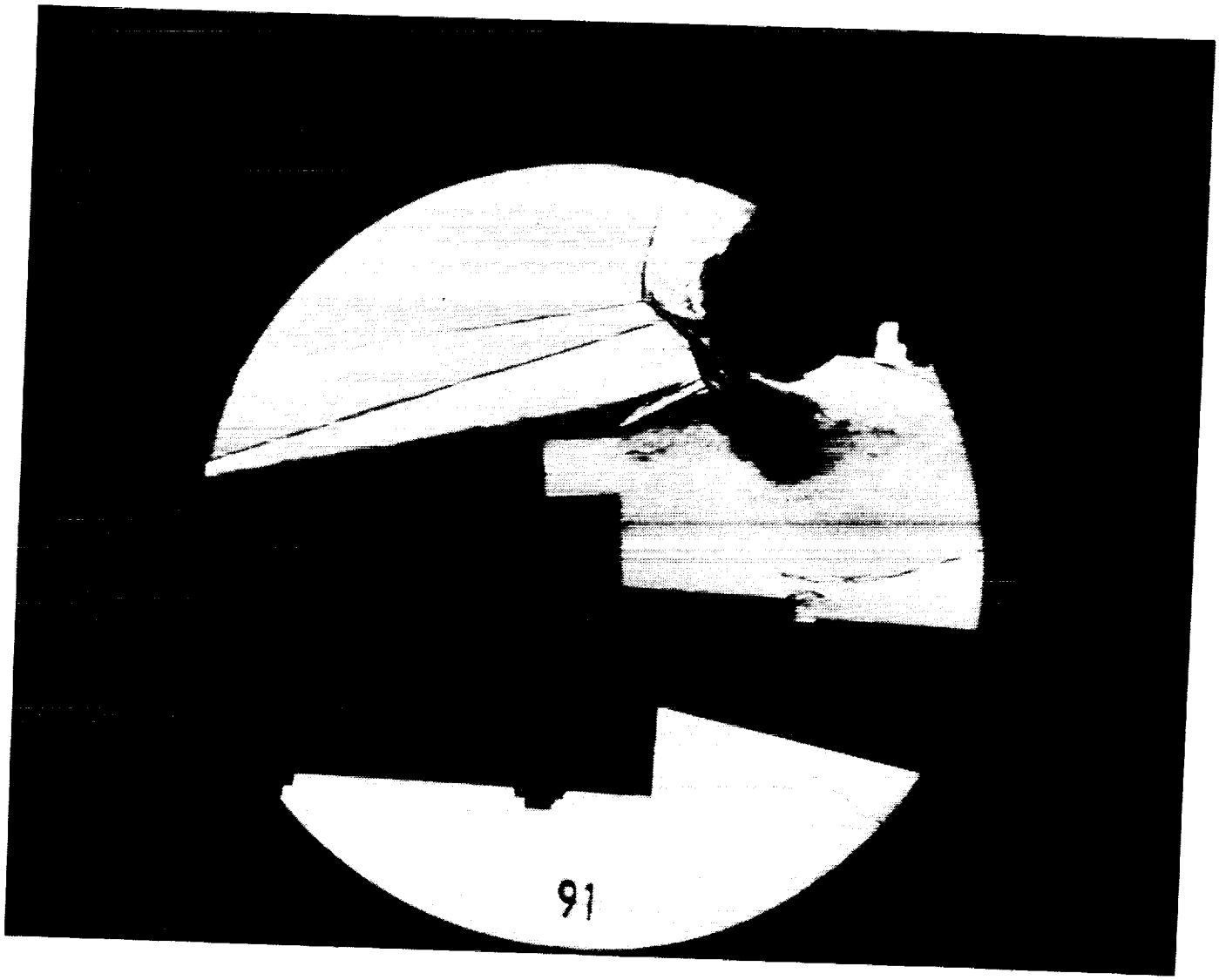

Test Conditions for Run 91 :

Po	= 1.389E+03 PSIA	Reservoir Total Pressure	
Ho	= 1.851E-07 (Ft/sec)²	Reservoir Total Enthalpy	
To	= 2.812E-03 °R	Reservoir Total Temperature	
M	= 8.040E-00	Freestream Mach Number	
U	= 5.864E+03 Ft/sec	Freestream Velocity	
T	= 2.212E-02 °R	Freestream Temperature	
P	= 1.215E-01 PSIA	Freestream Static Pressure	
Rho	= 4.609E-05 Slugs/Ft3	Freestream Density	
Mu	= 1.828E-07 Slugs/Ft-sec	Freestream Viscosity	
Re	= 1.478E+06 1/Ft	Freestream Reynolds Number	
Po'	= 1.020E+01 PSIA	Pitot Pressure	
Q	= 5.503E-00 PSIA	Dynamic Pressure (½·Rho·U²/144)	
Mi	= 3.412E+00	Shock Tube Incident Shock Mach Number	
Hw	= 3.183E+06 (Ft/sec)²	Wall Enthalpy (Cp·Tw)	
CPf	= 1.817E-01 1/PSIA	Pressure to CP factor (1/Q)	
CHf	= 1.879E-04 Ft²-s/BTU	Heat Rate to CH factor (778/(Rho·U·(Ho-Hw))	
QoFR	= 4.008E+01 BTU/Ft²-s	Fay-Riddell Heat Transfer to 3" Diam Sphere	

Model Configuration Parameter	Value
Stagnation Position (gauge label)	P21
Vertical Distance (inches)	4.00
Horizontal Distance (inches)	1.32
Plate Angle (degrees)	7.50
Plate Length (inches)	36.00
Sweep Angle (degrees)	0.00
BOW to BOP (inches)	-1.44
Wedge Angle (degrees)	6.00
Wedge Length (inches)	11.00

Run 91

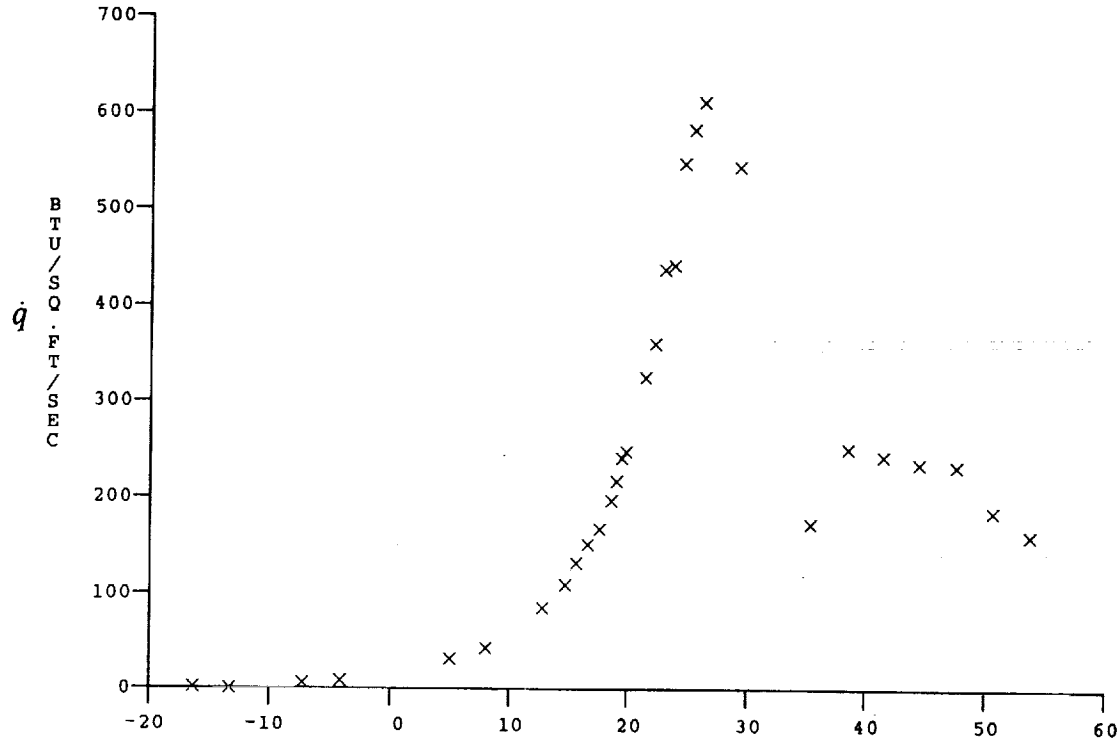

HEAT TRANSFER vs Gauge Position
Run 91

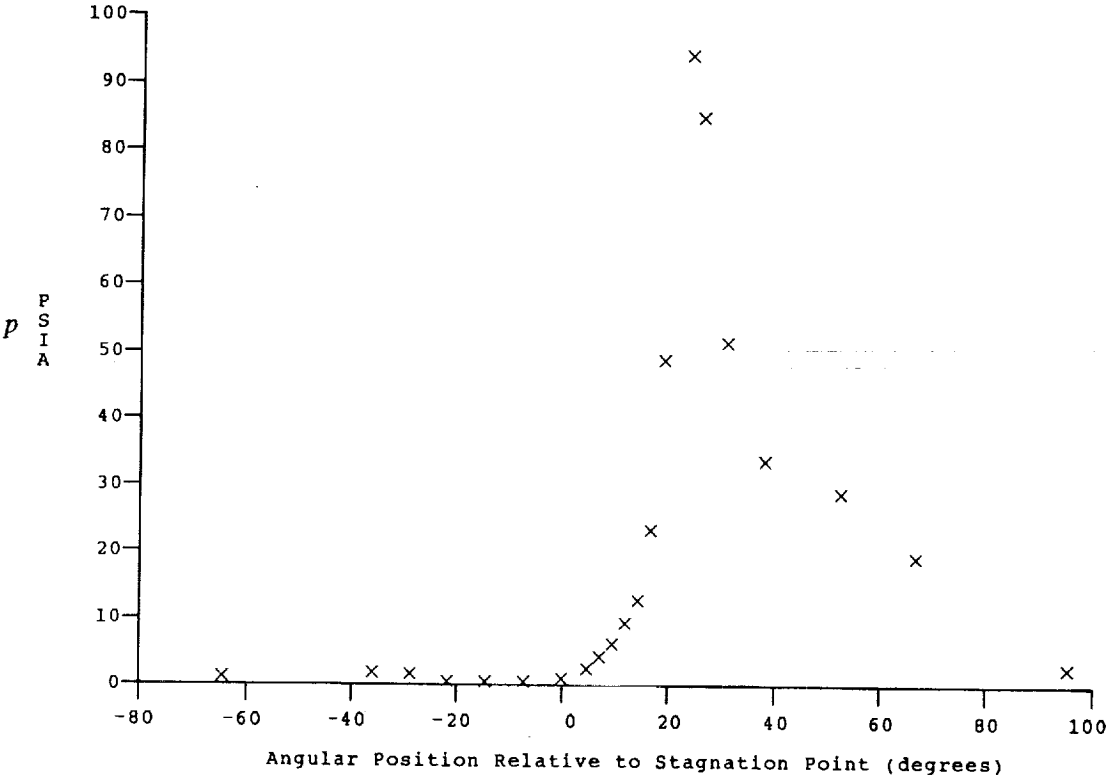

PRESSURE vs Gauge Position
Run 91

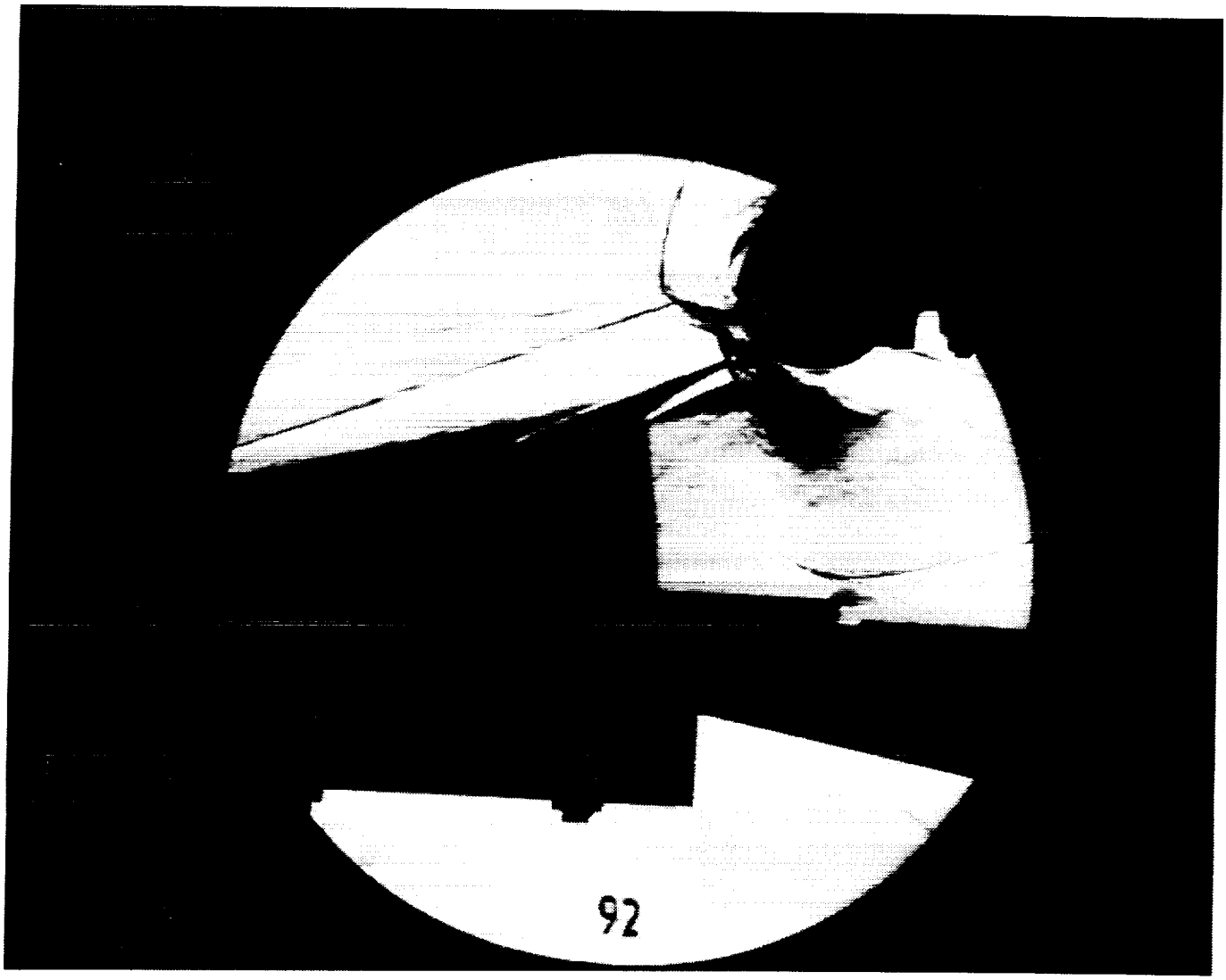

Test Conditions for Run 92 :

Po	= 1.400E+03 PSIA	Reservoir Total Pressure
Ho	= 1.824E+07 (Ft/sec)²	Reservoir Total Enthalpy
To	= 2.775E+03 °R	Reservoir Total Temperature
M	= 8.041E+00	Freestream Mach Number
U	= 5.823E+03 Ft/sec	Freestream Velocity
T	= 2.180E+02 °R	Freestream Temperature
P	= 1.230E-01 PSIA	Freestream Static Pressure
Rho	= 4.733E-05 Slugs/Ft3	Freestream Density
Mu	= 1.803E-07 Slugs/Ft-sec	Freestream Viscosity
Re	= 1.528E+06 1/Ft	Freestream Reynolds Number
Po'	= 1.033E+01 PSIA	Pitot Pressure
Q	= 5.572E+00 PSIA	Dynamic Pressure (½·Rho·U²/144)
Mi	= 3.411E+00	Shock Tube Incident Shock Mach Number
Hw	= 3.183E+06 (Ft/sec)²	Wall Enthalpy (Cp·Tw)
CPf	= 1.795E-01 1/PSIA	Pressure to CP factor (1/Q)
CHf	= 1.875E-04 Ft²-s/BTU	Heat Rate to CH factor (778/(Rho·U·(Ho-Hw))
QoFR	= 3.959E-01 BTU/Ft²-s	Fay-Riddell Heat Transfer to 3" Diam Sphere

Model Configuration Parameter	Value
Stagnation Position (gauge label)	P21
Vertical Distance (inches)	4.00
Horizontal Distance (inches)	1.32
Plate Angle (degrees)	7.50
Plate Length (inches)	36.00
Sweep Angle (degrees)	0.00
BOW to BOP (inches)	-2.69
Wedge Angle (degrees)	6.00
Wedge Length (inches)	13.25

Run 92

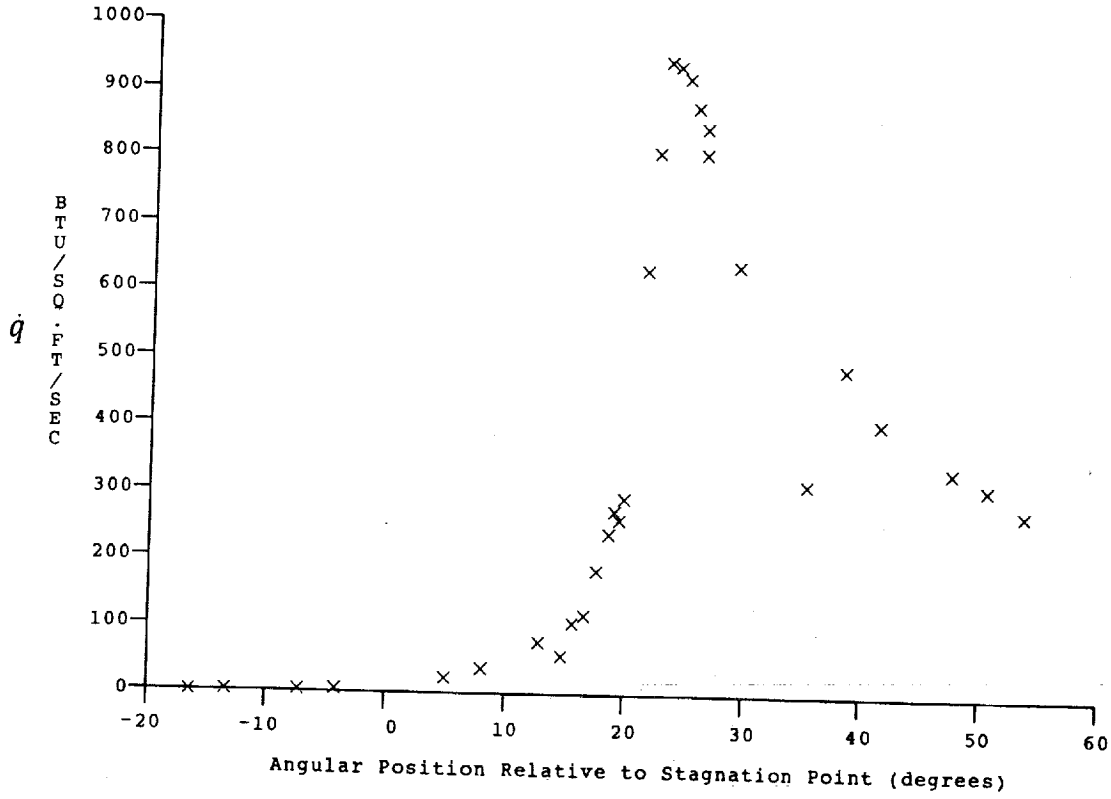

HEAT TRANSFER vs Gauge Position
Run 92

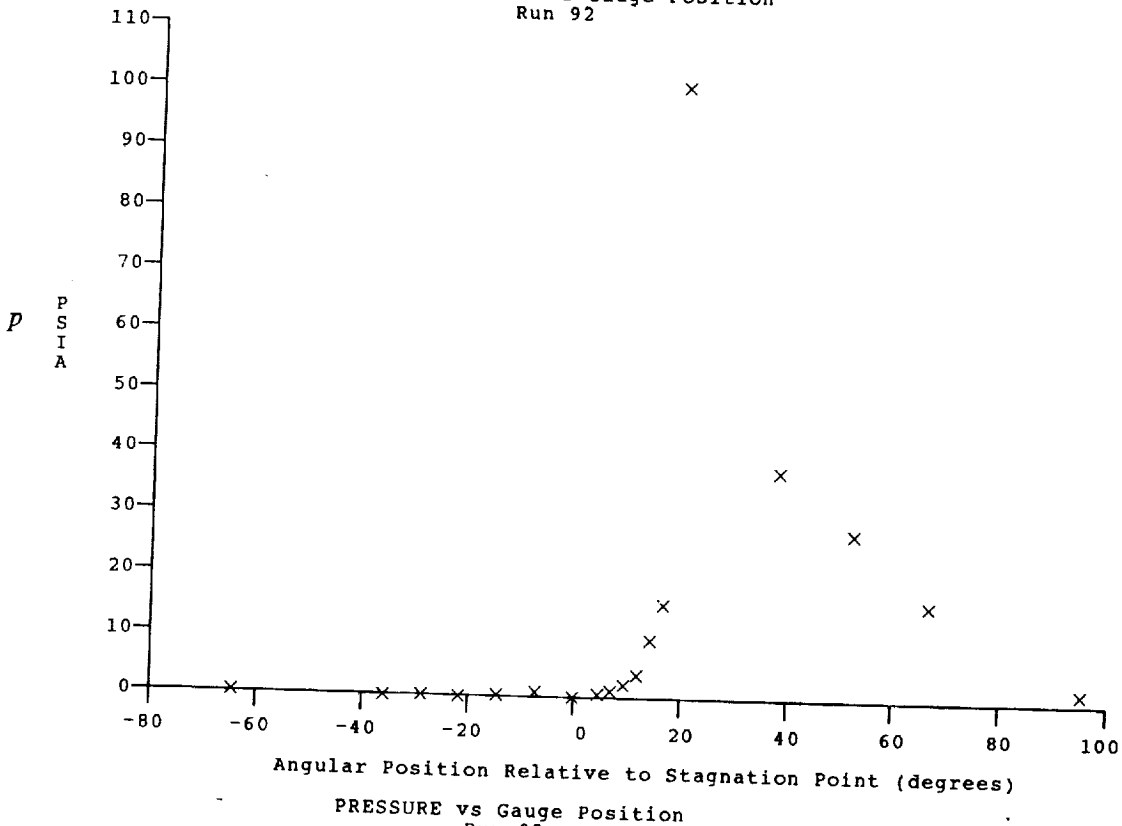

PRESSURE vs Gauge Position
Run 92

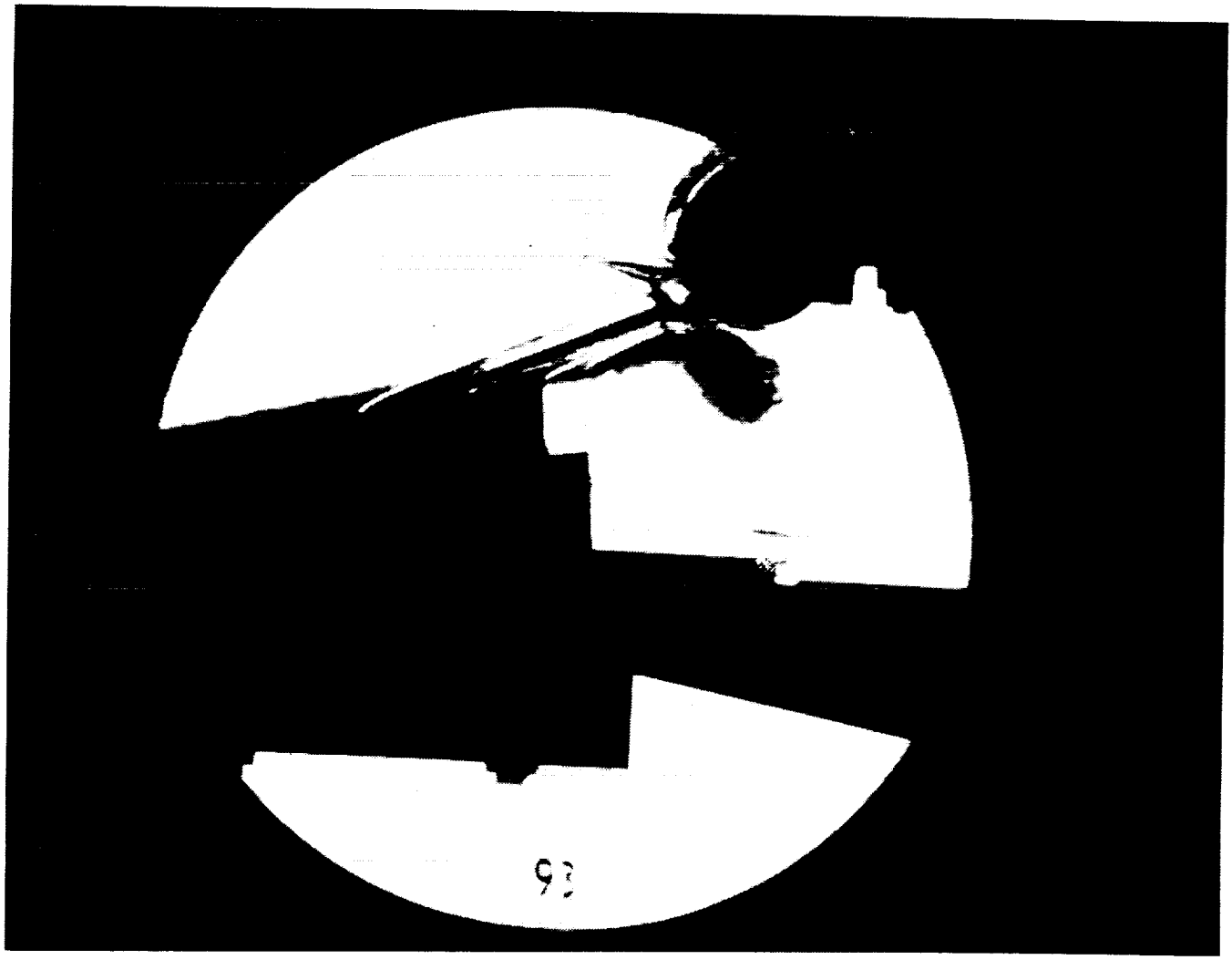

Test Conditions for Run 93 :

Po	= 1.353E+03	PSIA	Reservoir Total Pressure
Ho	= 1.831E+07	(Ft/sec)²	Reservoir Total Enthalpy
To	= 2.785E+03	°R	Reservoir Total Temperature
M	= 8.037E+00		Freestream Mach Number
U	= 5.833E+03	Ft/sec	Freestream Velocity
T	= 2.191E-02	°R	Freestream Temperature
P	= 1.190E-01	PSIA	Freestream Static Pressure
Rho	= 4.559E-05	Slugs/Ft3	Freestream Density
Mu	= 1.811E-07	Slugs/Ft-sec	Freestream Viscosity
Re	= 1.468E+06	1/Ft	Freestream Reynolds Number
Po'	= 9.984E+00	PSIA	Pitot Pressure
Q	= 5.386E+00	PSIA	Dynamic Pressure (½·Rho·U²/144)
Mi	= 3.410E+00		Shock Tube Incident Shock Mach Number
Hw	= 3.183E+06	(Ft/sec)²	Wall Enthalpy (Cp·Tw)
CPf	= 1.857E-01	1/PSIA	Pressure to CP factor (1/Q)
CHf	= 1.934E-04	Ft²-s/BTU	Heat Rate to CH factor (778/(Rho·U·(Ho-Hw))
QoFR	= 3.912E+01	BTU/Ft²-s	Fay-Riddell Heat Transfer to 3" Diam Sphere

Model Configuration Parameter	Value
Stagnation Position (gauge label)	P21
Vertical Distance (inches)	4.00
Horizontal Distance (inches)	1.32
Plate Angle (degrees)	7.50
Plate Length (inches)	36.00
Sweep Angle (degrees)	0.00
BOW to BOP (inches)	-3.44
Wedge Angle (degrees)	6.00
Wedge Length (inches)	13.25

Run 93

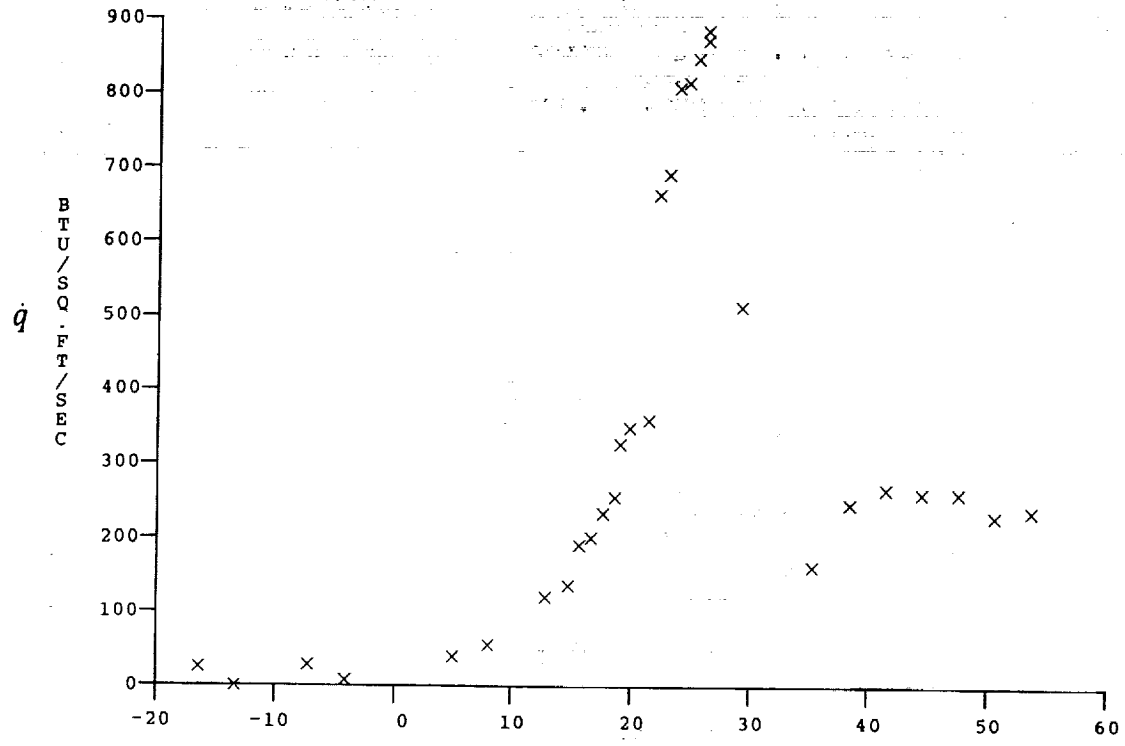

HEAT TRANSFER vs Gauge Position
Run 93

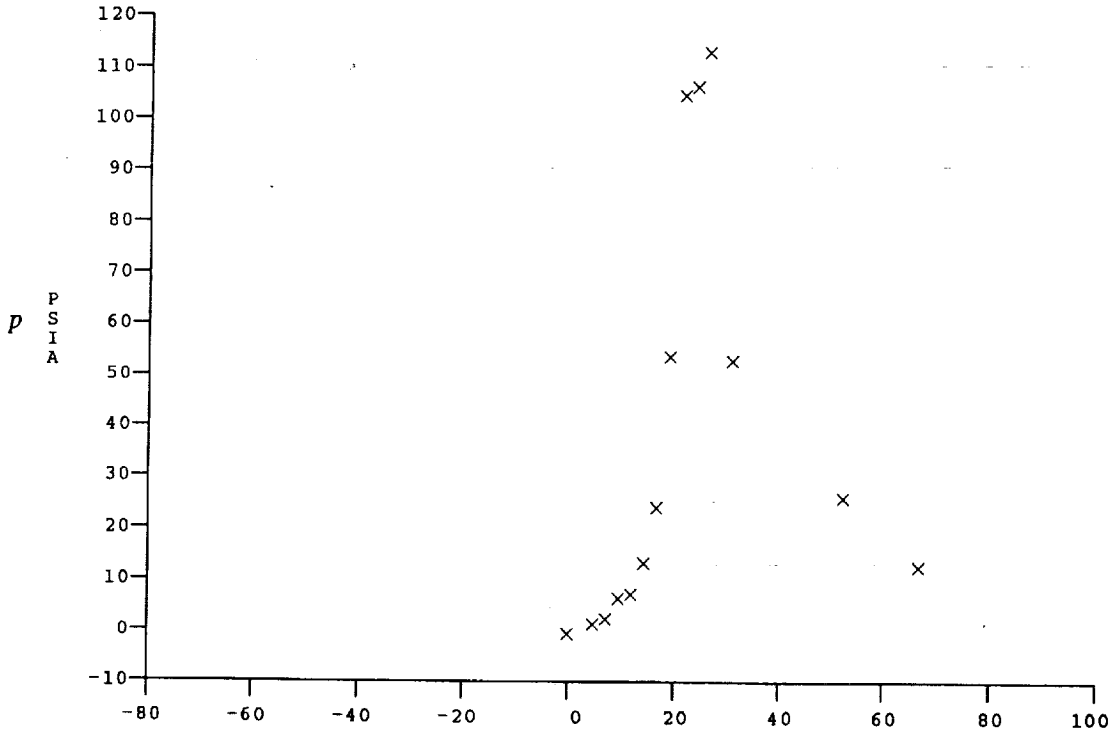

PRESSURE vs Gauge Position
Run 93

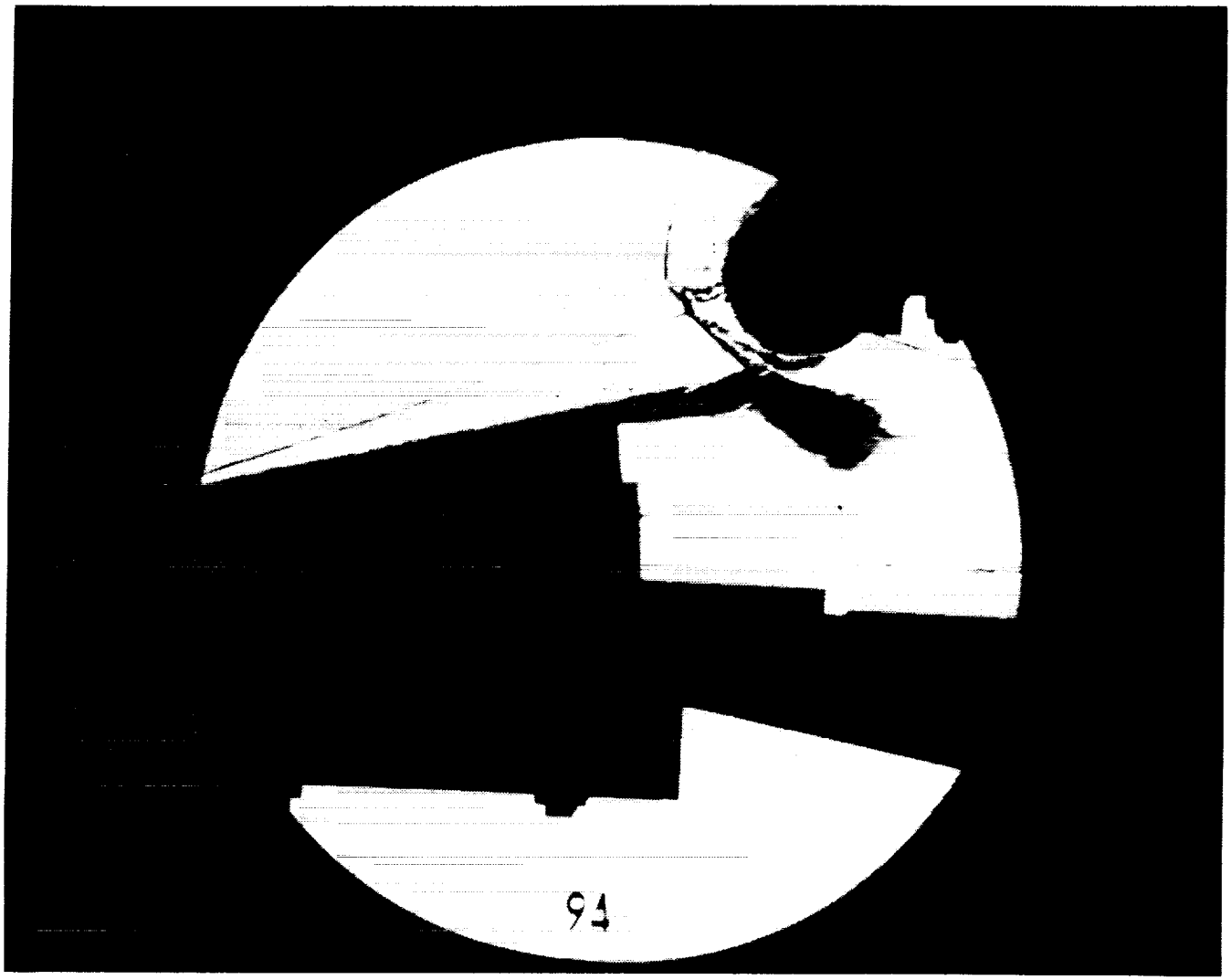

Test Conditions for Run 94 :

Po	= 1.372E+03	PSIA	Reservoir Total Pressure
Ho	= 1.825E+07	(Ft/sec)²	Reservoir Total Enthalpy
To	= 2.775E+03	°R	Reservoir Total Temperature
M	= 8.036E+00		Freestream Mach Number
U	= 5.823E+03	Ft/sec	Freestream Velocity
T	= 2.184E+02	°R	Freestream Temperature
P	= 1.209E-01	PSIA	Freestream Static Pressure
Rho	= 4.647E-05	Slugs/Ft3	Freestream Density
Mu	= 1.806E-07	Slugs/Ft-sec	Freestream Viscosity
Re	= 1.499E+06	1/Ft	Freestream Reynolds Number
Po'	= 1.014E+01	PSIA	Pitot Pressure
Q	= 5.472E+00	PSIA	Dynamic Pressure (½·Rho·U²/144)
Mi	= 3.415E+00		Shock Tube Incident Shock Mach Number
Hw	= 3.183E-06	(Ft/sec)²	Wall Enthalpy (Cp·Tw)
CPf	= 1.827E-01	1/PSIA	Pressure to CP factor (1/Q)
CHf	= 1.908E-04	Ft²-s/BTU	Heat Rate to CH factor (778/(Rho·U·(Ho-Hw))
QoFR	= 3.926E+01	BTU/Ft²-s	Fay-Riddell Heat Transfer to 3" Diam Sphere

Model Configuration Parameter	Value
Stagnation Position (gauge label)	P21
Vertical Distance (inches)	4.00
Horizontal Distance (inches)	1.32
Plate Angle (degrees)	7.50
Plate Length (inches)	36.00
Sweep Angle (degrees)	0.00
BOW to BOP (inches)	-0.25
Wedge Angle (degrees)	6.00
Wedge Length (inches)	11.00

Run 94

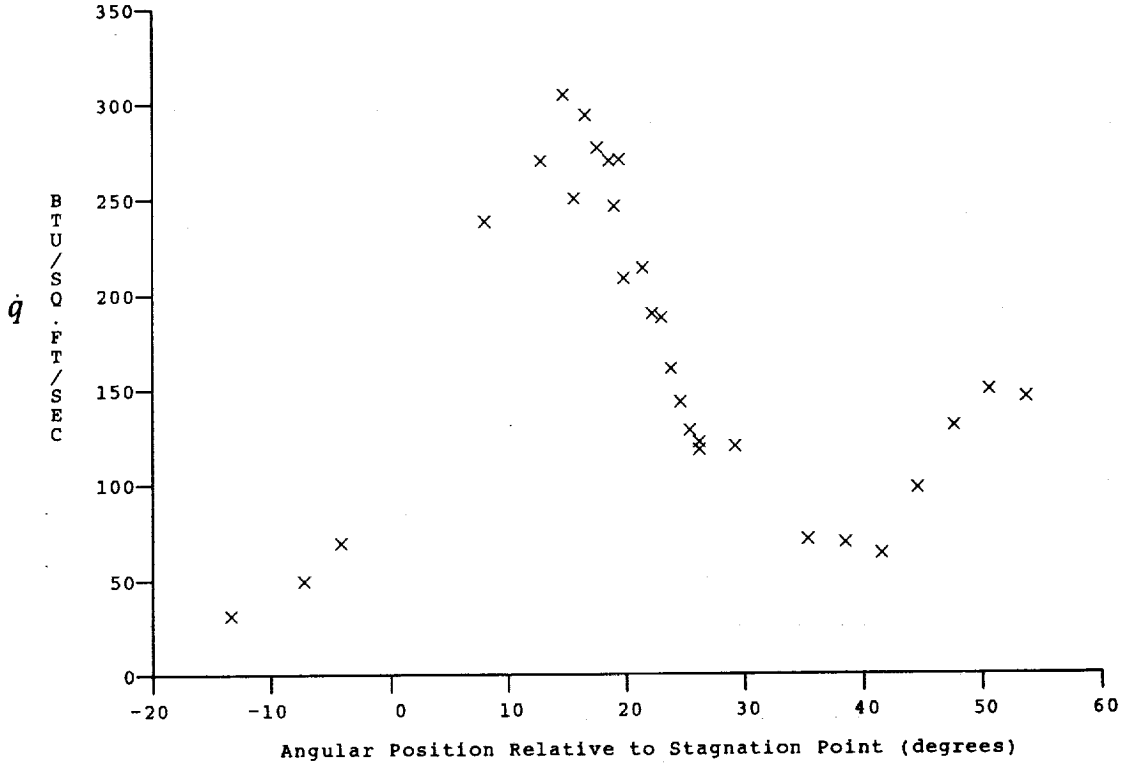

HEAT TRANSFER vs Gauge Position
Run 94

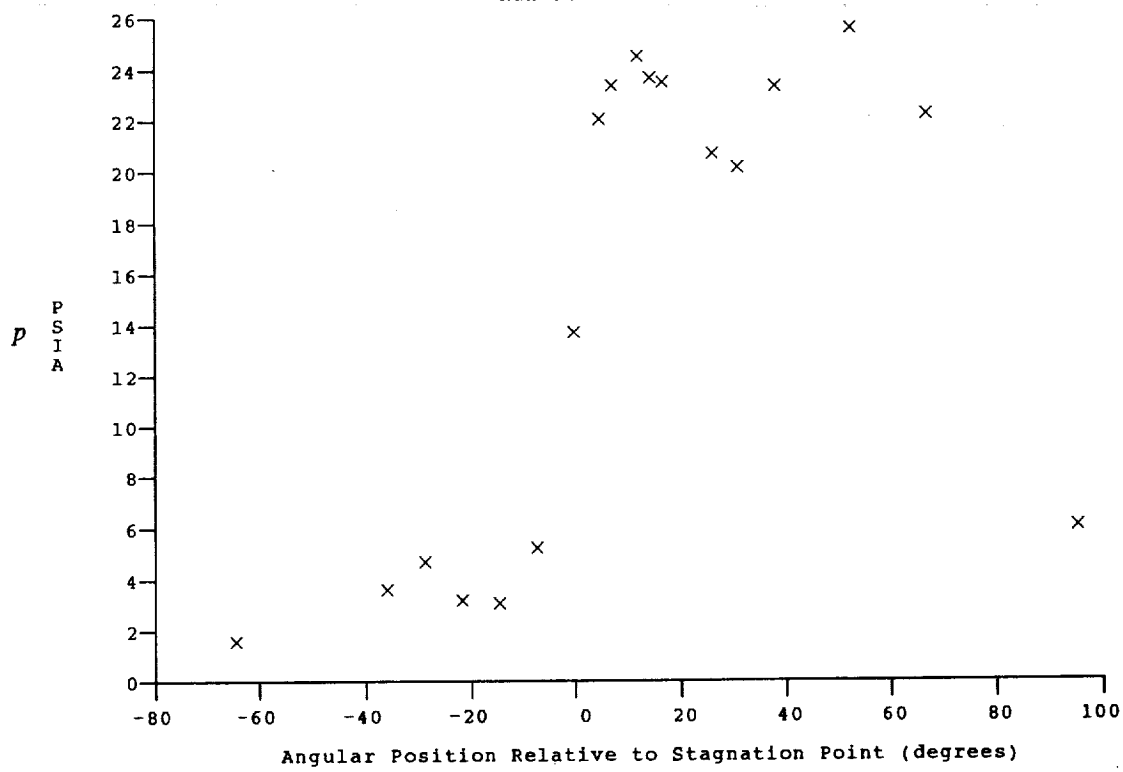

PRESSURE vs Gauge Position
Run 94

C-4

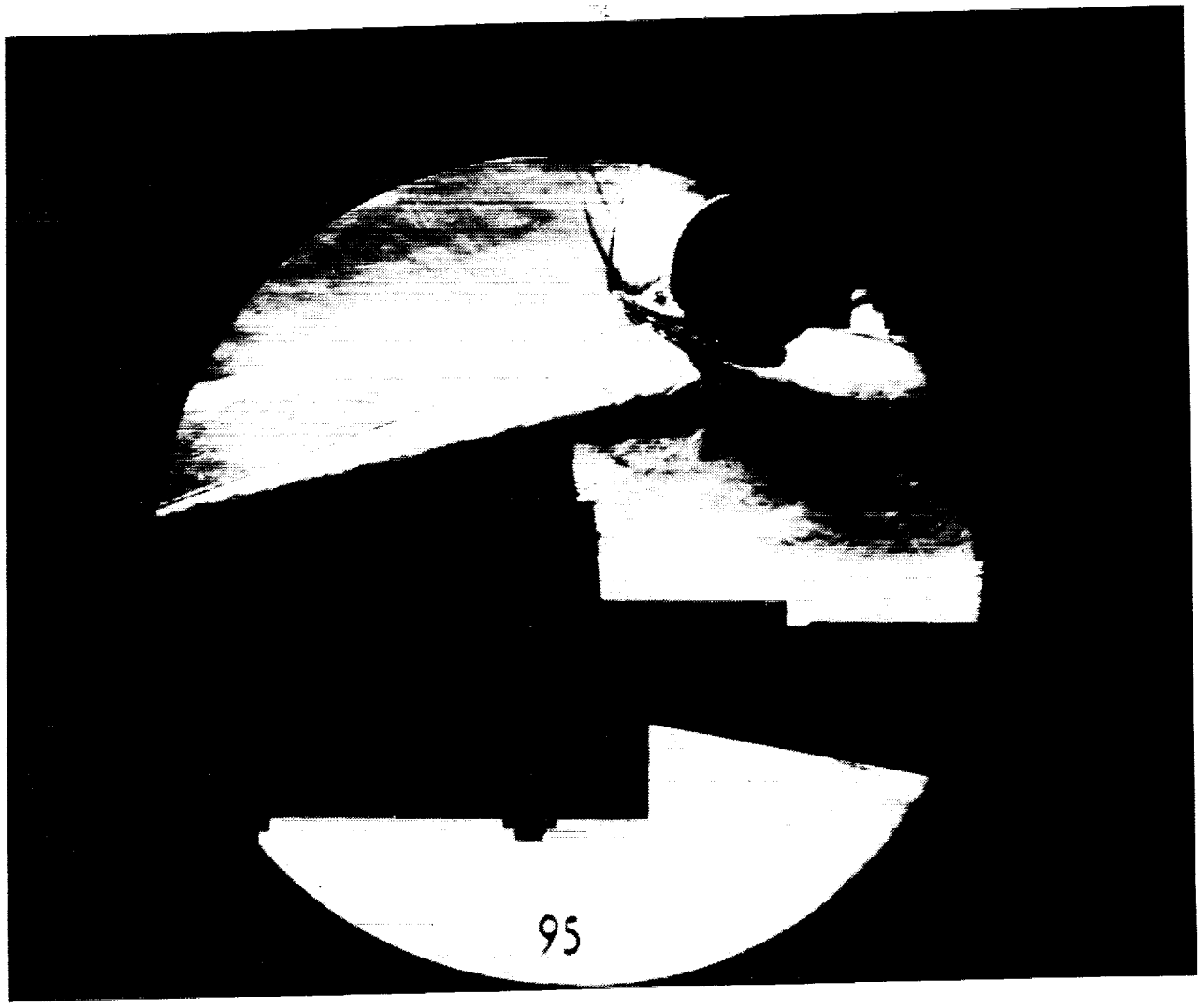

Test Conditions for Run 95 :

Po	= 1.395E+03 PSIA	Reservoir Total Pressure
Ho	= 1.858E+07 (Ft/sec)²	Reservoir Total Enthalpy
To	= 2.821E-03 °R	Reservoir Total Temperature
M	= 8.032E+00	Freestream Mach Number
U	= 5.875E+03 Ft/sec	Freestream Velocity
T	= 2.225E-02 °R	Freestream Temperature
P	= 1.226E-01 PSIA	Freestream Static Pressure
Rho	= 4.626E-05 Slugs/Ft3	Freestream Density
Mu	= 1.838E-07 Slugs/Ft-sec	Freestream Viscosity
Re	= 1.479E+06 1/Ft	Freestream Reynolds Number
Po'	= 1.028E+01 PSIA	Pitot Pressure
Q	= 5.544E+00 PSIA	Dynamic Pressure (½·Rho·U²/144)
Mi	= 3.430E+00	Shock Tube Incident Shock Mach Number
Hw	= 3.183E+06 (Ft/sec)²	Wall Enthalpy (Cp·Tw)
CPf	= 1.804E-01 1/PSIA	Pressure to CP factor (1/Q)
CHf	= 1.860E-04 Ft²-s/BTU	Heat Rate to CH factor (778/(Rho·U·(Ho-Hw))
QoFR	= 4.042E+01 BTU/Ft²-s	Fay-Riddell Heat Transfer to 3" Diam Sphere

Model Configuration Parameter	Value
Stagnation Position (gauge label)	P24
Vertical Distance (inches)	4.25
Horizontal Distance (inches)	1.32
Plate Angle (degrees)	7.50
Plate Length (inches)	36.00
Sweep Angle (degrees)	0.00
BOW to BOP (inches)	-0.25
Wedge Angle (degrees)	6.00
Wedge Length (inches)	13.25

Run 95

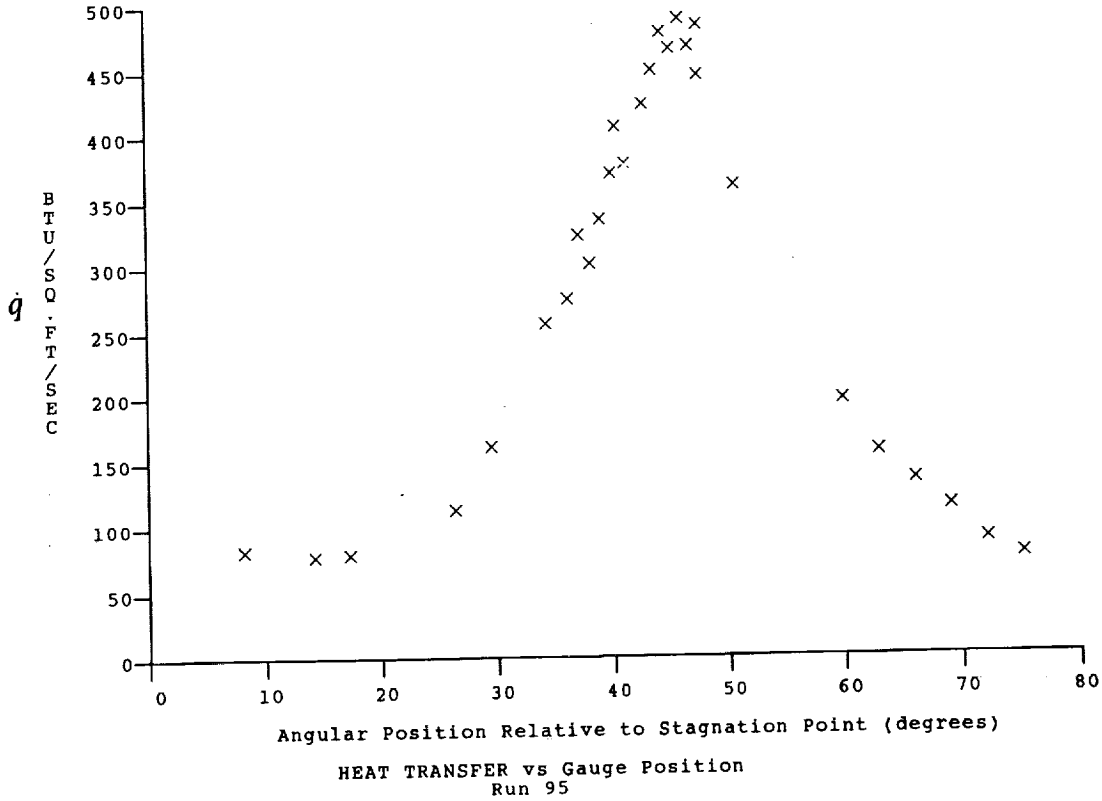

HEAT TRANSFER vs Gauge Position
Run 95

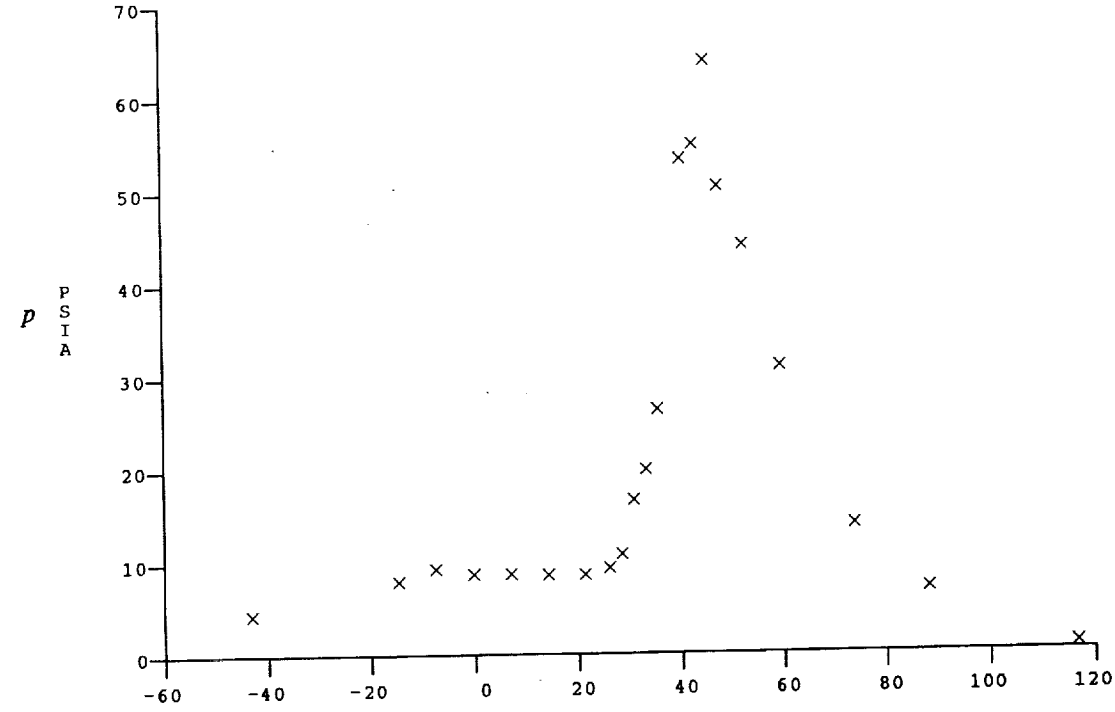

PRESSURE vs Gauge Position
Run 95

Gauge Label	Angle (deg)	Value (PSIA) or (BTU/Ft2-Sec)	T Surf (DegR)	Gauge Label	Angle (deg)	Value (PSIA) or (BTU/Ft2-Sec)	T Surf (DegR)	Gauge Label	Angle (deg)	Value (PSIA) or (BTU/Ft2-Sec)	T Surf (DegR)
P 30	-64.40	1.804(0)		P 9	38.22	1.798(1)		HT 71	19.60	9.038(1)	645.76
P 28	-50.11	3.087(0)		P 7	52.54	1.360(1)		HT 9	19.90	8.983(1)	637.99
P 26	-35.79	4.289(0)		P 5	66.86	8.723(0)		HT 7	21.51	8.840(1)	636.57
P 25	-28.63	4.190(0)		P 3	81.19	4.335(0)		HT 6	22.30	8.438(1)	633.95
P 24	-21.47	4.192(0)		P 1	95.51	2.044(0)		HT 5	23.09	1.019(2)	646.64
P 23	-14.30	6.781(0)		HT 32	-16.31	5.744(1)	599.20	HT 4	23.89	8.232(1)	629.20
P 22	-7.14	1.455(1)		HT 31	-13.25	7.592(1)	614.10	HT 3	24.69	8.608(1)	633.36
P 21	.02	2.571(1)		HT 29	-7.14	1.403(2)	665.52	HT 2	25.49	8.741(1)	632.02
P 20	4.79	2.678(1)		HT 28	-4.09	1.808(2)	694.80	HT 1	26.29	8.465(1)	629.85
P 15	7.18	2.467(1)		HT 25	5.08	1.312(2)	674.27	HT 62	26.29	9.190(1)	634.63
P 19	9.57	2.625(1)		HT 24	8.14	1.095(2)	656.83	HT 61	29.35	8.104(1)	623.39
P 14	11.96	2.676(1)		HT 64	12.91	1.120(2)	657.84	HT 59	35.46	Null	Null
P 18	14.34	2.296(1)		HT 65	13.87	Null	Null	HT 58	38.51	6.443(1)	608.03
P 13	16.73	2.054(1)		HT 66	14.82	1.069(2)	661.48	HT 57	41.57	6.048(1)	605.37
P 17	19.12	Null		HT 67	15.78	1.007(2)	654.63	HT 56	44.63	6.200(1)	603.36
P 12	21.51	Null		HT 68	16.73	9.720(1)	650.58	HT 55	47.68	5.528(1)	598.24
P 16	23.89	Null		HT 69	17.69	9.911(1)	651.42	HT 54	50.74	5.147(1)	595.60
P 11	26.28	2.033(1)		HT 70	18.64	9.100(1)	644.11	HT 53	53.79	4.828(1)	587.98
P 10	31.05	1.847(1)		HT 10	19.10	9.677(1)	650.46				

Run 82 Reduced Data Tabulation

Gauge Label	Angle (deg)	Value (PSIA) or (BTU/Ft2-Sec)	T Surf (DegR)	Gauge Label	Angle (deg)	Value (PSIA) or (BTU/Ft2-Sec)	T Surf (DegR)	Gauge Label	Angle (deg)	Value (PSIA) or (BTU/Ft2-Sec)	T Surf (DegR)
P 30	-64.40	1.423(0)		P 9	38.22	3.324(1)		HT 71	19.60	3.476(2)	818.17
P 28	-50.11	Null		P 7	52.54	2.741(1)		HT 9	19.90	3.788(2)	840.55
P 26	-35.79	3.216(0)		P 5	66.86	1.847(1)		HT 7	21.51	5.143(2)	895.78
P 25	-28.63	1.866(0)		P 3	81.19	7.946(0)		HT 6	22.30	5.665(2)	907.65
P 24	-21.47	8.120(-1)		P 1	95.51	3.044(0)		HT 5	23.09	6.920(2)	955.60
P 23	-14.30	7.449(-1)		HT 32	-16.31	2.039(0)	549.94	HT 4	23.89	7.359(2)	955.52
P 22	-7.14	7.081(-1)		HT 31	-13.25	4.110(0)	551.65	HT 3	24.69	7.554(2)	949.94
P 21	.02	-4.861(-1)		HT 29	-7.14	5.844(0)	553.11	HT 2	25.49	7.749(2)	953.98
P 20	4.79	1.901(0)		HT 28	-4.09	1.089(1)	558.04	HT 1	26.29	7.392(2)	939.80
P 15	7.18	3.738(0)		HT 25	5.08	3.672(1)	591.44	HT 62	26.29	6.153(2)	907.38
P 19	9.57	7.401(0)		HT 24	8.14	4.915(1)	607.77	HT 61	29.35	3.231(2)	799.67
P 14	11.96	1.348(1)		HT 64	12.91	1.195(2)	682.38	HT 59	35.46	1.686(2)	686.08
P 18	14.34	1.567(1)		HT 65	13.87	Null	Null	HT 58	38.51	2.832(2)	738.19
P 13	16.73	2.911(1)		HT 66	14.82	1.409(2)	706.60	HT 57	41.57	2.504(2)	724.37
P 17	19.12	6.390(1)		HT 67	15.78	1.864(2)	736.82	HT 56	44.63	2.150(2)	718.62
P 12	21.51	1.104(2)		HT 68	16.73	2.130(2)	747.70	HT 55	47.68	1.879(2)	697.43
P 16	23.89	1.141(2)		HT 69	17.69	2.668(2)	780.70	HT 54	50.74	1.956(2)	688.53
P 11	26.28	7.175(1)		HT 70	18.64	2.904(2)	799.19	HT 53	53.79	1.619(2)	672.49
P 10	31.05	3.134(1)		HT 10	19.10	3.778(2)	840.91				

Run 83 Reduced Data Tabulation

Gauge Label	Angle (deg)	Value (PSIA) or (BTU/Ft2-Sec)	T Surf (DegR)	Gauge Label	Angle (deg)	Value (PSIA) or (BTU/Ft2-Sec)	T Surf (DegR)	Gauge Label	Angle (deg)	Value (PSIA) or (BTU/Ft2-Sec)	T Surf (DegR)
P 30	-64.40	1.475(0)		P 9	38.22	2.832(1)		HT 71	19.60	Null	Null
P 28	-50.11	Null		P 7	52.54	3.471(1)		HT 9	19.90	Null	Null
P 26	-35.79	3.342(0)		P 5	66.86	2.105(1)		HT 7	21.51	1.621(2)	705.56
P 25	-28.63	4.158(0)		P 3	81.19	9.464(0)		HT 6	22.30	1.475(2)	698.20
P 24	-21.47	3.988(0)		P 1	95.51	4.015(0)		HT 5	23.09	1.744(2)	721.02
P 23	-14.30	5.122(0)		HT 32	-16.31	4.543(1)	593.97	HT 4	23.89	1.654(2)	711.72
P 22	-7.14	8.287(0)		HT 31	-13.25	5.411(1)	596.98	HT 3	24.69	1.570(2)	703.51
P 21	.02	1.875(1)		HT 29	-7.14	8.055(1)	613.92	HT 2	25.49	1.444(2)	700.22
P 20	4.79	2.275(1)		HT 28	-4.09	1.354(2)	640.51	HT 1	26.29	1.543(2)	708.36
P 15	7.18	2.526(1)		HT 25	5.08	Null	Null	HT 62	26.29	1.529(2)	693.52
P 19	9.57	2.508(1)		HT 24	8.14	3.110(2)	739.65	HT 61	29.35	1.805(2)	714.15
P 14	11.96	2.418(1)		HT 64	12.91	2.834(2)	739.75	HT 59	35.46	1.806(2)	700.06
P 18	14.34	2.304(1)		HT 65	13.87	Null	Null	HT 58	38.51	2.824(2)	761.43
P 13	16.73	2.095(1)		HT 66	14.82	2.569(2)	728.93	HT 57	41.57	2.976(2)	760.92
P 17	19.12	Null		HT 67	15.78	2.495(2)	726.18	HT 56	44.63	3.075(2)	762.72
P 12	21.51	Null		HT 68	16.73	Null	Null	HT 55	47.68	2.648(2)	741.31
P 16	23.89	Null		HT 69	17.69	1.725(2)	691.21	HT 54	50.74	2.568(2)	737.06
P 11	26.28	2.229(1)		HT 70	18.64	1.983(2)	702.36	HT 53	53.79	1.938(2)	703.19
P 10	31.05	2.142(1)		HT 10	19.10	1.917(2)	719.38				

Run 84 Reduced Data Tabulation

Gauge Label	Angle (deg)	Value (PSIA) or (BTU/Ft2-Sec)	T Surf (DegR)	Gauge Label	Angle (deg)	Value (PSIA) or (BTU/Ft2-Sec)	T Surf (DegR)	Gauge Label	Angle (deg)	Value (PSIA) or (BTU/Ft2-Sec)	T Surf (DegR)
P 30	-64.40	1.485(0)		P 9	38.22	3.050(1)		HT 71	19.60	1.832(2)	785.82
P 28	-50.11	Null		P 7	52.54	2.527(1)		HT 9	19.90	2.305(2)	808.81
P 26	-35.79	6.121(0)		P 5	66.86	1.752(1)		HT 7	21.51	Null	Null
P 25	-28.63	7.656(0)		P 3	81.19	Null		HT 6	22.30	4.162(2)	885.06
P 24	-21.47	6.409(0)		P 1	95.51	3.871(0)		HT 5	23.09	4.805(2)	915.60
P 23	-14.30	4.020(0)		HT 32	-16.31	6.985(1)	587.61	HT 4	23.89	5.818(2)	929.80
P 22	-7.14	1.662(0)		HT 31	-13.25	4.297(1)	573.65	HT 3	24.69	6.093(2)	938.43
P 21	.02	1.176(0)		HT 29	-7.14	1.214(1)	558.61	HT 2	25.49	6.370(2)	942.53
P 20	4.79	2.463(0)		HT 28	-4.09	9.687(0)	557.90	HT 1	26.29	6.500(2)	940.48
P 15	7.18	3.547(0)		HT 25	5.08	1.949(1)	582.80	HT 62	26.29	6.833(2)	946.46
P 19	9.57	5.607(0)		HT 24	8.14	3.641(1)	602.93	HT 61	29.35	4.508(2)	856.14
P 14	11.96	7.027(0)		HT 64	12.91	6.106(1)	654.11	HT 59	35.46	1.867(2)	710.21
P 18	14.34	1.074(1)		HT 65	13.87	Null	Null	HT 58	38.51	2.375(2)	735.64
P 13	16.73	1.253(1)		HT 66	14.82	7.773(1)	680.00	HT 57	41.57	2.386(2)	732.24
P 17	19.12	Null		HT 67	15.78	9.987(1)	707.57	HT 56	44.63	2.075(2)	716.28
P 12	21.51	Null		HT 68	16.73	1.132(2)	718.95	HT 55	47.68	1.763(2)	705.55
P 16	23.89	Null		HT 69	17.69	1.097(2)	711.91	HT 54	50.74	1.635(2)	690.73
P 11	26.28	Null		HT 70	18.64	1.532(2)	767.36	HT 53	53.79	1.535(2)	673.49
P 10	31.05	4.681(1)		HT 10	19.10	2.125(2)	796.48				

Run 85 Reduced Data Tabulation

Gauge Label	Angle (deg)	Value (PSIA) or (BTU/Ft2-Sec)	T Surf (DegR)	Gauge Label	Angle (deg)	Value (PSIA) or (BTU/Ft2-Sec)	T Surf (DegR)	Gauge Label	Angle (deg)	Value (PSIA) or (BTU/Ft2-Sec)	T Surf (DegR)
P 30	-64.40	1.693(0)		P 9	38.22	2.221(1)		HT 71	19.60	Null	Null
P 28	-50.11	Null		P 7	52.54	2.303(1)		HT 9	19.90	1.176(2)	681.63
P 26	-35.79	3.413(0)		P 5	66.86	1.861(1)		HT 7	21.51	1.025(2)	674.22
P 25	-28.63	3.469(0)		P 3	81.19	Null		HT 6	22.30	9.789(1)	664.31
P 24	-21.47	2.840(0)		P 1	95.51	5.958(0)		HT 5	23.09	1.032(2)	678.95
P 23	-14.30	3.530(0)		HT 32	-16.31	3.279(1)	591.07	HT 4	23.89	1.037(2)	658.56
P 22	-7.14	6.704(0)		HT 31	-13.25	4.114(1)	603.88	HT 3	24.69	8.611(1)	660.22
P 21	.02	1.798(1)		HT 29	-7.14	7.521(1)	647.19	HT 2	25.49	9.892(1)	660.79
P 20	4.79	2.406(1)		HT 28	-4.09	1.087(2)	685.04	HT 1	26.29	1.062(2)	666.41
P 15	7.18	2.600(1)		HT 25	5.08	2.728(2)	805.47	HT 62	26.29	9.450(1)	664.34
P 19	9.57	2.714(1)		HT 24	8.14	2.557(2)	794.44	HT 61	29.35	7.964(1)	652.90
P 14	11.96	2.325(1)		HT 64	12.91	2.125(2)	768.73	HT 59	35.46	7.029(1)	640.03
P 18	14.34	2.203(1)		HT 65	13.87	Null	Null	HT 58	38.51	5.627(1)	630.96
P 13	16.73	1.959(1)		HT 66	14.82	1.837(2)	740.39	HT 57	41.57	6.595(1)	637.09
P 17	19.12	Null		HT 67	15.78	1.917(2)	740.01	HT 56	44.63	7.355(1)	653.34
P 12	21.51	Null		HT 68	16.73	1.513(2)	716.51	HT 55	47.68	9.114(1)	667.69
P 16	23.89	Null		HT 69	17.69	1.339(2)	706.25	HT 54	50.74	7.849(1)	662.32
P 11	26.28	2.166(1)		HT 70	18.64	1.293(2)	703.06	HT 53	53.79	9.199(1)	667.38
P 10	31.05	2.001(1)		HT 10	19.10	1.264(2)	694.69				

Run 86 Reduced Data Tabulation

Gauge Label	Angle (deg)	Value (PSIA) or (BTU/Ft2-Sec)	T Surf (DegR)	Gauge Label	Angle (deg)	Value (PSIA) or (BTU/Ft2-Sec)	T Surf (DegR)	Gauge Label	Angle (deg)	Value (PSIA) or (BTU/Ft2-Sec)	T Surf (DegR)
P 30	-64.40	5.832(-1)		P 9	38.22	3.199(1)		HT 71	19.60	4.939(2)	953.04
P 28	-50.11	Null		P 7	52.54	2.655(1)		HT 9	19.90	5.686(2)	981.08
P 26	-35.79	4.933(-1)		P 5	66.86	1.717(1)		HT 7	21.51	6.893(2)	976.73
P 25	-28.63	5.419(-1)		P 3	81.19	Null		HT 6	22.30	9.438(2)	998.61
P 24	-21.47	2.988(-1)		P 1	95.51	2.397(0)		HT 5	23.09	1.135(3)	1046.20
P 23	-14.30	4.612(-1)		HT 32	-16.31	2.908(0)	546.79	HT 4	23.89	1.190(3)	1034.30
P 22	-7.14	8.491(-1)		HT 31	-13.25	3.529(0)	548.09	HT 3	24.69	1.055(3)	980.01
P 21	.02	1.420(0)		HT 29	-7.14	9.870(0)	551.97	HT 2	25.49	1.041(3)	966.70
P 20	4.79	5.959(0)		HT 28	-4.09	1.493(1)	559.05	HT 1	26.29	9.352(2)	939.79
P 15	7.18	7.860(0)		HT 25	5.08	4.668(1)	605.20	HT 62	26.29	6.301(2)	891.91
P 19	9.57	1.469(1)		HT 24	8.14	8.545(1)	650.63	HT 61	29.35	3.198(2)	786.52
P 14	11.96	2.301(1)		HT 64	12.91	1.614(2)	776.16	HT 59	35.46	1.904(2)	698.66
P 18	14.34	3.268(1)		HT 65	13.87	Null	Null	HT 58	38.51	2.522(2)	727.33
P 13	16.73	4.220(1)		HT 66	14.82	1.890(2)	830.42	HT 57	41.57	2.645(2)	723.96
P 17	19.12	8.614(1)		HT 67	15.78	2.412(2)	869.34	HT 56	44.63	2.361(2)	713.33
P 12	21.51	1.360(2)		HT 68	16.73	3.613(2)	914.61	HT 55	47.68	2.052(2)	701.92
P 16	23.89	1.423(2)		HT 69	17.69	3.514(2)	910.53	HT 54	50.74	1.938(2)	685.59
P 11	26.28	7.202(1)		HT 70	18.64	4.755(2)	947.92	HT 53	53.79	1.550(2)	665.39
P 10	31.05	3.394(1)		HT 10	19.10	5.048(2)	973.67				

Run 87 Reduced Data Tabulation

Gauge Label	Angle (deg)	Value (PSIA) or (BTU/Ft2-Sec)	T Surf (DegR)	Gauge Label	Angle (deg)	Value (PSIA) or (BTU/Ft2-Sec)	T Surf (DegR)	Gauge Label	Angle (deg)	Value (PSIA) or (BTU/Ft2-Sec)	T Surf (DegR)
P 30	-64.40	2.133(0)		P 9	38.22	4.974(1)		HT 71	19.60	4.190(2)	771.99
P 28	-50.11	Null		P 7	52.54	3.170(1)		HT 9	19.90	Null	Null
P 26	-35.79	6.905(0)		P 5	66.86	2.062(1)		HT 7	21.51	5.568(2)	836.37
P 25	-28.63	8.029(0)		P 3	81.19	Null		HT 6	22.30	6.277(2)	849.43
P 24	-21.47	6.360(0)		P 1	95.51	4.389(0)		HT 5	23.09	8.101(2)	907.28
P 23	-14.30	3.974(0)		HT 32	-16.31	6.439(1)	591.68	HT 4	23.89	8.173(2)	905.26
P 22	-7.14	2.556(0)		HT 31	-13.25	4.356(1)	580.65	HT 3	24.69	7.857(2)	898.52
P 21	.02	2.242(0)		HT 29	-7.14	1.794(1)	565.19	HT 2	25.49	7.912(2)	895.27
P 20	4.79	3.806(0)		HT 28	-4.09	1.400(1)	563.13	HT 1	26.29	7.456(2)	891.02
P 15	7.18	1.296(1)		HT 25	5.08	4.944(1)	592.29	HT 62	26.29	6.595(2)	875.19
P 19	9.57	9.095(0)		HT 24	8.14	6.151(1)	604.11	HT 61	29.35	4.036(2)	811.42
P 14	11.96	3.515(1)		HT 64	12.91	1.731(2)	673.95	HT 59	35.46	1.962(2)	687.33
P 18	14.34	1.650(1)		HT 65	13.87	Null	Null	HT 58	38.51	2.905(2)	725.32
P 13	16.73	3.538(1)		HT 66	14.82	2.282(2)	695.94	HT 57	41.57	2.747(2)	724.41
P 17	19.12	7.349(1)		HT 67	15.78	2.849(2)	719.21	HT 56	44.63	2.417(2)	711.53
P 12	21.51	8.020(1)		HT 68	16.73	2.811(2)	718.18	HT 55	47.68	2.187(2)	699.73
P 16	23.89	1.132(2)		HT 69	17.69	3.257(2)	737.30	HT 54	50.74	2.037(2)	689.24
P 11	26.28	5.151(1)		HT 70	18.64	3.776(2)	767.15	HT 53	53.79	1.724(2)	668.91
P 10	31.05	4.237(1)		HT 10	19.10	4.338(2)	794.60				

Run 88 Reduced Data Tabulation

Gauge Label	Angle (deg)	Value (PSIA) or (BTU/Ft2-Sec)	T Surf (DegR)	Gauge Label	Angle (deg)	Value (PSIA) or (BTU/Ft2-Sec)	T Surf (DegR)	Gauge Label	Angle (deg)	Value (PSIA) or (BTU/Ft2-Sec)	T Surf (DegR)
P 30	-64.40	1.876(0)		P 7	52.54	1.293(1)		HT 9	19.90	7.154(2)	889.25
P 28	-50.11	Null		P 5	66.86	8.094(0)		HT 7	21.51	Null	Null
P 26	-35.79	5.618(0)		P 3	81.19	Null		HT 6	22.30	4.741(2)	873.36
P 25	-28.63	6.778(0)		P 1	95.51	1.745(0)		HT 5	23.09	4.510(2)	894.02
P 24	-21.47	7.351(0)		HT 32	-16.31	9.392(1)	620.47	HT 4	23.89	3.394(2)	866.27
P 23	-14.30	7.171(0)		HT 31	-13.25	7.693(1)	623.96	HT 3	24.69	2.861(2)	862.06
P 22	-7.14	8.347(0)		HT 29	-7.14	1.115(2)	640.09	HT 2	25.49	2.423(2)	851.64
P 21	.02	8.182(0)		HT 28	-4.09	1.434(2)	654.42	HT 1	26.29	2.107(2)	844.48
P 20	4.79	6.451(0)		HT 25	5.08	4.680(1)	613.73	HT 62	26.29	2.438(2)	880.02
P 15	7.18	5.275(0)		HT 24	8.14	7.982(1)	622.91	HT 61	29.35	1.858(2)	794.26
P 19	9.57	8.334(0)		HT 64	12.91	1.673(2)	693.34	HT 59	35.46	1.145(2)	660.30
P 14	11.96	1.035(1)		HT 65	13.87	Null	Null	HT 58	38.51	1.418(2)	670.30
P 18	14.34	1.854(1)		HT 66	14.82	2.699(2)	742.83	HT 57	41.57	1.265(2)	664.71
P 13	16.73	4.599(1)		HT 67	15.78	3.719(2)	781.42	HT 56	44.63	1.148(2)	661.23
P 17	19.12	6.684(1)		HT 68	16.73	4.670(2)	809.59	HT 55	47.68	1.160(2)	654.51
P 16	23.89	4.414(1)		HT 69	17.69	5.480(2)	832.94	HT 54	50.74	1.006(2)	646.58
P 11	26.28	2.236(1)		HT 70	18.64	6.481(2)	866.11	HT 53	53.79	8.423(1)	627.62
P 10	31.05	1.748(1)		HT 10	19.10	7.124(2)	890.33				
P 9	38.22	1.724(1)		HT 71	19.60	7.073(2)	881.64				

Run 89 Reduced Data Tabulation

Gauge Label	Angle (deg)	Value (PSIA) or (BTU/Ft2-Sec)	T Surf (DegR)	Gauge Label	Angle (deg)	Value (PSIA) or (BTU/Ft2-Sec)	T Surf (DegR)	Gauge Label	Angle (deg)	Value (PSIA) or (BTU/Ft2-Sec)	T Surf (DegR)
P 30	-64.40	1.523(0)		P 7	52.54	2.995(1)		HT 9	19.90	2.722(2)	735.13
P 28	-50.11	Null		P 5	66.86	1.920(1)		HT 7	21.51	3.794(2)	784.74
P 26	-35.79	2.751(0)		P 3	81.19	Null		HT 6	22.30	4.237(2)	800.92
P 25	-28.63	2.145(0)		P 1	95.51	2.844(0)		HT 5	23.09	5.239(2)	849.20
P 24	-21.47	1.041(0)		HT 32	-16.31	4.153(0)	557.68	HT 4	23.89	5.795(2)	866.64
P 23	-14.30	8.175(-1)		HT 31	-13.25	6.655(0)	556.06	HT 3	24.69	6.814(2)	895.12
P 22	-7.14	7.417(-1)		HT 29	-7.14	6.474(0)	555.46	HT 2	25.49	7.366(2)	911.72
P 21	.02	1.632(0)		HT 28	-4.09	7.500(0)	556.19	HT 1	26.29	7.753(2)	934.49
P 20	4.79	2.685(0)		HT 25	5.08	2.849(1)	575.03	HT 62	26.29	8.057(2)	966.45
P 15	7.18	4.215(0)		HT 24	8.14	4.002(1)	583.54	HT 61	29.35	4.657(2)	924.17
P 19	9.57	5.455(0)		HT 64	12.91	8.539(1)	622.31	HT 59	35.46	1.609(2)	694.36
P 14	11.96	9.138(0)		HT 65	13.87	Null	Null	HT 58	38.51	2.378(2)	728.16
P 18	14.34	1.311(1)		HT 66	14.82	1.080(2)	639.13	HT 57	41.57	2.842(2)	748.50
P 13	16.73	1.685(1)		HT 67	15.78	1.333(2)	652.99	HT 56	44.63	2.420(2)	742.21
P 17	19.12	4.365(1)		HT 68	16.73	1.668(2)	662.96	HT 55	47.68	2.097(2)	725.13
P 16	23.89	9.248(1)		HT 69	17.69	1.671(2)	674.10	HT 54	50.74	2.138(2)	715.18
P 11	26.28	1.011(2)		HT 70	18.64	2.350(2)	703.54	HT 53	53.79	1.898(2)	694.45
P 10	31.05	5.194(1)		HT 10	19.10	2.556(2)	723.95				
P 9	38.22	3.321(1)		HT 71	19.60	2.503(2)	717.99				

Run 90 Reduced Data Tabulation

Gauge Label	Angle (deg)	Value (PSIA) or (BTU/Ft2-Sec)	T Surf (DegR)	Gauge Label	Angle (deg)	Value (PSIA) or (BTU/Ft2-Sec)	T Surf (DegR)	Gauge Label	Angle (deg)	Value (PSIA) or (BTU/Ft2-Sec)	T Surf (DegR)
P 30	-64.40	1.408(0)		P 7	52.54	2.897(1)		HT 9	19.90	2.483(2)	751.19
P 28	-50.11	Null		P 5	66.86	1.943(1)		HT 7	21.51	3.266(2)	812.14
P 26	-35.79	2.072(0)		P 3	81.19	Null		HT 6	22.30	3.611(2)	827.93
P 25	-28.63	1.889(0)		P 1	95.51	2.815(0)		HT 5	23.09	4.388(2)	880.11
P 24	-21.47	8.086(-1)		HT 32	-16.31	2.425(0)	546.04	HT 4	23.89	4.437(2)	891.18
P 23	-14.30	7.437(-1)		HT 31	-13.25	2.276(0)	545.54	HT 3	24.69	5.489(2)	925.38
P 22	-7.14	7.207(-1)		HT 29	-7.14	7.007(0)	549.65	HT 2	25.49	5.849(2)	932.18
P 21	.02	1.264(0)		HT 28	-4.09	9.703(0)	551.07	HT 1	26.29	6.133(2)	950.39
P 20	4.79	2.685(0)		HT 25	5.08	3.211(1)	571.46	HT 62	26.29	Null	Null
P 15	7.18	4.430(0)		HT 24	8.14	4.413(1)	584.48	HT 61	29.35	5.458(2)	895.56
P 19	9.57	6.355(0)		HT 64	12.91	8.550(1)	623.14	HT 59	35.46	1.732(2)	695.02
P 14	11.96	9.439(0)		HT 65	13.87	Null	Null	HT 58	38.51	2.518(2)	738.66
P 18	14.34	1.290(1)		HT 66	14.82	1.096(2)	643.49	HT 57	41.57	2.439(2)	744.17
P 13	16.73	2.348(1)		HT 67	15.78	1.322(2)	664.96	HT 56	44.63	2.367(2)	731.51
P 17	19.12	4.908(1)		HT 68	16.73	1.514(2)	675.22	HT 55	47.68	2.338(2)	723.42
P 16	23.89	9.437(1)		HT 69	17.69	1.679(2)	691.91	HT 54	50.74	1.858(2)	704.08
P 11	26.28	8.514(1)		HT 70	18.64	1.972(2)	715.46	HT 53	53.79	1.608(2)	683.04
P 10	31.05	5.169(1)		HT 10	19.10	2.178(2)	734.95				
P 9	38.22	3.386(1)		HT 71	19.60	2.422(2)	740.15				

Run 91 Reduced Data Tabulation

Gauge Label	Angle (deg)	Value (PSIA) or (BTU/Ft2-Sec)	T Surf (DegR)	Gauge Label	Angle (deg)	Value (PSIA) or (BTU/Ft2-Sec)	T Surf (DegR)	Gauge Label	Angle (deg)	Value (PSIA) or (BTU/Ft2-Sec)	T Surf (DegR)
P 30	-64.40	4.399(-1)		P 7	52.54	2.762(1)		HT 9	19.90	2.957(2)	771.22
P 28	-50.11	Null		P 5	66.86	1.607(1)		HT 7	21.51	6.355(2)	980.36
P 26	-35.79	1.364(-1)		P 3	81.19	Null		HT 6	22.30	8.101(2)	1022.00
P 25	-28.63	2.359(-1)		P 1	95.51	2.133(0)		HT 5	23.09	9.471(2)	1061.00
P 24	-21.47	1.625(-1)		HT 32	-16.31	1.903(0)	536.66	HT 4	23.89	9.412(2)	1042.80
P 23	-14.30	5.020(-1)		HT 31	-13.25	3.664(0)	538.49	HT 3	24.69	9.232(2)	1022.80
P 22	-7.14	1.049(0)		HT 29	-7.14	5.237(0)	538.77	HT 2	25.49	8.783(2)	996.17
P 21	.02	2.272(-1)		HT 28	-4.09	7.347(0)	540.44	HT 1	26.29	8.095(2)	966.74
P 20	4.79	7.998(-1)		HT 25	5.08	2.541(1)	560.14	HT 62	26.29	8.486(2)	1004.20
P 15	7.18	1.309(0)		HT 24	8.14	3.921(1)	572.70	HT 61	29.35	6.438(2)	948.34
P 19	9.57	2.388(0)		HT 64	12.91	7.884(1)	618.00	HT 59	35.46	3.174(2)	789.33
P 14	11.96	4.029(0)		HT 65	13.87	Null	Null	HT 58	38.51	4.905(2)	856.73
P 18	14.34	9.783(0)		HT 66	14.82	5.917(1)	595.21	HT 57	41.57	4.095(2)	826.98
P 13	16.73	1.573(1)		HT 67	15.78	1.077(2)	642.70	HT 56	44.63	Null	Null
P 17	19.12	1.010(2)		HT 68	16.73	1.189(2)	651.12	HT 55	47.68	3.384(2)	785.51
P 16	23.89	Null		HT 69	17.69	1.861(2)	711.89	HT 54	50.74	3.139(2)	764.41
P 11	26.28	Null		HT 70	18.64	2.407(2)	739.14	HT 53	53.79	2.766(2)	743.56
P 10	31.05	Null		HT 10	19.10	2.749(2)	766.63				
P 9	38.22	3.758(1)		HT 71	19.60	2.618(2)	752.56				

Run 92 Reduced Data Tabulation

Gauge Label	Angle (deg)	Value (PSIA) or (BTU/Ft2-Sec)	T Surf (DegR)	Gauge Label	Angle (deg)	Value (PSIA) or (BTU/Ft2-Sec)	T Surf (DegR)	Gauge Label	Angle (deg)	Value (PSIA) or (BTU/Ft2-Sec)	T Surf (DegR)
P 30	-64.40	Null		P 9	38.22	Null		HT 71	19.60	Null	Null
P 28	-50.11	Null		P 7	52.54	2.626(1)		HT 9	19.90	3.505(2)	986.67
P 26	-35.79	Null		P 5	66.86	1.293(1)		HT 7	21.51	3.601(2)	981.55
P 25	-28.63	Null		P 3	81.19	Null		HT 6	22.30	6.648(2)	1056.80
P 24	-21.47	Null		P 1	95.51	Null		HT 5	23.09	6.927(2)	1104.70
P 23	-14.30	Null		HT 32	-16.31	2.706(1)	540.64	HT 4	23.89	8.081(2)	1101.00
P 22	-7.14	Null		HT 31	-13.25	2.381(0)	540.29	HT 3	24.69	8.161(2)	1089.90
P 21	.02	-2.786(-1)		HT 29	-7.14	2.997(1)	549.62	HT 2	25.49	8.473(2)	1076.50
P 20	4.79	1.467(0)		HT 28	-4.09	9.306(0)	539.53	HT 1	26.29	8.736(2)	1058.90
P 15	7.18	2.487(0)		HT 25	5.08	4.193(1)	593.58	HT 62	26.29	8.854(2)	1026.00
P 19	9.57	6.501(0)		HT 24	8.14	5.772(1)	633.59	HT 61	29.35	5.146(2)	869.91
P 14	11.96	7.533(0)		HT 64	12.91	1.216(2)	730.96	HT 59	35.46	1.651(2)	720.95
P 18	14.34	1.358(1)		HT 65	13.87	Null	Null	HT 58	38.51	2.484(2)	760.66
P 13	16.73	2.439(1)		HT 66	14.82	1.388(2)	777.28	HT 57	41.57	2.692(2)	759.50
P 17	19.12	5.406(1)		HT 67	15.78	1.925(2)	842.87	HT 56	44.63	2.625(2)	749.93
P 12	21.51	1.051(2)		HT 68	16.73	2.026(2)	858.54	HT 55	47.68	2.620(2)	739.21
P 16	23.89	1.069(2)		HT 69	17.69	2.347(2)	863.58	HT 54	50.74	2.314(2)	719.84
P 11	26.28	1.136(2)		HT 70	18.64	2.562(2)	924.11	HT 53	53.79	2.386(2)	721.96
P 10	31.05	5.340(1)		HT 10	19.10	3.281(2)	972.18				

Run 93 Reduced Data Tabulation

Gauge Label	Angle (deg)	Value (PSIA) or (BTU/Ft2-Sec)	T Surf (DegR)	Gauge Label	Angle (deg)	Value (PSIA) or (BTU/Ft2-Sec)	T Surf (DegR)	Gauge Label	Angle (deg)	Value (PSIA) or (BTU/Ft2-Sec)	T Surf (DegR)
P 30	-64.40	1.620(0)		P 9	38.22	2.335(1)		HT 71	19.60	2.710(2)	695.74
P 28	-50.11	Null		P 7	52.54	2.565(1)		HT 9	19.90	2.091(2)	681.23
P 26	-35.79	3.677(0)		P 5	66.86	2.224(1)		HT 7	21.51	2.143(2)	678.17
P 25	-28.63	4.705(0)		P 3	81.19	Null		HT 6	22.30	1.906(2)	669.88
P 24	-21.47	3.239(0)		P 1	95.51	6.064(0)		HT 5	23.09	1.878(2)	683.79
P 23	-14.30	3.089(0)		HT 32	-16.31	Null	Null	HT 4	23.89	1.615(2)	664.35
P 22	-7.14	5.244(0)		HT 31	-13.25	3.184(1)	578.68	HT 3	24.69	1.438(2)	660.76
P 21	.02	1.377(1)		HT 29	-7.14	4.951(1)	604.93	HT 2	25.49	1.290(2)	658.52
P 20	4.79	2.209(1)		HT 28	-4.09	6.964(1)	629.25	HT 1	26.29	1.189(2)	658.66
P 15	7.18	2.338(1)		HT 25	5.08	Null	Null	HT 62	26.29	1.229(2)	671.46
P 19	9.57	Null		HT 24	8.14	2.386(2)	765.06	HT 61	29.35	1.205(2)	661.66
P 14	11.96	2.456(1)		HT 64	12.91	2.704(2)	745.92	HT 59	35.46	7.153(1)	621.90
P 18	14.34	2.368(1)		HT 65	13.87	Null	Null	HT 58	38.51	6.963(1)	628.51
P 13	16.73	2.353(1)		HT 66	14.82	3.053(2)	730.65	HT 57	41.57	6.398(1)	633.10
P 17	19.12	Null		HT 67	15.78	2.506(2)	794.79	HT 56	44.63	9.812(1)	658.72
P 12	21.51	Null		HT 68	16.73	2.944(2)	713.44	HT 55	47.68	1.312(2)	682.91
P 16	23.89	Null		HT 69	17.69	2.773(2)	702.81	HT 54	50.74	1.500(2)	691.49
P 11	26.28	2.075(1)		HT 70	18.64	2.707(2)	699.62	HT 53	53.79	1.462(2)	684.25
P 10	31.05	2.018(1)		HT 10	19.10	2.467(2)	693.91				

Run 94 Reduced Data Tabulation

Gauge Label	Angle (deg)	Value (PSIA) or (BTU/Ft2-Sec)	T Surf (DegR)	Gauge Label	Angle (deg)	Value (PSIA) or (BTU/Ft2-Sec)	T Surf (DegR)	Gauge Label	Angle (deg)	Value (PSIA) or (BTU/Ft2-Sec)	T Surf (DegR)
P 30	-42.93	4.507(0)		P 9	59.68	3.096(1)		HT 71	41.06	Null	Null
P 28	-28.65	Null		P 7	74.01	1.396(1)		HT 9	41.37	3.787(2)	831.40
P 26	-14.32	7.994(0)		P 5	88.33	6.997(0)		HT 7	42.97	4.242(2)	856.20
P 25	-7.16	9.404(0)		P 3	102.65	Null		HT 6	43.76	4.498(2)	861.80
P 24	.00	8.810(0)		P 1	116.98	8.867(-1)		HT 5	44.56	4.784(2)	882.82
P 23	7.16	8.819(0)		HT 32	5.16	Null	Null	HT 4	45.36	4.662(2)	869.99
P 22	14.32	8.705(0)		HT 31	8.21	8.304(1)	616.26	HT 3	46.16	4.889(2)	873.55
P 21	21.49	8.694(0)		HT 29	14.32	7.865(1)	615.11	HT 2	46.96	4.679(2)	870.07
P 20	26.26	9.410(0)		HT 28	17.38	7.973(1)	615.38	HT 1	47.76	4.843(2)	879.83
P 15	28.65	1.082(1)		HT 25	26.55	1.141(2)	650.97	HT 62	47.76	4.459(2)	870.38
P 19	31.04	1.662(1)		HT 24	29.60	1.625(2)	682.60	HT 61	50.81	3.612(2)	830.38
P 14	33.42	1.994(1)		HT 64	34.38	2.568(2)	757.08	HT 59	56.93	Null	Null
P 18	35.81	2.652(1)		HT 65	35.33	Null	Null	HT 58	59.98	1.969(2)	723.45
P 13	38.20	Null		HT 66	36.29	2.751(2)	771.26	HT 57	63.04	1.576(2)	698.16
P 17	40.58	5.348(1)		HT 67	37.24	3.241(2)	799.53	HT 56	66.09	1.353(2)	676.17
P 12	42.97	5.504(1)		HT 68	38.20	3.021(2)	801.37	HT 55	69.15	1.148(2)	659.10
P 16	45.36	6.392(1)		HT 69	39.15	3.360(2)	814.93	HT 54	72.20	8.971(1)	635.75
P 11	47.75	5.044(1)		HT 70	40.11	3.711(2)	832.89	HT 53	75.26	7.760(1)	621.56
P 10	52.52	4.413(1)		HT 10	40.57	4.069(2)	842.69				

Run 95 Reduced Data Tabulation

Appendix D
SWEPT-SHOCK/SHOCK-INTERACTION STUDY DATA

Test Conditions, Heat Transfer and
Pressure Measurements, Schlieren Photographs,
and Reduced Data Tabulations

Test Conditions

Mi	= 3.4510	
Po	= 7.0200X10+2	PSIA
Ho	= 1.9394X10+7	(Ft/sec)^2
To	= 2.9408X10+3	Degrees R
M	= 7.9432	
U	= 5.9980X10+3	Ft/sec
T	= 2.3710X10+2	Degrees R
P	= 6.4509X10-2	PSIA
Q	= 2.8522	PSIA
Rho	= 2.2832X10-5	Slugs/Ft^3
Mu	= 1.9506X10-7	Slugs/Ft-sec
Re	= 7.0210X10+5	1/Ft
Po'	= 5.2915	PSIA

Model Configuration Parameter	Value
Stagnation Position (gauge label)	P21
Vertical Distance (inches)	3.19
Horizontal Distance (inches)	1.81
Plate Angle (degrees)	12.50
Plate Length (inches)	26.50
Sweep Angle (degrees)	15.00

Run 66

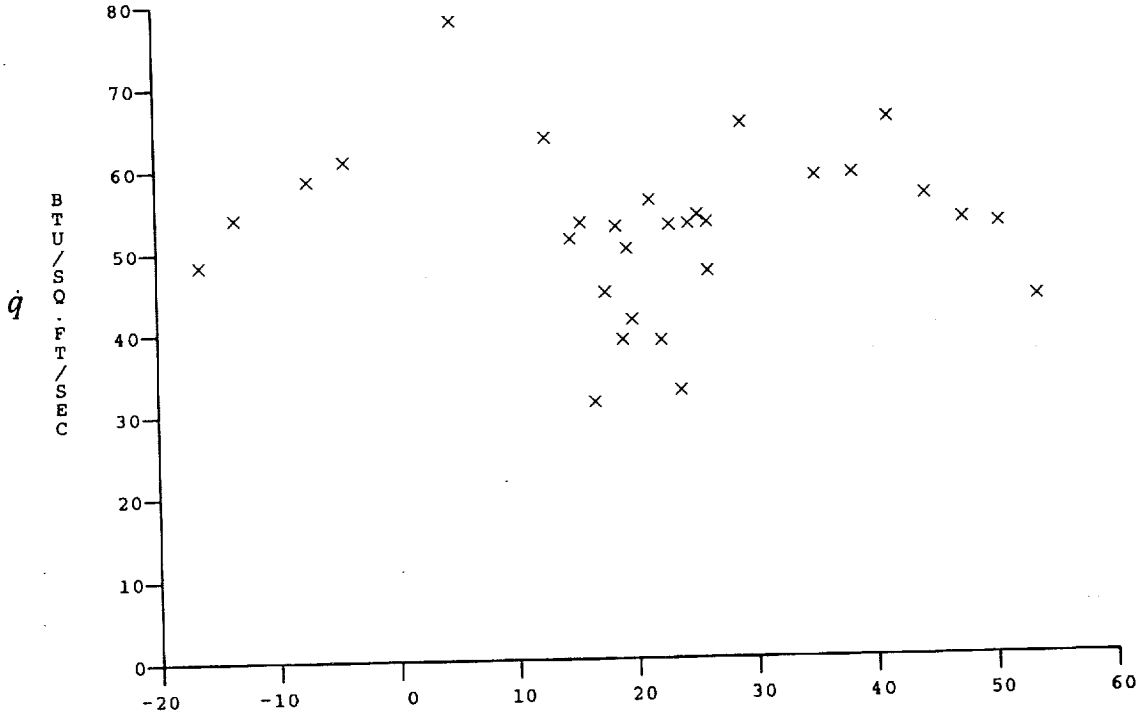

HEAT TRANSFER vs Gauge Position
Run 66

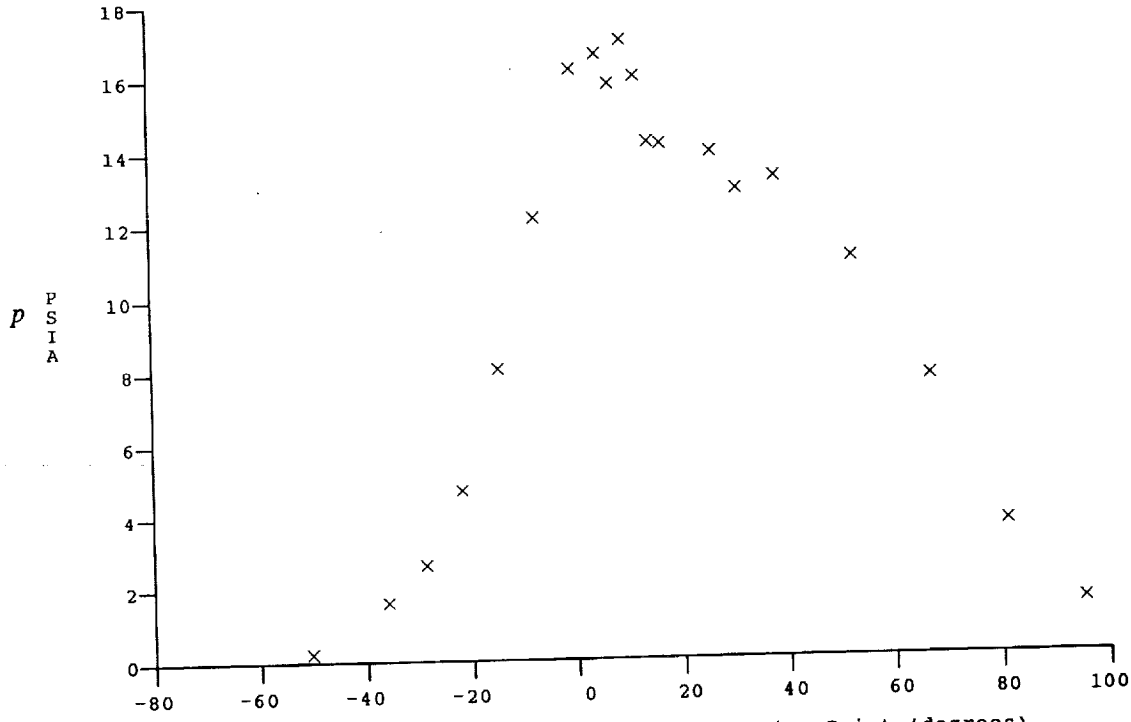

PRESSURE vs Gauge Position
Run 66

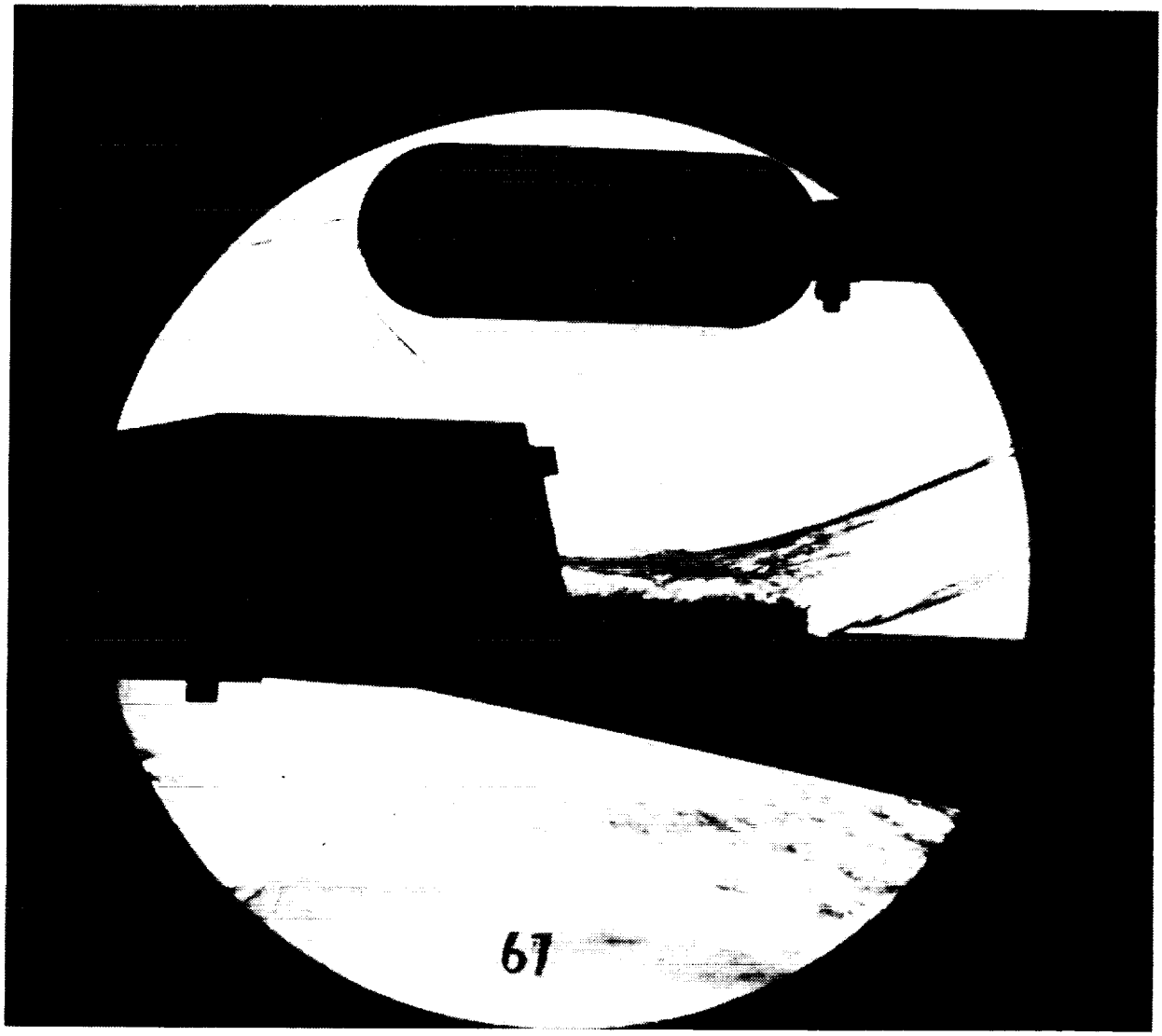

Test Conditions for Run 67 :

Po	= 1.440E+03 PSIA	Reservoir Total Pressure
Ho	= 1.889E-07 (Ft/sec)²	Reservoir Total Enthalpy
To	= 2.864E+03 °R	Reservoir Total Temperature
M	= 8.027E+00	Freestream Mach Number
U	= 5.924E+03 Ft/sec	Freestream Velocity
T	= 2.265E+02 °R	Freestream Temperature
P	= 1.264E-01 PSIA	Freestream Static Pressure
Rho	= 4.682E-05 Slugs/Ft3	Freestream Density
Mu	= 1.869E-07 Slugs/Ft-sec	Freestream Viscosity
Re	= 1.484E+06 1/Ft	Freestream Reynolds Number
Po'	= 1.058E+01 PSIA	Pitot Pressure
Q	= 5.706E+00 PSIA	Dynamic Pressure (½·Rho·U²/144)
Mi	= 3.451E+00	Shock Tube Incident Shock Mach Number
Hw	= 3.183E+06 (Ft/sec)²	Wall Enthalpy (Cp·Tw)
CPf	= 1.753E-01 1/PSIA	Pressure to CP factor (1/Q)
CHf	= 1.786E-04 Ft²-s/BTU	Heat Rate to CH factor (778/(Rho·U·(Ho-Hw))
QoFR	= 4.190E+01 BTU/Ft²-s	Fay-Riddell Heat Transfer to 3" Diam Sphere

Model Configuration Parameter	Value
Stagnation Position (gauge label)	P21
Vertical Distance (inches)	3.19
Horizontal Distance (inches)	1.81
Plate Angle (degrees)	12.50
Plate Length (inches)	26.50
Sweep Angle (degrees)	15.00

Run 67

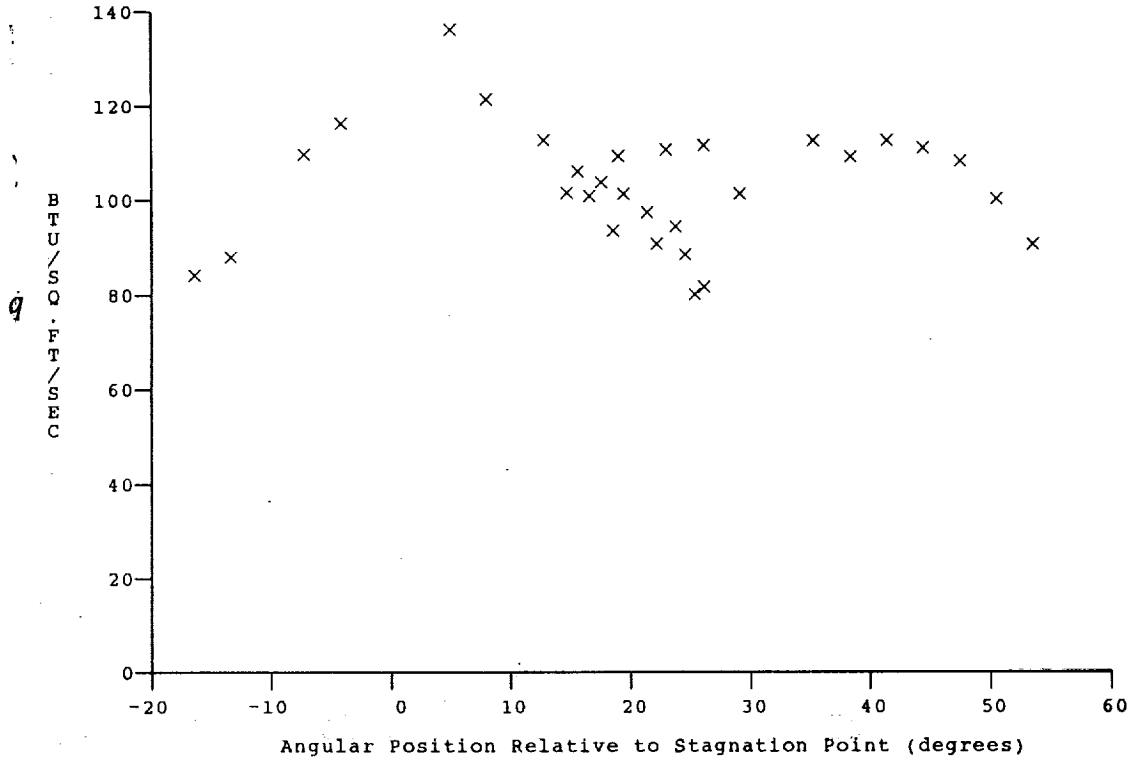

HEAT TRANSFER vs Gauge Position
Run 67

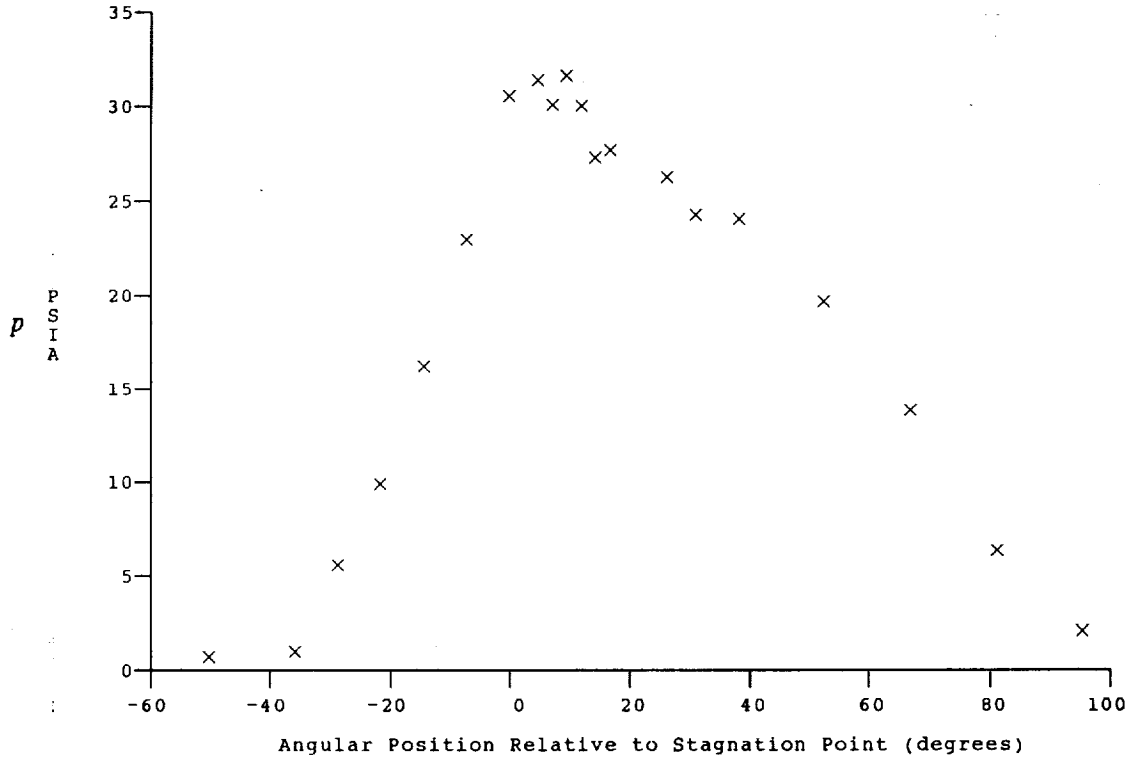

PRESSURE vs Gauge Position
Run 67

Test Conditions		
Mi	= 3.3752	
Po	= 1.3200X10+3	PSIA
Ho	= 1.8009X10+7	(Ft/sec)^2
To	= 2.7440X10+3	Degrees R
M	= 8.0494	
U	= 5.7854X10+3	Ft/sec
T	= 2.1481X10+2	Degrees R
P	= 1.1555X10-1	PSIA
Q	= 5.2464	PSIA
Rho	= 4.5142X10-5	Slugs/Ft^3
Mu	= 1.7783X10-7	Slugs/Ft-sec
Re	= 1.4686X10+6	1/Ft
Po'	= 9.7218	PSIA

Model Configuration Parameter	Value
Stagnation Position (gauge label)	P24
Vertical Distance (inches)	3.43
Horizontal Distance (inches)	1.43
Plate Angle (degrees)	12.50
Plate Length (inches)	26.50
Sweep Angle (degrees)	15.00

Run 68

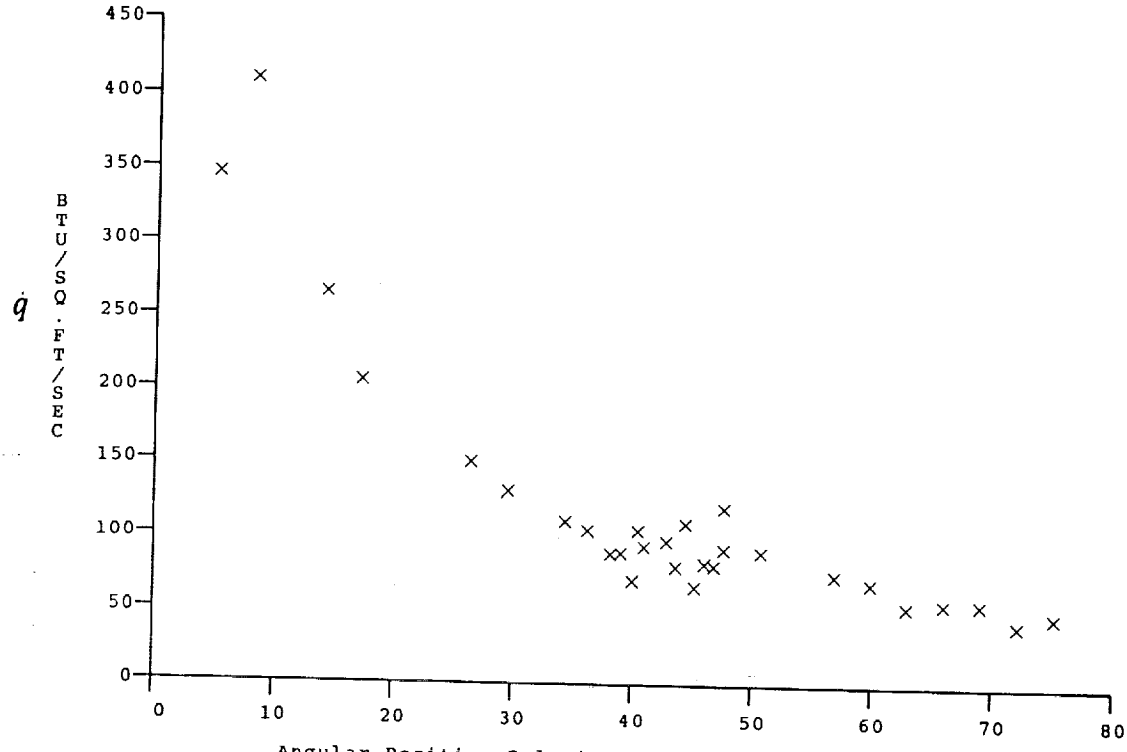

HEAT TRANSFER vs Gauge Position
Run 68

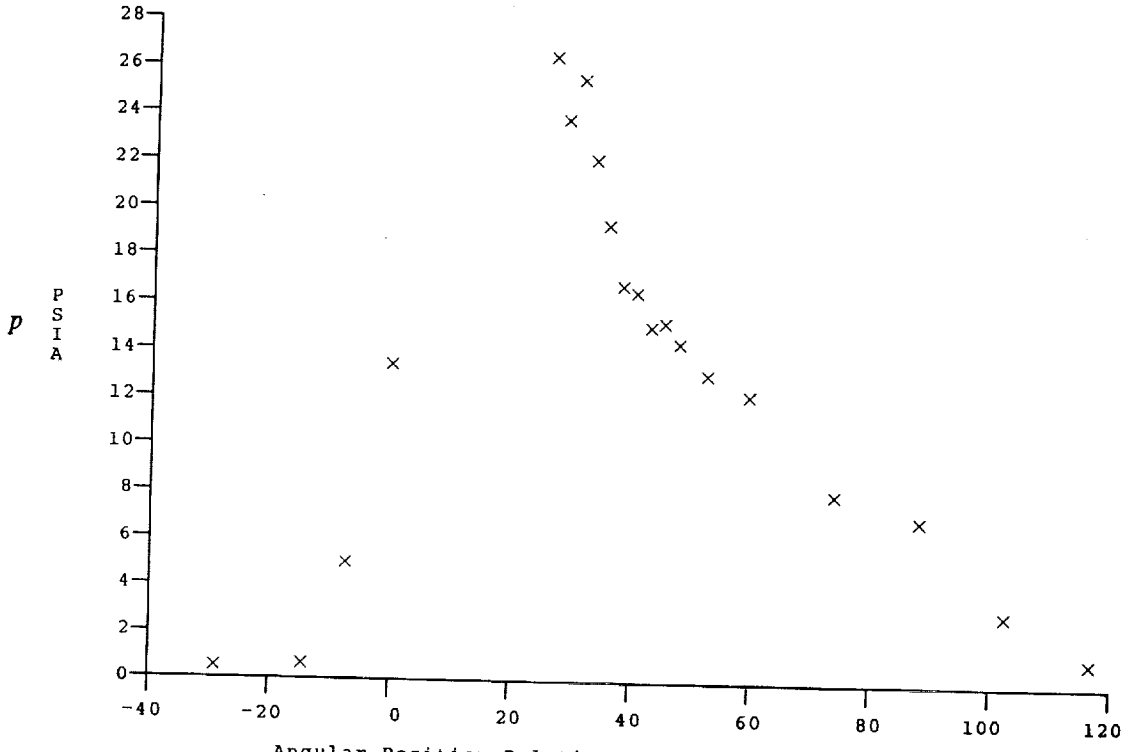

PRESSURE vs Gauge Position
Run 68

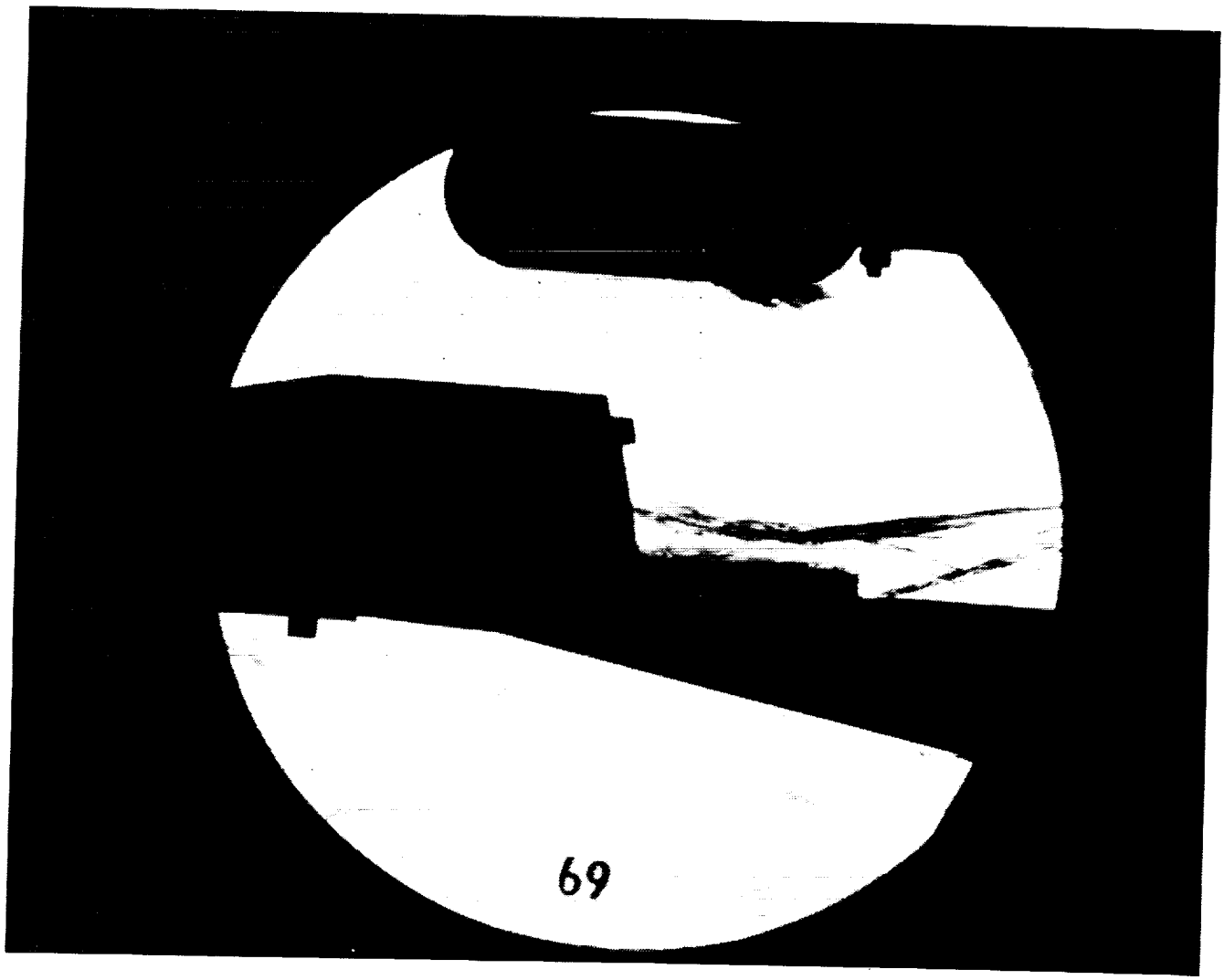

Test Conditions for Run 69 :

Po	= 1.432E-03	PSIA
Ho	= 1.866E-07	(Ft/sec)²
To	= 2.833E-03	°R
M	= 8.041E-00	
U	= 5.888E-03	Ft/sec
T	= 2.230E-02	°R
P	= 1.248E-01	PSIA
Rho	= 4.696E-05	Slugs/Ft3
Mu	= 1.842E-07	Slugs/Ft-sec
Re	= 1.501E+06	1/Ft
Po'	= 1.048E+01	PSIA
Q	= 5.653E+00	PSIA
Mi	= 3.417E+00	
Hw	= 3.183E+06	(Ft/sec)²
CPf	= 1.769E-01	1/PSIA
CHf	= 1.818E-04	Ft²-s/BTU
QoFR	= 4.105E+01	BTU/Ft²-s

Reservoir Total Pressure
Reservoir Total Enthalpy
Reservoir Total Temperature
Freestream Mach Number
Freestream Velocity
Freestream Temperature
Freestream Static Pressure
Freestream Density
Freestream Viscosity
Freestream Reynolds Number
Pitot Pressure
Dynamic Pressure (½·Rho·U²/144)
Shock Tube Incident Shock Mach Number
Wall Enthalpy (Cp·Tw)
Pressure to CP factor (1/Q)
Heat Rate to CH factor (778/(Rho·U·(Ho-Hw))
Fay-Riddell Heat Transfer to 3" Diam Sphere

Model Configuration Parameter	Value
Stagnation Position (gauge label)	P21
Vertical Distance (inches)	3.63
Horizontal Distance (inches)	1.43
Plate Angle (degrees)	12.50
Plate Length (inches)	26.50
Sweep Angle (degrees)	15.00

Run 69

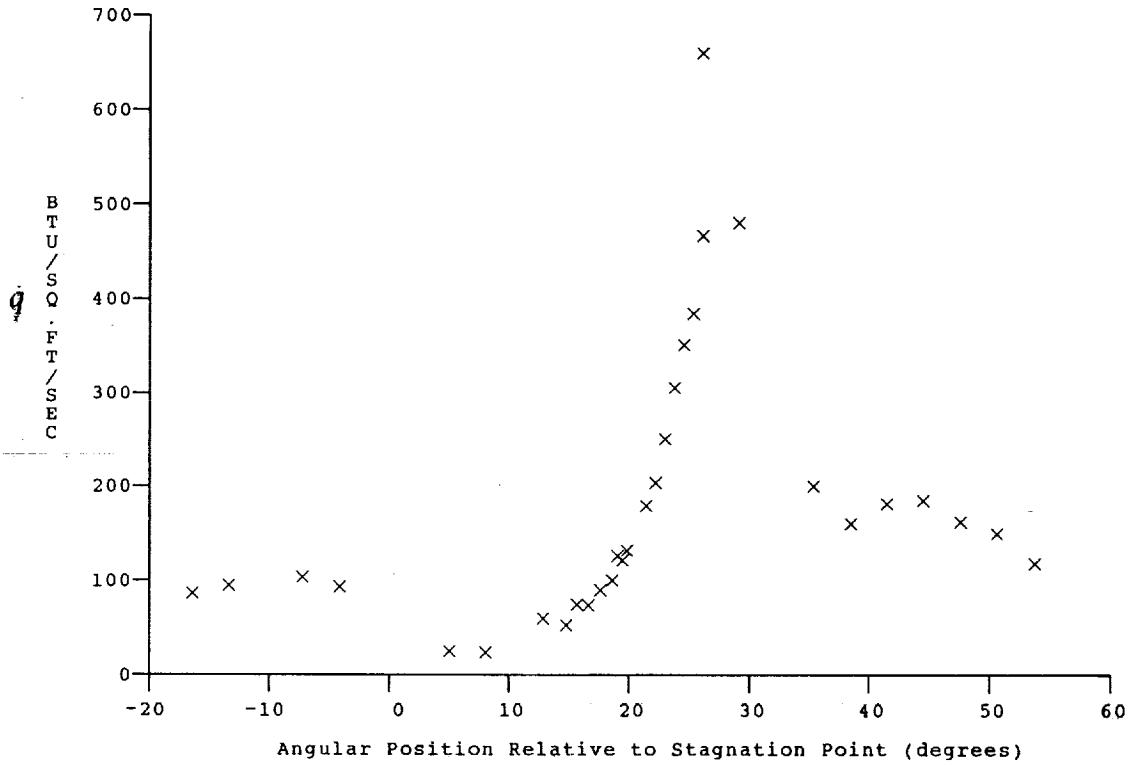

HEAT TRANSFER vs Gauge Position
Run 69

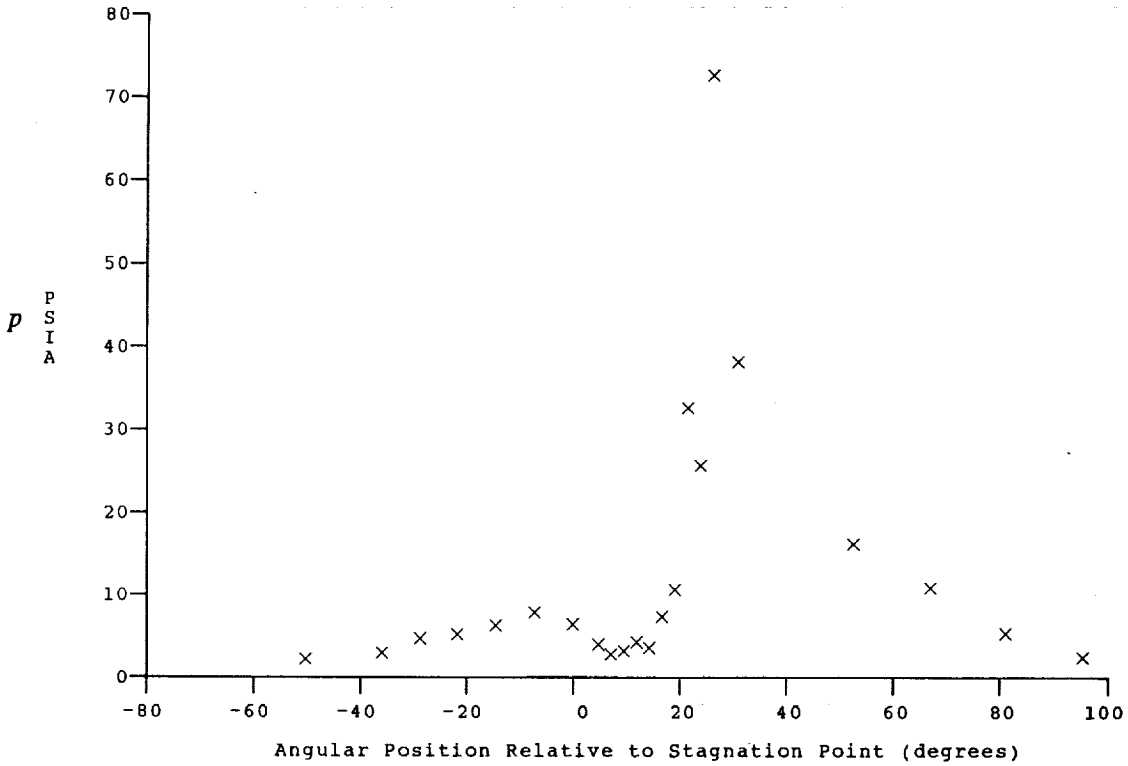

PRESSURE vs Gauge Position
Run 69

Test Conditions for Run 70 :

Po	= 1.403E+03	PSIA	Reservoir Total Pressure
Ho	= 1.865E+07	(Ft/sec)²	Reservoir Total Enthalpy
To	= 2.833E-03	°R	Reservoir Total Temperature
M	= 8.042E+00		Freestream Mach Number
U	= 5.887E+03	Ft/sec	Freestream Velocity
T	= 2.228E+02	°R	Freestream Temperature
P	= 1.221E-01	PSIA	Freestream Static Pressure
Rho	= 4.600E-05	Slugs/Ft3	Freestream Density
Mu	= 1.840E-07	Slugs/Ft-sec	Freestream Viscosity
Re	= 1.471E+06	1/Ft	Freestream Reynolds Number
Po'	= 1.026E+01	PSIA	Pitot Pressure
Q	= 5.536E+00	PSIA	Dynamic Pressure (½·Rho·U²/144)
Mi	= 3.408E+00		Shock Tube Incident Shock Mach Number
Hw	= 3.183E+06	(Ft/sec)²	Wall Enthalpy (Cp·Tw)
CPf	= 1.807E-01	1/PSIA	Pressure to CP factor (1/Q)
CHf	= 1.858E-04	Ft²-s/BTU	Heat Rate to CH factor (778/(Rho·U·(Ho-Hw))
QoFR	= 4.060E+01	BTU/Ft²-s	Fay-Riddell Heat Transfer to 3" Diam Sphere

Model Configuration Parameter	Value
Stagnation Position (gauge label)	P24
Vertical Distance (inches)	3.63
Horizontal Distance (inches)	-0.33
Plate Angle (degrees)	12.50
Plate Length (inches)	26.50
Sweep Angle (degrees)	15.00

Run 70

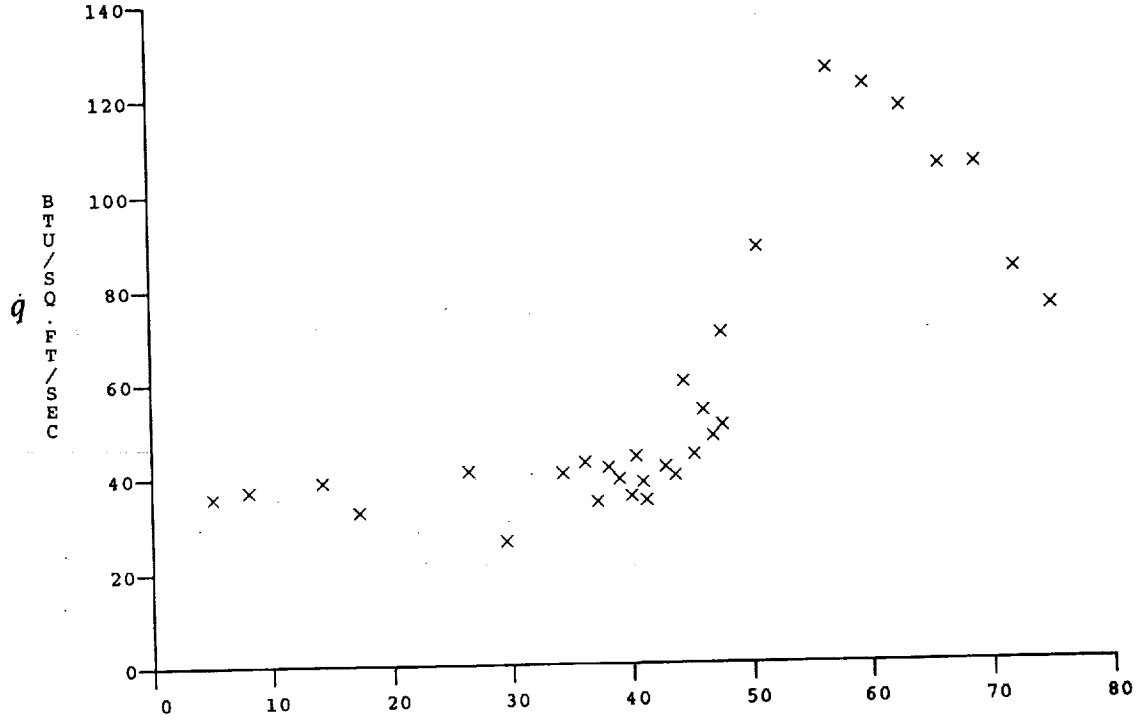

HEAT TRANSFER vs Gauge Position
Run 70

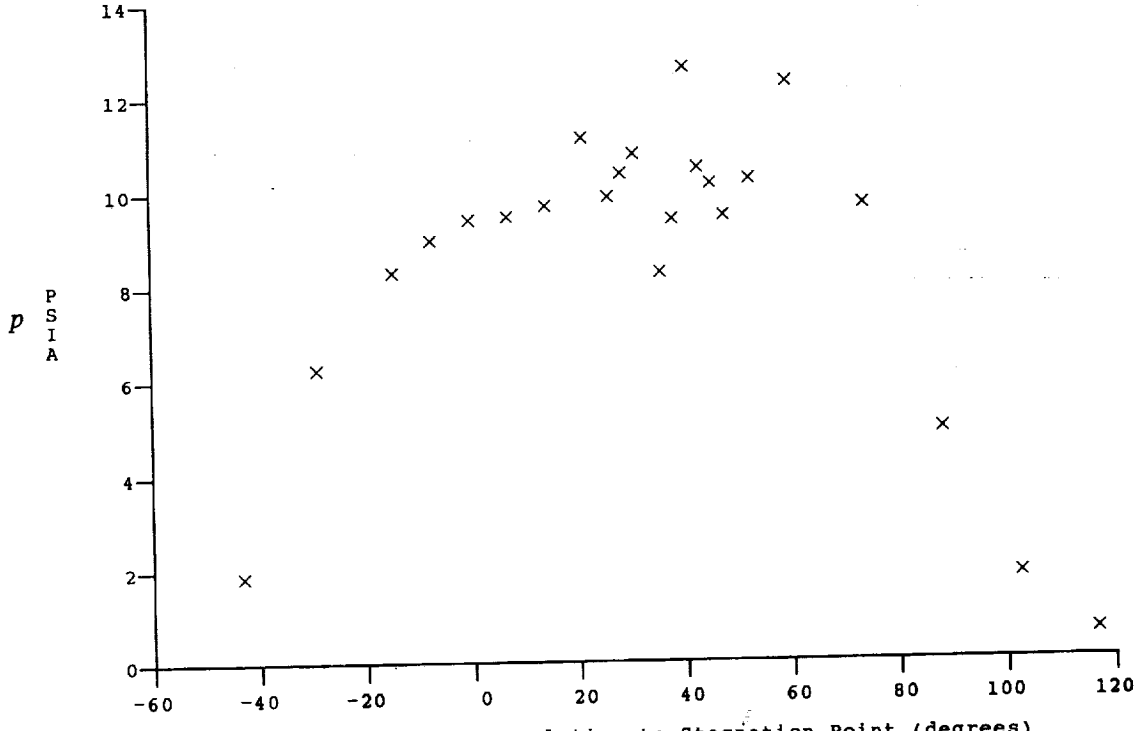

PRESSURE vs Gauge Position
Run 70

Test Conditions for Run 71 :

Po	= 1.288E+03 PSIA	Reservoir Total Pressure
Ho	= 1.841E+07 (Ft/sec)²	Reservoir Total Enthalpy
To	= 2.803E+03 °R	Reservoir Total Temperature
M	= 8.050E+00	Freestream Mach Number
U	= 5.850E+03 Ft/sec	Freestream Velocity
T	= 2.196E+02 °R	Freestream Temperature
P	= 1.118E-01 PSIA	Freestream Static Pressure
Rho	= 4.271E-05 Slugs/Ft3	Freestream Density
Mu	= 1.816E-07 Slugs/Ft-sec	Freestream Viscosity
Re	= 1.376E+06 1/Ft	Freestream Reynolds Number
Po'	= 9.409E+00 PSIA	Pitot Pressure
Q	= 5.076E+00 PSIA	Dynamic Pressure (½·Rho·U²/144)
Mi	= 3.367E+00	Shock Tube Incident Shock Mach Number
Hw	= 3.183E+06 (Ft/sec)²	Wall Enthalpy (Cp·Tw)
CPf	= 1.970E-01 1/PSIA	Pressure to CP factor (1/Q)
CHf	= 2.044E-04 Ft²-s/BTU	Heat Rate to CH factor (778/(Rho·U·(Ho-Hw))
QoFR	= 3.825E+01 BTU/Ft²-s	Fay-Riddell Heat Transfer to 3" Diam Sphere

Model Configuration Parameter	Value
Stagnation Position (gauge label)	P24
Vertical Distance (inches)	3.31
Horizontal Distance (inches)	-0.33
Plate Angle (degrees)	12.50
Plate Length (inches)	26.50
Sweep Angle (degrees)	15.00

Run 71

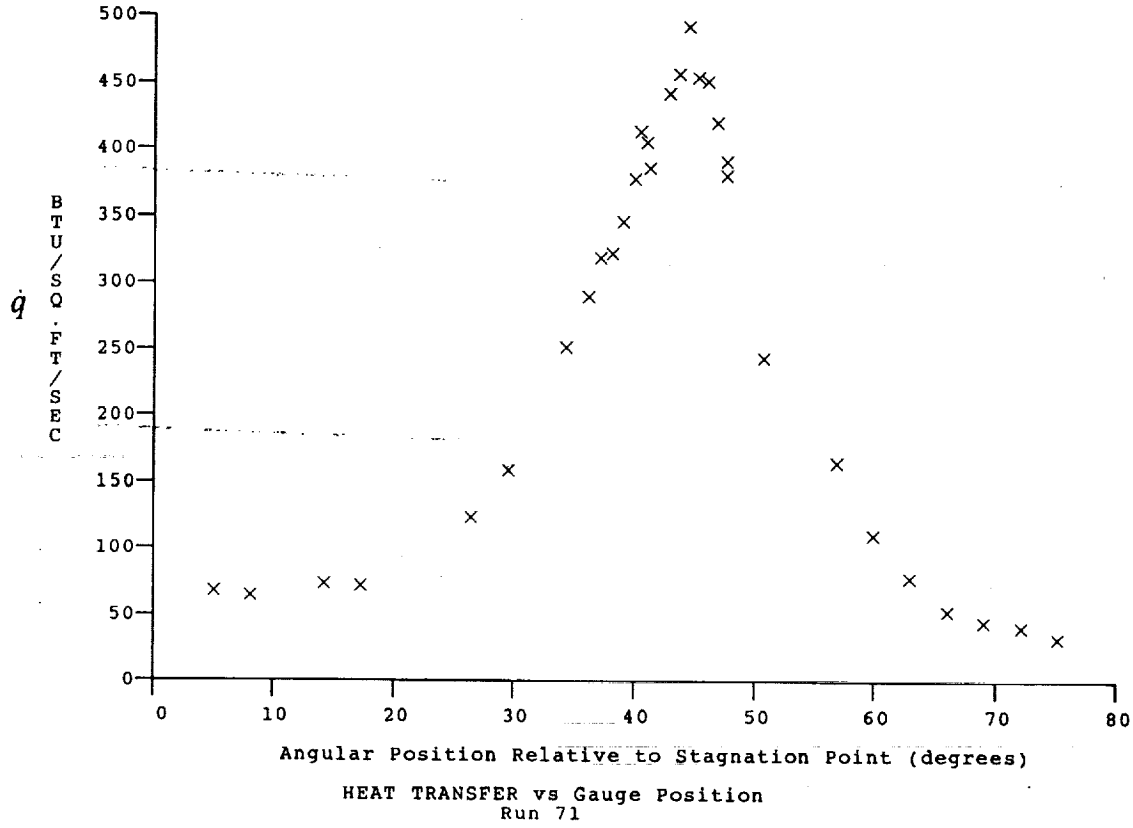

HEAT TRANSFER vs Gauge Position
Run 71

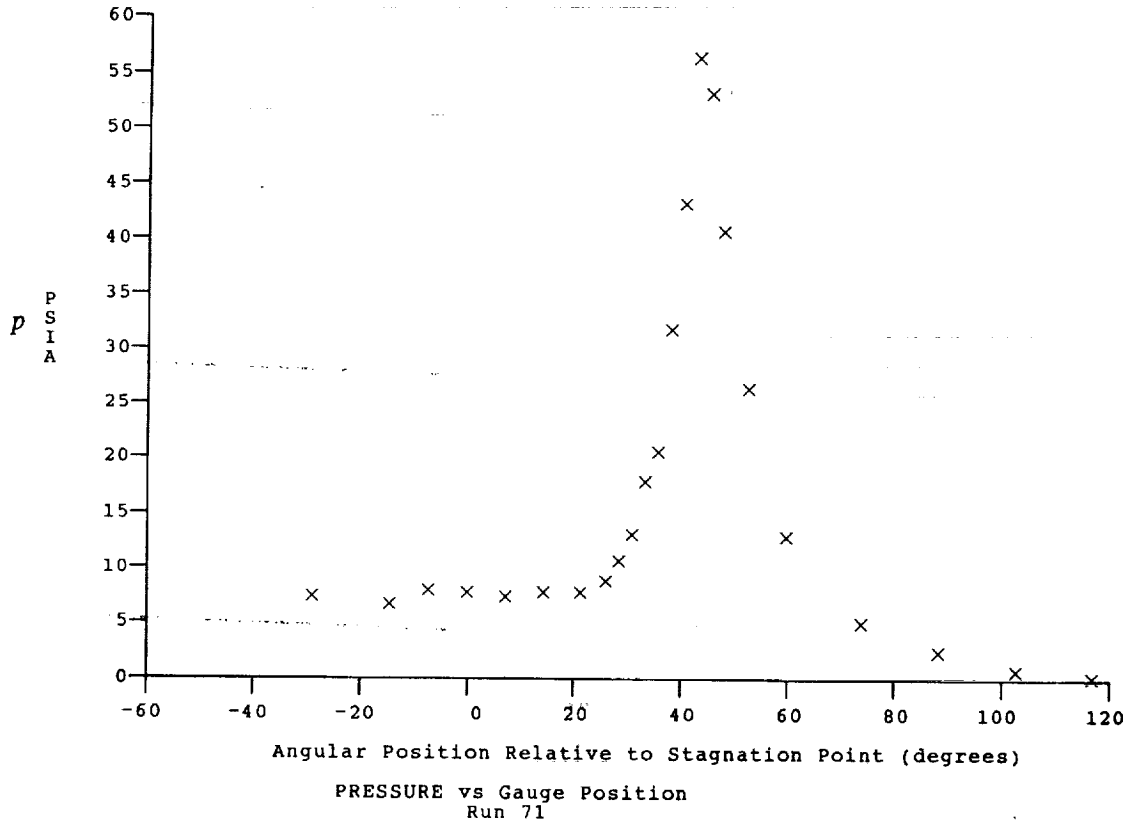

PRESSURE vs Gauge Position
Run 71

Test Conditions for Run 72 :

Po	= 1.875E-03 PSIA	Reservoir Total Pressure	
Ho	= 1.921E-07 (Ft/sec)²	Reservoir Total Enthalpy	
To	= 2.905E-03 °R	Reservoir Total Temperature	
M	= 8.064E+00	Freestream Mach Number	
U	= 5.975E+03 Ft/sec	Freestream Velocity	
T	= 2.283E+02 °R	Freestream Temperature	
P	= 1.607E-01 PSIA	Freestream Static Pressure	
Rho	= 5.906E-05 Slugs/Ft3	Freestream Density	
Mu	= 1.883E-07 Slugs/Ft-sec	Freestream Viscosity	
Re	= 1.874E+06 1/Ft	Freestream Reynolds Number	
Po'	= 1.358E-01 PSIA	Pitot Pressure	
Q	= 7.322E+00 PSIA	Dynamic Pressure (½·Rho·U²/144)	
Mi	= 3.467E+00	Shock Tube Incident Shock Mach Number	
Hw	= 3.183E+06 (Ft/sec)²	Wall Enthalpy (Cp·Tw)	
CPf	= 1.366E-01 1/PSIA	Pressure to CP factor (1/Q)	
CHf	= 1.376E-04 Ft²-s/BTU	Heat Rate to CH factor (778/(Rho·U·(Ho-Hw))	
QoFR	= 4.848E+01 BTU/Ft²-s	Fay-Riddell Heat Transfer to 3" Diam Sphere	

Model Configuration Parameter	Value
Stagnation Position (gauge label)	P24
Vertical Distance (inches)	3.31
Horizontal Distance (inches)	-0.33
Plate Angle (degrees)	12.50
Plate Length (inches)	26.50
Sweep Angle (degrees)	15.00

Run 72

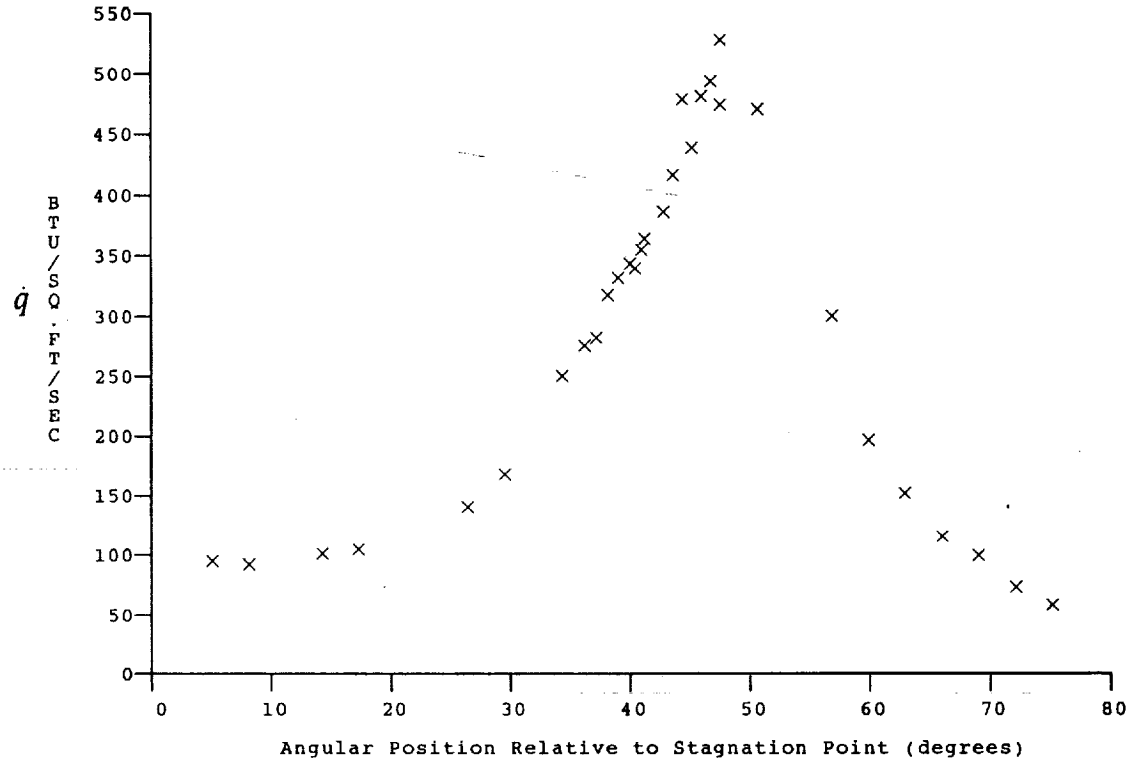

HEAT TRANSFER vs Gauge Position
Run 72

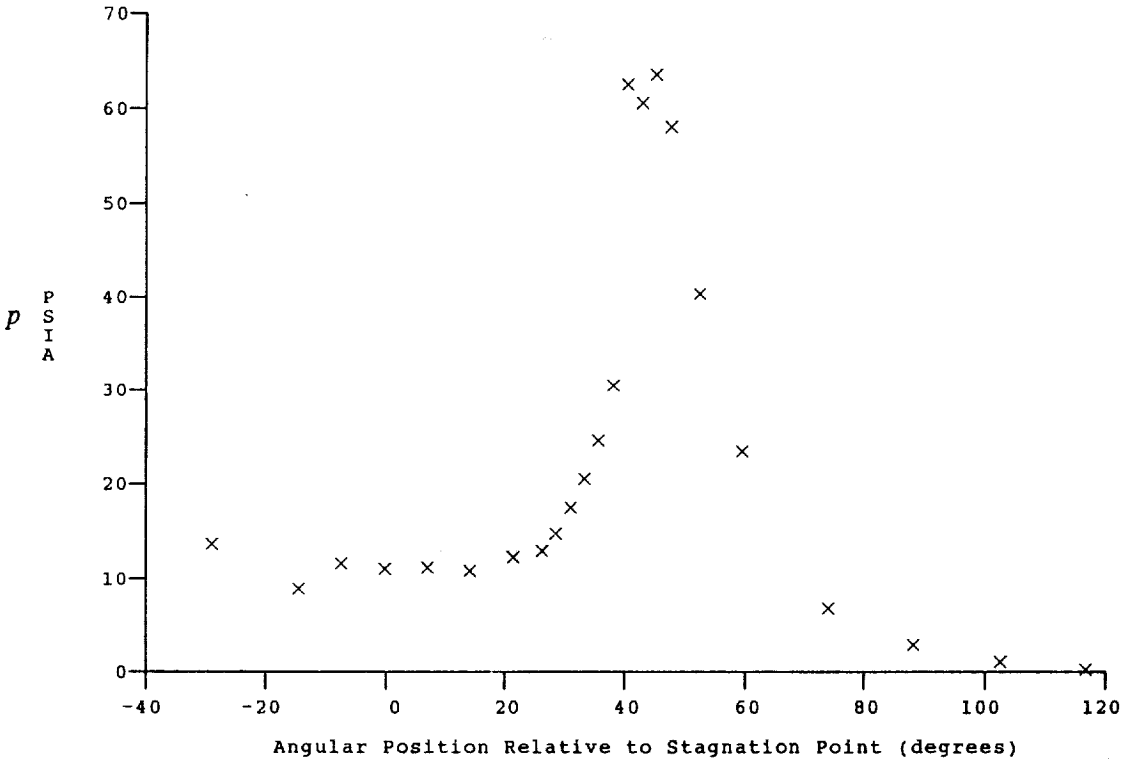

PRESSURE vs Gauge Position
Run 72

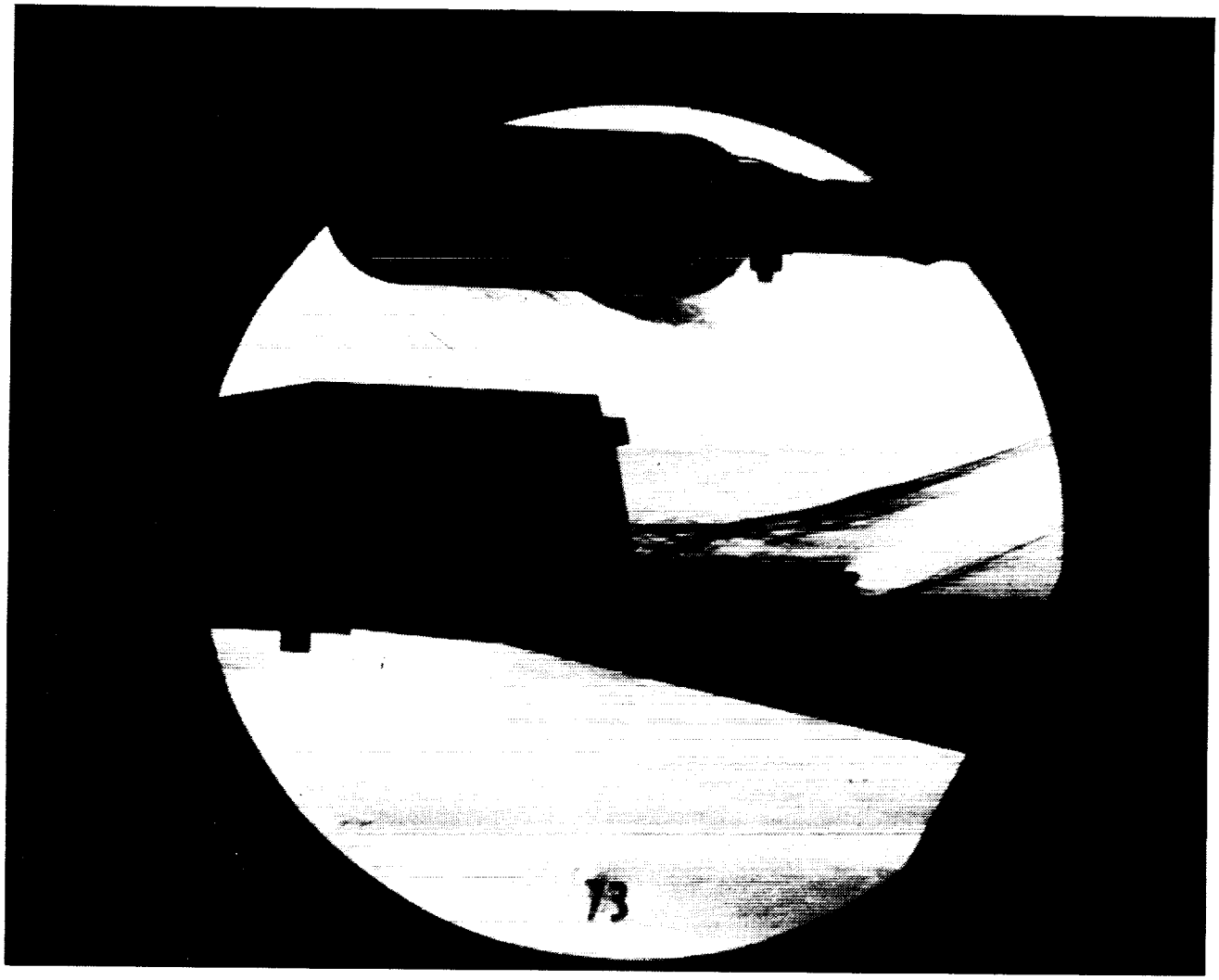

Test Conditions for Run 73 :

Po	= 6.564E+02	PSIA	Reservoir Total Pressure
Ho	= 1.844E-07	(Ft/sec)²	Reservoir Total Enthalpy
To	= 2.809E-03	°R	Reservoir Total Temperature
M	= 7.965E+00		Freestream Mach Number
U	= 5.850E-03	Ft/sec	Freestream Velocity
T	= 2.243E-02	°R	Freestream Temperature
P	= 6.024E-02	PSIA	Freestream Static Pressure
Rho	= 2.254E-05	Slugs/Ft3	Freestream Density
Mu	= 1.852E-07	Slugs/Ft-sec	Freestream Viscosity
Re	= 7.120E+05	1/Ft	Freestream Reynolds Number
Po'	= 4.965E+00	PSIA	Pitot Pressure
Q	= 2.678E+00	PSIA	Dynamic Pressure (½·Rho·U²/144)
Mi	= 3.388E+00		Shock Tube Incident Shock Mach Number
Hw	= 3.183E+06	(Ft/sec)²	Wall Enthalpy (Cp·Tw)
CPf	= 3.734E-01	1/PSIA	Pressure to CP factor (1/Q)
CHf	= 3.867E-04	Ft²-s/BTU	Heat Rate to CH factor (778/(Rho·U·(Ho-Hw))
QoFR	= 2.784E+01	BTU/Ft²-s	Fay-Riddell Heat Transfer to 3" Diam Sphere

Model Configuration Parameter	Value
Stagnation Position (gauge label)	P24
Vertical Distance (inches)	3.31
Horizontal Distance (inches)	-0.33
Plate Angle (degrees)	12.50
Plate Length (inches)	26.50
Sweep Angle (degrees)	15.00

Run 73

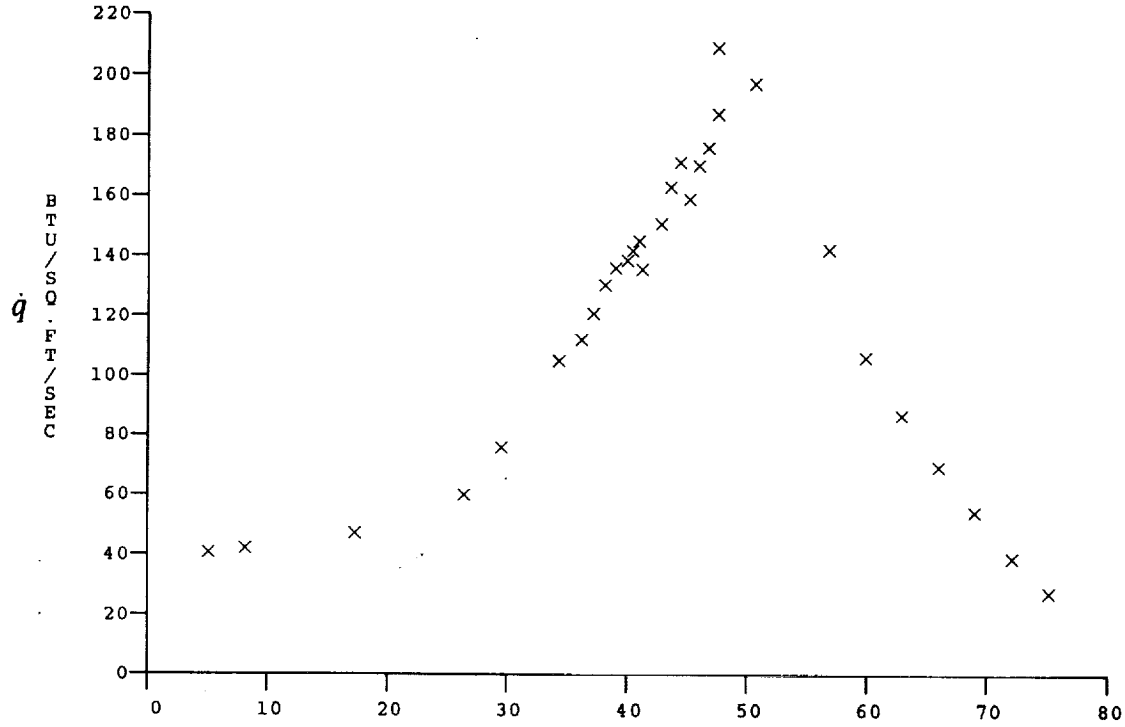

HEAT TRANSFER vs Gauge Position
Run 73

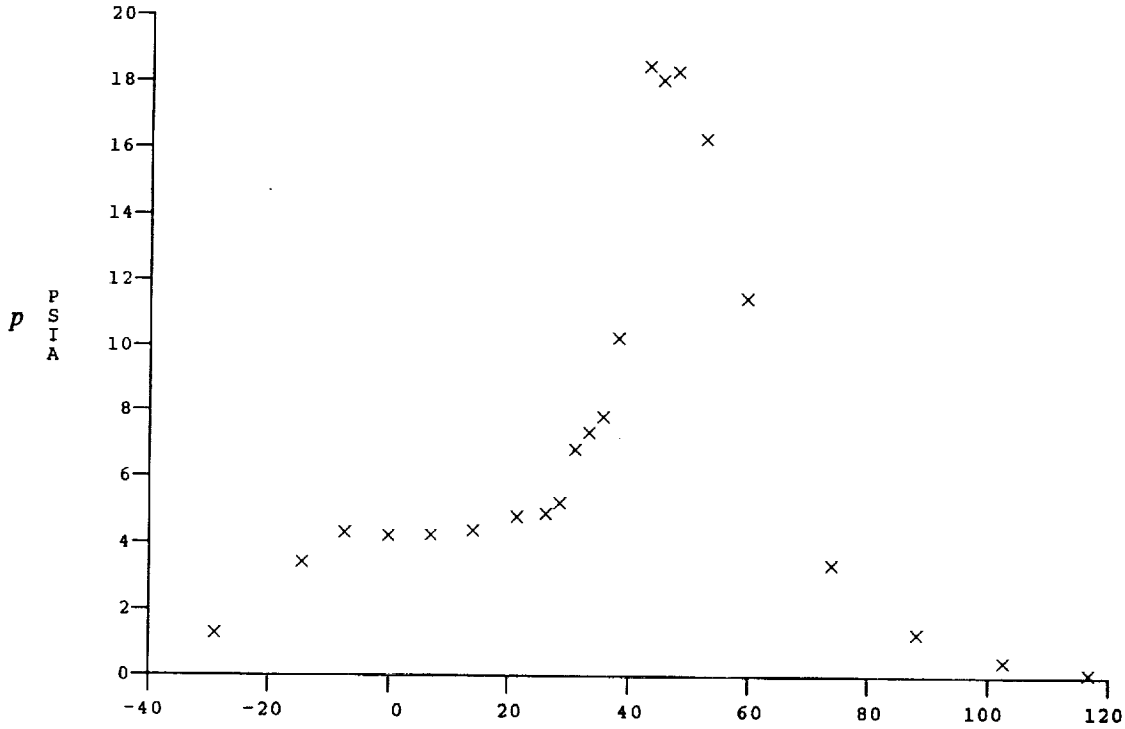

PRESSURE vs Gauge Position
Run 73

Test Conditions		
Mi	= 3.3875	
Po	= 1.3370X10+3	PSIA
Ho	= 1.8396X10+7	(Ft/sec)^2
To	= 2.7985X10+3	Degrees R
M	= 8.0455	
U	= 5.8471X10+3	Ft/sec
T	= 2.1963X10+2	Degrees R
P	= 1.1657X10-1	PSIA
Q	= 5.2875	PSIA
Rho	= 4.4542X10-5	Slugs/Ft^3
Mu	= 1.8159X10-7	Slugs/Ft-sec
Re	= 1.4342X10+6	1/Ft
Po'	= 9.8013	PSIA

Model Configuration Parameter	Value
Stagnation Position (gauge label)	P24
Sweep Angle (degrees)	15.00

Run 74

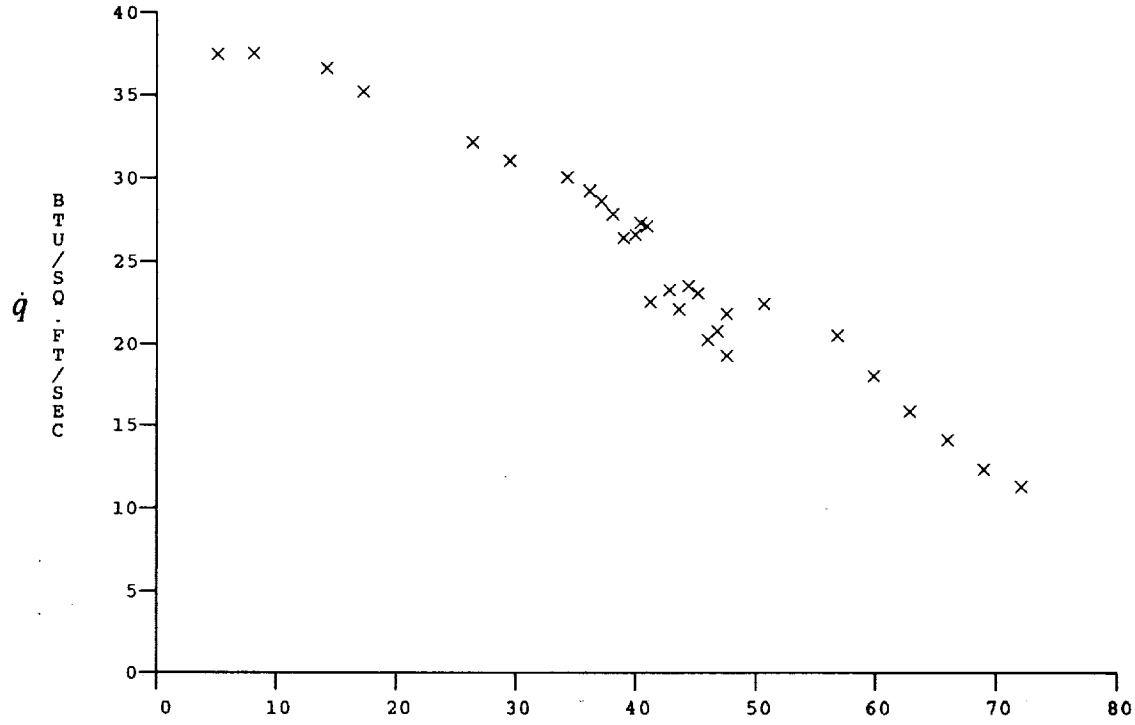

HEAT TRANSFER vs Gauge Position
Run 74

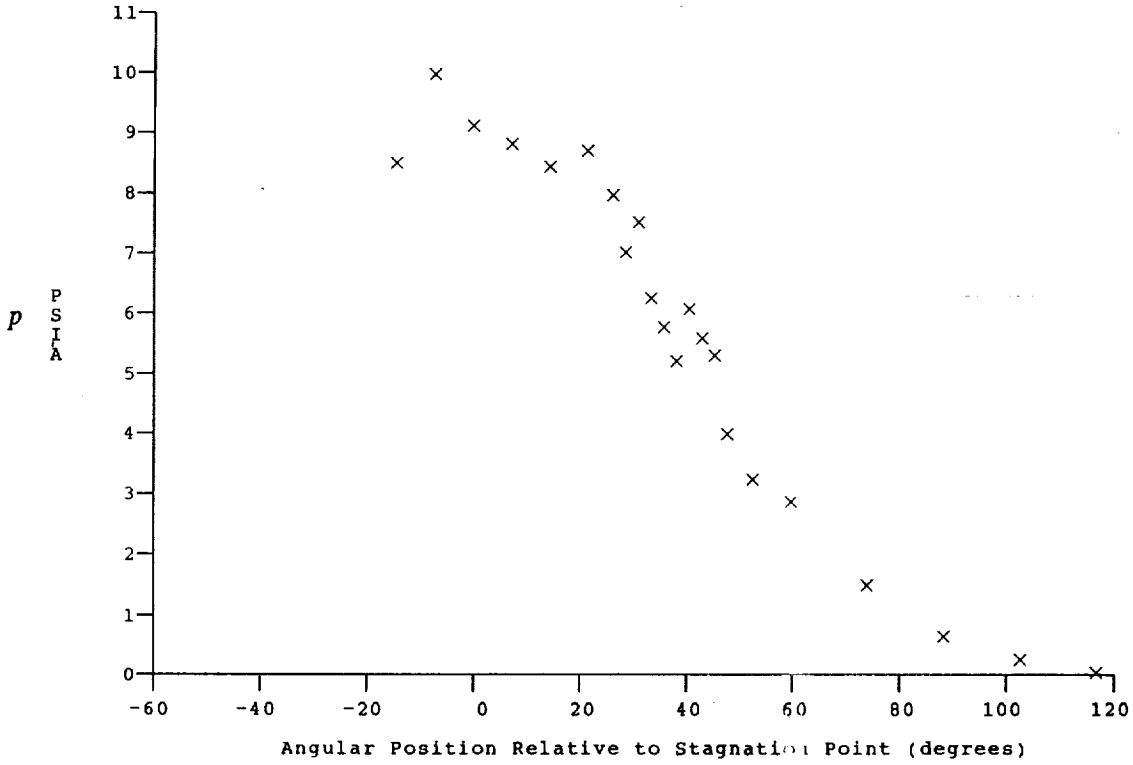

PRESSURE vs Gauge Position
Run 74

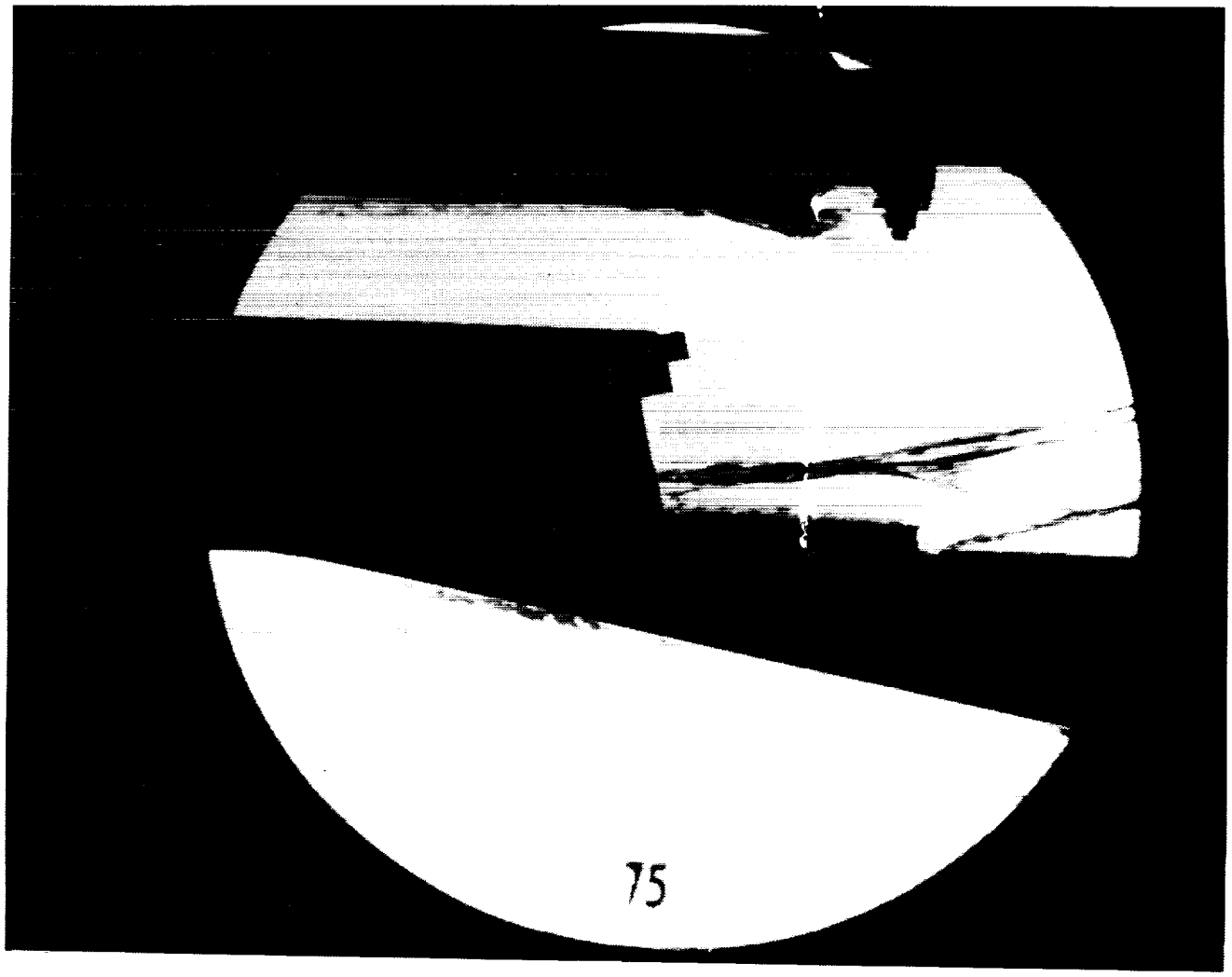

Test Conditions for Run 75 :

Po	= 1.416E+03 PSIA	Reservoir Total Pressure	
Ho	= 1.869E+07 (Ft/sec)²	Reservoir Total Enthalpy	
To	= 2.839E-03 °R	Reservoir Total Temperature	
M	= 8.041E-00	Freestream Mach Number	
U	= 5.894E-03 Ft/sec	Freestream Velocity	
T	= 2.234E+02 °R	Freestream Temperature	
P	= 1.233E-01 PSIA	Freestream Static Pressure	
Rho	= 4.633E-05 Slugs/Ft3	Freestream Density	
Mu	= 1.845E-07 Slugs/Ft-sec	Freestream Viscosity	
Re	= 1.480E+06 1/Ft	Freestream Reynolds Number	
Po'	= 1.036E+01 PSIA	Pitot Pressure	
Q	= 5.588E+00 PSIA	Dynamic Pressure (½·Rho·U²/144)	
Mi	= 3.414E-00	Shock Tube Incident Shock Mach Number	
Hw	= 3.183E+06 (Ft/sec)²	Wall Enthalpy (Cp·Tw)	
CPf	= 1.790E-01 1/PSIA	Pressure to CP factor (1/Q)	
CHf	= 1.837E-04 Ft²-s/BTU	Heat Rate to CH factor (778/(Rho·U·(Ho-Hw))	
QoFR	= 4.091E+01 BTU/Ft²-s	Fay-Riddell Heat Transfer to 3" Diam Sphere	

Model Configuration Parameter	Value
Stagnation Position (gauge label)	P21
Vertical Distance (inches)	3.44
Horizontal Distance (inches)	1.34
Plate Angle (degrees)	12.50
Plate Length (inches)	26.00
Sweep Angle (degrees)	30.00

Run 75

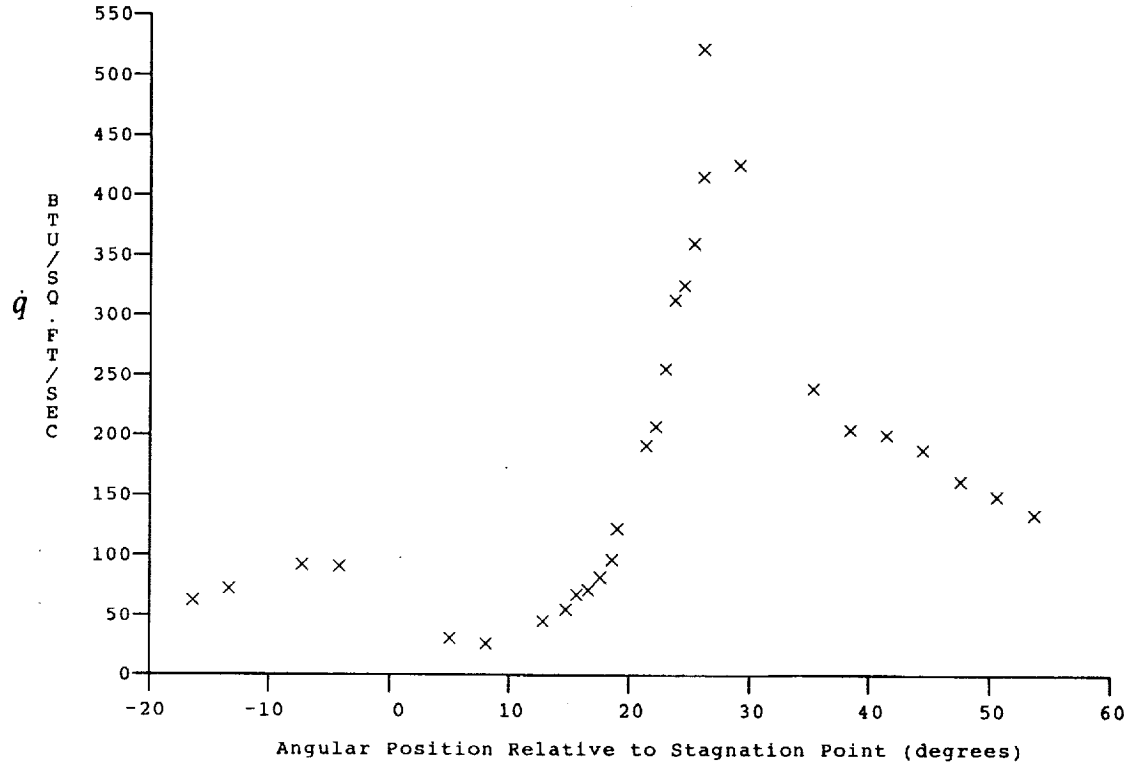

HEAT TRANSFER vs Gauge Position
Run 75

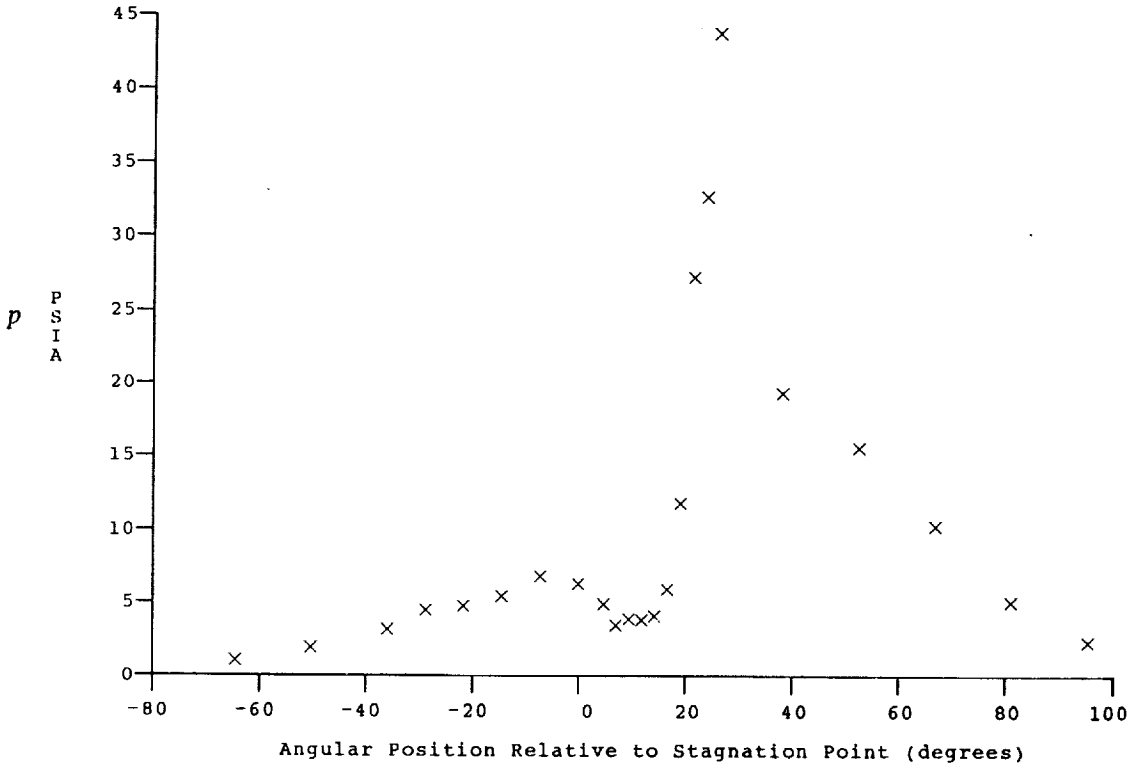

PRESSURE vs Gauge Position
Run 75

Test Conditions for Run 76 :

Po	= 1.382E+03	PSIA	Reservoir Total Pressure
Ho	= 1.865E+07	(Ft/sec)²	Reservoir Total Enthalpy
To	= 2.831E+03	°R	Reservoir Total Temperature
M	= 8.033E+00		Freestream Mach Number
U	= 5.886E+03	Ft/sec	Freestream Velocity
T	= 2.232E+02	°R	Freestream Temperature
P	= 1.212E-01	PSIA	Freestream Static Pressure
Rho	= 4.554E-05	Slugs/Ft3	Freestream Density
Mu	= 1.844E-07	Slugs/Ft-sec	Freestream Viscosity
Re	= 1.454E+06	1/Ft	Freestream Reynolds Number
Po'	= 1.016E+01	PSIA	Pitot Pressure
Q	= 5.479E+00	PSIA	Dynamic Pressure (½·Rho·U²/144)
Mi	= 3.423E+00		Shock Tube Incident Shock Mach Number
Hw	= 3.183E+06	(Ft/sec)²	Wall Enthalpy (Cp·Tw)
CPf	= 1.825E-01	1/PSIA	Pressure to CP factor (1/Q)
CHf	= 1.877E-04	Ft²-s/BTU	Heat Rate to CH factor (778/(Rho·U·(Ho-Hw))
QoFR	= 4.038E+01	BTU/Ft²-s	Fay-Riddell Heat Transfer to 3" Diam Sphere

Model Configuration Parameter	Value
Stagnation Position (gauge label)	P21
Vertical Distance (inches)	3.09
Horizontal Distance (inches)	1.34
Plate Angle (degrees)	12.50
Plate Length (inches)	26.00
Sweep Angle (degrees)	30.00

Run 76

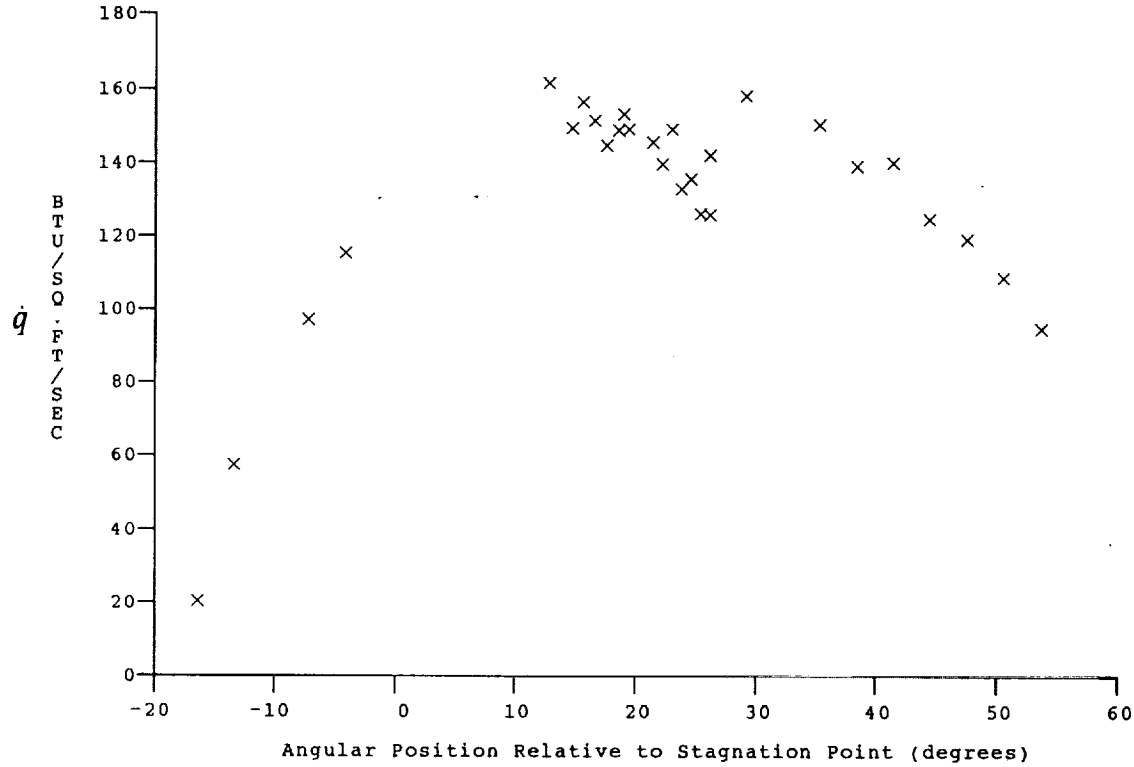

HEAT TRANSFER vs Gauge Position
Run 76

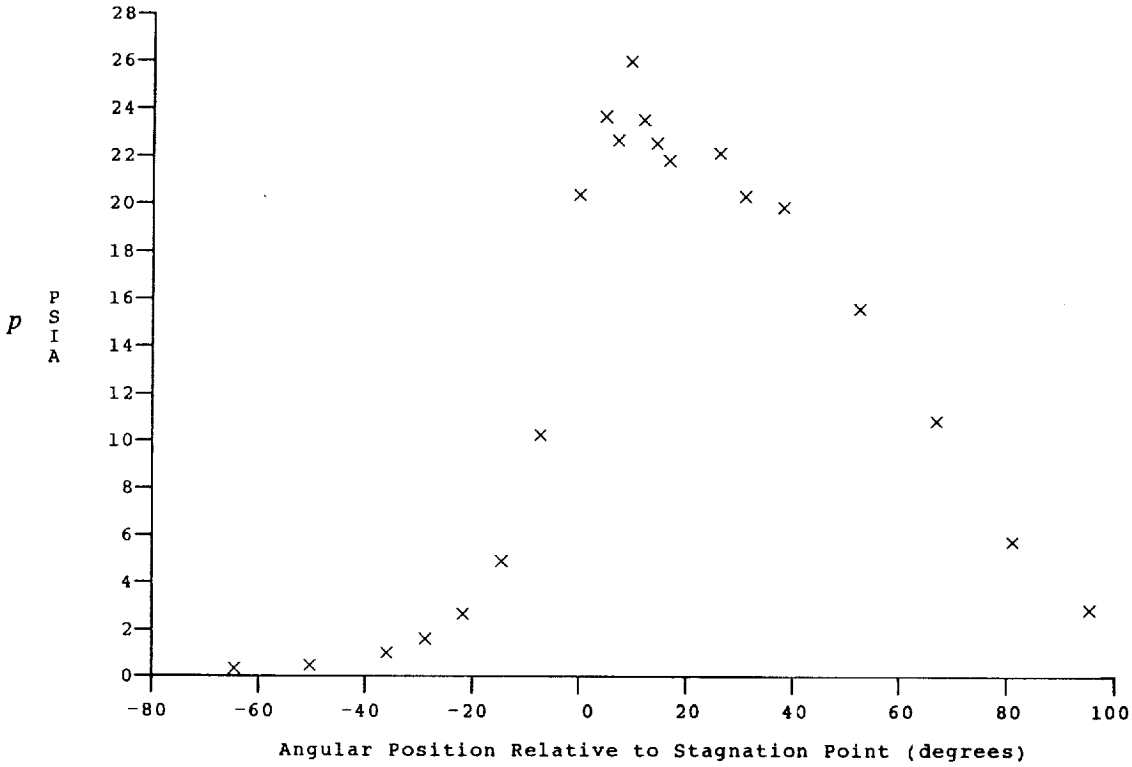

PRESSURE vs Gauge Position
Run 76

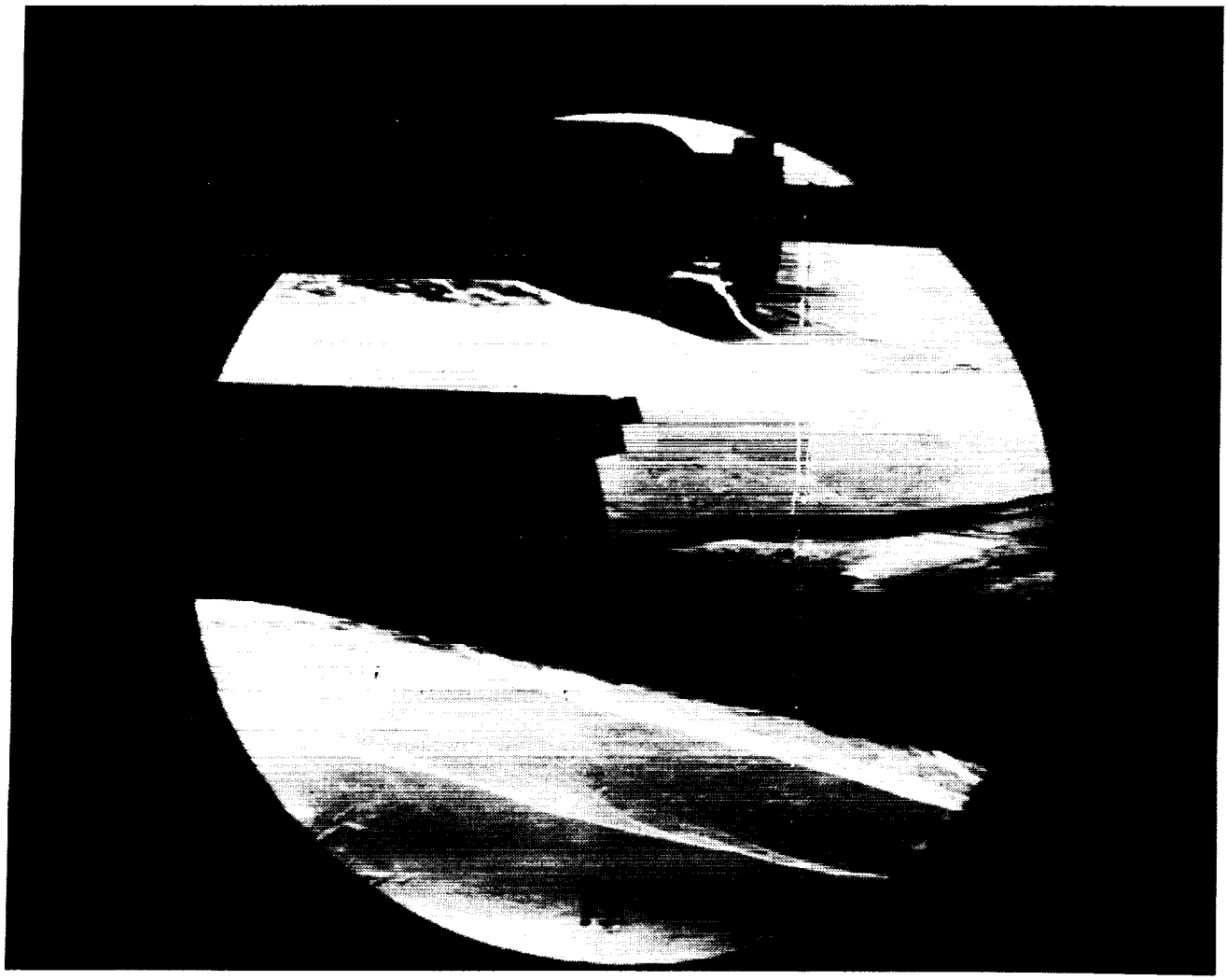

Test Conditions for Run 77 :

Po	= 1.410E-03 PSIA	Reservoir Total Pressure
Ho	= 1.832E+07 (Ft/sec)²	Reservoir Total Enthalpy
To	= 2.785E-03 °R	Reservoir Total Temperature
M	= 8.040E+00	Freestream Mach Number
U	= 5.834E+03 Ft/sec	Freestream Velocity
T	= 2.189E+02 °R	Freestream Temperature
P	= 1.237E-01 PSIA	Freestream Static Pressure
Rho	= 4.742E-05 Slugs/Ft3	Freestream Density
Mu	= 1.810E-07 Slugs/Ft-sec	Freestream Viscosity
Re	= 1.528E+06 1/Ft	Freestream Reynolds Number
Po'	= 1.039E+01 PSIA	Pitot Pressure
Q	= 5.604E+00 PSIA	Dynamic Pressure (½·Rho·U²/144)
Mi	= 3.414E+00	Shock Tube Incident Shock Mach Number
Hw	= 3.183E+06 (Ft/sec)²	Wall Enthalpy (Cp·Tw)
CPf	= 1.785E-01 1/PSIA	Pressure to CP factor (1/Q)
CHf	= 1.858E-04 Ft²-s/BTU	Heat Rate to CH factor (778/(Rho·U·(Ho-Hw))
QoFR	= 3.991E+01 BTU/Ft²-s	Fay-Riddell Heat Transfer to 3" Diam Sphere

Model Configuration Parameter	Value
Stagnation Position (gauge label)	P21
Vertical Distance (inches)	3.44
Horizontal Distance (inches)	-0.25
Plate Angle (degrees)	12.50
Plate Length (inches)	26.00
Sweep Angle (degrees)	30.00

Run 77

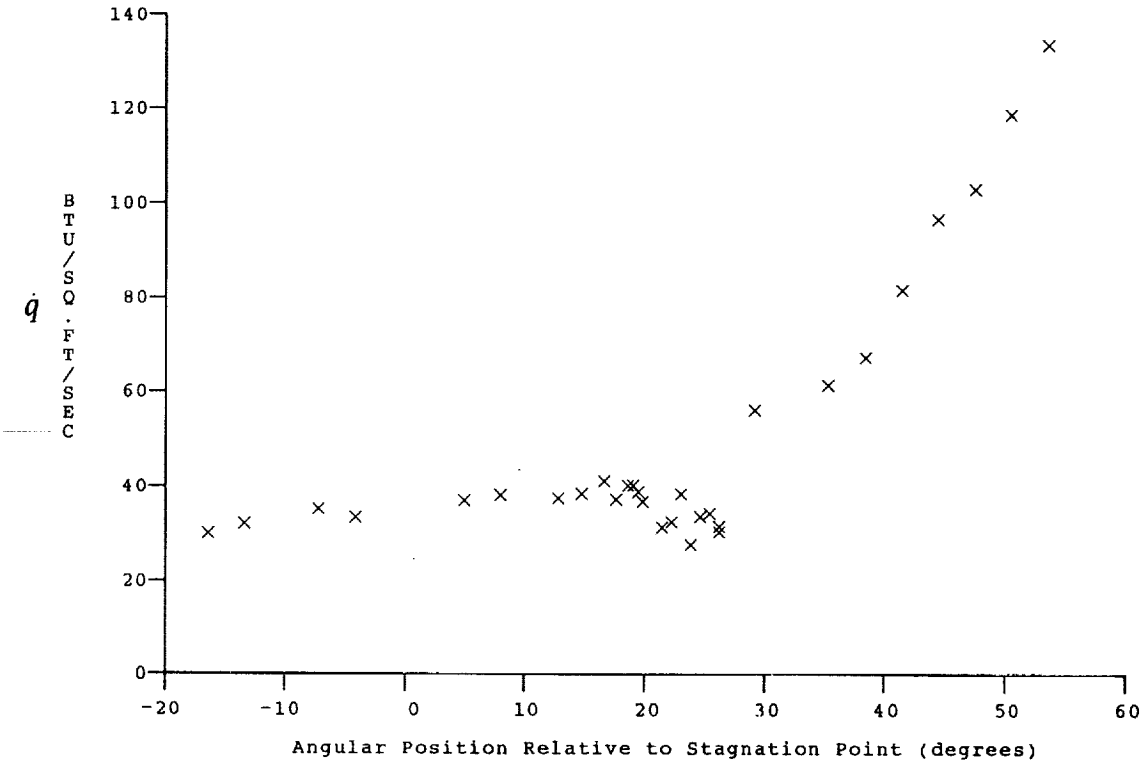

HEAT TRANSFER vs Gauge Position
Run 77

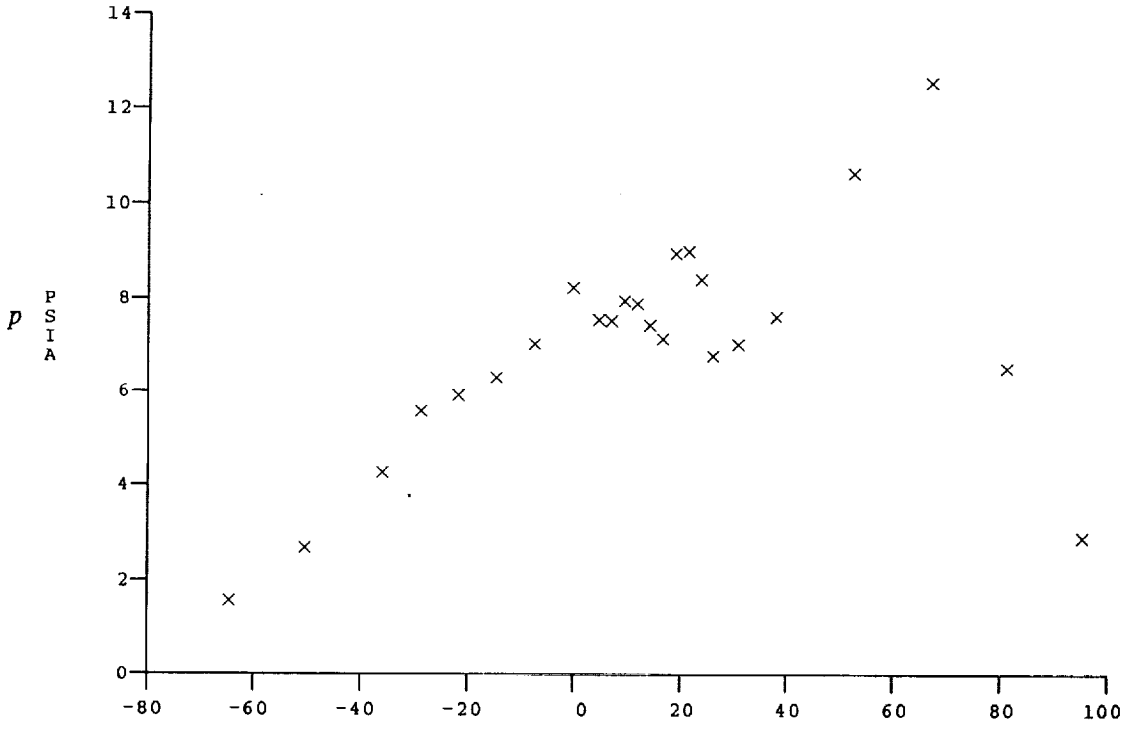

PRESSURE vs Gauge Position
Run 77

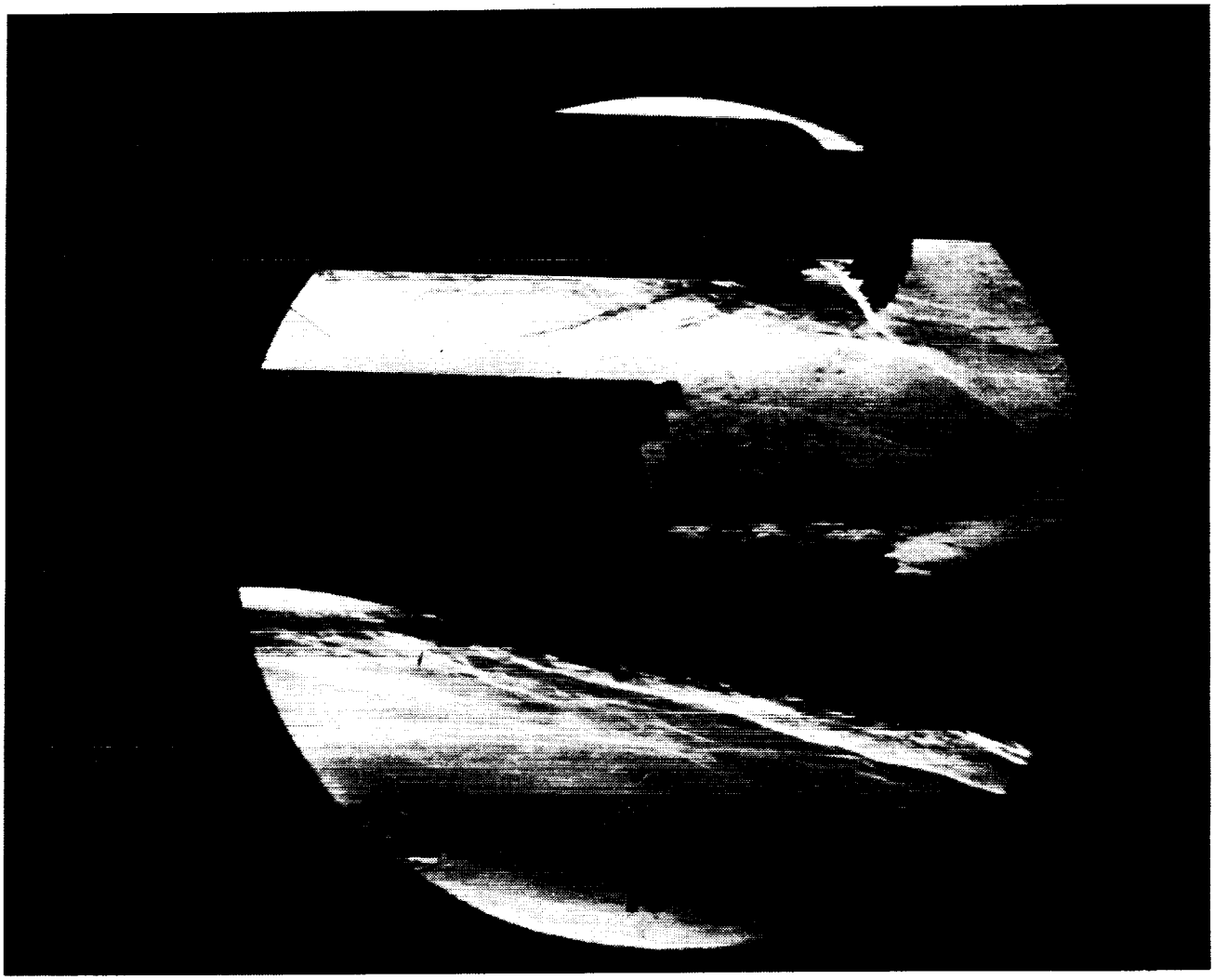

Test Conditions for Run 78 :

Po	= 1.397E+03 PSIA	Reservoir Total Pressure	
Ho	= 1.854E+07 (Ft/sec)²	Reservoir Total Enthalpy	
To	= 2.816E+03 °R	Reservoir Total Temperature	
M	= 8.033E+00	Freestream Mach Number	
U	= 5.870E+03 Ft/sec	Freestream Velocity	
T	= 2.220E+02 °R	Freestream Temperature	
P	= 1.227E-01 PSIA	Freestream Static Pressure	
Rho	= 4.639E-05 Slugs/Ft3	Freestream Density	
Mu	= 1.835E-07 Slugs/Ft-sec	Freestream Viscosity	
Re	= 1.484E+06 1/Ft	Freestream Reynolds Number	
Po'	= 1.029E+01 PSIA	Pitot Pressure	
Q	= 5.550E+00 PSIA	Dynamic Pressure (½·Rho·U²/144)	
Mi	= 3.428E+00	Shock Tube Incident Shock Mach Number	
Hw	= 3.183E+06 (Ft/sec)²	Wall Enthalpy (Cp·Tw)	
CPf	= 1.802E-01 1/PSIA	Pressure to CP factor (1/Q)	
CHf	= 1.860E-04 Ft²-s/BTU	Heat Rate to CH factor (778/(Rho·U·(Ho-Hw))	
QoFR	= 4.036E-01 BTU/Ft²-s	Fay-Riddell Heat Transfer to 3" Diam Sphere	

Model Configuration Parameter	Value
Stagnation Position (gauge label)	P21
Vertical Distance (inches)	3.24
Horizontal Distance (inches)	1.34
Plate Angle (degrees)	12.50
Plate Length (inches)	26.00
Sweep Angle (degrees)	30.00

Run 78

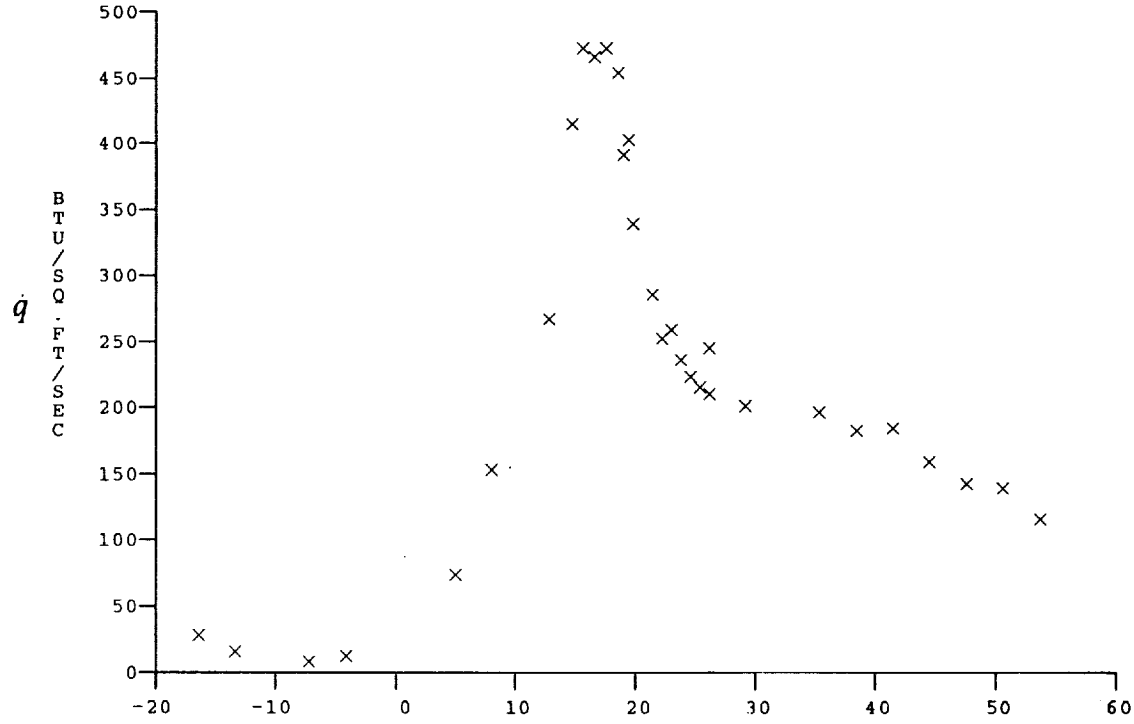

HEAT TRANSFER vs Gauge Position
Run 78

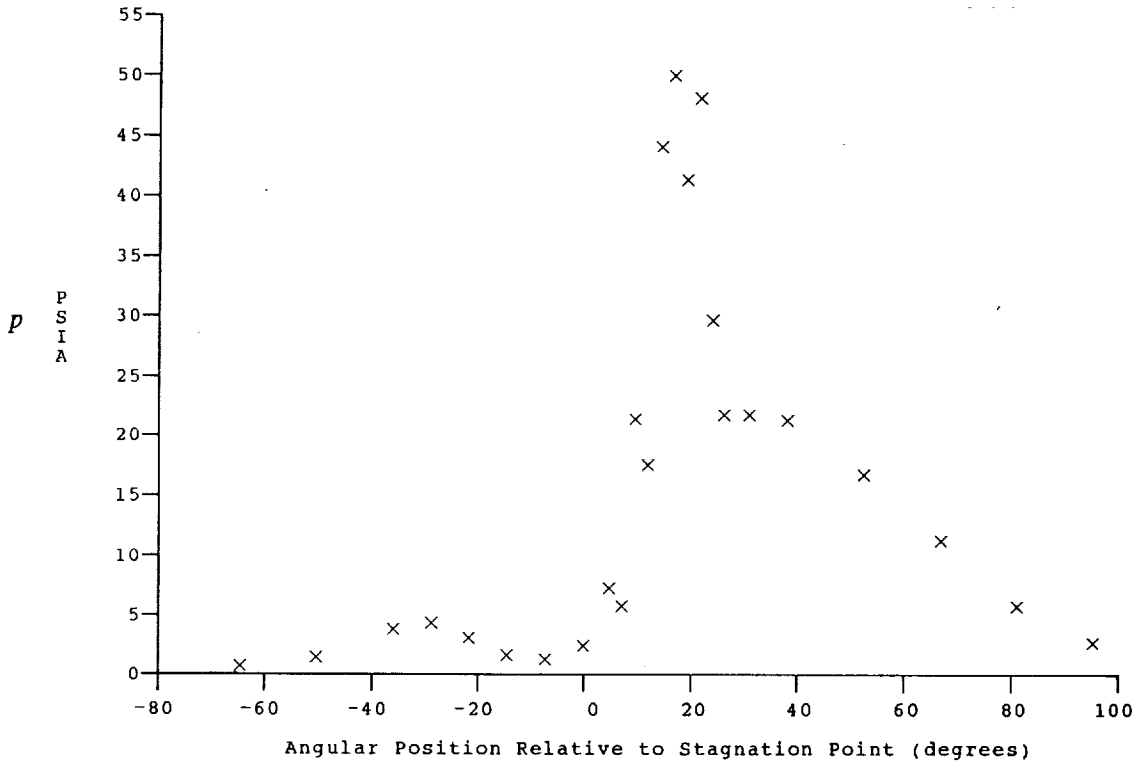

PRESSURE vs Gauge Position
Run 78

Test Conditions

Mi	= 3.4844	
Po	= 1.8020X10+3	PSIA
Ho	= 1.9072X10+7	(Ft/sec)^2
To	= 2.8845X10+3	Degrees R
M	= 8.0486	
U	= 5.9538X10+3	Ft/sec
T	= 2.2754X10+2	Degrees R
P	= 1.5642X10-1	PSIA
Q	= 7.1007	PSIA
Rho	= 5.7691X10-5	Slugs/Ft^3
Mu	= 1.8772X10-7	Slugs/Ft-sec
Re	= 1.8298X10+6	1/Ft
Po'	= 1.3170X10+1	PSIA

Model Configuration Parameter	Value
Stagnation Position (gauge label)	P21
Vertical Distance (inches)	3.44
Horizontal Distance (inches)	1.34
Plate Angle (degrees)	12.50
Plate Length (inches)	26.00
Sweep Angle (degrees)	30.00

Run 79

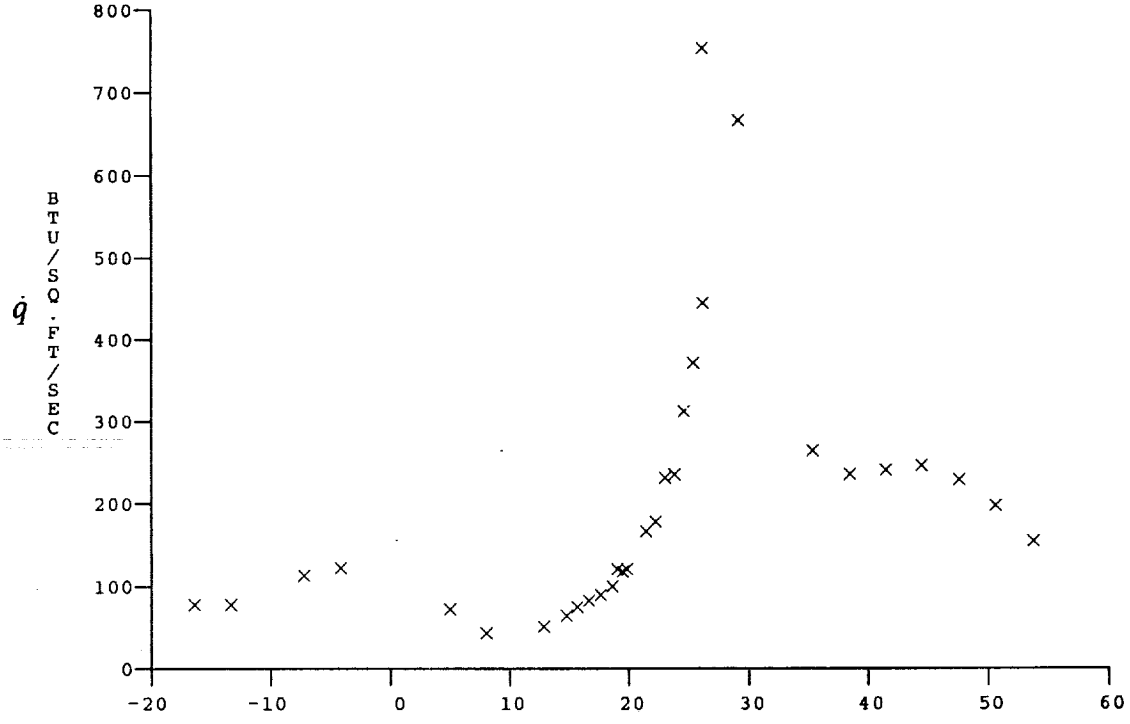

HEAT TRANSFER vs Gauge Position
Run 79

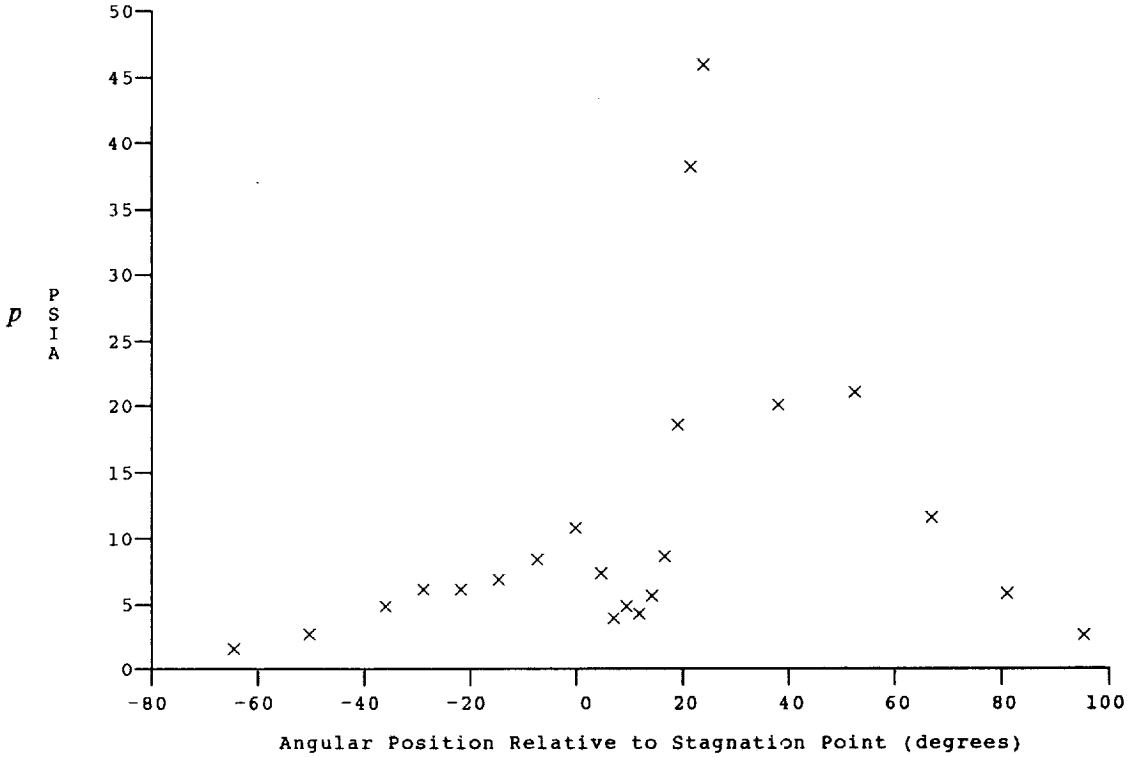

PRESSURE vs Gauge Position
Run 79

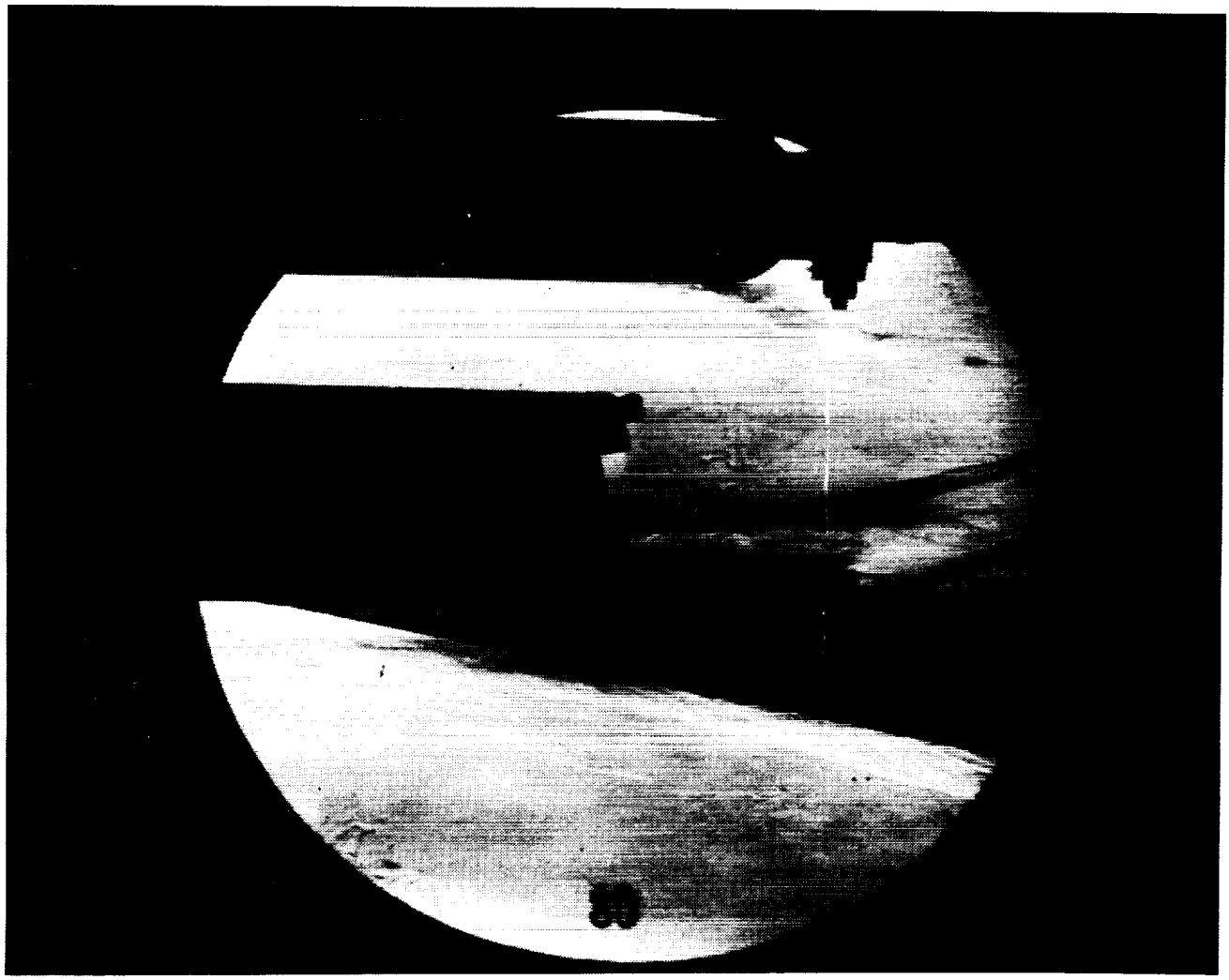

Test Conditions for Run 80 :

Po	= 6.160E+02 PSIA	Reservoir Total Pressure	
Ho	= 1.765E+07 (Ft/sec)²	Reservoir Total Enthalpy	
To	= 2.702E+03 °R	Reservoir Total Temperature	
M	= 7.991E+00	Freestream Mach Number	
U	= 5.725E+03 Ft/sec	Freestream Velocity	
T	= 2.134E+02 °R	Freestream Temperature	
P	= 5.611E-02 PSIA	Freestream Static Pressure	
Rho	= 2.206E-05 Slugs/Ft3	Freestream Density	
Mu	= 1.768E-07 Slugs/Ft-sec	Freestream Viscosity	
Re	= 7.146E+05 1/Ft	Freestream Reynolds Number	
Po'	= 4.651E+00 PSIA	Pitot Pressure	
Q	= 2.511E+00 PSIA	Dynamic Pressure (½·Rho·U²/144)	
Mi	= 3.319E+00	Shock Tube Incident Shock Mach Number	
Hw	= 3.183E+06 (Ft/sec)²	Wall Enthalpy (Cp·Tw)	
CPf	= 3.983E-01 1/PSIA	Pressure to CP factor (1/Q)	
CHf	= 4.257E-04 Ft²-s/BTU	Heat Rate to CH factor (778/(Rho·U·(Ho-Hw))	
QoFR	= 2.548E+01 BTU/Ft²-s	Fay-Riddell Heat Transfer to 3" Diam Sphere	

Model Configuration Parameter	Value
Stagnation Position (gauge label)	P21
Vertical Distance (inches)	3.44
Horizontal Distance (inches)	1.34
Plate Angle (degrees)	12.50
Plate Length (inches)	26.00
Sweep Angle (degrees)	30.00

Run 80

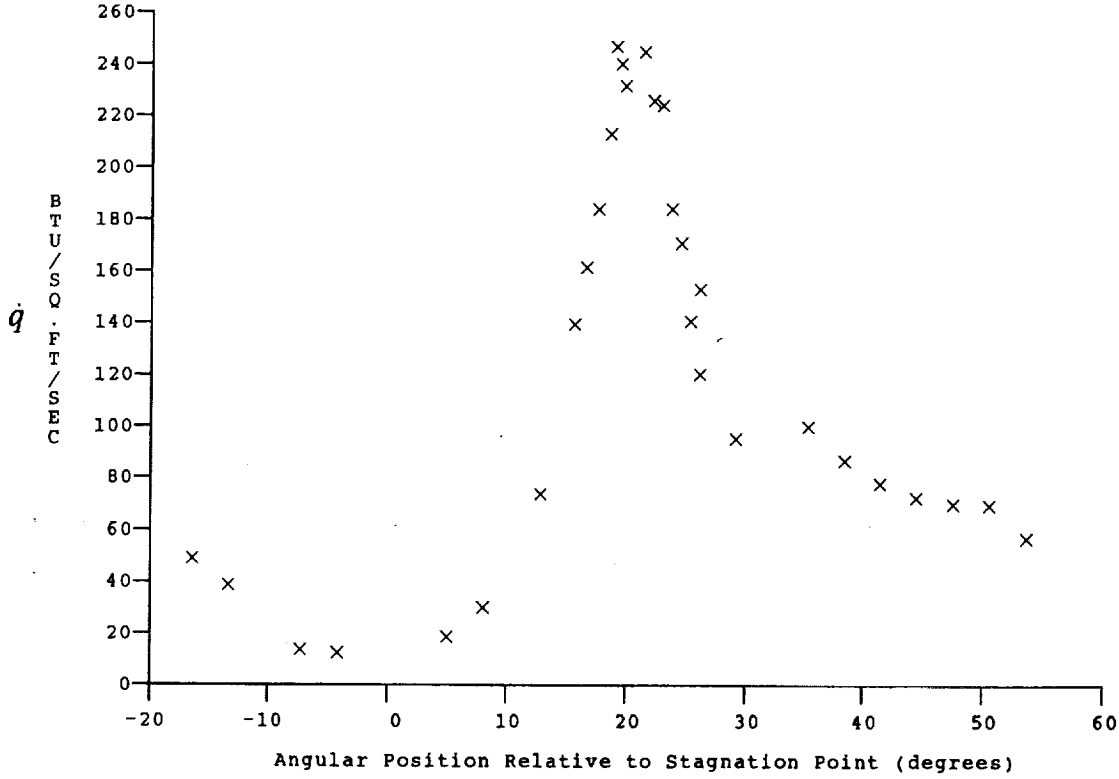

HEAT TRANSFER vs Gauge Position
Run 80

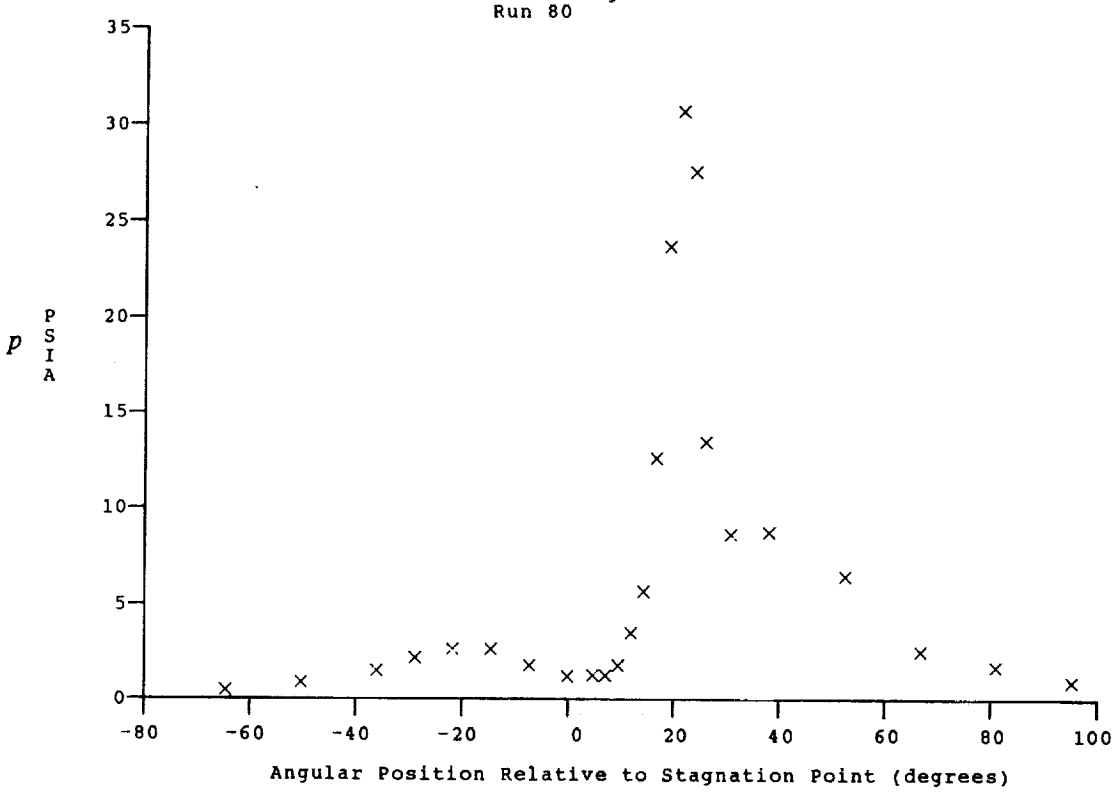

PRESSURE vs Gauge Position
Run 80

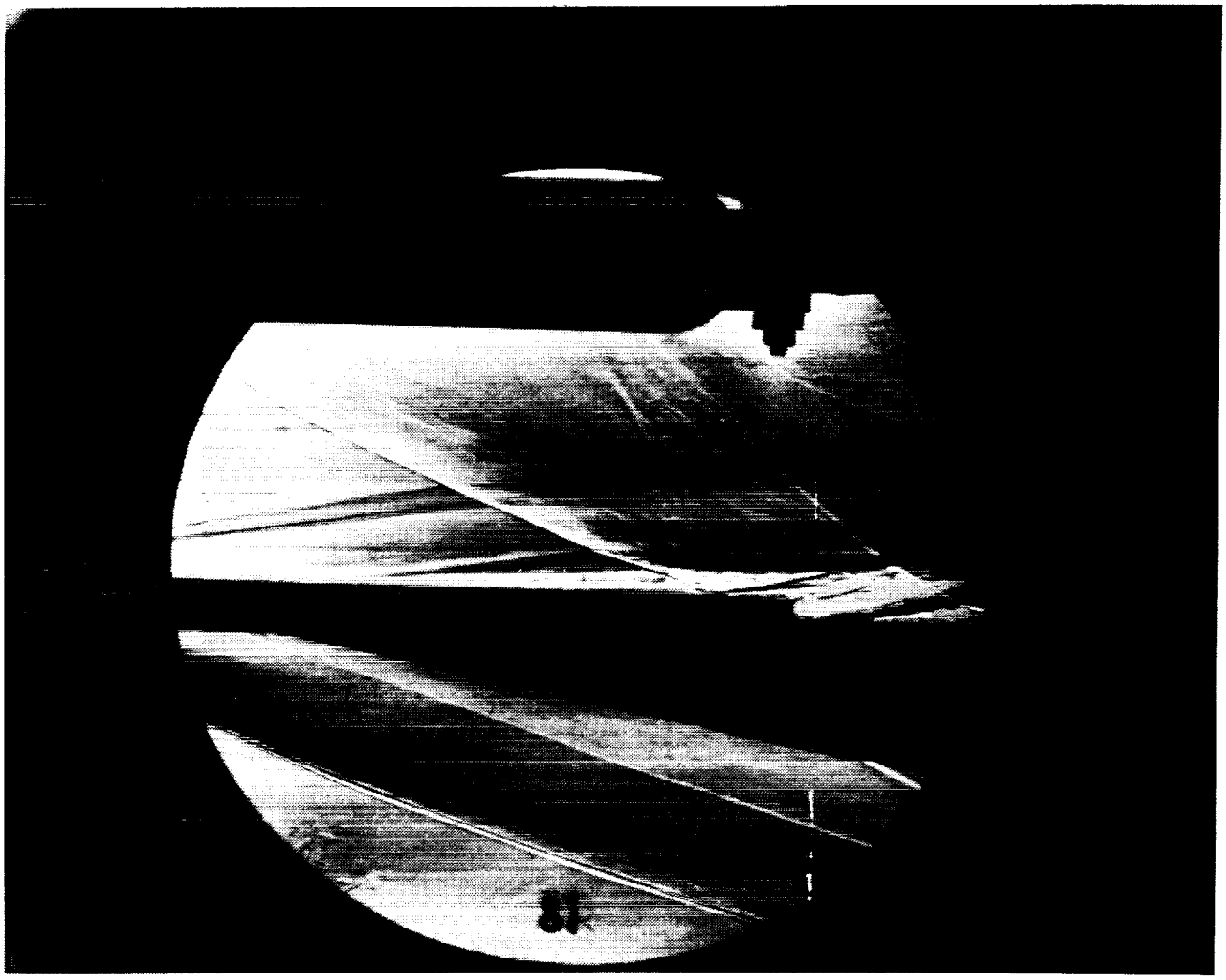

Test Conditions for Run 81 :

Po	= 1.413E+03 PSIA	Reservoir Total Pressure	
Ho	= 1.869E+07 (Ft/sec)²	Reservoir Total Enthalpy	
To	= 2.839E+03 °R	Reservoir Total Temperature	
M	= 8.041E+00	Freestream Mach Number	
U	= 5.894E+03 Ft/sec	Freestream Velocity	
T	= 2.234E+02 °R	Freestream Temperature	
P	= 1.231E-01 PSIA	Freestream Static Pressure	
Rho	= 4.624E-05 Slugs/Ft3	Freestream Density	
Mu	= 1.845E-07 Slugs/Ft-sec	Freestream Viscosity	
Re	= 1.477E+06 1/Ft	Freestream Reynolds Number	
Po'	= 1.034E+01 PSIA	Pitot Pressure	
Q	= 5.576E+00 PSIA	Dynamic Pressure (½·Rho·U²/144)	
Mi	= 3.414E+00	Shock Tube Incident Shock Mach Number	
Hw	= 3.183E+06 (Ft/sec)²	Wall Enthalpy (Cp·Tw)	
CPf	= 1.793E-01 1/PSIA	Pressure to CP factor (1/Q)	
CHf	= 1.841E-04 Ft²-s/BTU	Heat Rate to CH factor (778/(Rho·U·(Ho-Hw))	
QoFR	= 4.087E+01 BTU/Ft²-s	Fay-Riddell Heat Transfer to 3" Diam Sphere	

Model Configuration Parameter	Value
Stagnation Position (gauge label)	P21
Sweep Angle (degrees)	30.00

Run 81

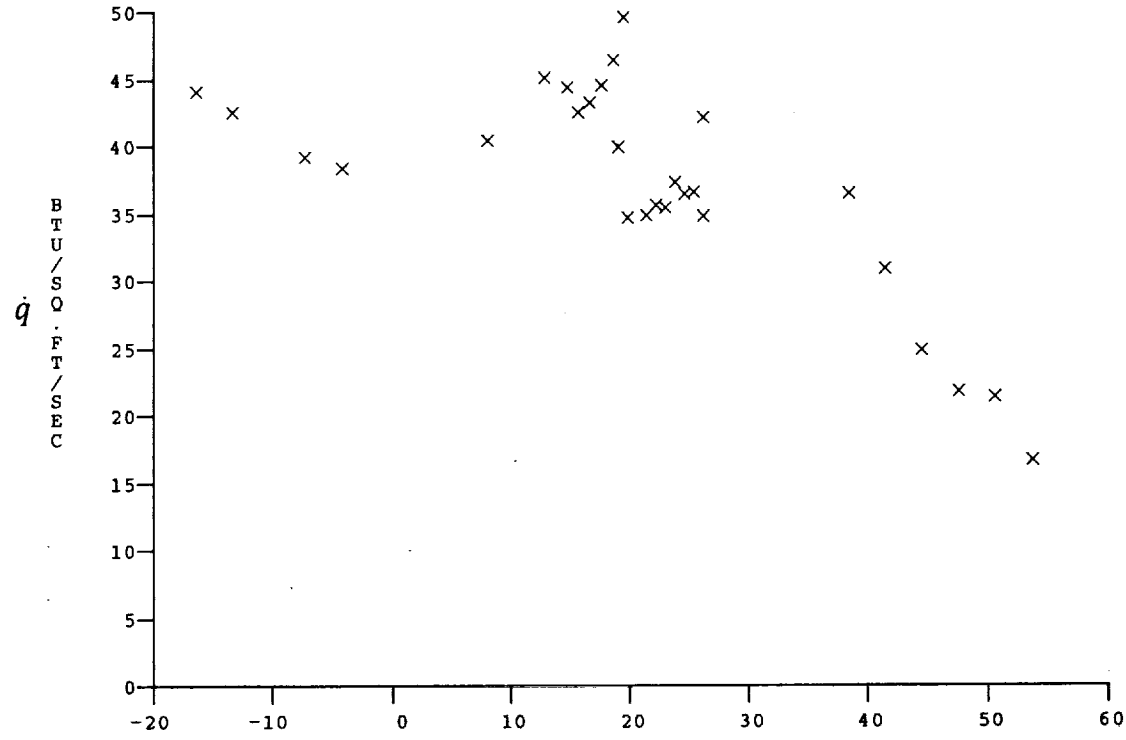

HEAT TRANSFER vs Gauge Position
Run 81

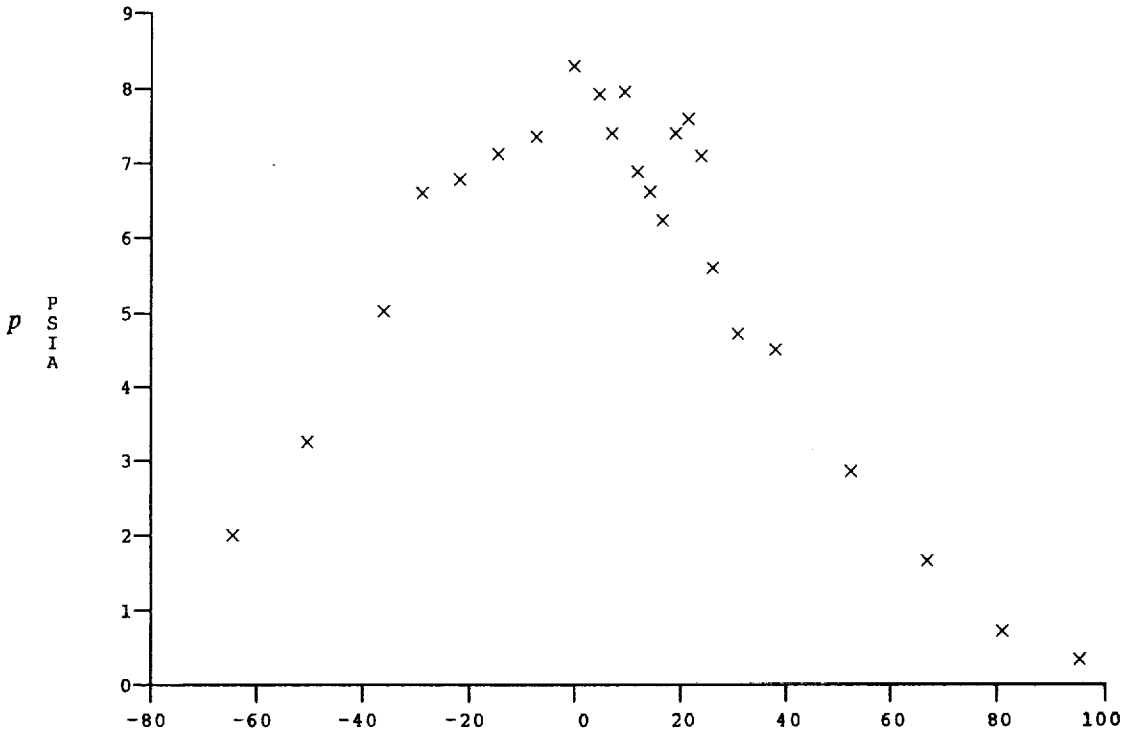

PRESSURE vs Gauge Position
Run 81

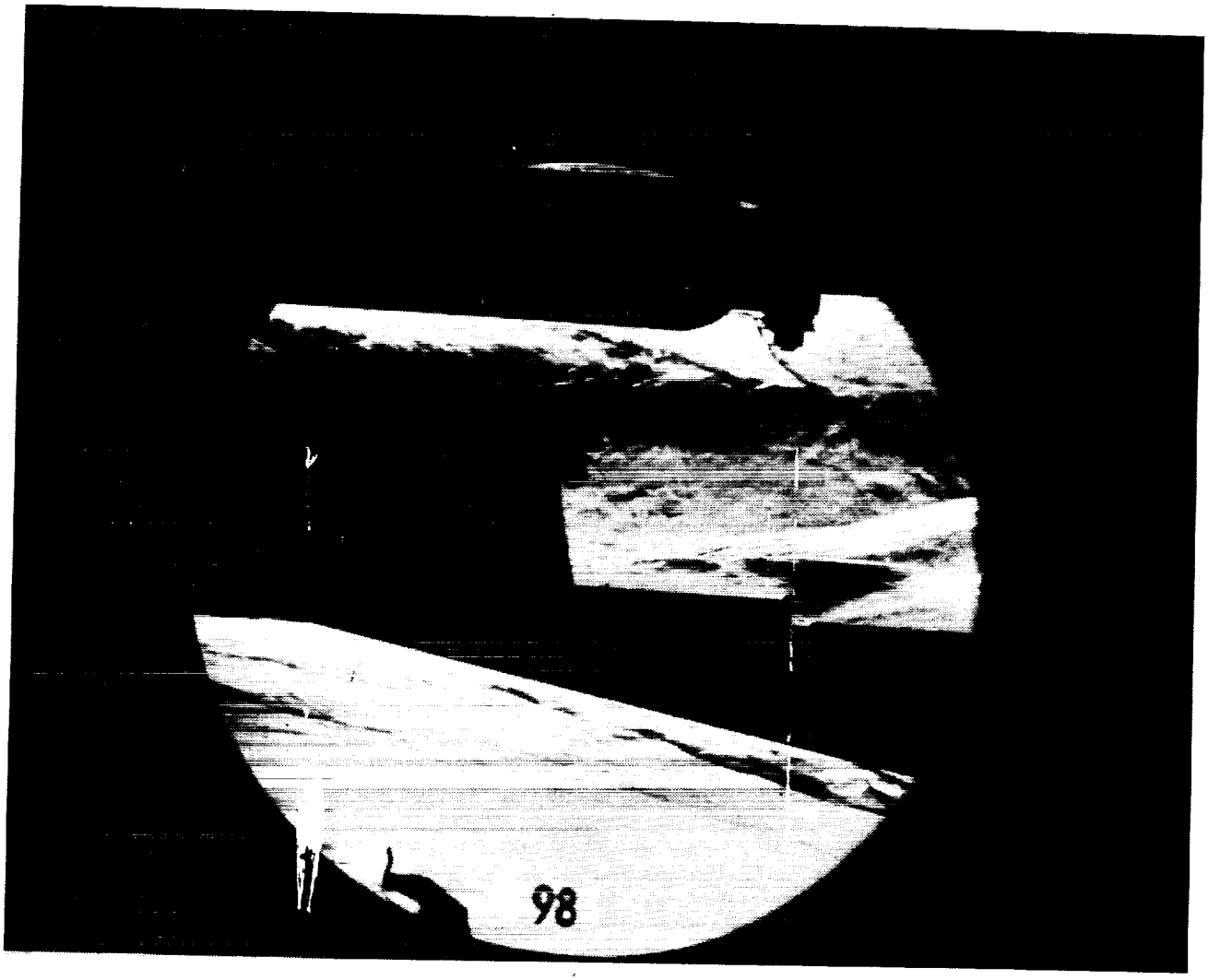

Test Conditions for Run 98 :

Po	= 1.353E+03 PSIA	Reservoir Total Pressure
Ho	= 1.834E+07 (Ft/sec)²	Reservoir Total Enthalpy
To	= 2.788E+03 °R	Reservoir Total Temperature
M	= 8.031E+00	Freestream Mach Number
U	= 5.838E+03 Ft/sec	Freestream Velocity
T	= 2.197E+02 °R	Freestream Temperature
P	= 1.195E-01 PSIA	Freestream Static Pressure
Rho	= 4.564E-05 Slugs/Ft3	Freestream Density
Mu	= 1.816E-07 Slugs/Ft-sec	Freestream Viscosity
Re	= 1.467E+06 1/Ft	Freestream Reynolds Number
Po'	= 1.001E+01 PSIA	Pitot Pressure
Q	= 5.400E+00 PSIA	Dynamic Pressure (½·Rho·U²/144)
Mi	= 3.422E+00	Shock Tube Incident Shock Mach Number
Hw	= 3.183E+06 (Ft/sec)²	Wall Enthalpy (Cp·Tw)
CPf	= 1.852E-01 1/PSIA	Pressure to CP factor (1/Q)
CHf	= 1.927E-04 Ft²-s/BTU	Heat Rate to CH factor (778/(Rho·U·(Ho-Hw))
QoFR	= 3.925E-01 BTU/Ft²-s	Fay-Riddell Heat Transfer to 3" Diam Sphere

Model Configuration Parameter	Value
Stagnation Position (gauge label)	P21
Vertical Distance (inches)	3.41
Horizontal Distance (inches)	1.22
Plate Angle (degrees)	12.50
Plate Length (inches)	26.00
Sweep Angle (degrees)	30.00

Run 98

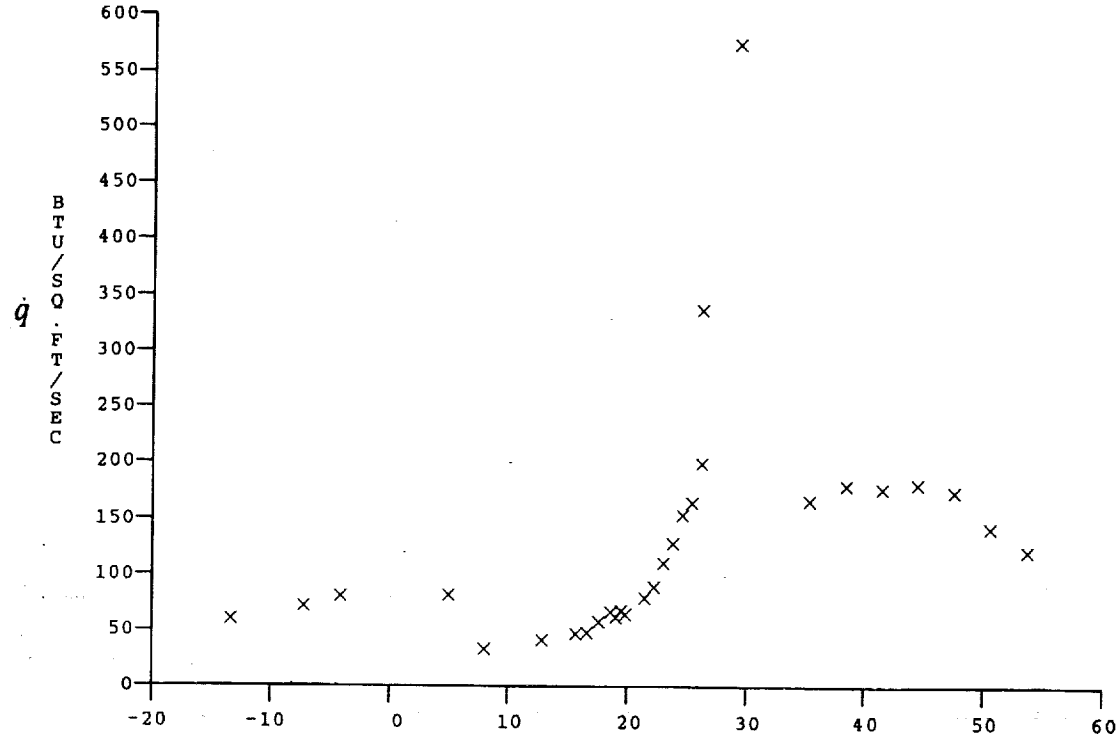

HEAT TRANSFER vs Gauge Position
Run 98

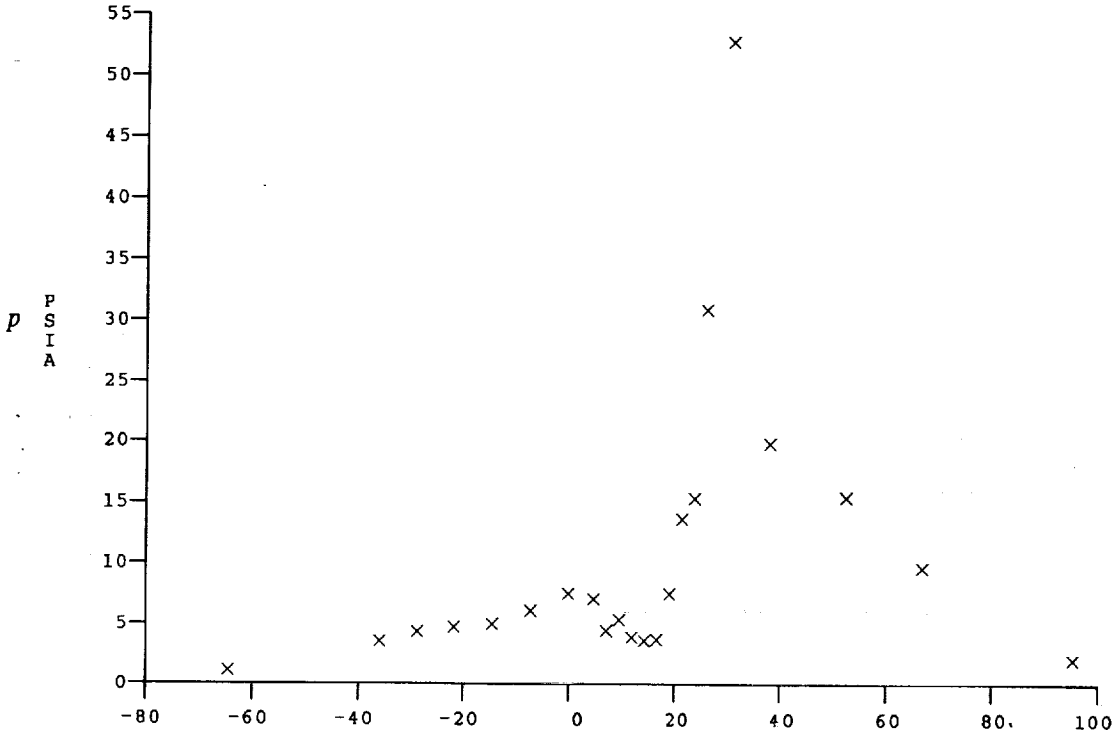

PRESSURE vs Gauge Position
Run 98

Gauge Label	Angle (deg)	Value (PSIA) or (BTU/Ft2-Sec)	T Surf (DegR)	Gauge Label	Angle (deg)	Value (PSIA) or (BTU/Ft2-Sec)	T Surf (DegR)	Gauge Label	Angle (deg)	Value (PSIA) or (BTU/Ft2-Sec)	T Surf (DegR)
P 30	-64.40	Null		P 9	38.22	1.323(1)		HT 71	19.60	4.995(1)	597.61
P 28	-50.11	2.868(-1)		P 7	52.54	1.101(1)		HT 9	19.90	4.134(1)	589.45
P 26	-35.79	1.666(0)		P 5	66.86	7.766(0)		HT 7	21.51	5.589(1)	593.42
P 25	-28.63	2.673(0)		P 3	81.19	3.706(0)		HT 6	22.30	3.876(1)	587.42
P 24	-21.47	4.748(0)		P 1	95.51	1.500(0)		HT 5	23.09	5.293(1)	598.79
P 23	-14.30	8.087(0)		HT 32	-16.31	4.848(1)	590.60	HT 4	23.89	3.259(1)	583.16
P 22	-7.14	1.218(1)		HT 31	-13.25	5.413(1)	595.26	HT 3	24.69	5.301(1)	595.17
P 21	.02	1.622(1)		HT 29	-7.14	5.874(1)	600.72	HT 2	25.49	5.408(1)	591.12
P 20	4.79	1.663(1)		HT 28	-4.09	6.110(1)	601.30	HT 1	26.29	4.716(1)	587.38
P 15	7.18	1.583(1)		HT 25	5.08	7.800(1)	609.02	HT 62	26.29	5.314(1)	597.81
P 19	9.57	1.702(1)		HT 24	8.14	Null	Null	HT 61	29.35	6.513(1)	605.80
P 14	11.96	1.604(1)		HT 64	12.91	6.361(1)	605.59	HT 59	35.46	5.856(1)	602.19
P 18	14.34	1.424(1)		HT 65	13.87	Null	Null	HT 58	38.51	5.881(1)	598.87
P 13	16.73	1.418(1)		HT 66	14.82	5.128(1)	595.40	HT 57	41.57	6.556(1)	600.47
P 17	19.12	Null		HT 67	15.78	5.323(1)	596.69	HT 56	44.63	5.614(1)	600.76
P 12	21.51	Null		HT 68	16.73	3.129(1)	579.36	HT 55	47.68	5.311(1)	601.13
P 16	23.89	Null		HT 69	17.69	4.474(1)	593.38	HT 54	50.74	5.258(1)	593.55
P 11	26.28	1.396(1)		HT 70	18.64	5.278(1)	594.14	HT 53	53.79	4.351(1)	585.40
P 10	31.05	1.293(1)		HT 10	19.10	3.887(1)	587.31				

Run 66 Reduced Data Tabulation

Gauge Label	Angle (deg)	Value (PSIA) or (BTU/Ft2-Sec)	T Surf (DegR)	Gauge Label	Angle (deg)	Value (PSIA) or (BTU/Ft2-Sec)	T Surf (DegR)	Gauge Label	Angle (deg)	Value (PSIA) or (BTU/Ft2-Sec)	T Surf (DegR)
P 28	-50.11	7.489(-1)		P 7	52.54	1.978(1)		HT 9	19.90	Null	Null
P 26	-35.79	1.066(0)		P 5	66.86	1.390(1)		HT 7	21.51	9.747(1)	617.12
P 25	-28.63	5.580(0)		P 3	81.19	6.404(0)		HT 6	22.30	9.104(1)	615.20
P 24	-21.47	9.925(0)		P 1	95.51	2.139(0)		HT 5	23.09	1.107(2)	624.03
P 23	-14.30	1.630(1)		HT 32	-16.31	8.437(1)	607.51	HT 4	23.89	9.466(1)	614.48
P 22	-7.14	2.310(1)		HT 31	-13.25	8.826(1)	610.85	HT 3	24.69	8.867(1)	614.08
P 21	.02	3.067(1)		HT 29	-7.14	1.098(2)	625.32	HT 2	25.49	8.024(1)	608.67
P 20	4.79	3.148(1)		HT 28	-4.09	1.165(2)	628.65	HT 1	26.29	8.177(1)	609.51
P 15	7.18	3.020(1)		HT 25	5.08	1.364(2)	640.88	HT 62	26.29	1.115(2)	631.67
P 19	9.57	3.174(1)		HT 24	8.14	1.215(2)	629.61	HT 61	29.34	1.013(2)	625.83
P 14	11.96	3.016(1)		HT 64	12.91	1.129(2)	630.16	HT 59	35.46	1.125(2)	635.04
P 18	14.34	2.743(1)		HT 65	13.87	Null	Null	HT 58	38.51	1.091(2)	630.03
P 13	16.73	2.782(1)		HT 66	14.82	1.016(2)	622.71	HT 57	41.57	1.125(2)	633.70
P 17	19.12	Null		HT 67	15.78	1.062(2)	624.90	HT 56	44.63	1.109(2)	631.75
P 12	21.51	Null		HT 68	16.73	1.010(2)	619.20	HT 55	47.68	1.083(2)	629.82
P 16	23.89	Null		HT 69	17.69	1.039(2)	621.48	HT 54	50.73	1.004(2)	624.70
P 11	26.28	2.639(1)		HT 70	18.64	9.363(1)	617.02	HT 53	53.78	9.069(1)	613.90
P 10	31.05	2.438(1)		HT 10	19.10	1.095(2)	626.96				
P 9	38.22	2.418(1)		HT 71	19.60	1.013(2)	618.25				

Run 67 Reduced Data Tabulation

Gauge Label	Angle (deg)	Value (PSIA) or (BTU/Ft2-Sec)	T Surf (DegR)	Gauge Label	Angle (deg)	Value (PSIA) or (BTU/Ft2-Sec)	T Surf (DegR)	Gauge Label	Angle (deg)	Value (PSIA) or (BTU/Ft2-Sec)	T Surf (DegR)
P 28	-28.65	5.766(-1)		P 7	74.01	8.110(0)		HT 9	41.37	Null	Null
P 26	-14.32	7.138(-1)		P 5	88.33	7.072(0)		HT 7	42.97	9.739(1)	609.32
P 25	-7.16	5.012(0)		P 3	102.65	3.078(0)		HT 6	43.76	8.114(1)	605.72
P 24	.00	1.349(1)		P 1	116.98	1.094(0)		HT 5	44.56	1.102(2)	618.34
P 23	7.16	Null		HT 32	5.16	3.472(2)	759.13	HT 4	45.36	6.799(1)	594.84
P 22	14.32	Null		HT 31	8.21	4.110(2)	768.44	HT 3	46.16	8.334(1)	598.49
P 21	21.49	Null		HT 29	14.32	2.669(2)	692.53	HT 2	46.96	8.150(1)	599.35
P 20	26.26	2.660(1)		HT 28	17.38	2.066(2)	671.09	HT 1	47.76	9.289(1)	600.05
P 15	28.65	2.394(1)		HT 25	26.55	1.510(2)	647.57	HT 62	47.76	1.209(2)	621.12
P 19	31.04	2.564(1)		HT 24	29.60	1.314(2)	630.77	HT 61	50.80	9.087(1)	606.46
P 14	33.42	2.225(1)		HT 64	34.38	1.109(2)	623.79	HT 59	56.93	7.597(1)	596.97
P 18	35.81	1.948(1)		HT 65	35.33	Null	Null	HT 58	59.98	7.061(1)	589.27
P 13	38.20	1.691(1)		HT 66	36.29	1.050(2)	619.83	HT 57	63.04	5.523(1)	581.97
P 17	40.58	1.662(1)		HT 67	37.24	Null	Null	HT 56	66.09	5.773(1)	580.45
P 12	42.97	1.520(1)		HT 68	38.20	8.898(1)	608.31	HT 55	69.15	5.760(1)	579.40
P 16	45.36	1.537(1)		HT 69	39.15	8.954(1)	608.58	HT 54	72.19	4.331(1)	571.24
P 11	47.75	1.450(1)		HT 70	40.11	7.126(1)	604.99	HT 53	75.25	4.971(1)	569.94
P 10	52.52	1.319(1)		HT 10	40.57	1.047(2)	620.35				
P 9	59.68	1.234(1)		HT 71	41.06	9.402(1)	609.26				

Run 68 Reduced Data Tabulation

Gauge Label	Angle (deg)	Value (PSIA) or (BTU/Ft2-Sec)	T Surf (DegR)	Gauge Label	Angle (deg)	Value (PSIA) or (BTU/Ft2-Sec)	T Surf (DegR)	Gauge Label	Angle (deg)	Value (PSIA) or (BTU/Ft2-Sec)	T Surf (DegR)
P 30	-64.40	Null		P 9	38.22	Null		HT 71	19.60	1.225(2)	609.43
P 28	-50.11	2.387(0)		P 7	52.54	1.639(1)		HT 9	19.90	1.331(2)	615.83
P 26	-35.79	3.130(0)		P 5	66.86	1.094(1)		HT 7	21.51	1.802(2)	636.98
P 25	-28.63	4.865(0)		P 3	81.19	5.519(0)		HT 6	22.30	2.048(2)	643.80
P 24	-21.47	5.416(0)		P 1	95.51	2.651(0)		HT 5	23.09	2.512(2)	671.91
P 23	-14.30	6.398(0)		HT 32	-16.31	8.703(1)	593.13	HT 4	23.89	3.065(2)	687.65
P 22	-7.14	7.949(0)		HT 31	-13.25	9.521(1)	597.11	HT 3	24.69	3.520(2)	714.10
P 21	.02	6.530(0)		HT 29	-7.14	1.045(2)	603.14	HT 2	25.49	3.847(2)	724.56
P 20	4.79	4.280(0)		HT 28	-4.09	9.406(1)	600.00	HT 1	26.29	4.682(2)	756.89
P 15	7.18	3.087(0)		HT 25	5.08	2.703(1)	573.14	HT 62	26.29	6.618(2)	823.72
P 19	9.57	3.507(0)		HT 24	8.14	2.546(1)	564.71	HT 61	29.35	4.822(2)	813.62
P 14	11.96	4.470(0)		HT 64	12.91	6.065(1)	583.14	HT 59	35.46	2.014(2)	693.97
P 18	14.34	3.845(0)		HT 65	13.87	Null	Null	HT 58	38.51	1.609(2)	654.31
P 13	16.73	7.481(0)		HT 66	14.82	5.395(1)	576.70	HT 57	41.57	1.823(2)	654.38
P 17	19.12	1.076(1)		HT 67	15.78	7.571(1)	588.98	HT 56	44.63	1.857(2)	654.20
P 12	21.51	3.287(1)		HT 68	16.73	7.488(1)	587.00	HT 55	47.68	1.628(2)	646.65
P 16	23.89	2.576(1)		HT 69	17.69	9.035(1)	594.87	HT 54	50.74	1.508(2)	642.22
P 11	26.28	7.304(1)		HT 70	18.64	1.006(2)	601.02	HT 53	53.79	1.186(2)	622.70
P 10	31.05	3.840(1)		HT 10	19.10	1.273(2)	613.69				

Run 69 Reduced Data Tabulation

Gauge Label	Angle (deg)	Value (PSIA) or (BTU/Ft2-Sec)	T Surf (DegR)	Gauge Label	Angle (deg)	Value (PSIA) or (BTU/Ft2-Sec)	T Surf (DegR)	Gauge Label	Angle (deg)	Value (PSIA) or (BTU/Ft2-Sec)	T Surf (DegR)
P 30	-42.93	1.868(0)		P 9	59.68	1.233(1)		HT 71	41.06	3.868(1)	574.49
P 28	-28.65	6.264(0)		P 7	74.01	9.725(0)		HT 9	41.37	3.468(1)	569.82
P 26	-14.32	8.323(0)		P 5	88.33	4.961(0)		HT 7	42.97	4.188(1)	571.37
P 25	-7.16	8.994(0)		P 3	102.65	1.850(0)		HT 6	43.76	4.006(1)	575.69
P 24	.00	9.432(0)		P 1	116.98	6.358(-1)		HT 5	44.56	5.975(1)	579.88
P 23	7.16	9.511(0)		HT 32	5.16	3.581(1)	570.39	HT 4	45.36	4.432(1)	574.41
P 22	14.32	9.723(0)		HT 31	8.21	3.731(1)	571.07	HT 3	46.16	5.372(1)	578.21
P 21	21.49	1.118(1)		HT 29	14.32	3.896(1)	572.14	HT 2	46.96	4.813(1)	576.29
P 20	26.26	9.923(0)		HT 28	17.38	3.269(1)	568.99	HT 1	47.76	5.035(1)	578.50
P 15	28.65	1.041(1)		HT 25	26.55	4.103(1)	574.52	HT 62	47.76	7.018(1)	593.86
P 19	31.04	1.081(1)		HT 24	29.60	2.632(1)	564.97	HT 61	50.81	8.817(1)	608.14
P 14	33.42	Null		HT 64	34.38	4.060(1)	574.31	HT 59	56.93	1.255(2)	625.54
P 18	35.81	8.289(0)		HT 65	35.33	Null	Null	HT 58	59.98	1.221(2)	626.58
P 13	38.20	9.447(0)		HT 66	36.29	4.298(1)	575.10	HT 57	63.04	1.173(2)	629.08
P 17	40.58	1.265(1)		HT 67	37.24	3.454(1)	571.12	HT 56	66.09	1.053(2)	625.63
P 12	42.97	1.053(1)		HT 68	38.20	4.170(1)	571.76	HT 55	69.15	1.055(2)	617.95
P 16	45.36	1.020(1)		HT 69	39.15	3.935(1)	572.82	HT 54	72.20	8.332(1)	607.68
P 11	47.75	9.515(0)		HT 70	40.11	3.567(1)	572.22	HT 53	75.26	7.532(1)	601.15
P 10	52.52	1.029(1)		HT 10	40.57	4.414(1)	572.52				

Run 70 Reduced Data Tabulation

Gauge Label	Angle (deg)	Value (PSIA) or (BTU/Ft2-Sec)	T Surf (DegR)	Gauge Label	Angle (deg)	Value (PSIA) or (BTU/Ft2-Sec)	T Surf (DegR)	Gauge Label	Angle (deg)	Value (PSIA) or (BTU/Ft2-Sec)	T Surf (DegR)
P 30	-42.93	Null		P 9	59.68	1.306(1)		HT 71	41.06	4.057(2)	743.39
P 28	-28.65	7.464(0)		P 7	74.01	5.094(0)		HT 9	41.37	3.869(2)	741.26
P 26	-14.32	6.752(0)		P 5	88.33	2.541(0)		HT 7	42.97	4.427(2)	763.95
P 25	-7.16	8.096(0)		P 3	102.65	9.746(-1)		HT 6	43.76	4.577(2)	769.95
P 24	.00	7.817(0)		P 1	116.98	3.516(-1)		HT 5	44.56	4.932(2)	788.53
P 23	7.16	7.506(0)		HT 32	5.16	6.852(1)	594.56	HT 4	45.36	4.546(2)	780.93
P 22	14.32	7.806(0)		HT 31	8.21	6.543(1)	593.16	HT 3	46.16	4.514(2)	781.22
P 21	21.49	7.898(0)		HT 29	14.32	7.423(1)	598.43	HT 2	46.96	4.208(2)	774.75
P 20	26.26	8.924(0)		HT 28	17.38	7.295(1)	598.66	HT 1	47.76	3.915(2)	772.14
P 15	28.65	1.081(1)		HT 25	26.55	1.248(2)	626.14	HT 62	47.76	3.810(2)	774.24
P 19	31.04	1.321(1)		HT 24	29.60	1.596(2)	638.55	HT 61	50.81	2.439(2)	743.30
P 14	33.42	1.797(1)		HT 64	34.38	2.522(2)	687.00	HT 59	56.93	1.656(2)	692.48
P 18	35.81	2.074(1)		HT 65	35.33	Null	Null	HT 58	59.98	1.113(2)	652.25
P 13	38.20	3.197(1)		HT 66	36.29	2.903(2)	703.19	HT 57	63.04	7.823(1)	630.59
P 17	40.58	4.347(1)		HT 67	37.24	3.200(2)	713.20	HT 56	66.09	5.440(1)	610.68
P 12	42.97	5.661(1)		HT 68	38.20	3.234(2)	714.15	HT 55	69.15	4.594(1)	597.85
P 16	45.36	5.343(1)		HT 69	39.15	3.466(2)	722.90	HT 54	72.20	4.186(1)	584.97
P 11	47.75	4.097(1)		HT 70	40.11	3.784(2)	733.41	HT 53	75.26	3.372(1)	574.28
P 10	52.52	2.660(1)		HT 10	40.57	4.145(2)	750.35				

Run 71 Reduced Data Tabulation

Gauge Label	Angle (deg)	Value (PSIA) or (BTU/Ft2-Sec)	T Surf (DegR)	Gauge Label	Angle (deg)	Value (PSIA) or (BTU/Ft2-Sec)	T Surf (DegR)	Gauge Label	Angle (deg)	Value (PSIA) or (BTU/Ft2-Sec)	T Surf (DegR)
P 28	-28.65	1.367(1)		P 7	74.01	6.914(0)		HT 9	41.37	3.648(2)	748.83
P 26	-14.32	8.963(0)		P 5	88.33	3.028(0)		HT 7	42.97	3.869(2)	773.16
P 25	-7.16	1.163(1)		P 3	102.65	1.159(0)		HT 6	43.76	4.169(2)	781.78
P 24	.00	1.108(1)		P 1	116.98	3.796(-1)		HT 5	44.56	4.785(2)	810.49
P 23	7.16	1.117(1)		HT 32	5.16	9.523(1)	606.06	HT 4	45.36	4.391(2)	795.85
P 22	14.32	1.083(1)		HT 31	8.21	9.253(1)	606.87	HT 3	46.16	4.816(2)	800.87
P 21	21.49	1.231(1)		HT 29	14.32	1.012(2)	610.68	HT 2	46.96	4.939(2)	802.89
P 20	26.26	1.306(1)		HT 28	17.38	1.048(2)	614.70	HT 1	47.76	4.744(2)	804.51
P 15	28.65	1.483(1)		HT 25	26.55	1.408(2)	636.17	HT 62	47.76	5.289(2)	808.83
P 19	31.04	1.759(1)		HT 24	29.60	1.687(2)	651.15	HT 61	50.81	4.705(2)	802.91
P 14	33.42	2.069(1)		HT 64	34.38	2.508(2)	694.42	HT 59	56.93	3.008(2)	747.77
P 18	35.81	2.472(1)		HT 65	35.33	Null	Null	HT 58	59.98	1.968(2)	699.43
P 13	38.20	3.066(1)		HT 66	36.29	2.765(2)	709.34	HT 57	63.04	1.522(2)	676.53
P 17	40.58	6.280(1)		HT 67	37.24	2.826(2)	718.95	HT 56	66.09	1.157(2)	651.51
P 12	42.97	6.087(1)		HT 68	38.20	3.175(2)	731.40	HT 55	69.15	1.000(2)	634.71
P 16	45.36	6.381(1)		HT 69	39.15	3.323(2)	735.86	HT 54	72.20	7.358(1)	612.36
P 11	47.75	5.834(1)		HT 70	40.11	3.441(2)	743.37	HT 53	75.26	5.874(1)	594.83
P 10	52.52	4.060(1)		HT 10	40.57	3.407(2)	750.70				
P 9	59.68	2.367(1)		HT 71	41.06	3.553(2)	752.30				

Run 72 Reduced Data Tabulation

Gauge Label	Angle (deg)	Value (PSIA) or (BTU/Ft2-Sec)	T Surf (DegR)	Gauge Label	Angle (deg)	Value (PSIA) or (BTU/Ft2-Sec)	T Surf (DegR)	Gauge Label	Angle (deg)	Value (PSIA) or (BTU/Ft2-Sec)	T Surf (DegR)
P 28	-28.65	1.332(0)		P 7	74.01	3.439(0)		HT 9	41.37	1.361(2)	644.63
P 26	-14.32	3.469(0)		P 5	88.33	1.355(0)		HT 7	42.97	1.512(2)	654.94
P 25	-7.16	4.385(0)		P 3	102.65	5.110(-1)		HT 6	43.76	1.634(2)	659.61
P 24	.00	4.266(0)		P 1	116.98	1.482(-1)		HT 5	44.56	1.715(2)	667.21
P 23	7.16	4.322(0)		HT 32	5.16	4.101(1)	570.55	HT 4	45.36	1.593(2)	660.06
P 22	14.32	4.433(0)		HT 31	8.21	4.251(1)	571.14	HT 3	46.16	1.704(2)	663.58
P 21	21.49	4.861(0)		HT 29	14.32	Null	Null	HT 2	46.96	1.765(2)	662.30
P 20	26.26	4.950(0)		HT 28	17.38	4.747(1)	574.40	HT 1	47.76	1.876(2)	670.33
P 15	28.65	5.277(0)		HT 25	26.55	6.037(1)	588.58	HT 62	47.76	2.095(2)	674.93
P 19	31.04	6.866(0)		HT 24	29.60	7.619(1)	601.33	HT 61	50.81	1.977(2)	669.21
P 14	33.42	7.395(0)		HT 64	34.38	1.052(2)	622.03	HT 59	56.93	1.425(2)	640.06
P 18	35.81	7.893(0)		HT 65	35.33	Null	Null	HT 58	59.98	1.063(2)	616.02
P 13	38.20	1.033(1)		HT 66	36.29	1.127(2)	628.50	HT 57	63.04	8.718(1)	607.93
P 17	40.58	Null		HT 67	37.24	1.212(2)	635.72	HT 56	66.09	6.951(1)	593.85
P 12	42.97	1.857(1)		HT 68	38.20	1.306(2)	640.02	HT 55	69.15	5.459(1)	583.74
P 16	45.36	1.813(1)		HT 69	39.15	1.365(2)	642.35	HT 54	72.20	3.919(1)	572.31
P 11	47.75	1.838(1)		HT 70	40.11	1.391(2)	645.95	HT 53	75.26	2.761(1)	564.57
P 10	52.52	1.638(1)		HT 10	40.57	1.422(2)	648.46				
P 9	59.68	1.157(1)		HT 71	41.06	1.453(2)	649.78				

Run 73 Reduced Data Tabulation

Gauge Label	Angle (deg)	Value (PSIA) or (BTU/Ft2-Sec)	T Surf (DegR)	Gauge Label	Angle (deg)	Value (PSIA) or (BTU/Ft2-Sec)	T Surf (DegR)	Gauge Label	Angle (deg)	Value (PSIA) or (BTU/Ft2-Sec)	T Surf (DegR)
P 30	-42.93	Null		P 9	59.68	2.883(0)		HT 71	41.06	2.720(1)	565.89
P 28	-28.65	Null		P 7	74.01	1.503(0)		HT 9	41.37	2.261(1)	560.87
P 26	-14.32	8.527(0)		P 5	88.33	6.755(-1)		HT 7	42.97	2.333(1)	560.62
P 25	-7.16	1.001(1)		P 3	102.65	2.858(-1)		HT 6	43.76	2.216(1)	560.80
P 24	.00	9.141(0)		P 1	116.98	6.913(-2)		HT 5	44.56	2.359(1)	561.90
P 23	7.16	8.842(0)		HT 32	5.16	3.754(1)	578.97	HT 4	45.36	2.310(1)	559.80
P 22	14.32	8.472(0)		HT 31	8.21	3.760(1)	577.57	HT 3	46.16	2.034(1)	558.61
P 21	21.49	8.736(0)		HT 29	14.32	3.673(1)	576.45	HT 2	46.96	2.084(1)	558.86
P 20	26.26	8.009(0)		HT 28	17.38	3.528(1)	573.71	HT 1	47.76	1.932(1)	558.05
P 15	28.65	7.060(0)		HT 25	26.55	3.226(1)	572.62	HT 62	47.76	2.186(1)	558.88
P 19	31.04	7.551(0)		HT 24	29.60	3.115(1)	569.41	HT 61	50.81	2.250(1)	560.51
P 14	33.42	6.287(0)		HT 64	34.38	3.017(1)	570.04	HT 59	56.93	2.062(1)	558.48
P 18	35.81	5.797(0)		HT 65	35.33	Null	Null	HT 58	59.98	1.813(1)	554.85
P 13	38.20	5.246(0)		HT 66	36.29	2.932(1)	568.65	HT 57	63.04	1.591(1)	553.42
P 17	40.58	6.104(0)		HT 67	37.24	2.874(1)	568.27	HT 56	66.09	1.411(1)	551.48
P 12	42.97	5.622(0)		HT 68	38.20	2.791(1)	566.25	HT 55	69.15	1.238(1)	549.22
P 16	45.36	5.336(0)		HT 69	39.15	2.652(1)	565.59	HT 54	72.20	1.132(1)	547.32
P 11	47.75	4.007(0)		HT 70	40.11	2.671(1)	565.10	HT 53	75.26	Null	Null
P 10	52.52	3.270(0)		HT 10	40.57	2.740(1)	564.95				

Run 74 Reduced Data Tabulation

Gauge Label	Angle (deg)	Value (PSIA) or (BTU/Ft2-Sec)	T Surf (DegR)	Gauge Label	Angle (deg)	Value (PSIA) or (BTU/Ft2-Sec)	T Surf (DegR)	Gauge Label	Angle (deg)	Value (PSIA) or (BTU/Ft2-Sec)	T Surf (DegR)
P 30	-64.40	1.161(0)		P 9	38.22	1.941(1)		HT 71	19.60	Null	Null
P 28	-50.11	1.996(0)		P 7	52.54	1.573(1)		HT 9	19.90	Null	Null
P 26	-35.79	3.228(0)		P 5	66.86	1.035(1)		HT 7	21.51	1.920(2)	708.84
P 25	-28.63	4.559(0)		P 3	81.19	5.190(0)		HT 6	22.30	2.082(2)	719.43
P 24	-21.47	4.863(0)		P 1	95.51	2.436(0)		HT 5	23.09	2.564(2)	742.37
P 23	-14.30	5.522(0)		HT 32	-16.31	6.266(1)	595.01	HT 4	23.89	3.136(2)	757.18
P 22	-7.14	6.919(0)		HT 31	-13.25	7.297(1)	600.38	HT 3	24.69	3.261(2)	767.10
P 21	.02	6.429(0)		HT 29	-7.14	9.278(1)	606.42	HT 2	25.49	3.608(2)	775.71
P 20	4.79	4.984(0)		HT 28	-4.09	9.128(1)	603.71	HT 1	26.29	4.161(2)	790.23
P 15	7.18	3.566(0)		HT 25	5.08	3.156(1)	576.76	HT 62	26.29	5.228(2)	838.58
P 19	9.57	3.955(0)		HT 24	8.14	2.752(1)	566.50	HT 61	29.35	4.264(2)	813.90
P 14	11.96	3.938(0)		HT 64	12.91	4.589(1)	588.69	HT 59	35.46	2.402(2)	722.08
P 18	14.34	4.226(0)		HT 65	13.87	Null	Null	HT 58	38.51	2.049(2)	694.80
P 13	16.73	6.058(0)		HT 66	14.82	5.583(1)	599.17	HT 57	41.57	2.005(2)	690.82
P 17	19.12	1.190(1)		HT 67	15.78	6.801(1)	610.33	HT 56	44.63	1.885(2)	683.28
P 12	21.51	2.739(1)		HT 68	16.73	7.223(1)	617.89	HT 55	47.68	1.628(2)	671.85
P 16	23.89	3.283(1)		HT 69	17.69	8.258(1)	629.75	HT 54	50.74	1.501(2)	662.79
P 11	26.28	4.397(1)		HT 70	18.64	9.663(1)	642.17	HT 53	53.79	1.346(2)	647.27
P 10	31.05	Null		HT 10	19.10	1.230(2)	660.54				

Run 75 Reduced Data Tabulation

Gauge Label	Angle (deg)	Value (PSIA) or (BTU/Ft2-Sec)	T Surf (DegR)	Gauge Label	Angle (deg)	Value (PSIA) or (BTU/Ft2-Sec)	T Surf (DegR)	Gauge Label	Angle (deg)	Value (PSIA) or (BTU/Ft2-Sec)	T Surf (DegR)
P 30	-64.40	3.688(-1)		P 9	38.22	1.996(1)		HT 71	19.60	1.493(2)	663.04
P 28	-50.11	5.068(-1)		P 7	52.54	1.567(1)		HT 9	19.90	Null	Null
P 26	-35.79	1.070(0)		P 5	66.86	1.095(1)		HT 7	21.51	1.459(2)	661.43
P 25	-28.63	1.640(0)		P 3	81.19	5.817(0)		HT 6	22.30	1.401(2)	656.46
P 24	-21.47	2.690(0)		P 1	95.51	2.899(0)		HT 5	23.09	1.493(2)	666.71
P 23	-14.30	4.930(0)		HT 32	-16.31	2.075(1)	561.71	HT 4	23.89	1.334(2)	651.24
P 22	-7.14	1.030(1)		HT 31	-13.25	5.794(1)	583.53	HT 3	24.69	1.359(2)	651.40
P 21	.02	2.048(1)		HT 29	-7.14	9.729(1)	619.11	HT 2	25.49	1.266(2)	646.38
P 20	4.79	2.379(1)		HT 28	-4.09	1.158(2)	628.56	HT 1	26.29	1.262(2)	647.46
P 15	7.18	2.277(1)		HT 25	5.08	Null	Null	HT 62	26.29	1.424(2)	658.90
P 19	9.57	2.609(1)		HT 24	8.14	Null	Null	HT 61	29.35	1.586(2)	672.82
P 14	11.96	2.363(1)		HT 64	12.91	1.620(2)	672.20	HT 59	35.46	1.506(2)	666.07
P 18	14.34	2.264(1)		HT 65	13.87	Null	Null	HT 58	38.51	1.394(2)	658.19
P 13	16.73	2.193(1)		HT 66	14.82	1.497(2)	665.42	HT 57	41.57	1.404(2)	656.33
P 17	19.12	Null		HT 67	15.78	1.567(2)	669.95	HT 56	44.63	1.253(2)	649.71
P 12	21.51	Null		HT 68	16.73	1.518(2)	664.25	HT 55	47.68	1.195(2)	642.80
P 16	23.89	Null		HT 69	17.69	1.449(2)	662.51	HT 54	50.74	1.090(2)	634.75
P 11	26.28	2.222(1)		HT 70	18.64	1.492(2)	660.53	HT 53	53.79	9.508(1)	625.39
P 10	31.05	2.042(1)		HT 10	19.10	1.535(2)	665.69				

Run 76 Reduced Data Tabulation

Gauge Label	Angle (deg)	Value (PSIA) or (BTU/Ft2-Sec)	T Surf (DegR)	Gauge Label	Angle (deg)	Value (PSIA) or (BTU/Ft2-Sec)	T Surf (DegR)	Gauge Label	Angle (deg)	Value (PSIA) or (BTU/Ft2-Sec)	T Surf (DegR)
P 30	-64.40	1.582(0)		P 9	38.22	7.657(0)		HT 71	19.60	3.907(1)	566.38
P 28	-50.11	2.689(0)		P 7	52.54	1.071(1)		HT 9	19.90	3.688(1)	563.19
P 26	-35.79	4.292(0)		P 5	66.86	1.262(1)		HT 7	21.51	3.147(1)	560.59
P 25	-28.63	5.614(0)		P 3	81.19	6.578(0)		HT 6	22.30	3.264(1)	559.76
P 24	-21.47	5.962(0)		P 1	95.51	2.923(0)		HT 5	23.09	3.851(1)	566.07
P 23	-14.30	6.342(0)		HT 32	-16.31	3.009(1)	559.77	HT 4	23.89	2.794(1)	557.78
P 22	-7.14	7.057(0)		HT 31	-13.25	3.216(1)	561.12	HT 3	24.69	3.375(1)	557.37
P 21	.02	8.271(0)		HT 29	-7.14	3.543(1)	562.56	HT 2	25.49	3.445(1)	557.24
P 20	4.79	7.587(0)		HT 28	-4.09	3.353(1)	562.95	HT 1	26.29	3.063(1)	556.27
P 15	7.18	7.564(0)		HT 25	5.08	3.723(1)	567.17	HT 62	26.29	3.184(1)	558.68
P 19	9.57	8.010(0)		HT 24	8.14	3.833(1)	563.20	HT 61	29.35	5.623(1)	573.10
P 14	11.96	7.940(0)		HT 64	12.91	3.764(1)	566.42	HT 59	35.46	6.169(1)	584.49
P 18	14.34	7.474(0)		HT 65	13.87	Null	Null	HT 58	38.51	6.745(1)	583.64
P 13	16.73	7.187(0)		HT 66	14.82	3.869(1)	567.19	HT 57	41.57	8.192(1)	588.53
P 17	19.12	9.001(0)		HT 67	15.78	Null	Null	HT 56	44.63	9.676(1)	604.60
P 12	21.51	9.057(0)		HT 68	16.73	4.121(1)	565.93	HT 55	47.68	1.032(2)	604.82
P 16	23.89	8.460(0)		HT 69	17.69	3.734(1)	565.48	HT 54	50.74	1.189(2)	619.55
P 11	26.28	6.821(0)		HT 70	18.64	4.036(1)	564.37	HT 53	53.79	1.336(2)	628.41
P 10	31.05	7.059(0)		HT 10	19.10	4.052(1)	564.66				

Run 77 Reduced Data Tabulation

Gauge Label	Angle (deg)	Value (PSIA) or (BTU/Ft2-Sec)	T Surf (DegR)	Gauge Label	Angle (deg)	Value (PSIA) or (BTU/Ft2-Sec)	T Surf (DegR)	Gauge Label	Angle (deg)	Value (PSIA) or (BTU/Ft2-Sec)	T Surf (DegR)
P 30	-64.40	8.747(-1)		P 9	38.22	2.144(1)		HT 71	19.60	4.035(2)	845.22
P 28	-50.11	1.593(0)		P 7	52.54	1.686(1)		HT 9	19.90	3.401(2)	816.08
P 26	-35.79	3.900(0)		P 5	66.86	1.143(1)		HT 7	21.51	2.868(2)	792.78
P 25	-28.63	4.401(0)		P 3	81.19	5.832(0)		HT 6	22.30	2.534(2)	778.42
P 24	-21.47	3.177(0)		P 1	95.51	2.779(0)		HT 5	23.09	2.598(2)	791.82
P 23	-14.30	1.779(0)		HT 32	-16.31	2.848(1)	564.95	HT 4	23.89	2.368(2)	772.69
P 22	-7.14	1.344(0)		HT 31	-13.25	1.684(1)	561.78	HT 3	24.69	2.237(2)	763.18
P 21	.02	2.553(0)		HT 29	-7.14	9.393(0)	575.94	HT 2	25.49	2.157(2)	754.66
P 20	4.79	7.379(0)		HT 28	-4.09	1.311(1)	597.67	HT 1	26.29	2.112(2)	751.70
P 15	7.18	5.894(0)		HT 25	5.08	7.417(1)	742.07	HT 62	26.29	2.461(2)	785.34
P 19	9.57	2.153(1)		HT 24	8.14	1.538(2)	800.46	HT 61	29.35	2.016(2)	767.34
P 14	11.96	1.762(1)		HT 64	12.91	2.681(2)	858.18	HT 59	35.46	1.972(2)	759.20
P 18	14.34	4.428(1)		HT 65	13.87	Null	Null	HT 58	38.51	1.836(2)	744.05
P 13	16.73	5.026(1)		HT 66	14.82	4.159(2)	887.80	HT 57	41.57	1.846(2)	741.94
P 17	19.12	4.154(1)		HT 67	15.78	4.737(2)	902.64	HT 56	44.63	1.597(2)	726.04
P 12	21.51	4.830(1)		HT 68	16.73	4.669(2)	888.00	HT 55	47.68	1.438(2)	716.74
P 16	23.89	2.981(1)		HT 69	17.69	4.738(2)	879.87	HT 54	50.74	1.401(2)	706.75
P 11	26.28	2.190(1)		HT 70	18.64	4.545(2)	866.79	HT 53	53.79	1.169(2)	684.95
P 10	31.05	2.183(1)		HT 10	19.10	3.921(2)	841.57				

Run 78 Reduced Data Tabulation

Gauge Label	Angle (deg)	Value (PSIA) or (BTU/Ft2-Sec)	T Surf (DegR)	Gauge Label	Angle (deg)	Value (PSIA) or (BTU/Ft2-Sec)	T Surf (DegR)	Gauge Label	Angle (deg)	Value (PSIA) or (BTU/Ft2-Sec)	T Surf (DegR)
P 30	-64.40	1.633(0)		P 9	38.22	2.019(1)		HT 71	19.60	1.184(2)	692.02
P 28	-50.11	2.835(0)		P 7	52.54	2.120(1)		HT 9	19.90	1.210(2)	700.56
P 26	-35.79	4.920(0)		P 5	66.86	1.176(1)		HT 7	21.51	1.672(2)	754.06
P 25	-28.63	6.250(0)		P 3	81.19	5.931(0)		HT 6	22.30	1.783(2)	765.18
P 24	-21.47	6.241(0)		P 1	95.51	2.708(0)		HT 5	23.09	2.321(2)	797.42
P 23	-14.30	6.928(0)		HT 32	-16.31	7.823(1)	601.77	HT 4	23.89	2.362(2)	796.95
P 22	-7.14	8.536(0)		HT 31	-13.25	7.814(1)	607.33	HT 3	24.69	3.124(2)	824.13
P 21	.02	1.094(1)		HT 29	-7.14	1.134(2)	622.21	HT 2	25.49	3.715(2)	831.98
P 20	4.79	7.420(0)		HT 28	-4.09	1.227(2)	618.27	HT 1	26.29	4.457(2)	849.19
P 15	7.18	4.030(0)		HT 25	5.08	7.408(1)	586.99	HT 62	26.29	7.552(2)	903.74
P 19	9.57	4.894(0)		HT 24	8.14	4.546(1)	578.20	HT 61	29.35	6.672(2)	838.89
P 14	11.96	4.332(0)		HT 64	12.91	5.293(1)	601.31	HT 59	35.46	2.651(2)	729.32
P 18	14.34	5.770(0)		HT 65	13.87	Null	Null	HT 58	38.51	2.366(2)	713.73
P 13	16.73	8.777(0)		HT 66	14.82	6.630(1)	615.51	HT 57	41.57	2.414(2)	717.12
P 17	19.12	1.867(1)		HT 67	15.78	7.587(1)	630.25	HT 56	44.63	2.468(2)	701.74
P 12	21.51	3.835(1)		HT 68	16.73	8.390(1)	640.57	HT 55	47.68	2.299(2)	690.05
P 16	23.89	4.603(1)		HT 69	17.69	9.046(1)	654.32	HT 54	50.74	1.981(2)	674.31
P 11	26.28	Null		HT 70	18.64	1.011(2)	673.97	HT 53	53.79	1.560(2)	654.83
P 10	31.05	Null		HT 10	19.10	1.212(2)	693.26				

Run 79 Reduced Data Tabulation

Gauge Label	Angle (deg)	Value (PSIA) or (BTU/Ft2-Sec)	T Surf (DegR)	Gauge Label	Angle (deg)	Value (PSIA) or (BTU/Ft2-Sec)	T Surf (DegR)	Gauge Label	Angle (deg)	Value (PSIA) or (BTU/Ft2-Sec)	T Surf (DegR)
P 30	-64.40	5.587(-1)		P 9	38.22	8.765(0)		HT 71	19.60	2.409(2)	686.51
P 28	-50.11	9.275(-1)		P 7	52.54	6.497(0)		HT 9	19.90	2.321(2)	689.76
P 26	-35.79	1.583(0)		P 5	66.86	2.566(0)		HT 7	21.51	2.456(2)	714.95
P 25	-28.63	2.228(0)		P 3	81.19	1.807(0)		HT 6	22.30	2.266(2)	715.58
P 24	-21.47	2.691(0)		P 1	95.51	1.023(0)		HT 5	23.09	2.248(2)	724.17
P 23	-14.30	2.726(0)		HT 32	-16.31	4.910(1)	578.51	HT 4	23.89	1.847(2)	716.25
P 22	-7.14	1.830(0)		HT 31	-13.25	3.927(1)	578.88	HT 3	24.69	1.715(2)	715.54
P 21	.02	1.290(0)		HT 29	-7.14	1.398(1)	564.66	HT 2	25.49	1.416(2)	700.84
P 20	4.79	1.322(0)		HT 28	-4.09	1.292(1)	557.25	HT 1	26.29	1.206(2)	692.16
P 15	7.18	1.321(0)		HT 25	5.08	1.920(1)	555.15	HT 62	26.29	1.537(2)	709.40
P 19	9.57	1.821(0)		HT 24	8.14	3.084(1)	559.35	HT 61	29.35	9.567(1)	651.41
P 14	11.96	3.559(0)		HT 64	12.91	7.437(1)	593.54	HT 59	35.46	1.003(2)	638.42
P 18	14.34	5.691(0)		HT 65	13.87	Null	Null	HT 58	38.51	8.737(1)	629.43
P 13	16.73	1.267(1)		HT 66	14.82	Null	Null	HT 57	41.57	7.835(1)	624.29
P 17	19.12	2.375(1)		HT 67	15.78	1.400(2)	630.68	HT 56	44.63	7.285(1)	616.44
P 12	21.51	3.077(1)		HT 68	16.73	1.622(2)	643.32	HT 55	47.68	7.042(1)	611.68
P 16	23.89	2.763(1)		HT 69	17.69	1.847(2)	655.86	HT 54	50.74	6.976(1)	610.64
P 11	26.28	1.352(1)		HT 70	18.64	2.136(2)	671.52	HT 53	53.79	5.746(1)	598.28
P 10	31.05	8.679(0)		HT 10	19.10	2.474(2)	693.03				

Run 80 Reduced Data Tabulation

Gauge Label	Angle (deg)	Value (PSIA) or (BTU/Ft2-Sec)	T Surf (DegR)	Gauge Label	Angle (deg)	Value (PSIA) or (BTU/Ft2-Sec)	T Surf (DegR)	Gauge Label	Angle (deg)	Value (PSIA) or (BTU/Ft2-Sec)	T Surf (DegR)
P 30	-64.40	2.019(0)		P 9	38.22	4.535(0)		HT 71	19.60	4.976(1)	576.01
P 28	-50.11	3.265(0)		P 7	52.54	2.881(0)		HT 9	19.90	3.482(1)	566.54
P 26	-35.79	5.043(0)		P 5	66.86	1.680(0)		HT 7	21.51	3.497(1)	565.94
P 25	-28.63	6.618(0)		P 3	81.19	7.320(-1)		HT 6	22.30	3.572(1)	566.00
P 24	-21.47	6.795(0)		P 1	95.51	3.583(-1)		HT 5	23.09	3.557(1)	566.03
P 23	-14.30	7.138(0)		HT 32	-16.31	4.418(1)	572.72	HT 4	23.89	3.741(1)	566.14
P 22	-7.14	7.371(0)		HT 31	-13.25	4.265(1)	572.34	HT 3	24.69	3.653(1)	565.40
P 21	.02	8.323(0)		HT 29	-7.14	3.929(1)	571.53	HT 2	25.49	3.673(1)	565.45
P 20	4.79	7.944(0)		HT 28	-4.09	3.849(1)	572.37	HT 1	26.29	3.492(1)	564.36
P 15	7.18	7.411(0)		HT 25	5.08	Null	Null	HT 62	26.29	4.222(1)	572.38
P 19	9.57	7.963(0)		HT 24	8.14	4.052(1)	572.79	HT 61	29.35	Null	Null
P 14	11.96	6.896(0)		HT 64	12.91	4.521(1)	575.38	HT 59	35.46	Null	Null
P 18	14.34	6.643(0)		HT 65	13.87	Null	Null	HT 58	38.51	3.660(1)	568.55
P 13	16.73	6.254(0)		HT 66	14.82	4.451(1)	573.77	HT 57	41.57	3.099(1)	562.67
P 17	19.12	7.406(0)		HT 67	15.78	4.262(1)	572.95	HT 56	44.63	2.503(1)	558.17
P 12	21.51	7.610(0)		HT 68	16.73	4.335(1)	572.55	HT 55	47.68	2.191(1)	555.22
P 16	23.89	7.110(0)		HT 69	17.69	4.469(1)	573.33	HT 54	50.74	2.153(1)	555.42
P 11	26.28	5.605(0)		HT 70	18.64	4.654(1)	574.69	HT 53	53.79	1.679(1)	551.41
P 10	31.05	4.727(0)		HT 10	19.10	4.003(1)	569.47				

Run 81 Reduced Data Tabulation

Gauge Label	Angle (deg)	Value (PSIA) or (BTU/Ft2-Sec)	T Surf (DegR)	Gauge Label	Angle (deg)	Value (PSIA) or (BTU/Ft2-Sec)	T Surf (DegR)	Gauge Label	Angle (deg)	Value (PSIA) or (BTU/Ft2-Sec)	T Surf (DegR)
P 30	-64.40	1.237(0)		P 9	38.22	1.987(1)		HT 71	19.60	6.899(1)	583.22
P 28	-50.11	Null		P 7	52.54	1.550(1)		HT 9	19.90	6.537(1)	578.37
P 26	-35.79	3.661(0)		P 5	66.86	9.691(0)		HT 7	21.51	8.024(1)	589.23
P 25	-28.63	4.391(0)		P 3	81.19	Null		HT 6	22.30	8.989(1)	595.09
P 24	-21.47	4.769(0)		P 1	95.51	2.182(0)		HT 5	23.09	1.114(2)	611.36
P 23	-14.30	5.095(0)		HT 32	-16.31	Null	Null	HT 4	23.89	1.291(2)	616.29
P 22	-7.14	6.084(0)		HT 31	-13.25	6.113(1)	580.26	HT 3	24.69	1.546(2)	625.48
P 21	.02	7.584(0)		HT 29	-7.14	7.282(1)	584.23	HT 2	25.49	1.650(2)	628.76
P 20	4.79	7.104(0)		HT 28	-4.09	8.105(1)	588.03	HT 1	26.29	2.004(2)	648.08
P 15	7.18	4.561(0)		HT 25	5.08	8.245(1)	615.45	HT 62	26.29	3.378(2)	702.28
P 19	9.57	5.435(0)		HT 24	8.14	3.474(1)	570.02	HT 61	29.35	5.751(2)	801.35
P 14	11.96	3.936(0)		HT 64	12.91	4.214(1)	572.24	HT 59	35.46	1.669(2)	711.20
P 18	14.34	3.711(0)		HT 65	13.87	Null	Null	HT 58	38.51	1.815(2)	707.38
P 13	16.73	3.825(0)		HT 66	14.82	Null	Null	HT 57	41.57	1.780(2)	678.15
P 17	19.12	7.567(0)		HT 67	15.78	4.860(1)	574.79	HT 56	44.63	1.816(2)	651.42
P 12	21.51	1.372(1)		HT 68	16.73	4.949(1)	573.98	HT 55	47.68	1.751(2)	650.22
P 16	23.89	1.541(1)		HT 69	17.69	5.933(1)	578.08	HT 54	50.74	1.433(2)	637.77
P 11	26.28	3.095(1)		HT 70	18.64	6.817(1)	582.36	HT 53	53.79	1.227(2)	626.91
P 10	31.05	5.289(1)		HT 10	19.10	6.301(1)	579.40				

Run 98 Reduced Data Tabulation

NASA
National Aeronautics and Space Administration

Report Documentation Page

1. Report No.	2. Government Accession No.	3. Recipient's Catalog No.
NASA CR-181893		

4. Title and Subtitle
Studies of Aerothermal Loads Generated in Regions of Shock/Shock Interaction in Hypersonic Flow

5. Report Date
October 1991

6. Performing Organization Code

7. Author(s)
Michael S. Holden, John R. Moselle, and Jinho Lee

8. Performing Organization Report No.

10. Work Unit No.
506-40-21-01

9. Performing Organization Name and Address
Calspan-UB Research Center
P.O. Box 400
Buffalo, NY 14225

11. Contract or Grant No.
NAS1-17721

13. Type of Report and Period Covered
Contractor Report

12. Sponsoring Agency Name and Address
National Aeronautics and Space Administration
Langley Research Center
Hampton, VA 23665-5225

14. Sponsoring Agency Code

15. Supplementary Notes
Langley Technical Monitor: L. Roane Hunt
Final Report

16. Abstract

Studies are presented of the aerothermal characteristics of shock/shock/boundary layer interactions generated by single and multiple incident shocks. An extensive review made of the literature on this subject showed that there was significant lack of detailed high-quality experimental data in the high Mach number and Reynolds number flow regime. The experimental studies presented here were conducted over a Mach number range from 6 to 19 for a range of Reynolds numbers to obtain both laminar and turbulent interaction regions. Detailed heat transfer and pressure measurements were made for a range of interaction types and incident shock strengths over a transverse cylinder, with emphasis on the types III and IV interaction regions. These measurements indicated that the peak heat transfer and pressure increased with the occurrence of transition in the shear layer generated in both type III and type IV interactions, and with increasing Mach number. For some type IV interactions with flowfield configurations close to those for maximum heating, a flow instability was observed that caused large temporal variations in the peak heating. The measurements made in this study were compared with the simple Edney, Keyes and Hains models for a range of interaction configurations and freestream conditions. The effect of sweeping the interaction is to lower the heating and pressure levels in roughly the same proportions to the reductions observed when sweeping a cylinder in the absence of the interaction. The studies of multiple-shock interaction demonstrated that the largest heat loads are generated on the cylinder if the shocks coalesce before they are incident on the cylinder. The complex flowfields and aerothermal loads generated by multiple-shock impingement, while not generating as large peak loads, provide important test cases for code prediction. It will be difficult to accurately predict the maximum heating in shock/shock-interaction regions over a large and important part of the flight regime, because free-shear-layer transition can take place at low Reynolds numbers, in either single- or multiple-shock/shock interactions, and because of the occurrence of flow instabilities for type IV interactions.

17. Key Words (Suggested by Author(s))	18. Distribution Statement
Hypersonic Interference Heating Shock/Shock Interaction	Unclassified - Unlimited Subject Category 34

19. Security Classif. (of this report)	20. Security Classif. (of this page)	21. No. of pages	22. Price
Unclassified	Unclassified	341	A15

NASA FORM 1626 OCT 86